FUNDAMENTALS OF ACOUSTICS

FUNDAMENTALS OF ACOUSTICS

SECOND EDITION

LAWRENCE E. KINSLER
Professor of Physics
United States Naval Postgraduate School
Monterey, California

AUSTIN R. FREY
Professor of Physics
United States Naval Postgraduate School
Monterey, California

John Wiley & Sons, Inc., New York · London

Library of Congress Catalog Card Number: 62-16151
Printed in the United States of America

PREFACE

One purpose of this book is to present, in as simple and concise a form as possible, the fundamental principles underlying the generation, transmission, and reception of acoustic waves. A second purpose is to apply these principles to a number of important fields of applied acoustics. The extensive developments of the past few decades have so broadened these fields that an exhaustive treatment of all their aspects could not be contained in any single volume, and it has therefore been necessary to restrict the number of topics considered and to limit the extent to which each is carried.

In making this selection our primary aim has been to familiarize the student with the fundamental concepts and terminology of the subject and with the analytical methods that are available for attacking acoustical problems. The first nine chapters of the book provide an analysis of the various types of vibration of solid bodies, and of the propagation of sound waves through fluid media. These nine chapters will suffice for a one-semester course in the fundamentals of theoretical acoustics, and they may also be used for the first semester of a full-year course in theoretical and applied acoustics. The remaining six chapters are concerned with a limited number of applications of acoustics. Those discussed have been selected either because of their outstanding importance, as concrete illustrations of the practical application of mathematical techniques developed in the earlier chapters, or because adequate treatments are not readily available in other books. Since each of these last six chapters is an independent, self-contained unit, an instructor presenting a two-semester course may omit any one or more of these chapters and substitute material from the more specialized textbooks of acoustics.

One factor that has been kept in mind in writing this book is the close association that exists between acoustics and electrical engineering. Not only do nearly all modern devices used in the generation and reception of acoustic waves depend for their operation on a conversion of electrical into acoustical energy, or vice versa, but the mathematical formulation of many acoustical problems is also quite similar to that employed in corresponding problems involving the transmission of high-frequency currents through lines or networks. In addition, it has been found that the design and analysis of many acoustical devices is facilitated by converting their mechanical or acoustical properties, such as mass or pressure, into analogous electrical quantities, and then carrying through either a theoretical or an experimental analysis of the resulting analogous electrical circuit. In view of these factors, the mechanical and acoustical notation employed has been chosen to emphasize the similarity between these fields and the conversion of results from one to the other. The interchange of concepts and techniques between acoustics and electrical engineering has also been enhanced through the consistent use of MKS (meter-kilogram-second) units in this book.

The book may be studied with equal facility by advanced undergraduate or graduate students in Physics, Electrical Engineering, Electronic Engineering, and similar disciplines. The essential requirements are a knowledge of the fundamental principles of mechanics and electricity and an understanding of the methods of calculus, including partial derivatives. Since this book is intended primarily as a textbook for classroom use, rather than as an encyclopedic reference work, no attempt has been made to include a complete bibliography, although numerous references are given, either where the treatment is necessarily incomplete or to provide an interested reader with a source of more detailed information. We have attempted to derive each important equation from the fundamental laws of physics and to show in some detail not only the mathematical steps but also the logical processes involved in these derivations. The derivations of a few of the less important equations have been intentionally omitted and are, instead, included as exercises for the student among the problems given at the end of each chapter.

Considerable attention has been paid to the selection of a comprehensive set of problems, for the ultimate check on the student's understanding of the subject is his ability to apply his knowledge to new situations. In order to assist those engaged in self-study of this book, answers are provided in the appendix for the odd-numbered problems. Tables of physical constants and functions are given in the Appendix.

As far as possible, the recommended standards of acoustical terminology of the American Standards Association have been used throughout this book, and a glossary of symbols is incorporated in the Appendix as a further aid in clarifying the confusion that might result from the multiplicity of physical quantities represented by certain of the more commonly used symbols.

The writing of a second edition of this book has been largely the responsibility and work of one of the authors (L. E. Kinsler). It differs from the first edition in the following important respects. The MKS system of units is used instead of the CGS system (see Section 1.3). Considerable new material has been added to the chapters on Transmission Phenomena, Hearing, and Architectural Acoustics. The chapter on Absorption of Sound Waves has been completely rewritten at a more advanced level and brought up to date. Much of the material on horn speakers contained in a separate chapter in the first edition has been deleted, the remainder being incorporated in a single unified chapter on Loudspeakers. The chapter on Ultrasonics has been deleted since a single chapter on this broad topic tends to be encyclopedic rather than fundamental. A new chapter on Ultrasonic and Sonar Transducers has been added. The chapter on Underwater Acoustics has been greatly expanded in keeping with the growing importance of this branch of acoustics. Finally, many minor changes have been made as a result of comments and suggestions received from users of the first edition. We hereby express our sincere appreciation for such assistance.

LAWRENCE E. KINSLER
AUSTIN R. FREY

Monterey, Calif.
July 1962

CONTENTS

chapter 1

FUNDAMENTALS OF VIBRATION

1.1 Introduction. In a broad sense, acoustics may be defined as the generation, transmission, and reception of energy in the form of vibrational waves in matter. As the atoms or molecules of a fluid or solid are displaced from their normal configuration an internal elastic restoring force of stiffness arises. Typical examples of such a force include the tensile force produced when a spring is stretched, the increase in pressure produced when a fluid is compressed into a lesser volume, and the transverse restoring force produced when a point on a stretched wire is displaced in a direction normal to its length. It is the action of this elastic restoring force, coupled with the inertia of the system, that enables matter to participate in oscillatory vibrations and thereby generate and transmit acoustic waves.

Many different types of vibration occur in the generation and propagation of acoustic waves. In a narrow sense, their frequency is limited to the range from about 20 cycles/sec to 15,000 cycles/sec, which produce the auditory sensation of sound for the average person. However, in a broader sense they also include both the *ultrasonic* frequencies above 15,000 cycles/sec, which although inaudible have important practical applications in numerous fields, and the inaudible *infrasonic* frequencies below 20 cycles/sec. The modes of vibration range from the simple sinusoidal vibrations produced in the adjacent air by a mounted tuning fork vibrating at its fundamental frequency, through the complex pattern of vibrations generated by a bowed violin string, to the nonperiodic vibrations associated with a noise or an explosion. In studying such vibrations it is advisable to begin with the simplest type, i.e., a sinusoidal vibration that has only a single frequency component.

1.2 Simple Oscillator. If a mass m, fastened to some sort of spring and constrained to move back and forth in just one direction, is displaced from its central or rest position and is then released, the mass will be observed to vibrate. Measurement shows that the frequency of vibration is constant and that the displacement of the mass from its rest position is a sinusoidal function of time. Sinusoidal vibrations of this type are called *simple harmonic vibrations.* It can be shown, both experimentally and theoretically, that the mass will vibrate with simple harmonic motion whenever the restoring force resulting from the stiffness of the spring is directly proportional to the displacement of the mass from its rest position. A very large number of vibrators used in acoustics are of this type, or are approximately equivalent to it. Loaded tuning forks and loudspeaker diaphragms, which are so constructed that at low frequencies their mass moves as a unit and may be considered to be concentrated near their center, are but two examples. Even more complex vibrating systems have many of the characteristics of the simple system and may be studied to a first approximation by being reduced to simple oscillators.

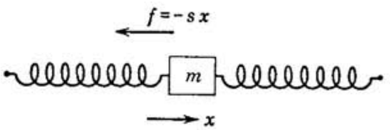

Fig. 1.1. Simple oscillator.

The only physical restriction placed upon the equations shortly to be developed for the motion of a simple oscillator is that the restoring force be directly proportional to the displacement. Whenever the amplitude of vibration is sufficiently small so that the *elastic limit* of the spring is not exceeded, the frequency of vibration is independent of amplitude and the motion is simple harmonic, but this is not true if this limit is exceeded. A similar restriction applies to more complex types of vibration, such as those corresponding to the transmission of an acoustic wave through a fluid medium. If the resulting acoustic pressures are so large that they are no longer proportional to the displacement of the particles of the fluid, it becomes necessary to modify the normal acoustic equations. With sounds of ordinary intensity this is not necessary, for even the noise generated by a large crowd at a football game rarely causes the amplitude of motion of the air molecules to exceed one-tenth of a millimeter, which is within the limit given above. The amplitude of the shock wave generated by a large explosion is, however, well above this limit, and hence the normal acoustic equations are not applicable.

Returning now to a consideration of the simple oscillator, such as that shown in Fig. 1.1, let us assume that the restoring force f can be expressed by the equation

$$f = -sx \tag{1.1}$$

where x is the displacement of the mass m from its rest position, s is the *stiffness constant* of the spring, and the minus sign indicates that the force is directed oppositely to the displacement. Substituting this expression for force into the general equation of linear motion

$$f = m \frac{d^2x}{dt^2} \tag{1.2}$$

we obtain

$$\frac{d^2x}{dt^2} + \frac{s}{m} x = 0 \tag{1.3}$$

This equation is an important second-order linear differential equation whose solution is well known and may be obtained by several methods.

One method is to assume a solution of the type

$$x = A_1 \cos \gamma t$$

Differentiation and substitution of this expression in equation 1.3 shows that it is a solution if we identify γ with $\sqrt{s/m}$. Furthermore, it may similarly be shown that

$$x = A_2 \sin \sqrt{s/m}\, t$$

is also a solution. The complete general solution is the sum of these two solutions, i.e.,

$$x = A_1 \cos \sqrt{s/m}\, t + A_2 \sin \sqrt{s/m}\, t \tag{1.4}$$

where A_1 and A_2 are two arbitrary constants. This equation may be rewritten in a more convenient form as

$$x = A_1 \cos \omega_0 t + A_2 \sin \omega_0 t \tag{1.4a}$$

by replacing $\sqrt{s/m}$ with ω_0, a constant known as the *angular frequency* constant.

The frequency of vibration f_0 of the simple oscillator is related to the value of this angular frequency constant ω_0 by the equation $\omega_0 = 2\pi f_0$. Therefore, the frequency of vibration is given by

$$f_0 = \frac{\omega_0}{2\pi} = \frac{1}{2\pi}\sqrt{\frac{s}{m}} \tag{1.5}$$

It is to be noted that either decreasing the numerical value of the stiffness constant or increasing the mass of the oscillator results in a decreased frequency. This mathematical deduction is in agreement with what we would conclude from a logical consideration of the physical principles involved; i.e., increasing mass or decreasing stiffness would be expected to slow down the motion. The *period*, T, of one complete vibration is given by the reciprocal of equation 1.5.

1.3 Choice of Units. Before proceeding further in our discussion of vibrations, it is necessary to make a decision as to what system of physical units should be used in the above and in following equations. Unfortunately, acoustics encompasses such a wide range of scientific and engineering disciplines that this choice is a difficult one to make. For instance, a survey of the literature will reveal a great lack of uniformity; usually each writer uses the units which are most common in his particular field of interest. Historically, much of the fundamental experimental work in acoustics has been reported in a terminology related to the CGS (centimeter-gram-second) system of units. Considerable engineering work has also been carried out in a mixture of metric and English units. Much recent work in electroacoustics and underwater acoustics is commonly reported in the MKS (meter-kilogram-second) system of units. Unfortunately, this lack of uniformity has not been resolved by the most recent publication of an American Standard on Acoustical Terminology.[1]

However, it is becoming generally recognized that the array of basic equations pertinent to acoustics is simpler when expressed in MKS units than when expressed in CGS units. This is particularly true whenever equivalent electrical circuits are employed for an analysis of electromechanical or electroacoustic systems. Therefore, all equations in this book are derived primarily for use in MKS units. It is hoped that the consistent use of the MKS system throughout this book will make its merits clearer and enable the reader to use it to his fullest advantage. For the benefit of those who wish to continue using the CGS system, it is to be noted that all the basic equations in this book, other than those derived in Chapter 10 through 12, may be used with equal facility in a consistent set of CGS units. Finally, a conversion table relating the CGS and MKS system of units is incorporated in the Appendix in order to assist the reader in using data in the literature which is presented in CGS units.

Returning to equation 1.5, the frequency f_0 is given in cycles/sec when the MKS units of newtons/meter are used for the stiffness constant s and kilograms for the mass m. If CGS units were to be used in this equation, s would be expressed in dynes/centimeter and m in grams.

1.4 Initial Conditions. The constants A_1 and A_2 are determined by the manner in which the mass is started into motion, i.e., by the *initial conditions*. If at the time $t = 0$ the mass has an initial displacement x_0 and an initial velocity v_0, then the arbitrary constants A_1 and A_2 are fixed by these

[1] *Acoustical Terminology*, S1.1–1960, American Standards Association, (1960).

initial conditions, and the subsequent motion of the mass is completely determined. A direct substitution into equation 1.4*a* of $x = x_0$ at $t = 0$ will show that A_1 equals the initial displacement x_0. Differentiation of equation 1.4*a* and substitution of the initial velocity condition gives

$$v_0 = -\omega_0 A_1 \sin 0 + \omega_0 A_2 \cos 0$$

so that v_0 must equal $\omega_0 A_2$. Therefore $A_2 = v_0/\omega_0$, and equation 1.4*a* becomes

$$x = x_0 \cos \omega_0 t + \frac{v_0}{\omega_0} \sin \omega_0 t \tag{1.4b}$$

Another form of equation 1.4*a* may be obtained by letting $A_1 = A \cos \phi$ and $A_2 = -A \sin \phi$, where A and ϕ are two new arbitrary constants. Substitution and simplification then gives

$$x = A \cos (\omega_0 t + \phi) \tag{1.6}$$

where A is the *amplitude* of the motion and ϕ is the initial *phase angle* of the motion. Also we may show that A and ϕ have their values determined by the usual initial conditions and are

$$A = \left(x_0^2 + \frac{v_0^2}{\omega_0^2}\right)^{1/2}, \quad \text{and} \quad \phi = \tan^{-1} \frac{-v_0}{\omega_0 x_0} \tag{1.6a}$$

1.5 Complex Exponential Method of Solution. A second method of solving the original differential equation (1.3) is to assume a solution of the form

$$x = Ae^{\gamma t}$$

This expression will satisfy the equation if γ^2 is set equal to $-\omega_0^2$, which is equivalent to $\gamma = \pm j\omega_0$, where $j = \sqrt{-1}$. Letting γ equal both $+j\omega_0$ and $-j\omega_0$, the complete general solution may be written

$$x = A_1 e^{j\omega_0 t} + A_2 e^{-j\omega_0 t} \tag{1.7}$$

where A_1 and A_2 are constants to be determined from the initial conditions of motion. Utilizing the well-known relations between exponential and trigonometric quantities,

$$e^{j\omega_0 t} = \cos \omega_0 t + j \sin \omega_0 t$$

and

$$e^{-j\omega_0 t} = \cos \omega_0 t - j \sin \omega_0 t$$

equation 1.7 may be reduced to

$$x = (A_1 + A_2) \cos \omega_0 t + j(A_1 - A_2) \sin \omega_0 t \tag{1.7a}$$

From the physical considerations it is apparent that the displacement of the mass must be a *real* quantity (not involving j), and hence, if A_1 and A_2 are chosen as real numbers, this condition requires that $A_1 = A_2$. The solution then contains in effect only a single arbitrary constant, $A_1 + A_2 = 2A_1$, and is consequently incomplete. To obtain the complete solution we must assume that $\mathbf{A}_1$ and $\mathbf{A}_2$ are complex,[1] i.e.,

$$\mathbf{A}_1 = a_1 + jb_1 \quad \text{and} \quad \mathbf{A}_2 = a_2 + jb_2$$

where a_1, a_2, b_1, and b_2 are real numbers. Then equation 1.7 may be reduced to

$$x = (a_1 + a_2)\cos \omega_0 t - (b_1 - b_2)\sin \omega_0 t + j[(b_1 + b_2)\cos \omega_0 t + (a_1 - a_2)\sin \omega_0 t] \quad (1.7b)$$

and the displacement will be real at all values of t if the coefficients of the trigonometric expressions in the imaginary term are zero, i.e., if $b_1 + b_2 = 0$ and $a_1 - a_2 = 0$. Under these conditions $\mathbf{A}_1$ and $\mathbf{A}_2$ are complex conjugates, and equation 1.7*b* becomes

$$x = 2a_1 \cos \omega_0 t - 2b_1 \sin \omega_0 t \quad (1.7c)$$

which is identical in form with equation 1.4*a*.

In actual practice it is unnecessary to go through the mathematical steps required to make the imaginary part of the general solution vanish, for it is sufficient to adopt the convention that the *real part of the complex solution is by itself a complete general solution* of the physical problem indicated by the original differential equation. It is self-evident that the real part of the above complex solution (equation 1.7*b*) is a complete solution. Similarly, the real part of either $\mathbf{A}_1 e^{j\omega_0 t}$ or $\mathbf{A}_2 e^{-j\omega_0 t}$ is likewise a complete solution.

It will be the general practice in this textbook to analyze problems by the complex exponential method. The chief advantages of the procedure, as compared with the trigonometric method of solution, are its greater mathematical simplicity and the relative ease with which the phase relationships between the various mechanical and acoustic variables can be determined. In addition, many of the problems that arise in acoustics are similar to those encountered in alternating-current electrical theory, so that the results and techniques of electrical theory may be used in solving acoustic problems. Whenever possible, the notation used in this textbook is chosen to emphasize this similarity. The chief disadvantage of the complex exponential method is that the solutions obtained do not represent the *true* values of the various acoustic variables, and care must be taken

[1] In this book **boldface type** will be used to indicate **complex** quantities; *italic type* will represent *real* quantities.

to obtain the *real* part of the complex solution in order to arrive at the correct physical equation or numerical solution.

1.6 Physical Characteristics of Simple Harmonic Motion. Differentiation of equation 1.6 shows that the velocity is given by

$$v = \frac{dx}{dt} = -\omega_0 A \sin(\omega_0 t + \phi) \tag{1.8}$$

and the acceleration by

$$a = \frac{d^2x}{dt^2} = -\omega_0^2 A \cos(\omega_0 t + \phi) = -\omega_0^2 x \tag{1.8a}$$

From these equations it will be seen that the displacement lags 90° or $\pi/2$ radians behind the velocity and that the acceleration is out of phase with the displacement by 180° or π radians, as shown in Fig. 1.2.

Consideration of the complex form of the equation representing this type of motion leads to similar results. The expression $e^{j\omega_0 t}$ may be thought of as a vector of unit length, rotating in a counterclockwise direction in the complex plane with an angular velocity ω_0. Similarly, any complex quantity **A** having the components a and jb may be represented by $Ae^{j\phi}$, a vector of length $A = (a^2 + b^2)^{1/2}$ making a phase angle ϕ, whose tangent is b/a, with the axis of reals. It can readily be shown that the product of any two complex quantities is then represented by a vector whose length is

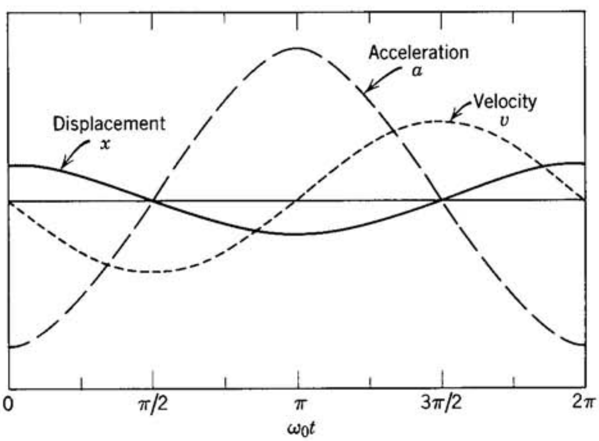

Fig. 1.2. The velocity v always leads the displacement x by a time interval corresponding to $\pi/2$ radians of phase-angle difference. Acceleration a and displacement x are always π radians out of phase with each other. Plotted curves correspond to $\phi = 0$ and $\omega_0 = 2$.

the product of the lengths of the individual vectors, and whose phase angle is the sum of their phase angles. The expression $\mathbf{A}e^{j\omega_0 t}$ consequently is equivalent to $Ae^{j(\omega_0 t+\phi)}$ and represents a vector of length A and initial phase angle ϕ, rotating counterclockwise in the complex plane with the angular velocity ω_0, Fig. 1.3. The real part of this rotating vector, i.e., its projection on the axis of reals, has the magnitude

$$A \cos (\omega_0 t + \phi)$$

and, therefore, varies with time in a simple harmonic manner. The reader may similarly show that the real part of $\mathbf{A}e^{-j\omega_0 t}$ also varies in a simple harmonic manner.

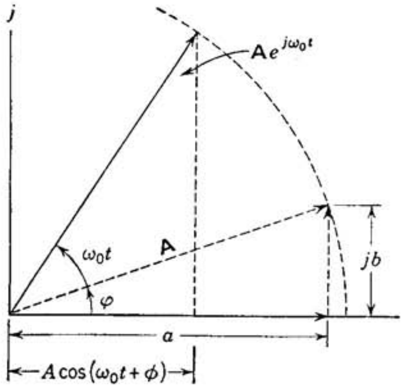

Fig. 1.3. Physical representation of a rotating complex vector $\mathbf{A}e^{j\omega_0 t}$.

If the displacement x is represented by the complex equation

$$\mathbf{x} = \mathbf{A}e^{j\omega_0 t}$$

differentiation with respect to time gives $\mathbf{v} = j\omega_0 \mathbf{x}$, and hence the complex vector representing velocity *leads* that representing displacement by j, i.e., by a phase angle of 90°. The projection of this vector on the axis of reals then represents the instantaneous velocity of motion, the velocity amplitude being $\omega_0 A$. A further differentiation shows that the complex vector representing acceleration is out of phase with the displacement vector by -1, or 180°.

1.7 Energy of Vibration. The energy of a mass oscillating with simple harmonic motion of amplitude A and angular frequency ω_0 is the sum of the system's potential energy E_p and its kinetic energy E_k. The potential energy is the work done in distorting the spring as the mass moves from its position of static equilibrium. Since the force exerted by the mass on the spring is in the direction of the displacement and equals $+sx$, the potential energy E_p stored in the spring is

$$E_p = \int_0^x sx\, dx = \tfrac{1}{2}sx^2 = \tfrac{1}{2}m\omega_0^{\,2}x^2 \tag{1.9}$$

This energy is expressed in *joules* in the MKS system of units. An alternative form of this equation may be obtained if the value of x as given by equation 1.6 is substituted in equation 1.9. Then

$$E_p = \tfrac{1}{2}m\omega_0^{\,2}A^2 \cos^2(\omega_0 t + \phi) \tag{1.9a}$$

Using the usual expression for kinetic energy, we have

$$E_k = \tfrac{1}{2}mv^2 = \tfrac{1}{2}m\omega_0^{\,2}A^2 \sin^2(\omega_0 t + \phi) \tag{1.10}$$

The total energy E of the system at all times is, therefore,

$$E = E_p + E_k = \tfrac{1}{2}m\omega_0^{\,2}A^2[\cos^2(\omega_0 t + \phi) + \sin^2(\omega_0 t + \phi)]$$

or

$$E = \tfrac{1}{2}m\omega_0^{\,2}A^2 = \tfrac{1}{2}sA^2 \tag{1.11}$$

so that the total energy is constant. Since the system was assumed to be nondissipative, i.e., to have no frictional losses, this result is to be expected. The magnitude of the total energy is seen to be equal to the potential energy ($\frac{1}{2}sA^2$), when the mass has its greatest displacement, and is also equal to the kinetic energy ($\frac{1}{2}m\omega_0^{\,2}A^2$) when the mass has its greatest velocity. Expressed in terms of ω_0 and A, it is to be noted that E depends on the product of the squares of these two quantities. This particular dependence of energy on frequency and displacement amplitude recurs frequently in acoustics, both for sound sources and sound waves. For instance, a specified acoustic output may be obtained at high frequencies with an amplitude of vibration of the sound source that is small as compared to that required at low frequencies.

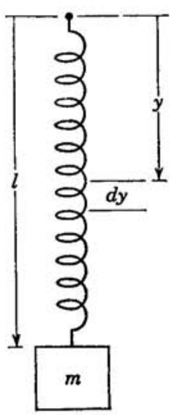

Fig. 1.4. Effect of mass of spring.

1.8 Effect of Including Mass of Spring. If the mass m_s of the spring is not negligible as compared with the mass m attached to the spring, it is to be expected that this additional inertia of the system will result in a reduced frequency of vibration. Let the length of the spring be l, and assume the velocity of any element dy of the spring, Fig. 1.4, to be proportional to its distance y from the fixed end of the spring. Then the velocity of this element is given by vy/l, where v is the velocity of the free end of the spring to which the mass is attached. The total kinetic energy of the spring can be obtained by integrating the kinetic energy of a length dy, along the entire spring. Then

$$E_k \text{ of spring} = \frac{1}{2}\int_0^l \left(\frac{m_s}{l}\,dy\right)\left(\frac{y}{l}\,v\right)^2 = \frac{1}{6}\,m_s v^2$$

and hence the total kinetic energy of the system is given by

$$E_k \text{ of system} = \frac{1}{2}\left(m + \frac{m_s}{3}\right)v^2$$

Assuming that the stiffness constant s is measured with the spring hanging in a vertical position, the potential energy ($\frac{1}{2}sx^2$) is the same as for a massless spring.

Since the system is nondissipative the total energy must be constant. Therefore,

$$E = \frac{1}{2}\left(m + \frac{m_s}{3}\right)v^2 + \tfrac{1}{2}\bar{s}x^2 = \text{constant} \tag{1.12}$$

Setting $v = dx/dt$ and differentiating with respect to time, we have

$$\left(m + \frac{m_s}{3}\right)\frac{d^2x}{dt^2} + sx = 0 \tag{1.12a}$$

as the differential equation representing the motion. Upon comparing this equation with equation 1.3, it is seen to be equivalent if ω_0 is now given by

$$\omega_0{}^2 = \frac{s}{m + (m_s/3)} \tag{1.12b}$$

When the mass of the spring is not negligible, the frequency of vibration may, therefore, be determined by adding to the suspended mass one-third of the mass of the spring. This example illustrates how a somewhat complicated vibrating system, having both mass and variation in motion distributed along the length of the spring, may to a first approximation be represented by an equivalent simple oscillator.

1.9 Linear Combinations of Simple Harmonic Vibrations. In many important situations that arise in acoustics the motion of a body is a linear combination of the vibrations induced separately by two or more simple harmonic motions. The displacement of the body is then the *algebraic* sum of the individual displacements.

One important example is the combination of two such motions that have the same angular frequency ω. Thus, if the two individual displacements are given by

$$x_1 = A_1 \cos(\omega t + \phi_1) \quad \text{and} \quad x_2 = A_2 \cos(\omega t + \phi_2)$$

then their linear combination along one direction is $x = x_1 + x_2$. By the use of the familiar trigonometric relations involving the sums and differences of angles it is possible to convert this expression for the displacement into the more convenient form

$$x = A \cos(\omega t + \phi) \tag{1.13}$$

where

$$A^2 = A_1^{\,2} + A_2^{\,2} + 2A_1A_2 \cos(\phi_1 - \phi_2) \tag{1.13a}$$

and

$$\tan \phi = \frac{A_1 \sin \phi_1 + A_2 \sin \phi_2}{A_1 \cos \phi_1 + A_2 \cos \phi_2} \tag{1.13b}$$

Therefore, the linear combination of two simple harmonic vibrations of identical frequency results in a new simple harmonic vibration of this same frequency, having a new amplitude A and a new phase angle ϕ. It is to be noted that upon the combination of two such vibrations that have identical initial phase angles, i.e., $\phi_1 = \phi_2$, the above equations simplify to a new motion of amplitude $A = A_1 + A_2$ and phase angle $\phi = \phi_1 = \phi_2$. This result is to be anticipated from fundamental physical principles. In general, the vibration resulting from the linear combination of two simple harmonic vibrations of identical frequency is another simple harmonic vibration of this same frequency, having a different phase angle ϕ, and an amplitude A in the range of the absolute values given by

$$|A_1 + A_2| \geq A \geq |A_1 - A_2|$$

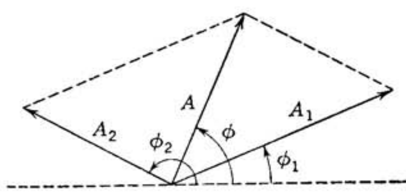

Fig. 1.5. Complex vector combination, $\mathbf{A} = \mathbf{A}_1 + \mathbf{A}_2$, of two simple harmonic motions having identical frequencies.

It is possible to combine two simple harmonic vibrations of identical frequency by graphical methods. Polar coordinates are used, with the radius representing the amplitude of the vibration and the polar angle representing the phase angle. The vector sum of the two separate vibrations then represents the resultant combination vibration, Fig. 1.5. An extension of this method may be applied to the linear combination of any number of simple harmonic vibrations of identical frequency.

It may readily be shown that the resultant vibration, representing a combination of any number n of simple harmonic vibrations of identical frequency, has the amplitude given by

$$A^2 = (\sum A_n \cos \phi_n)^2 + (\sum A_n \sin \phi_n)^2 \tag{1.14}$$

and the phase angle ϕ whose tangent is

$$\tan \phi = \frac{\sum A_n \sin \phi_n}{\sum A_n \cos \phi_n} \tag{1.14a}$$

Thus any linear combination of simple harmonic vibrations of identical frequency produces a new simple harmonic vibration of this same frequency. Furthermore, upon the combination of such vibrations into one resultant vibration, it is impossible to resolve this vibration by physical means into its original component vibrations.

When two or more sound waves are simultaneously acting at a point in a fluid medium, the periodic sound pressures of the individual waves combine in a linear fashion similar to that described above for simple harmonic vibrations. Many common acoustic observations may be explained by means of this type of linear combination. For instance, the simultaneous sounding of a number of sources that produce sounds of the same frequency cannot be distinguished, except possibly in loudness or directional characteristics, from any one of the sources sounded alone. The analysis also shows that sounds from two sources of the same frequency may completely cancel each other at some particular point, if they arrive at the point with identical amplitudes but are exactly opposite in phase.

1.10 Linear Combination of Different Frequencies. The general expression for the linear combination of two simple harmonic vibrations of different frequency is

$$x = A_1 \cos (\omega_1 t + \phi_1) + A_2 \cos (\omega_2 t + \phi_2) \tag{1.15}$$

where ω_1 is the angular frequency of one vibration, and ω_2 that of the other. The resulting motion is complex, rather than simple harmonic; i.e., it cannot be represented by a simple sine or cosine function. However, if ω_1 and ω_2 are commensurable, i.e., if the ratio of ω_1 to ω_2 is a rational number, the motion is periodic with a frequency given by the greatest common divisor of $\omega_1/2\pi$ and $\omega_2/2\pi$. If ω_1 and ω_2 are incommensurable, not only is the resulting motion no longer simple harmonic, but in addition it is no longer periodic, and is instead a complex oscillation which never exactly repeats itself.

In contrast to the combination of vibrations of identical frequency, the combination of vibrations of any two different frequencies is reversible; i.e., the complex vibration is capable of being uniquely resolved into its two component simple harmonic vibrations. A physical illustration of this characteristic is the ability of various types of sound analyzers to analyze a complex sound into its component frequencies. It is to be noted that the

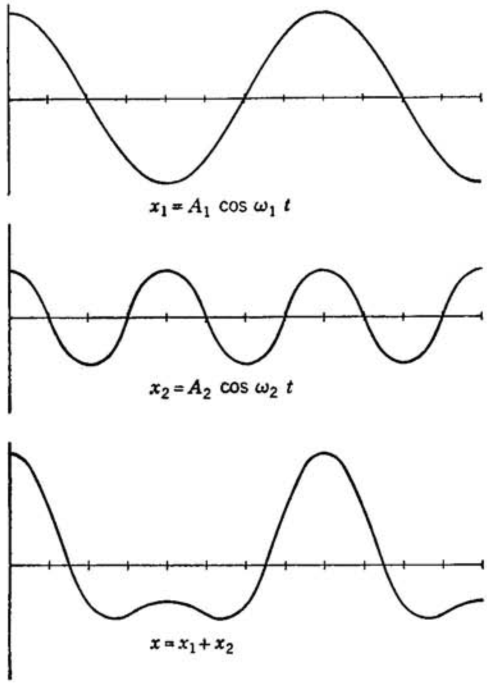

Fig. 1.6. Linear combination of two simple harmonic motions of different frequencies. Curves correspond to $A_1 = 2A_2$, $\omega_2 = 2\omega_1$, and $\phi_1 = \phi_2 = 0$.

linear combination of two different frequencies does not necessarily result in any periodicity of the nature of the summation or difference of the two component frequencies, Fig. 1.6.

The linear combination of three or more simple harmonic vibrations that have different frequencies is carried out in a manner and has characteristics similar to those discussed above for two. This method of combining the effects of individual vibrations by linear addition of their individual values is characteristic of the majority of vibrations encountered in acoustics. In general, the presence of one vibration does not alter the vibrating body or medium to such an extent that the characteristics of other vibrations are disturbed. Consequently, the total vibration is obtained by a linear superposition of the individual vibrations.

1.11 Beats. The linear combination of two simple harmonic vibrations of nearly the same frequency results in the phenomenon of *beats*. Without any loss of generality it is possible to simplify equation 1.15 by choosing an origin of time such that $\phi_2 = 0$ at $t = 0$. If, in addition, the angular frequency ω_2 is written as $\omega_2 = \omega_1 + \Delta\omega$, where $\Delta\omega$ may be either positive or negative, then the equation for the combination of the two vibrations becomes

$$x = A_1 \cos(\omega_1 t + \phi_1) + A_2 \cos(\omega_1 t + \Delta\omega t)$$

This equation may be simplified by the usual trigonometric methods to the form

$$x = A \cos(\omega_1 t + \phi) \tag{1.16}$$

where

$$A^2 = A_1^2 + A_2^2 + 2A_1A_2 \cos(\phi_1 - \Delta\omega t) \tag{1.16a}$$

and

$$\tan \phi = \frac{A_1 \sin \phi_1 + A_2 \sin \Delta\omega t}{A_1 \cos \phi_1 + A_2 \cos \Delta\omega t} \tag{1.16b}$$

The resulting vibration may be regarded as approximately simple harmonic, with an angular frequency ω_1, but with both amplitude A and phase ϕ varying slowly at a frequency of $\Delta\omega/2\pi$.

From equation 1.16*a* it can be seen that the amplitude of the vibration waxes and wanes between the limits $|A_1 + A_2|$ and $|A_1 - A_2|$ at a frequency of $\Delta\omega/2\pi$. In the acoustical case of the simultaneous sounding of two pure tones of slightly different frequency, this variation in amplitude results in a rhythmic pulsing of the loudness of the sound, which occurs at a rate corresponding to the difference in frequency, $\Delta\omega/2\pi$, of the two components, and is known as *beating*. The effect of the variation in phase angle is somewhat more complicated. It modifies the vibration rate in such a manner that its frequency is not strictly constant, but the average angular vibration rate may be shown to lie somewhere between ω_1 and ω_2, depending on the relative magnitudes of the amplitudes A_1 and A_2.

As an example let us consider the special case in which the two amplitudes A_1 and A_2 are equal. If, in addition, we choose as the time for which t is zero an instant when the two motions are in phase, then $\phi_1 = \phi_2 = 0$, so that the amplitude equation (1.16*a*) reduces to

$$A = A_1(2 + 2\cos \Delta\omega t)^{1/2} \tag{1.16c}$$

Therefore, the amplitude ranges between $2A_1$ and zero, and the phenomenon of beating is very pronounced. The phase angle ϕ is given by the equation

$$\tan \phi = \frac{\sin \Delta\omega t}{1 + \cos \Delta\omega t} \tag{1.16d}$$

It may be shown that this variation in phase angle with time is equivalent to an additional frequency term in equation 1.16 and that, furthermore, the oscillations are no longer sinusoidal. However, it may also be shown that the average value of the angular frequency is $\omega_1 + \Delta\omega/2$, i.e., that the resulting average frequency of oscillation is the arithmetic average of the two frequencies being combined.

Audible beats are heard whenever two sounds of nearly the same frequency strike the ear, and when the frequency of each component is within the audible range. If their frequency difference is small, about 10 or less cycles/sec, the resulting sound waxes and wanes at this rate, with an apparent pitch corresponding to the average frequency. If, on the other hand, their frequency difference is about 200 cycles/sec or more, a combination tone may be observed whose frequency is equal to the difference between that of the two sounds. For intermediate frequency differences the sound has a rough or discordant character. A further discussion of beats is given in Sect. 13.9 in connection with the subject of hearing.

1.12 Analysis of Complex Vibrations by Fourier's Theorem. In the immediately preceding sections it has been noted that a linear combination of two or more simple harmonic vibrations which have commensurable frequencies leads to a complex vibration that has a frequency determined by the greatest common divisor of these frequencies. Conversely, by means of a powerful mathematical theorem, originated by Fourier, it is possible to analyze any complex periodic vibration into a harmonic array of component frequencies.

Stated briefly, this theorem asserts that any single-valued periodic and continuous function may be expressed as a summation of simple harmonic terms, finite or infinite in number depending on the form of the function, whose frequencies are integral multiples of the repetition rate of the given function. The above restrictions are normally satisfied in the case of the vibrations of material bodies and, therefore, the theorem is widely used in acoustics.

If a certain complex vibration of period T is represented by the function $x = f(t)$, then Fourier's theorem states that x may be represented by the harmonic series

$$x = f(t) = A_0 + A_1 \cos \omega t + A_2 \cos 2\omega t + \cdots + A_n \cos n\omega t + \cdots$$
$$+ B_1 \sin \omega t + B_2 \sin 2\omega t + \cdots + B_n \sin n\omega t + \cdots \quad (1.17)$$

where $\omega = 2\pi/T$ and the A's and B's are constants to be determined.

Depending on the nature of the function being expanded, some terms in this series may be absent. If the function $f(t)$ is symmetrical with respect to $x = 0$, the constant term A_0 will be absent. If the function $f(t)$ is *even*, i.e., $f(t) = f(-t)$, then all sine terms will be missing. An *odd* function, $f(t) = -f(-t)$, will cause all cosine terms to be absent. The presence or absence of a term will become known when we determine the constants A_0, A_n, and B_n.

Formulas for determining these constants, as derived in standard mathematical treatises on Fourier's theorem, are as follows:

$$A_0 = \frac{1}{T}\int_0^T f(t)\,dt \tag{1.18}$$

$$A_n = \frac{2}{T}\int_0^T f(t)\cos n\omega t\,dt \tag{1.18a}$$

$$B_n = \frac{2}{T}\int_0^T f(t)\sin n\omega t\,dt \tag{1.18b}$$

Whether or not the integrations represented by equations 1.18, 1.18*a*, and 1.18*b* are feasible will depend on the nature and complexity of the function, $x = f(t)$. If this function exactly represents the combination of a finite number of pure sine and cosine vibrations, the series obtained by computing the above constants will contain only these terms. Analysis, for instance, of the vibration effect known as beats will yield only the two frequencies present. Similarly, the complex vibration constituting the sum of three pure musical tones will analyze into those frequencies alone. On the other hand, if the vibration is characterized by abrupt changes in slope, e.g., saw-tooth waves or square waves, then the entire infinite series must be considered for a complete equivalence of motion. Although it is possible to show that the harmonic series is always convergent, i.e., A_n and B_n become progressively smaller as the frequency rises, functions such as the latter two will require the inclusion of a large number of terms merely to achieve a reasonably good equivalence to the original function. Fortunately, the majority of vibrations encountered in acoustics are relatively smooth functions, $f(t)$, of time. In such cases, the convergence is rather rapid and only a few terms must be computed. Another factor that enables us to reduce the number of higher frequency terms that must be computed is that the characteristics of the human ear are such that the subjective audible interpretation of a complex sound vibration is often only slightly altered if the higher frequencies are removed or ignored.

As an example, let us apply the above equations in an analysis of the function represented by a saw-tooth vibration as shown graphically in Fig. 1.7*a*. This function may be defined analytically as

$$x = f(t) = a\left(1 - \frac{2t}{T}\right)$$

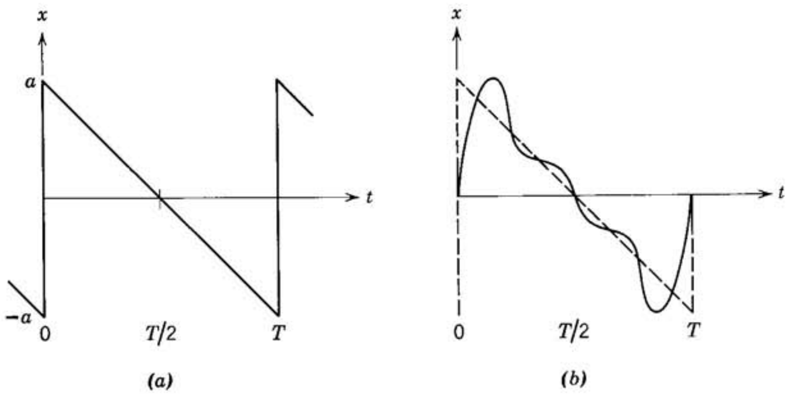

Fig. 1.7. Fourier series representation of a saw-tooth vibration.

for the time interval $t = 0$ to $t = T$. A substitution of this function into equations 1.18, 1.18*a*, and 1.18*b* leads respectively to

$$A_0 = 0, \quad A_n = 0, \quad \text{and} \quad B_n = \frac{a}{n\pi}$$

It should be noted that A_0 is zero because of symmetry of the motion about the x-axis. All A_n's are zero since the function is odd, as will be noted if the saw-tooth graph of Fig. 1.7*a* is repeated to the left of the origin, where t is negative.

Therefore, the complete harmonic series equivalent to the saw-tooth vibration is

$$x = f(t) = \frac{a}{\pi}\left(\sin \omega t + \frac{\sin 2\omega t}{2} + \cdots + \frac{\sin n\omega t}{n} + \cdots\right)$$

Plotted in Fig. 1.7*b* are results obtained by including only the first three terms of the series. Differences between the plots of Fig. 1.7*a* and 1.7*b* are quite apparent. It would be necessary to include at least 20 terms in plotting the series function if it were not to differ by more than 5 per cent from a plot of the original analytical function. Additional applications of Fourier's theorem will be found in the problems at the end of this chapter and in sections in subsequent chapters.

1.13 Damped Oscillations. Whenever a body is set into oscillation, dissipative (frictional) forces arise. These frictional forces are of many types, depending on the particular oscillating system, but they will always result in a *damping* of the oscillation, i.e., a decrease in the amplitude of free oscillations with time. Let us first consider the effect of a viscous type of frictional force upon a simple oscillator. Such a study will then enable us to deduce by analogy the effect of frictional forces upon more complex systems.

The frictional force that is of greatest importance in most vibrational problems is the resistance to motion that the fluid surrounding the body manifests. This resistance arises from the radiation of sound waves, and from the presence of fluid forces of viscosity. It depends on the velocity of the body, and in many important practical applications is directly proportional to this velocity. It can then be expressed mathematically as

$$f_r = -R_m \frac{dx}{dt} \tag{1.19}$$

where R_m is a positive constant called the *mechanical resistance* of the system. From equation 1.19 it is evident that mechanical resistance R_m has the units of newtons per meter/sec or of its equivalent, kilograms per second. If the effect of resistance is included, the equation of motion of the simple oscillator constrained by a stiffness force $-sx$ becomes

$$m \frac{d^2x}{dt^2} + R_m \frac{dx}{dt} + sx = 0 \tag{1.20}$$

It is interesting to note that the equation for the free oscillation of charge in a series circuit containing inductance, resistance, and capacitance has the same form as equation 1.20. The inductance is analogous to mass m, the resistance to the mechanical resistance R_m, and the capacitance to the reciprocal of the stiffness constant s, i.e., to the mechanical compliance C_m as defined by $C_m = 1/s$.

Equation 1.20 may be conveniently solved by the complex exponential method, i.e., by assuming a solution of the form

$$\mathbf{x} = \mathbf{A}e^{\gamma t}$$

Substitution in equation 1.20 shows that

$$(m\gamma^2 + R_m\gamma + s)\mathbf{A}e^{\gamma t} = 0$$

for all times t. Therefore,

$$m\gamma^2 + R_m\gamma + s = 0$$

or

$$\gamma = -\frac{R_m}{2m} \pm \sqrt{\left(\frac{R_m}{2m}\right)^2 - \left(\frac{s}{m}\right)} = -\alpha \pm \beta \tag{1.21}$$

where

$$\alpha = \frac{R_m}{2m} \tag{1.21a}$$

and

$$\beta = \sqrt{\left(\frac{R_m}{2m}\right)^2 - \left(\frac{s}{m}\right)} = \sqrt{\alpha^2 - \omega_0{}^2} \tag{1.21b}$$

using the previous definition of $\omega_0{}^2$ as being equal to s/m. In all cases of importance in acoustics the mechanical resistance R_m is of such a magnitude that $\omega_0{}^2 > \alpha^2$, so that β is imaginary, and γ is consequently complex. It is then advantageous to let

$$\beta = j\sqrt{\omega_0{}^2 - \alpha^2} = j\omega_d \tag{1.21c}$$

where ω_d is the damped value of the angular frequency of vibration. It is to be noted that for small damping the damped frequency of vibration is very nearly equal to, although slightly less than, the undamped frequency.

The complete solution is the sum of the two solutions (equation 1.21) obtained above; hence

$$\mathbf{x} = e^{-\alpha t}(\mathbf{A}_1 e^{j\omega_d t} + \mathbf{A}_2 e^{-j\omega_d t}) \tag{1.22}$$

As in the nondissipative case, the constants $\mathbf{A}_1$ and $\mathbf{A}_2$ are in general complex. Following the convention established in Sect. 1.5, it is necessary to consider only the real part of the complex solution as being a complete general solution. One convenient form of this general solution is

$$x = Ae^{-\alpha t} \cos (\omega_d t + \phi) \tag{1.22a}$$

where A and ϕ are real constants determined by the initial conditions. The amplitude $Ae^{-\alpha t}$ is no longer constant, but instead decreases exponentially with time. As was true with the undamped oscillator, the frequency is independent of the amplitude of oscillation, but it is always lower than that of a corresponding undamped oscillator.

One measure of the rapidity with which the oscillations are damped out by friction is the time required for the amplitude to decrease to $1/e$ of its initial value. This time τ is called the *decay modulus* and is given by the expression

$$\tau = \frac{1}{\alpha} = \frac{2m}{R_m} \tag{1.22b}$$

The smaller R_m is, the larger τ is, indicating that it takes a longer time for the oscillations to damp out.

If the mechanical resistance R_m is large enough, then β is real and the system is no longer oscillatory. When the mass is displaced it merely returns to its rest position without crossing this point. If β is zero, the system is also nonoscillatory and this condition is known as *critical damping*.

1.14 Forced Oscillations. A simple oscillator, or some equivalent system, is often maintained in a condition of vibration by the application of a *sinusoidal* driving force. Representing this force by the expression $f = F \cos \omega t$, the differential equation for the motion of a damped oscillator becomes

$$m \frac{d^2x}{dt^2} + R_m \frac{dx}{dt} + sx = F \cos \omega t \tag{1.23}$$

The solution of this equation is the sum of two parts, a *transient* term containing two arbitrary constants and a *steady-state* term which depends on F but does not contain any arbitrary constants. The transient term is obtained by setting F in equation 1.23 equal to zero. Since the resulting equation is identical with equation 1.20, the transient term is given by equation 1.22, or the equivalent expression, equation 1.22*a*. Its frequency of vibration is the damped frequency ω_d,[1] and, as previously, the arbitrary constants are determined by the initial conditions. After a sufficient time interval, such that $\alpha t \gg 1$, the damping term $e^{-\alpha t}$ makes this portion of the solution negligible, leaving only the steady-state term whose frequency ω is that of the driving force.

To obtain the steady-state (particular) solution of equation 1.23 it will be advantageous to replace the real driving force $F \cos \omega t$ by its equivalent complex driving force $Fe^{j\omega t}$. The equation then becomes

$$m \frac{d^2\mathbf{x}}{dt^2} + R_m \frac{d\mathbf{x}}{dt} + s\mathbf{x} = Fe^{j\omega t} \tag{1.23a}$$

The solution of this equation gives the displacement $\mathbf{x}$ as a complex quantity. Since the real part of the complex driving force represents the actual driving force, it is to be expected that the real part of the complex displacement will represent the actual displacement. This is in agreement with the convention previously adopted of taking the real part of a complex solution as the actual solution.

Assuming an exponential solution of the form $\mathbf{x} = \mathbf{A}e^{j\omega t}$, where $\mathbf{A}$ is in general complex, equation 1.23*a* becomes

$$(-\mathbf{A}\omega^2 m + j\mathbf{A}\omega R_m + \mathbf{A}s)e^{j\omega t} = Fe^{j\omega t}$$

For this equation to be true at all times t, $\mathbf{A}$ must satisfy

$$\mathbf{A} = \frac{F}{j\omega R_m + (s - \omega^2 m)} \tag{1.24}$$

[1] Note that, although ω_d is, strictly speaking, the *angular* frequency of vibration, it differs from the actual frequency f by the constant factor 2π, and for convenience the adjective "angular" will be omitted, except where this omission may cause confusion.

Then the complex displacement $\mathbf{x}$ is

$$\mathbf{x} = \frac{Fe^{j\omega t}}{j\omega R_m + (s - \omega^2 m)} = \frac{-jFe^{j\omega t}}{\omega[R_m + j(\omega m - s/\omega)]} \tag{1.25}$$

Before solving for the real part of this equation, the analogy with electric circuits can be made more apparent, and the equation can be thrown into simpler form, if we define the *complex mechanical impedance* $\mathbf{Z}_m$ of the system as

$$\mathbf{Z}_m = R_m + j\left(\omega m - \frac{s}{\omega}\right) = R_m + jX_m = Z_m e^{j\phi} \tag{1.26}$$

where the *mechanical reactance* X_m is defined as $\omega m - s/\omega$. The magnitude of the mechanical impedance is

$$Z_m = \sqrt{R_m^{\,2} + \left(\omega m - \frac{s}{\omega}\right)^2} = \sqrt{R_m^{\,2} + X_m^{\,2}} \tag{1.27}$$

and its phase angle ϕ is

$$\phi = \tan^{-1}\frac{\omega m - s/\omega}{R_m} = \tan^{-1}\frac{X_m}{R_m} \tag{1.27a}$$

This definition of $\mathbf{Z}_m$ is exactly analogous to that for the complex electrical impedance of a series circuit, with the mechanical resistance R_m analogous to the electrical resistance, the mass m analogous to the electrical inductance, and the mechanical stiffness s analogous to the reciprocal of the electrical capacitance. The dimensions of mechanical impedance are the same as those of mechanical resistance and may be expressed in the same units as the latter, i.e., kilograms per second. This unit may be defined as a *mechanical ohm*.[1] It is to be emphasized that, although the mechanical ohm is analogous to the electrical ohm, these two quantities do not have the same fundamental units. The electrical ohm has the dimensions of a voltage divided by a current, whereas the mechanical ohm has the dimensions of a force divided by a velocity.

Using the definition of $\mathbf{Z}_m$ from equation 1.26, we may write equation 1.25 in the simplified form

$$\mathbf{x} = \frac{-jFe^{j(\omega t - \phi)}}{\omega Z_m} \tag{1.25a}$$

[1] In a strict sense, this quantity should be referred to as an MKS mechanical ohm in order to distinguish it from a similarly defined CGS mechanical ohm that has the units of grams per second. However, for the sake of simplicity, the prefix MKS will not be used in this book.

The actual displacement is given by the real part of equation 1.25*a*, which is

$$x = \frac{F \sin(\omega t - \phi)}{\omega Z_m} = \frac{F \sin(\omega t - \phi)}{\omega\sqrt{R_m^{\,2} + (\omega m - s/\omega)^2}} \tag{1.28}$$

In many mechanical and acoustical problems a knowledge of the velocity is more important than a knowledge of the displacement. Differentiation of equation 1.25 shows that the *complex velocity* is

$$\mathbf{v} = \frac{Fe^{j\omega t}}{R_m + j(\omega m - s/\omega)} = \frac{Fe^{j(\omega t - \phi)}}{Z_m} \tag{1.29}$$

The actual velocity is now given by the real part of equation 1.29, which is

$$v = \frac{F \cos(\omega t - \phi)}{Z_m} = \frac{F \cos(\omega t - \phi)}{\sqrt{R_m^{\,2} + (\omega m - s/\omega)^2}} \tag{1.30}$$

The ratio F/Z_m gives the numerical magnitude of the maximum velocity of the driven oscillator and is known as the *velocity amplitude*. Of course, it would also be possible to obtain equation 1.30 by direct differentiation of equation 1.28.

Equation 1.29 shows that the phase angle ϕ, as defined in equation 1.27*a*, is the angle of phase between the velocity and the driving force. When this angle is positive it indicates that the velocity lags the driving force in the cycle of motion by the angle ϕ, and when this angle is negative it indicates that the velocity leads the driving force. At very high frequencies the angle of lag approaches 90°; at very low frequencies the angle of lead approaches 90°. At some intermediate frequency the mechanical reactance X_m vanishes, and the velocity and driving force are then in phase with each other. At this frequency the velocity amplitude also has its maximum value, F/R_m.

1.15 Power Relations. The *instantaneous* power in *watts* supplied to the system by the driving force is equal to the product of the instantaneous driving force and the resulting velocity. Substituting the appropriate expressions for force and velocity,

$$W_i = F \cos \omega t \, \frac{F \cos(\omega t - \phi)}{Z_m} = \frac{F^2}{Z_m} \cos \omega t \cos(\omega t - \phi) \tag{1.31}$$

It should be noted that the instantaneous power W_i is *not* in general equal to the real part of the product of the complex driving force $Fe^{j\omega t}$ and the complex velocity **v**.

In most situations the average power W being supplied to the system is of more significance than the instantaneous power. This average power is equal to the total work done per complete vibration, divided by the time of one vibration. Therefore

$$W = \frac{\int_0^T W_i \, dt}{T}$$

Substitution of equation 1.31 in this equation gives

$$\begin{aligned} W &= \frac{F^2}{Z_m T}\int_0^T \cos \omega t \cos (\omega t - \phi) \, dt \\ &= \frac{F^2}{Z_m T}\int_0^T [\cos^2 \omega t \cos \phi + \cos \omega t \sin \omega t \sin \phi] \, dt \\ &= \frac{F^2}{2Z_m} \cos \phi \qquad (1.32) \end{aligned}$$

This average power supplied to the system by the driving force is not permanently stored in the system but is, instead, dissipated in the form of work expended in moving the system against the frictional force $R_m(dx/dt)$. It is to be noted that the expression for the average power is analogous in form to that expressing the power dissipation in a series electrical circuit containing resistance, inductance, and capacitance. One slight difference, i.e., the presence of a multiplicative factor of $\frac{1}{2}$ in equation 1.32, is a consequence of the use of peak amplitude for force F, rather than rms (root mean square) force as is customary for voltage in the analogous electrical equation. In conformity with electrical nomenclature, the expression $\cos \phi$ is defined as the *mechanical power factor*.

Since $\cos \phi = R_m/Z_m$, equation 1.32 may be written as

$$W = \frac{F^2 R_m}{2{Z_m}^2} \qquad (1.32a)$$

This alternative form may be derived directly by considering the power dissipated in working against the mechanical resistance R_m. Then the instantaneous power is given by

$$W_i = R_m \left(\frac{dx}{dt}\right)^2 = \frac{F^2 R_m}{{Z_m}^2} \cos^2 (\omega t - \phi) \qquad (1.31a)$$

If this expression for power is averaged over one complete cycle we obtain equation 1.32*a*. As a result, one may say that in the steady state the amplitude and the phase of a driven oscillator so adjust themselves that the average power being supplied by the driving force is just equal to that being dissipated by the frictional force.

The average power is seen to have its maximum value when the mechanical reactance X_m vanishes. Considering equation 1.32, it is evident that for the frequency at which $X_m = 0$, i.e., the frequency ω_0 at which $\omega_0 m = s/\omega_0$, W is a maximum, since at this frequency $\cos \phi$ has its maximum value of unity and Z_m its minimum value R_m.

1.16 Frequency of Mechanical Resonance. The frequency of *mechanical resonance* is defined as that at which the mechanical reactance X_m vanishes, i.e., $\omega_0 = (s/m)^{1/2}$. As has just been noted, this is the frequency at which a driving force will supply maximum power to the oscillator. In Sect. 1.2 it was also found to be the frequency of free oscillation of a similar undamped oscillator. It is the frequency at which the mechanical impedance has its minimum value of $Z_m = R_m$, and is a pure real quantity. It is also the frequency of maximum velocity amplitude, as has been shown in Sect. 1.14. At this frequency equation 1.30 reduces to

$$v_{\text{res}} = \frac{F}{R_m} \cos \omega_0 t \tag{1.33}$$

where F/R_m is the resonance velocity amplitude.

At the resonance frequency the equation for displacement (1.28) reduces to

$$x_{\text{res}} = \frac{F}{\omega_0 R_m} \sin \omega_0 t \tag{1.33a}$$

It is to be noted that this frequency does not give the maximum displacement amplitude, which occurs at the frequency ω that makes $\omega[R_m{}^2 + (\omega m - s/\omega)^2]^{1/2}$ a minimum. It can be shown that the latter frequency is

$$\omega = \sqrt{\omega_0{}^2 - 2\alpha^2}$$

However, unless the mechanical resistance is very large, $2\alpha^2$ is negligible in comparison with $\omega_0{}^2$, and hence it is usually sufficient to assume that the displacement has its maximum amplitude at the resonance frequency ω_0, and that this amplitude is $F/\omega_0 R_m$.

If the average power supplied to the system as given by equation 1.32*a* is plotted as a function of the frequency of a driving force of constant amplitude, a curve similar to the corresponding power curve for a series *RLC* circuit is obtained, Fig. 1.8. It has a maximum value of $F^2/2R_m$ at the resonance frequency ω_0 and falls off more or less gradually at lower and higher frequencies. The sharpness of the peak of the power curve is primarily determined by R_m. If R_m is small, the curve falls off very rapidly and the mechanical system is one of *sharp resonance*. If, on the other hand, R_m is large, the curve falls off more slowly and the system is one of *broad*

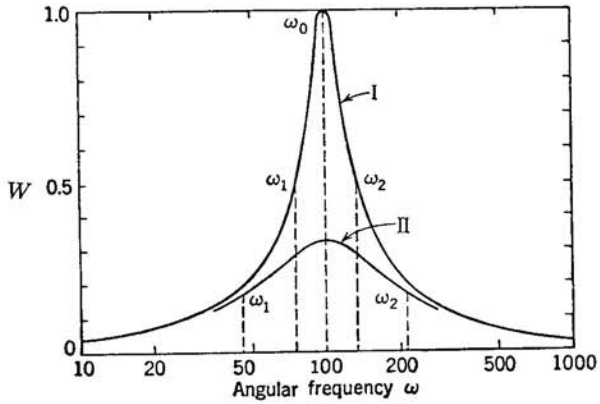

Fig. 1.8. Resonance curves of a simple mechanical system. Curve I corresponds to $Q = 3$. Increasing R_m by a factor of 3 gives curve II with $Q = 1$.

resonance. A more precise definition of the sharpness of resonance can be given in terms of the *quality factor*, Q, of the system, which is defined by

$$Q = \frac{\omega_0}{\omega_2 - \omega_1} \tag{1.34}$$

where ω_0 is the resonance frequency, and ω_2 and ω_1 are the two frequencies respectively above and below resonance at which the average power has dropped to one-half its resonance value.

It is also possible to express Q in terms of the mechanical constants of the system. From equation 1.32*a* it is evident that the average power will be one-half of its resonance value whenever $Z_m^2 = 2R_m^2$. This corresponds to

$$R_m^2 + X_m^2 = 2R_m^2 \quad \text{or} \quad X_m = \pm R_m$$

Since $X_m = \omega m - s/\omega$, the two frequencies ω_2 and ω_1 that satisfy this requirement are given by

$$\omega_2 m - \frac{s}{\omega_2} = R_m \quad \text{and} \quad \omega_1 m - \frac{s}{\omega_1} = -R_m$$

The elimination of s between these equations gives

$$\omega_2 - \omega_1 = \frac{R_m}{m}$$

and, hence,

$$Q = \frac{\omega_0 m}{R_m} \tag{1.35}$$

which is similar to the corresponding expression $\omega_0 L/R$ giving the quality factor of an inductance coil. It should also be noted that $Q/2\pi$ is a measure of the ratio of the maximum energy of the driven oscillator at its resonant frequency to the energy dissipated per cycle of vibration. Proof of this statement is left as an exercise for the reader.

1.17 Equivalent Electrical Circuit for a Simple Oscillator. Many vibrating mechanical and acoustical systems are mathematically equivalent to corresponding electrical systems. As an example, consider a simple series circuit containing inductance L, resistance R, and capacitance C, driven by an impressed sinusoidal voltage $E \cos \omega t$. The differential equation for the current i in this circuit is

$$L\frac{di}{dt} + Ri + \frac{q}{C} = E\cos\omega t \tag{1.36}$$

where q is the charge on the condenser. Since the current i is the time rate of change of the charge q, i.e., since $i = dq/dt$, this equation may be written

$$L\frac{d^2q}{dt^2} + R\frac{dq}{dt} + \frac{q}{C} = E\cos\omega t \tag{1.36a}$$

Equation 1.36*a* is of the same form as equation 1.23 for a driven mechanical system, where L is equivalent to m, R to R_m, $1/C$ to s, and E to F, so that its steady-state solution is

$$q = \frac{E}{\omega Z}\sin(\omega t - \phi) \quad \text{or} \quad i = \frac{E}{Z}\cos(\omega t - \phi)$$

where $Z^2 = R^2 + X^2$, $X = \omega L - 1/\omega C$, and $\phi = \tan^{-1} X/R$. Therefore, the current i in the electrical system is equivalent to the velocity v in the mechanical system, and the charge q is equivalent to the displacement x.

By direct comparison it can be seen that the resonance frequency of the electrical circuit is

$$\omega_0 = \frac{1}{\sqrt{LC}} \tag{1.36b}$$

and the average power is

$$W = \frac{E^2}{2Z}\cos\phi \tag{1.36c}$$

If a simple mechanical oscillator is driven by a sinusoidal force applied to the normally fixed end of the spring, rather than to the end attached to the mass, it may be shown that the resulting system is equivalent to an electric circuit consisting of a coil and condenser connected in parallel. The velocity of the driven end of the spring is then equivalent to the current entering the parallel circuit.

1.18 Phase and Impedance Relations. Since the phase angle ϕ is zero at resonance, the resonance velocity is in phase with the driving force F, while the displacement x lags F by 90°. When the frequency ω is greater than ω_0, both the mechanical reactance and phase angle are positive, so that the velocity lags F by an angle that approaches 90° as ω becomes infinite, while the lag of the displacement with respect to F approaches 180°. When ω is less than ω_0, both the mechanical reactance and phase angle are negative, so that as ω approaches zero the velocity leads F by an angle that approaches 90°, while the lag of the displacement with respect to F is reduced, and approaches zero. In systems having relatively small mechanical resistance the phase angles of both velocity and displacement vary rapidly with small changes in ω in the vicinity of the resonance frequency ω_0.

Mechanical systems driven by periodic forces can be grouped into three different classes. Sometimes it is desired that the system respond strongly to only *one* particular frequency. If the mechanical resistance of a simple oscillator is small, its impedance will be relatively large at all frequencies except those in the immediate vicinity of resonance, and such an oscillator will consequently respond strongly, with large velocity amplitudes, in the vicinity of resonance. Some common examples are tuning forks, the resonators below the bars of a xylophone, and magnetostrictive sonar transducers.

In other applications it is desired that the system respond strongly to a series of discrete frequencies. The simple oscillator does not have this property, but mechanical systems that do behave in this manner can be designed. These will be considered in subsequent chapters of this book.

A third type of use requires that the system respond more or less uniformly to a wide range of frequencies. Examples include the vibrator elements of many electro-acoustic transducers, e.g., microphones, loudspeakers, hydrophones, and crystal sonar transducers, and the sounding board of a piano. In different applications, the quantity whose amplitude is supposed to be independent of frequency may be different. In some cases it is desired that the displacement amplitude be independent of frequency, in others it is the velocity amplitude that is to be held constant, whereas in still others it is the amplitude of the acceleration that is to be invariant. By a suitable choice of the stiffness, mass, and mechanical resistance, a simple oscillator can be made to satisfy any of these requirements over a limited frequency range.

These three special types of frequency-independent driven oscillators are known as *stiffness-controlled, resistance-controlled,* and *mass-controlled* systems, respectively. A *stiffness-controlled* system is characterized by a large value of the ratio s/ω for the frequency range over which the response is to be flat. Then in this range both ωm and R_m are negligible in comparison with s/ω, and $\mathbf{Z}_m$ is very nearly equal to $-js/\omega$, so that

$$x \approx \frac{F}{s} \cos \omega t \quad \text{and} \quad v \approx -\frac{\omega F}{s} \sin \omega t \tag{1.37}$$

It should be noted that, although the displacement amplitude is independent of frequency, the velocity amplitude is not.

A *resistance-controlled* system is one for which R_m is large in comparison with the reactance X_m. This will be true when an oscillator of relatively high mechanical resistance is operated in the vicinity of resonance. Then

$$x \approx \frac{F}{\omega R_m} \sin \omega t \quad \text{and} \quad v \approx \frac{F}{R_m} \cos \omega t \tag{1.38}$$

so that the velocity amplitude is essentially independent of frequency, although both the displacement amplitude and the acceleration are not.

A *mass-controlled* system is characterized by a large value of ωm over the desired frequency range. Then s/ω and R_m are negligible, and $\mathbf{Z}_m$ is approximately equal to $j\omega m$, so that

$$x \approx -\frac{F}{\omega^2 m} \cos \omega t \quad \text{and} \quad v \approx \frac{F}{\omega m} \sin \omega t \tag{1.39}$$

It will be seen that neither the displacement amplitude nor the velocity amplitude is independent of frequency. Computing the acceleration, however, we have

$$a = \frac{d^2x}{dt^2} \approx \frac{F}{m} \cos \omega t \tag{1.39a}$$

which is independent of frequency.

All driven mechanical vibrator elements are resistance-controlled for frequencies nearly equal to their resonant frequency, but for vibrators of low mechanical resistance the range of relatively flat response is extremely narrow. Similarly, all driven vibrators are stiffness-controlled for frequencies well below ω_0, and mass-controlled for frequencies well above ω_0. A suitable choice of mechanical constants will place any of these systems in the desired part of the frequency range, but the computed values are sometimes very difficult to attain in practice.

1.19 Transient Response of an Oscillator. Before concluding the discussion of the simple oscillator it will be well to consider the effect of superimposing the transient respone upon the steady-state condition. The complete general solution of equation 1.23 is

$$x = Ae^{-\alpha t}\cos(\omega_d t + \phi_d) + \frac{F}{\omega Z_m}\sin(\omega t - \phi) \tag{1.40}$$

where A and ϕ_d are two arbitrary constants whose values are determined by the initial conditions, i.e., by the displacement x_0 and the velocity v_0 at the time $t = 0$.

As a special case let us assume that the displacement and velocity are both zero at the time $t = 0$ when the driving force is first applied, and that α is small compared to ω and ω_d. Application of these conditions to equation 1.40 gives

$$A = \frac{F}{Z_m^{\,2}}\left(\frac{X_m^{\,2}}{\omega^2} + \frac{R_m^{\,2}}{\omega_d^{\,2}}\right)^{1/2} \tag{1.41}$$

and

$$\tan\phi_d = \frac{\omega R_m}{\omega_d X_m} \tag{1.42}$$

Representative curves, showing the relative importance of the steady-state and transient motions in producing a combined motion for frequencies corresponding to $\omega = \omega_0$ and $\omega = \omega_0/2$, are plotted in Fig. 1.9. The effect of the transient is apparent in the left-hand portion of these curves, but near the right-hand end the transient has been so damped that the final steady state is nearly reached. Curves for other initial conditions are

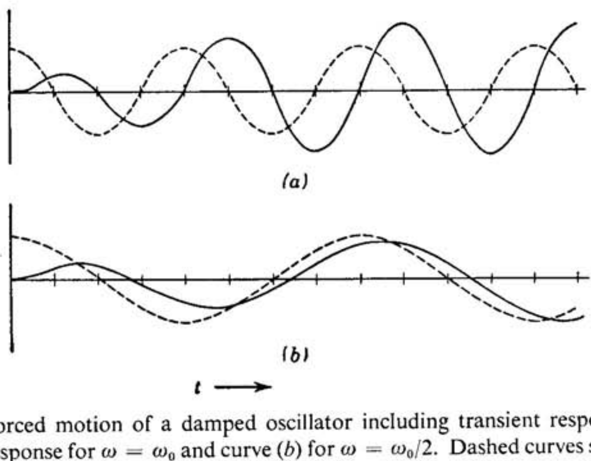

Fig. 1.9. Forced motion of a damped oscillator including transient response. Curve (*a*) shows response for $\omega = \omega_0$ and curve (*b*) for $\omega = \omega_0/2$. Dashed curves show applied force as a function of time; solid curves show resulting displacement.

analogous, in that the wave form is always somewhat irregular immediately after the application of the driving force, but it soon smooths down into the steady state.

Another important transient is the *decay transient* which results when the driving force is abruptly removed. The equation of this motion is that of the damped oscillator, equation 1.22*a*, and its frequency of oscillation is ω_d, not ω. The constants giving the amplitude and phase angle of this motion depend on the part of its cycle in which the driving force is removed. It is impossible to remove the driving force without the appearance of a decay transient, although the effect will be negligible if the amplitude of the driving force is very slowly reduced to zero. The decay transient characteristics of mechanical vibrator elements are of particular importance when considering the fidelity of response of sound reproduction components such as loudspeakers and microphones. An example of an overly slow decay is a noticeable "hangover" of the fundamental frequency produced by some loudspeaker systems.

PROBLEMS

1.1. Given that the real part of $\mathbf{x} = \mathbf{A}e^{j\omega_0 t}$ represents $x = A\cos(\omega_0 t + \phi)$, show that the real part of $\mathbf{x}^2$ does not equal x^2.

1.2. Show that $x = A\cos(\omega_0 t + \phi)$ is equivalent to $x = A_1 \cos \omega_0 t + A_2 \sin \omega_0 t$.

1.3. A mass m is fastened to a string of length l as indicated. The string is stretched to a tension T between two rigid supports. (*a*) When the mass is displaced a small distance x as indicated, what is the restoring force f? Assume the

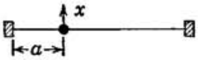

tension T to remain constant and neglect the effects of gravitational forces. (*b*) Derive an expression giving the frequency of vertical vibration of the mass for such small amplitudes that the sines and tangents of the angles between segments of the string and the horizontal may be considered equal. (*c*) For what position a of the mass will this frequency be a minimum?

1.4. A vibrating system consists of a mass m hanging from a spring whose force constant is s_1 and whose original length is l_1, and which in turn hangs from a second spring whose force constant is s_2 and whose original length is l_2. The system is hanging vertically down under the influence of gravity. (*a*) Neglecting the mass of the springs, calculate the increase in length of the system caused by the gravitational force mg acting on the mass. (*b*) Derive a general expression giving the fundamental frequency of vibration of the system.

1.5. A long round wooden spar of 0.1-m radius is weighted at one end so that it rides vertically in the water. If the upper end of the spar is pushed down and released, the spar is observed to oscillate vertically with a period of 4 seconds. Calculate the mass of the weighted spar.

1.6. (*a*) Plot one complete cycle of the displacements that correspond to the equation $x = 2 \cos 6\pi t + 5 \sin 5\pi t$. (*b*) At what time is the displacement a maximum? (*c*) At what time is the velocity a maximum? (*d*) What is this maximum velocity?

1.7. Show that the amplitude A_n of the displacement resulting from the linear addition of n simple harmonic vibrations all of the same amplitude A and frequency ω but having different initial phase angles of $\phi_1 = \epsilon$, $\phi_2 = 2\epsilon$, $\phi_3 = 3\epsilon, \cdots, \phi_n = n\epsilon$, is given by the equation

$$A_n = \frac{A \sin (n\epsilon/2)}{\sin (\epsilon/2)} .$$

1.8. (*a*) Determine the constants for the Fourier series equivalent to a square wave function specified by $x = a$, from $t = 0$ to $t = T/2$, and $x = -a$, from $t = T/2$ to $t = T$. (*b*) Make a graphical plot of the function represented by the sum of the first four terms in the above solution and compare with that of the original square wave.

1.9. Compute the first few terms of the Fourier series equivalent to the function $x = a$ from $t = 0$ to $t = T/2$, and $x = 0$ from $t = T/2$ to $t = T$.

1.10. A mass of 0.25 kg hangs on a spring of 0.3-kg mass. The stiffness constant of the spring is 100 newtons/m, and the mechanical resistance of the system is 7.0 kg/sec. (*a*) What is the damped free oscillation frequency of the system? (*b*) What is the resulting displacement amplitude of the mass when driven at this frequency by a sinusoidal force having an amplitude of 2 newtons? (*c*) What is the maximum kinetic energy of the system when driven by the force of part (*b*)?

1.11. A mass of 0.5 kg hangs on a spring of negligible mass. When an additional mass of 0.2 kg is attached to the spring, the spring is observed to stretch an additional 0.04 m. When the 0.2-kg mass is abruptly removed, the amplitude of the ensuing oscillations of the 0.5-kg mass is observed to decrease by 63.4 per cent, i.e., to $1/e$ of its initial value, in a time of 1 sec. Compute numerical values for the constant R_m, ω_d, A, and ϕ for this motion.

1.12. A mass of 0.5 kg hangs on a spring of negligible mass. The stiffness constant of the spring is 100 newtons/m, and the mechanical resistance of the system is 1.4 kg/sec. The force driving the system is represented by $f = 2 \cos 5t$. (*a*) What will be the steady-state values of the displacement amplitude, velocity amplitude, and average power dissipation? (*b*) What is the phase angle between velocity and force? (*c*) What is the resonant frequency and what would be the values of displacement amplitude, velocity amplitude, and average power dissipation at this frequency and for the same force magnitude as in (*a*)? (*d*) What is the Q of the system, and over what range of frequencies will the power loss be at least 50 per cent of its resonance value?

1.13. Show that $x = (At + B)e^{-\alpha t}$ is the equation governing the motion of a simple oscillator under conditions of critical damping. Show that the displacement of a critically damped oscillator is always less than the displacement amplitude of a simple oscillator of equal mass and stiffness but lesser mechanical resistance, when started under identical initial conditions.

1.14. (*a*) Derive an expression that gives the relationship between the decay modulus τ and the quality factor Q of a damped mechanical oscillator. (*b*) When a simple oscillator is being driven at its resonant frequency, show that the ratio of the energy dissipated per cycle to the total mechanical energy present is equal to $2\pi/Q$.

1.15. Derive equations that give the two frequencies corresponding to the half-power points on the power output curve of a driven simple oscillator. Show that they are approximately given by $\omega_0 \pm R_m/2m$.

1.16. A mass m is fastened to one end of a horizontal spring of negligible mass and stiffness s, and a horizontal driving force $F \sin \omega t$ is applied to the other end of the spring. (*a*) Assuming no damping, determine the equation giving the motion of the driven end of the spring as a function of time t. (*b*) Show that the expression for the velocity of this end of the spring is analogous to that giving the current into a parallel LC electrical circuit. (*c*) If the constants of the above system are $F = 3$ newtons, $s = 200$ newtons/m, and $m = 0.5$ kg, compute and plot curves showing the manner in which the displacement and velocity amplitude of the driven end of the spring varies with frequency in the range $0 < \omega < 100$.

1.17. (*a*) What is the general expression for the acceleration of a simple damped oscillator driven by a force $F \cos \omega t$? (*b*) Derive an expression that gives the frequency ω' which gives a maximum value to this acceleration. (*c*) Show that, if $R_m = \sqrt{sm}$, the acceleration amplitude at the frequency of velocity resonance ω_0 equals the limiting acceleration amplitude at high frequencies.

chapter 2

VIBRATING STRINGS

2.1 Vibrations of Material Bodies. In the previous chapter it was assumed that the entire mass of the vibrating system is concentrated near one point and that the motion of the system can be completely specified by giving the displacement of this point as a function of time. Most vibrating bodies are not of such a simple nature. The total mass of a simple oscillator is not actually concentrated at the end of a massless spring, a part of it being instead distributed along the spring. A method of making allowance for the mass of the spring was formulated in Sect. 1.8, but this was only an approximation, as it did not take into account the finite time required for the propagation of the stretching force along the spring. Similarly, a loudspeaker diaphragm has a considerable portion of its mass spread uniformly over its surface, and, since each part of the diaphragm vibrates with a somewhat different motion from that of the other parts, it becomes necessary to give the displacement of each point as a function of time in order to specify the motion completely. Rather than beginning with the study of such complex vibrations as those of a speaker diaphragm, it will be wise to consider first some simpler modes of vibration, such as those of a vibrating string or bar. The transverse vibrations of a uniform string are, undoubtedly, the most readily visualized physical system involving the propagation of waves and will provide an excellent starting point for our discussion. Actually, even this simple system is a hypothetical one, in that certain simplifying assumptions must be made which cannot be completely realized in practical cases. Nevertheless, the results obtained are extremely important because of the understanding of fundamental wave phenomena which they yield.

2.2 Transverse Wave Propagation on a String. One method of analyzing the transverse vibrations of a string is to consider the motion of a finite number of identical masses, equally spaced at points along an idealized massless string, and then to extend the analysis to an infinite number of infinitesimally spaced masses. The resulting infinite set of equations can be solved to obtain the position of every point on the string as a function of time, and the solution shows that there are an infinite number of allowed frequencies of vibration. However, the same results can be obtained more readily by an indirect attack on the problem, i.e., through a consideration of the propagation of transverse waves along the string, and this indirect method will be used in the following analysis.

Consider a long, heavy string, stretched to a moderate tension between two rigid supports. If a part of the string is displaced from its equilibrium position by the application of a momentary force, it is observed that the displacement does not remain fixed in its initial position, but instead breaks up into two separate disturbances which are propagated along the string, one moving to the right and the other to the left with equal velocities, Fig. 2.1. Furthermore, it is observed that the velocity of propagation of all *small* displacements is independent of the shape and amplitude of the initial displacement and depends only on the mass and the tension of the string. Both experiment and theory show that this velocity is given by $c = \sqrt{T/\delta}$, where c is the velocity in meters per second, T is the tension in newtons, and δ is the linear density of the string in kilograms per meter. The propagation of such a transverse disturbance along a string is commonly referred to as the propagation of a *transverse wave*.

2.3 Transverse Wave Equation. By considering the forces tending to return the string to its equilibrium position it is possible to derive a *wave equation*, first derived by Euler in 1748, whose solution agrees with the observed motion. Assume that a string of negligible stiffness and of uniform linear density δ is rigidly supported at both ends and is stretched to a tension T. Also assume that there are no dissipative forces, such as those associated with the radiation of energy in the form of acoustic waves.

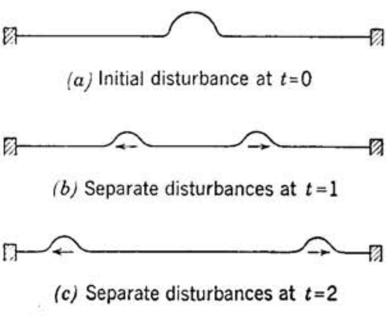

Fig. 2.1. Propagation of a transverse disturbance along a stretched string.

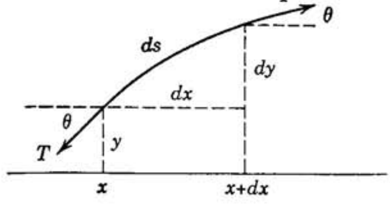

Fig. 2.2. String segment.

Let the x coordinate of a point on the string represent its horizontal distance measured along the string from the left-hand support, and its y coordinate a transverse displacement measured from the equilibrium position. For small transverse displacements the tension may be assumed to be constant throughout the string. (Actually $T\cos\theta$, where at any point on the string θ is the angle between the tangent to the string and the horizontal, is more nearly constant.) Consider a segment of the string of infinitesimal length, as indicated in Fig. 2.2, then the difference between the y components of the tension at the two ends of the element *ds* is the *net* transverse force, which is given by

$$dF_y = (T\sin\theta)_{x+dx} - (T\sin\theta)_x \tag{2.1}$$

where $(T\sin\theta)_{x+dx}$ is the value of $T\sin\theta$ at $x + dx$, and $(T\sin\theta)_x$ is its value at x. Applying the well-known mathematical relation expressing a function in terms of the first two terms of its Taylor's series expansion, i.e.,

$$f(x + dx) = f(x) + \frac{\partial f(x)}{\partial x}\,dx \tag{2.2}$$

equation 2.1 may be written

$$dF_y = (T\sin\theta)_x + \frac{\partial(T\sin\theta)}{\partial x}\,dx - (T\sin\theta)_x = \frac{\partial(T\sin\theta)}{\partial x}\,dx$$

Since we have already assumed that the displacement y of the string is small, and correspondingly that θ is small, we may replace $\sin\theta$ with $\tan\theta$, which is in turn equal to $\partial y/\partial x$. Then the net transverse force on the element *ds* becomes

$$dF_y = \frac{\partial\left(T\dfrac{\partial y}{\partial x}\right)}{\partial x}\,dx = T\frac{\partial^2 y}{\partial x^2}\,dx \tag{2.1a}$$

The mass of the element of the string is $\delta\,dx$, so that upon equating the transverse force dF_y to the product of the element's mass and its acceleration,

$$T\frac{\partial^2 y}{\partial x^2}\,dx = \delta\,dx\,\frac{\partial^2 y}{\partial t^2} \tag{2.3}$$

is obtained. Setting

$$c = \sqrt{T/\delta} \tag{2.4}$$

the equation of motion becomes

$$\frac{\partial^2 y}{\partial t^2} = c^2\,\frac{\partial^2 y}{\partial x^2} \tag{2.5}$$

As will be shown, solutions of this equation represent wave disturbances, propagated along the string at a velocity equal to c, and for this reason it is known as a *wave equation*.

2.4 General Solution of the Wave Equation. The most general solution of the wave equation (2.5) is

$$y = f_1(ct - x) + f_2(ct + x) \tag{2.6}$$

where $f_1(ct - x)$ and $f_2(ct + x)$ are completely arbitrary functions of the arguments $(ct - x)$ and $(ct + x)$, respectively. Possible examples of such arbitrary functions include $\log(ct - x)$, $(ct - x)^2$, $\sin \omega(t - x/c)$, $e^{j\omega(t-x/c)}$, etc.

Equation 2.5 is a second-order partial differential equation, and hence its complete general solution contains *two* arbitrary functions. Let us now prove that $f_1(ct - x)$ and $f_2(ct + x)$ are these two functions. Consider the function $f_1(ct - x)$. Its first partial derivative with respect to time is

$$\frac{\partial f_1(ct - x)}{\partial t} = f_1'(ct - x)\frac{\partial(ct - x)}{\partial t} = cf_1'(ct - x)$$

where f_1' is another function of $(ct - x)$, defined by

$$f_1'(ct - x) = \frac{df_1(ct - x)}{d(ct - x)}$$

Repeating this partial differentiation with respect to time gives

$$\frac{\partial^2 f_1(ct - x)}{\partial t^2} = c^2 f_1''(ct - x) \tag{2.7}$$

where $f_1''(ct - x)$ is yet another function of $(ct - x)$, defined by

$$f_1''(ct - x) = \frac{df_1'(ct - x)}{d(ct - x)} = \frac{d^2 f_1(ct - x)}{d(ct - x)^2}$$

In a like manner, differentiation of the function $f_1(ct - x)$ with respect to x gives

$$\frac{\partial^2 f_1(ct - x)}{\partial x^2} = -\frac{\partial f_1'(ct - x)}{\partial x} = +f_1''(ct - x) \tag{2.7a}$$

where $f_1'(ct - x)$ and $f_1''(ct - x)$ are the same functions of $(ct - x)$ as in equation 2.7. Direct substitution of these two second-order partial derivatives into the original equation 2.5 shows that $f_1(ct - x)$ is a solution.

In a similar manner it can be shown that $f_2(ct + x)$ is also a solution of equation 2.5. Hence the sum of these two functions is the complete general solution of the wave equation.

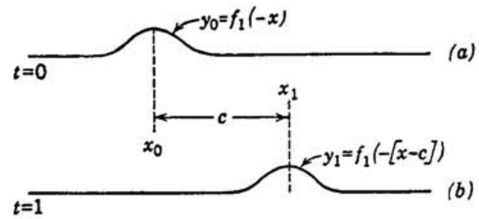

Fig. 2.3. Velocity of transverse wave propagation.

2.5 Wave Nature of the General Solution. Consider the solution $f_1(ct - x)$. If $y = f_1(ct - x)$ is plotted at the instant $t = 0$, the resulting curve, $y_0 = f_1(-x)$, may be assumed to have the general form of that shown in Fig. 2.3*a*. At a later time for which $t = 1$ the curve representing this function will be given by

$$y_1 = f_1(c - x) = f_1(-[x - c])$$

It is clearly evident that Fig. 2.3*b*, which represents the function at $t = 1$, is identical with that for $t = 0$, except that each particular value of the displacement y occurs at $x - c$, rather than at x. For example, the displacement y_1 at x_1 is the same as that of y_0 at x_0 if $x_1 - c = x_0$. Rewriting this equation, it becomes $x_1 = x_0 + c$, which shows that the entire curve has been shifted a distance c to the right in a time of one second. Consequently, $y = f_1(ct - x)$ represents a wave moving to the right, i.e., in the positive x direction, with a velocity c. Similarly, it may be shown that $y = f_2(ct + x)$ represents a wave moving to the left with the velocity c.

It is to be noted that the wave shape corresponding to each of the two arbitrary functions remains constant as the initial disturbance progresses along the string. It should be emphasized, however, that this mathematical conclusion is never completely realized in practice, since the assumptions made in deriving the wave equation are never strictly fulfilled for actual strings. These always have some stiffness and are acted on by dissipative forces, with the result that the waves traveling along them become somewhat distorted. For the relatively flexible strings and low damping normally encountered in musical instruments, however, the rate of distortion is quite slight if the amplitude of the disturbance is small. For large amplitudes, on the other hand, the rate of change of wave shape is always pronounced.

2.6 Initial and Boundary Conditions. In practice, the functions $f_1(ct - x)$ and $f_2(ct + x)$ are not completely arbitrary but are limited by various kinds of initial and boundary conditions. For the freely vibrating string, their initial mathematical forms, i.e., their values at $t = 0$, are determined by the type and point of application of the exciting force applied to the string. For example, the initial wave shape set up by striking a string, as when a piano is played, is quite different from that established by plucking a string, such as that of a harp or guitar, or in bowing a violin string, and the initial functions representing the wave shape are consequently different.

These functions are further limited by the boundary conditions existing at the ends of the string. Actual strings are always finite in length and must be fixed in some manner at their ends. If, for example, the supports of the string are rigid, as is approximately true for most strings, the sum of the functions $f_1 + f_2$ is constrained to have a zero value at all times at the points of support. The most important effect of this kind of boundary condition is to require that the motion of the freely vibrating string be *periodic*.

Finally, when a string is driven to steady-state conditions by a periodic external driving force, periodic functions f_1 and f_2, having the same frequency as the driving force, are produced but some of their other characteristics, such as amplitude of vibration, are also determined by the point of application of the force and by boundary conditions at the ends of the string.

2.7 Reflection at a Boundary. Assume that a string of length l is rigidly supported at $x = 0$ and at $x = l$. Then the solutions $y_1 = f_1(ct - x)$ and $y_2 = f_2(ct + x)$ are no longer completely arbitrary, since, as has just been pointed out, their sum must be zero at all times at the ends of the string. Considering first the left end of the string, this condition requires that

$$y = f_1(ct - 0) + f_2(ct + 0) = 0$$

so that

$$f_2(ct) = -f_1(ct) \tag{2.8}$$

Therefore, the two functions are of the same form but opposite sign, and hence the general expression for the net displacement at any point on the string may be written

$$y = f_1(ct - x) - f_1(ct + x) \tag{2.9}$$

As may be seen in Fig. 2.4, this represents a wave $y_1 = f_1(ct - x)$ traveling to the right, plus another wave $y_2 = -f_1(ct + x)$ of similar shape but opposite displacement traveling to the left. The process of reflection at the boundary $x = 0$ may be considered as one in which wave (B) does not pass this boundary but is instead reflected into a similarly shaped wave of opposite displacement traveling to the right.

The presence of a rigid support at $x = l$ results in another reflection.

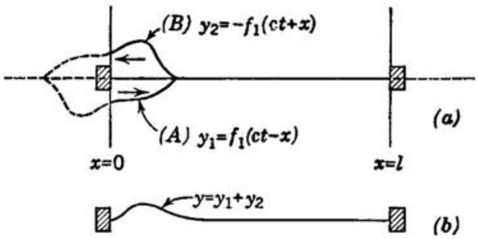

Fig. 2.4. In (*a*) the dashed-line segment of wave (*B*) is shown as being reflected to become the solid-line segment of wave (*A*). The resultant wave, shown in (*b*), has no displacement at $x = 0$.

Here a wave traveling to the right is reflected into a similar wave of opposite displacement traveling to the left. An important effect of these two reflections is to cause the motion of the freely vibrating string to become periodic. A pulse originating at $x = 0$ reaches $x = l$ after an interval of l/c seconds. There it is reflected and returns to $x = 0$, where it is again reflected, the total time of travel being $2l/c$ seconds. The shape of the pulse after its second reflection is identical with that of the original pulse. The particular type of periodicity just discussed results from the particular set of boundary conditions that has been assumed, i.e., rigid supports. Many other kinds of boundary conditions may exist in practical cases, and each establishes its own particular type of reflections and periodicity. Some of these will be considered in later sections and in the problems.

2.8 Simple Harmonic Solution of the Wave Equation. An important type of periodic motion that frequently occurs in nature is simple harmonic motion. We shall now show that simple harmonic vibrations are propagated along a string and that any vibration, no matter how complex, may be resolved into an equivalent pattern of simple harmonic vibrations. This problem of determining the pattern of harmonic modes of vibration is not merely an academic exercise. There is a physiological reason for studying the problem, for the ear itself analyzes a complex sound into its simple harmonic components. One is able to distinguish between the sound emitted by a piano string and a note of the same pitch from a bell by this type of analysis. If all the frequencies present in a sound are integral multiples of some fundamental frequency, as they are for a note from a piano string, the resulting sound seems more harmonious than when the frequencies are not so simply related, as in a note of the same pitch from a bell.

As can be readily shown by direct substitution into equation 2.5, the displacement of any point on a string vibrating with simple harmonic motion of angular frequency ω may be represented by the following special solution of the wave equation,

$$y = a_1 \sin(\omega t - kx) + a_2 \sin(\omega t + kx) + b_1 \cos(\omega t - kx) + b_2 \cos(\omega t + kx) \quad (2.10)$$

where a_1, a_2, b_1, and b_2 are arbitrary constants and k is a constant defined by

$$k = \frac{\omega}{c} \quad (2.11)$$

and is known as the *wavelength constant*. If the string is rigidly supported at $x = 0$, then at this point equation 2.10 reduces to

$$0 = (a_1 + a_2) \sin \omega t + (b_1 + b_2) \cos \omega t$$

Since this equation is applicable at all times t, there must be the following relations between the constants,

$$a_1 + a_2 = 0 \quad \text{and} \quad b_1 + b_2 = 0$$

or

$$a_2 = -a_1 \quad \text{and} \quad b_2 = -b_1$$

These two restrictions on the arbitrary constants of equation 2.10 are equivalent to the single restriction of equation 2.8 on the general wave solution (equation 2.6); i.e., the two waves must be of equal and opposite displacement and must consequently differ in phase by 180° at $x = 0$.

Introducing these restrictions, equation 2.10 becomes

$$y = a_1[\sin(\omega t - kx) - \sin(\omega t + kx)] + b_1[\cos(\omega t - kx) - \cos(\omega t + kx)] \quad (2.12)$$

and, using the standard trigonometric transformations for the sines and cosines of the sums and differences of angles, equation 2.12 simplifies to

$$y = [-2a_1 \cos \omega t + 2b_1 \sin \omega t] \sin kx \quad (2.13)$$

It is to be noted that the dependence of y in equation 2.13 is expressed as the product of two terms, one dependent only on time t, and the other only on the coordinate position x. This alternative form of the solution of the original wave equation 2.5 could have been obtained directly by application of the technique for solving partial differential equations known as "separation of variables." In later chapters applications of the latter technique will be encountered.

Substitution into equation 2.13 of the condition that $y = 0$ at all times at $x = l$ introduces the further restriction that

$$\sin kl = 0$$

and consequently k is limited to a discrete set of values such that kl always equals an integral multiple of π or

$$k_n l = n\pi \qquad n = 1, 2, 3, \cdots \tag{2.14}$$

As a consequence, the string cannot sustain free vibrations of arbitrary frequency, but can instead have only a discrete set of frequencies given by

$$\omega_n = \frac{n\pi c}{l} \qquad n = 1, 2, 3, \cdots \tag{2.14a}$$

or

$$f_n = \frac{nc}{2l} \qquad n = 1, 2, 3, \cdots \tag{2.14b}$$

2.9 Standing Waves. The application of boundary conditions at $x = 0$ and at $x = l$ has reduced the general harmonic wave solution (equation 2.10) to a pattern of *standing waves* on the string. The equation representing the mode of vibration corresponding to the lowest frequency, where $n = 1$, is

$$y_1 = (A_1 \cos \omega_1 t + B_1 \sin \omega_1 t) \sin k_1 x \tag{2.15}$$

where $k_1 = \pi/l$ and A_1 and B_1 are arbitrary constants replacing $(-2a_1)$ and $(2b_1)$, respectively. The numerical values of A_1 and B_1 are determined by the initial conditions, i.e., by the type of excitation. This mode of vibration is called the *fundamental* mode, and its frequency $f_1 = c/(2l)$ is called the fundamental or *first harmonic* frequency.

Similarly, the mode of vibration corresponding to the nth harmonic frequency is represented by

$$y_n = (A_n \cos \omega_n t + B_n \sin \omega_n t) \sin k_n x \tag{2.16}$$

where A_n and B_n are, as before, constants determined by the initial conditions, and the frequency is $f_n = nc/2l$, or n times the fundamental frequency.

A consideration of the term $\sin k_n x$ which is equivalent to $\sin n\pi x/l$, shows that the displacement y_n is zero at all times for values of x such that $\sin n\pi x/l = 0$, i.e., for

$$\frac{n\pi x}{l} = m\pi \qquad m = 0, 1, 2, 3, \cdots, n$$

The cases for which $m = 0$ and $m = n$ correspond to the original boundary conditions that $y = 0$ at the ends of the string. However, there are $n - 1$ additional coordinate positions along the string for which the displacement produced by the nth harmonic mode of vibration is always zero, Fig. 2.5.

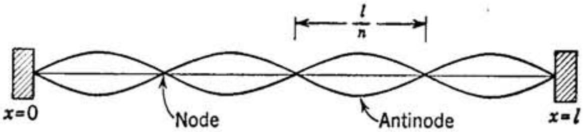

Fig. 2.5. Standing wave pattern for fourth harmonic, $n = 4$.

These positions are called *nodal points*, or *nodes*, of the standing-wave pattern. At each of these points the harmonic wave progressing to the right exactly cancels the harmonic wave moving to the left at all times t. It is because of the existence of these fixed points of zero displacement amplitude that such a wave pattern is known as a set of *standing waves*. The distance between nodal points for the nth harmonic mode of vibration is seen to be l/n. Points of maximum amplitude of vibration, called *antinodes* or *loops*, are spaced evenly between the nodes.

2.10 Wavelength of Harmonic Waves. Let us next consider the displacements resulting from just one of the terms of equation 2.10 when the string is vibrating in its nth mode. Taking, for example, the term $a_1 \sin(\omega_n t - k_n x)$ and substituting $n\pi c/l$ and $n\pi/l$, respectively, for ω_n and k_n, this expression becomes

$$a_1 \sin\left(\frac{n\pi ct}{l} - \frac{n\pi x}{l}\right)$$

It indicates that, as far as this term is concerned, each point of the string goes through a simple harmonic vibration of amplitude a_1 and frequency $nc/2l$. Similarly, each of the other three terms expresses a simple harmonic motion of the same frequency, and, since the linear combination of simple harmonic motions of the same frequency is also simple harmonic, the vibration of every point on the string is simple harmonic. It should be noted, however, that the resultant amplitude of vibration varies from point to point, being zero at the nodes and having its maximum value at the antinodes.

If, instead of observing the motion of one part of the string over a period of time, an instantaneous observation is made of the transverse displacements along the entire string at some particular time, a pattern such as that of Fig. 2.6 is obtained. This pattern is a sinusoidal function of x, which repeats itself whenever the x coordinate is increased by an amount $2l/n$. This distance is known as the *wavelength* λ_n of the harmonic waves. It is related to the velocity of wave propagation c by

$$\lambda_n = \frac{c}{f_n} \tag{2.17}$$

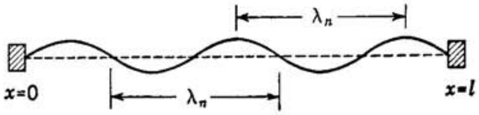

Fig. 2.6. Wavelength $\lambda_n = 2l/n$ for fifth harmonic, $n = 5$.

where f_n is the frequency of vibration of the nth mode, and to the wavelength constant k_n by the relation $k_n = 2\pi/\lambda_n$. Introducing equation 2.14*b*, we have

$$\lambda_n = \frac{2l}{n} \tag{2.18}$$

and the wavelength is consequently exactly twice the nodal distance of the corresponding standing-wave pattern. A physical measurement of the nodal distance is one of the best methods available for determining the wavelength of harmonic waves.

2.11 Overtones and Harmonics. As has been noted previously, the lowest natural frequency of a vibrating system is known as its fundamental frequency; the higher frequency modes are called *overtones*. As can be seen from equation 2.14*b*, the frequencies of all the overtones of a rigidly supported ideal string are integral multiples of its fundamental frequency. Overtones bearing this simple relation to the fundamental are called *harmonics*, the fundamental frequency being the first harmonic, an overtone of twice this frequency being the second harmonic, etc. Only a few vibrating systems have harmonic overtones, but these few form the basis of nearly all musical instruments.

2.12 Initial Conditions. The complete general harmonic solution for a rigidly supported freely vibrating string is the sum of all the individual modes of vibration represented by equation 2.16. It is

$$y = \sum_{n=1}^{\infty} (A_n \cos \omega_n t + B_n \sin \omega_n t) \sin k_n x \tag{2.19}$$

where A_n and B_n are amplitude coefficients, which are determined by the method of setting the string in vibration. The actual amplitude a_n of the nth mode is

$$a_n = \sqrt{A_n^2 + B_n^2} \tag{2.20}$$

Assume that at the time $t = 0$ the string is distorted from its normal linear configuration in such a manner that the displacement of each point is given by the function

$$y_{(t=0)} = y_0(x) \tag{2.21}$$

and the corresponding velocity by

$$v_{(t=0)} = \left(\frac{\partial y}{\partial t}\right)_{(t=0)} = v_0(x) \tag{2.21a}$$

Now, if equation 2.19 is to represent the position of the string at all times, it must represent it at $t = 0$, so that

$$y_0(x) = \sum_{n=1}^{\infty} A_n \sin k_n x \tag{2.22}$$

Its derivative with respect to time must also represent the velocity at $t = 0$, and hence

$$v_0(x) = \sum_{n=1}^{\infty} \omega_n B_n \sin k_n x \tag{2.22a}$$

The Fourier series method of expressing an arbitrary function as a series of sine and cosine terms, as previously discussed in Sect. 1.12, is ideally suited to the evaluation of the coefficients A_n and B_n. Applying the Fourier theorem to equation 2.22 gives

$$A_n = \frac{2}{l}\int_0^l y_0(x) \sin k_n x \, dx \tag{2.23}$$

and similarly, from equation 2.22*a*, we have

$$B_n = \frac{2}{\omega_n l}\int_0^l v_0(x) \sin k_n x \, dx \tag{2.23a}$$

2.13 Plucked String. As an illustration of the application of the Fourier series method, consider a string that is initially pulled aside a distance h at its center and is then released. Here $v_0(x)$ is zero, and hence all the coefficients B_n will be zero. The coefficients A_n are given by

$$A_n = \frac{2}{l}\left[\int_0^{l/2} \frac{2hx}{l} \sin k_n x \, dx + \int_{l/2}^{l} \frac{2h}{l}(l - x) \sin k_n x \, dx\right]$$

or

$$A_n = \frac{8h}{n^2\pi^2} \sin \frac{n\pi}{2} \tag{2.24}$$

Therefore

$$A_2 = A_4 = A_6 = \cdots = 0$$

and

$$A_1 = \frac{8h}{\pi^2}, \qquad A_3 = -\frac{8h}{9\pi^2}, \qquad A_5 = \frac{8h}{25\pi^2}, \qquad \text{etc.}$$

The numerical values of the coefficients A_n determine the amplitudes of the various harmonic modes of vibration of the string. Here, for example, all vibrations corresponding to the second, fourth, sixth, etc., harmonics are absent, and as a result no sounds of these frequencies are produced. The absent harmonics correspond to standing waves having a node at the center, where the string was initially pulled aside. In general, no harmonics are produced having a node at the point of the string initially plucked. The amplitude A_1 of the fundamental is 9 times the amplitude A_3 of the third harmonic, 25 times the amplitude A_5 of the fifth harmonic, etc.

If the string is initially struck a blow such that $v_0(x)$ has values along the string, but there is no initial displacement, then all the coefficients A_n are zero, and the coefficients B_n are given by equation 2.23*a*. As with the plucked string, those harmonics will be absent whose modes of vibration have a node at the point initially struck. Pianos are commonly designed so that the point of impact of the hammer is one-seventh of the way from one end of the string, thus eliminating the seventh harmonic. This is desirable, since the presence of this harmonic would produce somewhat discordant effects when a chord was struck.

A detailed mathematical formulation of the initial conditions for a struck string is much more involved than for a plucked string, for the impact of the hammer not only produces a slight displacement but also establishes an initial velocity distribution. Neither the initial displacement nor the initial velocity is a linear function of position along the string but, instead, depends on such factors as the force of impact, the width and hardness of the hammer, and the relation between its mass and the linear density of the string. A complete analysis of the struck string is beyond the scope of this book.

2.14 Energy of Vibration. The energy of vibration of a string can be computed in much the same manner as that for the simple harmonic oscillator, Sect. 1.7. However, it is easier to take advantage of the fact that for any nondissipative system the total energy is constant and is equal to the maximum kinetic energy. Assuming that the string is vibrating in its *n*th harmonic mode, the maximum value of the kinetic energy of a segment of length dx is

$$dE_n = \frac{\omega_n^2 \delta}{2} (A_n^2 + B_n^2) \sin^2 k_n x \, dx$$

where δ is the linear density of the string. Integrating from zero to l, we have for the the maximum kinetic energy of the entire string

$$E_n = \frac{\omega_n^2 \delta}{2} (A_n^2 + B_n^2) \frac{l}{2} = \frac{m}{4} \omega_n^2 (A_n^2 + B_n^2) \tag{2.25}$$

where m is the total mass of the string and $(A_n^2 + B_n^2)^{1/2}$ is the maximum displacement amplitude of the nth harmonic. From a consideration of the conservation of energy it is apparent that, for a conservative system, equation 2.25 is also the maximum potential energy and the total energy of the nth harmonic. As with the simple oscillator, the total energy is proportional to the square of the product of amplitude and frequency.

For the plucked string of Sect. 2.13 it is apparent that the energy of the nth mode of vibration is

$$E_n = \frac{m}{4}\,\omega_n^{\,2}A_n^{\,2} = \frac{m}{4}\left(\frac{n\pi c}{l}\right)^2\left(\frac{8h}{n^2\pi^2}\right)^2 = \frac{16mh^2c^2}{n^2\pi^2l^2} \tag{2.26}$$

Therefore, the energy of the fundamental mode of vibration is 9 times that of the third harmonic, 25 times that of the fifth harmonic, etc. If all this energy were radiated in the form of acoustic waves, the sound intensities corresponding to each of the harmonic modes would be similarly related. It is quite evident that variations in the position at which the string is plucked will alter the *quality* of the sound produced, i.e., its harmonic content. It may be shown that the series representing the summation of all the energy in the various harmonic modes of vibration is equal to the work performed in initially plucking the string. Such a result is obviously to be expected from the law of conservation of energy.

2.15 Forced Vibrations of an Infinite String. The simplest type of forced vibrations that can be set up in a string is that resulting from the application of a transverse sinusoidal driving force to one end of an ideal string of infinite length. Since all real strings are of finite length this particular problem is one of purely academic interest, but its analysis is fully justified, as it not only furnishes a simple introduction to the study of forced vibrations of strings of finite length but also aids in the understanding of the transmission of acoustic waves. The radiation of acoustic energy, which will be discussed in later chapters, has many characteristics in common with the forced vibrations of an infinite string.

Consider an ideal string of infinite length, stretched to a tension T, with a transverse driving force $F \cos \omega t$ applied at the end where $x = 0$, and with the other end fastened to a rigid support at $x = \infty$. Assume that the support at $x = 0$ is rigid to displacements in the x direction but is free to move in the y direction. A hinge would be a good approximation to such a support. Since the transverse driving force will move the hinge as well as the string, the total mechanical impedance offered to this force is the sum of the mechanical impedance of the hinge and the mechanical impedance offered by the string. In the following analysis it will be assumed that the mechanical impedance of the hinge is negligible, as it may be for a light hinge having no stiffness and little friction. If the mechanical impedance of the hinge is not negligible, it can be computed by the methods of Chapter 1.

Since the string is of infinite length, there are no waves reflected from its far end, and hence none traveling to the left. The displacement of any point on the string may therefore be represented by the general expression for a harmonic wave traveling to the right, i.e.,

$$y = a_1 \sin(\omega t - kx) + b_1 \cos(\omega t - kx) \tag{2.27}$$

or in complex form,

$$\mathbf{y} = \mathbf{A}e^{j(\omega t - kx)} \tag{2.27a}$$

where $\mathbf{A}$ is a complex constant whose magnitude gives the displacement amplitude of the wave motion, and whose phase angle gives the phase of the motion with respect to the driving force.

The complex expression for the harmonic driving force is

$$\mathbf{f} = Fe^{j\omega t} \tag{2.28}$$

Consider the force applied to the support by the left end of the string to be as shown in Fig. 2.7, where θ, the angle the string makes with the horizontal, is given by

$$\tan\theta = \left(\frac{\partial y}{\partial x}\right)_{x=0} \tag{2.29}$$

Then the horizontal force exerted by the support on the end of the string is $-T\cos\theta$, and, since all displacements have been assumed to be small, the magnitude of this force is essentially equal to the constant tension T in the string. Similarly, the transverse force exerted by the support on the string is $-T\sin\theta$, or to a first approximation

$$\mathbf{f} = -T\tan\theta = -T\left(\frac{\partial \mathbf{y}}{\partial x}\right)_{x=0} \tag{2.30}$$

In effect, this equation implies that, for any applied transverse force, the slope of the string at $x = 0$ so adjusts itself that equation 2.30 is satisfied.

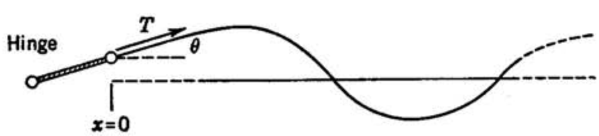

Fig. 2.7. Force of string on hinge.

Substitution of the expressions for **f** and **y** from equations 2.28 and 2.27*a* gives for this boundary condition

$$Fe^{j\omega t} = -T(-jk)\,\mathbf{A}e^{j(\omega t - k0)}$$

or

$$\mathbf{A} = \frac{F}{jkT} \tag{2.31}$$

The magnitude of this complex amplitude is $A = F/kT$. Substitution of equation 2.31 into equation 2.27*a* and differentiation with respect to time gives the complex velocity

$$\mathbf{v} = F\left(\frac{c}{T}\right)e^{j(\omega t - kx)} \tag{2.32}$$

Now let us define the input *mechanical* or *wave impedance* $\mathbf{Z}_s$ of the string as the ratio of the driving force to the transverse velocity of the string at $x = 0$. Then

$$\mathbf{Z}_s = \frac{T}{c} = \sqrt{T\delta} = \delta c \tag{2.33}$$

The input impedance of an infinite string is consequently a real quantity, having no imaginary component, and the mechanical load offered by the string to the driving force is therefore purely resistive. The input impedance is a function of the linear density and tension of the string and is independent of the driving force applied to the string. It is thus a characteristic property of the string, and not of the particular waves being propagated along the string. For this reason it is sometimes called the *characteristic mechanical impedance* (*resistance*) of the string. It is analogous to the characteristic electrical impedance of an infinite transmission line.

The average power input to the string is the average value of the instantaneous power $W_i = fv$, evaluated at $x = 0$, or

$$W = \frac{F^2}{2\delta c} = \frac{\delta c V_0^{\,2}}{2} \tag{2.34}$$

where V_0 is the velocity amplitude of the string at $x = 0$.

2.16 Forced Vibrations of a String of Finite Length. The input impedance of a string of finite length is considerably more complicated than that of an infinite string. Reflections from the support at the far end establish resonance frequencies which cause the input impedance to vary widely with the frequency of the driving force. If the support at the far end is rigid and if there are no dissipative forces in the string, the input impedance becomes a pure reactance, and no power is consumed by the system.

The complex expression for transverse waves on a finite string must include a term representing the reflected wave, so that instead of equation 2.27*a* we have

$$\mathbf{y} = \mathbf{A}e^{j(\omega t - kx)} + \mathbf{B}e^{j(\omega t + kx)} \tag{2.35}$$

At the left end of the string the boundary condition is

$$Fe^{j\omega t} = -T\left(\frac{\partial \mathbf{y}}{\partial x}\right)_{x=0} \tag{2.36}$$

at all times t. Substitution of equation 2.35 into this boundary condition gives

$$F = -T(-jk\mathbf{A} + jk\mathbf{B}) \tag{2.37}$$

If the string is rigidly supported at $x = l$, the deflection at this point is always zero, and hence

$$0 = \mathbf{A}e^{-jkl} + \mathbf{B}e^{jkl} \tag{2.38}$$

Solving equations 2.37 and 2.38 simultaneously for **A** and **B**, we have

$$\mathbf{A} = \frac{F}{jkT} \cdot \frac{e^{jkl}}{e^{jkl} + e^{-jkl}} = \frac{Fe^{jkl}}{2jkT \cos kl} \tag{2.39}$$

and

$$\mathbf{B} = -\frac{F}{jkT} \cdot \frac{e^{-jkl}}{e^{jkl} + e^{-jkl}} = -\frac{Fe^{-jkl}}{2jkT \cos kl} \tag{2.39a}$$

Substitution of these constants into equation 2.35 gives

$$\mathbf{y} = \frac{Fe^{j\omega t}}{jkT} \cdot \frac{e^{jk(l-x)} - e^{-jk(l-x)}}{2 \cos kl}$$

or

$$\mathbf{y} = \frac{Fe^{j\omega t}}{kT} \cdot \frac{\sin k(l - x)}{\cos kl} \tag{2.40}$$

The real part of this expression represents a pattern of standing waves on the string, with nodes at those positions for which $\sin k(l - x) = 0$. It will be seen that as a result of the original boundary conditions there will always be a node at $x = l$ but that the displacement amplitude Y_0 at $x = 0$ will in general have a finite value given by

$$Y_0 = \frac{F \tan kl}{kT} \tag{2.41}$$

The displacement amplitude Y of the standing waves, i.e., the maximum value of the displacement which occurs at the antinodes, is given by

$$Y = \frac{F}{kT \cos kl} \tag{2.41a}$$

The denominator of this expression becomes zero at frequencies such that $\cos kl = 0$, i.e., when

$$kl = \frac{\omega l}{c} = \frac{(2n-1)\pi}{2} \qquad n = 1, 2, 3, \cdots$$

or

$$\omega_n = \frac{(2n-1)\pi c}{2l} \quad \text{and} \quad f_n = \frac{(2n-1)c}{4l} \tag{2.42}$$

The theoretically infinite amplitudes of vibration predicted by this equation do not occur in actual strings, where there are always dissipative forces which have been neglected in the foregoing analysis. However, the amplitude will be a maximum at these frequencies.

Similarly, the set of frequencies for which the amplitude is a minimum is determined by the condition $\cos kl = \pm 1$, i.e.,

$$kl = \frac{\omega l}{c} = n\pi \qquad n = 1, 2, 3, \cdots$$

or

$$\omega_n = \frac{n\pi c}{l} \quad \text{and} \quad f_n = \frac{nc}{2l} \tag{2.43}$$

It will be observed that these minimum amplitudes decrease progressively with increasing frequency. A comparison with equation 2.14 shows that the frequencies of minimum amplitude for a driven string are identical with its frequencies of free vibration. These frequencies may therefore be called *antiresonant* frequencies, by analogy with the terminology used for a similar behavior of parallel electric circuits or transmission lines.

Differentiation of equation 2.40 with respect to time gives

$$\mathbf{v} = \frac{jFe^{j\omega t}}{(T/c)} \cdot \frac{\sin k(l-x)}{\cos kl} \tag{2.44}$$

for the complex velocity of the string. Then the input mechanical impedance is

$$\mathbf{Z}_s = \frac{Fe^{j\omega t}}{\mathbf{v}} = \frac{(T/c)\cos kl}{j\sin kl} = -j\delta c \cot kl \tag{2.45}$$

This impedance is a pure reactance, and consequently no power is absorbed by the string.

A consideration of the variations in input impedance leads to the same conclusions as those arrived at from amplitude considerations. Whenever $\cot kl = 0$ the input impedance is zero, and the amplitude of vibration is consequently a maximum. This will occur at the frequencies given by equation 2.42. At the frequencies given by equation 2.43, $\cot kl$ is infinite and the motion of the driven end of the string is infinitesimally small, although the remainder of the string is in motion. The input impedance of a nondissipative string having a rigid support at its far end is analogous to the input impedance of a resistanceless electric transmission line which is open-circuited at its far end, and any conclusions arrived at from a consideration of one system are applicable to the other.

For very low frequencies the input impedance has the limiting value

$$\mathbf{Z}_s = -j\,\frac{\delta c}{kl} = -j\,\frac{T}{\omega l} \tag{2.46}$$

which is identical with the input impedance of a simple spring having a stiffness constant $s = T/l$, and corresponds to a capacitive reactance in the equivalent electric circuit or transmission line.

2.17 Free Vibration of Actual Strings. The free vibration of an actual string differs to some extent from that of an ideal string. If the string has appreciable stiffness, as is true of a stretched steel wire, the observed frequencies are higher than those given by equation 2.14. This increase results from the existence of the elastic bending forces in the wire in addition to the tensile forces previously considered, the net effect being an increase in the restoring force. The effect of stiffness on frequency becomes more important with increasing frequency, and consequently the relative increase in frequency of the higher harmonics is greater than that of the fundamental. As a result, the overtones of a stiff string no longer form an exact harmonic series.

Any yielding of the supports also modifies the motion of the string, for the boundary conditions are then no longer that $y = 0$ at its ends, but rather that at these points the wave impedance of the string must be equal to the transverse mechanical impedance of the support. An investigation of the motion of a hinged support, such as that described in Sect. 2.15, will confirm the validity of this statement.

Assume that the left end of the string where $x = 0$ is attached to such a hinge. Then the transverse force $\mathbf{f}_0$ exerted by the string on the hinge is given by

$$\mathbf{f}_0 = T\sin\theta \approx T\left(\frac{\partial \mathbf{y}}{\partial x}\right)_{x=0} \tag{2.47}$$

where $\mathbf{y}$ is the general complex expression for the transverse waves on the string, as given in equation 2.35. Since the motion of the hinge is constrained to match that of the end of the string, its velocity is

$$\mathbf{v}_0 = \left(\frac{\partial \mathbf{y}}{\partial t}\right)_{x=0} = j\omega\mathbf{y}_0 \tag{2.48}$$

Letting $\mathbf{Z}_0$ be the transverse mechanical impedance of the hinge at $x = 0$, we have

$$\mathbf{Z}_0 = \frac{\mathbf{f}_0}{\mathbf{v}_0} = \frac{T}{j\omega} \cdot \frac{(\partial \mathbf{y}/\partial x)_{x=0}}{\mathbf{y}_0} \tag{2.49}$$

and hence the boundary condition at $x = 0$ is

$$\mathbf{y}_0 = \frac{T(\partial \mathbf{y}/\partial x)_{x=0}}{j\omega \mathbf{Z}_0} \tag{2.50}$$

Similarly it may be shown that the condition at $x = l$ is

$$\mathbf{y}_l = \frac{-T(\partial \mathbf{y}/\partial x)_{x=l}}{j\omega \mathbf{Z}_l} \tag{2.50a}$$

where $\mathbf{Z}_l$ is the mechanical impedance of the hinge at $x = l$. With rigid supports, the mechanical impedances $\mathbf{Z}_0$ and $\mathbf{Z}_l$ are infinite, and the boundary conditions reduce to the usual ones that $\mathbf{y}$ is zero at the ends of the string.

If the transverse impedances of the supports are mass-controlled positive reactances, the above boundary conditions result in an increase of all the natural frequencies of vibration relative to those for rigid supports. As is characteristic of all mass-controlled systems, the motion of the supports lags behind the driving force, with the result that the nodes shift from their positions at the supports to points a short distance in along the string. This decreases the wavelength of the vibration and, consequently, increases its frequency.

If the transverse impedances of the supports are stiffness-controlled negative reactances, they move in phase with the driving forces exerted on them by the string. The outer nodes then become virtual nodes located at points somewhat beyond the supports, and the resulting increase in wavelength corresponds to a decrease in the frequency of vibration.

If the transverse mechanical impedances of the supports have finite resistances, energy will be dissipated by the system. Here the amplitude of vibration at the nodes will no longer be zero but will instead have a finite value.

Up to this point we have neglected the effects of the surrounding medium on the motion of the string. One of the effects of the medium is to provide a resistive force which opposes the motion. As with a simple oscillator, the effect of this frictional force is to damp out the free vibrations and to reduce their frequency slightly. Of the energy being dissipated by the string, part heats the surrounding medium, the amount depending on its viscosity, and part goes into the radiation of sound energy.

Another effect of the medium is to add an effective additional mass per unit length to the string. This may not be negligible in a liquid medium, or at low frequencies in a gaseous medium. An analytical treatment of the effect of the medium on the vibrating string is not warranted; however, in Chapter 10 we shall consider the much more important case of its effect on the vibrations of a loudspeaker diaphragm. The conclusions arrived at will be found similar to those stated above.

It is just this similarity between the vibrations of a string and those of more complicated mechanical or acoustic systems that warrants such a thorough treatment of the vibrating string as has been given in this chapter. A knowledge of the various modes of vibration and other characteristics of a simple string will facilitate the future study of more complicated systems, where the mathematical difficulties might otherwise obscure the physical ideas. All the methods of attack employed in this chapter will be used over and over again in the more complex situations to be encountered.

PROBLEMS

2.1. A steel wire of 0.01-kg mass and 2-m length is stretched to a tension of 10 newtons. (*a*) What is the frequency of fundamental vibrations? (*b*) If the displacement amplitude of the fundamental is 0.02 m at the center of the wire, what is the total energy of the fundamental mode of vibration? (*c*) What is the velocity amplitude at a point 0.5 m from either end of the wire?

2.2. By direct substitution show that $\log(ct - x)$, $(ct - x)^2$, and $\cos(ct + x)$ are all solutions of equation 2.5.

2.3. Show that the function $y = Ae^{-a(t-x/c)}$ satisfies equation 2.5. If $A = 3$ cm, $a = 2\ \text{sec}^{-1}$, and $c = 0.03$ m/sec, plot this function for positive values of the argument $(t - x/c)$ at $t = 0$, $t = 1$ sec and $t = 2$ sec, respectively. What is the significance of the respective displacements of the three plotted curves?

2.4. A certain harp string has a linear density of 0.5 kg/m, a length of 1 meter, and is stretched to a tension of 50 newtons. (*a*) What is its fundamental frequency? (*b*) If it is plucked at a point 0.25 m from one end, find the frequencies and the relative amplitudes of the first five existing modes of vibration?

2.5. A stretched string of length l is plucked at the position $l/3$ by producing an initial displacement h and then releasing the string. Determine the resulting amplitude constants A_n for the fundamental and the first three harmonic overtones. Sketch the wave shapes of these individual waves and the shape of the string resulting from the linear combination of these waves at $t = 0$. Repeat for $t = l/c$, where c is the transverse wave velocity of the string.

2.6. Show that the work done in displacing the center of a stretched string by an amount h equals the sum of the energies present in the various modes of vibration when the string is released.

2.7. A stretched string of length l is struck a blow such that its initial velocity is zero from 0 to $l/4$ and from $3l/4$ to l. Its initial velocity from $l/4$ to $l/2$ is $4v_0(x - l/4)$, and from $l/2$ to $3l/4$ it is $-4v_0(x - 3l/4)$. Determine the resulting amplitude constants B_n for the fundamental and the first three harmonic overtones.

2.8. A uniform string is stretched between rigid supports a distance l apart. It is driven by a force $F \cos \omega t$ located at its midpoint. (*a*) Show that the amplitude of the midpoint is $(F/2kT)\tan(kl/2)$. (*b*) What is the mechanical impedance at the midpoint? (*c*) What is the amplitude of the displacement of the point $x = l/4$?

2.9. A string of density 0.01 kg/m is stretched with a tension of 5 newtons from a rigid support at one end to a device for producing transverse periodic vibrations at the other end. The length of the string is 0.44 m, and it is observed that, when the driving frequency has a given value, the nodes are spaced 0.1 m apart, and the maximum amplitude is 0.02 m. What are the (*a*) frequency and (*b*) amplitude of the driving force?

2.10. A large mass m is attached to the center of an infinite string of linear density δ, which is stretched to a tension T. (*a*) Derive an expression for the transverse mechanical impedance at the mass. (*b*) What is the fundamental frequency of the mass, if any? (*c*) Answer the same two questions, if the string is of a finite length l which is small compared to a wavelength in the string.

2.11. A string of linear density 0.01 kg/m and of 0.2-m length is stretched between rigid supports to a tension of 10 newtons. It is loaded at its center with a mass of 0.001 kg. (*a*) What is the fundamental frequency of the system? (*b*) What is the first overtone frequency of the system?

2.12. A mass of 0.2 kg is hung from a string of 0.05-kg mass and 1.0-m length. (*a*) What is the velocity of transverse waves in the string? Neglect weight of string in computing tension in string. (*b*) What are the frequencies of the fundamental and first overtone modes of transverse vibration of the string? (*c*) When the string is vibrating at its first overtone frequency, what is the relative amplitude of its displacement at the anti-node to that of the mass?

chapter 3

VIBRATIONS OF BARS

3.1 Longitudinal Vibrations of a Bar. Another important type of wave motion is the propagation of *longitudinal waves* in a bar or rod. As a longitudinal wave disturbance moves along such a bar, the displacement of particles of the bar is parallel to its axis. When the lateral dimensions of the bar are small compared with its length, each cross-sectional plane of the bar may be considered to move as a unit. Actually the bar shrinks somewhat in a lateral direction as it expands longitudinally, but for thin bars this lateral motion may be neglected.

It is possible to list a number of acoustic devices that utilize longitudinal vibrations in a bar. A set of frequency standards used for producing sounds of definite pitches may be constructed from circular rods of varying lengths. When longitudinal vibrations are excited in such rods, the frequency of vibration is observed to be inversely proportional to the length of the rod. Longitudinal vibrations in nickel tubes are often used to drive the vibrating diaphragm of a sonar transducer. Piezoelectric crystals are sometimes cut so that the frequency of longitudinal vibration in the direction of the longest axis of the crystal may be used either to control the frequency of an oscillating electric current or to drive an electroacoustic transducer.

A further reason for studying the longitudinal vibrations of a bar is that it aids in the understanding of acoustic waves. Not only are the mathematical expressions for the transmission of acoustic plane waves through fluid media very similar to those for the transmission of compressional waves along a bar, but if the fluid is confined to a rigid pipe there is also a close correlation between the boundary conditions in the two cases.

3.2 Longitudinal Strain. Consider a bar of length l and uniform cross-sectional area S, which is subjected to longitudinal forces. The application of these forces will produce a longitudinal displacement ξ of each of the particles in the bar, and for long thin bars this displacement will be the same at all points in any particular cross section. If the forces are steady, the displacement ξ of any particle is independent of time and is a function only of the distance x measured along the bar. For the varying forces corresponding to wave disturbances, however, ξ is a function of both x and t, although it may be assumed to be independent of the lateral coordinates y and z. Then

$$\xi = \xi(x, t) \tag{3.1}$$

Let the coordinates of the left and right ends of the bar be $x = 0$ and $x = l$, respectively, and consider a short segment dx of the unstrained bar lying between x and $x + dx$. Assume that the application of forces to the bar causes the plane originally located at x to move a distance ξ to the right, and that similarly a plane originally located at $x + dx$ moves a distance $\xi + d\xi$ to the right, Fig. 3.1. The convention adopted in this book is that a positive value of ξ signifies a displacement to the right, and a negative value a displacement to the left.

Since dx is assumed to be small, the displacement at $x + dx$ can be represented by the first two terms of a Taylor's series expansion of ξ about x, i.e.,

$$\xi + d\xi = \xi + \left(\frac{\partial \xi}{\partial x}\right) dx$$

and, since the left end of the segment has been displaced a distance ξ, and the right end a distance $\xi + d\xi$, the increase in length of the segment is given by

$$(\xi + d\xi) - \xi = d\xi = \left(\frac{\partial \xi}{\partial x}\right) dx$$

Now the *strain* in the segment is defined as the ratio of its increase in length to its original length, or

$$\text{Strain} = \frac{\left(\dfrac{\partial \xi}{\partial x}\right) dx}{dx} = \frac{\partial \xi}{\partial x} \tag{3.2}$$

Note that since ξ is a function of both x and t we must use partial derivatives, rather than total derivatives. It should also be observed that in

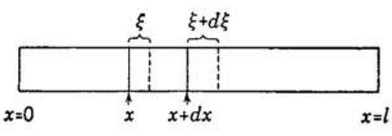

Fig. 3.1. Longitudinal strain $d\xi/dx$ in a bar.

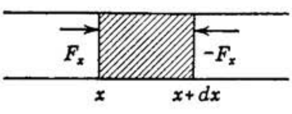

Fig. 3.2. Compressional forces in a bar.

contrast with the application of static forces to a uniform bar, where the strain is the same at all points and is independent of time, the strain in the dynamic case varies both with the coordinate x of the cross-sectional plane being considered and with the time t at which the observation is made. The effect of this kind of variation in the strain is to produce a longitudinal wave motion in the bar, analogous to the transverse waves on a string.

3.3 Longitudinal Wave Equation. Whenever a bar is strained, elastic forces are produced. These forces act across each cross-sectional plane in the bar and hold the bar together. Let $F_x = F_x(x, t)$ represent these longitudinal forces, where the convention is adopted of choosing a *positive* value of F_x to represent forces of *compression*, as indicated in Fig. 3.2, and a *negative* value, forces of *tension*. This particular choice of sign for a compressional force is adopted so as to make the compression of a solid by a positive force analogous to the compression of a fluid by a positive increment in pressure.

The *stress* in the bar is defined as

$$\text{Stress} = \frac{F_x}{S} \tag{3.3}$$

where S is the cross-sectional area of the bar. Applying Hooke's law,

$$\frac{F_x/S}{\partial\xi/\partial x} = -Y \tag{3.4}$$

where Y is an elastic constant known as Young's modulus. This constant is a characteristic property of the material used in the bar. Since a positive stress results in a negative strain, the minus sign in equation 3.4 ensures a positive value for the constant Y. Values of Y for a number of common solids are given in Table I of the appendix. Rewriting equation 3.4, we obtain

$$F_x = -SY\frac{\partial\xi}{\partial x} \tag{3.5}$$

as an expression for the internal longitudinal forces in the bar.

In the static case, where the strain $\partial\xi/\partial x$ is constant throughout the bar, the force F_x is also constant. In the dynamic case, however, both the strain and F_x vary, so that a net force will act on the segment dx. If F_x represents the internal force at x, then $F_x + (\partial F_x/\partial x)\, dx$ represents the force at $x + dx$, and the net force to the right is

$$dF_x = F_x - \left(F_x + \frac{\partial F_x}{\partial x}\, dx\right) = -\frac{\partial F_x}{\partial x}\, dx \tag{3.6}$$

A substitution of the expression 3.5 for F_x yields

$$dF_x = SY \frac{\partial^2 \xi}{\partial x^2} dx \tag{3.6a}$$

The mass of the segment dx is $\rho S\, dx$, where ρ is the volume density of the bar. Therefore, the equation of motion governing the acceleration $\partial^2\xi/\partial t^2$ of the segment is

$$(\rho S\, dx) \frac{\partial^2 \xi}{\partial t^2} = SY \frac{\partial^2 \xi}{\partial x^2} dx$$

Setting $c^2 = Y/\rho$, this equation becomes

$$\frac{\partial^2 \xi}{\partial t^2} = c^2 \frac{\partial^2 \xi}{\partial x^2} \tag{3.7}$$

A comparison of this equation with the corresponding equation 2.5 for the transverse motion of a segment of a string shows that they are of identical form, with a longitudinal displacement ξ replacing the transverse displacement y. Equation 3.7, therefore, represents a *one-dimensional longitudinal wave equation.*

3.4 Solutions of the Longitudinal Wave Equation. The general solution of equation 3.7 is identical in form with that of the transverse wave equation. It is

$$\xi = f_1(ct - x) + f_2(ct + x) \tag{3.8}$$

where the velocity of wave propagation is now determined by the square root of the ratio of the stiffness modulus Y to the volume density ρ of the material,

$$c = \sqrt{\frac{Y}{\rho}} \tag{3.8a}$$

Let us assume a complex harmonic solution of equation 3.7, i.e.,

$$\boldsymbol{\xi} = \mathbf{A}e^{j(\omega t - kx)} + \mathbf{B}e^{j(\omega t + kx)} \tag{3.9}$$

where $\mathbf{A}$ and $\mathbf{B}$ are complex amplitude constants, and $k = \omega/c$ is the wavelength constant. The real part of this expression can readily be shown to be of the same form as equation 2.10 for transverse waves on a string.

Let us now apply boundary conditions to a bar considered rigidly fixed at both ends, so that $\boldsymbol{\xi} = 0$ at $x = 0$ and at $x = l$ at all times t. The resulting expressions will be found identical with those obtained in Sect. 2.8 for a rigidly supported vibrating string. However, as will be seen, the mathematical process is less involved when the complex form of the harmonic solution is used.

Application of the condition that $\boldsymbol{\xi} = 0$ at $x = 0$ gives $0 = \mathbf{A} + \mathbf{B}$, so that $\mathbf{B} = -\mathbf{A}$ and equation 3.9 becomes

$$\boldsymbol{\xi} = \mathbf{A}e^{j\omega t}(e^{-jkx} - e^{jkx}) \tag{3.10}$$

The condition that $\boldsymbol{\xi} = 0$ at $x = l$ now gives

$$e^{-jkl} - e^{jkl} = 0 \tag{3.11}$$

However, since

$$\sin kl = \tfrac{1}{2}j(e^{-jkl} - e^{jkl})$$

the condition of equation 3.11 is equivalent to

$$\sin kl = 0 \tag{3.12}$$

or

$$k_n l = n\pi \qquad n = 1, 2, 3, \cdots \tag{3.12a}$$

which is identical with equation 2.14 for a rigidly supported string. Therefore, the frequencies of the allowed modes of vibration are

$$\omega_n = \frac{n\pi c}{l} \quad \text{or} \quad f_n = \frac{nc}{2l} \qquad n = 1, 2, 3, \cdots \tag{3.13}$$

which are the same as equations 2.14*a* and 2.14*b*.

The complex displacement $\boldsymbol{\xi}$ corresponding to the *n*th mode of vibration as obtained upon simplifying equation 3.10 is

$$\boldsymbol{\xi}_n = -2j\mathbf{A}_n e^{j\omega_n t} \sin k_n x \tag{3.14}$$

and the real part of equation 3.14 is

$$\xi_n = (A_n \cos \omega_n t + B_n \sin \omega_n t) \sin k_n x \tag{3.14a}$$

where the real amplitude constants A_n and B_n are related to the complex constant $\mathbf{A}_n$ of equation 3.14 by $2\mathbf{A}_n = B_n + jA_n$.

The complete solution is the sum of all separate harmonic solutions, therefore

$$\xi = \sum_{n=1}^{\infty} (A_n \cos \omega_n t + B_n \sin \omega_n t) \sin k_n x \tag{3.15}$$

If the initial conditions as to the displacement and velocity of the bar are known, the Fourier theorem can be used, as in Sect. 2.13, to evaluate the constants A_n and B_n.

3.5 Additional Boundary Conditions. Since a solid bar is itself very rigid, it is difficult to provide supports of greater rigidity, and hence the boundary conditions assumed in Sect. 3.14 are difficult to realize in practice. By contrast, a free-end condition (impossible in a string) may be achieved quite readily by supporting the bar on soft supports placed some distance in from the ends. When the bar is free to move at an end, there can be no internal elastic force at the end, and hence $F_x = 0$ at this point. Since

$$F_x = -SY\frac{\partial \xi}{\partial x}$$

this condition is equivalent to

$$\frac{\partial \xi}{\partial x} = 0 \tag{3.16}$$

at a free end.

Let us now consider the so-called free-free bar, i.e., a bar that is free to move at both ends. Then the condition $\partial \boldsymbol{\xi}/\partial x = 0$, applied to equation 3.9 at $x = 0$, gives

$$0 = -\mathbf{A} + \mathbf{B} \quad \text{or} \quad \mathbf{B} = \mathbf{A}$$

so that

$$\boldsymbol{\xi} = \mathbf{A}e^{j\omega t}(e^{-jkx} + e^{jkx}) \tag{3.17}$$

A further application of $\partial \boldsymbol{\xi}/\partial x = 0$ at $x = l$ gives

$$-e^{-jkl} + e^{jkl} = 0 \quad \text{or} \quad \sin kl = 0 \tag{3.18}$$

The frequencies of allowed vibration for a free-free bar are identical with those of equation 3.13 for a fixed-fixed bar.

The complex displacements corresponding to the nth mode of vibration are given by

$$\boldsymbol{\xi}_n = 2\mathbf{A}_n e^{j\omega_n t} \cos k_n x \tag{3.19}$$

where $2 \cos kx$ replaces $e^{-jkx} + e^{jkx}$. The actual physical vibrations are given by the real part of equation 3.19 which is

$$\xi_n = (A_n \cos \omega_n t + B_n \sin \omega_n t) \cos k_n x \tag{3.19a}$$

In contrast with the fixed-fixed bar which has nodes at either end, the free-free bar has antinodes at either end as is indicated by the presence of the $\cos k_n x$ term in the above equation. A comparison of the nodal patterns for these two types of support is given in Fig. 3.3. It should be observed that, whenever an antinode occurs at the center of the bar, the vibrations are symmetrical with respect to the center; i.e., when a segment of the bar to the left of center is displaced to the left, the corresponding segment to the right is displaced the same distance to the left. Similarly, whenever there is a node at the center, the vibrations are asymmetrical.

A bar may be rigidly clamped at any of its nodal positions without interfering with the modes of vibration having a node at this position. However, those modes of vibration not having a node at this position will be suppressed. It is impossible to find a position for clamping a free-free

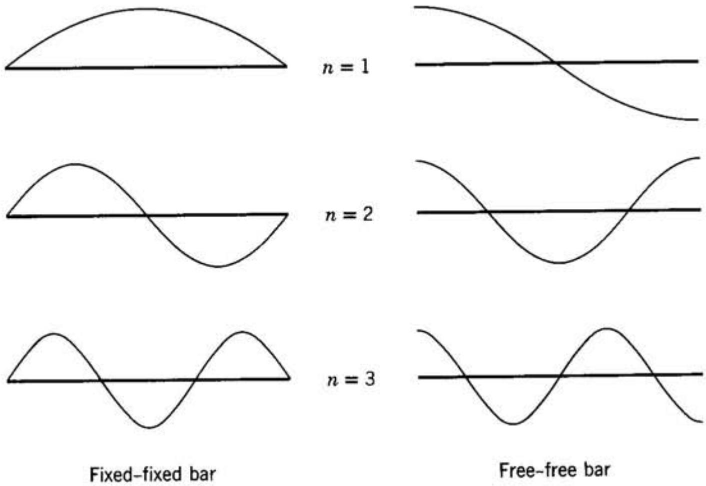

Fig. 3.3. Standing wave patterns in a bar.

bar that will not eliminate at least some of the frequencies given by equation 3.13.

Next consider a free-fixed bar, i.e., one free at $x = 0$ and rigidly fixed at $x = l$. Application to equation 3.9 of the first condition $\partial\xi/\partial x = 0$ at $x = 0$, gives equation 3.17, and application of the second condition, $\xi = 0$ at $x = l$ leads to

$$e^{-jkl} + e^{jkl} = 0 \quad \text{or} \quad \cos kl = 0 \tag{3.20}$$

The allowed frequencies are those satisfying

$$k_n l = (2n - 1)\frac{\pi}{2} \qquad n = 1, 2, 3, \cdots$$

or

$$\omega_n = \frac{(2n - 1)\pi c}{2l}, \qquad f_n = \frac{(2n - 1)c}{4l} \tag{3.21}$$

The frequency of the fundamental is half that of a similar free-free bar, and only the odd-numbered harmonic overtones are present. For example, the frequency of the first overtone of a free-fixed bar is three times that of its fundamental. This is to be expected, since the effect of clamping a free-free bar at its center is to suppress all its even harmonics. Because of the absence of even harmonics, the quality of the sound produced by a vibrating free-fixed bar differs from that produced by a free-free bar.

3.6 Mass-Loaded Bar. In many practical applications, a vibrating bar is neither rigidly fixed nor completely free to move at its ends. Instead, it may be loaded with some kind of mechanical impedance, most commonly one of the mass-controlled type. In one form of sonar transducer, for example, the mass of the diaphragm may be considered as a distributed mass loading of one end of the vibrating nickel tubes.

To analyze this type of constraint, consider a bar that is free at $x = 0$ and is loaded with a concentrated mass m at $x = l$. Ideally, this mass should be a point mass, for otherwise it will not move as a unit but will instead have waves propagated through it. The boundary condition $\partial\boldsymbol{\xi}/\partial x = 0$, applied to equation 3.9 at $x = 0$, gives $\mathbf{B} = \mathbf{A}$, and leads to equation 3.17.

The boundary condition at $x = l$ is given by

$$(\mathbf{F}_x)_{(x=l)} = m\left(\frac{\partial^2\boldsymbol{\xi}}{\partial t^2}\right)_{(x=l)} \tag{3.22}$$

Since a positive value for F_x was chosen to indicate compression of the bar, the reaction to such a force will accelerate the mass attached to the right end of the bar toward the right. Also, since the mass is rigidly attached to the bar, the accelerations of the mass and of the end of the bar must be identical. If the mass had been fastened to the left end of the bar, a positive compression force F_x would correspond to a reaction force to the left on the attached mass. Therefore, the appropriate boundary conditions for such a mass would be

$$(-\mathbf{F}_x)_{(x=0)} = m\left(\frac{\partial^2\boldsymbol{\xi}}{\partial t^2}\right)_{(x=0)} \tag{3.22a}$$

Applying the boundary condition (equation 3.22) to equation 3.17 gives

$$-SY\mathbf{A}e^{j\omega t}(-jke^{-jkl} + jke^{jkl}) = m\mathbf{A}e^{j\omega t}(-\omega^2)(e^{-jkl} + e^{jkl})$$

or

$$jkSY(e^{-jkl} - e^{jkl}) = -m\omega^2(e^{-jkl} + e^{jkl})$$

which reduces to

$$kSY\sin kl = -m\omega^2\cos kl$$

or

$$\tan kl = -\frac{\omega mc}{SY} \tag{3.23}$$

There is no explicit solution of this transcendental equation. For very small mass loading, however, $m \approx 0$, so that $\tan kl \approx 0$, or $kl \approx n\pi$, which is the condition for the allowed frequencies of a free-free bar. Such a result is obviously to be expected, since, for very light loadings, the bar is essentially free at both ends. Similarly, for heavy mass loadings the mass acts very much like a rigid support, and the allowed frequencies approach those of a free-fixed bar.

It should be noted that in practice the process of "fixing" the end of a bar actually consists in loading it with a large mass, the mass of the support. For light bars a heavy support will act essentially like an infinite mass, and hence like a rigid clamp, but for heavy bars it may be very difficult, if not impossible, to approximate the rigidly clamped condition closely.

The general case of intermediate mass loading can be most readily solved by graphical means. It will be convenient to replace Y by its equivalent expression ρc^2, as given by equation 3.8a, and to let $m_b = \rho Sl$ represent the mass of the bar. Then equation 3.23 becomes

$$\frac{\tan kl}{kl} = -\frac{m}{m_b} \tag{3.24}$$

If we now plot the functions $y_1 = \tan kl$ and $y_2 = -(m/m_b)kl$ as functions of kl, the allowed frequencies of vibration will correspond to the values of kl for which the curves intersect. Taking as an illustration the mass loading for which $m = m_b$, the values of kl satisfying equation 3.24 are

$$kl = 2.03, 4.91, 7.98, \cdots$$

The fundamental frequency, which is given by $k_1 l = 2.03$, is $f_1 = (2.03/2\pi)(c/l)$. This is intermediate between the fundamental frequency $f_1 = \frac{1}{2}c/l$ of a free-free bar and the fundamental frequency $f_1 = \frac{1}{4}c/l$ of a free-fixed bar.

It should also be noted that the overtones are not harmonics of the fundamental. For example, the ratio of the frequency of the first overtone to that of the fundamental is $4.91/2.03 = 2.42$. The presence of non-harmonic overtones is sometimes advantageous in practical applications of longitudinally vibrating bars. As an illustration, consider a mass-loaded nickel tube which is driven magnetostrictively by alternating currents in a coil mounted on the tube and is intended to generate a pure tone. Unless the current produced by the oscillator-amplifier unit driving the tube is well filtered, harmonic frequency components other than the desired fundamental will be present in the output. However, since the overtone frequencies of the mass-loaded tube are not harmonics of the fundamental, they will not be resonant with the harmonics of the driving current, and hence will be weakly excited, if at all.

The locations of the nodal points of a bar are also altered by the presence of mass loading. In general the nodes corresponding to a particular mode of vibration will occur where

$$\cos kx = 0 \tag{3.25}$$

In the example just considered, where $m = m_b$, the fundamental mode of vibration is given by $kl = 2.03$, and a node will occur at

$$\frac{2.03x}{l} = \frac{\pi}{2} \quad \text{or} \quad x = 0.77l$$

In contrast with the free-free bar, the node is no longer at the center but has instead shifted toward the loading mass, Fig. 3.4. Such a bar could be supported at this nodal position without interfering with the fundamental mode of vibration.

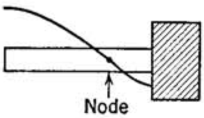

Fig. 3.4. Fundamental mode of vibration of a mass-loaded bar.

3.7 General Boundary Conditions. The problem of the mass-loaded bar can be solved with equal facility by considering the bar as having a mechanical impedance $\mathbf{Z}_l$ at its right end, where

$$\mathbf{Z}_l = j\omega m \tag{3.26}$$

Similarly, the mechanical impedance corresponding to a mass attached to the left end of the bar is given by

$$\mathbf{Z}_0 = -j\omega m \tag{3.26a}$$

where the minus sign is required to take into account the 180° difference in phase between a positive force acting on the mass and on the bar.

If the loading at one end of a vibrating bar supplies dissipative as well as reactive forces, the mechanical impedance $\mathbf{Z}_l$ or $\mathbf{Z}_0$ is a complex quantity, rather than a pure imaginary. This type of loading occurs when the bar is attached to a sounding board or to some similar radiator of acoustic waves. The general method of attack on the problem of an impedance-loaded bar is similar to that for a reactance-loaded bar, but the mathematical difficulties are much greater. One effect of the loading is obviously to damp the free vibrations, and, as for a simple oscillator, the resistive forces also produce slight changes in the frequencies of the various natural modes of vibration. However, in nearly all practical applications the effect of the dissipative forces on the natural frequencies is negligible in comparison with the effect of the mass reactance of the load. A general analysis of impedance-loaded bars is very similar to the corresponding analysis of acoustic plane waves in pipes, and, consequently, a detailed consideration of the mathematical techniques involved will be deferred until Sect. 8.7.

Whenever one end of a longitudinal vibrator is attached to another vibrating body, e.g., to a vibrating diaphragm or machinery component, it is driven into modes of vibration having the same frequency as the latter. Since the mathematical techniques used in solving such problems are similar to those previously encountered in the case of driven transverse vibrations of a string, no further discussion is required. It also is to be noted that certain materials may be set into longitudinal vibrations by internal forces associated with the magnetostrictive and piezoelectric effects. Examples of these types of driven longitudinal vibrators are discussed in Chapter 12.

3.8 Transverse Vibrations of a Bar. A bar is capable of vibrating transversely, as well as longitudinally, and the internal coupling between longitudinal and bending strains often makes it difficult to produce one motion without also exciting the other. For example, if a long thin bar is supported at its center and is set into vibration by a hammer blow directed as nearly as possible along the axis of the bar, it is usually found that the unavoidable slight eccentricity of the blow results in the establishment of predominantly transverse vibrations, rather than the desired longitudinal vibrations.

There is also no sharp distinction between the transverse vibrations of strings and bars. In the previous chapter the strings considered were assumed to be perfectly flexible, so that the restoring forces could be attributed to tension alone. As has been pointed out, this is never strictly true, although in most strings the restoring force does result primarily from tension, rather than from stiffness. On the other hand, if a long thin bar is stretched between rigid supports, the restoring force may be due to both effects acting at once, the question of which type predominates being determined by the particular physical conditions. The study of the limiting case of the ideal string has supplied much useful information, and similarly we shall find it advantageous to study the other limiting case, i.e., the transverse vibrations of a stiff bar which is not subjected to longitudinal forces.

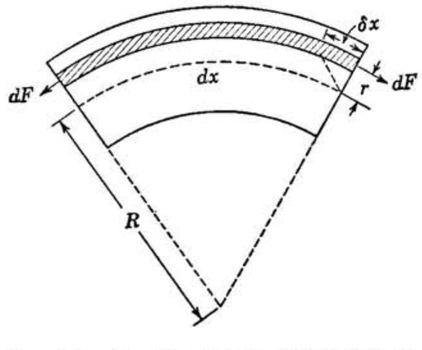

Fig. 3.5. Bending strains and stresses in a bar.

3.9 Bending Strains in a Uniform Bar. Consider a straight bar of length l, having a uniform cross section of area S, which is symmetrical about a vertical plane through the axis of the bar. Let the x coordinate measure positions along the bar, and the y coordinate the transverse displacements of the bar from its normal configuration. When the bar is bent as indicated in Fig. 3.5, the lower part is compressed and the upper part is stretched.

Somewhere between the top and the bottom of the bar there will be a *neutral axis* whose length remains unchanged. If the cross section of the bar is symmetrical about a horizontal plane, this neutral axis will coincide with the central axis of the bar.

Now consider a segment of the bar of length dx, measured along the neutral axis, and assume that the bending of the bar is measured by the radius of curvature R of the neutral axis. Let $\delta x = (\partial\xi/\partial x)\,dx$ be the increment in length, due to bending, of a filament of the bar located at a distance r from the neutral axis. Then the longitudinal force dF is given by

$$dF = -Y\,dS\,\frac{\delta x}{dx} = -Y\,dS\,\frac{\partial\xi}{\partial x} \tag{3.27}$$

where dS is the cross-sectional area of the filament. The value of δx for the particular filament considered in Fig. 3.5 is positive, so that dF is a force of tension, and is consequently negative. For filaments below the neutral axis δx is negative, giving a positive force of compression.

Now

$$\frac{dx + \delta x}{R + r} = \frac{dx}{R}$$

hence

$$\frac{\delta x}{dx} = \frac{r}{R} \tag{3.28}$$

A substitution of this relation into equation 3.27 yields

$$dF = -\frac{Y}{R}\,r\,dS \tag{3.27a}$$

The total longitudinal force $F_x = \int dF$ is zero, negative forces above the neutral axis being canceled by positive forces below the neutral axis. However, a bending moment M is present in the bar. This bending moment is given by

$$M = \int r\,dF = -\frac{Y}{R}\int r^2\,dS$$

If we define a constant κ by

$$\kappa^2 = \frac{\int r^2\,dS}{S}$$

then

$$M = -\frac{YS\kappa^2}{R} \tag{3.29}$$

The constant κ can be thought of as the radius of gyration of the cross-sectional area S, by analogy with the definition of the radius of gyration of a solid. The value of κ for a bar of rectangular cross section is $t/\sqrt{12}$, where t is the thickness of the bar measured in the y direction. For a circular rod of radius a, $\kappa = a/2$.

The radius of curvature R is not in general a constant but is rather a function of position along the neutral axis. A general analytical expression for the radius of curvature of a line is

$$R = \frac{[1 + (\partial y/\partial x)^2]^{3/2}}{\partial^2 y/\partial x^2} \tag{3.30}$$

If the displacements y of the bar are limited to small values, the slope of the bar at any point will always be small compared to unity, i.e., $\partial y/\partial x \ll 1$. Then we may use the approximate relation

$$R = \frac{1}{\partial^2 y/\partial x^2} \tag{3.30a}$$

A substitution of equation 3.30*a* into equation 3.29 yields

$$M = -YS\kappa^2 \frac{\partial^2 y}{\partial x^2} \tag{3.31}$$

In the situation illustrated in Fig. 3.5, the curvature is such as to make $\partial^2 y/\partial x^2$ negative, and the bending moment M is consequently positive. It is apparent that to obtain the curvature illustrated, the torque applied to the *left* end of the segment dx must act in a counterclockwise or *positive* angular direction, so that equation 3.31 gives the torque acting on the left end of the segment both as to magnitude and as to direction. Similarly, the torque acting on the *right* end of the segment must be clockwise, with the result that it is *negative* and is therefore represented both in direction and in magnitude by $-M$. This situation is analogous to that previously discussed in connection with the longitudinal vibrations of a bar, where F_x, as given by equation 3.5, represented a positive force acting on the left end of the bar, and $-F_x$, the associated negative force acting on the right end of the bar. If the bar of Fig. 3.5 were bent upward, the directions of both applied torques would be reversed.

3.10 Transverse Wave Equation. The effect of distorting the bar is to produce not only bending moments but also shear forces. Let us choose to consider an upward shear force F_y acting on the *left* end of the segment dx as positive, Fig. 3.6. Then the associated shear force acting on the right end of the segment must be downward, and is consequently negative. When a bent bar is in a condition of *static* equilibrium, the torques and shear forces acting on any segment must be so related as to produce no net

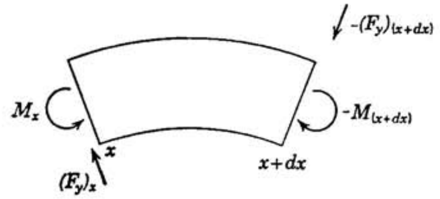

Fig. 3.6. Bending moments and shear forces in a bar.

turning moment. Taking moments about the left end of the segment of Fig. 3.6, this condition becomes

$$M_x - M_{(x+dx)} - (F_y)_{(x+dx)}\,dx = 0 \tag{3.32}$$

For segments of small length dx,

$$M_{(x+dx)} = M_x + \frac{\partial M}{\partial x}\,dx$$

and

$$(F_y)_{(x+dx)} = (F_y)_x + \frac{\partial F_y}{\partial x}\,dx$$

Substitution of these expressions into equation 3.32 gives

$$M_x - M_x - \frac{\partial M}{\partial x}\,dx - (F_y)_x\,dx - \left(\frac{\partial F_y}{\partial x}\,dx\right)dx = 0$$

and, neglecting the second order term involving $(dx)^2$,

$$F_y = -\frac{\partial M}{\partial x} = YS\kappa^2\frac{\partial^3 y}{\partial x^3} \tag{3.33}$$

This relation between the shear force F_y and the bending moment M has been derived for a condition of static equilibrium. In the actual case of the transverse vibrations of a bar the equilibrium is dynamic, rather than static, and the right-hand member of equation 3.32 will then equal the rate of increase of angular momentum of the segment, rather than zero. However, if the displacement and the slope of the bar are limited to small values, the variations in angular momentum may be neglected, and equation 3.33 serves as an adequate approximation for the relation between F_y and y.

The net upward force dF_y acting on the segment dx is then given by

$$dF_y = (F_y)_x - (F_y)_{(x+dx)} = -\frac{\partial F_y}{\partial x}\,dx = -YS\kappa^2\frac{\partial^4 y}{\partial x^4}\,dx \tag{3.34}$$

This force will give the segment an upward acceleration, and, since the mass of the segment is $\rho S\, dx$, the equation of motion is

$$(\rho S\, dx)\frac{\partial^2 y}{\partial t^2} = -YS\kappa^2 \frac{\partial^4 y}{\partial x^4}\, dx$$

or

$$\frac{\partial^2 y}{\partial t^2} = -\kappa^2 c^2 \frac{\partial^4 y}{\partial x^4} \tag{3.35}$$

where, as for longitudinal waves, we define c by

$$c = \sqrt{\frac{Y}{\rho}} \tag{3.8a}$$

One significant difference between this differential equation and the simpler equation 2.5 for the transverse waves on a string is the presence of a fourth partial derivative with respect to x, rather than a second partial. As a result of this difference, functions of the form $f(ct - x)$ are *not* solutions of equation 3.35, a fact that can be shown by direct substitution of $f(ct - x)$ as an assumed solution, and hence transverse waves *do not* travel along the bar with a constant velocity c and unchanging shape.

3.11 Periodic Form of the General Solution. As a first step toward obtaining a solution of equation 3.35, let us assume that it may be solved by the method of "separation of variables," in that the complex transverse displacement may be expressed by

$$\mathbf{y} = \psi(x)e^{j\omega t} \tag{3.36}$$

as the product of two terms, $\psi(x)$ or for short ψ, a complex function of x alone, and $e^{j\omega t}$, a function of t alone, the usual harmonic function for periodic vibrations. Then

$$\frac{\partial^2 \mathbf{y}}{\partial t^2} = \psi(j\omega)^2 e^{j\omega t}$$

and

$$\frac{\partial^4 \mathbf{y}}{\partial x^4} = \frac{\partial^4 \psi}{\partial x^4}\, e^{j\omega t}$$

Upon substitution of these expressions into equation 3.35, the exponential function of time cancels out, leaving a new *total* differential equation involving ψ as a function of x only. This equation is

$$\frac{d^4\psi}{dx^4} = \frac{\omega^2}{\kappa^2 c^2}\psi$$

or letting

$$v = \sqrt{\omega c \kappa} \tag{3.37}$$

it becomes

$$\frac{d^4\psi}{dx^4} = \frac{\omega^4}{v^4}\psi \tag{3.38}$$

Now assume that ψ can be expressed as an exponential of the form $\psi = \mathbf{A}e^{\gamma x}$, and substitute into equation 3.38. Then

$$\gamma^4\mathbf{A}e^{\gamma x} = \frac{\omega^4}{v^4}\mathbf{A}e^{\gamma x}$$

so that

$$\gamma = \pm\frac{\omega}{v} \quad \text{or} \quad \gamma = \pm j\frac{\omega}{v}$$

The complete solution is then given by the sum of these four solutions, i.e.,

$$\psi = \mathbf{A}e^{\omega x/v} + \mathbf{B}e^{-(\omega x/v)} + \mathbf{C}e^{j\omega x/v} + \mathbf{D}e^{-(j\omega x/v)} \tag{3.38a}$$

where **A**, **B**, **C**, and **D** are complex amplitude constants. The solution for the displacements **y** is therefore

$$\mathbf{y} = e^{j\omega t}(\mathbf{A}e^{\omega x/v} + \mathbf{B}e^{-(\omega x/v)} + \mathbf{C}e^{j\omega x/v} + \mathbf{D}e^{-(j\omega x/v)}) \tag{3.39}$$

None of the individual terms in equation 3.39 represents waves moving with a velocity c. For example, consider the last term, and write it as

$$\mathbf{y} = \mathbf{D}e^{j\omega(t - x/v)} \tag{3.40}$$

This represents a wave disturbance moving to the right with a velocity v, but from equation 3.37 it can be seen that v is itself a function of frequency, so that waves of different frequencies travel with different velocities. In a complex wave containing various frequency components, the high-frequency components travel with greater velocities and hence outrun the low-frequency components, thereby altering the shape of the wave. A precise definition of what is meant by the velocity of such a wave is consequently difficult. However, each frequency component of the complex wave progresses at its own velocity v, the so-called *phase velocity* of the component. This situation is analogous to the transmission of light through glass, where the different component frequencies, i.e., colors, of a complex light beam travel with different velocities, and dispersion results. Therefore, a vibrating bar may be thought of as a dispersive medium for transverse waves.

The actual solution of equation 3.35 is the real part of equation 3.39. It may be conveniently obtained by employing the hyperbolic and trigonometric identities

$$e^{\pm\theta} = \cosh\theta \pm \sinh\theta \tag{3.41}$$

and

$$e^{\pm j\theta} = \cos\theta \pm j\sin\theta \tag{3.41a}$$

Then

$$y = \cos(\omega t + \phi)\left[A\cosh\frac{\omega x}{v} + B\sinh\frac{\omega x}{v} + C\cos\frac{\omega x}{v} + D\sin\frac{\omega x}{v}\right] \tag{3.42}$$

where A, B, C, and D are real constants. Although these constants are related to the complex constants **A**, **B**, **C**, and **D**, the relationships are unimportant, since in practice A, B, C, and D are always directly evaluated through the application of initial and boundary conditions to equation 3.42.

3.12 Boundary Conditions. Since equation 3.42 contains twice as many arbitrary constants as the corresponding equation for the transverse vibrations of a string, the determination of these constants requires twice as many boundary conditions. This need is fulfilled by the existence of pairs of boundary conditions at the ends of the bar. The particular forms of these conditions depend on the nature of the support, and include:

(*a*) *Clamped end.* If the end of the bar is rigidly clamped, both the displacement and the slope must be zero at the end at all times t. The boundary conditions are therefore

$$y = 0 \quad \text{and} \quad \frac{\partial y}{\partial x} = 0 \tag{3.43}$$

(*b*) *Free end.* At a free end there can be neither an externally applied torque nor a shearing force, and hence both M and F_y are zero in a plane located an infinitesimal distance from the end. However, the displacement and slope are not constrained, except by the general restriction that their values must be small. Then from equations 3.31 and 3.33, the boundary conditions are

$$\frac{\partial^2 y}{\partial x^2} = 0 \quad \text{and} \quad \frac{\partial^3 y}{\partial x^3} = 0 \tag{3.43a}$$

3.13 Bar Clamped at One End. A type of constraint that occurs frequently in practice is that of the so-called *clamped-free* bar. Assume that such a bar of length l is rigidly clamped at $x = 0$ and is free at $x = l$. Then applying the two conditions of equation 3.43 at $x = 0$ to the general solution of equation 3.42 we obtain

$$y = 0 = A + C$$

and

$$\frac{\partial y}{\partial x} = 0 = B + D$$

so that the general solution reduces to

$$y = \cos(\omega t + \phi)\left[A\left(\cosh\frac{\omega x}{v} - \cos\frac{\omega x}{v}\right) + B\left(\sinh\frac{\omega x}{v} - \sin\frac{\omega x}{v}\right)\right] \quad (3.44)$$

A further application of the two conditions of equation 3.43*a* at $x = l$ gives

$$\frac{\partial^2 y}{\partial x^2} = 0 = \cos(\omega t + \phi)\left(\frac{\omega}{v}\right)^2\left[A\left(\cosh\frac{\omega l}{v} + \cos\frac{\omega l}{v}\right) + B\left(\sinh\frac{\omega l}{v} + \sin\frac{\omega l}{v}\right)\right]$$

and

$$\frac{\partial^3 y}{\partial x^3} = 0 = \cos(\omega t + \phi)\left(\frac{\omega}{v}\right)^3\left[A\left(\sinh\frac{\omega l}{v} - \sin\frac{\omega l}{v}\right) + B\left(\cosh\frac{\omega l}{v} + \cos\frac{\omega l}{v}\right)\right]$$

From these two expressions we obtain the following relationships between A and B:

$$A\left(\cosh\frac{\omega l}{v} + \cos\frac{\omega l}{v}\right) = -B\left(\sinh\frac{\omega l}{v} + \sin\frac{\omega l}{v}\right)$$

and

$$A\left(\sinh\frac{\omega l}{v} - \sin\frac{\omega l}{v}\right) = -B\left(\cosh\frac{\omega l}{v} + \cos\frac{\omega l}{v}\right)$$

It is impossible for both of these equations to be true for all frequencies, although at certain frequencies they become equivalent. To determine these allowed frequencies, divide one equation by the other, thus cancelling out the constants A and B. Then cross-multiply and simplify by using the identities $\cos^2\theta + \sin^2\theta = 1$ and $\cosh^2\theta - \sinh^2\theta = 1$. This gives

$$\cosh\frac{\omega l}{v}\cos\frac{\omega l}{v} = -1 \quad (3.45)$$

It would be possible to obtain the roots of this transcendental equation by plotting curves of cosh $(\omega l/v)$ and $-\sec(\omega l/v)$ as functions of $\omega l/v$, and then determining their intersections. However, such a procedure is impractical except for small values of $\omega l/v$, since the hyperbolic cosine increases in an approximately exponential manner with increasing $\omega l/v$. A more convenient form of equation 3.45 can be obtained by application of the identities

$$\tan\frac{\theta}{2} = \sqrt{\frac{1-\cos\theta}{1+\cos\theta}} \quad \text{and} \quad \tanh\frac{\theta}{2} = \sqrt{\frac{\cosh\theta - 1}{\cosh\theta + 1}}$$

Then

$$\cot\frac{\omega l}{2v} = \pm\tanh\frac{\omega l}{2v} \tag{3.45a}$$

Figure 3.7 is a graph of the functions $\cot(\omega l/2v)$ and $\pm\tanh(\omega l/2v)$, plotted against $\omega l/2v$. From the points of intersection of these curves it is apparent that the frequencies corresponding to the allowed modes of vibration are given by

$$\frac{\omega l}{2v} = \frac{\pi}{4}(1.194, 2.988, 5, 7, \cdots) \tag{3.46}$$

The numerical value of the hyperbolic tangent approaches unity for all

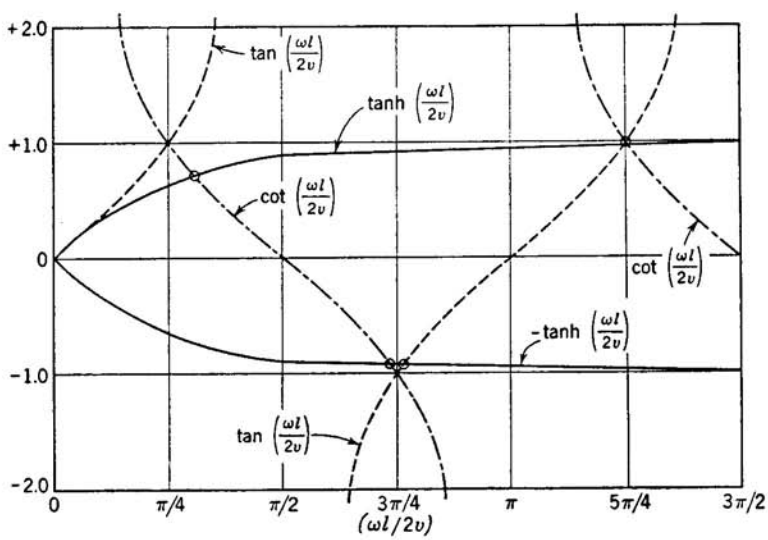

Fig. 3.7. Curves showing tangent, cotangent, and hyperbolic tangent functions.

angles greater than π. Therefore, for such angles the roots of equation 3.45*a* are given to a close approximation by the angles $\omega l/2v = (2n - 1)\pi/4$, where $n = 3, 4, 5, \cdots$, and the cotangent of $\omega l/2v$ is consequently equal to ± 1. The accurate values $1.194\pi/4$ and $2.988\pi/4$ must be used for the two lowest allowed frequencies.

Substituting $v = \sqrt{\omega c\kappa}$ into equation 3.46 and squaring both sides, we have

$$\omega = \frac{\pi^2 c\kappa}{4l^2}(1.194^2, 2.988^2, 5^2, 7^2, \cdots) \tag{3.47}$$

or

$$f = \frac{\pi c\kappa}{8l^2}(1.194^2, 2.988^2, 5^2, 7^2, \cdots) \tag{3.47a}$$

as the allowed frequencies of transverse vibration of a fixed-free bar. Therefore, the application of boundary conditions limits the allowed modes of free vibration of a finite bar to a discrete set of frequencies, just as it does for a vibrating string. However, in contrast with the string, the overtone frequencies of a bar are not harmonics of its fundamental, since equation 3.47*a* shows that

$$f_2 = \left(\frac{2.988}{1.194}\right)^2 f_1 = 6.267f_1$$

$$f_3 = 17.55f_1$$

$$f_4 = 34.39f_1$$

Etc.

The first overtone has a frequency higher than the sixth harmonic of a string of the same fundamental frequency. If a bar is struck in such a manner that the amplitudes of vibration of some of the overtones are appreciable, the sound produced has a metallic quality. However, these high-frequency overtones are rapidly damped out, so that the initial sound is soon mellowed into a nearly pure tone, whose frequency is that of the fundamental. A struck tuning fork exhibits the above characteristics of an initial metallic sound, which rapidly dies out, leaving a nearly pure tone.

The vibrating reeds used as frequency standards in frequency meters, and as components in low-frequency electrical filters, are other applications of fixed-free bars. It is possible to adjust the fundamental resonance frequency of such reeds either by varying their thickness, and thereby κ, or by varying their length. It is to be noted that as the length is doubled, the frequency is divided by four.

The distribution of nodal points along a transversely vibrating fixed-free bar is much more complex than in the examples previously considered, for the nodes are not evenly spaced at intervals of $\lambda/2$ but have instead an irregular spacing.[1] Furthermore there are *three* distinct types of nodal points, i.e., positions where $y = 0$ at all times. The point at which the bar is clamped is one node. This node is characterized by the conditions $y = 0$ and $\partial y/\partial x = 0$. The next group of nodal points is characterized by $y = 0$ and $\partial^2 y/\partial x^2 \approx 0$. These so-called *true* nodes are located near points of inflection of the bar. Also, the spacing between *true* nodes is very nearly $\lambda/2$. A third type of nodal point is that occurring at the node adjacent to the

Table 3.1 Transverse vibration characteristics of a fixed-free bar

Frequency	Phase Velocity (cm/sec)	Wavelength (cm)	Nodal Positions (cm from clamped end)
f_1	v_1	335.0	0
$6.267f_1$	$2.50v_1$	133.4	0, 78.3
$17.55f_1$	$4.18v_1$	80.0	0, 50.4, 86.8
$34.39f_1$	$5.87v_1$	57.2	0, 35.8, 64.4, 90.6

free end of the bar, where $y = 0$. A point of inflection, $\partial^2 y/\partial x^2 = 0$, does not occur near this nodal position but instead is shifted out to the free end. It is also to be noted that the vibrational amplitude at the various antinodal positions is not the same for each antinode, because that at the free end is always the greatest.

Table 3.1 gives the nodal positions for transverse vibrations of a bar 100 cm in length, which is clamped at $x = 0$, and is free at $x = 100$. The ratios of the frequency f and the phase velocity v to their fundamental values are also tabulated, together with the wavelength $\lambda = v/f$ in centimeters for each frequency component. The increase in velocity with frequency of the overtone is quite apparent. It should also be noted that the wavelengths are not in general equal to twice the distance between nodes. However, the nodal spacing between *true* nodes for the third overtone mode of vibration is 28.6 cm (64.4 − 35.8) which, within the accuracy of the data supplied, equals $\lambda/2$.

3.14 Bar Free at Both Ends. Another important type of transverse vibration is that of a *free-free* bar. The boundary conditions at both ends of the bar are

$$\partial^2 y/\partial x^2 = 0 \quad \text{and} \quad \partial^3 y/\partial x^3 = 0$$

These two conditions are satisfied at $x = 0$ if

$$A - C = 0 \quad \text{and} \quad B - D = 0$$

[1] Heller, *J. Acoust. Soc. Am.*, **24**, 273 (1952).

Application of the same conditions at $x = l$ restricts the allowed frequencies to those satisfying

$$\cosh\left(\frac{\omega l}{v}\right)\cos\left(\frac{\omega l}{v}\right) = 1 \tag{3.48}$$

or

$$\tan\left(\frac{\omega l}{2v}\right) = \pm\tanh\left(\frac{\omega l}{2v}\right) \tag{3.48a}$$

A consideration of Fig. 3.7 shows that the allowed frequencies are given by

$$\frac{\omega l}{2v} = \frac{\pi}{4}(3.0112, 5, 7, 9, \cdots) \tag{3.49}$$

or

$$f = \frac{\pi c\kappa}{8l^2}(3.0112^2, 5^2, 7^2, 9^2, \cdots) \tag{3.50}$$

and again the overtones are not harmonics of the fundamental.

Table 3.2, which is similar to Table 3.1, gives information concerning the frequencies, phase velocities, and nodal positions of a free-free bar 100 cm long. An inspection of Fig. 3.8*b* shows that the modes of vibration corresponding to the fundamental f_1 and all additional odd-numbered

Table 3.2 Transverse vibration characteristics of a free-free bar

Frequency	Phase Velocity (cm/sec)	Wavelength (cm)	Nodal Positions (cm from end)
f_1	v_1	133.0	22.4, 77.6
$2.756f_1$	$1.66v_1$	80.0	13.2, 50.0, 86.8
$5.404f_1$	$2.32v_1$	57.2	9.4, 35.6, 64.4, 90.6
$8.933f_1$	$2.99v_1$	44.5	7.3, 27.7, 50.0, 72.3, 92.7

frequencies, f_3, f_5, etc., are symmetrical about the center. The slope $\partial x/\partial y$ at the center is always zero, giving a true antinode. In contrast, the even-numbered frequencies f_2, f_4, f_6, etc., correspond to asymmetrical modes of vibration with respect to the center. The curvature $\partial^2 y/\partial x^2$ at the center is always zero, giving a true node. In all modes the nodal positions are symmetrically distributed about the center. The bar may be supported on a knife edge, or clamped by knife-edge clamps, at any nodal point without interfering with the mode of vibration having a node at this point. A knife-edge type of support or clamp is required, since it must merely restrict the displacement to zero and must not restrict the changes in slope that occur at a node.

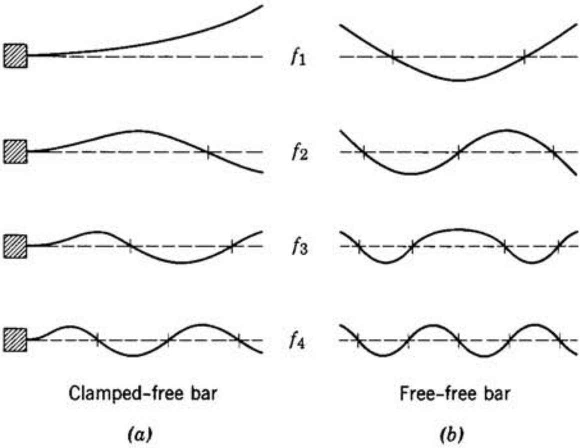

Fig. 3.8. Transverse modes of vibration of a bar.

The bars of a xylophone are supported at points corresponding to the nodal positions of the fundamental. Since the nodes of the accompanying overtones will not in general be located at these same two points, the overtones will be rapidly damped out, leaving the pure tone of the fundamental. This is one of a number of factors that contribute to the mellow pure tonal quality of a xylophone.

The theory of a free-free bar may be used qualitatively to explain the behavior of tuning forks. Such a fork is essentially a bar bent into the shape of a letter U. This bending as well as the mass-loading effect of the stem attached to the center of the bar brings about a closer spacing of the two nodes present, when vibrating at its fundamental frequency. Compare Fig. 3.9 with Fig. 3.8*b*. As has been previously mentioned, when a tuning fork is struck, the frequencies corresponding to the higher modes of vibration rapidly damp out, leaving a pure sinusoidal vibration at the fundamental frequency. Since the stem partakes of the antinodal motion at the center of the original free-free bar, the radiation efficiency of a tuning fork is greatly enhanced by either touching its stem to a surface of large area, such as a table top, or by attaching it to a resonator box tuned to its fundamental frequency.

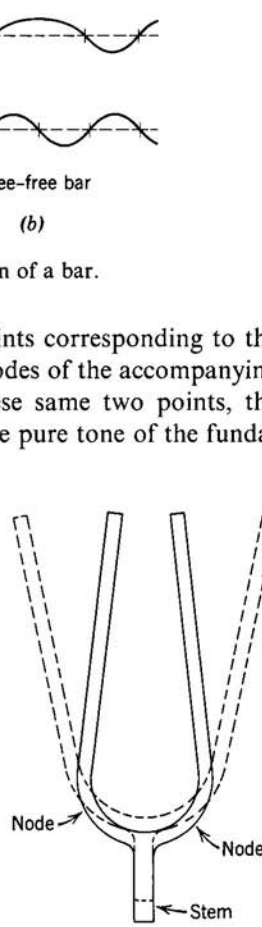

Fig. 3.9. Vibration of a tuning fork.

If a bar is rigidly clamped at both ends, the boundary conditions that $y = 0$ and $\partial y/\partial x = 0$ at $x = 0$ and at $x = l$ lead to the same set of allowed frequencies as for a free-free bar. However, as is to be expected, the arrangement of the nodal positions is different.

3.15 Initial Conditions. As with the transverse vibrations of a string, the amplitudes of the various modes of vibration of a bar are determined by the type of excitation, i.e., by the initial conditions. The technique of determining these amplitudes is similar to the Fourier series method used in Sect. 2.13, but the practical applications are so limited that a treatment is not justified in this book. There is one point, however, that is worthy of note. If the bar is initially distorted and is then released, it is possible to find a series of functions of the nature of equation 3.42 whose sum represents the initial shape of the bar, but, since the various overtones have a pattern of frequencies that are not commensurable, the bar will never again return to this initial shape, and the motion does not become truly periodic until all the overtones are damped out, leaving only the fundamental mode of vibration. For a more detailed discussion of the above as well as of the forced transverse vibrations of a bar, the reader is referred to more advanced treatises.[1]

PROBLEMS

3.1. A bar of length l is rigidly clamped at $x = 0$ and free to move at $x = l$. (*a*) Starting with the basic equation for longitudinal harmonic vibrations, apply boundary conditions to the bar and determine the allowed frequencies of vibration. (*b*) Show that only odd integral harmonic overtones are allowed. (*c*) Determine the fundamental frequency of the bar, if it is composed of steel and has a length of 0.5 m. (*d*) If a static force F is applied to the free end of the bar so as to displace this end an amount h, show that, when the bar vibrates longitudinally subsequent to the release of this force, the amplitudes of the various harmonic vibrations are given by $A_n = \frac{8h}{n^2\pi^2}\sin(n\pi/2)$. (*e*) Determine these amplitudes for the above steel bar, if the force is 5000 newtons and the cross-sectional area of the bar is 0.00005 m^2.

3.2. Determine the expressions giving the energies of the various modes of vibration for the bar of Problem 3.1.

3.3. A long thin bar of length l is driven by a longitudinal force $F\cos\omega t$ at $x = 0$ and is free at $x = l$. (*a*) Derive the equation that gives the amplitude of the standing waves set up in the bar. (*b*) What is the expression giving the input mechanical impedance of such a bar of length l. (*c*) What is the input mechanical impedance of a similar bar of infinite length? (*d*) If the material of the bar is aluminum, the length is 1.0 m, the cross-sectional area is 0.0001 m^2, and the amplitude of the driving force is 10 newtons, plot the amplitude of the driven

[1] Morse, *Vibration and Sound*, Chapter IV, McGraw-Hill Book Company, Inc., (1948).

end of the bar of part (*a*) as a function of frequency over the range from 200 to 2000 cycles/sec.

3.4. A bar of length l is clamped at $x = 0$ and loaded with a mass m at $x = l$. (*a*) Apply these boundary conditions to equation 3.9 and thereby determine an equation from which the fundamental frequency of longitudinal vibrations may be computed. (*b*) Determine the fundamental frequency of such a system composed of a steel bar of 0.5-m length and 0.0001-m^2 cross-sectional area to which is fastened a mass of 0.15 kg. (*c*) When a bar is vibrating in this manner, what position along the bar has the maximum longitudinal displacement amplitude?

3.5. A steel bar of 0.8-cm^2 cross-sectional area and 50-cm length is rigidly clamped at $x = 0$ and loaded with a mass of 0.14 kg at $x = 50$ cm. (*a*) Using the results of Problem 3.4*a* compute the fundamental frequency of longitudinal vibrations for the above mass-loaded bar. (*b*) What is the amplitude of the force acting upon the 0.14-kg mass when the above bar is vibrating at its fundamental frequency with a displacement amplitude of 0.002 cm at the mass-loaded end? (*c*) Replace the bar of the above system by a spring of equal stiffness and mass and compute the system's frequency when considered to vibrate as a simple oscillator.

3.6. Given a 2-kg mass to be hanging on a steel wire of 0.00001-m^2 cross-sectional area and 1.0-m length. (*a*) Compute the fundamental frequency of vertical oscillation of the mass by considering it to be a simple oscillator. (*b*) Compute the fundamental frequency of vertical oscillation of the mass by considering the system to be that of a longitudinally vibrating bar fixed at one end and mass-loaded at the other, i.e., apply the equation derived in Problem 3.4*a* (*c*) Show that for $kl < 0.2$, that the equation derived in Problem 3.4*a* is approximately equal to equation 1.5.

3.7. A steel bar of 0.0001-m^2 cross-sectional area and 0.25-m length is free to move at $x = 0$ and loaded with a mass of 0.15 kg at $x = 0.25$. (*a*) Compute the fundamental frequency of longitudinal vibrations of the above mass-loaded bar. (*b*) Determine the position at which the bar may be clamped so as to cause the least interference with its fundamental mode of vibration. (*c*) When this bar is vibrating in its fundamental mode, what is the ratio of the displacement amplitude of the free end to that of the mass-loaded end? (*d*) What is the frequency of the first overtone mode of vibration of this bar?

3.8. Given a steel bar of 0.2-m length and 0.04-kg mass to be loaded at one end with a mass of 0.027 kg and at the other end with a mass of 0.054 kg. (*a*) Calculate the fundamental frequency of longitudinal vibration of this system. (*b*) Calculate the position of the node in the bar. (*c*) Calculate the ratio of the displacement amplitudes at the two ends of the bar.

3.9. A thin bar of length l and mass M is rigidly clamped at one end and free at the other. What mass m must be attached to the free end in order to decrease the fundamental frequency of longitudinal vibration by 25 per cent from its fixed-free value?

3.10. Determine an expression giving the fundamental frequency of longitudinal vibrations of a clamped-free bar of length l and mass m, if the reaction of the clamp corresponds to a mechanical reactance $-js/\omega$, i.e., one of stiffness.

3.11. Show that $y = f(ct - x)$ does not satisfy equation 3.35.

3.12. Show that $v = \sqrt{\omega c \kappa}$ has the dimensions of a velocity. For what frequency will the transverse vibrations of an aluminum rod of 0.01-m diameter have the same velocity as that of longitudinal vibrations in the rod?

3.13. Given that

$$y = \cos \omega t[A \cosh (\omega x/v) + B \sinh (\omega x/v) + C \cos (\omega x/v) + D \sin (\omega x/v)]$$

where $\omega = 1.88\, v/l$ is the fundamental frequency of transverse vibrations of a bar clamped at one end and free at the other. If the amplitude at the free end $x = l$ is a, determine the constants A, B, C, and D in terms of a. Plot a curve showing the shape of such a bar of 100-cm length when the displacement is 5 cm at the free end.

3.14. A steel rod of 0.005-m radius has a length of 0.5 m. (*a*) What is its fundamental frequency of free-free transverse vibrations? (*b*) If the displacement amplitude at the center of the rod is 2 cm when vibrating in its fundamental mode, what is the displacement amplitude at the ends?

3.15. Show that, when a free-free bar is vibrating transversely, the nodal positions corresponding to the second overtone are located as indicated in Table 3.2.

3.16. A steel rod is of 0.002-m radius and has a length of 2-m. (*a*) What is its fundamental frequency of free-free transverse vibrations? (*b*) If the displacement amplitude at the center of the rod when vibrating in its fundamental mode is 2.0 cm, what is the corresponding amplitude at either end? (*c*) Show that when this rod is vibrating in its fundamental mode, that the nodes are located as indicated in Table 3.2.

3.17. Given a steel rod of 1.0-m length and 0.004-m radius rigidly clamped at both ends. (*a*) What is its fundamental frequency of transverse vibrations? (*b*) Neglecting the effects of elastic stiffness, to what tension would this same rod need to be stretched if its fundamental frequency of transverse vibrations, due to the restoring force of tension alone, is to be the same as that of part (*a*) above?

3.18. A steel rod is of 0.004-m radius and has a length of 0.4 m. The rod is rigidly clamped at one end and free at the other. (*a*) What is the ratio of its fundamental frequency of longitudinal vibration to its fundamental frequency of transverse vibration? (*b*) While vibrating longitudinally at its fundamental frequency, what is the ratio of its displacement amplitude at its midpoint to that at the free end? (*c*) While vibrating transversely at its fundamental frequency, what is the ratio of its displacement amplitude at its midpoint to that at the free end?

chapter 4

CIRCULAR MEMBRANES AND PLATES

4.1 Vibrations of a Plane Surface. Let us next consider the vibrations of systems extended in two dimensions. These range from the complex modes of vibration of Chladni plates to the relatively simple modes of the drumhead of a kettledrum. Detailed analysis will be restricted to two such systems that are of particular importance in the design of electroacoustic transducers. One is the uniformly stretched *circular membrane*, where the restoring force due to stiffness is negligible in comparison with that due to tension. This type of system includes as typical examples the parchment membranes used for drumheads, and the diaphragms of condenser microphones. The other is the *thin circular plate*, where stiffness is the important factor. This type includes as examples the diaphragms of ordinary telephone transmitters and receivers, and the steel faces of some types of sonar transducers.

A general analysis of the transverse motions of a membrane or plate is much more complicated than the analysis of the previously considered one-dimensional systems of a string or a bar. For transverse waves on a string, the expression giving the manner in which the displacement of a particular point on the string varies with time is a sinusoidal function, similar to that giving the shape of the string at any instant of time. In contrast, the function giving the motion of a point on a membrane has no simple relationship to that expressing the shape of the membrane at an instant of time, since the former is a one-dimensional function of time, whereas the latter gives the shape of a two-dimensional surface. There is, however, one case in which a membrane behaves like an assemblage of parallel strings. This occurs when the wave crests are in parallel lines, perpendicular to their direction of propagation. The behavior of such waves is exactly like the behavior of waves on a flexible string. However, this special case is of little practical importance.

In the two previous chapters we have noted that the application of boundary conditions limits the allowed frequencies to a discrete set. Similar restrictions apply to the free vibrations of membranes and plates, but in such two-dimensional systems the boundary conditions include not only the type of support but also the shape of the bounding curve.

4.2 Wave Equation for a Stretched Membrane. Before deriving the wave equation for transverse vibrations of a stretched membrane, we must decide upon what coordinate system to use in locating points on the membrane. Depending on this choice, the results may appear to be different, but are actually equivalent as may be shown by transformation from one coordinate system to another. Although the examples to be discussed in detail will require the use of polar coordinates, the wave equation is more readily derived in Cartesian coordinates in which the transverse displacement y at a point is expressed as

$$y = y(x, z, t) \tag{4.1}$$

Let us now set up the equation of motion for a rectangular element of area, $dS = dx\, dz$. The membrane will be assumed to be thin and uniform, to have negligible stiffness, to be perfectly elastic, to have no damping, and to vibrate with small displacement amplitudes. Let σ be the *area density* of the membrane, i.e., its mass per unit area, expressed in kilograms per square meter, and let T be the tension in newtons per meter of length to which the edge of the membrane is stretched. This tension will be distributed uniformly throughout the membrane, so that the material on opposite sides of a line segment of length ds will tend to be pulled apart with a force of $T\, ds$ newtons.

Our first task is to find an expression for the restoring force acting on any element of the membrane, Fig. 4.1, that bulges away from the equilibrium plane. By argument analogous to that used in Sect. 2.3 for the transverse force acting on a segment of string, the net force on the element $dx\, dz$ due to the pair of tensions $T\, dz$ is

$$T\, dz \left[\left(\frac{\partial y}{\partial x}\right)_{x+dx} - \left(\frac{\partial y}{\partial x}\right)_{x} \right] = T \frac{\partial^2 y}{\partial x^2}\, dx\, dz$$

and that due to the pair of tensions $T\, dx$ is $T(\partial^2 y/\partial z^2)\, dx\, dz$. Equating the sum of these two terms to the product of the element's mass $\sigma\, dx\, dz$ by its acceleration $\partial^2 y/\partial t^2$ gives

$$T \left(\frac{\partial^2 y}{\partial x^2} + \frac{\partial^2 y}{\partial z^2}\right) dx\, dz = \sigma\, dx\, dz\, \frac{\partial^2 y}{\partial t^2}$$

or

$$\frac{\partial^2 y}{\partial t^2} = c^2\left(\frac{\partial^2 y}{\partial x^2} + \frac{\partial^2 y}{\partial z^2}\right) \tag{4.2}$$

where

$$c = \sqrt{\frac{T}{\sigma}} \tag{4.3}$$

By direct substitution, the reader may show that

$$y = f(ct - x\cos\theta - z\sin\theta) \tag{4.4}$$

is a general solution of the *two-dimensional* wave equation (4.2). This solution represents a parallel wave traveling with a velocity c in a direction making an angle θ with respect to the x-axis.

The harmonic form of equation 4.4, appropriate for the discussion of periodic waves present on a stretched membrane having rectangular boundaries is

$$\mathbf{y} = \mathbf{A}e^{j(\omega t - k_x x - k_z z)} \tag{4.4a}$$

where the constants k_x and k_z must satisfy

$$k = \frac{\omega}{c} = \sqrt{{k_x}^2 + {k_z}^2} \tag{4.4b}$$

as the reader may show by direct substitution of equation 4.4a into equation 4.2. Furthermore, k_x/k and k_z/k represent the direction cosines made by the direction of propagation of the wave with respect to the x and z axes. If we replace either one or both of the negative signs in equation

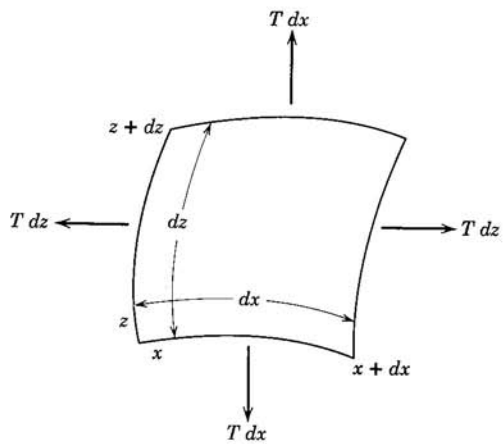

Fig. 4.1. Element of a vibrating membrane.

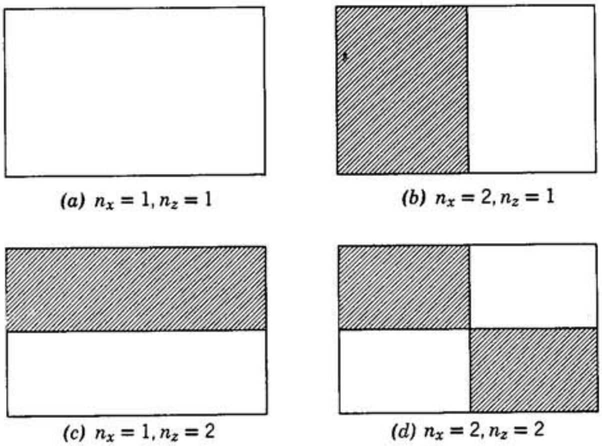

Fig. 4.2. Vibration modes of a rectangular membrane.

4.4*a* with positive signs, three additional solutions of the wave equation similar to equation 4.4*a* are obtained, all having identical values of k_x and k_z. This array of four equations represents the family of parallel waves generated by the original wave as successive reflections occur at the four bounding sides of the membrane.

As an example, let us assume that the boundaries of the stretched membrane lie along the lines $x = 0$, $x = l_x$, $z = 0$, and $z = l_z$. Application of the condition that $y = 0$ along these lines at all times t, to the sum of the array of four equations discussed above, leads to

$$\mathbf{y} = \mathbf{Y} \sin k_x x \sin k_z z \, e^{j\omega t} \tag{4.4c}$$

where $\mathbf{Y}$ is the maximum amplitude of transverse displacement, and

$$k_x = \frac{n_x \pi}{l_x} \qquad n_x = 1, 2, 3, \cdots \tag{4.4d}$$

$$k_z = \frac{n_z \pi}{l_z} \qquad n_z = 1, 2, 3, \cdots \tag{4.4e}$$

These two equations are seen to limit the *component* wavelength constants k_x and k_z to the same discrete set of integral values, as does equation 2.14 for the single wavelength constant k of a stretched string. This limitation, in turn, restricts the characteristic frequencies for the allowed modes of free vibration, as given by equation 4.4*b*, to

$$f = \frac{\omega}{2\pi} = \frac{c}{2}\sqrt{\left(\frac{n_x}{l_x}\right)^2 + \left(\frac{n_z}{l_z}\right)^2} \tag{4.4f}$$

The fundamental frequency is obtained by substitution of $n_x = 1$ and $n_z = 1$ into equation 4.4*f*. Those overtones corresponding to $n_x = n_z$ will be harmonics of the fundamental, while those for which $n_x \neq n_z$ will not be harmonics of the fundamental. Figure 4.2 illustrates a number of the possible modes for a rectangular membrane. The light areas vibrate 180° out of time phase with the shaded areas. Since the nodal lines are lines of zero displacement, it is possible to insert rigid supports along any of them without affecting the nodal pattern for the particular frequency involved.

4.3 Wave Equation for a Circular Membrane. In solving the wave equation for transverse vibrations of a membrane, it is essential to utilize space coordinate systems in which the geometrical shape of the membrane's boundary can be simply expressed. Hence, as we have seen, the use of Cartesian coordinates facilitates the discussion of a rectangular membrane. Similarly, polar coordinates will facilitate the discussion of a circular membrane. Unfortunately, the available number of coordinate systems is strictly limited and, consequently, the number of solvable membrane problems is similarly limited.

Equation 4.2 may be expressed in a general form, appropriate to any coordinate system, as

$$\frac{\partial^2 y}{\partial t^2} = c^2 \nabla^2 y \tag{4.5}$$

in which the operation $(\partial^2/\partial x^2 + \partial^2/\partial z^2)$ has been replaced by its symbolic equivalent ∇^2, the two-dimensional Laplacian operator.

For a circular membrane having a fixed boundary of radius a, it is necessary to express the Laplacian operator in polar coordinates, r and θ, where $x = r\cos\theta$ and $z = r\sin\theta$. By partial differentiation with respect to r and θ, regarding r and θ as implicit functions of x and z, the Laplacian in polar coordinates is found to be

$$\nabla^2 = \frac{\partial^2}{\partial r^2} + \frac{1}{r}\frac{1}{\partial r} + \frac{1}{r^2}\frac{\partial^2}{\partial \theta^2} \tag{4.6}$$

A substitution of this relationship into equation 4.5 leads to

$$\frac{\partial^2 y}{\partial t^2} = c^2\left(\frac{\partial^2 y}{\partial r^2} + \frac{1}{r}\frac{\partial y}{\partial r} + \frac{1}{r^2}\frac{\partial^2 y}{\partial \theta^2}\right) \tag{4.5a}$$

as the most general wave equation appropriate for discussing transverse vibrations of a circular membrane. In almost all cases of practical importance in acoustics, the membrane vibrates with circular symmetry, i.e., $y = y(r, t)$ alone, and is independent of the azimuthal coordinate θ. In this case, equation 4.5*a* simplifies to

$$\frac{\partial^2 y}{\partial t^2} = c^2 \left(\frac{\partial^2 y}{\partial r^2} + \frac{1}{r}\frac{\partial y}{\partial r}\right) \tag{4.5b}$$

and only its solution will be discussed in detail.

4.4 Symmetrical Free Vibrations of a Circular Membrane. As with the transverse vibrations of a bar, the solution of equation 4.5*b* can most readily be obtained by assuming that the displacement may be expressed as the product of separable time and space dependent terms. Thus, for harmonic vibrations, let us assume that

$$\mathbf{y} = \boldsymbol{\psi} e^{j\omega t} \tag{4.7}$$

where $\boldsymbol{\psi} = \boldsymbol{\psi}(r)$ is a function of r only, and not a function of the time t. A substitution of equation 4.7 into equation 4.5*b* reduces the latter equation to

$$\frac{d^2\boldsymbol{\psi}}{dr^2} + \frac{1}{r}\frac{d\boldsymbol{\psi}}{dr} + k^2\boldsymbol{\psi} = 0 \tag{4.8}$$

where

$$k^2 = \frac{\omega^2}{c^2} = \frac{\sigma\omega^2}{T}$$

Equation 4.8 can be solved by assuming a series solution of the form

$$\boldsymbol{\psi} = \mathbf{a}_0 + \mathbf{a}_1 r + \mathbf{a}_2 r^2 + \mathbf{a}_3 r^3 + \mathbf{a}_4 r^4 + \cdots \tag{4.9}$$

Then

$$\frac{1}{r}\frac{d\boldsymbol{\psi}}{dr} = \frac{\mathbf{a}_1}{r} + 2\mathbf{a}_2 + 3\mathbf{a}_3 r + 4\mathbf{a}_4 r^2 + \cdots$$

and

$$\frac{d^2\boldsymbol{\psi}}{dr^2} = 2\mathbf{a}_2 + 3\cdot 2\mathbf{a}_3 r + 4\cdot 3\mathbf{a}_4 r^2 + \cdots$$

After substituting these expressions into equation 4.8 we obtain

$$0 = \frac{\mathbf{a}_1}{r} + (2\mathbf{a}_2 + 2\mathbf{a}_2 + k^2\mathbf{a}_0) + (3\cdot 2\mathbf{a}_3 + 3\mathbf{a}_3 + k^2\mathbf{a}_1)r + (4\cdot 3\mathbf{a}_4 + 4\mathbf{a}_4 + k^2\mathbf{a}_2)r^2 + \cdots$$

Since this summation must be zero for all values of r, each coefficient multiplying a particular power of r must be zero, and hence

$$\mathbf{a}_1 = 0 \quad \text{and} \quad 9\mathbf{a}_3 + k^2\mathbf{a}_1 = 0$$

so that $\mathbf{a}_3 = 0$. Similarly, all the remaining odd-numbered constants, $\mathbf{a}_5$,

$\mathbf{a}_7$, etc., may be shown to equal zero. However, in considering the even-numbered constants we see that

$$4\mathbf{a}_2 + k^2\mathbf{a}_0 = 0 \quad \text{so that} \quad \mathbf{a}_2 = -k^2\frac{\mathbf{a}_0}{2^2}$$

and

$$4^2\mathbf{a}_4 + k^2\mathbf{a}_2 = 0 \quad \text{so that} \quad \mathbf{a}_4 = -k^2\frac{\mathbf{a}_2}{4^2} = \frac{k^4\mathbf{a}_0}{2^2 \cdot 4^2}$$

Similarly,

$$\mathbf{a}_6 = -\frac{k^6\mathbf{a}_0}{2^2 \cdot 4^2 \cdot 6^2}, \text{ etc.}$$

Hence the series solution of equation 4.8 is

$$\psi = \mathbf{a}_0\left[1 - \frac{(kr)^2}{2^2} + \frac{(kr)^4}{2^2 \cdot 4^2} - \frac{(kr)^6}{2^2 \cdot 4^2 \cdot 6^2} + \cdots\right] \tag{4.10}$$

The series included in brackets is the well-known *Bessel function* of the first kind and of zero order, which is customarily written as $J_0(kr)$. Values of the J_0 function, together with values of other useful Bessel functions, are given in Table III in the appendix, and a graph of $J_0(x)$ is shown in Fig. 4.3.

The function

$$\psi = \mathbf{A}J_0(kr) \tag{4.11}$$

is not the complete solution of equation 4.8, for, since the latter is a second-order differential equation, its complete solution must contain two arbitrary constants. It can be shown that there is another solution, $\psi = \mathbf{B}N_0(kr)$, where $N_0(kr)$ is one of the Bessel functions of the second kind and zero order. However, $N_0(kr)$ becomes infinite for $r = 0$ and hence does not satisfy the limitation of small displacements unless $\mathbf{B} = 0$.

4.5 Bessel's Equation. Equation 4.8 is a particular form of Bessel's differential equation

$$\frac{d^2y}{dx^2} + \frac{1}{x}\frac{dy}{dx} + \left(1 - \frac{m^2}{x^2}\right)y = 0 \tag{4.12}$$

Equation 4.12 becomes identical with equation 4.8 if y is replaced by ψ, x is replaced by kr, and m is set equal to zero.

If, in equation 4.12, m is an integer other than zero, the solution is another Bessel function, known as a function of the first kind and of order m, and is represented by $J_m(x)$. The $J_1(x)$ and $J_2(x)$ functions are the only higher order functions that we will use and are plotted along with $J_0(x)$ in Fig. 4.3. It will be observed that the J_0 Bessel function resembles a damped cosine function, whereas the J_1 and J_2 functions resemble a damped sine function.

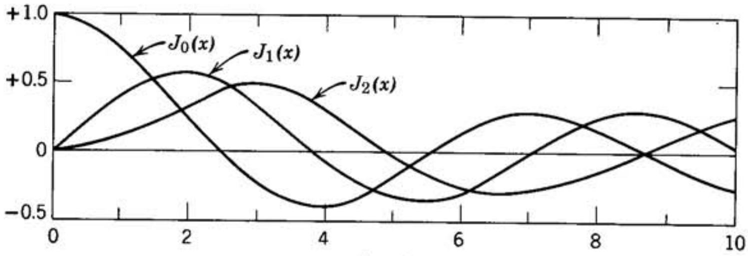

Fig. 4.3. Bessel functions, $J_0(x)$, $J_1(x)$, and $J_2(x)$.

The values of x for which the J_0 function is zero are

$$x = 2.405,\ 5.520,\ 8.654,\ 11.792, \cdots$$

which may be written as

$$x = 0.766\pi,\ 1.757\pi,\ 2.754\pi,\ 3.754\pi, \cdots$$

or approximately

$$x = (n - \tfrac{1}{4})\pi \qquad n = 1, 2, 3, \cdots$$

with the approximation becoming better as the magnitude of x increases.

Some useful relationships and properties of Bessel functions are given in Table 4.1. For proof the reader is referred to any textbook on Bessel functions.

Table 4.1 Properties of Bessel functions

$$J_0(x) \to 1 - \frac{x^2}{4}, \text{ as } x \to 0$$

$$J_1(x) \to \frac{x}{2}\left(1 - \frac{x^2}{8}\right), \text{ as } x \to 0$$

$$J_0(x) \to \sqrt{\frac{2}{\pi x}} \cos\left(x - \frac{\pi}{4}\right), \text{ as } x \to \infty$$

$$J_1(x) \to \sqrt{\frac{2}{\pi x}} \sin\left(x - \frac{\pi}{4}\right), \text{ as } x \to \infty$$

$$\int x J_0(x)\, dx = x J_1(x)$$

$$\int x J_0^2(x)\, dx = \frac{x^2}{2}[J_0^2(x) + J_1^2(x)]$$

$$\int J_1(x)\, dx = -J_0(x)$$

$$J_0(x) + J_2(x) = \frac{2}{x} J_1(x)$$

4.6 Boundary Conditions. The boundary condition at the edge of a circular membrane is $y = 0$ at $r = a$, so that $J_0(ka) = 0$, and hence

$$ka = 2.405,\ 5.520,\ 8.654,\ 11.792,\ \cdots \tag{4.13}$$

The fundamental frequency is therefore

$$f_1 = \frac{\omega_1}{2\pi} = \frac{k_1 c}{2\pi} = \frac{2.405}{2\pi a} c = \frac{2.405}{2\pi a}\sqrt{\frac{T}{\sigma}} \tag{4.14}$$

The ratios of the overtone to fundamental frequencies are

$$f_2 = \frac{5.520}{2.405} f_1 = 2.295 f_1 \tag{4.14a}$$

$$f_3 = 3.598 f_1$$

$$f_4 = 4.90 f_1$$

Etc.

As in the case of the transverse vibrations of a bar, the overtones are not harmonics of the fundamental.

Taking the real part of $\mathbf{y}_1 = \mathbf{A}_1 J_0(k_1 r) e^{j\omega_1 t}$, we obtain the general expression for the displacement of the membrane when it is vibrating in its fundamental mode:

$$y_1 = A_1 \cos(\omega_1 t + \phi_1) J_0\left(\frac{2.405 r}{a}\right) \tag{4.15}$$

where A_1 is the displacement amplitude at the center of the membrane and k_1 has been replaced by $2.405/a$. The complete solution is

$$y = \sum A_n \cos(\omega_n t + \phi_n) J_0(k_n r) \tag{4.16}$$

For all modes of vibration other than the fundamental, inner nodal circles will occur at those radial distances for which $J_0(k_n r)$ vanishes. Considering, for example, the first overtone, the J_0 function is zero for

$$k_2 r = \frac{5.520}{a} r = 2.405$$

or

$$r = 0.436a$$

An inspection of the $J_0(x)$ function of Fig. 4.3 shows that the displacements of the segments of the membrane immediately inside and outside of a nodal circle are always in phase opposition. When the central part is displaced up, the adjacent ring is displaced down, and vice versa. Consequently, a membrane vibrating at frequencies other than its fundamental produces little net displacement of the surrounding air. For this reason, the vibrating drumhead of a kettledrum has a low efficiency of sound production for its overtone frequencies.

The *average* amplitude of displacement of the surface of the membrane provides one parameter for judging the efficiency of sound production for each particular mode of vibration. It may be defined as

$$\bar{\psi}_n = \frac{\int_s \psi_n(r)\, dS}{\pi a^2} \tag{4.17}$$

Since all parts of a ring-shaped surface element, $dS = 2\pi r\, dr$, contained between r and $r + dr$, have the same displacement amplitude ψ_n, it is possible to carry out the indicated surface integration by merely integrating over r from 0 to a. Then

$$\bar{\psi}_n = \frac{\int_0^a A_n J_0(k_n r) \cdot 2\pi r\, dr}{\pi a^2}$$

which upon integration (see Table 4.1) becomes

$$\bar{\psi}_n = \frac{2A_n}{k_n a} J_1(k_n a) \tag{4.18}$$

As an example, let us determine the value of $\bar{\psi}_1$ for the fundamental mode of vibration.

$$\bar{\psi}_1 = \frac{2A_1}{k_1 a} J_1(k_1 a) = \frac{2A_1}{2.405} J_1(2.405) = 0.432A_1$$

Consequently, a rigid flat piston of radius a and displacement amplitude $0.432A_1$, will displace the same volume of air as will the membrane when vibrating at its fundamental frequency. Similarly, the reader may show that $\bar{\psi}_2 = -0.123A_2$, where the negative sign indicates that the average displacement amplitude is oppositely directed to the displacement at the center. These examples show that when the displacement amplitudes at the center are equal, i.e., $A_1 = A_2$, the fundamental mode of vibration is more than three times as effective for displacing air as is the first overtone.

In many problems encountered in the study of sources of sound waves, the characteristics of the sound wave are found to depend on the amount of air displaced, i.e., the volume displacement amplitude, and not on the exact shape of the moving surface. The radiating source may then be replaced by an *equivalent simple piston*, such that the product of its area, S_{eq}, and displacement amplitude, ξ_{eq}, equals the volume displacement amplitude of the true source. The volume displacement amplitude of a simple piston which is equivalent to the above membrane is therefore

$$S_{eq}\xi_{eq} = 0.432A_1\pi a^2$$

Real membranes do not vibrate with each mode having constant amplitude A_n such as is indicated by equation 4.16. The effect of damping forces, such as those arising within the membrane from internal frictional forces as well as external forces associated with the radiation of energy in the form of sound waves, causes the amplitude of each mode to decrease exponentially as $e^{-\alpha_n t}$. This decrease may be derived in a manner similar to that used in Sect. 1.13 for a simple oscillator. In general, the damping constant α_n increases with frequency so that the higher frequencies damp out more quickly than does the fundamental.

4.7 The Kettledrum. The resistive damping force just mentioned is but one of a number of forces that may act upon the surface of a membrane and influence its vibration. Another is that caused by changes in pressure occurring within a closed space behind the drumhead of a drum or the diaphragm of a condenser microphone as the volume of the entrapped gas is altered by vibration of the membrane. As an example, consider a kettledrum, which consists of a membrane stretched tightly over the open end of a hemispherical vessel. As the drumhead vibrates, the air in the vessel is alternately compressed and expanded. If the radial velocity of transverse waves along the membrane is considerably less than the speed of sound in air, the pressure resulting from the compression and expansion of the air in the vessel is nearly uniform over the entire extent of the membrane, i.e., it is not a function of radial position and depends only on the average displacement $\bar{y}$.

When the surface of the membrane is displaced an average amount $\bar{y}$, the increment in volume of the enclosed air is $dV = \pi a^2\bar{y}$, where a is the radius of the drumhead. If the equilibrium volume inside the vessel is V_0 and the equilibrium pressure is P_0, then, assuming that the alternations of volume are *adiabatic*, the new pressures P and volumes V are related by the equation

$$PV^\gamma = P_0V_0^\gamma = \text{constant} \tag{4.19}$$

where γ here represents the ratio of the specific heat of the entrapped air at constant pressure to its specific heat at constant volume. By differentiation of this equation it is possible to show that the excess pressure dP inside the vessel will be

$$dP = -\frac{\gamma P_0}{V_0}dV = -\frac{\gamma P_0}{V_0}\pi a^2\bar{y} \tag{4.20}$$

The introduction of a force given by equation 4.20 as acting upon each square meter of surface area of the membrane modifies equation 4.5*b*, which now becomes

$$\frac{\partial^2 y}{\partial t^2} + \frac{\gamma P_0}{\sigma V_0}\pi a^2 \bar{y} = c^2 \nabla_r{}^2 y \tag{4.21}$$

where for the sake of brevity, the symbol $\nabla_r{}^2$ has replaced the operation $(\partial^2/\partial r^2 + \partial/r\partial r)$, the form the two-dimensional Laplacian operator assumes in polar coordinates for a function having circular symmetry.

In this equation $\bar{y}$ is an integral function of all the allowed modes of vibration, including their relative amplitudes and phases (equation 4.16), and a general solution of equation 4.21 is consequently too involved to be considered. However, if only one mode of vibration is present, the solution of equation 4.21 is greatly simplified.

If only one frequency ω is present, we may assume a solution of the form

$$\mathbf{y} = \psi e^{j\omega t}$$

where, as previously, ψ is a function of r only. Then equation 4.21 becomes

$$\frac{d^2\psi}{dr^2} + \frac{1}{r}\frac{d\psi}{dr} + k^2\psi = \frac{\gamma P_0}{TV_0}\int_0^a \psi 2\pi r\, dr \tag{4.22}$$

To solve this differential equation we shall assume that it is satisfied by a function of the form

$$\psi = \mathbf{A}[J_0(kr) - J_0(ka)] \tag{4.23}$$

A solution of this type is suggested by the fact that, if the right-hand integral term of equation 4.22 were not present, the resulting solution would involve $J_0(kr)$, whereas the presence of this integral term involving the radius a may be expected to introduce some function of a, such as $J_0(ka)$, as an additional term in the solution. The assumed solution has the further desirable property of satisfying the boundary condition that $\psi = 0$ when $r = a$, regardless of the particular value assigned to k.

With this assumption, the right-hand term of equation 4.22 may be integrated and beomes

$$\frac{2\pi\gamma P_0}{TV_0}\mathbf{A}\left[\frac{rJ_1(kr)}{k} - \frac{r^2}{2}J_0(ka)\right]_0^a$$
$$= \frac{\pi a^2\gamma P_0}{TV_0}\mathbf{A}\left[\frac{2J_1(ka)}{ka} - J_0(ka)\right] = \frac{\pi a^2\gamma P_0}{TV_0}\mathbf{A}J_2(ka) \tag{4.24}$$

where $J_2(ka)$ is a second-order Bessel function of the first kind.

Direct substitution of equation 4.23 into equation 4.22 then shows that the assumed solution (equation 4.23) is an allowed solution, provided that

$$-k^2 J_0(ka) = \frac{\pi a^2 \gamma P_0}{T V_0} J_2(ka)$$

or

$$J_0(ka) = -\alpha \frac{J_2(ka)}{(ka)^2} \tag{4.25}$$

where

$$\alpha = \frac{\pi a^4 \gamma P_0}{T V_0}$$

is a nondimensional constant measuring the relative importance of the restoring forces, owing to the compression of the air in the vessel and to the tension applied to the membrane. This constant α is small if either the volume of the vessel or the tension in the membrane is large. In the limit, where this constant approaches zero, the allowed frequencies are those corresponding to $J_0(ka) = 0$, as previously determined for free vibrations of the membrane.

Table 4.2 Frequencies of a kettledrum

α	k_1a	k_2a	k_3a
0	2.405	5.520	8.654
1	2.545	5.54	8.657
2	2.68	5.55	8.660
5	3.02	5.59	8.67
10	3.485	5.67	8.69

Table 4.2 lists the values of ka satisfying equation 4.25 for selected values of α ranging from 0 to 10. It will be seen that the presence of the vessel has raised the numerical magnitudes of the allowed values of ka, and consequently those of the allowed frequencies. This is to be expected, since the additional term in equation 4.21 is proportional to the displacement and is therefore one of stiffness. It is also to be noted that the effect on the fundamental frequency is much more pronounced than it is on the other modes of vibration. This is also to be expected, since the average displacement amplitude becomes smaller and smaller as the membrane vibrates in higher modes and consequently in a greater number of oppositely phased segments.

4.8 Forced Vibrations of a Membrane. Let us next consider a circular membrane that is acted upon by a sinusoidal driving force. Assume that the membrane is of the ideal type defined in Sect. 4.3 and that the pressure exerted by the driving force is uniformly distributed over one side only. Then this pressure is $p = P \cos \omega t$, or in complex notation,

$$\mathbf{p} = Pe^{j\omega t} \tag{4.26}$$

and the equation of motion becomes

$$\frac{\partial^2 \mathbf{y}}{\partial t^2} = c^2 \nabla_r^{\ 2} \mathbf{y} + \frac{P}{\sigma} e^{j\omega t} \tag{4.27}$$

If we assume a steady-state solution of the form

$$\mathbf{y} = \boldsymbol{\psi} e^{j\omega t} \tag{4.28}$$

then

$$\nabla_r^{\ 2} \boldsymbol{\psi} + k^2 \boldsymbol{\psi} = -\frac{P}{\sigma c^2} = -\frac{P}{T} \tag{4.29}$$

where

$$k = \frac{\omega}{c}$$

It should be noted that for the driven membrane, the frequency ω and the wavelength constant k may have any value, depending on the driving frequency, and are not restricted to the discrete sets of values discussed in preceding sections for free vibrations.

The complete solution of equation 4.29 is the sum of two terms, one being the general solution of the equation $\nabla^2 \boldsymbol{\psi} + k^2 \boldsymbol{\psi} = 0$ and the other being the particular solution

$$\boldsymbol{\psi} = -\frac{P}{k^2 T}$$

Then

$$\boldsymbol{\psi} = \mathbf{A} J_0(kr) - \frac{P}{k^2 T} \tag{4.30}$$

Application of the boundary condition that $\boldsymbol{\psi} = 0$ when $r = a$ gives for the constant $\mathbf{A}$

$$\mathbf{A} = \frac{P}{k^2 T} \cdot \frac{1}{J_0(ka)} \tag{4.31}$$

Substituting these respective expressions into equation 4.28, the assumed equation for the displacement of the membrane then becomes

$$\mathbf{y} = \frac{P}{k^2 T} \left[\frac{J_0(kr)}{J_0(ka)} - 1 \right] e^{j\omega t} \tag{4.32}$$

Correspondingly, the amplitude of displacement at any coordinate position on the membrane is given by

$$\psi = \frac{P}{T}\left[\frac{J_0(kr) - J_0(ka)}{k^2 J_0(ka)}\right] \tag{4.33}$$

An inspection of this equation shows that the amplitude of the displacement is directly proportional to that of the driving force and is inversely proportional to the tension T. The dependence of amplitude of vibration, at any coordinate position, on frequency is given by the relatively complicated expression within the square bracket of equation 4.33. Whenever the driving frequency ω corresponds to any of the free oscillation frequencies of equation 4.14 or 4.14*a*, the function $J_0(ka) = 0$, so that an infinite amplitude is indicated. However, in all practical cases there are damping forces, which may be represented in equation 4.27 by a term of the type $-(R/\sigma)(\partial y/\partial t)$, and which limit the amplitudes at these frequencies to finite maximum values.

The most important practical application of a driven membrane is that of the circular diaphragm of a condenser microphone. Here the incident sound wave, acting upon a tightly stretched metallic membrane placed above a metal plate, produces an approximately uniform driving force. As the membrane is displaced, the electrical capacitance between the membrane and the adjacent plate is varied in such a manner as to generate an output voltage which is a linear function of the average displacement of the membrane. The constructional details of this microphone, together with the schematic of its associated electrical circuit, will be considered in Chapter 11.

The average displacement of the driven membrane is

$$\bar{y} = \frac{e^{j\omega t}\int_0^a \frac{P}{k^2 T}\left[\frac{J_0(kr)}{J_0(ka)} - 1\right]2\pi r\,dr}{\pi a^2} = \frac{P}{k^2 T}\frac{J_2(ka)}{J_0(ka)}e^{j\omega t} \tag{4.33}$$

At low frequencies, such that ka is smaller than unity,

$$J_0(ka) \approx 1 - \frac{(ka)^2}{4}$$

and

$$J_2(ka) \approx \frac{(ka)^2}{8}\left[1 - \frac{(ka)^2}{12}\right]$$

giving

$$\frac{J_2(ka)}{J_0(ka)} \approx \frac{(ka)^2}{8}\left[1 + \frac{(ka)^2}{6}\right]$$

Substitution of this expression into equation 4.33 gives for the average displacement at low frequencies

$$\bar{\mathbf{y}} \approx \frac{Pa^2}{8T}\left[1 + \frac{(ka)^2}{6}\right]e^{j\omega t} \tag{4.34}$$

Therefore, as long as the driving frequency is low enough so that ka is smaller than unity, the output of a condenser microphone is nearly independent of frequency. In this frequency range there are also no resonance difficulties, which first arise when $ka = 2.405$. Replacing k by

$$k = \frac{2\pi f}{c} = \frac{2\pi f}{\sqrt{T/\sigma}}$$

and assuming that the limiting frequency of uniform response of an ideal condenser microphone is given by $ka < 1$, then

$$f < \frac{1}{2\pi a}\sqrt{\frac{T}{\sigma}} \tag{4.35}$$

This upper frequency limit may be increased either by increasing the tension T or by decreasing the radius a. Excellent small condenser microphones having uniform output over a wide range of frequencies have been produced. However, it should be noted that either an increase in T or a decrease in a reduces the amplitude of the average displacement $\bar{y}$ and, consequently, the voltage output of the microphone.

If a damping force $-(R/\sigma)(\partial y/\partial t)$ is introduced into equation 4.27, the resulting solution for the displacement $\mathbf{y}$ is identical in form with equation 4.32. However, in this case $k \neq \omega/c$, but is instead given by

$$k^2 = \frac{\sigma\omega^2 - j\omega R}{T} \tag{4.36}$$

It can be shown that the presence of the term $-j\omega R/T$ in this expression reduces the average displacement at resonance to a finite value.[1] By a proper choice of damping resistance it is possible to take advantage of this reduction in the amplitude near resonance so as to extend the range of fairly uniform output up to, and somewhat beyond, the first resonance frequency. Commercial microphones are available in which this method of extending the frequency range is actually employed.

A response curve showing the average displacement amplitude $\bar{\mathbf{\Psi}}$ of a driven membrane without dissipation as computed by means of equation 4.33 is given in Fig. 4.4. It will be noted that the amplitude becomes infinite for $ka = 2.405$. The graph also gives a typical curve illustrating

[1] Morse, *Vibration and Sound*, pp. 200–203, McGraw-Hill Book Co., (1948).

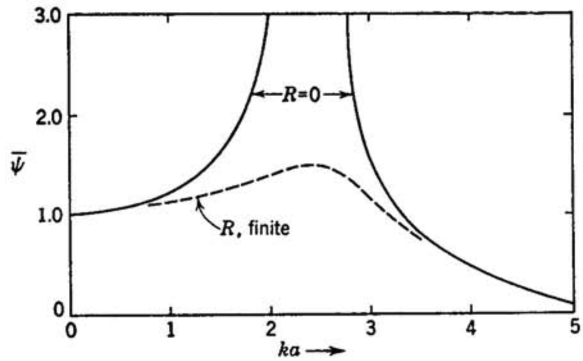

Fig. 4.4. Average displacement response $\bar{\psi}$ of a driven membrane as a function of frequency.

the reduction in amplitude resulting from the presence of a damping force. Both these curves indicate zero response at the frequency for which $ka = 5.136$, the value making $J_2(ka) = 0$. At a frequency about 60 per cent above the first resonance frequency a circular nodal line appears at the outer edge of the membrane, and as the frequency is further increased this line shrinks towards the center. The displacement of the central part of the membrane is out of phase with the driving force, while that of the outer part is in phase, so that as the driving frequency increases and the nodal circle shrinks there is an increasing tendency for the average displacement of the two zones to cancel each other. When $ka = 5.136$ there is complete cancellation, so that the average displacement, and hence the output, is zero.

4.9 Asymmetrical Free Vibrations of a Circular Membrane. When the drumhead of a drum is set into vibration by being struck at its center, the resulting vibration is a superposition of the various symmetrical modes as given by equation 4.16. By contrast, when it is struck off center, asymmetrical modes of vibration are excited in which $y = y(r, \theta, t)$. In order to solve equation 4.5*a*, a general form of the two-dimensional wave equation appropriate to this situation, let us assume that its harmonic solution may be expressed as

$$\mathbf{y} = \boldsymbol{\psi}(r) \cdot \boldsymbol{\theta}(\theta) \cdot e^{j\omega t} \tag{4.37}$$

which is the product of three terms, each a function of only one variable.

Upon making this substitution, equation 4.5*a* becomes

$$\boldsymbol{\theta} \frac{d^2\boldsymbol{\psi}}{dr^2} + \frac{\boldsymbol{\theta}}{r} \frac{d\boldsymbol{\psi}}{dr} + k^2\boldsymbol{\psi}\boldsymbol{\theta} + \frac{\boldsymbol{\psi}}{r^2} \frac{d^2\boldsymbol{\theta}}{d\theta^2} = 0 \tag{4.38}$$

Next, multiply each term in this equation by $r^2/\boldsymbol{\theta}\boldsymbol{\psi}$ and move terms containing r to one side of the equality sign and those containing θ to the other. The result is

$$\frac{r^2}{\boldsymbol{\psi}}\left(\frac{d^2\boldsymbol{\psi}}{dr^2} + \frac{1}{r}\frac{d\boldsymbol{\psi}}{dr}\right) + k^2r^2 = -\frac{1}{\boldsymbol{\theta}}\frac{d^2\boldsymbol{\theta}}{d\theta^2} \tag{4.38a}$$

The left-hand side of this equation, a function of r alone, cannot be equal to the right-hand side, a function of θ alone, if both functions really vary with r and θ. Consequently, both sides of equation 4.38a must separately be equal to some constant. If we let this constant be m^2, then the right-hand side becomes

$$\frac{d^2\boldsymbol{\theta}}{d\theta^2} = -m^2\boldsymbol{\theta} \tag{4.39}$$

having a harmonic solution of the type

$$\boldsymbol{\theta} = \mathbf{A}e^{jm\theta} \tag{4.39a}$$

The azimuthal coordinate θ is a periodic one, repeating itself after 2π, 4π, etc. Consequently, if the displacement y is to be a single valued function of position, then $y(r, \theta, t)$ must equal $y(r, \theta + 2\pi, t)$, which in turn restricts the constant m of equation 4.39a to integral values ($m = 0, 1, 2, 3, \cdots$).

The reader may show that, when the left-hand side of equation 4.38a is equated to m^2, it takes on the form of Bessel's differential equation (4.12) and has solutions of the type

$$\boldsymbol{\psi} = \mathbf{A}J_m(kr) \tag{4.40}$$

The complete harmonic solution for y in complex form is, therefore,

$$\mathbf{y} = \mathbf{A}J_m(kr)e^{jm\theta}e^{j\omega t} \tag{4.41}$$

or in equivalent analytical form

$$y = AJ_m(kr)\cos m(\theta - \alpha)\cos(\omega t + \phi) \tag{4.42}$$

The azimuthal phase angle α present in equation 4.42 is one of the arbitrary constants of the solution. For each value of m it determines those directions θ along which radial nodal lines of zero displacement will appear and in its turn depends on the azimuthal angle at which the membrane is initially excited.

Figure 4.5 illustrates a number of the simpler modes of vibration corresponding to equation 4.42 with $\alpha = 0$. In designating these modes of free vibration, the integer m determines the number of radial nodal lines while the integer n determines the number of azimuthal nodal circles. It

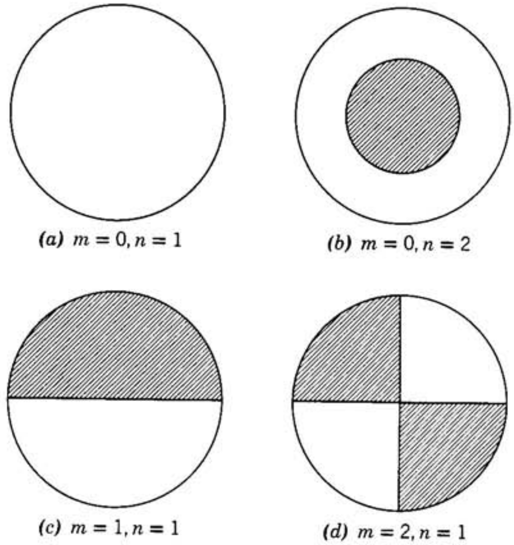

Fig. 4.5. Vibration modes of a circular membrane.

should be noted that $n = 1$ is the minimum value of n and corresponds to a mode of vibration in which the azimuthal nodal circle occurs only at the boundary of the membrane where $r = a$.

For each integral value of m there exists a whole sequence of allowed radial modes of vibration of increasing frequency. When $m = 0$, the allowed frequencies are those previously given for this symmetrical case by equations 4.14 and 4.14*a* and correspond to the condition that $J_0(ka) = 0$. For $m = 1$, the sequence of allowed frequencies is determined by $J_1(ka) = 0$, for $m = 2$ by $J_2(ka) = 0$, etc. Table 4.3 contains a few of these frequencies f_{mn}, expressed relative to the fundamental frequency f_{01} as given by equation 4.14. It is to be noted that none of the overtone modes are harmonics of the fundamental.

Table 4.3 Relative frequencies of a circular membrane

$f_{01} = 1.0$	$f_{11} = 1.593$	$f_{21} = 2.135$
$f_{02} = 2.295$	$f_{12} = 2.917$	$f_{22} = 3.500$
$f_{03} = 3.598$	$f_{13} = 4.230$	$f_{23} = 4.832$

The mathematical technique used in this section in solving equation 4.5*a* is generally referred to as the method of "separation of variables." It could equally well have been utilized in obtaining equation 4.4*c* for the square membrane.[1]

[1] Morse, *Vibration and Sound*, p. 179, McGraw-Hill Book Co., (1948).

4.10 Vibration of Thin Plates. The essential difference between the vibrations of a membrane and a thin plate is that in a membrane the restoring force is due entirely to the tension applied to the membrane, whereas in a thin plate the restoring force is due entirely to the stiffness of the diaphragm, no tension being applied. This same difference exists between the transverse restoring forces in strings and bars.

Our analysis of the plate will be limited to the symmetrical vibrations of a uniform circular diaphragm. Since a rigorous development of the equation of motion applicable to this case is too involved to be given here, the resulting equation will merely be written down and will then be justified by analogy with the equations for bars and membranes. This equation is

$$\frac{\partial^2 y}{\partial t^2} = -\frac{\kappa^2 Y}{\rho(1-\sigma^2)}\nabla_r^{\,4} y \tag{4.43}$$

where ρ is the volume density of the material in kilograms per cubic meter, σ is its Poisson's ratio, Y is Young's modulus, and κ is a surface radius of gyration. For a plate of uniform thickness t, $\kappa = t/\sqrt{12}$.

Since the restoring force acting upon a circular plate depends on its elastic resistance to bending we would expect the coefficient of the right-hand term in the above differential equation to be similar to that for the transverse vibration of a bar (equation 3.35); i.e., it would be of the form $-\kappa^2 Y/\rho$. This assumption is not strictly correct, for in a broad sheet there is a tendency for the sheet to curl up sidewise when it is bent down lengthwise. This curling results from the lateral expansion that accompanies a longitudinal compression and produces an increase in the effective stiffness of the sheet. The negative ratio of the lateral strain $\partial\zeta/\partial z$ which accompanies a longitudinal strain $\partial\xi/\partial x$ is known as Poisson's ratio σ, or

$$\sigma = -\frac{\partial\zeta/\partial z}{\partial\xi/\partial x} \tag{4.44}$$

Since a positive longitudinal strain of tension is always accompanied by a negative lateral strain of compression, the negative ratio is required to ensure that σ be a positive number. Values of Poisson's ratio for a number of solid materials are given in Table I in the appendix. It will be seen that σ is approximately equal to 0.3 for most materials. The effective increase in stiffness of the sheet resulting from the curling corresponds to the factor $1/(1 - \sigma^2)$, so that the coefficient of the right-hand term is actually as given in equation 4.43.

For a circular plate one would expect the differential portion of the right-hand term of equation 4.43 to involve partial derivatives of the fourth order, as for the transverse vibration of a bar, but to be in polar form, as for the vibration of a membrane. This is seen to be true, since the differential member of equation 4.43 is $\nabla_r^4 y$.

4.11 Simple Harmonic Vibrations. Let us assume periodic vibrations, such that **y** may be expressed as

$$\mathbf{y} = \boldsymbol{\psi} e^{j\omega t} \tag{4.45}$$

where $\boldsymbol{\psi}$ is a function of r, and not of t. Then equation 4.43 reduces to

$$\nabla_r^4 \boldsymbol{\psi} = \frac{\omega^2 \rho (1 - \sigma^2)}{\kappa^2 Y} \boldsymbol{\psi} = K^4 \boldsymbol{\psi} \tag{4.46}$$

where

$$K^4 = \frac{\omega^2 \rho (1 - \sigma^2)}{\kappa^2 Y} \tag{4.47}$$

This differential equation may be expressed in the following operator form

$$(\nabla_r^4 - K^4)\boldsymbol{\psi} = 0 \tag{4.48}$$

The operator $(\nabla_r^4 - K^4)$ is of such a form that it may be split into two parts by a process similar to the factoring of an algebraic equation, giving

$$(\nabla_r^2 + K^2)(\nabla_r^2 - K^2)\boldsymbol{\psi} = 0 \tag{4.48a}$$

Therefore $\boldsymbol{\psi}$ can be a solution of either $(\nabla_r^2 + K^2)\boldsymbol{\psi} = 0$ or $(\nabla_r^2 - K^2)\boldsymbol{\psi} = 0$, and the complete solution of equation 4.46 is the sum of these two solutions.

The first of these equations is identical in form with equation 4.8, which was derived for a circular membrane, and its solution is therefore

$$\boldsymbol{\psi} = \mathbf{A} J_0(Kr) \tag{4.49}$$

The solution of the second equation is obtained from the first by replacing K by jK, and is therefore

$$\boldsymbol{\psi} = \mathbf{B} J_0(jKr) \tag{4.49a}$$

which is customarily written

$$\boldsymbol{\psi} = \mathbf{B} I_0(Kr) \tag{4.49b}$$

The introduction here of the so-called *hyperbolic Bessel functions*, whose independent variable has imaginary values, necessitates a brief discussion of their more important properties. They are not solutions of Bessel's equation, but rather of a related equation

$$\frac{d^2y}{dx^2} + \frac{1}{x}\frac{dy}{dx} - \left(1 + \frac{m^2}{x^2}\right)y = 0$$

They are defined in terms of the ordinary Bessel functions by the equation

$$I_m(x) = j^{-m} J_m(jx) \tag{4.50}$$

Hence

$$I_0(x) = J_0(jx) = 1 + \frac{x^2}{2^2} + \frac{x^4}{2^2 \cdot 4^2} + \frac{x^6}{2^2 \cdot 4^2 \cdot 6^2} + \cdots \tag{4.50a}$$

It should be noted that whereas $J_0(x)$ is an alternating function, $I_0(x)$ increases continuously with x, so that in contrast to $J_0(x)$, which resembles a damped cosine function, $I_0(x)$ resembles a hyperbolic cosine. Additional useful relationships include

$$\int x I_0(x)\, dx = x I_1(x) \tag{4.51}$$

$$\int I_1(x)\, dx = I_0(x) \tag{4.51a}$$

$$I_0(x) - I_2(x) = \frac{2}{x} I_1(x) \tag{4.51b}$$

Values of the functions I_0, I_1, and I_2 are given in Table III of the appendix.

The solution of equation 4.48 is

$$\psi = \mathbf{A} J_0(Kr) + \mathbf{B} I_0(Kr) \tag{4.52}$$

Since this equation contains only two, rather than four, arbitrary constants, it is not the complete solution of the differential equation, but the other two functions are ruled out by the requirement that the amplitude remain finite for $r = 0$.

4.12 Boundary Conditions. In order to evaluate the constants **A** and **B** we must know the manner in which the diaphragm is supported. The most common type of support is rigid clamping of the diaphragm all around its circumference, where $r = a$. This is equivalent to the conditions

$$\psi = 0 \quad \text{and} \quad \frac{\partial \psi}{\partial r} = 0 \tag{4.53}$$

For $r = a$ the first of these conditions gives the relation

$$0 = \mathbf{A} J_0(Ka) + \mathbf{B} I_0(Ka) \tag{4.54}$$

and the second is satisfied if

$$0 = -\mathbf{A} K J_1(Ka) + \mathbf{B} K I_1(Ka) \tag{4.55}$$

since

$$\frac{dJ_0(Kr)}{dr} = -KJ_1(Kr)$$

and

$$\frac{dI_0(Kr)}{dr} = KI_1(Kr)$$

Rewriting these two boundary conditions as

$$\mathbf{A}J_0(Ka) = -\mathbf{B}I_0(Ka)$$

and

$$\mathbf{A}J_1(Ka) = \mathbf{B}I_1(Ka)$$

and dividing one by the other gives

$$\frac{J_0(Ka)}{J_1(Ka)} = -\frac{I_0(Ka)}{I_1(Ka)} \tag{4.56}$$

as the condition that determines the allowed values of K.

Since both the I_0 and I_1 functions are positive for all values of Ka, solutions occur only when J_0 and J_1 are of opposite sign. From the tables of Bessel functions it can be seen that this equation is satisfied by

$$Ka = 3.20,\ 6.30,\ 9.44,\ 12.57,\ \cdots \tag{4.57}$$

or approximately by

$$Ka = n\pi \qquad n = 1, 2, 3, \cdots$$

with the approximation becoming increasingly better with increasing values of n.

From equation 4.47 it is evident that

$$\omega = \kappa K^2 \sqrt{\frac{Y}{\rho(1-\sigma^2)}}$$

and substituting $3.20/a$ for K, the fundamental frequency is given by

$$f_1 = \frac{\omega_1}{2\pi} = \frac{3.2^2}{2\pi a^2}\frac{t}{\sqrt{12}}\sqrt{\frac{Y}{\rho(1-\sigma^2)}} = 0.47\,\frac{t}{a^2}\sqrt{\frac{Y}{\rho(1-\sigma^2)}} \tag{4.58}$$

where t is the thickness of the diaphragm. The frequencies of the other modes of allowed vibration are not harmonics of the fundamental and are given by

$$f_2 = \left(\frac{6.3}{3.2}\right)^2 f_1 = 3.88 f_1$$

$$f_3 = 8.70 f_1$$

Etc.

It will be observed that the allowed frequencies are spread much farther apart than are those of the circular membrane.

The actual displacement of a thin circular plate, vibrating in its fundamental mode, is

$$y_1 = \cos(\omega_1 t + \phi_1)\left[A_1 J_0\left(\frac{3.2}{a}r\right) + B_1 I_0\left(\frac{3.2}{a}r\right)\right] \tag{4.59}$$

However, the boundary condition (equation 4.54) may be expressed as

$$B_1 = -A_1\frac{J_0(K_1 a)}{I_0(K_1 a)} = -A_1\frac{J_0(3.2)}{I_0(3.2)} = +0.0555A_1 \tag{4.60}$$

and therefore

$$y_1 = A_1\cos(\omega_1 t + \phi_1)\left[J_0\left(\frac{3.2}{a}r\right) + 0.0555 I_0\left(\frac{3.2}{a}r\right)\right] \tag{4.61}$$

It is to be noted that the amplitude at the center is not A_1, but is instead $1.0555A_1$.

A comparison of the shape function

$$J_0\left(\frac{3.2}{a}r\right) + 0.0555 I_0\left(\frac{3.2}{a}r\right)$$

for a thin circular plate vibrating in its fundamental mode, with the corresponding shape function

$$J_0\left(\frac{2.405}{a}r\right)$$

for a membrane, shows that the relative displacement of the plate near its edge is much smaller than that of a similar membrane. Consequently, we should expect the ratio of its average amplitude to the amplitude at the center to be less than for the membrane. This can be shown by using equation 4.17 which gives for the average displacement amplitude

$$\bar{\Psi}_1 = 0.326A_1 = 0.309y_0 \tag{4.62}$$

where $y_0 = 1.0555A_1$ is the amplitude at the center of the plate. The circular plate may therefore be replaced by an equivalent flat piston such that

$$S_{\text{eq}}\xi_{\text{eq}} = 0.309y_0\pi a^2 \tag{4.63}$$

4.13 Loaded and Driven Plates. The treatment of loaded and driven plates is analogous to that of membranes, and the response curves for a uniform driving force are similar to those shown in Fig. 4.4 with large amplitudes occurring at the fundamental resonance frequency unless there is a considerable damping force. Condenser microphones may be constructed with a thin circular plate instead of a stretched membrane. However, it is difficult to design a vibrating-plate type of microphone having adequate sensitivity and at the same time a sufficiently high resonant frequency. For this reason membranes are used in most condenser microphones, although plate diaphragms have been successful in miniature condenser microphones.

The most important utilization of the vibrating thin plate is in the diaphragms of ordinary telephone microphones and receivers. Although the response of these devices is not uniform over a wide range of frequencies, they give adequate intelligibility and are simple and rugged in their construction. Another application is that in sonar transducers used for producing sounds in water at frequencies below 1000 cycles/sec, in which sound is generated by the motion of relatively thin circular steel plates driven by alternations in the magnetic field of an adjacent electromagnet.

Whenever either a membrane or thin plate is vibrating, the surrounding fluid medium reacts upon it with a type of loading which is usually assumed to be some kind of mechanical impedance uniformly distributed over its surface. Such impedances consist both of resistive types which result in the dissipation of energy, primarily in the form of sound waves, and mass reactive types which lower the fundamental frequency of free vibration. Before we can discuss such effects in detail, we must next investigate some of the characteristics of sound waves in fluids and their reactions upon vibrating surfaces. After thoroughly investigating these phenomena, we shall, in Chapters 11 and 12, devoted respectively to microphones and sonar transducers, again consider the motions of circular membranes and plates.

PROBLEMS

4.1. Given a square membrane of width a to vibrate at its fundamental frequency with an amplitude A at its center. (*a*) Derive a general expression that gives its average displacement amplitude. (*b*) Derive a general expression for locating points on the membrane having an amplitude of 0.5 A. (*c*) Compute and plot a few points as given by the equation derived in part (*b*). Do they form a circle?

4.2. Given a rectangular membrane of width a and length b. If $b = 2a$, compute the ratio of each of the first four overtone frequencies relative to the fundamental frequency.

4.3. A membrane is made from material having a density of 1.0 kg/m^2 and is stretched to a linear tension of 1000 newtons/m. It is wished to have the membrane vibrate at a fundamental frequency of 250 cycles/sec. (*a*) If the membrane is square, what must be the length of a side? (*b*) If the membrane is circular, what must be its radius? (*c*) What are the frequencies of each of the first two overtones for the membranes of parts (*a*) and (*b*)?

4.4. Given a circular membrane to be acted upon uniformly over its surface by a damping force per unit area of $-(R\,\partial y/\partial t)$. Introduce this term into equation 4.5*b* in a manner consistent with the dimensions of the terms in the latter and solve the resulting equation so as to show that the amplitude of the resulting free vibrations are damped exponentially as $e^{-(Rt/2\sigma)}$.

4.5. Show that the total energy of a circular membrane when vibrating in its fundamental mode is given by $0.135\pi a^2\sigma\omega^2 A_1^2$, where a is its radius, σ the area density, ω the angular frequency of vibration, and A_1 the amplitude at its center.

4.6. A circular membrane of 1-cm radius and 0.2-kg/m² area density is stretched to a linear tension of 4000 newtons/m. When vibrating in its fundamental mode, the amplitude at the center is observed to be 0.01 cm. (*a*) What is its fundamental frequency? (*b*) What is the maximum volume of air displaced by the membrane?

4.7. A steel membrane of 0.02-m radius and 0.0001-m thickness is stretched to a tension of 20,000 newtons/m. (*a*) For circularly symmetrical vibration, what is the frequency of the second overtone mode? (*b*) What are the radii of the two nodal circles when the membrane is vibrating at the above frequency? (*c*) When the membrane is vibrating at the above frequency, the displacement amplitude at the center is observed to be 0.0001 m. What is the average displacement amplitude?

4.8. The maximum tensile stress that may be applied to aluminum is 2×10^8 newtons/m² and to steel is 10^9 newtons/m². (*a*) What is the maximum fundamental frequency of a stretched aluminum membrane of 0.01-m radius? (*b*) of a steel membrane of equal radius? (Note that for thin membranes these maximum frequencies are independent of the thickness.)

4.9. The diaphragm of a condenser microphone consists of a circular sheet of aluminum of 0.03-m diameter and 0.00002-m thickness. It may be stretched to a maximum tensile stress of 2×10^8 newtons/m². (*a*) What is the maximum tension T in newtons per meter to which this aluminum sheet may be stretched? (*b*) What will be its fundamental frequency when stretched to this tension? (*c*) What will be the displacement amplitude at its center when acted upon by a sound wave of 500 cycles/sec frequency having a pressure amplitude of 2.0 newtons/m²? (*d*) What will be the average displacement amplitude under these conditions?

4.10. If the volume of air trapped behind the diaphragm of the condenser microphone of Problem 4.9 is 3×10^{-7} m³, by what percentage will its fundamental frequency be raised? Assume $P_0 = 10^5$ newtons/m² and $\gamma = 1.4$.

4.11. The circular membrane of a kettledrum has a radius of 0.25 m, its area density is 1.0 kg/m², and it is stretched to a tension of 10,000 newtons/m. (*a*) What is its fundamental frequency without a backing vessel? (*b*) What is its fundamental frequency if the backing vessel is a hemispherical bowl of 0.25-m radius? Assume the backing vessel to be filled with air at a pressure of 10^5 newtons/m² having a ratio of specific heats of 1.4.

4.12. An undamped circular membrane of 0.02-m radius, having an area density of 1.5 kg/m² and stretched to a tension of 950 newtons/m, is driven by a pressure $6000 \cos \omega t$ newtons/m² acting uniformly over its surface. (*a*) Compute and plot the amplitude of the displacement at the center as a function of frequency in the interval from 0 to 1000 cycles/sec. (*b*) Compute and plot the shape of the membrane when driven at a frequency of 400 cycles/sec. (*c*) Repeat part (*b*) for a frequency of 1000 cycles/sec.

4.13. (*a*) Plot the amplitude of a driven membrane as a function of ka in the interval from $0 < ka < 2$ as computed from equation 4.33. (*b*) Similarly plot amplitudes as computed from the approximation equation 4.34. (*c*) What is the percentage of error of the latter equation at $ka = 1$? At $ka = 2$? (*d*) What is the frequency corresponding to $ka = 2$ for the membrane of Problem 4.12?

4.14. (*a*) Compute and plot the shape of the driven circular membrane when being driven at a frequency one-half of its fundamental frequency. (*b*) Similarly, compute and plot the shape of the membrane when being driven at twice its fundamental frequency.

4.15. A circular membrane of 0.25-m radius has an area density of 1.0 kg/m^2 and is stretched to a tension of 25,000 newtons/m. (*a*) Compute the four lowest frequencies of free vibration. (*b*) For each of these frequencies locate any nodal circles.

4.16. By integration over its surface show that the average displacement amplitude of a thin plate when vibrating in its fundamental mode of vibration equals $0.309A$, where A is the displacement amplitude at the center of the circular plate. Assume the plate to be rigidly clamped at its rim.

4.17. The diaphragm of a telephone receiver consists of a circular sheet of steel, 4 cm in diameter and 0.02 cm thick. (*a*) If it is rigidly clamped at its rim, what is its fundamental frequency of vibration? (*b*) What will be the effect on this frequency of doubling the thickness of the diaphragm? (*c*) Of doubling the diameter?

4.18. To what tension would the diaphragm of Problem 4.17 need to be stretched if its fundamental frequency, considered as resulting from the restoring forces of tension alone, were to equal that resulting from stiffness forces alone?

4.19. (*a*) Determine the ratio of the constants B_2/A_2 for a thin circular plate clamped at its rim and vibrating in its first overtone mode of vibration. (*b*) Express the resulting motion in the form of an equation analogous to equation 4.61. (*b*) Plot the shape function of the diaphragm when vibrating in this mode. (*d*) What is the ratio of the radius of the nodal circle to the radius of the plate when vibrating in this mode?

4.20. Given the vibrating circular steel plate of an electromagnetic drive type of sonar transducer to be rigidly clamped at its rim, to have a radius of 0.1 m and to have a thickness of 0.005 m. What is its fundamental frequency of vibration?

chapter 5
ACOUSTIC PLANE WAVES

5.1 Introduction. The acoustic waves that produce the sensation of sound are but one of a variety of pressure disturbances that can be propagated through any compressible fluid. In addition there are ultrasonic waves whose frequencies are above the audible limit, high intensity waves such as those present in the immediate vicinity of jet engines and missiles, which may produce a sensation of pain rather than one of sound, and single pulse shock waves as generated by explosions and high speed aircraft.

Acoustic waves in fluids differ in several respects from the waves that we have discussed in the preceding chapters. They are waves in three dimensions and, as such, can be more complicated in behavior than waves in one or two dimensions. They are *longitudinal* waves, since the molecules transmitting the wave move back and forth in the direction of propagation of the wave, producing alternate regions of compression and rarefaction similar to those produced by longitudinal waves in a bar, rather than crests and troughs as for transverse waves. Fluids exhibit fewer types of constraints relative to possible physical deformations than do solids and, consequently, the restoring force responsible for propagating a wave is simply the nondirectional elastic opposition that arises when a fluid is compressed.

Because of the numerous points of difference between the wave phenomena discussed earlier and the more complicated forms of acoustic waves, it is well not to introduce all the complications at once. Accordingly, we shall first study *plane waves* of sound, the simplest type of wave motion propagated through a fluid medium. The characteristic property of such waves is that the acoustic pressures, particle displacements, density changes, etc., have common phases and amplitudes at all points on any given plane perpendicular to the direction of wave propagation. Plane waves may be readily produced in a fluid confined in a rigid pipe, through the action of a vibrating piston located at one end of the pipe. The wave fronts of any type of divergent wave in a homogeneous medium also assume the characteristics of plane waves as they proceed to great distances from their source.

5.2 Elastic Behavior of Fluids. Plane acoustic waves have many characteristics in common with the longitudinal waves that are propagated along a thin bar. Consequently, it is possible to derive a wave equation for the propagation of plane waves through a fluid medium that is assumed to be confined within a rigid pipe of constant cross-section, in essentially the same manner as that previously employed in the analysis of the transmission of longitudinal waves along a bar (Sect. 3.3). In order to carry out this derivation, it is first necessary to derive a relationship between pressure changes within the fluid and deformation of the fluid, analogous to equation 3.5 for longitudinal deformation of a bar. Such an equation may be evolved through a combination of equations expressing *thermodynamic* properties of a fluid along with one expressing the basic principle of *conservation of mass.*

The following symbols and abbreviations will be used in the derivation and solution of subsequent equations appropriate to the propagation of plane waves along the x-axis:

- x equilibrium coordinate of a particle of the medium
- ξ particle displacement from equilibrium position, along x-axis
- u particle velocity, $u = \partial\xi/\partial t$
- ρ instantaneous density at any point
- ρ_0 constant equilibrium density of medium
- s condensation at any point, as defined by

$$s = \frac{\rho - \rho_0}{\rho_0} \quad \text{or} \quad \rho = \rho_0(1 + s) \tag{5.1}$$

- P instantaneous pressure at any point
- P_0 constant equilibrium pressure in medium
- p excess pressure or acoustic pressure at any point, as defined by

$$p = P - P_0 \tag{5.2}$$

- c velocity of propagation of the wave

The term *particle* of the medium is to be understood as meaning a volume element large enough to contain millions of molecules so that it may be thought of as a continuous fluid, yet small enough so that such acoustic variables as pressure, density, and velocity may be considered as constant throughout the volume element. In the following analysis, the effects of gravitational forces will be neglected, and hence ρ_0 and P_0 have been assumed to have uniform values throughout the medium. The medium is also assumed to be homogeneous, isotropic, and perfectly elastic, i.e., no dissipative forces, such as those arising from viscosity or heat conduction losses, are present. Finally, the analysis will be limited to waves of relatively small amplitude so that changes in density of the medium will be small compared with its equilibrium value.

As a plane wave moves along the x-axis, adjacent planes of molecules in the fluid are displaced from their equilibrium positions, as shown in Fig. 5.1. In general, these displacements are a function of both coordinate position and of time and may be represented by a function $\xi(x, t)$. Our first task is to derive an equation relating these displacements to density changes in the medium. To accomplish this we may apply the principle of conservation of mass to a cross-sectional area S of undisturbed fluid contained between planes positioned at x and $x + dx$. The mass of this fluid is $\rho_0 S\,dx$. Next, let us assume that upon passage of a sound wave, the plane originally at x is displaced a distance ξ to the right and that originally at $x + dx$, a distance $\xi + (\partial\xi/\partial x)\,dx$. The volume enclosed is therefore changed to $S\,dx(1 + \partial\xi/\partial x)$. Consequently, the density of the fluid contained between the planes must be altered so that the total mass can remain unchanged, as is expressed by the equation

$$\rho S\,dx\left(1 + \frac{\partial\xi}{\partial x}\right) = \rho_0 S\,dx$$

If we use equation 5.1 to replace ρ with $\rho_0(1 + s)$ and cancel the common term $\rho_0 S\,dx$ from the resulting equation, it becomes

$$(1 + s)\left(1 + \frac{\partial\xi}{\partial x}\right) = 1 \tag{5.3}$$

Since both density changes and molecular displacements have been assumed to be small, (even for those intense sounds in air which are painful to the

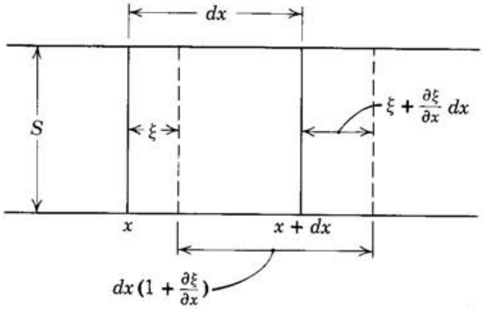

Fig. 5.1. Longitudinal displacements in a plane sound wave.

human ear, neither s nor $\partial\xi/\partial x$ exceed 10^{-4}), we can neglect the product of s and $\partial\xi/\partial x$, so that equation 5.3 simplifies to

$$s = -\frac{\partial\xi}{\partial x} \tag{5.3a}$$

This equation is a special form of a very important hydrodynamic equation known as the *equation of continuity*. It states that when a plane of molecules in the fluid to the right of a given point is displaced more to the right than is a similar plane to the left of the point, i.e., when these two planes are separated by a greater distance than their equilibrium separation, $\partial\xi/\partial x$ is positive and the density of the fluid is diminished.

A second property of fluids which is used in deriving the wave equation is a thermodynamic one relating changes in pressure and density. In general, many such relationships exist, depending on what particular thermodynamic process is involved. For example, the equation governing the *isothermal* process in a perfect gas is $(P/P_0) = (\rho/\rho_0)$, while that for the *adiabatic* process is $(P/P_0) = (\rho/\rho_0)^\gamma$.

We must now decide which particular thermodynamic process is most appropriate to the alternate expansions and compressions of the small volume element $S\,dx$ of Fig. 5.1, when acted upon by acoustic waves. In general, any compression of a fluid volume element requires the expenditure of work which is converted into heat energy and will increase its temperature unless the process is so slow that this energy may flow into the surrounding fluid. When a fluid is transmitting acoustic waves, the temperature gradients between adjacent compressed and expanded parts of the fluid are relatively small. Consequently, little heat energy flows away from a compressed part of the fluid before this part is no longer compressed. Under such circumstances, the thermodynamic process may be said to be *adiabatic*. Therefore, we shall assume that it is this process that most nearly applies to acoustic pressure and density changes in fluids.

In order to generalize our derivation so that it may apply equally well to all fluids, i.e., to liquids and real gases as well as to perfect gases, let us represent the adiabatic process by the symbolic equation $P = P(\rho)$. Differentiation of this equation gives

$$dP = \left(\frac{dP}{d\rho}\right)_0 d\rho \tag{5.4}$$

where $(dP/d\rho)_0$ is the slope measured at the coordinate point, $P_0\rho_0$, of an adiabatic plot of pressure versus density. For the small changes taking place in acoustic waves, we may replace the incremental pressure change dP with the acoustic pressure p and the incremental density change $d\rho$ by

$\rho_0 s$ (see equation 5.1) leading to

$$p = \left(\frac{dP}{d\rho}\right)_0 \rho_0 s \tag{5.4a}$$

Letting

$$c^2 = \left(\frac{dP}{d\rho}\right)_0 \tag{5.5}$$

we have

$$p = \rho_0 c^2 s \tag{5.4b}$$

an important equation relating acoustic pressure and condensation. Finally, upon replacing s with its equivalent $-(\partial\xi/\partial x)$, from equation 5.3*a*,

$$p = -\rho_0 c^2 \frac{\partial \xi}{\partial x} \tag{5.6}$$

is obtained. A comparison of this equation with equation 3.5 will emphasize the similarity of the relationship between stress and strain for longitudinal plane waves in a fluid and in a bar.

5.3 Plane Wave Equation. When a fluid medium is deformed in the manner described in the preceding section, the resulting pressures on the two faces of the volume element $S\,dx$ will be slightly different, producing a net force which will accelerate the element. Since the external force acting on each face is equal to the product of the pressure and the area of the face, the net force acting upon $S\,dx$ in the positive x direction is

$$dF_x = \left[p - \left(p + \frac{\partial p}{\partial x}\,dx\right)\right]S = -\frac{\partial p}{\partial x}\,dx\,S \tag{5.7}$$

In deriving this equation, forces caused by the equilibrium pressure P_0 have been ignored since they always cancel. It is only the gradient $\partial p/\partial x$ of the acoustic pressure that is instrumental in producing a net force upon the volume element. Setting this net force equal to the product of the element's mass $\rho_0 S\,dx$ by its acceleration gives

$$-\frac{\partial p}{\partial x} = \rho_0 \frac{\partial^2 \xi}{\partial t^2} \tag{5.8}$$

In deriving this equation we have neglected second order differences between accelerations $\partial^2\xi/\partial t^2$ occurring in the medium at the fixed point in space x and actual accelerations $d^2\xi/dt^2$ of the moving volume element.

Equation 5.8 may be combined with equation 5.6 either to eliminate p or ξ, giving, respectively

$$\frac{\partial^2 \xi}{\partial t^2} = c^2 \frac{\partial^2 \xi}{\partial x^2} \tag{5.9}$$

or

$$\frac{\partial^2 p}{\partial t^2} = c^2 \frac{\partial^2 p}{\partial x^2} \tag{5.9a}$$

as two particular forms of the *acoustic plane wave* equation. Similar equations also apply to such acoustic variables as particle velocity u and condensation s. Fortunately, it is unnecessary to solve each of these equations. A solution just for ξ will suffice. Once its solution has been obtained, the behavior of the other acoustic variables readily can be obtained by using the relationships developed above such as

$$p = -\rho_0 c^2 \frac{\partial \xi}{\partial x}, \quad s = -\frac{\partial \xi}{\partial x}, \quad u = \frac{\partial \xi}{\partial t}, \quad \text{etc.}$$

A fluid is not, of course, made up of molecules having fixed mean positions in the medium, as has been assumed above in deriving the wave equation. Even without the presence of a wave, the molecules are in constant motion, with average velocities far in excess of any particle velocities associated with the wave motion. However, from a statistical point of view, a small volume element may be treated as an unchanging unit, since those molecules leaving its confines are replaced by an equal number possessing on the average identical properties, thus keeping the macroscopic properties of the element unchanged. As a consequence, it is possible to speak of *particle* displacements and velocities when discussing acoustic waves in a fluid in much the same manner as is done for elastic waves in solids. Nevertheless, it is to be emphasized that a statistical variable such as acoustic pressure more adequately represents acoustic waves and is used almost exclusively for their measurement.

5.4 Harmonic Solution of the Plane Wave Equation. Equation 5.9 is identical in form with equation 3.7 for the longitudinal vibrations of a bar and has the general solution

$$\xi = f_1(ct - x) + f_2(ct + x) \tag{5.10}$$

where c is the velocity of wave propagation.

The most important specific type of solution is that expressing motion of particles of the fluid as a function of harmonic waves. In complex form this is

$$\boldsymbol{\xi} = \mathbf{A}e^{j(\omega t - kx)} + \mathbf{B}e^{j(\omega t + kx)} \tag{5.11}$$

where **A** is the complex displacement amplitude of a plane wave of frequency ω and wavelength constant k traveling in the positive x direction with a velocity c, and **B** is the amplitude of a similar wave traveling in the negative x direction. In complex form, the other important acoustic variables are given by

$$\mathbf{p} = -\rho_0 c^2 \frac{\partial \boldsymbol{\xi}}{\partial x} = j\rho_0 c\omega(\boldsymbol{\xi}_+ - \boldsymbol{\xi}_-) \tag{5.12}$$

$$\mathbf{s} = -\frac{\partial \boldsymbol{\xi}}{\partial x} = jk(\boldsymbol{\xi}_+ - \boldsymbol{\xi}_-) \tag{5.13}$$

$$\mathbf{u} = \frac{\partial \boldsymbol{\xi}}{\partial t} = j\omega(\boldsymbol{\xi}_+ + \boldsymbol{\xi}_-) \tag{5.14}$$

where for purposes of simplification

$$\boldsymbol{\xi}_+ = \mathbf{A}e^{j(\omega t - kx)} \tag{5.15}$$

and

$$\boldsymbol{\xi}_- = \mathbf{B}e^{j(\omega t + kx)} \tag{5.15a}$$

are the functions representing displacements produced by waves traveling in the positive and negative x directions, respectively.

These complex relationships show that, when plane waves are traveling in the positive x direction, acoustic pressure p, condensation s, and particle velocity u are in phase with each other and lead the displacement ξ by j, i.e., by a quarter of a cycle or 90° of phase angle. On the other hand, when plane waves are traveling in the negative x direction, the particle velocity leads the displacement by 90° but condensation and pressure lag by 90°. This difference of phase relationship between the various acoustic variables for waves moving in opposite directions arises from the fact that pressure

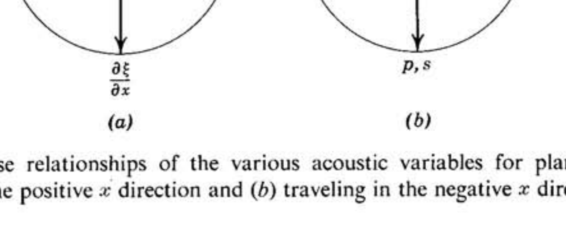

Fig. 5.2. Phase relationships of the various acoustic variables for plane waves (*a*) traveling in the positive x direction and (*b*) traveling in the negative x direction.

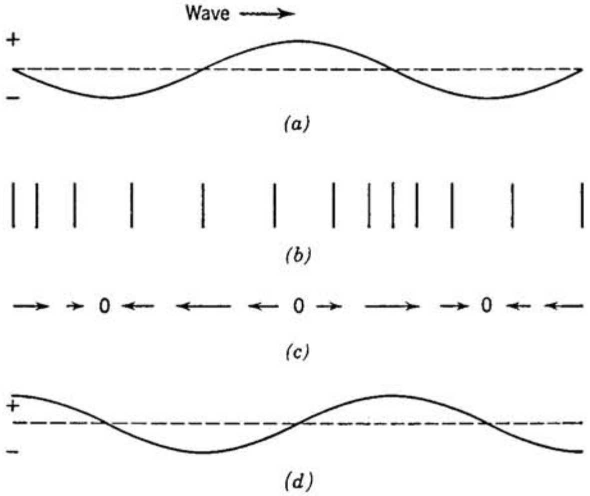

Fig. 5.3. Phase relationships of acoustic variables for a plane wave traveling in the positive x direction. (*a*) Displacement ξ as a function of position. (*b*) Spacing of particles when displaced as indicated in (*a*). (*c*) Particle velocity u as a function of position. (*d*) Pressure and condensation as a function of position.

and condensation are scalar quantities whereas velocity and displacement are vector quantities. It is to be noted that irrespective of the direction of propagation, a maximum of pressure and condensation is associated with a maximum of particle velocity in the direction of wave propagation and that all three lead the displacement maximum in this direction by 90° of phase angle. These phase relations are shown in Figs. 5.2 and 5.3.

Analytical equations giving instantaneous values for the above acoustic variables are provided by the real parts of equations 5.11 through 5.14. As an example, consider the special case where **A** and **B** are real constants, A and B, respectively. Then

$$\xi = A \cos(\omega t - kx) + B \cos(\omega t + kx) \tag{5.11a}$$

$$p = -\rho_0 c\omega A \sin(\omega t - kx) + \rho_0 c\omega B \sin(\omega t + kx) \tag{5.12a}$$

$$s = -kA \sin(\omega t - kx) + kB \sin(\omega t + kx) \tag{5.13b}$$

$$u = -\omega A \sin(\omega t - kx) - \omega B \sin(\omega t + kx) \tag{5.14a}$$

5.5 Velocity of Sound in Fluids. The constant c, representing the velocity with which an acoustic wave is propagated through a fluid medium, was defined in Sect. 5.3 as

$$c = \sqrt{\frac{dP}{d\rho}} \tag{5.5}$$

where $dP/d\rho$ is evaluated for an adiabatic process at equilibrium conditions of pressure and density. It is a characteristic property of the medium dependent on the elastic nature of the latter and as well on such thermodynamic variables as temperature, pressure, and density. It is independent of frequency and the amplitude of pressure or displacement for ordinary acoustic waves, corresponding to those normally audible to the human ear.

When a sound wave is being propagated through a gas, the adiabatic gas law relating pressure and density may be utilized to derive an important special form of equation 5.5. Let us express the adiabatic gas law in the form

$$\frac{P}{\rho^{\gamma}} = K \tag{5.16}$$

where γ is the ratio of the specific heat of the gas at constant pressure to that at constant volume and K is a constant. Then, direct differentiation of equation 5.16 leads to

$$\frac{dP}{d\rho} = \frac{\gamma P}{\rho} \tag{5.17}$$

If this expression for $dP/d\rho$ is now substituted into equation 5.5 at the point P_0, ρ_0, corresponding to equilibrium conditions of pressure and density

$$c = \sqrt{\frac{\gamma P_0}{\rho_0}} \tag{5.18}$$

is obtained.

Included in Table I in the appendix are values of γ and ρ_0 for various gases at 0°C and at a standard barometric pressure of $P_0 = 1.013 \times 10^5$ newtons/m². Substitution of the appropriate values for air gives

$$c_0 = \sqrt{\frac{1.402 \times 1.013 \times 10^5}{1.293}} = 331.6 \text{ meters/sec}$$

as the theoretical value for the velocity of sound in air at 0°C. This is in excellent agreement with measured values and thereby supports our earlier assumption that acoustic compressions and expansions in a fluid are adiabatic.

For most gases the ratio of P_0/ρ_0 is nearly independent of pressure; i.e., a doubling of pressure is accompanied by a doubling of the density of the gas, so that the velocity of sound in air does not change with variations in the barometric pressure. Furthermore, if the atmosphere were homogeneous and isothermal, the velocity would be independent of altitude. In actual practice neither of these two assumptions is correct, but the changes in velocity that result from the changes in temperature are of much greater significance than those resulting from the inhomogeneity in composition.

One form of the general gas law states that

$$\frac{P}{\rho} = rT$$

where r is a constant whose value depends on the particular gas involved, and T is the absolute temperature of the gas in °K (Kelvin), i.e., $T = t + 273$, where t is the temperature in °C (centigrade). An alternative expression for the velocity of sound in a gas is therefore

$$c = \sqrt{\gamma r T}$$

which clearly indicates that the velocity is proportional to the square root of the absolute temperature, or that the velocity at any temperature is related to the velocity c_0 at 0°C by

$$c = c_0\sqrt{\frac{T}{273}} = c_0\sqrt{1 + \frac{t}{273}} \tag{5.19}$$

When the centigrade temperature is small in comparison with 273, we may replace equation 5.19 by the approximate relation

$$c \approx c_0\left(1 + \frac{1}{2}\cdot\frac{t}{273}\right) = c_0 + \frac{c_0 t}{546} \tag{5.19a}$$

Substituting for c_0 the velocity in air at 0°C this becomes

$$c = 331.6 + 0.6t \tag{5.20}$$

A theoretical prediction of the velocity of sound in liquids is considerably more difficult than it is for gases. Nevertheless, it is possible to derive an equation similar to equation 5.18, for use with liquids. This equation is

$$c = \sqrt{\frac{\gamma B_T}{\rho_0}} \tag{5.21}$$

where B_T is the isothermal bulk modulus, an elastic modulus measuring the difficulty of compressing a liquid. Numerical values for the various quantities appearing in equation 5.21 are given in Table I in the appendix for a few common liquids.

Since all of these quantities depend upon both the temperature and the pressure of the liquid, it is to be expected that the velocity of sound in liquids likewise will vary both with temperature and pressure. No simple theory is available for predicting these variations. Consequently, it becomes necessary to measure them experimentally. An empirical equation giving the velocity of sound in distilled water as a function of temperature at a pressure of one atmosphere, as derived from experimental data,[1] is

$$c = 1403 + 5t - 0.06t^2 + 0.0003t^3 \tag{5.22}$$

where t is the temperature of the water in °C and c is in meters per second. This empirical equation fits the measured data over temperatures ranging from 0°C to 60°C, with errors of less than 0.2 per cent. Additional factors such as pressure and salinity increase the velocity of sound as measured in sea water. A detailed discussion of this phenomenon and its consequences will be given in Chapter 15, which is devoted to underwater acoustics.

5.6 Energy Density of Plane Waves. The energy involved in the propagation of acoustic waves through a fluid medium is of two forms, the kinetic energy of the moving particles and the potential energy inherent in a compressed fluid.

Consider a small volume element, similar to the one previously discussed in Sect. 5.2, of such a thickness dx that all particles of the element may be considered as having the same velocity u. Then the kinetic energy of this volume element is

$$\Delta E_k = \tfrac{1}{2}\rho_0 u^2 V_0 \tag{5.23}$$

where V_0, the volume of the element in the undisturbed fluid, equals $S\,dx$. As the fluid is compressed and expanded during the transmission of an acoustic wave, the volume V of this element will vary in accordance with the equation

$$V = V_0\left(1 + \frac{\partial \xi}{\partial x}\right) \tag{5.24}$$

as was previously explained in Sect. 5.2. The change in potential energy associated with this volume change is given by

$$\Delta E_p = -\int p\,dV \tag{5.25}$$

The negative sign in this equation is required so that the potential energy will increase as work is done on the element when its volume is decreased by action of a positive acoustic pressure p. In order to carry out the integration expressed by equation 5.25, it is necessary to express all variables behind the integral sign in terms of one variable, p for example. If we replace $\partial\xi/\partial x$ in equation 5.24 by $-p/\rho_0 c^2$ as obtained from equation 5.6, then

$$V = V_0\left(1 - \frac{p}{\rho_0 c^2}\right)$$

[1] Wilson, *J. Acoust. Soc. Am.*, **31**, 1067 (1959).

which upon differentiation becomes

$$dV = -\frac{V_0\,dp}{\rho_0 c^2} \tag{5.26}$$

Substitution of equation 5.26 into 5.25 and integration of the acoustic pressure from 0 to p gives

$$\Delta E_p = \frac{V_0}{\rho_0 c^2}\int_0^p p\,dp = \frac{1}{2}\frac{p^2}{\rho_0 c^2}V_0 \tag{5.27}$$

The total acoustic energy of the volume element is

$$\Delta E = \Delta E_k + \Delta E_p = \frac{1}{2}\rho_0\left(u^2 + \frac{p^2}{\rho_0^2 c^2}\right)V_0 \tag{5.28}$$

and the energy density $\mathcal{E}$ in joules per cubic meter is

$$\mathcal{E} = \frac{\Delta E}{V_0} = \frac{1}{2}\rho_0\left(u^2 + \frac{p^2}{\rho_0^2 c^2}\right) \tag{5.29}$$

In order to determine the instantaneous energy density associated with waves traveling in both the positive and the negative x directions, it is necessary to substitute the values of u and p as given by equations 5.14*a* and 5.12*a* into equation 5.29. However, this determination is greatly simplified if the two waves are considered separately. For example, when a plane wave is traveling in the positive x direction a comparison of equation 5.12*a* with 5.14*a* shows that, $p = \rho_0 cu$, and therefore

$$\mathcal{E}_+ = \rho_0 u_+^2 \tag{5.30}$$

where the subscript + indicates a wave traveling in the positive x direction. On the other hand, when a wave is traveling in the negative x direction, $p = -\rho_0 cu$, and therefore

$$\mathcal{E}_- = \rho_0 u_-^2 \tag{5.30a}$$

The instantaneous energy density corresponding to the presence of both plane waves is consequently

$$\mathcal{E} = \mathcal{E}_+ + \mathcal{E}_- = \rho_0(u_+^2 + u_-^2) \tag{5.31}$$

The instantaneous particle velocity corresponding to a single progressive plane wave, one traveling in the positive x direction for instance, is a function of both position and time, and consequently the energy density $\mathcal{E}_+$ is not constant throughout the medium. The time average of this energy density at any point in the medium is given by

$$\overline{\mathcal{E}}_+^{\,t} = \frac{1}{T}\int_0^T \mathcal{E}_+\,dt \tag{5.32}$$

where the integration is to be taken over a time T corresponding to the period of one complete cycle of the harmonic wave motion. From equation 5.14a it is apparent that

$$u_+ = -\omega A \sin(\omega t - kx)$$

and therefore

$$\begin{aligned}\overline{\mathcal{E}}_+{}^t &= \frac{1}{T}\int_0^T \rho_0[-\omega A \sin(\omega t - kx)]^2\, dt \\ &= \frac{\rho_0\omega^2 A^2}{T}\int_0^T \left[\sin^2 \omega t \cos^2 kx + \cos^2 \omega t \sin^2 kx - \frac{\sin(2\omega t)\sin(2kx)}{2}\right] dt\end{aligned}$$

so that

$$\overline{\mathcal{E}}_+{}^t = \frac{\rho_0\omega^2 A^2}{2} \tag{5.33}$$

If $-\omega A$ is replaced by U_+, the velocity amplitude corresponding to this wave, then

$$\overline{\mathcal{E}}_+{}^t = \frac{\rho_0 U_+{}^2}{2} \tag{5.33a}$$

Similarly, replacing $-\omega A$ by $P_+/\rho_0 c$, where P_+ is the pressure amplitude of the wave,

$$\overline{\mathcal{E}}_+{}^t = \frac{P_+{}^2}{2\rho_0 c^2} \tag{5.33b}$$

If, instead of determining the time average of the energy density at a particular point, we determine the space average of the energy density at some particular time, which can be obtained by integrating over one complete wavelength λ with t constant, i.e.,

$$\overline{\mathcal{E}}_+{}^x = \frac{1}{\lambda}\int_0^\lambda \mathcal{E}_+\, dx$$

the latter can be shown to be identical with the time average.

Therefore

$$\overline{\mathcal{E}}_+{}^x = \frac{\rho_0\omega^2 A^2}{2} = \frac{\rho_0 U_+{}^2}{2}, \text{ etc.} \tag{5.34}$$

Similarly, it can be shown that the average energy density of a plane wave traveling in the negative x direction is given by

$$\overline{\mathcal{E}}_-{}^t = \overline{\mathcal{E}}_-{}^x = \frac{\rho_0\omega^2 B^2}{2} = \frac{\rho_0 U_-{}^2}{2}, \text{ etc.} \tag{5.35}$$

Although equation 5.29 has been derived for plane waves, it also applies to other types of waves such as diverging spherical waves, cylindrical waves, etc. However, in deriving equations 5.30 and 5.30*a* it was necessary to use the relations $p = \pm\rho_0 cu$. Neither of the latter relations can be applied to spherical waves, except at such great distances from their source that the wave fronts are essentially plane, and hence equations 5.33 and 5.35 are not generally applicable to spherical waves, as we shall discuss further in Chapter 7.

5.7 Acoustic Intensity. The *acoustic intensity* I of a sound wave is defined as the *average* rate of flow of energy through a unit area normal to the direction of wave propagation. Its fundamental units are those of joules per second per square meter, and since this has the dimensions of power transmitted per unit area it can also be expressed in watts per square meter. All of the acoustic energy contained in a column $c\,dt$ meters in length, i.e., $\mathcal{E}c\,dt$, will pass through unit area in a time interval dt. Consequently, the instantaneous rate of flow of acoustic energy through unit area is

$$\frac{dE}{dt} = \mathcal{E}c \tag{5.36}$$

and the *intensity* or average rate of flow is

$$I = \frac{\overline{dE}^t}{dt} = \overline{\mathcal{E}}^t c \tag{5.37}$$

The intensity of a plane wave traveling in the positive x direction is therefore

$$I_+ = c\overline{\mathcal{E}}_+ \tag{5.37a}$$

Alternative forms of this relation include

$$I_+ = \frac{\rho_0 c\omega^2 A^2}{2} = \frac{\rho_0 c U_+^{\,2}}{2} = \frac{P_+^{\,2}}{2\rho_0 c} = \frac{P_+ U_+}{2} \tag{5.38}$$

In order to emphasize the similarity of equations 5.38 with corresponding ones for electromagnetic waves and for voltage waves on transmission lines and as well to write them in a more practical form, let us express them in terms of *effective* (root mean square) amplitudes as defined by

$$A_e = \frac{A}{\sqrt{2}}, \quad P_e = \frac{P}{\sqrt{2}}, \quad U_e = \frac{U}{\sqrt{2}} \tag{5.39}$$

Then

$$I_+ = \rho_0 c\omega^2 A_e^{\,2} = \rho_0 c U_e^{\,2} = \frac{P_e^{\,2}}{\rho_0 c} = P_e U_e \tag{5.38a}$$

When a plane wave is progressing in the negative x direction the intensity I_- is also in the negative x direction, so that

$$I_- = -c\bar{\mathcal{E}}_- \tag{5.37b}$$

and

$$I_- = -\frac{\rho_0 c\omega^2 B^2}{2} = -\frac{\rho_0 c U_-^2}{2} = -\frac{P_-^2}{2\rho_0 c} = -\frac{P_- U_-}{2} \tag{5.40}$$

or

$$I_- = -\rho_0 c\omega^2 B_e^2 = -\rho_0 c U_e^2, \text{ etc.} \tag{5.40a}$$

5.8 Specific Acoustic Impedance. The ratio of acoustic pressure in a medium to the associated particle velocity is defined as the *specific acoustic impedance*, **z**, of the medium for the particular type of wave motion present. For plane waves traveling in the positive x direction this ratio is given by

$$\mathbf{z}_+ = \frac{\mathbf{p}_+}{\mathbf{u}_+} = \frac{j\rho_0 c\omega\boldsymbol{\xi}_+}{j\omega\boldsymbol{\xi}_+} = \rho_0 c \tag{5.41}$$

and for plane waves traveling in the negative x direction by

$$\mathbf{z}_- = \frac{\mathbf{p}_-}{\mathbf{u}_-} = \frac{-j\rho_0 c\omega\boldsymbol{\xi}_-}{j\omega\boldsymbol{\xi}_-} = -\rho_0 c \tag{5.41a}$$

The specific acoustic impedance for plane waves traveling in either direction is a *real* quantity of magnitude $\rho_0 c$. The MKS unit of specific acoustic impedance is a kilogram/meter^2 second or *rayl* (MKS rayl).[1]

It will be observed that this product $\rho_0 c$ occurs in most forms of the equations giving the intensity of the wave, and in later sections (see, for example, Sect. 6.2) it will become apparent that the product of these two quantities has greater significance as a characteristic property of the medium than does either ρ_0 or c, individually. For this reason $\rho_0 c$ is called the *characteristic impedance* (*resistance*) of the medium.

Although the specific acoustic impedance of the medium is a real quantity for progressive plane waves, this is not true for standing plane waves or for diverging waves. In general **z** will be found to have both a real part, r, and an imaginary part, jx, so that

$$\mathbf{z} = \frac{\mathbf{p}}{\mathbf{u}} = r + jx \tag{5.42}$$

where r is called the *specific acoustic resistance* and x the *specific acoustic reactance* of the medium for the particular wave motion being considered. From equations 5.41 and 5.41*a* it is apparent that the specific acoustic

[1] Named in honor of Lord Rayleigh.

resistance of a medium for a plane progressive wave is

$$r = \pm\rho_0 c \text{ rayls} \tag{5.43}$$

where the positive sign is to be used for waves traveling in the positive x direction and the negative sign for those traveling in the negative x direction. It is also apparent that for this type of wave the specific acoustic reactance is zero.

The characteristic impedance of a medium for acoustic waves is analogous to the index of refraction n of a transparent medium for light waves, to the wave impedance $\sqrt{\mu/\epsilon}$ of a dielectric medium for electromagnetic waves, and to the characteristic impedance Z_0 of an electric transmission line.

Numerical values of $\rho_0 c$ for various fluids, and also for plane waves in some solids, are given in Table I in the appendix.

5.9 Acoustic Standards and Reference Conditions. It is customary to specify air at a temperature of 20°C and at standard atmospheric pressure in defining standards of acoustic intensity, specific acoustic impedance, pressure, etc. Under these conditions the density of air is 1.21 kg/m^3 and the velocity of sound is 343 m/sec, giving for the standard characteristic impedance of air

$$(\rho_0 c)_{20} = 415 \text{ rayls}$$

Therefore, unless other conditions of temperature and pressure are specified in a particular situation, we shall use the above value in illustrative examples or for the solution of problems.

The commonly used reference standard of intensity for airborne sounds is that of 10^{-12} watt/m^2 (10^{-16} watt/cm^2), which is approximately the intensity of a 1000-cycles/sec pure tone that is just barely audible to normal human ears. Substitution of this intensity into equation 5.38 shows that it corresponds to a peak pressure amplitude of

$$P = \sqrt{2\rho_0 c I} = \sqrt{2 \times 415 \times 10^{-12}} = 0.0000289 \text{ newton/m}^2$$

or a corresponding *effective* (root mean square) pressure of

$$P_e = \frac{P}{\sqrt{2}} = 0.0000204 \text{ newton/m}^2$$

As we shall discuss in the following section, the latter pressure, rounded off to 0.00002 newton/m^2, is the commonly used reference pressure for specifying sound pressure levels in air. Equivalent expressions for this reference pressure include 0.0002 dyne/cm^2 and 0.0002 microbar.[1]

[1] A microbar = 1 dyne/cm^2 = 0.1 newton/m^2 $\approx 10^{-6}$ atmosphere.

The velocity of sound in water varies with the temperature and, consequently, the specific acoustic impedance will vary similarly. At 20°C the velocity of sound in distilled water, as computed from equation 5.22, is 1481.4 m/sec and its density is 998.2 kg/m³, resulting in a characteristic impedance of

$$(\rho_0 c)_{20} = 1{,}480{,}000 \text{ rayls}$$

We shall adopt this value as a standard for making computations in this book.

Two different pressures are commonly used as reference pressures for specifying sound pressure levels in underwater acoustic measurements. One is an effective pressure of 0.00002 newton/m² or the equivalent pressures of either 0.0002 dyne/cm² or 0.0002 microbar. This pressure corresponds to an intensity in water of $(0.00002)^2/1{,}480{,}000 = 2.7 \times 10^{-16}$ watt/m². The other is an effective pressure of 0.1 newton/m² or the equivalent pressures of 1 dyne/cm² or 1 microbar. This pressure corresponds to an intensity in water of $0.1^2/1{,}480{,}000 = 6.75 \times 10^{-9}$ watt/m².

From the above discussion it is to be noted that an acoustic pressure of 0.00002 newton/m² in air corresponds to a much higher intensity than does the same acoustic pressure in water. More precisely, equation 5.38 shows that for a given pressure amplitude, intensity is inversely proportional to the characteristic impedance of the medium. Therefore, the ratio of intensities in air and water for the same acoustic pressure is 1,480,000/415 = 3560. On the other hand, another one of the various forms of equation 5.38 shows that if we compare two acoustic waves of the same frequency and particle displacement amplitude A, the intensity of the one in water is 3560 times the intensity of that in air.

5.10 Decibel Scales. In theoretical investigations of acoustic phenomena it is convenient to express sound pressures in newtons/m² and sound intensities in watts/m². However, in practical engineering work and in experimental work it is customary to describe these same quantities through the use of logarithmic scales known as *sound levels*. One reason for doing this is a consequence of the very wide range of sound pressures and intensities encountered in our acoustical environment, e.g., audible intensities range from approximately 10^{-12} to 10 watts/m². The use of a logarithmic scale compresses the range of numbers required to describe this wide range of intensities. A second reason, is that the human ear subjectively judges the relative loudness of two sounds by the ratio of their intensities, a logarithmic behavior. A minor consequence of this use in acoustics of logarithmic type sound levels is that multiplicative factors in fundamental equations for pressure and intensity become additive terms in equations for their logarithmic equivalents.

The most generally used logarithmic scale for describing sound levels is the *decibel* scale. The *intensity level* (IL) of a sound of intensity I is defined by

$$\mathrm{IL} = 10 \log (I/I_0) \tag{5.44}$$

where IL is expressed in decibels (db) and I_0 is a reference intensity.[1] Only one intensity level is commonly used, that in air with a reference intensity of $I_0 = 10^{-12}$ watt/m^2.

We have shown in Sect. 5.7 that intensities and effective pressures of plane waves are related by the equation, $I = P_e^2/\rho_0 c$. Consequently, the expressions for intensity in equation 5.44 may be replaced by expressions for pressure, leading to

$$\mathrm{SPL} = 20 \log (P_e/P_0) \tag{5.45}$$

In this equation, SPL is known as a *sound pressure level* and also is expressed in decibels, P_e is the measured effective pressure of the sound wave, and P_0 is the reference effective pressure. A reference pressure of $P_0 =$ 0.00002 newton/m^2, or the equivalent pressures of 0.0002 dyne/cm^2 or 0.0002 microbar, is commonly used for computing sound pressure levels in air. Since this pressure is almost exactly equivalent to the effective pressure corresponding to the reference intensity $I_0 = 10^{-12}$ watt/m^2 used in equation 5.44, essentially identical numerical results are obtained by use of either of the above equations when plane progressive waves are being measured in air. However, in certain more complex sound fields, such as standing wave patterns and omnidirectional noise fields, intensity and pressure are no longer simply related by equation 5.38*a* and, as a consequence, equations 5.44 and 5.45 will not yield identical results. Since the voltage outputs of the microphones and hydrophones commonly used in acoustic measurements are proportional to pressure, acoustic pressure is the most readily measured variable in a sound field. For this reason, sound pressure levels as given by equation 5.45 are more widely used in specifying sound levels than are intensity levels as given by equation 5.44.

The term intensity level is *not* used in referring to the measurement of acoustic waves in water. However, unfortunately two reference pressures are commonly used for specifying sound pressure levels in water. An effective reference pressure of 0.0002 microbar (0.00002 newton/m^2) is normally used for equipment designed for the measurement of the noise output of ships and other underwater noises, while an effective reference pressure of 1 microbar (0.1 newton/m^2) is used for equipment designed to calibrate and otherwise investigate the acoustic characteristics of sonar transducers and hydrophones. This duality of reference pressures may

[1] In this book log is used for logarithms to the base 10 and ln for those to the base e.

lead to confusion unless care is taken by always specifying the reference pressure being used as *re* (reference) 0.0002 microbar or *re* 1 microbar. It is to be noted that the same numerical value of a sound pressure level relative to these two reference pressures actually corresponds to two sounds whose levels of intensity differ by almost exactly 74 db. In this book, pressure levels of underwater sounds will usually be expressed relative to a reference pressure of *one* microbar.

Table 5.1 Sound levels in decibels

Medium	Type	I_0 watts/m^2	P_0(rms) microbars	Relative Intensity of 0 db Reading	Relative Level of 0 db Reading
Air	Intensity	10^{-12}	—	1	0
Air	Pressure	—	0.0002	1	0
Water	Pressure	—	0.0002	0.00027	−35.5
Water	Pressure	—	1.0	6700	38.5

Table 5.1 summarizes the various methods of expressing the level of a sound in decibels. The first column gives the medium in which the particular decibel scale is commonly used. The second column gives the type of reference level, i.e., intensity or pressure. In either the third or fourth column is listed the reference condition corresponding to 0 db. The fifth column gives relative intensities of the various 0-db levels with respect to an intensity of 10^{-12} watt/m^2. Strictly speaking, this column applies only to plane waves, but it serves the useful purpose of showing the approximate magnitudes of the differences in intensity between the various 0-db reference levels. Evidently, a given numerical decibel level with reference to 1 microbar in water, corresponds to a higher intensity sound wave than does the same numerical level when referred to any other reference level. The final column in the table essentially expresses the same information as the fifth column and is obtained by taking 10 log of each number in the latter column.

PROBLEMS

5.1. By direct substitution show that $p = A(ct - x)e^{-a(ct-x)}$ satisfies equation 5.9*a* for plane waves. Derive an expression relating acoustic pressure p and particle velocity u for this type of function.

5.2. In the derivation of the plane wave equation, differences between du/dt, the acceleration of a particle moving with the fluid, and $\partial u/\partial t$, the acceleration of particles at a fixed point in space, were ignored. (*a*) Show that $du/dt = \partial u/\partial t + u(\partial u/\partial x)$. (*b*) Show that for plane waves the ratio of $u(\partial u/\partial x)$ to $\partial u/\partial t$ is equal to the condensation s. (*c*) What is this ratio for a sound of 130 db intensity level in air?

5.3. (*a*) Derive an equation expressing the adiabatic temperature rise ΔT produced in a gas by an acoustic pressure p. (*b*) What is the amplitude of the temperature fluctuations produced by a sound of 10 watts/m^2 intensity in air at 20°C and standard atmospheric pressure?

5.4. The intensity of a sound wave may be obtained by averaging over time the rate at which work is being done per unit area in the fluid, $I = \frac{1}{T}\int_0^T pu\,dt$. Show that for harmonic waves, this definition leads to equations 5.38.

5.5. Replace the expressions for acoustic pressure p and particle velocity u in equation 5.29 by their analytical forms from equations 5.12*a* and 5.14*a* and show that the result is equivalent to equation 5.31.

5.6. (*a*) Show that a plane wave having an effective acoustic pressure of 1 microbar in air has an intensity level of 74 db. (*b*) Find the intensity in watts/m^2 produced by an acoustic plane wave in water of 120 db sound pressure level relative to 1 microbar. (*c*) What is the ratio of the sound pressure in water for a plane wave to that of a similar wave in air of equal intensity?

5.7. Given a beam of plane waves in water to contain 100 watts of acoustic power distributed uniformly over a circular cross section of 40-cm diameter. The frequency of the waves is 24 kc/sec. Determine: (*a*) the intensity of the beam in watts/cm^2; (*b*) the sound pressure amplitude; (*c*) the acoustic particle velocity amplitude; (*d*) the acoustic particle displacement amplitude; (*e*) the condensation amplitude; (*f*) the effective or rms pressure; (*g*) the sound pressure level *re* 1 microbar.

5.8. A plane sound wave in air of 100 cycles/sec frequency has a peak acoustic pressure amplitude of 2 newtons/m^2. (*a*) What is its intensity? Its intensity level? (*b*) What is its peak particle displacement amplitude? (*c*) What is its peak particle velocity amplitude? (*d*) What is its effective or rms pressure? (*e*) What is its sound pressure level *re* 0.0002 microbar?

5.9. (*a*) Determine the energy density and effective pressure of a plane wave in air of 70-db intensity level. (*b*) Determine the energy density and effective pressure of a plane wave in water, if its sound pressure level is 70 db *re* 1 microbar.

5.10. (*a*) By means of equation 5.22, determine the velocity of sound in distilled water at a temperature of 30°C. (*b*) What is the rate of change of the velocity of sound in water with respect to temperature change at this temperature?

5.11. (*a*) Show that the characteristic impedance $\rho_0 c$ of a gas is inversely proportional to the square root of its absolute temperature T. (*b*) What is the characteristic impedance of air at 0°C? At 80°C? (*c*) If the pressure amplitude of a sound wave remains constant, what is its per cent change in intensity as the temperature increases from 0°C to 80°C? (*d*) What would be the corresponding change in measured intensity level? In pressure level?

5.12. Cavitation may take place at the face of a sonar transducer when the sound pressure amplitude being produced exceeds the hydrostatic pressure in the water. (*a*) For a hydrostatic pressure of 200,000 newtons/m^2, what is the highest intensity that may be radiated without producing cavitation? (*b*) What is the pressure level of this sound *re* 1 microbar?

chapter 6
TRANSMISSION PHENOMENA

6.1 Changes in Media. When a progressive plane wave in a fluid medium impinges on the boundary of a contiguous second medium, a *reflected* wave is generated in the first medium and a *transmitted* wave in the second medium. The ratios of the respective intensities and pressure amplitudes of the reflected and transmitted waves to those of the incident wave depend on the characteristic impedances of the two media and on the angle of incidence of the incident wave. The theory for transmission from one fluid to another across a plane interface and at normal incidence is relatively simple and will be treated first.

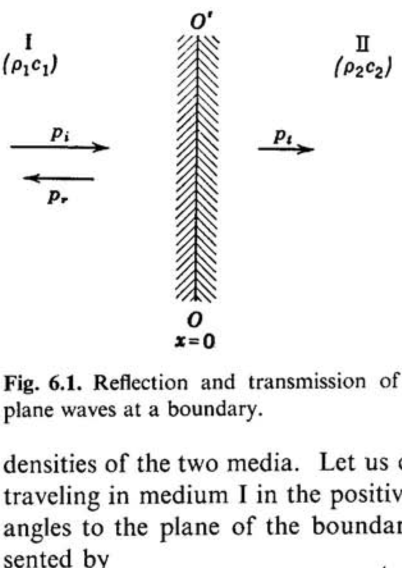

Fig. 6.1. Reflection and transmission of plane waves at a boundary.

6.2 Transmission from One Fluid Medium to Another; Normal Incidence. Let OO' of Fig. 6.1 denote the plane of the boundary between medium I, of characteristic impedance $\rho_1 c_1$, and medium II, of characteristic impedance $\rho_2 c_2$, where ρ_1 and ρ_2 respectively represent the undisturbed equilibrium densities of the two media. Let us consider an incident plane wave to be traveling in medium I in the positive x direction which in turn is at right angles to the plane of the boundary. This *incident wave* may be represented by

$$\mathbf{p}_i = A_1 e^{j(\omega t - k_1 x)} \tag{6.1}$$

where A_1 is a real constant representing the pressure amplitude of this wave. Upon striking the plane of the boundary between the two media, which is for convenience chosen at $x = 0$, a *reflected wave*

$$\mathbf{p}_r = \mathbf{B}_1 e^{j(\omega t + k_1 x)} \tag{6.2}$$

and a *transmitted wave*

$$\mathbf{p}_t = \mathbf{A}_2 e^{j(\omega t - k_2 x)} \tag{6.3}$$

are produced. The transmitted wave always has the same frequency as the incident wave, but, as a result of the difference between the velocities c_1 and c_2 in the two media, the values of the wavelength constants, $k_1 = \omega/c_1$ in medium I and $k_2 = \omega/c_2$ in medium II, are different.

There are two boundary conditions that must be satisfied at all times and at all points on the plane surface separating the two media: (1) the acoustic pressures on the two sides of the boundary are equal, and (2) the particle velocities normal to the interface are equal. The first condition of continuity of pressure results from the fundamental law that pressure in a fluid is a continuous, single-valued, scalar function, and the second condition is equivalent to the requirement that the two media remain in constant contact at the boundary.

Since pressure is a scalar quantity, the pressure at a point in medium I is given by $\mathbf{p}_i + \mathbf{p}_r$. Upon setting this expression equal to $\mathbf{p}_t$ at the boundary, where $x = 0$, we obtain

$$A_1 e^{j\omega t} + \mathbf{B}_1 e^{j\omega t} = \mathbf{A}_2 e^{j\omega t}$$

so that

$$A_1 + \mathbf{B}_1 = \mathbf{A}_2 \tag{6.4}$$

An inspection of equations 5.41 and 5.41*a* shows that the particle velocities $\mathbf{u}_i$, $\mathbf{u}_r$, and $\mathbf{u}_t$ associated with these three waves can be represented by

$$\mathbf{u}_i = \frac{\mathbf{p}_i}{\rho_1 c_1}, \quad \mathbf{u}_r = \frac{\mathbf{p}_r}{-\rho_1 c_1}, \quad \text{and} \quad \mathbf{u}_t = \frac{\mathbf{p}_t}{\rho_2 c_2} \tag{6.5}$$

The velocity of a particle in medium I is $\mathbf{u}_i + \mathbf{u}_r$, and therefore the second boundary condition is $\mathbf{u}_i + \mathbf{u}_r = \mathbf{u}_t$ at $x = 0$. Substituting from equation 6.5

$$\frac{\mathbf{p}_i}{\rho_1 c_1} - \frac{\mathbf{p}_r}{\rho_1 c_1} = \frac{\mathbf{p}_t}{\rho_2 c_2}$$

and introducing the respective expressions for the pressure at $x = 0$ this equation can be reduced to

$$\rho_2 c_2 (A_1 - \mathbf{B}_1) = \rho_1 c_1 \mathbf{A}_2 \tag{6.6}$$

Equations 6.4 and 6.6 can be combined to eliminate $\mathbf{A}_2$, giving

$$\mathbf{B}_1 = A_1 \frac{\rho_2 c_2 - \rho_1 c_1}{\rho_2 c_2 + \rho_1 c_1} \tag{6.7}$$

It is apparent from equation 6.7 that the assumed complex constant $\mathbf{B}_1$ is actually a real constant B_1, positive when $\rho_2c_2 > \rho_1c_1$ and negative when $\rho_2c_2 < \rho_1c_1$. Consequently, the acoustic pressure of the reflected wave at the boundary is either in phase with that of the incident wave at the boundary, or is 180° out of phase, depending on whether B_1 is a positive or negative constant. When the characteristic impedance of medium II is greater than that of medium I, as is true when a plane wave in air is incident upon an air-water interface, a positive excess pressure in the incident wave is reflected as a positive excess pressure; i.e., a condensation is reflected as a condensation. On the other hand, if $\rho_2c_2 < \rho_1c_1$, as is true for a wave in water incident on a water-air boundary, a positive excess pressure in the incident wave is reflected as a negative excess pressure; i.e., a condensation is reflected as a rarefaction.

In general, the ratio of the pressure amplitude of the reflected wave to that of the incident wave as given by equation 6.7 is less than unity, except for the limiting cases of $\rho_2c_2/\rho_1c_1 \rightarrow \infty$, i.e., reflection from a highly incompressible or very dense medium, and $\rho_2c_2/\rho_1c_1 \rightarrow 0$, i.e., reflection from an easily compressed or rarefied medium. Therefore, when $\rho_2c_2/\rho_1c_1 \rightarrow \infty$, the wave is reflected with only a slight reduction in amplitude and no change in phase, and a pattern of standing waves having a pressure antinode at the boundary will be set up in medium I. The pressure amplitude at this antinode will be almost double the amplitude of the incident wave. When $\rho_2c_2/\rho_1c_1 \rightarrow 0$, the amplitude of the reflected wave is also almost equal to that of the incident wave, and again a pattern of standing waves is established in medium I, but this time with a pressure node of nearly zero amplitude at the boundary, as is to be expected since the rarefied medium II cannot support large changes in pressure. As the ratio ρ_2c_2/ρ_1c_1, either decreases from large values or increases from small values so as to approach unity, the amplitude B_1 decreases toward zero and the pattern of standing waves becomes less pronounced, i.e., the pressure amplitudes at both antinodes and nodes approach the amplitude of the incident wave.

The acoustic pressure p_1 at any point in medium I is the sum of the real part of equation 6.1 and the real part of equation 6.2. Therefore,

$$p_1 = A_1 \cos(\omega t - k_1x) + B_1 \cos(\omega t + k_1x) \tag{6.8}$$

By the use of trigonometric identities such as

$$\cos(\omega t - k_1x) = \cos\omega t \cos k_1x + \sin\omega t \sin k_1x,$$

this equation may be converted to

$$p_1 = [(A_1 + B_1)^2 \cos^2 k_1x + (A_1 - B_1)^2 \sin^2 k_1x]^{1/2} \cos(\omega t + \phi) \tag{6.8a}$$

a form which is more useful for describing standing waves. When the amplitude constant B_1 is positive, pressure antinodes of amplitude $(A_1 + B_1)$ will occur at those places where $\cos^2 k_1x = 1$, i.e., at $x = 0, -\lambda_1/2, -2\lambda_1/2, -3\lambda_1/2$, etc. Pressure nodes of amplitude $(A_1 - B_1)$ will correspondingly occur at those places where $\sin^2 k_1x = 1$, i.e., at $x = -\lambda_1/4, -3\lambda_1/4, -5\lambda_1/4$, etc. By contrast, when B_1 is a negative constant, the coordinate positions of nodes and antinodes are reversed from those given above.

An interesting special case is that of $\rho_2c_2 = \rho_1c_1$, for which $B_1 = 0$, indicating the existence of *no* reflected wave. It is therefore possible to transmit sound from one fluid medium into another without any reflection of acoustic energy, providing $\rho_2c_2 = \rho_1c_1$.

Since the intensity of a plane wave as given by equation 5.38 is

$$I = \frac{P^2}{2\rho_0c}$$

it is evident that the ratio of the reflected flow of sound energy to the incident flow of sound energy is

$$\alpha_r = \frac{I_r}{I_i} = \frac{B_1^{\ 2}}{A_1^{\ 2}} = \left(\frac{\rho_2c_2 - \rho_1c_1}{\rho_2c_2 + \rho_1c_1}\right)^2 \tag{6.9}$$

where α_r is known as the *sound power reflection coefficient.*

If equations 6.4 and 6.6 are combined so as to eliminate $\mathbf{B}_1$, then

$$\mathbf{A}_2 = A_1 \frac{2\rho_2c_2}{\rho_2c_2 + \rho_1c_1} \tag{6.10}$$

It is evident that, the assumed complex constant $\mathbf{A}_2$ is actually a real *positive* constant A_2, irrespective of the relative magnitudes of ρ_2c_2 and ρ_1c_1. Consequently, the acoustic pressure of the transmitted wave at the boundary is always in phase with that of the incident wave at the boundary. Furthermore, the pressure amplitude A_2 of the transmitted wave ranges from nearly $2A_1$ when the ratio ρ_2c_2/ρ_1c_1 is large, as for air to water, to nearly zero when the ratio is small, e.g., water to air.

The *sound power transmission coefficient* α_t is given by

$$\alpha_t = \frac{I_t}{I_i} = \frac{A_2^{\ 2}/2\rho_2c_2}{A_1^{\ 2}/2\rho_1c_1} = \frac{\rho_1c_1}{\rho_2c_2} \cdot \frac{A_2^{\ 2}}{A_1^{\ 2}}$$

or

$$\alpha_t = \frac{4\rho_2c_2\rho_1c_1}{(\rho_2c_2 + \rho_1c_1)^2} \tag{6.11}$$

It should be noted that whenever ρ_2c_2 and ρ_1c_1 have widely separated magnitudes, the sound power transmission coefficient is small. Furthermore, from the symmetry of equation 6.11, it is apparent that the sound transmission coefficient is independent of the direction of wave motion, i.e., it is the same from water into air as it is from air into water. This reciprocal property of transmission is but a special case of a very much more general principle of reciprocity applicable to acoustic phenomena.

A substitution of the respective standard characteristic impedance of water and air in equation 6.11 gives

$$\alpha_t = \frac{4 \times 1{,}480{,}000 \times 415}{(1{,}480{,}000 + 415)^2} = 0.00112$$

so that the intensity of a plane wave passing at normal incidence either from water into air or from air into water is reduced by a factor of 0.00112. This corresponds to a decrease in intensity level of 10 log 0.00112 = −29.5 db.

6.3 Reflection at the Surface of a Solid; Normal Incidence. The reflection of plane waves in a fluid as produced at the surface of a solid is somewhat more involved than that produced at the interface between two fluids. In order to generalize our analysis of reflection from a solid surface, let us ignore the characteristics of the plane wave that penetrates into the solid. Instead, we will characterize the behavior of this wave by a parameter $\mathbf{z}_n$, the normal specific acoustic impedance of the solid, where $\mathbf{z}_n$ is defined as the ratio of acoustic pressure acting on the surface of the solid to the associated velocity of fluid normal to the surface. Since acoustic pressure is not always in phase with fluid velocity at the surface of a solid, the normal specific acoustic impedance may be complex and consequently

$$\mathbf{z}_n = r_n + jx_n \tag{6.12}$$

where r_n is its resistive component and x_n is its reactive component.

Let us now replace fluid medium II of Fig. 6.1 by a solid medium. The separate boundary conditions of continuity of pressure and of particle velocity at $x = 0$ as utilized in Sect. 6.2 become instead a condition of continuity of their ratio, i.e.,

$$\frac{\mathbf{p}_i + \mathbf{p}_r}{\mathbf{u}_i + \mathbf{u}_r} = \mathbf{z}_n \tag{6.13}$$

at $x = 0$. Upon substitution into this equation of the expressions for pressure and particle velocity as obtained from equations 6.1, 6.2, and 6.5, it becomes

$$\frac{(A_1 + \mathbf{B}_1)\rho_1 c_1}{(A_1 - \mathbf{B}_1)} = \mathbf{z}_n \tag{6.13a}$$

Solving equation 6.13*a* for $\mathbf{B}_1$ gives

$$\mathbf{B}_1 = A_1 \frac{\mathbf{z}_n - \rho_1 c_1}{\mathbf{z}_n + \rho_1 c_1} \tag{6.14}$$

or upon substitution for $\mathbf{z}_n$ from equation 6.12

$$\mathbf{B}_1 = A_1 \frac{(r_n - \rho_1 c_1) + jx_n}{(r_n + \rho_1 c_1) + jx_n} \tag{6.14a}$$

It is to be noted that when $\mathbf{z}_n$ is real, equation 6.14 becomes equivalent to equation 6.7. Excepting in those cases where $\mathbf{z}_n$ is real, the pressure amplitude constant $\mathbf{B}_1$ is complex and consequently the reflected wave at the boundary may either lead or lag the incident wave by angles ranging from 0° to 180°. By taking the magnitude of the right-hand side of equation 6.14*a* we obtain

$$B_1 = A_1 \left[\frac{(r_n - \rho_1 c_1)^2 + x_n^2}{(r_n + \rho_1 c_1)^2 + x_n^2}\right]^{1/2} \tag{6.14b}$$

as an expression for determining the magnitude of the reflected pressure amplitude.

The sound power reflection coefficient is now

$$\alpha_r = \frac{B_1^2}{A_1^2} = \frac{(r_n - \rho_1 c_1)^2 + x_n^2}{(r_n + \rho_1 c_1)^2 + x_n^2} \tag{6.15}$$

The sound power transmission coefficient may most readily be obtained from the equation

$$\alpha_t = (1 - \alpha_r) \tag{6.16}$$

The latter equation is in effect a statement of the law of conservation of acoustic energy, namely that the sum of the reflected and transmitted power must equal the incident power. Then

$$\alpha_t = \frac{4 r_n \rho_1 c_1}{(r_n + \rho_1 c_1)^2 + x_n^2} \tag{6.17}$$

The wave transmitted into the solid is in many cases an attenuated wave which is absorbed in the solid. Consequently, the coefficient of equation 6.17 is frequently referred to as α_n, the sound power absorption coefficient of the surface for normally incident waves.

Let us now consider reflection from the surfaces of relatively rigid nonporous solids such as steel, glass, sealed concrete, etc. In an infinite solid material and also in finite solids of such a width that the wave front extends over a number of wavelengths, three types of elastic waves may be propagated including both plane longitudinal and plane shear waves. In an isotropic solid having a large cross section at right angles to the direction of propagation, the so-called *bulk* or *plate* velocity of longitudinal waves is given by

$$c = \sqrt{\frac{B + \frac{4}{3}G}{\rho_0}} \tag{6.18}$$

where B and G are respectively the bulk and the shear modulus of the solid and ρ_0 is its density. Numerical values for the *bulk* velocity for various solids are given in Table I in the appendix along with the corresponding characteristic impedances $\rho_0 c$. It should be noted that the bulk velocity given for each material is always higher than that given for longitudinal waves in thin bars as previously discussed in Chapter 3. Consequently, the above equations may be used to discuss reflection and transmission phenomena occurring at the surfaces of the solids listed in the appendix by substitution of the listed numerical values of the bulk characteristic impedances $\rho_0 c$ for $\mathbf{z}_n$.

The above method for determining $\mathbf{z}_n$ is not applicable if the solid body is so thin or so flexible that it vibrates as a unit in the manner of a membrane or thin plate. In these cases, the surface must be considered as having a normal specific acoustic impedance, i.e., a ratio of driving acoustic pressure to resulting velocity of the surface, as determined by methods similar to that used for the driven membrane previously discussed in Sect. 4.8.

Finally, for such porous solid materials as acoustic tile, mineral wool, porous bricks, felt, etc., the action of an acoustic pressure on the surface is not solely one of elastic compression of the solid but also one of moving fluid back and forth in voids within the solid. Here, the normal specific acoustic impedance at the surface has both resistive and reactive components, both of which in turn usually depend upon frequency. Further discussion of factors influencing $\mathbf{z}_n$ including frequency, thickness, porosity, and density of the material is contained in the reference given below.[1]

6.4 Standing Wave Patterns. The formation of a reflected wave at any plane boundary of a fluid medium will, of course, generate a pattern of standing waves in the fluid. When the pressure amplitude constant $\mathbf{B}_1$ of the reflected wave is complex, it is possible to show by methods similar to those previously utilized in Sect 6.2, that the amplitude P_1 of the standing wave pattern is given by

$$P_1 = [(A_1 + B_1)^2 \cos^2 (k_1 x + \theta/2) + (A_1 - B_1)^2 \sin^2 (k_1 x + \theta/2)]^{1/2} \tag{6.19}$$

[1] Zwikker and Kosten, *Sound Absorbing Materials*, Elsevier Publishing Co., (1949).

where θ is a phase angle defined by

$$\mathbf{B}_1 = B_1 e^{j\theta} \tag{6.20}$$

This angle θ measures the amount by which the reflected pressure at the surface of a solid leads or lags the incident pressure.

The formation of these standing waves makes it difficult if not impossible to measure the pressure amplitude of the initially incident plane progressive wave when reflecting walls are present. Consequently, it has been necessary to develop types of nonreflecting treatments for the walls of both *anechoic chambers*, used for accurate measurement of sound waves in air, and *anechoic tanks*, used for similar measurements of sound waves in water.

On the other hand, when we desire to measure the normal specific acoustic impedance of a surface, measurement of the pattern of standing waves generated by a plane wave normally incident on the surface, will enable us to calculate $\mathbf{z}_n$. The technique for doing this is essentially the same as that used for measuring an unknown terminating impedance on a transmission line relative to the characteristic impedance of the line. If we can determine both the magnitude and the phase of the reflected pressure amplitude $\mathbf{B}_1$ relative to the incident pressure amplitude A_1, then substitution into equation 6.13*a* will determine $\mathbf{z}_n$ in terms of $\rho_1 c_1$, the characteristic impedance of the fluid. The magnitude of B_1 relative to A_1 is determined by measurement of the so-called *standing wave ratio* SWR, the ratio of the pressure amplitude at an antinode to the pressure amplitude at a node or

$$\text{SWR} = \frac{A_1 + B_1}{A_1 - B_1} \tag{6.21}$$

This equation may be rewritten in a form more convenient for computing the ratio B_1/A_1 as

$$\frac{B_1}{A_1} = \frac{\text{SWR} - 1}{\text{SWR} + 1} \tag{6.21a}$$

Finally, by measurement of the position of either the first antinode or the first node relative to the reflecting wall, it is possible to compute the phase angle θ by which $\mathbf{B}_1$ leads A_1. For example, equation 6.19 indicates that all nodes will be located at coordinate positions such that $\sin(k_1 x + \theta/2)$ has its maximum magnitude of unity. In particular, the first node is located at a position such that $(k_1 x + \theta/2) = -\pi/2$, which may be solved for θ to give

$$\theta = -\pi - 2k_1 x \tag{6.22}$$

As an illustration of this method of determining $\mathbf{z}_n$, let us assume a pattern of standing waves in which the standing wave ratio is $\text{SWR} = 2$ and the first node is located at a distance of $\frac{3}{8}$ of a wavelength from the reflecting surface, i.e., $x = -3\lambda_1/8$. The negative sign is required for the coordinate position of the node since the reflecting surface has been assumed at $x = 0$. A substitution of this value of x into equation 6.22 leads to $\theta = -\pi - 2(2\pi/\lambda_1)(-3\lambda_1/8) = \pi/2$. A substitution of SWR = 2 into equation 6.21 leads to $B_1/A_1 = \frac{1}{3}$. Therefore $\mathbf{B}_1 = (A_1/3)e^{j\pi/2} = j(A_1/3)$. Finally, a substitution of this value of $\mathbf{B}_1$ into equation 6.13*a* leads to $\mathbf{z}_n = (0.8 + j0.6)\rho_1 c_1$.

In actual practice it is unnecessary to carry out the lengthy calculations for θ, $\mathbf{B}_1$, and $\mathbf{z}_n$ as outlined above. Instead it is possible to use a "Smith chart," a nomographic device which enables one rapidly to determine $r_n/\rho_1 c_1$ and $x_n/\rho_1 c_1$ from measurements of the standing wave ratio and position of the node nearest the reflecting surface.[1]

6.5 Transmission through Three Media; Normal Incidence. Let us now consider the transmission of a plane acoustic wave from one medium through a second and into a third medium. Assume that the initial wave is traveling in the positive x direction, that the boundary between medium I and medium II is the plane OO', located at $x = 0$, and that the boundary between medium II and medium III is the plane PP' located at $x = l$ as shown in Fig. 6.2. Let the characteristic impedances of the media be $\rho_1 c_1$, $\rho_2 c_2$, and $\rho_3 c_3$, respectively.

The incident wave in medium I may be represented by

$$(\mathbf{p}_i)_1 = A_1 e^{j(\omega t - k_1 x)} \tag{6.23}$$

When this wave first arrives at the boundary between media I and II, some of the energy is reflected and some is transmitted into the second medium. After passing through medium II a part of this transmitted wave is reflected at $x = l$ and is returned to $x = 0$, where it is again partially reflected, the

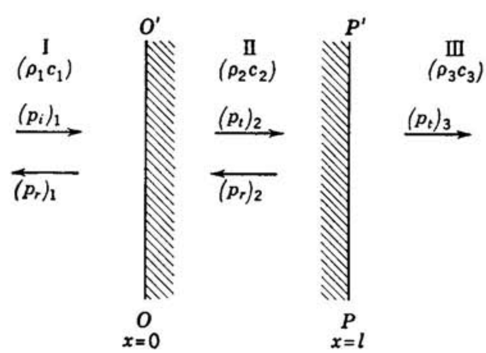

Fig. 6.2. Transmission of plane waves across two boundaries.

[1] Beranek, *Acoustic Measurements*, 317–321, John Wiley and Sons, (1949).

reflected portion combining with the wave being initially transmitted into the second medium, and the transmitted portion combining with the wave being initially reflected at the boundary. This process is then repeated, and after a sufficient number of transits of medium II the conditions will reach a steady state, in which the rate at which energy is reflected back into medium I plus the rate at which it is transmitted into medium III is equal to the rate of arrival of the incident energy. Under these steady-state conditions the wave reflected into medium I may be represented by

$$(\mathbf{p}_r)_1 = \mathbf{B}_1 e^{j(\omega t + k_1 x)} \tag{6.24}$$

the transmitted and reflected waves in medium II by

$$(\mathbf{p}_t)_2 = \mathbf{A}_2 e^{j(\omega t - k_2 x)} \tag{6.25}$$

and

$$(\mathbf{p}_r)_2 = \mathbf{B}_2 e^{j(\omega t + k_2 x)} \tag{6.26}$$

respectively, and the wave transmitted into medium III by

$$(\mathbf{p}_t)_3 = \mathbf{A}_3 e^{j[\omega t - k_3(x - l)]} \tag{6.27}$$

It should be noted that the steady-state waves established in media I and II differ in both amplitude and phase from those *initially* reflected and transmitted at the first boundary.

The boundary condition of continuity of pressure at $x = 0$ gives

$$A_1 + \mathbf{B}_1 = \mathbf{A}_2 + \mathbf{B}_2 \tag{6.28}$$

and that of continuity of particle velocity gives

$$\rho_2 c_2 (A_1 - \mathbf{B}_1) = \rho_1 c_1 (\mathbf{A}_2 - \mathbf{B}_2) \tag{6.29}$$

Similarly, at $x = l$, the condition of continuity of pressure gives

$$\mathbf{A}_2 e^{-jk_2 l} + \mathbf{B}_2 e^{jk_2 l} = \mathbf{A}_3 \tag{6.30}$$

and that of continuity of particle velocity gives

$$\rho_3 c_3 (\mathbf{A}_2 e^{-jk_2 l} - \mathbf{B}_2 e^{jk_2 l}) = \rho_2 c_2 \mathbf{A}_3 \tag{6.31}$$

In order to determine the complex amplitude $\mathbf{A}_3$ of the transmitted wave in medium III it is necessary to eliminate $\mathbf{B}_1$, $\mathbf{A}_2$, and $\mathbf{B}_2$ from these four equations. In carrying out this procedure equations 6.28 and 6.29 may be combined to eliminate $\mathbf{B}_1$ and give

$$A_1 = \frac{(\rho_2 c_2 + \rho_1 c_1)\mathbf{A}_2 + (\rho_2 c_2 - \rho_1 c_1)\mathbf{B}_2}{2\rho_2 c_2} \tag{6.32}$$

Similarly, equations 6.30 and 6.31 may be combined to give

$$\mathbf{A}_2 = \frac{(\rho_3 c_3 + \rho_2 c_2)}{2\rho_3 c_3} \mathbf{A}_3 e^{jk_2 l} \tag{6.33}$$

and

$$\mathbf{B}_2 = \frac{(\rho_3 c_3 - \rho_2 c_2)}{2\rho_3 c_3} \mathbf{A}_3 e^{-jk_2 l} \tag{6.34}$$

A substitution of these two equations into equation 6.32 gives

$$A_1 = \frac{[(\rho_2 c_2 + \rho_1 c_1)(\rho_3 c_3 + \rho_2 c_2)e^{jk_2 l} + (\rho_2 c_2 - \rho_1 c_1)(\rho_3 c_3 - \rho_2 c_2)e^{-jk_2 l}]}{4\rho_3 c_3 \rho_2 c_2} \mathbf{A}_3$$

which may be reduced to

$$\frac{A_1}{\mathbf{A}_3} = \frac{(\rho_3 c_3 + \rho_1 c_1)\cos k_2 l}{2\rho_3 c_3} + \frac{j(\rho_2{}^2 c_2{}^2 + \rho_3 c_3 \rho_1 c_1)\sin k_2 l}{2\rho_3 c_3 \rho_2 c_2} \tag{6.35}$$

The *magnitude* of the complex ratio $A_1/\mathbf{A}_3$ is a measure of the ratio of the pressure amplitude of the incident wave to that of the transmitted wave, and the *phase angle* of this complex ratio is a measure of the amount by which the phase of the incident wave at $x = 0$ leads that of the transmitted wave at $x = l$.

The sound power transmission coefficient α_t from medium I through II into III is

$$\alpha_t = \frac{\dfrac{(P_t{}^2)_3}{2\rho_3 c_3}}{\dfrac{(P_i{}^2)_1}{2\rho_1 c_1}} = \frac{\rho_1 c_1}{\rho_3 c_3} \frac{A_3{}^2}{A_1{}^2}$$

The magnitude of $(A_1/A_3)^2$ may be obtained from equation 6.35 by squaring its real and imaginary parts and adding which upon substitution into the equation immediately above leads to

$$\alpha_t = \frac{4\rho_3 c_3 \rho_1 c_1}{(\rho_3 c_3 + \rho_1 c_1)^2 \cos^2 k_2 l + (\rho_2 c_2 + \rho_3 c_3 \rho_1 c_1/\rho_2 c_2)^2 \sin^2 k_2 l} \tag{6.36}$$

There exist a number of special forms of equation 6.36 which are of particular interest. One is that for which the final fluid medium is the same as the initial fluid medium and consequently, $\rho_1 c_1 = \rho_3 c_3$. Then,

$$\alpha_t = \frac{4}{4\cos^2 k_2 l + \left(\dfrac{\rho_2 c_2}{\rho_1 c_1} + \dfrac{\rho_1 c_1}{\rho_2 c_2}\right)^2 \sin^2 k_2 l} \tag{6.37}$$

If in addition, $\rho_2 c_2 \gg \rho_1 c_1$, equation 6.37 further simplifies to

$$\alpha_t \approx \frac{4}{4\cos^2 k_2 l + (\rho_2 c_2/\rho_1 c_1)^2 \sin^2 k_2 l} \tag{6.37a}$$

The latter situation applies, for example, to the transmission of sound waves from air in one room through a solid wall into air in an adjacent room. It also applies to sound waves in water passing through a steel plate into water on the opposite side of the plate.

Actually, the solid materials forming the walls of rooms have such large characteristic impedances relative to air that $(\rho_2 c_2/\rho_1 c_1)\sin k_2 l \gg 2\cos k_2 l$ for all reasonable frequencies and thicknesses of walls. Therefore, when the fluid medium is air, equation 6.37*a* further simplifies to

$$\alpha_t \approx \frac{4\rho_1^{\,2}c_1^{\,2}}{\rho_2^{\,2}c_2^{\,2}\sin^2 k_2 l} \tag{6.37b}$$

Finally, for all situations excepting those of high frequencies and very thick walls, $k_2 l \ll 1$ and consequently $\sin k_2 l$ may be replaced by $k_2 l$ so that equation 6.37*b* becomes

$$\alpha_t \approx \frac{4\rho_1^{\,2}c_1^{\,2}}{\rho_2^{\,2}c_2^{\,2}k_2^{\,2}l^2} \tag{6.37c}$$

In order to check the validity of the above assumption it is to be noted that at 1000 cycles/sec, the value of $k_2 l$ for a 0.1-m thick concrete wall is $k_2 l = 2\pi \times 1000 \times 0.1/3100 = 0.2$. An equation identical with equation 6.37*c* may be obtained by ignoring any wave transmission through medium II and instead considering that at $x = 0$ it merely adds a specific acoustic reactance $j\omega\rho_2 l$ to the characteristic impedance $\rho_1 c_1$ of the continuing medium. Equations derived in Sect. 6.3 may then be used to derive expressions for α_t and α_r. The presence of a solid wall is thus seen to exert essentially the same influence on the propagation of sound waves normally incident on the wall as does the insertion of an inductance in a transmission line. Equation 6.37*c* may be written in a form which is more readily used in making calculations if we replace the product $\rho_2 l$ by σ, where σ is the area density of the wall in kg/m^2, and replace $c_2 k_2$ by $2\pi f$. Then

$$\alpha_t \approx \left(\frac{\rho_1 c_1}{\pi}\right)^2 \cdot \frac{1}{\sigma^2 f^2} \tag{6.38}$$

The transmission characteristics of the walls of a room are usually expressed in terms of a *transmission loss* TL in decibels. This transmission loss is defined as

$$\mathrm{TL} = 10\log\frac{I_i}{I_t} \tag{6.39}$$

where I_i is the incident intensity and I_t is the transmitted intensity. However, since $\alpha_t = I_t/I_i$, we may substitute equation 6.38 into equation 6.39 with the result

$$\mathrm{TL} = 20\log\frac{\pi}{\rho_1 c_1} + 20\log\sigma f \tag{6.40}$$

Finally, upon substituting 415, the characteristic impedance of air, for $\rho_1 c_1$, and converting units so that σ is expressed in lb/ft^2 rather than in kg/m^2, a practical engineering form of the equation is obtained as

$$\text{TL} = -31.4 + 20 \log \sigma f \tag{6.40a}$$

Experimental results for sound waves normally incident on solid walls are in good agreement with the predictions of this equation. It should be noted that the predicted transmission loss increases by 6 db for a doubling either of frequency or of mass per unit area.

Table 6.1 Transmission loss for solid wall materials

Material	Thickness, in.	Area Density, lb/ft^2	Frequency, cycles/sec	Transmission Loss, db
Gypsum wall board	1	4.5	500	31
Gypsum wall board	2	9.0	500	34
Gypsum wall board	2	9.0	250	32
Gypsum wall board	2	9.0	1000	40
Glass	0.25	3.0	500	31
Concrete	4	53.5	500	45
Brick	12	121	500	53

In actual situations, the sound waves in a room are nearly randomly incident on the walls of a room rather than normally incident, resulting in a lesser transmission loss than that predicted by equation 6.40*a*. Table 6.1 contains measured values for the transmission loss of *randomly* incident sound waves through typical wall materials. An empirical equation fitted to this and other data for the transmission loss of randomly incident sound waves on solid walls is

$$\text{TL} = -17 + 15 \log \sigma f \tag{6.41}$$

Discussions about the influence of double-wall construction, panel vibration, random versus normal incidence, as well as voluminous data on transmission loss through various materials, may be found in the *Handbook of Noise Control*[1] and other publications.[2]

In the case of solid panels in water, both terms occurring in the denominator of equation 6.37*a* usually are significant so that the complete equation must be used. However, for either such thin panels or such low

[1] Harris, *Handbook of Noise Control*, Ch. 20, McGraw-Hill Book Co., (1957).

[2] London, *J. Acoust. Soc. Am.*, **22**, 270 (1950).

frequencies that $(\rho_2 c_2/\rho_1 c_1) \sin k_2 l \ll 1$, equation 6.37*a* simplifies to $\alpha_t \approx 1$. This behavior is used in the design of free-flooding streamlined domes for housing sonar transducers. These domes are constructed of reinforced panels of either stainless steel or rubber of such a small thickness that little loss takes place as sound is transmitted through the dome into exterior sea water.

Another special form of equation 6.36 is obtained by assuming that the intermediate medium has a larger characteristic impedance than either medium I or medium III yet is of such a small thickness and moderate characteristic impedance that $\rho_2 c_2 \sin k_2 l \ll 1$ and $\cos k_2 l \approx 1$. Then, equation 6.36 is reduced to

$$\alpha_t \approx \frac{4\rho_3 c_3 \rho_1 c_1}{(\rho_3 c_3 + \rho_1 c_1)^2} \tag{6.42}$$

This equation is equivalent to equation 6.11 which gives the sound power transmission coefficient for a wave moving directly from medium I into medium III. It is therefore apparent that a *thin* membrane of solid material of appropriate characteristic impedance may be used in preventing two gases or two liquids from mixing with each other and yet not interfere with sound transmission between them.

Similarly, if the intermediate medium is of such a thickness that $k_2 l \approx n\pi$, where n is any integer, we obtain the same expression for α_t as with a thin layer. It should be noted, however, that the transmission of sound is independent of the presence of a *thick* intervening layer only for bands of frequencies centered about the particular frequencies given by $f = nc_2/2l$. This is in contrast with the transmission through a thin layer, where α_t is independent of the intervening medium for *all* frequencies below some upper limit determined by $\rho_2 c_2 \sin k_2 l \ll 1$.

Finally, if $k_2 l \approx (2n - 1)\pi/2$, where n is any integer, then $\cos k_2 l \approx 0$ and $\sin k_2 l \approx 1$, so that equation 6.36 becomes

$$\alpha_t \approx \frac{4\rho_1 c_1 \rho_3 c_3}{\left(\rho_2 c_2 + \dfrac{\rho_1 c_1 \rho_3 c_3}{\rho_2 c_2}\right)^2} \tag{6.43}$$

This ratio becomes equal to unity when

$$\rho_2 c_2 = \sqrt{\rho_1 c_1 \rho_3 c_3} \tag{6.44}$$

It is therefore possible to obtain 100 per cent transmission of acoustic power from one medium to another of different characteristic impedance, through the use of an intermediate medium whose characteristic impedance is the geometric mean of the other two. However, this action is selective, since it occurs only for bands of frequencies centered about the particular frequencies for which

$$f = (2n - 1)\frac{c_2}{4l}$$

i.e., only when the thickness of the intervening layer is such that

$$l = (2n - 1)\frac{\lambda_2}{4}$$

This technique for obtaining 100 per cent transmission of acoustic power through the use of a quarter-wavelength thick intermediate layer is similar to the method of making glass lenses nonreflecting by coating them with a quarter-wavelength thick layer of some suitable material, such as an alkali fluoride.

The phase angle θ of the complex quantity $A_1/\mathbf{A}_3$ is a measure of the difference in phase between the incident and transmitted waves, and is given by

$$\tan\theta = \frac{(\rho_2{}^2c_2{}^2 + \rho_1c_1\rho_3c_3)}{\rho_2c_2(\rho_1c_1 + \rho_3c_3)}\tan k_2l \tag{6.45}$$

On first thought one might expect the difference in phase between these two waves to be merely k_2l, which represents the time required for the wave to travel through medium II. However, as can be seen from equation 6.45, this is not in general true, the reason being that in the steady state there is usually a shift in phase between the incident and transmitted waves at the boundary $x = 0$.

6.6 Transmission from One Fluid Medium to Another; Oblique Incidence. Before discussing the transmission of acoustic waves across a plane boundary between two media when the angle of incidence is not 0°, it is necessary to derive an expression for the pressure in a medium through which plane waves are traveling in an arbitrary direction, making an angle θ with the positive x axis. Without loss of generality we may assume that the direction of propagation of the waves is in the xy plane, so that the excess pressure is everywhere independent of the z coordinate.

Now consider the plane wave fronts AA', BB', etc., of Fig. 6.3. The excess pressure is constant over each of these wave fronts, and may be represented by

$$\mathbf{p} = \mathbf{A}e^{j(\omega t - kd)} \tag{6.46}$$

where d is the distance from the z axis to the wave front, measured in the direction of propagation of the wave. One form of the equation for a plane corresponding to the wave front AA' is

$$d = x\cos\theta + y\sin\theta \tag{6.47}$$

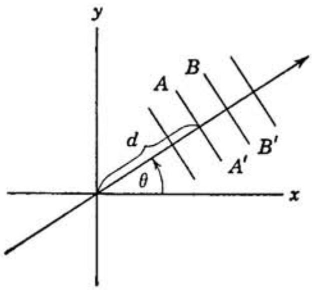

Fig. 6.3. Plane wave fronts for a direction of propagation θ.

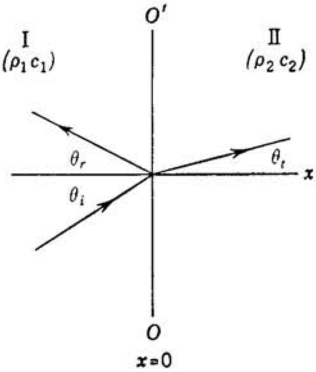

Fig. 6.4. Oblique incidence of plane waves.

so that we may eliminate d from equation 6.46 and obtain a general expression for the excess pressure at any point in the medium as a function of the coordinates and of the direction of wave propagation,

$$\mathbf{p} = \mathbf{A}e^{j(\omega t - kx\cos\theta - ky\sin\theta)} \tag{6.48}$$

Assume that the boundary separating two media is a plane OO' passing through the origin normal to the x axis, as shown in Fig. 6.4. Then the equation for the pressure in the incident wave traveling through medium I in a direction making an angle θ_i with the positive x axis is

$$\mathbf{p}_i = A_1 e^{j(\omega t - k_1 x\cos\theta_i - k_1 y\sin\theta_i)} \tag{6.49}$$

The corresponding expressions for the reflected wave in medium I making an angle $(180 - \theta_r)$ with the positive x axis and the transmitted wave in medium II making an angle θ_t with the positive x axis are, respectively,

$$\mathbf{p}_r = \mathbf{B}_1 e^{j(\omega t + k_1 x\cos\theta_r - k_1 y\sin\theta_r)} \tag{6.50}$$

and

$$\mathbf{p}_t = \mathbf{A}_2 e^{j(\omega t - k_2 x\cos\theta_t - k_2 y\sin\theta_t)} \tag{6.51}$$

Applying the condition of continuity of pressure at the boundary $(x = 0)$ between the two media, we have, after elimination of the common factor $e^{j\omega t}$,

$$A_1 e^{-jk_1 y\sin\theta_i} + \mathbf{B}_1 e^{-jk_1 y\sin\theta_r} = \mathbf{A}_2 e^{-jk_2 y\sin\theta_t} \tag{6.52}$$

This expression can be simplified by using the well-known laws of reflection and refraction of plane waves, i.e., the angle of incidence θ_i is equal to the angle of reflection θ_r, and Snell's law

$$\frac{\sin\theta_i}{\sin\theta_t} = \frac{c_1}{c_2} \tag{6.53}$$

These laws may be derived for acoustic waves in exactly the same manner as for the more familiar analysis of the reflection and refraction of light waves. Since $c_1/c_2 = k_2/k_1$, an alternative form of the law of refraction is

$$\frac{\sin \theta_i}{\sin \theta_t} = \frac{k_2}{k_1} \tag{6.53a}$$

From the relations $\theta_i = \theta_r$ and equation 6.53*a* it is apparent that the three exponential terms of equation 6.52 are identical, so that

$$A_1 + \mathbf{B}_1 = \mathbf{A}_2 \tag{6.54}$$

The condition for continuity of the normal or x component of velocity at the boundary is

$$\mathbf{u}_i \cos \theta_i + \mathbf{u}_r \cos (180° - \theta_r) = \mathbf{u}_t \cos \theta_t$$

Replacing each velocity by the appropriate value of $\mathbf{p}/\rho_0 c$, this condition reduces to

$$\frac{A_1}{\rho_1 c_1} \cos \theta_i - \frac{\mathbf{B}_1}{\rho_1 c_1} \cos \theta_r = \frac{\mathbf{A}_2}{\rho_2 c_2} \cos \theta_t \tag{6.55}$$

Equations 6.54 and 6.55 can be combined to eliminate $\mathbf{A}_2$, giving

$$\mathbf{B}_1 = A_1 \frac{\rho_2 c_2 \cos \theta_i - \rho_1 c_1 \cos \theta_t}{\rho_2 c_2 \cos \theta_i + \rho_1 c_1 \cos \theta_t} \tag{6.56}$$

It should be noted that for normal incidence both θ_i and θ_t are zero, so that equation 6.56 reduces to equation 6.7.

The sound power reflection coefficient α_r is given by

$$\alpha_r = \left(\frac{\rho_2 c_2 \cos \theta_i - \rho_1 c_1 \cos \theta_t}{\rho_2 c_2 \cos \theta_i + \rho_1 c_1 \cos \theta_t} \right)^2 \tag{6.57}$$

It is possible to determine the ratio $\mathbf{A}_2/A_1$ and the ratio of transmitted intensity to incident intensity for an oblique wave in a manner similar to that used in deriving equation 6.11. The resulting expression for the *intensity* transmission coefficient α_i is

$$\alpha_i = \frac{4\rho_1 c_1 \rho_2 c_2 \cos^2 \theta_i}{(\rho_2 c_2 \cos \theta_i + \rho_1 c_1 \cos \theta_t)^2} \tag{6.58}$$

Since a sound beam is either widened or narrowed upon oblique transmission into a second medium, equation 6.58 does not give the correct expression for the ratio of the total power transmitted to that incident. The latter ratio is usually of greater significance than α_i and is defined as the sound power transmission coefficient α_t. It can be most readily computed from equation 6.16 giving

$$\alpha_t = \frac{4\rho_1 c_1 \rho_2 c_2 \cos\theta_i \cos\theta_t}{(\rho_2 c_2 \cos\theta_i + \rho_1 c_1 \cos\theta_t)^2} \tag{6.59}$$

It would be possible to eliminate $\cos\theta_t$ from equation 6.59 by using the law of refraction (equation 6.53), but the resulting equation is so involved that it is more expeditious to calculate the numerical value of $\cos\theta_t$ from equation 6.53 for each particular angle of incidence, and then to substitute into equation 6.59.

There are a number of interesting special cases that arise as the angle of incidence is increased. For example, when $\rho_2 c_2 \cos\theta_i = \rho_1 c_1 \cos\theta_t$, the power reflection ratio is zero, i.e., all the incident power is transmitted. If this condition is combined with equation 6.53 to eliminate θ_t, then

$$\cot^2\theta_i = \frac{(c_1/c_2)^2 - 1}{(\rho_2/\rho_1)^2 - (c_1/c_2)^2} \tag{6.60}$$

gives the angle of incidence for which there is 100 per cent transmission. This angle is commonly referred to as the angle of *intromission*. Since $\cot^2\theta_i$ is always a positive, real quantity, this angle will exist only if either $\rho_2/\rho_1 > c_1/c_2 > 1$ or $\rho_2/\rho_1 < c_1/c_2 < 1$.

If $c_1 < c_2$, then for some *critical angle* of incidence, θ_c, the refracted ray makes an angle of 90° with the normal to the interface. This critical angle is given by

$$\sin\theta_c = \frac{c_1}{c_2} \tag{6.61}$$

If the angle of incidence is equal to or greater than the critical angle, no acoustic energy is transmitted into the second medium.

If $c_1 > c_2$ and if the angle of incidence θ_i approaches 90°, the condition of *grazing incidence*, then $\cos\theta_i \to 0$ and equation 6.57 is reduced to

$$\alpha_r \approx \left(-\frac{\rho_1 c_1 \cos\theta_t}{\rho_1 c_1 \cos\theta_t}\right)^2 = 1$$

Consequently, as the angle of incidence approaches 90° there is complete reflection of the incident acoustic energy, irrespective of the relative characteristic impedances of the two media.

Table 6.2 gives an illustrative set of values showing how the angle of refraction θ_t and the sound transmission coefficient α_t vary with the angle of incidence for waves traveling from oil into water. The table is computed for an oil having a density ρ_1 of 900 kg/m^3, a sound velocity c_1 of 1300 m/sec, and a resulting characteristic impedance of 1,117,000 rayls. It should be noted that, in spite of the fact that the characteristic impedance of the oil differs from that of water by more than 20 per cent, the sound transmission coefficient is very nearly equal to unity for all angles of incidence except those approaching the critical angle of 61.4°.

Table 6.2 Transmission from oil to water

θ_i (oil), degrees	θ_t (water), degrees	α_t
0	0	0.986
30	34.8	0.979
45	54.8	0.953
50	61.2	0.935
55	69.0	0.885
60	81.0	0.63
61.4	90.0	0.00

6.7 Reflection at the Surface of a Solid; Oblique Incidence. No single simple method is available for analyzing the reflection of plane waves obliquely incident on the surface of a solid. Because of differences in the porosity and of the internal elastic structure of various solids, the nature of the transmitted wave varies widely and thereby influences the reflected wave. For instance, the wave transmitted into the solid may be (1) refracted so that it is propagated effectively only at right angles to the surface, (2) refracted in a manner similar to plane waves entering a second fluid as has been discussed above in Sect. 6.6, or (3) refracted into two waves, longitudinal bulk waves traveling in one direction and transverse shear waves traveling at a lower velocity and in a different direction.

The first type of refraction occurs for the so-called *normally reacting* or *locally acting* surfaces. One example of this type of refraction is that occurring in anisotropic solids where waves propagated parallel to the surface travel with a much lower velocity than those propagated perpendicular to the surface. This type of propagation is typical of solids having a honeycomb structure in which the velocity of compressional waves through the fluid contained in capillary pores oriented at right angles to the surface is much higher than that at right angles to this direction from pore to pore through the solid material of the structure. This type of refraction also will occur in an isotropic solid when the velocity of longitudinal wave propagation in the solid is small compared with that in the fluid. When $c_2 \ll c_1$, Snell's law (equation 6.53) requires that $\theta_t \ll \theta_i$, resulting in a marked bending of the transmitted wave toward the normal direction. Many of the highly sound absorbing materials used in building

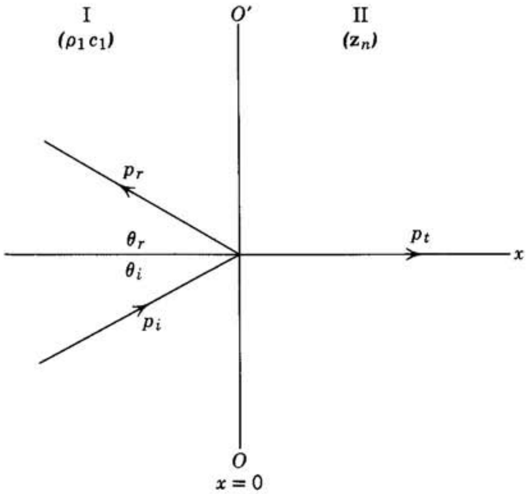

Fig. 6.5. Oblique incidence of plane waves on a normally reacting solid.

construction, such as acoustic tile, perforated panels, etc., appear to behave as normally reacting surfaces.

Since for such surfaces, the refracted ray travels nearly normal to the surface irrespective of the particular angle of incidence, it is reasonable to assume that the ratio of acoustic pressure acting upon the surface to the fluid velocity normal to the surface will be independent of the direction of the incident wave. Consequently, refraction from such a surface is most readily discussed in terms of the normal specific acoustic impedance $\mathbf{z}_n$ of its surface as defined by equation 6.12. The condition of continuity of normal specific acoustic impedance applied at the surface OO' of Fig. 6.5 may therefore be expressed as

$$\frac{\mathbf{p}_i + \mathbf{p}_r}{\mathbf{u}_i \cos\theta_i + \mathbf{u}_r \cos(180 - \theta_r)} = \mathbf{z}_n \tag{6.62}$$

If we replace $\mathbf{u}_i$ by $\mathbf{p}_i/\rho_1 c_1$ and $\mathbf{u}_r$ by $\mathbf{p}_r/\rho_1 c_1$ and substitute from equations 6.49 and 6.50 respectively for $\mathbf{p}_i$ and $\mathbf{p}_r$

$$\frac{(A_1 + \mathbf{B}_1)\rho_1 c_1}{(A_1 - \mathbf{B}_1)} = \mathbf{z}_n \cos\theta_i \tag{6.63}$$

is obtained. Solving this equation for $\mathbf{B}_1$ gives

$$\mathbf{B}_1 = A_1 \frac{(\mathbf{z}_n \cos\theta_i - \rho_1 c_1)}{(\mathbf{z}_n \cos\theta_i + \rho_1 c_1)} \tag{6.64}$$

This equation is similar in form to equation 6.14 and differs only in that $\mathbf{z}_n \cos\theta_i$ replaces $\mathbf{z}_n$. As a consequence, equations for the reflection and transmission coefficients applicable to this more general case may be obtained from those developed in Sect. 6.3 by replacing $\mathbf{z}_n$ with $\mathbf{z}_n \cos \theta_i$. For instance, the sound power reflection coefficient is

$$\alpha_r = \frac{(r_n \cos \theta_i - \rho_1 c_1)^2 + x_n^{\ 2} \cos^2 \theta_i}{(r_n \cos \theta_i + \rho_1 c_1)^2 + x_n^{\ 2} \cos^2 \theta_i} \tag{6.65}$$

and the sound power transmission (or absorption) coefficient is

$$\alpha_t = \frac{4 r_n \cos \theta_i \rho_1 c_1}{(r_n \cos \theta_i + \rho_1 c_1)^2 + x_n^{\ 2} \cos^2 \theta_i} \tag{6.66}$$

For most solid materials $r_n > \rho_1 c_1$, i.e., the resistive component of its normal specific acoustic impedance is greater than the characteristic impedance of fluids in contact with it, and consequently as the angle of incidence θ_i increases an angle will be reached where $r_n \cos \theta_i = \rho_1 c_1$. When this occurs, the sound reflection coefficient will be near its minimum value. In particular, if x_n were zero, α_r would be zero and α_t would be one

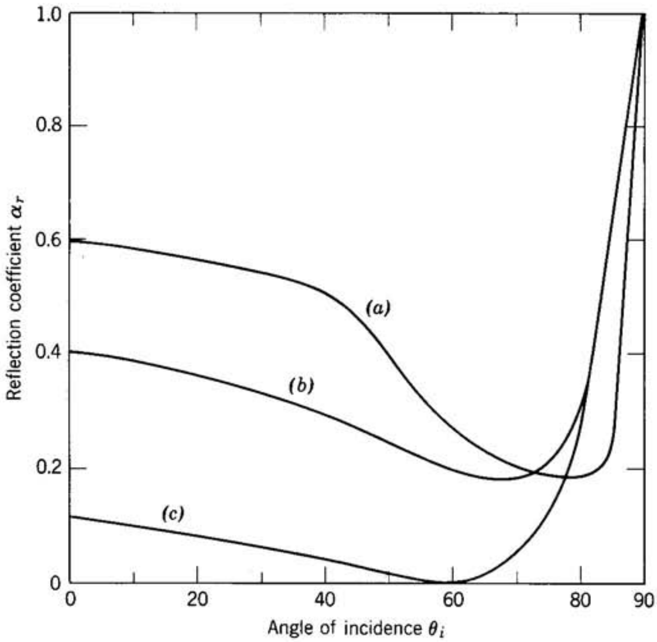

Fig. 6.6. Dependence of reflection coefficient upon angle of incidence for typical normally reacting solids. Curve (*a*) corresponds to $r_n/\rho_1 c_1 = x_n/\rho_1 c_1 = 4$. Curve (*b*) corresponds to $r_n/\rho_1 c_1 = x_n/\rho_1 c_1 = 2$. Curve (*c*) corresponds to $r_n/\rho_1 c_1 = 2, x_n/\rho_1 c_1 = 0$.

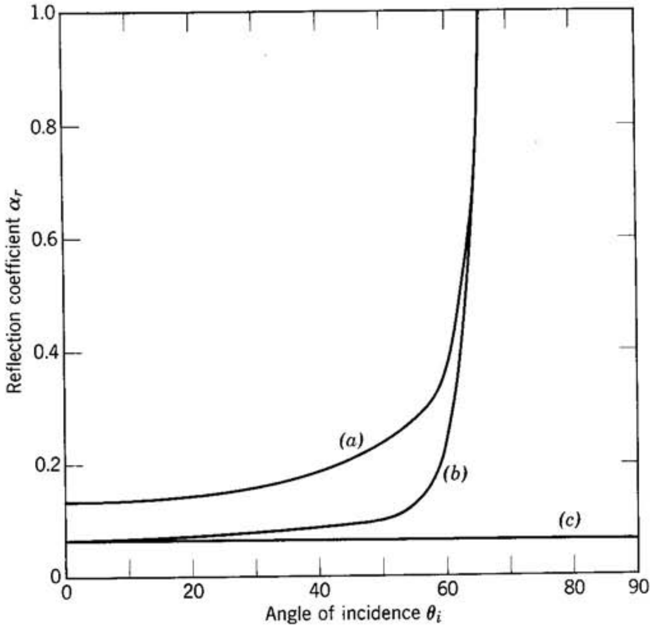

Fig. 6.7. Dependence of reflection coefficient upon angle of incidence for Rayleigh type of reflection. Curve (*a*) corresponds to $\rho_2 = 2\rho_1$, $c_2 = 1.1c_1$. Curve (*b*) corresponds to $\rho_2 = 1.5\rho_1$, $c_2 = 1.1c_1$. Curve (*c*) corresponds to $\rho_2 = 1.5\rho_1$, $c_2 = c_1$.

for $r_n \cos\theta_i = \rho_1 c_1$. For very large values of θ_i, i.e., as the incident angle approaches grazing incidence of $\theta_i \approx 90^\circ$, α_r approaches a value of one. Plotted in Fig. 6.6 are curves for the reflection coefficient α_r as a function of the angle of incidence θ_i for a few assumed values of the nondimensional parameters $r_n/\rho_1 c_1$ and $x_n/\rho_1 c_1$.

The second type of refraction and associated reflection that occurs in solids in contact with a fluid is similar to the so-called *Rayleigh* type of refraction occurring between two fluids as has been discussed in Sect. 6.6. The reflection that takes place in sea water from a sand or silt bottom is a good example of reflection associated with this type of refraction. Such a behavior is to be anticipated in that the saturated sand or silt is more like a fluid than a solid in its inability effectively to transmit shear waves. As a first order of approximation, equation 6.57 may be used for computing a reflection coefficient in which the sand or silt is assumed to be of a density ρ_2 and to transmit unattenuated plane waves with a velocity c_2. Measured values of ρ_2 for sand and silt range from 1.5 ρ_1 to 2.0 ρ_1, where ρ_1 is the density of sea water, and of c_2 range from 0.9 c_1 to 1.1 c_1, where c_1 is the velocity of sound in sea water. Use of the various equations of Sect. 6.6

indicate 100 per cent reflection for grazing incidence or for angles of incidence greater than that of the critical angle θ_c as determined by $\sin \theta_c = c_1/c_2$ followed by a gradual decrease in the reflection coefficient until its value for normal incidence is reached as θ_i approaches zero. It should be noted that if $c_2 < c_1$, an angle of intromission may occur for which the coefficient of reflection will be zero, i.e., all of the incident acoustic energy will enter the second medium. Plotted in Fig. 6.7 are curves for the reflection coefficient α_r as a function of the angle of incidence θ_i as computed for a few assumed values of the ratios ρ_2/ρ_1 and c_2/c_1, typical of those existing between a sand or silt bottom and sea water. Still more accurate predictions may be made, if in deriving an equation similar to equation 6.57, allowance is made for the fact that the wave transmitted into the sea bottom is of an attenuated nature similar to those which are discussed in Chapter 9.[1]

A third type of reflection of plane waves is that which occurs in fluids at the surface of a rigid elastic solid. A detailed discussion of this type of reflection requires a consideration of the propagation of both elastic shear and compressional waves in the solid and is not warranted in a general textbook on acoustics. Information on this type of reflection is available in the following references.[2,3]

PROBLEMS

6.1. A plane wave of 50 newtons/m^2 effective (rms) pressure and 1000-cycles/sec frequency is incident normally on the water-air boundary at the surface of the water. (*a*) What is the effective pressure of the plane wave transmitted into the air? (*b*) What is the intensity of the incident wave in the water and of the wave transmitted into the air? (*c*) Express, as a decibel reduction, the ratio of the intensity of the transmitted wave in air to that of the incident wave in water. (*d*) Answer the same three questions for the above sound wave assumed incident on a thick layer of ice. (*e*) What is the sound power reflection coefficient from the layer of ice?

6.2. A sound wave in air having a frequency of 500 cycles/sec and a pressure level of 60 db *re* 0.0002 microbar is normally incident on a boundary between the air and a second medium having a characteristic impedance of 830 rayls. (*a*) What is the effective (rms) pressure amplitude of the reflected waves? (*b*) of the transmitted waves? (*c*) At what distance from the boundary is the pressure amplitude in the pattern of standing waves equal to that of the incident wave?

6.3. Plane waves in water are normally incident on a flat concrete wall which may be considered to absorb all of the sound energy transmitted into it. The velocity of sound in the water is 1480 m/sec and the frequency of the waves is

[1] Mackenzie, *J. Acoust. Soc. Am.*, **32**, 221 (1960).

[2] Officer, *Introduction to the Theory of Sound Transmission*, pp. 207–211, McGraw-Hill Book Co., (1958).

[3] Ewing, Jardetzky, Press, *Elastic Waves in Layered Media*, pp. 79–83, McGraw-Hill Book Co., (1957).

1480 cycles/sec. The pattern of standing waves has a peak pressure amplitude of 15 newtons/m^2 at the wall and a pressure amplitude of 5 newtons/m^2 at the nearest pressure node at a distance of 0.25 m from the wall. (*a*) What is the ratio of the intensity of the reflected wave to that of the incident wave? (*b*) What is the specific acoustic impedance of the wall?

6.4. Given plane waves in water of 1000-cycles/sec frequency to be normally incident on a concrete wall. (*a*) What is the resulting standing wave ratio? (*b*) To what difference in pressure levels in decibels is this equivalent? (*c*) Where are the first three nodes located?

6.5. Given plane waves in air having a frequency of 200 cycles/sec to be normally incident on an acoustic tile panel having a normal specific acoustic impedance of $1000-j2000$ rayls. (*a*) What is the standing wave ratio in the resulting pattern of standing waves? (*b*) Where are the first two nodes located?

6.6. (*a*) What must be the thickness of, and the velocity of sound in, a plastic layer having a density of 1500 kg/m^3, if it is to transmit plane waves at a frequency of 20 kc/sec from water into steel with no reflection? (*b*) What would be the reflection coefficient back into water for normally incident waves impinging on an infinitely thick layer of this plastic?

6.7. Given a plane wave in water, having a frequency of 2000 cycles/sec, to impinge normally on a wide steel plate of 1.5-cm thickness. (*a*) What is the transmission loss expressed in decibels through the steel plate into water on the opposite side. (*b*) What is the sound power reflection coefficient of this plate? (*c*) Repeat the calculations of parts (*a*) and (*b*) for a 1.5-cm thick slab of sponge rubber having a density of 500 kg/m^3 and which propagates longitudinal waves with a velocity of 1000 m/sec.

6.8. Given the task of maximizing the transmission of sound waves from water into steel. (*a*) What is the optimum characteristic impedance of the material to be placed between the water and the steel? (*b*) What must be the density of and sound velocity in a layer of 1-cm thickness which will produce 100 per cent transmission at a frequency of 20 kc/sec?

6.9. Calculate the pressure level in water in db *re* 1 microbar of normally incident plane waves that is required if they are to be heard by an observer inside a submarine at a pressure level of 60 db *re* 0.0002 microbar. Assume a frequency of 500 cycles/sec and that the thickness of the steel hull is 0.015 m.

6.10. Given the velocity of sound in water to change suddenly from 1480 m/sec to 1470 m/sec along a horizontal plane at a depth of 25 meters. Assume the density to remain constant at 1000 kg/m^3. Compute numerical values for the sound power reflection coefficient for sound rays incident from above on the interface between the two velocities at angles of incidence of (*a*) 0°, (*b*) 80°, (*c*) 88°, and (*d*) 89.5°.

6.11. (*a*) What is the critical angle of incidence for plane waves traveling from oil into water? Assume the oil to have a velocity of sound of 1350 m/sec and a density of 850 kg/m^3. (*b*) If the sound beam is incident at an angle of 45° in the oil, what is the sound transmission coefficient into the water?

6.12. A plane wave traveling from air into hydrogen gas, across a thin membrane separating the two gases, is refracted by 40° from its original direction. (*a*) What is the angle of incidence in the air? (*b*) What is the sound power transmission coefficient into the hydrogen?

6.13. Given a plane wave in water of 100 newtons/m^2 peak pressure amplitude to be incident at 45° on a mud bottom having a density of 2000 kg/m^3 and a sound velocity of 1000 m/sec. Compute (*a*) the angle at which the refracted ray is transmitted into the mud, (*b*) the peak pressure amplitude of the transmitted ray, (*c*) the peak pressure amplitude of the reflected ray, and (*d*) the sound power reflection coefficient.

6.14. Plane waves in water of 100 newtons/m^2 effective (rms) pressure are incident normally on a sand bottom. The sand has a density of 2000 kg/m^3 and a sound velocity of 2000 m/sec. (*a*) What is the effective pressure of the wave reflected back into the water? (*b*) What is the effective pressure of the wave transmitted into the sand? (*c*) What is the sound power coefficient of reflection from the sand? (*d*) What is the smallest angle of incidence at which all of the sound energy will be reflected?

6.15. Given a sand bottom in sea water to be characterized by a density of 1700 kg/m^3 and a sound velocity of 1600 m/sec. (*a*) What is the critical angle of incidence corresponding to total reflection. (*b*) For what angle of incidence is the sound power reflection coefficient equal to 0.25? (*c*) What is the reflection coefficient for normal incidence?

6.16. Given a certain acoustic tile panel to be characterized by a normal specific acoustic impedance of $900 - j1200$ rayls. (*a*) For what angle of incidence in air will the sound power reflection coefficient be a minimum? (*b*) What is the reflection coefficient for an angle of incidence of 80°? (*c*) What is the reflection coefficient for normal incidence?

6.17. By considering a wall to reflect plane waves in a manner similar to a normally reacting surface of normal specific acoustic impedance $z_n = \rho_1 c_1 + j\omega\sigma$, where $\rho_1 c_1$ is the characteristic impedance of the air and σ is the area density of the wall in kg/m^2, derive a general equation for its sound power reflection coefficient as a function of the incident angle θ. For a wall of area density $\sigma = 2$ kg/m^2, compute and plot the reflection coefficient at 100 cycles/sec as a function of θ.

chapter 7

SPHERICAL ACOUSTIC WAVES

7.1 Introduction. The acoustic wave equations 5.9 and 5.9a derived in Sect. 5.3 for plane waves, although simple in form, unfortunately apply only to a limited number of situations. For instance, many kinds of sound sources produce diverging spherical waves in which the acoustic energy spreads over an increasingly larger area as it recedes from the source. As a consequence, both the intensity and the pressure amplitude of such waves decrease as their distance from the source increases.

Our first task in discussing spherical waves is that of obtaining a *general* acoustic wave equation in a form valid for discussing any three-dimensional type of nondissipative acoustic wave. Such an equation can be derived directly in spherical coordinates. However, it is more readily derived in Cartesian coordinates. Upon consulting the various books on acoustics, a reader will find a wide variety of methods used for deriving the general wave equation. At first glance some developments may appear quite simple and others either more complicated or more rigorous. It is to be noted that all developments require a combination of three basic equations expressing respectively the *equation of continuity*, the *elastic properties*, and the *force equation* for fluids. Furthermore, in all cases the same ultimate simplifying assumptions regarding small amplitudes of density change, condensation, particle displacement, and particle velocity must be made. The following development of the general acoustic wave equation, utilizing Cartesian coordinates, is a generalization of the argument previously used in Sects. 5.2 and 5.3 for a one-dimensional plane wave.

7.2 General Wave Equation. Consider a particle of the fluid medium as having equilibrium coordinates x, y, and z. In general, this particle can move in any direction and its displacement must therefore be represented by a vector, **d**, for example, having components ξ, η, and ζ in the x, y, and z directions, respectively. The corresponding vector particle velocity,

$\mathbf{q} = \partial\mathbf{d}/\partial t$, may be assumed to have components $u = \partial\xi/\partial t$, $v = \partial\eta/\partial t$, and $w = \partial\zeta/\partial t$. All of these quantities, together with the acoustic pressure p and condensation s, are functions of x, y, z, and t.

Let us now assume that upon passage of a sound wave each pair of parallel planes of the rectangular volume element of the medium, $dx\,dy\,dz$, shown in Fig. 7.1 experience parallel displacements similar to those described in Sect. 5.2 for the one-dimensional case. The volume of the element then becomes

$$dx\,dy\,dz\left(1+\frac{\partial\xi}{\partial x}\right)\times\left(1+\frac{\partial\eta}{\partial y}\right)\left(1+\frac{\partial\zeta}{\partial z}\right)$$

Correspondingly, the counterpart of equation 5.3, expressing conservation of mass within this volume element, is

$$(1+s)\left(1+\frac{\partial\xi}{\partial x}\right)\times\left(1+\frac{\partial\eta}{\partial y}\right)\left(1+\frac{\partial\zeta}{\partial z}\right)=1 \quad (7.1)$$

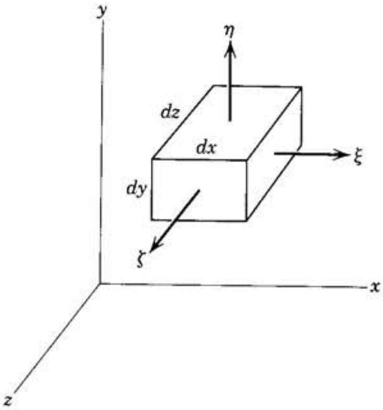

Fig. 7.1. Rectangular parallelepiped volume element.

Similarly, upon assuming both density changes and particle displacements to be small, product terms such as $s\dfrac{\partial\xi}{\partial x}$, $\dfrac{\partial\xi}{\partial x}\dfrac{\partial\eta}{\partial y}$, etc., may be neglected and equation 7.1 simplifies to

$$s=-\left(\frac{\partial\xi}{\partial x}+\frac{\partial\eta}{\partial y}+\frac{\partial\zeta}{\partial z}\right) \quad (7.2)$$

This equation is one special three-dimensional form of the more general hydrodynamical *equation of continuity*. It may be written in equivalent vector form as

$$s=-\nabla\cdot\mathbf{d} \quad (7.2a)$$

where $\nabla\cdot\mathbf{d}=\left(\dfrac{\partial\xi}{\partial x}+\dfrac{\partial\eta}{\partial y}+\dfrac{\partial\zeta}{\partial z}\right)$ represents the *divergence* of the vector displacement **d**.

By use of equation 5.4*b* which expresses certain elastic properties of a fluid, the expression for condensation s may be eliminated from each of the above two equations leading either to

$$p = -\rho_0 c^2\left(\frac{\partial\xi}{\partial x} + \frac{\partial\eta}{\partial y} + \frac{\partial\zeta}{\partial z}\right) \tag{7.3}$$

or

$$p = -\rho_0 c^2(\nabla \cdot \mathbf{d}) \tag{7.3a}$$

Upon considering the differences in external pressure acting upon each pair of parallel planes of the volume element $dx\,dy\,dz$ of Fig. 7.1, three *force* equations, each a counterpart of equation 5.8 as derived in the one-dimensional case, are obtained. They are

$$-\frac{\partial p}{\partial x} = \rho_0 \frac{\partial^2\xi}{\partial t^2} \qquad -\frac{\partial p}{\partial y} = \rho_0 \frac{\partial^2\eta}{\partial t^2} \qquad -\frac{\partial p}{\partial z} = \rho_0 \frac{\partial^2\zeta}{\partial t^2} \tag{7.4}$$

If the first of these equations is differentiated partially with respect to x, the second with respect to y, the third with respect to z, and then all are added together,

$$-\left(\frac{\partial^2 p}{\partial x^2} + \frac{\partial^2 p}{\partial y^2} + \frac{\partial^2 p}{\partial z^2}\right) = \rho_0 \frac{\partial^2}{\partial t^2}\left(\frac{\partial\xi}{\partial x} + \frac{\partial\eta}{\partial y} + \frac{\partial\zeta}{\partial z}\right) \tag{7.5}$$

is obtained. The latter equation may be expressed more simply in vector form as

$$-\nabla^2 p = \rho_0 \frac{\partial^2(\nabla \cdot \mathbf{d})}{\partial t^2} \tag{7.5a}$$

where $\nabla^2 = \left(\frac{\partial^2}{\partial x^2} + \frac{\partial^2}{\partial y^2} + \frac{\partial^2}{\partial z^2}\right)$ is a symbolic operator known as the *Laplacian* operator.

Finally, if $\nabla \cdot \mathbf{d}$ is eliminated between equations 7.3*a* and 7.5*a*,

$$\frac{\partial^2 p}{\partial t^2} = c^2\nabla^2 p \tag{7.6}$$

is obtained as representing the general acoustic wave equation. It should be noted that, when the acoustic pressure p is independent of both the y and z coordinates, the general equation 7.6 reduces to the one-dimensional plane wave equation 5.9*a* as previously derived in Sect. 5.3.

Although Cartesian coordinates have been used in deriving equation 7.6, it may be applied to solve problems in any coordinate system, provided the appropriate form of the Laplacian operator is used in each situation. Of the many possible coordinate systems, only three have been found of much significance to acoustical problems. Cartesian coordinates are commonly used for discussing plane waves, either in unbounded space or in rectangular enclosures. On the other hand, an analysis of cylindrical waves, such as those generated by a long cylindrical source or those present in cylindrical enclosures, is facilitated by expressing equation 7.6 in cylindrical coordinates. Finally, the treatment of spherical waves such as those diverging from a small central source is greatly simplified by expressing equation 7.6 in spherical coordinates.

7.3 Spherical Wave Equation. When expressed in spherical coordinates the Laplacian operator is represented by

$$\nabla^2 = \frac{\partial^2}{\partial r^2} + \frac{2}{r}\frac{\partial}{\partial r} + \frac{1}{r^2 \sin\theta}\frac{\partial}{\partial\theta}\left(\sin\theta\frac{\partial}{\partial\theta}\right) + \frac{1}{r^2\sin^2\theta}\frac{\partial^2}{\partial\psi^2} \tag{7.7}$$

where $x = r\sin\theta\cos\psi$, $y = r\sin\theta\sin\psi$, and $z = r\cos\theta$, as shown in Fig. 7.2. If the waves have spherical symmetry, i.e., if the acoustic pressure $p = p(r, t)$ is a function of radial distance and of time but not of the angular coordinates θ and ψ, a substitution of equation 7.7 into equation 7.6 leads to

$$\frac{\partial^2 p}{\partial t^2} = c^2\left(\frac{\partial^2 p}{\partial r^2} + \frac{2}{r}\frac{\partial p}{\partial r}\right) \tag{7.8}$$

or

$$\frac{\partial^2 p}{\partial t^2} = c^2\left(\frac{1}{r}\cdot\frac{\partial^2(rp)}{\partial r^2}\right) \tag{7.8a}$$

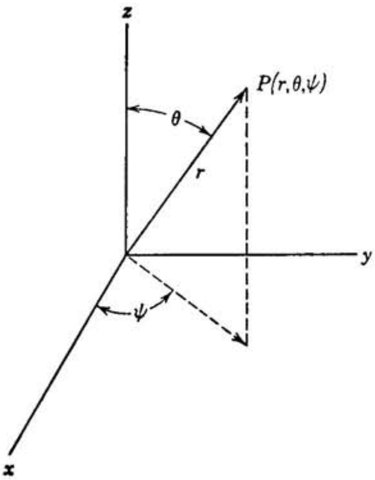

Fig. 7.2. Spherical coordinates.

Since the spatial coordinate r is an independent variable which is not a function of time, the partial derivative $\partial^2 p/\partial t^2$ may be written as

$$\frac{\partial^2 p}{\partial t^2} = \frac{1}{r}\cdot\frac{\partial^2(rp)}{\partial t^2}$$

Substituting this expression into equation 7.8a leads to

$$\frac{\partial^2(rp)}{\partial t^2} = c^2\frac{\partial^2(rp)}{\partial r^2} \tag{7.9}$$

If the product rp in this equation is considered as a single variable, the equation is of the same form as the plane wave equation (5.9), and its general solution is therefore

$$rp = f_1(ct - r) + f_2(ct + r)$$

or

$$p = \frac{1}{r}f_1(ct - r) + \frac{1}{r}f_2(ct + r) \tag{7.10}$$

The first term of equation 7.10 represents a spherical wave *diverging* from the origin of coordinates with a velocity c; the second term represents a similar wave *converging* on the origin. Converging spherical waves are of so little importance in acoustics that they will not be given detailed consideration in this book. It should be noted, however, that, since r is zero at the origin, the equation predicts infinite values for the acoustic pressure at the focal point of a converging wave. In actual practice these values remain finite but become so large that many of the assumptions made in deriving the general wave equation are no longer valid.

In each of the three component equations 7.4 it is to be noted that the negative of the pressure gradient, $-\partial p/\partial x$, for example, is proportional to the particle acceleration in the specified direction. Correspondingly, these equations may be combined to show that for spherical waves, the radial pressure gradient $\partial p/\partial r$ is related to the radial acceleration by

$$-\frac{\partial p}{\partial r} = \rho_0 \frac{\partial^2 \xi}{\partial t^2} \tag{7.11}$$

where the symbol ξ here represents a radial particle displacement, rather than one in the x direction as was the case in Chapter 5 and in Sect. 7.2.

If equation 7.11 is integrated with respect to time,

$$u = \frac{\partial \xi}{\partial t} = -\frac{1}{\rho_0}\int \frac{\partial p}{\partial r}\, dt \tag{7.12}$$

is obtained, where u here represents a radial particle velocity. This is a general equation relating acoustic pressure and radial particle velocity. In the case of harmonic waves where the dependence of pressure on time is expressed by $e^{j\omega t}$, equation 7.12 may be expressed in complex form as

$$\mathbf{u} = -\frac{1}{j\omega\rho_0}\frac{\partial \mathbf{p}}{\partial r} \tag{7.12a}$$

Finally, expressions for the radial particle displacement may be obtained by integrating either equation 7.12 or 7.12*a* with respect to time. In particular, for harmonic waves

$$\boldsymbol{\xi} = \int \mathbf{u}\, dt = \frac{\mathbf{u}}{j\omega} = \frac{1}{\omega^2\rho_0}\frac{\partial \mathbf{p}}{\partial r} \tag{7.13}$$

7.4 Harmonic Spherical Waves. The most important type of diverging spherical wave is one whose vibrations are harmonic. Such a wave is represented in complex form by

$$\mathbf{p} = \frac{\mathbf{A}}{r} e^{j(\omega t - kr)} \tag{7.14}$$

Using relationships developed previously, the other important acoustic variables may be expressed in terms of pressure **p** by

$$\mathbf{s} = \frac{\mathbf{p}}{\rho_0 c^2} \tag{7.15}$$

$$\mathbf{u} = -\frac{1}{j\omega\rho_0}\frac{\partial \mathbf{p}}{\partial r} = \left(\frac{1}{r} + jk\right)\frac{\mathbf{p}}{j\omega\rho_0} \tag{7.16}$$

$$\boldsymbol{\xi} = \frac{1}{\omega^2\rho_0}\frac{\partial \mathbf{p}}{\partial r} = -\left(\frac{1}{r} + jk\right)\frac{\mathbf{p}}{\omega^2\rho_0} \tag{7.17}$$

The actual equations giving the various acoustic variables are obtained by taking the real parts of equations 7.14 through 7.17.

It is apparent from equation 7.16 that, in contrast with plane waves, the particle velocity is not in general in phase with the pressure, the phase relation between **p** and **u** being determined by equation 7.16 as

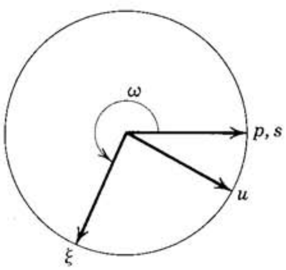

Fig. 7.3. Phase relationships of acoustic variables in a diverging spherical wave when $kr = 2$.

$$\frac{\mathbf{p}}{\mathbf{u}} = \frac{j\omega\rho_0}{\left(\frac{1}{r} + jk\right)} = \rho_0 c\,\frac{kr(kr + j)}{1 + k^2r^2}$$

$$= \frac{\rho_0 ckr}{\sqrt{1 + k^2r^2}}\,e^{j\theta} \tag{7.18}$$

where

$$\tan\theta = \frac{1}{kr} \tag{7.19}$$

It will be seen that the pressure leads the particle velocity by a phase angle θ, which varies from nearly 90° for small values of kr to practically zero for very large values of kr. As is true with many other acoustic phenomena, the product of k and r is the determining factor, rather than the magnitude of either of the individual parameters. Since $kr = 2\pi r/\lambda$, the phase angle is a function of the ratio of the source distance to the wavelength. When the distance from the source is only a small fraction of a wavelength, the phase difference between the pressure and the particle velocity is large. On the other hand, at distances corresponding to a considerable number of wavelengths, **p** and **u** are very nearly in phase, and the spherical wave then assumes some of the characteristics of a plane wave. This behavior is to be expected, since the wave fronts of all spherical waves become essentially plane at great distances from their source.

Equation 7.17 shows that the particle displacement lags the particle velocity by an angle of 90° for all values of kr. The phase relationship between the various acoustic variables for diverging spherical waves having $kr = 2$ is shown in Fig. 7.3.

7.5 Specific Acoustic Impedance. Since the specific acoustic impedance $\mathbf{z}$ is defined as $\mathbf{p}/\mathbf{u}$, it is apparent from equation 7.18 that the specific acoustic impedance of a medium for spherical waves is in general complex. Separating equation 7.18 into its real and imaginary parts, we have

$$\mathbf{z} = \rho_0 c \frac{k^2r^2}{1 + k^2r^2} + j\rho_0 c \frac{kr}{1 + k^2r^2} \quad (7.20)$$

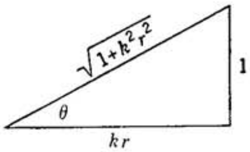

Fig. 7.4. Vector triangle, showing relations between θ and kr.

The first term of this expression represents the *specific acoustic resistance* of the medium, and the magnitude of the second term its *specific acoustic reactance*. Both terms approach zero for very small values of kr, but for very large values of kr the resistive term approaches $\rho_0 c$, while the reactive term approaches zero. When $kr = 1$, both the specific acoustic resistance and reactance are equal to $\rho_0 c/2$ and the specific acoustic reactance has its maximum value.

The absolute magnitude z of the specific acoustic impedance is equal to the ratio of the pressure amplitude P of the wave to its velocity amplitude U, and hence

$$z = \frac{P}{U} = \rho_0 c \frac{kr}{\sqrt{1 + k^2r^2}} \quad (7.21)$$

Since $\tan\theta = 1/kr$, it is apparent from Fig. 7.4 that

$$\cos\theta = \frac{kr}{\sqrt{1 + k^2r^2}} \quad (7.19a)$$

so that equation 7.21 may be rewritten as

$$z = \rho_0 c \cos\theta \quad (7.21a)$$

and the relation between pressure and velocity amplitude may be written as

$$P = \rho_0 c U \cos\theta \quad (7.22)$$

For large values of kr, $\cos\theta$ approaches unity, and the relation between pressure and velocity is then the same as that given by equation 5.41 for a plane wave. As the distance from the source of a spherical acoustic wave to the point of observation is decreased, both kr and $\cos\theta$ decrease, so that larger and larger particle velocities are associated with a given pressure amplitude. For very small distances from a *point source* of sound the particle velocities corresponding to even very low acoustic pressures become impossibly large, with the result that a small source of sound is inherently incapable of generating spherical waves of large intensity. Similarly, it is impossible to construct a sound source of moderate size that is capable of radiating large amounts of power at low frequencies.

As an illustration of these difficulties, let us calculate the velocity and displacement amplitudes required to produce a spherical wave in air, if the frequency is 20 cycles/sec and the pressure amplitude at a distance of 2.5 cm (0.025 m) from the source is to be 20 microbars (2 newtons/m^2). Since $kr \ll 1$,

$$\cos\theta \approx kr = \frac{2\pi \times 20 \times 0.025}{343} = 0.00915$$

and

$$U = \frac{P}{\rho_0 c \cos\theta} = \frac{2}{415 \times 0.00915} = 0.526 \text{ m/sec}$$

The corresponding displacement amplitude is

$$\xi = \frac{U}{\omega} = \frac{0.526}{2\pi \times 20} = 0.0042 \text{ m} = 0.42 \text{ cm}$$

Considered by themselves, these numerical values do not appear to be excessive, but if they are compared with the corresponding values for a plane wave of similar frequency and pressure they will be found to be greater by a factor of $1/\cos\theta$, or about 110.

7.6 Intensity of Spherical Waves. Let us rewrite equation 7.14 as

$$\mathbf{p} = \frac{A}{r} e^{j(\omega t - kr)} \tag{7.14a}$$

where without any loss in generality we may choose a new origin of time such that the complex amplitude constant **A** becomes a real constant A. Then A/r is the pressure amplitude of the wave. It should be noted that the pressure amplitude in an undamped spherical wave is *not* constant, as it is for an undamped plane wave, but instead decreases inversely with the distance r from the source. The actual pressure is given by the real part of equation 7.14a and is

$$p = \frac{A}{r} \cos(\omega t - kr) \tag{7.14b}$$

Since $\mathbf{u} = \mathbf{p}/\mathbf{z}$, the corresponding complex expression for the particle velocity is

$$\mathbf{u} = \frac{A}{r\mathbf{z}} e^{j(\omega t - kr)} \tag{7.23}$$

Replacing $\mathbf{z}$ by its value

$$\mathbf{z} = \frac{\rho_0 ckr}{\sqrt{1 + k^2r^2}} e^{j\theta}$$

as given in equation 7.18 and then taking the real part of the resulting expression, we have for the actual particle velocity

$$u = \frac{A}{\rho_0 cr} \cdot \frac{\sqrt{1 + k^2r^2}}{kr} \cos(\omega t - kr - \theta) \tag{7.23a}$$

It is apparent that the velocity amplitude

$$U = \frac{A}{\rho_0 ck} \cdot \frac{\sqrt{1 + k^2r^2}}{r^2} \tag{7.24}$$

is *not* inversely proportional to the distance from the source, and as a result it is usually advantageous to treat problems involving spherical waves in terms of pressure amplitude, rather than in terms of velocity amplitude. An alternative form of equation 7.23*a* may be obtained by using equation 7.19*a* to introduce the factor $\cos\theta$. Then

$$u = \frac{A}{\rho_0 cr \cos\theta} \cos(\omega t - kr - \theta) \tag{7.23b}$$

The instantaneous energy density $\mathcal{E}$ can be obtained from equation 5.29, which is applicable to both plane and spherical waves. It can be shown that the average kinetic energy density is

$$\overline{\mathcal{E}}_k = \frac{\rho_0 U^2}{4} = \frac{A^2(1 + k^2r^2)}{4\rho_0 c^2k^2r^4} \tag{7.25}$$

and that the average potential energy density is

$$\overline{\mathcal{E}}_p = \frac{P^2}{4\rho_0 c^2} = \frac{A^2}{4\rho_0 c^2r^2} \tag{7.25a}$$

giving for the average total energy density

$$\overline{\mathcal{E}} = \overline{\mathcal{E}}_k + \overline{\mathcal{E}}_p = \frac{A^2}{2\rho_0 c^2r^2}\left(1 + \frac{1}{2k^2r^2}\right) \tag{7.26}$$

or

$$\overline{\mathcal{E}} = \frac{P^2}{2\rho_0 c^2}\left(1 + \frac{1}{2k^2r^2}\right) \tag{7.26a}$$

Part of the kinetic energy density of a spherical wave results from a component of the particle velocity which is out of phase with the pressure, and which is analogous to the reactive power in an electrical circuit. Since this energy is not transmitted out of the system, the intensity of a spherical wave cannot be obtained by multiplying $\bar{\mathcal{E}}$ by c, as was done for plane waves. It can be shown, however, that the intensity of a spherical wave is given by the product of c and the first term of equation 7.26*a*, i.e.,

$$I = \frac{P^2}{2\rho_0 c} \tag{7.27}$$

which is identical with the corresponding equation for plane waves.

The intensity of a spherical wave may be obtained more readily by considering it as equal to the *average* rate at which unit area of a spherical wave does work on the external medium. In a fluid the instantaneous rate of doing work per unit area is equal to the product of pressure and velocity, and hence the average work over a complete cycle is

$$I = \frac{\int_0^T pu\,dt}{T} \tag{7.28}$$

or

$$I = \frac{1}{T}\int_0^T P\cos(\omega t - kr)\,U\cos(\omega t - kr - \theta)\,dt = \frac{PU\cos\theta}{2} \tag{7.28a}$$

where the factor $\cos\theta$ is analogous to the power factor of a reactive alternating current circuit. Since $U\cos\theta = P/\rho_0 c$, it is apparent that equations 7.28*a* and 7.27 are equivalent. Equation 7.27 is far more useful, since it does not involve the power factor, $\cos\theta$, which varies with both radial distance and frequency.

The average rate at which energy flows through a closed spherical surface of radius r surrounding a source of symmetrical spherical waves is

$$W = 4\pi r^2 I = \frac{4\pi r^2 P^2}{2\rho_0 c} \tag{7.29}$$

or since $P^2 = A^2/r^2$, as indicated by equation 7.14*a*,

$$W = \frac{2\pi A^2}{\rho_0 c} \tag{7.29a}$$

The average rate of energy flow through any spherical surface surrounding the origin is therefore independent of the radius of the surface, a conclusion that is consistent with the law of conservation of energy.

7.7 Spherical Radiation from a Simple Source. From a theoretical point of view the simplest type of source for generating spherical acoustic waves is a *pulsating sphere*, i.e., a sphere whose radius varies sinusoidally with time. It is obvious from its symmetry that such a source will set up harmonic spherical waves in any surrounding medium that is homogeneous and isotropic. Although this type of source is rarely used in actual practice, a consideration of some of its properties is justified, not only because it supplies a simple introduction to more practical sources but also because many acoustic radiators act, at least to a first approximation, like pulsating spheres, if their dimensions are small as compared with the wavelength of the radiated sound.

Let the average radius of a pulsating sphere be a, and assume that the radial velocity u_s of any point on its surface is given by

$$u_s = U_0 \cos \omega t \tag{7.30}$$

where U_0 is the velocity amplitude of the surface. The complex form of equation 7.30 is

$$\mathbf{u}_s = U_0 e^{j\omega t} \tag{7.31}$$

At other than those large velocity amplitudes where the associated acoustic pressure amplitudes approach or exceed the mean equilibrium pressure in the fluid, the fluid medium surrounding the sphere must remain in contact with the surface of the sphere at all times, and consequently the particle velocity of an acoustic wave of radius a must be equal to the surface velocity of the sphere. Referring to equation 7.23, this boundary condition is

$$\frac{\mathbf{A}}{a\mathbf{z}_a} e^{j(\omega t - ka)} = U_0 e^{j\omega t}$$

where $\mathbf{z}_a$ is the specific acoustic impedance of a spherical wave, evaluated at $r = a$. Then

$$\mathbf{A} = aU_0 \mathbf{z}_a e^{jka} \tag{7.32}$$

If the radius of the pulsating sphere is so small that $ka \ll 1$ at all operating frequencies,

$$\mathbf{A} = aU_0 \frac{\rho_0 cka(ka + j)}{1 + k^2a^2} (\cos ka + j \sin ka)$$

$$\approx a^2 U_0 \rho_0 ck \frac{(ka + j)(1 + jka)}{1 + k^2a^2}$$

or

$$\mathbf{A} \approx j\rho_0 cka^2 U_0 \tag{7.33}$$

The equation for the acoustic pressure is therefore

$$\mathbf{p} = \frac{j\rho_0 cka^2U_0}{r} e^{j(\omega t - kr)} \tag{7.34}$$

The real part of this expression

$$p = \frac{-\rho_0 cka^2U_0}{r} \sin(\omega t - kr) \tag{7.34a}$$

represents the actual pressure in the wave. Complex expressions for the other acoustic variables can be obtained from equations 7.15 through 7.17. For example, the complex particle velocity is given by

$$\mathbf{u} = \frac{j\rho_0 cka^2U_0}{\mathbf{z}r} e^{j(\omega t - kr)} \tag{7.35}$$

which reduces to $\mathbf{u} = U_0 e^{j\omega t}$ for $r = a$.

The equation for pressure (7.34) may be rewritten as

$$\mathbf{p} = \frac{j\rho_0 ck}{4\pi r} Q_s e^{j(\omega t - kr)} \tag{7.36}$$

where the quantity Q_s, which is known as the *strength* of the spherical source, is defined as the product of its surface area and velocity amplitude, i.e., $Q_s = 4\pi a^2 U_0$. The units of source strength are obviously cubic meters per second. In general, the strength of any source whose surface elements vibrate in phase is equal to the maximum rate of volume flow at its surface and is given by

$$Q = \int_S \mathbf{U} \cdot \mathbf{dS} \tag{7.37}$$

where $\mathbf{U}$ represents the vector velocity amplitude of a surface element $\mathbf{dS}$. For a uniformly vibrating body whose velocity is normal to its surface at all points, such as a pulsating sphere, equation 7.37 reduces to $Q = SU_0$, as previously indicated. However, if the velocity amplitude varies in direction or magnitude over the vibrating surface, the source strength must be obtained by evaluating the surface integral of the scalar product of the vector velocity amplitude and its corresponding surface element.

When the wavelength of the sound produced is much greater than the dimensions of the radiator, i.e., when $ka \ll 1$, the acoustic pressures measured at distances from the source such that $r \gg a$ are found to be the same for all sources of equal strength, regardless of the particular shape of the radiator, and hence equation 7.36 may be applied to any such *simple source*. For example, the open end of an organ pipe, or of any woodwind instrument, is usually small enough to be treated as a simple source.

Similarly, an ordinary telephone receiver radiates as a simple source having a strength corresponding to that of its *equivalent simple piston*.

The intensity of the acoustic waves produced by a simple source radiating spherical waves is

$$I = \frac{P^2}{2\rho_0 c} = \frac{\left(\dfrac{\rho_0 ckQ_s}{4\pi r}\right)^2}{2\rho_0 c} = \frac{\rho_0 ck^2}{32\pi^2 r^2} Q_s^{\ 2} \tag{7.38}$$

The average power W radiated through any closed spherical surface of radius r surrounding the source is the product of the intensity at the radial distance r and the surface area of the sphere, so that

$$W = \frac{\rho_0 ck^2}{8\pi} Q_s^{\ 2} \tag{7.39}$$

7.8 Infinite Baffle. The radiation characteristics of any source of sound are materially affected by the presence of any large rigid surface, located in the vicinity of the source. An important example is that of a simple source mounted in the surface of an infinite plane baffle, with the radiation confined to one side of the plane. A small hemispherical source mounted in an infinite baffle, as shown in Fig. 7.5, is an idealized example of this type of simple source. From the symmetry of this arrangement it is apparent that the acoustic pressures generated on the side of the baffle into which the hemisphere is radiating are identical with those which would be produced in free space by a spherical source having the same radius, frequency, and velocity amplitude. Equation 7.34 may therefore be used to determine the radiation characteristics of the hemispherical source.

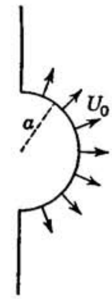

Fig. 7.5. Hemispherical source mounted in an infinite baffle.

If the characteristics of the source are expressed in terms of its source strength, rather than its velocity amplitude, it will be seen that the strength of a hemispherical source is only half as great as that of a similar spherical source having the same radius and velocity amplitude, i.e., $Q_H = 2\pi a^2 U_0$. Substitution into equation 7.34 gives for the acoustic pressure produced by a hemispherical source in an infinite baffle

$$\mathbf{p} = \frac{j\rho_0 ck}{2\pi r} Q_H e^{j(\omega t - kr)} \tag{7.40}$$

which is twice as great as that produced by a spherical source of the same strength. Similarly, any simple source of strength Q_H mounted in an infinite baffle and radiating hemispherically, will produce a sound field whose pressures are given by equation 7.40. The intensity of the diverging waves generated by such a simple source is

$$I = \frac{\rho_0 c k^2}{8\pi^2 r^2} Q_H{}^2 \tag{7.41}$$

and the total acoustic power radiated is $2\pi r^2 I$ or

$$W = \frac{\rho_0 c k^2}{4\pi} Q_H{}^2 \tag{7.42}$$

7.9 Radiation from a Piston. In general, the radiation produced by the vibration of an *extended surface* does not have the symmetric spherical radiation pattern characteristic of a simple source. The pressure produced at any point by such a source is, however, the sum of the pressures that would be produced by an equivalent assembly of simple sources. For example, each infinitesimal element of area $\mathbf{dS}$ of a vibrating surface mounted in an infinite baffle contributes an element of pressure $d\mathbf{p}$ given by

$$d\mathbf{p} = \frac{j\rho_0 c k}{2\pi r'} (\mathbf{U} \cdot \mathbf{dS}) e^{j(\omega t - kr')} \tag{7.43}$$

where r' is the distance from the surface element to the point in the medium at which $d\mathbf{p}$ is measured. In theory, an equation giving the acoustic pressure at any point in a medium can be obtained by integrating this expression over the surface of the vibrating body. In practice, however, the mathematical difficulties encountered in carrying out this integration limit its application to a few simple but important cases.

One type of extended radiator that is of particular interest is a rigid circular piston, mounted flush with the surface of an infinite baffle, and vibrating with simple harmonic motion, $u = U_0 \cos \omega t$. The solution in this particular example is applicable to a number of related problems, such as the radiation from the open end of a flanged organ pipe. It makes no difference, for the purposes of this analysis, whether the vibrating element is an actual piston or is merely a circular layer of air, provided only that all portions of the layer vibrate in phase, with the same amplitude and frequency. In actual practice this limitation is not strictly obeyed for an organ pipe, where the amplitude of vibration of the air near the edges of the pipe is somewhat less than at its center, but the results obtained by assuming that the radiation is similar to that from a rigid piston are in reasonably good agreement with observed values.

Assume that the radius of the piston is a and that its vibrating surface lies in the yz plane, with its center coinciding with the origin of coordinates.

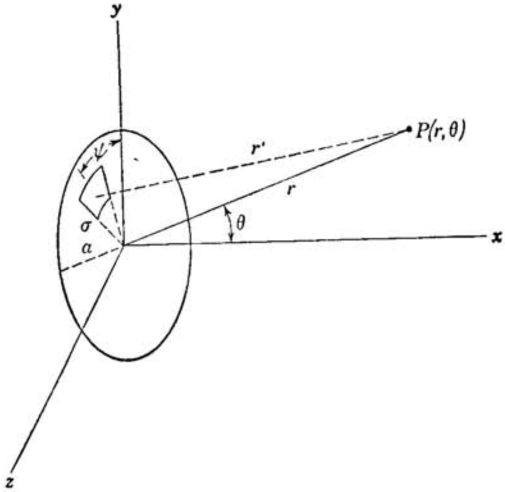

Fig. 7.6. Coordinate system used in deriving the radiation characteristics of a flat piston.

The radiation will then be symmetric about the x axis, so that it is sufficient to specify the position of a point in space by the spherical coordinates r and θ, where r is the radial distance from the center of the piston, and θ is the angle between the radius vector and the x axis, as in Fig. 7.6. Let positions on the surface of the piston be specified by the polar coordinates σ and ψ, where σ is the radial distance from the center of the piston and ψ is the angle between the corresponding radius vector and the y axis. Then the area dS of a surface element of the piston is $\sigma\, d\sigma\, d\psi$. Letting r' represent the distance from a surface element dS to a point $P(r, \theta)$ in the medium, the acoustic pressure $d\mathbf{p}$ produced at this point by the motion of dS is

$$d\mathbf{p} = \frac{j\rho_0 ck}{2\pi r'}\, U_0\, dS\, e^{j(\omega t - kr')} \tag{7.44}$$

Since the motion of every surface element of the piston is normal to its surface, the scalar product $\mathbf{U} \cdot \mathbf{dS}$ in equation 7.43 has been replaced by $U_0\, dS$. The total pressure $\mathbf{p}$ at the point $P(r, \theta)$ is the integral of this expression over the surface of the piston.

The distance r' is equal to

$$r' = (r^2 + \sigma^2 - 2r\sigma \sin\theta \cos\psi)^{1/2} \tag{7.45}$$

as can be shown by the methods of analytic geometry. If this exact expression for r' is substituted into equation 7.44, the resulting equation for $d\mathbf{p}$ is so complicated that it cannot be integrated. However, if the distance from the point $P(r, \theta)$ to the center of the piston is large as compared with the radius of the piston, we may use an approximate value of r', obtained by expanding equation 7.45 in a power series. The first two terms of this series are

$$r' = r - \sigma \sin\theta \cos\psi + \cdots \tag{7.45a}$$

At considerable distances from the piston the *amplitude* of the pressure produced by any particular surface element differs only very slightly from that produced by any other element, so that the distance r' in the denominator of equation 7.44 can be satisfactorily approximated by using only the first term of the series (7.45*a*) i.e., $r' = r$. On the other hand, the relative *phase* of the pressures produced at $P(r, \theta)$ by any two surface elements depends on the *difference* in distance of the two elements, and for distant points this difference is practically independent of r. As a consequence, we must use at least two terms of the series in substituting for the phase factor of equation 7.44, i.e., for the r' appearing in the exponential. The approximate expression for the pressure at considerable distances from the piston is therefore

$$d\mathbf{p} = \frac{j\rho_0 ck}{2\pi r} U_0 e^{j(\omega t - kr)} e^{jk\sigma \sin\theta \cos\psi}\, dS$$

or

$$\mathbf{p} = \frac{j\rho_0 ck}{2\pi r} U_0 e^{j(\omega t - kr)} \int_0^a \sigma\, d\sigma \int_0^{2\pi} e^{jk\sigma \sin\theta \cos\psi}\, d\psi \tag{7.46}$$

The expression $\int_0^{2\pi} e^{jk\sigma \sin\theta\cos\psi}\, d\psi$ can be integrated by expanding the exponential as a power series in $(k\sigma \sin\theta \cos\psi)$ and integrating term by term. The resulting series will be found to equal $2\pi J_0(k\sigma \sin\theta)$. The same result may be obtained by using the general relation

$$J_m(x) = \frac{(-j)^m}{2\pi} \int_0^{2\pi} e^{jx\cos\psi} \cos(m\psi)\, d\psi \tag{7.47}$$

which is proved in books treating Bessel functions.

The second integration of equation 7.46 can be carried out by using the relation $\int x J_0(x)\, dx = x J_1(x)$, as given in Table 4.1. Then

$$2\pi \int_0^a \sigma J_0(k\sigma \sin\theta)\, d\sigma = 2\pi a^2 \left[\frac{J_1(ka \sin\theta)}{ka \sin\theta}\right] \tag{7.48}$$

Substitution into equation 7.46 and simplification give for the complex pressure

$$\mathbf{p} = \frac{j\rho_0 cka^2 U_0}{2r} e^{j(\omega t - kr)} \left[\frac{2J_1(ka \sin\theta)}{ka \sin\theta}\right] \tag{7.49}$$

The real part of $\mathbf{p}$ is the actual pressure at $P(r, \theta)$. Expressions for the particle velocity, displacement, etc., can be obtained from the usual relations between the pressure and the other acoustic variables.

7.10 Pressure and Intensity Distribution. The source strength Q_p of the piston may be introduced into equation 7.49 by replacing U_0 with $Q_p/\pi a^2$, giving

$$\mathbf{p} = \frac{j\rho_0 ck}{2\pi r} Q_p e^{j(\omega t - kr)} \left[\frac{2J_1(ka \sin \theta)}{ka \sin \theta}\right] \tag{7.50}$$

A comparison of equation 7.50 with equation 7.40 shows that the acoustic pressures produced by a piston of source strength Q_p are identical with those produced by a hemispherically radiating simple source of equal strength Q_H, except for the presence of a *directivity* term

$$\frac{2J_1(ka \sin \theta)}{ka \sin \theta}$$

Values of the function $2J_1(x)/x$ can be computed from the $J_1(x)$ Bessel function and are listed in Table IV in the appendix. A simple expression for this directivity function, valid for fractional values of x, can be obtained by expanding $J_1(x)$ as a power series in x, and then neglecting all but the first two terms. Then

$$\frac{2J_1(x)}{x} \approx 1 - \frac{x^2}{8} \tag{7.51}$$

At points along the axis of the piston the polar angle θ, and hence $ka \sin \theta$, is zero, and consequently the directivity function is unity. The pressures produced by a piston at points along its axis are therefore equal to those produced by a hemispherical type of simple source of equal source strength.

Values of the directivity function, $2J_1(x)/x$, are plotted as a function of x in Fig. 7.7. It will be observed that the resulting curve crosses the axis for values of $x = 3.83$, 7.02, 10.15, etc. The pressure amplitude at points on a spherical surface of radius r therefore decreases with increasing polar angle θ, and becomes zero when $ka \sin \theta = 3.83$. The angle θ_1, which is given by

$$\sin \theta_1 = \frac{3.83}{ka} = 0.61 \frac{\lambda}{a} \tag{7.52}$$

marks the extreme angular beam width of the *major lobe* of acoustic pressure.

Since the pressure radiated by a piston source is a function of polar angle, as well as of distance from the source, the wave is not spherically

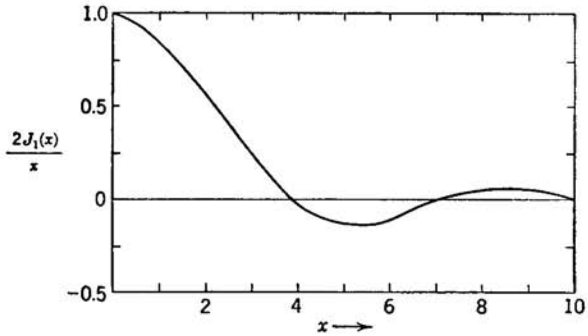

Fig. 7.7. Directivity function for a circular piston.

symmetrical. It still has, however, the characteristic property of a diverging spherical wave, namely, the pressure is inversely proportional to the radial distance from the center of the source. The phase of the pressure on any spherical wave front is also the same at all points included within the major lobe.

The *first side lobe* is included between the angles θ_1 and θ_2, where

$$\sin \theta_2 = \frac{7.02}{ka} = 1.12 \frac{\lambda}{a} \tag{7.53}$$

The acoustic pressures within this lobe are in general much smaller than those within the major lobe, the maximum value in this side lobe being equal to 0.133 of the maximum value in the major lobe. Frequently such ratios are stated as a difference in decibel level. In this case, the maximum sound pressure level of the side lobe is down 17.5 db (20 log 0.133) as compared to the major lobe. Furthermore, the pressures corresponding to any particular value of the radius r are 180° out of phase with those on the same wave front in the major lobe.

When the radius of the piston is large in comparison with the wavelength of the sound, i.e., when $ka \gg 1$, the radiation pattern has many side lobes and the angular width of the major lobe is small. On the other hand, if the ratio of the radius to the wavelength is small enough for ka to be less than 3.83, there is no real value of θ for which $\sin \theta = 3.83/ka$, and consequently only the major lobe will be present. For very small values of ka the directivity factor is nearly equal to unity for all angles, so that the pressure amplitudes are symmetrical about the center of the piston and are equal to those of a hemispherically radiating simple source of the same strength. This result was to have been anticipated, since for very small values of ka a flat piston is in effect a simple source.

The pressure amplitude P is

$$P = \frac{\rho_0 c k \pi a^2 U_0}{2\pi r}\left[\frac{2J_1(ka \sin\theta)}{ka \sin\theta}\right] \tag{7.54}$$

and the intensity I is

$$I = \frac{P^2}{2\rho_0 c} = \frac{\rho_0 c k^2 U_0^{\,2}(\pi a^2)^2}{8\pi^2 r^2}\left[\frac{2J_1(ka \sin\theta)}{ka \sin\theta}\right]^2 \tag{7.55}$$

Various forms in which the axial intensity I_0 may be expressed include

$$I_0 = \frac{\rho_0 c k^2}{8\pi^2 r^2} U_0^{\,2} S^2 = \frac{\rho_0 c k^2}{8\pi^2 r^2} Q_p^{\,2} = \frac{\rho_0 c}{2\lambda^2 r^2} Q_p^{\,2} \tag{7.56}$$

where S is the area of the surface of the piston and λ is the wavelength of the sound. It should be noted that for a source of constant strength Q_p, the axial intensity is directly proportional to the square of the frequency. On the other hand, if the velocity amplitude U_0 is maintained constant, this intensity is proportional to the square of the area of the piston, rather than to its first power, as one might expect.

Figure 7.8 shows polar plots illustrating the manner in which the radiation pattern of a piston of constant radius a and source strength Q_p varies with

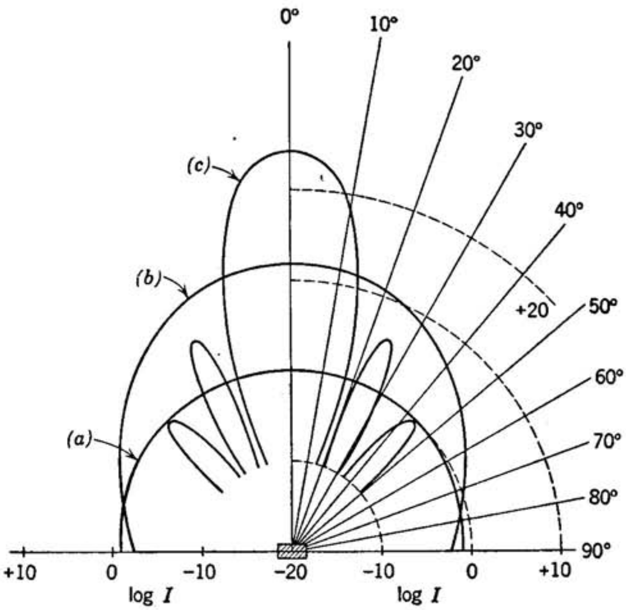

Fig. 7.8. Polar radiation patterns of a flat piston as plotted for three different frequencies. Log I is plotted against θ for (*a*) $\lambda = 8a$, (*b*) $\lambda = 2a$, and (*c*) $\lambda = a/2$.

frequency. Radial distances in this graph are proportional to log I, and the frequencies correspond to $\lambda = 8a$ in (a), $\lambda = 2a$ in (b), and $\lambda = a/2$ in (c). It will be observed that the axial intensity I_0 is much greater at high frequencies than it is at low frequencies, as is to be expected from equation 7.56. The maximum intensity I_1 of the first side lobe is

$$I_1 = 0.133^2 I_0 = 0.018 I_0$$

and the direction of this maximum is given by

$$\sin\theta = \frac{5.15}{ka}$$

The radiation patterns produced by piston type loudspeakers differ to some extent from these idealized patterns. One reason for this discrepancy is that the area of the baffle in which the speaker is mounted is necessarily finite, so that it does not always act like an infinite plane. At high frequencies, i.e., short wavelengths, even a baffle of small linear dimensions corresponds quite closely to an ideal infinite baffle, but at low frequencies, where the wavelength of the sound may be about the same as, or even greater than, the linear dimensions of the baffle, the assumption that each element of the piston radiates with the hemispherical divergence of a simple source will be in error. In addition, the radiation from the back of the speaker may be propagated into the region in front of the speaker, with the result that the actual radiation pattern approximates that of an acoustic doublet, rather than that of a piston in an infinite baffle. This subject will be considered further in Chapter 10 on loudspeakers.

Another reason for this discrepancy is that the material of which an actual speaker cone is constructed is not perfectly rigid. The effect of driving the speaker from its center is then to establish higher velocity amplitudes in the inner parts of the cone than near its rim, and at high driving frequencies the cone may even vibrate in zones similar to those of a flexible diaphragm. Under these circumstances U is a function of the radial distance σ and hence must be considered as a variable, rather than a constant, in the integration of equation 7.46. In general, the effect of decreasing U with increasing σ is to produce a slight broadening of the major lobe, with an accompanying decrease in the intensity of the side lobes. By a suitable choice of the relation between U and σ we may obtain a wide variety of radiation patterns, ranging from those in which the first side lobe is completely suppressed to those in which all side lobes are of equal intensity. However, there is an important fundamental restriction which makes it impossible to cause the null of the major lobe to occur at an angle of less than $\theta_1 = \sin^{-1} (0.61\ \lambda/a)$, regardless of the velocity distribution over the surface of the piston. The beam may be made broader by varying the velocity distribution, but for any given wavelength it can be made narrower only by increasing the diameter of the piston.

The increase in directionality that accompanies an increase in frequency sometimes produces wide variations in the relative intensities of the low-frequency and the high-frequency sounds generated by a single speaker, the relative intensity of the higher frequency components being much greater at points on or near the axis of the speaker than at larger angles. In rooms of moderate dimensions this effect is of little importance unless the walls have a high absorption coefficient, for reflections from the walls scatter the radiated sound to such an extent that the intensity distribution is nearly uniform. When public address systems are used outdoors or in large auditoriums, however, the scattering is negligible and uniform distribution of the high-frequency components can be obtained only by employing several speakers aimed in different directions.

7.11 Beam Width and Directivity Index. One method of specifying the directivity of a sound source, such as an idealized flat piston, is in terms of the *beam width* of the major lobe. In theory the intensity is zero at a polar angle θ that is given by $\sin \theta = 0.61\lambda/a$, and the beam width is therefore 2θ. In actual practice, however, an absolute null of zero intensity is never observed, and as a result it is customary to specify the beam width as the angle between the two directions at which the intensity I first drops to some particular fraction of its axial value I_0. The widths of the sonar beams used in echo ranging on underwater targets are commonly specified in this manner.

No standard value of the ratio I/I_0 has been agreed upon for measuring or calculating the angle θ that marks the extremity of a sound beam, and hence the particular value employed must be clearly stated when beam widths are specified in this manner. The ratios used by various authors and experimenters range from a maximum of 0.5 (down 3 db), through 0.25 (down 6 db), to a minimum of 0.1 (down 10 db). As an illustration of the ambiguity that arises if I/I_0 is not clearly specified, consider a flat piston that is radiating sound of wavelength $\lambda = a/4$, i.e., $ka = 8\pi$. The calculated beam widths corresponding to the three ratios given above are then 7.4° (down 3 db), 10.1° (down 6 db), and 12.9° (down 10 db), whereas the beam width corresponding to the first null of intensity is 17.3°. It should be noted that even when the outer limits of the beam are defined as being down 10 db in intensity level relative to the axial level, they still are some 7.5 db higher than the maximum level in the first minor lobe.

Other methods of specifying the directionality of a sound source are either in terms of the *directivity factor D*, which is defined by

$$D = \frac{I_0}{I_{\text{ref}}} \tag{7.57}$$

or the *directivity index d*, also called *directional gain*, which is defined by

$$d = 10 \log D = 10 \log \frac{I_0}{I_{\text{ref}}} \tag{7.58}$$

In these equations, I_0 is the axial intensity measured at some distance r from the source and I_{ref} is an arbitrary reference intensity defined by

$$I_{\text{ref}} = \frac{W}{4\pi r^2} \tag{7.59}$$

where $W = \iint I\,dS$ is the total acoustic power radiated by the source. Values of the directivity factor range from unity for a source of symmetrical spherical waves, such as an isolated simple source, to large numbers for highly directional sources. The directivity factor for a simple source radiating on *one* side of an infinite baffle is two.

A theoretical expression for the directivity factor of a flat piston radiating sound on one side of an infinite baffle can be derived. The intensity radiated in a direction θ by such a piston is

$$I = I_0 \frac{4J_1^2(ka \sin \theta)}{(ka \sin \theta)^2}$$

Consider an annular element of area $dS = 2\pi r^2 \sin \theta \, d\theta$ on the surface of a sphere of radius r centered on the piston. Since the intensity I is the same over all parts of this zone, it may be used as the element of area dS in computing the total acoustic output W. Then

$$W = 8\pi r^2 I_0 \int_0^{\pi/2} \frac{J_1{}^2(ka \sin \theta)}{(ka \sin \theta)^2} \sin \theta \, d\theta$$

Since it is assumed that no sound is radiated into the region corresponding to $\pi/2 < \theta < \pi$, the limits of integration are from $\theta = 0$ to $\theta = \pi/2$. Integration gives

$$W = \frac{4\pi r^2 I_0}{k^2 a^2} \left[1 - \frac{2J_1(2ka)}{2ka} \right] \tag{7.60}$$

Substitution of the above expression for W into equation 7.59, and the result in turn into equation 7.57, leads to

$$D = \frac{k^2 a^2}{1 - \dfrac{2J_1(2ka)}{2ka}} \tag{7.61}$$

When $2ka < 1$ this equation indicates a directivity factor of two and the piston is then equivalent to a simple source in an infinite baffle. On the other hand, when $ka \gg 1$

$$D \approx k^2a^2 = \frac{4\pi S}{\lambda^2} \tag{7.61a}$$

which clearly shows that the directivity factor is large for either short wavelengths or large piston areas.

Theoretical expressions for the directivity index of the above piston may be obtained by substitution of equations 7.61 and 7.61*a* into equation 7.58. In particular, when $ka \gg 1$

$$d \approx 20 \log ka \tag{7.62}$$

The directivity index is a measure of the increase in axial intensity level, expressed in decibels, relative to the uniform intensity level of a symmetrical spherical source that delivers the same total acoustic power. The directivity index of the piston previously considered, for which $ka = 8\pi$, is

$$d = 20 \log 8\pi = 28 \text{ db}$$

7.12 Sound Intensity Near a Piston Source. In the previous sections our discussion of the pressures and intensities produced by a piston source has been limited to distances from the source that are large in comparison with the radius of the piston, the treatment being mathematically analogous to the Fraunhofer diffraction of light through a circular aperture. Correspondingly, the pattern of pressures and intensities produced in the immediate vicinity of a vibrating piston is analogous to the Fresnel diffraction of light and can be analyzed by a consideration of half-period zones. As has been pointed out in Sect. 7.9, the general case of the pressures and intensities at points near a piston source is too difficult for mathematical analysis, and our discussion will therefore be limited to points on the axis of a circular piston. For such points $r' = (r^2 + \sigma^2)^{1/2}$, so that equation 7.44 becomes

$$d\mathbf{p} = \frac{j\rho_0 ck}{2\pi} U_0 e^{j\omega t}\left(\frac{e^{-jk\sqrt{r^2+\sigma^2}}}{\sqrt{r^2 + \sigma^2}}\right) dS$$

and integration over the surface of the piston gives

$$\mathbf{p} = -\rho_0 c U_0 e^{j\omega t}(e^{-jk\sqrt{r^2+a^2}} - e^{-jkr}) \tag{7.63}$$

The real part of this expression represents the actual pressure and may be used to derive an expression for the axial intensity I_0. Then

$$I_0 = 2\rho_0 c U_0^2 \sin^2 \frac{k}{2}(\sqrt{r^2 + a^2} - r) \tag{7.64}$$

At the center of the surface of the piston, where $r = 0$, the intensity is

$$I_{0(r=0)} = 2\rho_0 c U_0^2 \sin^2\left(\frac{ka}{2}\right) \tag{7.64a}$$

It is apparent that the pressure and the intensity are zero at the center of the piston whenever $ka/2 = n\pi$, where n is any integer. Similarly, the intensity is zero at points along the axis whose distance r from the center are given by

$$\frac{k}{2}(\sqrt{r^2 + a^2} - r) = n\pi \tag{7.65}$$

The largest value of r satisfying this equation is that corresponding to $n = 1$. If we replace k by $2\pi/\lambda$, then equation 7.65 reduces to

$$\sqrt{r^2 + a^2} - r = \lambda \tag{7.66}$$

If the frequency is so low that $a < \lambda$, this equation has no real solution, and consequently the intensity of the axis becomes zero only as r becomes infinite. At frequencies high enough so that $a \gg \lambda$, we may replace equation 7.66 by the approximate relation

$$r \approx a^2/2\lambda \tag{7.66a}$$

Finally it can readily be shown that for distances from the piston that are large in comparison with its radius, equation 7.64 reduces to

$$I_0 = \frac{\rho_0 c k^2 a^4 U_0^2}{8r^2} \tag{7.64b}$$

which is identical with the axial intensity as given by equation 7.56.

It should be noted that in general the axial intensity near the surface of a piston undergoes wide variations. With increasing distance from the surface this intensity runs through a series of maxima of constant amplitude, with intervening nulls. The last null occurs in the vicinity of $r = a^2/2\lambda$. At still greater distances the intensity goes through its final maximum and then, when $r > 2a^2/\lambda$, decreases inversely as the square of the distance. The equations developed in Sect. 7.9 through Sect. 7.11, which indicate spherical divergence of the sound beam, are therefore valid only for distances from the piston that are greater than $2a^2/\lambda$. For distances less than a^2/λ the radiated sound may be thought of as being confined within a cylinder of radius a, whereas beyond this point there is at least approximate spherical divergence. Figure 7.9 gives a rough picture of what occurs when $a = 4\lambda$ and also shows the manner in which the axial intensity varies with r. As a result of the fluctuations in intensity that occur

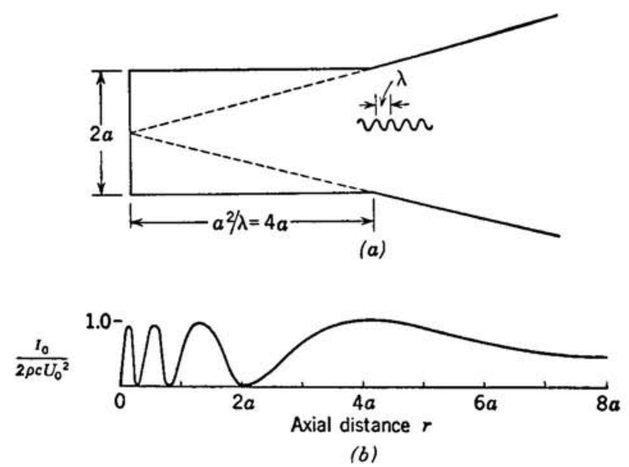

Fig. 7.9. (*a*) Sound beam in vicinity of a vibrating piston for $a = 4\lambda$. (*b*) Axial intensity as a function of radial distance r in the vicinity of a vibrating piston for $a = 4\lambda$.

in the immediate vicinity of any extended radiator, measurements of the acoustic radiation from a loudspeaker or sonar transducer should not be made with the measuring microphone placed close to the vibrating surface.

7.13 Reaction on a Vibrating Piston. In the preceding sections we have been primarily concerned with the pressure and intensity of the acoustic waves set up in a surrounding medium by a vibrating surface, the assumption being that both the amplitude and the frequency of vibration of the surface are known constants. In practice, however, it is often either the driving force or the driving power that is known, and under these circumstances the amplitude of vibration is a function of frequency. In writing the differential equation for the motion of the driver it is then necessary to include not only the dynamic constants of the driver itself, i.e., its mass, stiffness, and mechanical resistance, but also the force with which the medium reacts on the driving surface. This *reaction force* is required in order to transfer energy from the driver to the medium and can be computed from the expression for the acoustic pressure at points in the medium immediately adjacent to the driving surface. As in the previous discussion, our analysis will be limited to the reaction on a rigid circular piston mounted in an infinite baffle, but the solution will nevertheless be found useful in the study of several additional problems.

Consider an infinitesimal area dS of the surface of the piston, and let $d\mathbf{p}$ be the increment in pressure that the motion of dS produces in the medium at a point adjacent to some other element of area of the piston, dS'.

The total acoustic pressure **p** in the medium adjacent to dS' can then be obtained by integrating equation 7.44 over the surface of the piston, i.e.,

$$\mathbf{p} = \iint \frac{j\rho_0 ck}{2\pi r} U_0 e^{j(\omega t - kr)} dS \tag{7.67}$$

where r is the distance between dS and dS', measured along the surface of the piston.

The total reaction force acting on the piston is

$$\mathbf{f}_r = -\iint \mathbf{p}\, dS' \tag{7.68}$$

and substituting the value of **p** from equation 7.67

$$\mathbf{f}_r = -\frac{j\rho_0 ck}{2\pi} U_0 e^{j\omega t} \times \iint dS' \iint \frac{e^{-jkr}}{r} dS \tag{7.69}$$

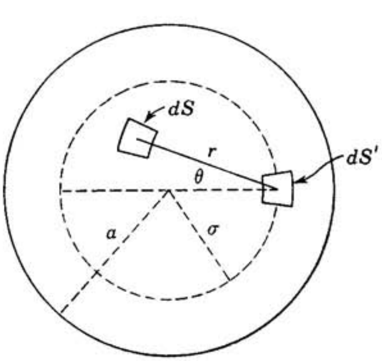

Fig. 7.10. Surface elements dS and dS' used in obtaining the reaction force acting on a vibrating piston.

The reaction force acting on an element dS', due to the motion of dS, is the same as the force acting on dS due to the motion of dS', so that the ultimate result of the double integration indicated by equation 7.69 is exactly *twice* as great as that which would be obtained if the limits of integration were so chosen as to include the force due to each pair of elements only *once*. This latter choice of limits leads to a considerable simplification of the problem and will be used in the following analysis, the value obtained from the integration being multiplied by two.

Referring to Fig. 7.10, let σ be the radial distance of the element dS' from the center of the piston. Then we may ensure that each pair of elements is used only once by integrating with respect to dS only over the area of the piston that is included within a concentric circle of radius σ. Let θ be the angle between the line from dS' to dS and a diameter through dS', and let $r\, d\theta\, dr$ represent the element of area dS. The maximum distance, in the direction θ, from dS' to any point within the circle of radius σ is $2\sigma \cos \theta$, so that the entire area within this circle will be covered if we integrate r from 0 to $2\sigma \cos \theta$, and θ from $-\pi/2$ to $\pi/2$. The integration of dS' is now to be extended over the entire surface of the piston, which will be accomplished by setting $dS' = \sigma\, d\sigma\, d\psi$ and then integrating

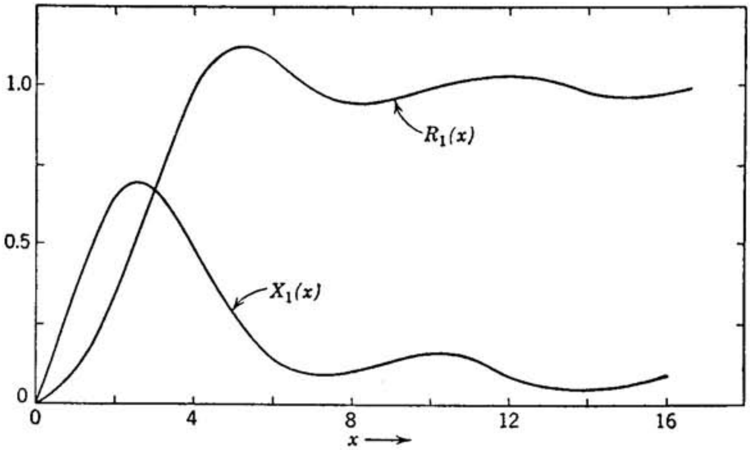

Fig. 7.11. Piston impedance functions.

ψ from 0 to 2π and σ from 0 to a. Therefore

$$\mathbf{f}_r = -\frac{j\rho_0 ck}{\pi} U_0 e^{j\omega t} \int_0^a \sigma \, d\sigma \int_0^{2\pi} d\psi \int_{-\pi/2}^{\pi/2} d\theta \int_0^{2\sigma \cos\theta} e^{-jkr} \, dr \quad (7.70)$$

The result of carrying out the above integration is

$$\mathbf{f}_r = -\rho_0 c\pi a^2 U_0 e^{j\omega t}[R_1(2ka) + jX_1(2ka)] \quad (7.71)$$

where $R_1(x)$ and $X_1(x)$ are two piston impedance functions defined, respectively, by

$$R_1(x) = \frac{x^2}{2 \cdot 4} - \frac{x^4}{2 \cdot 4^2 \cdot 6} + \frac{x^6}{2 \cdot 4^2 \cdot 6^2 \cdot 8} - \cdots \quad (7.72)$$

and

$$X_1(x) = \frac{4}{\pi}\left(\frac{x}{3} - \frac{x^3}{3^2 \cdot 5} + \frac{x^5}{3^2 \cdot 5^2 \cdot 7} - \cdots\right) \quad (7.73)$$

$R_1(x)$ is known as the *piston resistance function* and $X_1(x)$ as the *piston reactance function*. Values for these piston functions are given in Table IV of the appendix, and graphs of the functions are shown in Fig. 7.11.

At *small* values of x, such that $x < 1$, each of these functions can be replaced by the first term of its corresponding series, so that

$$R_1(x) \approx \frac{x^2}{8} \quad (7.72a)$$

and

$$X_1(x) \approx \frac{4x}{3\pi} \quad (7.73a)$$

On the other hand, when x is large it is possible to show that the above series expressions for the impedance functions converge in a manner such that

$$R_1(x) \approx 1 \tag{7.72b}$$

and

$$X_1(x) \approx \frac{4}{\pi x} \tag{7.73b}$$

7.14 Radiation Impedance. Let us now define a quantity $\mathbf{Z}_r$, called the *radiation impedance* of the piston, as the ratio of the force exerted by the piston on the medium to the velocity of the piston. In accordance with Newton's third law of equality of action and reaction, this force must be given by the negative of equation 7.71, i.e., by $-\mathbf{f}_r$. Therefore,

$$\mathbf{Z}_r = \frac{-\mathbf{f}_r}{U_0 e^{j\omega t}} = \rho_0 c \pi a^2 [R_1(2ka) + jX_1(2ka)] \tag{7.74}$$

The reaction force may readily be expressed in terms of this radiation impedance as

$$\mathbf{f}_r = -\mathbf{Z}_r U_0 e^{j\omega t} \tag{7.75}$$

If we include the reaction force of the medium, the differential equation governing the motion of a piston that is driven by a complex driving force $\mathbf{F}e^{j\omega t}$ is

$$m \frac{\partial^2 \xi}{\partial t^2} + R_m \frac{\partial \xi}{\partial t} + s\xi = \mathbf{F}e^{j\omega t} - \mathbf{Z}_r U_0 e^{j\omega t} = (\mathbf{F} - \mathbf{Z}_r U_0)e^{j\omega t} \tag{7.76}$$

where m is the mass, R_m the mechanical resistance constant, and s the stiffness constant of the piston. The solution of this equation is

$$\mathbf{u}_p = \frac{(\mathbf{F} - \mathbf{Z}_r U_0)e^{j\omega t}}{R_m + j(\omega m - s/\omega)} \tag{7.77}$$

Since the initial motion of the piston was assumed to be $\mathbf{u}_p = U_0 e^{j\omega t}$, equation 7.77 may be written in simpler form as

$$U_0 = \frac{\mathbf{F}}{R_m + j(\omega m - s/\omega) + \mathbf{Z}_r}$$

or

$$U_0 = \frac{\mathbf{F}}{\mathbf{Z}_m + \mathbf{Z}_r} \tag{7.78}$$

It is evident that the total impedance acting on the piston is the sum of its ordinary *mechanical impedance*, $\mathbf{Z}_m = R_m + j(\omega m - s/\omega)$, and the *radiation impedance*, $\mathbf{Z}_r$. Both of these quantities are functions of frequency, so that the velocity amplitude U_0 will not remain constant as the frequency is varied unless the driving force is also varied in such a manner as to keep $\mathbf{F}/(\mathbf{Z}_m + \mathbf{Z}_r)$ constant. Since the radiation impedance is the ratio of a force to a velocity, it is fundamentally identical with other kinds of mechanical impedance and has the dimensions of kilograms per second.

The real and imaginary components of the radiation impedance $\mathbf{Z}_r$ are defined as the *radiation resistance* R_r and the *radiation reactance* X_r, respectively, and hence for a circular piston mounted in an infinite baffle

$$R_r = \rho_0 c \pi a^2 R_1(2ka) \tag{7.79}$$

and

$$X_r = \rho_0 c \pi a^2 X_1(2ka) \tag{7.80}$$

The radiation reactance of a piston is always positive, and its effect is therefore equivalent to adding to the actual mass of the piston an additional mass m_r given by

$$m_r = \frac{X_r}{\omega} = \pi a^2 \rho_0 \frac{X_1(2ka)}{k} \tag{7.81}$$

At such low frequencies of vibration that $2ka < 1$, we may use equation 7.73*a* to replace the function $X_1(2ka)$ by

$$X_1(2ka) = \frac{4}{\pi} \cdot \frac{2ka}{3} = \frac{8ka}{3\pi} \tag{7.82}$$

so that for these frequencies

$$m_r = \tfrac{8}{3}\rho_0 a^3 \tag{7.83}$$

This mass is equivalent to that of an imaginary cylinder of the medium having the same radius as the piston and a length $\Delta l = 8a/3\pi$.

The result of mass loading is to decrease the resonant frequency of the piston from the usual value given by $\omega_0{}^2 = s/m$ to $\omega_0{}^2 = s/(m + m_r)$. Its effect is usually negligible for pistons operating in light media, such as air, but for a dense medium, such as that encountered in the transmission of underwater sound, the decrease in resonant frequency resulting from the presence of the medium may be quite marked.

At very high frequencies, such that $ka \gg 1$, the function $X_1(2ka)$ may be replaced by $2/\pi ka$, and then

$$m_r = \frac{2\rho_0 a^3}{k^2 a^2} = \frac{2\rho_0 a}{k^2} \tag{7.84}$$

so that the effect of the added mass is much less at high than at low frequencies. Computed values of the mass loading for a piston of 0.1-m radius radiating into water are plotted as a function of frequency in Fig. 7.12.

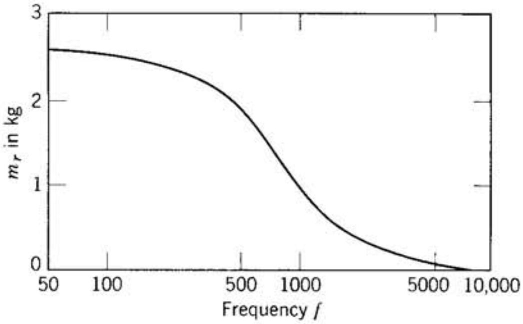

Fig. 7.12. Mass loading of a vibrating piston radiating into water.

The acoustic power radiated by a piston is equal to the rate at which work is done against the radiation resistance R_r. The average power expressed in watts is given by an equation similar to that derived for a simple oscillator (equation 1.32*a*), so that

$$W = \tfrac{1}{2}R_r U_0^2 \tag{7.85}$$

Substituting the value of R_r from equation 7.79,

$$W = \tfrac{1}{2}\rho_0 c\pi a^2 U_0^2 R_1(2ka) \tag{7.86}$$

Two special cases are of particular interest. When $2ka < 1$, i.e., for small pistons or for low frequencies, we may use the approximate relation of equation 7.72*a*,

$$R_1(2ka) = \frac{(2ka)^2}{8} = \frac{k^2a^2}{2} \tag{7.87}$$

and therefore

$$R_r \approx \frac{\rho_0 ck^2}{2\pi}(\pi a^2)^2 = \frac{\rho_0 ck^2}{2\pi} S^2 \tag{7.88}$$

The corresponding expression for the power radiated is

$$W = \frac{\rho_0 ck^2}{4\pi} S^2 U_0^2 \tag{7.89}$$

A comparison of this equation with equation 7.42 shows that the radiated power is identical with that of a simple source of strength $Q_H = SU_0$. This result is to be expected, since a small piston is in effect a simple source. In the region of low frequencies the power radiated as indicated by equation 7.89 is small, and increases with the square of the radiated frequency, provided that U_0 remains constant.

When $ka \gg 1$, i.e., for large pistons or for high frequencies, $R_1(2ka) \approx 1$ and $R_r \approx \rho_0 c\pi a^2$, so that

$$W \approx \tfrac{1}{2}\rho_0 c\pi a^2 U_0^{\,2} = \tfrac{1}{2}\rho_0 c S U_0^{\,2} \tag{7.90}$$

A comparison of this equation with equation 5.38 shows that the average power is the same as the plane-wave power that would be radiated by the piston into a pipe of radius a. Such behavior is to be anticipated, for when $ka \gg 1$ most of the sound energy is radiated in a narrow beam of small divergence. Finally, if the driving force can be varied in such a manner as to keep the velocity amplitude constant as the frequency is changed, the power radiated by the piston is directly proportional to the function $R_1(2ka)$ shown in Fig. 7.11.

Although the equations developed in this chapter are strictly applicable only to the particular situations for which they were derived, namely the simple source and the flat piston in an infinite baffle, they are basic to applied acoustics and will serve as a starting point for the discussion of the more complicated problems that will be considered in the following chapters.

PROBLEMS

7.1. Show that the component equations 7.4 may be combined into one vector equation, $-\nabla p = \rho_0(\partial \mathbf{q}/\partial t)$. Use this equation to derive equation 7.12.

7.2. Given the acoustic pressure in a spherical wave to be represented by $p = (A/r)\cos(\omega t - kr)$. (*a*) By direct substitution show that this equation satisfies equation 7.8. (*b*) For what value of kr is the specific acoustic reactance of a diverging spherical wave equal to one-tenth of its specific acoustic resistance?

7.3. Given a small source of spherical waves in air. For a radial distance of 10 cm, compute the difference in phase angle between pressure and particle velocity at frequencies of 10, 100, and 1000 cycles/sec. Similarly compute the magnitude of the specific acoustic impedance for these conditions.

7.4. A simple source of sound in air radiates spherical waves at a frequency of 400 cycles/sec and at an acoustic power of 10 milliwatts. Compute (*a*) the intensity at a radial distance of 0.5 m from the source, (*b*) the pressure amplitude at this distance, (*c*) the particle velocity amplitude at this distance, (*d*) the particle displacement amplitude at this distance, and (*e*) the condensation amplitude at this distance.

7.5. A hemisphere of 0.1-m radius is mounted in an infinite baffle and radiates spherical waves into water at a frequency of 250 cycles/sec. The measured pressure level at a distance of 2 m from the center of the hemisphere is 66 db *re* 1 microbar. (*a*) What is the effective acoustic pressure at this point? (*b*) What is the intensity at this point? (*c*) What is the total acoustic power radiated by the hemisphere? (*d*) What is the peak displacement amplitude of the surface of the hemisphere under these conditions?

7.6. A small source of sound is located near the center of a large body of water and radiates 20 watts of acoustic power at a frequency of 1000 cycles/sec. What is (*a*) the intensity, (*b*) the acoustic pressure amplitude, and (*c*) the particle velocity amplitude at a distance of 50 cm from the source? (*d*) By what phase angle does the pressure lead the particle velocity?

7.7. A pulsating sphere radiates spherical waves into air so as to produce an intensity of 50 milliwatt/m^2 at a distance of 1.0 m from the center of the sphere. (*a*) What is the acoustic power radiated in watts? (*b*) If the frequency is 100 cycles/sec, compute the intensity, the pressure amplitude, and the particle velocity amplitude at the surface of the sphere. (*c*) Repeat part (*b*) at a distance of 0.5 m from the center of the sphere.

7.8. Given a pulsating sphere of radius a and surface velocity amplitude U_0 to radiate uniformly in all directions. Derive a general expression, good for all frequencies, giving the intensity and pressure amplitude of the radiated spherical waves. Note that since ka is not necessarily small relative to unity, it may not be neglected as was done in Sect. 7.7.

7.9. Given a pulsating sphere of radius a to be vibrating with a surface velocity amplitude U_0 and at such a high frequency that $ka \gg 1$. Derive expressions for the pressure amplitude, the particle velocity amplitude, the intensity, and the total acoustic power radiated in the resulting acoustic wave.

7.10. A piston of radius a is mounted in an infinite plane baffle. By direct integration of equation 7.44 over the surface of the piston, derive a general expression for the acoustic pressure amplitude at the center of the piston.

7.11. By expanding $e^{jk\sigma \sin\theta \cos\psi}$ as a power series show that

$$\int_0^{2\pi} e^{jk\sigma \sin\theta \cos\psi}\, d\psi = 2\pi J_0(k\sigma \sin\theta)$$

7.12. A dynamic speaker cone having a diameter of 30 cm is mounted in an infinite baffle. Assuming that the cone may be regarded as a rigid circular piston of equal radius, compute the intensities relative to the axial intensity for a frequency of 1000 cycles/sec, and make a polar plot of this radiation pattern as a function of direction. What must be the velocity amplitude of the cone if the axial intensity level at a distance of 300 cm is to be 80 db?

7.13. A dynamic speaker cone having a diameter of 0.3 m is mounted in an infinite baffle. Assuming that the cone may be regarded as a rigid circular piston of equal radius, compute the pressure amplitudes relative to the axial pressure for a frequency of 3000 cycles/sec, and make a polar plot of this radiation pattern as a function of direction. At what frequency will the pressure amplitude along the wall be equal to one half of its axial value?

7.14. (*a*) Derive a general equation giving the beam width of the radiation pattern produced by a circular piston vibrating in an infinite baffle at the -3 db intensity level relative to the axial level. (*b*) Repeat for a -6 db level. (*c*) Repeat for a -10 db level.

7.15. A circular piston type of sonar transducer of 0.5-m radius radiates 5000 watts of acoustic power into water at a frequency of 10 kc/sec. (*a*) What is its beam width at the down 10 db direction? (*b*) What is the axial pressure level in db *re* 1 microbar at a distance of 10 m from the face of the transducer?

7.16. A piston of radius a is mounted so as to radiate on one side of an infinite baffle into air. The piston is driven at a frequency such that the wavelength of the radiated sound equals πa. (*a*) Compute and plot the relative axial intensities produced by the piston from its surface to a distance of 0.5 m. (*b*) Over what range of distances is the divergence approximately spherical?

7.17. A pulsating sphere of radius a is vibrating with a surface velocity amplitude U_0 and at a frequency such that $ka > 1$. (*a*) Derive a general expression for the radiation resistance and reactance acting upon the surface of the sphere. Note that since ka is not small relative to unity, it may not be neglected as was done in Sect. 7.7. (*b*) Derive a general expression for the total acoustic power radiated by the above sphere.

7.18. A pulsating sphere of 0.2-m diameter radiates 150 watts of acoustic power into water at a frequency of 5 kc/sec. (*a*) Using the results of problem 7.17, compute the required velocity amplitude of vibration of the surface of the sphere. (*b*) Compute the equivalent mass added to the sphere by the radiation reactance of the medium.

7.19. A piston is mounted so as to radiate on one side of an infinite baffle into air. The radius of the piston is a, and it is driven at a frequency such that the wavelength of the radiated sound equals πa. (*a*) If the radius $a = 0.1$ m, and the maximum displacement amplitude of the piston is 0.0002 m, how much acoustic power is radiated? (*b*) What is the axial intensity at a distance of 2.0 m? (*c*) What is the directivity index of the radiated beam? (*d*) What is the radiation mass loading acting on the piston?

7.20. A flat piston of 0.2-m radius radiates 100 watts of acoustic power at 20 kc/sec when immersed in water. (*a*) Assuming the radiation to be equivalent to that of a piston mounted in an infinite baffle and radiating on only one side, what is the velocity amplitude of the piston? (*b*) What is the radiation mass loading of the piston? (*c*) What is the beam width at the down 10-db direction? (*d*) What is the directivity index of the beam?

7.21. A flat piston of 0.15-m radius is mounted so as to radiate on one side of an infinite baffle into air. The frequency is 330 cycles/sec. (*a*) What must be the velocity amplitude of the piston, if it is to radiate 0.5 watts of acoustic power? (*b*) If the piston has a mass of 0.015 kg, a stiffness constant of 2000 newtons/m, and negligible internal mechanical resistance, what force amplitude is required in order to produce this velocity amplitude?

chapter 8

RESONATORS AND FILTERS

8.1 Helmholtz Resonator. The dimensions of the various elements of an acoustic system are often small in comparison with the wavelength of the sound, and, when this is true, the motion of the medium in the system is analogous to that of a mechanical system having lumped mechanical elements of mass, stiffness, and resistance. The simple Helmholtz resonator of Fig. 8.1*a* is one important acoustic system that may be discussed in terms of an analogous simple mechanical oscillator. Such a resonator consists of a rigid enclosure of volume V, communicating with the external medium through a small opening of radius a and length l. The gas in the opening is considered to move as a unit and provides the *mass* element of the system. The pressure of the gas within the cavity of the resonator changes as it is alternately compressed and expanded by the influx and efflux of gas through the opening and thus provides the *stiffness* element. At the opening, moreover, there is radiation of sound into the surrounding medium, which leads to the dissipation of acoustic energy and thus provides a *resistance* element. In addition, another resistance element is provided by the viscous forces associated with the influx and efflux of gas through the opening. In this chapter, we shall ignore those resistance terms associated with viscosity since the equations required for their computation are

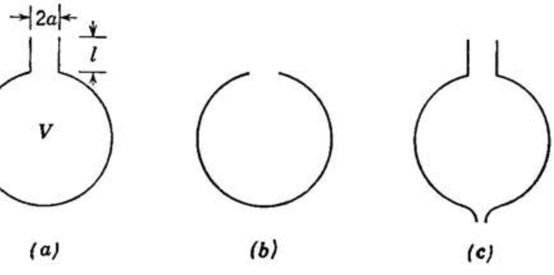

Fig. 8.1. Simple Helmholtz resonators.

not developed until the following chapter. However, it is to be noted that, generally speaking, resistance terms contributed by viscous forces through openings of one centimeter diameter or greater are less than those associated with the radiation of sound.

The gas in the opening has a total effective mass of $\rho_0 S l'$, where S is the cross-sectional area of the opening, and l' is its effective length. Since some of the gas beyond the ends of the actual constriction moves as a unit with the gas in the constriction, it is necessary to use an effective length l' which is greater than the true length l. In Sect. 7.14 we have seen that at low frequencies the adjacent medium loads a vibrating piston, mounted in an infinite baffle, with a mass equal to that of the fluid contained in a cylinder of area S and length $\Delta l = 8a/3\pi$. If the mass loading at each of the two ends of the opening of a Helmholtz resonator is assumed to be equivalent to that of such a piston, then

$$l' = l + 2\Delta l = l + \frac{16a}{3\pi} \tag{8.1}$$

Therefore, we may expect that even an opening consisting of a mere hole drilled in the thin wall of resonator, Fig. 8.1b, will have a finite effective length proportional to the radius of this hole.

The determination of the end correction Δl that must be applied to obtain the effective length of a given constriction has been carried through mathematically for relatively few types of opening. However, at low frequencies reasonably correct results are obtained by assuming that $\Delta l = 8a/3\pi = 0.85a$ for a constriction terminated in a wide flange and $\Delta l = 0.6a$ for an unflanged termination.

In order to determine the stiffness of the system it is necessary to calculate the force f acting on the area S of the opening when the gas in the constriction is displaced a distance ξ. The increase in pressure that results when a volume of gas $dV = S\xi$ flows in through the opening is given by equation 5.4b as

$$p = \rho_0 c^2 s = \rho_0 c^2 \frac{dV}{V} = \frac{\rho_0 c^2 S \xi}{V} \tag{8.2}$$

The resulting force of stiffness acting at the opening is therefore

$$f = -\frac{\rho_0 c^2 S^2}{V}\,\xi \tag{8.2a}$$

and the effective stiffness constant of the system is $\rho_0 c^2 S^2/V$.

If it is assumed that the moving mass of air in the opening radiates sound into the surrounding medium in the same manner as a simple source mounted in an infinite baffle, then the effective radiation resistance given by equation 7.88 is $\rho_0 ck^2S^2/2\pi$.

In complex form, the instantaneous acoustic pressure produced by a sound wave of amplitude P impinging on the resonator opening is

$$\mathbf{p} = Pe^{j\omega t} \tag{8.3}$$

and the corresponding driving force is

$$\mathbf{f} = SPe^{j\omega t} \tag{8.3a}$$

The resulting differential equation for the inward displacement $\boldsymbol{\xi}$ of the gas in the constriction is

$$\rho_0 l'S\frac{d^2\boldsymbol{\xi}}{dt^2} + \frac{\rho_0 ck^2S^2}{2\pi}\frac{d\boldsymbol{\xi}}{dt} + \frac{\rho_0 c^2S^2}{V}\boldsymbol{\xi} = SPe^{j\omega t} \tag{8.4}$$

Since this equation is analogous to that of a driven oscillator, its solution may be obtained by analogy from that of equation 1.23*a*.

8.2 Acoustic Impedance. Similarly, many other simple acoustic systems may be converted into an analogous mechanical system and solved. However, it is also possible to convert such a system into an analogous electrical system in which the motion of the fluid medium is equivalent to the behavior of current in an electric circuit having lumped elements of inductance, capacitance, and resistance. The electrical analogue of the pressure difference across an acoustic element is the voltage across the corresponding part of the electric circuit. The acoustic analogue of current at some point in the circuit is the *volume velocity* U of the fluid in the corresponding acoustic element. The latter quantity is readily defined in terms of the *volume displacement* X *of* fluid in the element. The displacement of fluid through any surface is given by the integral of the scalar product of the displacement and the corresponding surface element, i.e.,

$$X = \iint \boldsymbol{\xi}\cdot\mathbf{dS} \tag{8.5}$$

If the particle displacement is normal to the surface, and is the same at all points, equation 8.5 reduces to

$$X = \xi S \tag{8.5a}$$

and the volume velocity is then given by

$$U = \frac{\partial X}{\partial t} = \frac{\partial \xi}{\partial t}S \tag{8.5b}$$

The right-hand term of equation 8.4 may be converted into its analogous-electrical form by dividing both sides of the equation by S. Furthermore, if the expression for particle displacement ξ is replaced by X/S, then equation 8.4 becomes

$$\frac{\rho_0 l'}{S}\frac{d^2\mathbf{X}}{dt^2} + \frac{\rho_0 c k^2}{2\pi}\frac{d\mathbf{X}}{dt} + \frac{\rho_0 c^2}{V}\mathbf{X} = Pe^{j\omega t} \tag{8.6}$$

Finally, replacing $\rho_0 l'/S$ with M, $\rho_0 ck^2/2\pi$ with R, and $\rho_0 c^2/V$ with $1/C$, we obtain

$$M\frac{d^2\mathbf{X}}{dt^2} + R\frac{d\mathbf{X}}{dt} + \frac{\mathbf{X}}{C} = Pe^{j\omega t} \tag{8.7}$$

which is seen to be an acoustic analogue of the electrical equation for a series RLC circuit, Sect. 1.17. Its solution is

$$\mathbf{U} = \frac{d\mathbf{X}}{dt} = \frac{Pe^{j\omega t}}{\mathbf{Z}} \tag{8.8}$$

where

$$\mathbf{Z} = R + j\left(\omega M - \frac{1}{\omega C}\right) \tag{8.9}$$

represents the *acoustic impedance* of a Helmholtz resonator.

In general, the acoustic impedance $\mathbf{Z}$ of a fluid medium acting on or through a surface of given area S is the complex quotient of the acoustic pressure at the surface divided by the volume velocity at the surface, i.e.,

$$\mathbf{Z} = \frac{\mathbf{p}}{\mathbf{U}} \tag{8.10}$$

When concentrated, rather than distributed, impedances are considered, the impedance of a portion of the acoustic system is defined as the complex ratio of the pressure difference effective in driving that portion to the volume velocity. The acoustic impedance of any system is readily expressed in terms of mechanical impedance, being equal to mechanical impedance divided by the square of the area of the surface being considered. The unit of acoustic impedance is the *acoustic ohm*, which in the MKS system has the units of

$$\frac{\text{Pressure}}{\text{Volume velocity}} = \frac{\text{newtons/m}^2}{\text{m}^3\text{/sec}} = \frac{\text{kg}}{\text{m}^4\text{ sec}}$$

A complex acoustic impedance $\mathbf{Z}$ may be separated into its real and imaginary parts

$$\mathbf{Z} = R + jX \tag{8.11}$$

where the *acoustic resistance* R of a sound medium is defined as the *real* component of the acoustic impedance and is the component that is associated with the dissipation of energy. Similarly, the acoustic *reactance* X of a sound medium is the *imaginary* component of the acoustic impedance and is the component that results from the effective mass and stiffness of the medium.

We have now encountered three kinds of acoustic impedances, an inexcusable redundancy if it were not for the fact that these various impedances are useful in different kinds of calculations. The specific acoustic impedance $\mathbf{z}$ (pressure/particle velocity) is a characteristic property of the medium and of the type of waves that are being propagated through it. It is primarily useful in calculations involving the transmission of acoustic waves from one medium to another. The acoustic impedance $\mathbf{Z}$ (pressure/volume velocity) is primarily useful in discussing acoustic radiation from vibrating surfaces, and the transmission of this radiation through lumped acoustic elements at low frequencies, or through pipes and horns at all frequencies. The acoustic impedance is related to the specific acoustic impedance at a surface by $\mathbf{Z} = \mathbf{z}/S$. The radiation impedance $\mathbf{Z}_r$ (force/velocity) is used in calculating the coupling between acoustic waves and a driving source or driven load. It is the part of the mechanical impedance of a vibrating system associated with the radiation of sound. Radiation impedance is related to specific acoustic impedance at a surface by $\mathbf{Z}_r = \mathbf{z}S$ and to acoustic impedance by $\mathbf{Z}_r = \mathbf{Z}S^2$.

The acoustic impedance of the medium acting upon the flat piston of Sect. 7.13 is obtained by dividing its radiation impedance by the square of the surface area. The expression for the acoustic resistance of the piston is

$$R = \frac{\rho_0 c}{\pi a^2} R_1(2ka) \tag{8.12}$$

and that for the acoustic reactance is

$$X = \frac{\rho_0 c}{\pi a^2} X_1(2ka) \tag{8.13}$$

For frequencies low enough so that $2ka < 0.5$, the expression for acoustic resistance may be simplified by means of equation 7.87 to

$$R = \frac{\rho_0 c k^2}{2\pi} \tag{8.12a}$$

without producing an error in excess of one per cent.

8.3 Acoustic Analogues. The analogy between acoustic and electrical systems may be advantageously carried much further if we define the *acoustic inertance* M of the acoustic element as

$$M = m/S^2 \tag{8.14}$$

where m is the effective mass of the element. An application of this definition to the Helmholtz resonator gives

$$M = \frac{\rho_0 l' S}{S^2} = \frac{\rho_0 l'}{S}$$

which agrees with the substitution used in deriving equation 8.7. Acoustic inertance is analogous to electrical inductance and has the dimensions of kg/m^4 in the MKS system of units.

The *acoustic compliance* C of an acoustic element is defined as the volume displacement X that is produced by the application of unit pressure. It is the analogue of electrical capacitance, which is similarly defined as the charge appearing on a capacitor per unit of applied voltage. For an acoustic element having an enclosed volume V, such as a Helmholtz resonator, this definition leads to

$$C = \frac{V}{\rho_0 c^2} \tag{8.15}$$

The units of acoustic compliance are $m^4 sec^2/kg$.[1]

Finally, any element or characteristic of an acoustic system that leads to the dissipation of energy is analogous to electrical resistance. For instance, we have already seen that a major portion of the acoustic resistance of a Helmholtz resonator results from the radiation of sound energy and is given by $R = \rho_0 c k^2/2\pi$. It is also possible to derive expressions for the additional acoustic resistance associated with viscous forces in the fluid medium.

The three basic elements of acoustical, electrical, and mechanical systems are represented schematically in Fig. 8.2. The inertance M of an acoustic system is represented by the mass of fluid contained in a constriction which is short enough so that all particles may be assumed to move in phase when actuated by a sound pressure. The compliance C of the system is represented by an enclosed volume, with its associated stiffness. It should be noted that the mechanical analogue of acoustic compliance is not mechanical stiffness, but rather its reciprocal *mechanical compliance* C_m, defined by $C_m = 1/s$. Although resistance may be contributed to an acoustic system by a number of different factors, irrespective of its origin it is conveniently represented by narrow slits in a pipe, for the viscous forces that arise when the fluid is forced to flow through these slits always results in the dissipation of energy.

[1] It will be the general practice in this book to use the symbols R, C, Z, etc., without subscripts to represent acoustic quantities. If in any particular situation confusion is likely to result from the use of the same symbols for the analogous electrical quantities, the acoustic quantities will be written with subscripts as R_A, C_A, Z_A, etc.

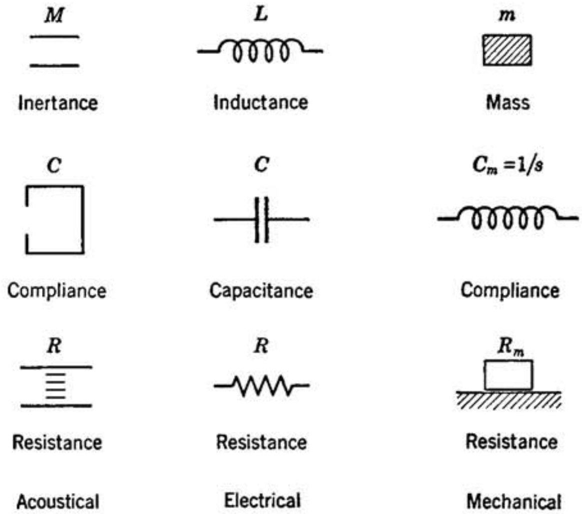

Fig. 8.2. Acoustical, electrical, and mechanical analogues.

A Helmholtz resonator may be graphically represented as in Fig. 8.3*a*. However, this simple acoustic system may be represented schematically with equal or greater facility by the circuit of the analogous electrical system, Fig. 8.3*b*. In general, if it is possible to replace a complicated acoustic system by the schematic circuit of its analogous electrical system, known solutions of the latter may be used to discuss the former. Section 8.12 contains a number of such representations of important acoustic systems.

The analogies just described are those most commonly used in acoustics. However, another system of analogies known as the *mobility* system is sometimes used with advantage. In the mobility system *acoustic mobility*, defined as the ratio of volume velocity across to pressure through the acoustic system, is analogous to electrical impedance, volume velocity to

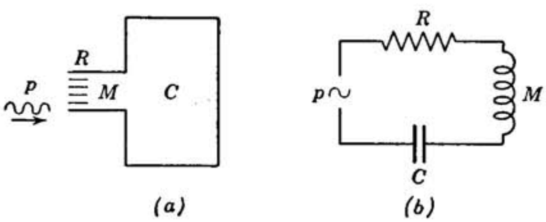

Fig. 8.3. Schematic representations of a Helmholtz resonator.

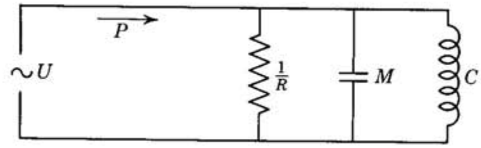

Fig. 8.4. Mobility analogue of a Helmholtz resonator.

voltage, pressure to current, inertance to capacitance, compliance to inductance, and the reciprocal of the acoustic resistance to electrical resistance. A schematic circuit representing the Helmholtz resonator in terms of its mobility type of analogous circuit is shown in Fig. 8.4. Readers acquainted with electrical network theory will recognize the circuit of Fig. 8.4 as being the *parallel* circuit that is *dual* with the *series* circuit of Fig. 8.3*b*. The mobility system of analogies has its principal applications where either electromechanical or electroacoustical coupling is involved.[2] Consequently, further discussion will be deferred to later chapters concerned with the various types of electroacoustic transducers such as loudspeakers, microphones, and sonar transducers.

8.4 Resonance of a Helmholtz Resonator. Resonance will occur when the acoustic reactance equals zero, i.e., when

$$\omega_0 M - \frac{1}{\omega_0 C} = 0$$

Therefore

$$\omega_0 = \sqrt{\frac{1}{MC}} = c\sqrt{\frac{S}{l'V}} \tag{8.16}$$

where M and C have been replaced by $\rho_0 l'/S$ and $V/\rho_0 c^2$, respectively. This equation also gives the frequency of undamped free oscillation. In actual resonators the damping due to viscosity and to the radiation of sound is so small that the frequency of damped free oscillation is also given, to a very close approximation, by the same expression.

A comparison of measured resonance frequencies with those predicted by equation 8.16 may be used to determine the effective length l' of the opening, which in turn may be used to calculate the effective end correction Δl. Table 8.1 gives the dimensions of four Helmholtz resonators, with their measured resonant frequencies and the resulting values of $\Delta l/a$. In making these calculations it has been assumed that the end corrections at both the inside and outside of the opening are the same.

[2] Olson, *Dynamical Analogies*, pp. 232–256, D. Van Nostrand Co. (1958).

These values are seen to lie in an intermediate range between the expected value of 0.6 for an unflanged pipe and 0.85 for a flanged pipe.

In deriving the equation for the resonant frequency of a Helmholtz resonator, no assumption has been made which restricts its shape to that of a sphere. For a given opening, it is the volume of the cavity, and not its shape, that is important. In fact, as long as the linear dimensions of the cavity are considerably less than a quarter of a wavelength and the opening is not too large, the resonant frequencies of cavities having the same opening and volume but having very different shapes are found to be identical.

Table 8.1 Data on Helmholtz resonators

V m^3	a m	l m	f_0 cycles/sec	l' m	$\Delta l/a$	Q	n_0 db
0.00266	0.019	0.006	192	0.034	0.74	52	34
0.00112	0.0155	0.006	256	0.03	0.78	52	34
0.000385	0.0095	0.007	320	0.0215	0.76	80	38
0.000115	0.0075	0.003	576	0.014	0.74	47	33

Helmholtz resonators are observed to have additional resonant frequencies which are higher than the fundamental frequency given by equation 8.16. The origin of these higher frequencies is quite different from that of the fundamental, for they result from the formation of patterns of standing waves in the cavity, rather than from the oscillatory motion of the mass of gas in the orifice. The overtone frequencies therefore depend on the shape of the cavity, rather than on its volume, and are not harmonically related to the fundamental. In general, the frequency of the first overtone is several times as great as that of the fundamental, a property that enhances the utility of a Helmholtz resonator as an acoustic measuring device, for it greatly simplifies the problem of distinguishing between fundamental and overtone responses.

The sharpness of resonance of a driven Helmholtz resonator as measured by its quality factor Q is theoretically given by

$$Q = \frac{\omega_0 M}{R} = 2\pi\sqrt{\frac{l'^3 V}{S^3}} \tag{8.17}$$

This expression is derived on the assumption that there are no losses except those resulting from the radiation of sound energy and that this radiation is similar to that of a simple source mounted in an infinite baffle, i.e., $R = \rho_0 c k^2/2\pi$. Computed values for the resonators listed in Table 8.1

range from 48 to 80, whereas actual measured values are somewhat higher. This is not surprising, since we might with equal justification have assumed that $R = \rho_0 ck^2/4\pi$, the acoustic resistance of an isolated simple source, which would have led to a theoretical quality factor double that of equation 8.17.

In his original investigations of the component frequencies present in complex musical tones, Helmholtz used a graduated series of resonators of the type pictured in Fig. 8.1*c*, with their individual volumes and areas of opening so chosen as to cover a wide range of frequencies. Whenever an incident sound wave has a frequency component corresponding to the resonant frequency of a particular resonator, greatly amplified sound pressures at this frequency will be produced within the cavity of the resonator. Such resonance may be audibly detected by connecting the small nipple opposite the mouth of the resonator to the ear, either directly or through a short rubber tube.

Let us define the *pressure amplification* of the resonator as the ratio of the acoustic pressure within the cavity to the external driving pressure of the incident sound wave. The pressure amplitude P_r within the cavity, as given by equation 8.2 combined with equations 8.15 and 8.16 is

$$P_r = \frac{\rho_0 c^2}{V} X = \frac{X}{C} = \omega_0^2 MX \tag{8.18}$$

where X is the amplitude of volume displacement in the opening. At resonance the latter is given by $X_0 = P/\omega_0 R$. When this value of X_0 is substituted into equation 8.18, the pressure amplification at resonance is given by

$$\left(\frac{P_r}{P}\right)_0 = \frac{\omega_0 M}{R} = Q = 2\pi\sqrt{\frac{l'^3 V}{S^3}} \tag{8.19}$$

This pressure amplification at resonance corresponds to a sound pressure level gain expressed in decibels of

$$n_0 = 20 \log (P_r/P)_0 = 20 \log Q = 10 \log \frac{4\pi^2 l'^3 V}{S^3} \tag{8.20}$$

Calculated values of sound pressure level gain are given for the resonators listed in Table 8.1.

Whenever a loudspeaker is mounted in a closed cabinet, the combined system may be treated as a Helmholtz resonator, in which both the reactance of the fluid medium and the mass of the speaker cone contribute to the effective inertance of the system. Similarly, both the stiffness of the cavity and that of the speaker cone contribute to the effective acoustic compliance. Finally, the effective acoustic resistance is the sum of that due to the radiation of acoustic energy and that due to the internal mechanical resistance of the speaker cone.

8.5 Distributed Acoustic Impedance. When the dimensions of elements of an acoustic system are not small as compared to a wavelength, it is no longer possible to treat the system as one having lumped constants, and it must instead be considered as one having distributed constants. The simplest system of this type is one in which plane waves are propagated through a long pipe. If the waves are propagated in the positive x direction, the ratio of acoustic pressure to particle velocity is given by the characteristic impedance $\rho_0 c$ of the medium, and hence the acoustic impedance at any cross section S in the pipe is

$$\mathbf{Z} = \frac{\mathbf{p}}{\mathbf{U}} = \frac{\mathbf{p}}{S\mathbf{u}} = \frac{\rho_0 c}{S} \tag{8.21}$$

The propagation of plane waves in such a pipe is analogous to the propagation of high-frequency currents along a transmission line. We may consider the medium in the pipe to possess a *distributed inertance* M_1 per unit length, where $M_1 = \rho_0/S$, and a *distributed compliance* C_1 per unit length, where $C_1 = S/\rho_0 c^2$. Application of the well-known equation for the characteristic impedance of a transmission line to the analogous acoustic problem gives for the acoustic impedance of plane waves in a pipe

$$Z = \sqrt{\frac{M_1}{C_1}} = \sqrt{\frac{\rho_0/S}{S/\rho_0 c^2}} = \frac{\rho_0 c}{S}$$

which is in agreement with equation 8.21. Furthermore, as will be shown in the following sections, the reflection and transmission of sound waves at a point where the acoustic impedance of a pipe changes is analogous to the behavior of current waves in a transmission line at a point where there is an abrupt change in its dimensions or where it is terminated in an impedance differing from the characteristic impedance of the line.

8.6 Reflection of Waves in a Pipe. Assume that at some point x along a pipe the acoustic impedance changes from its characteristic value of $\rho_0 c/S$, to $\mathbf{Z}_x$, where $\mathbf{Z}_x$ may be either real or complex, depending on the particular nature of the change occurring in the pipe. If an initial wave traveling in the positive x direction and represented by

$$\mathbf{p}_i = \mathbf{A}e^{j(\omega t - k)} \tag{8.22}$$

is incident at this point, a reflected wave

$$\mathbf{p}_r = \mathbf{B}e^{j(\omega t + kx)} \tag{8.23}$$

traveling in the negative x direction will in general be produced. The volume velocities of fluid flow corresponding to these two waves are given, respectively, by

$$\mathbf{U}_i = \frac{\mathbf{p}_i}{\rho_0 c/S} \quad \text{and} \quad \mathbf{U}_r = -\frac{\mathbf{p}_r}{\rho_0 c/S}$$

When both waves are present, the varying phase relationship between them causes the acoustic impedance to vary from point to point along the pipe, rather than remaining the same at all points as is true when only the incident wave is present. A general expression for acoustic impedance which includes the reflected wave is

$$\mathbf{Z} = \frac{\mathbf{p}_i + \mathbf{p}_r}{\mathbf{U}_i + \mathbf{U}_r} = \frac{\rho_0 c}{S} \cdot \frac{\mathbf{p}_i + \mathbf{p}_r}{\mathbf{p}_i - \mathbf{p}_r} \tag{8.24}$$

or

$$\mathbf{Z} = \frac{\rho_0 c}{S} \cdot \frac{\mathbf{A}e^{-jkx} + \mathbf{B}e^{jkx}}{\mathbf{A}e^{-jkx} - \mathbf{B}e^{jkx}} \tag{8.24a}$$

At the cross section of the pipe where the impedance changes, the usual conditions of continuity of pressure and volume velocity may be replaced by a condition of continuity of their ratio, i.e., continuity of acoustic impedance, and hence the phases and amplitudes of the incident and reflected waves must be so related as to cause equation 8.24*a* to be equal to $\mathbf{Z}_x$.

Without any loss in generality, the origin of coordinates may be chosen to coincide with the position of changing impedance. Then we may apply the condition that equation 8.24*a* equals $\mathbf{Z}_0$ when $x = 0$, giving

$$\mathbf{Z}_0 = \frac{\rho_0 c}{S} \cdot \frac{\mathbf{A} + \mathbf{B}}{\mathbf{A} - \mathbf{B}}$$

so that

$$\frac{\mathbf{B}}{\mathbf{A}} = \frac{\mathbf{Z}_0 - \rho_0 c/S}{\mathbf{Z}_0 + \rho_0 c/S} \tag{8.25}$$

The sound power reflection coefficient α_r, at a point where the acoustic impedance changes is given by

$$\alpha_r = \left(\frac{B}{A}\right)^2 = \frac{(R_0 - \rho_0 c/S)^2 + X_0^{\,2}}{(R_0 + \rho_0 c/S)^2 + X_0^{\,2}} \tag{8.26}$$

where $\mathbf{Z}_0$ has been replaced by $R_0 + jX_0$, its real and reactive components. Correspondingly, the sound power transmission coefficient α_t, which is equal to $1 - \alpha_r$, is given by

$$\alpha_t = \frac{4R_0\rho_0 c/S}{(R_0 + \rho_0 c/S)^2 + X_0^{\,2}} \tag{8.27}$$

It is to be noted that each of the above three equations is similar in form to equations derived in Sect. 6.3 expressing reflection of plane waves normally incident on a second medium of different characteristic specific impedance. The only difference between equations 8.25, 8.26, and 8.27 and the corresponding equations of Sect. 6.3 is that acoustic impedance parameters have replaced specific acoustic impedance parameters.

As one example, let us apply these equations to plane waves in a pipe of cross-sectional area S_1 as they enter a second pipe of area S_2, as shown in Fig. 8.5. When the wavelength is large compared to the diameters of each of the pipes, we may assume that the acoustic impedance seen by the waves incident on the junction is $Z_0 = \rho_0 c/S_2$, the acoustic impedance of plane waves in the second pipe. Note that this assumption requires that the second pipe be essentially either of infinite length or so terminated, that no reflected wave is returned from its far end to set up standing waves. Furthermore, distortions in the wave fronts as they either converge or diverge at the junction are ignored. Upon substitution of this expression for Z_0 into the general equations derived above, the following special equations are obtained.

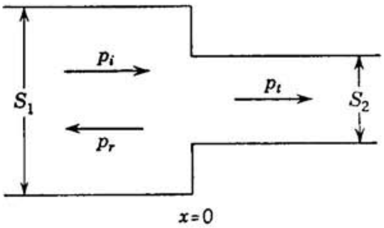

Fig. 8.5. Transmission and reflection of a plane wave at a junction between two pipes.

$$\frac{\mathbf{B}}{\mathbf{A}} = \frac{(S_1 - S_2)}{(S_1 + S_2)} \tag{8.28}$$

$$\alpha_r = \frac{(S_1 - S_2)^2}{(S_1 + S_2)^2} \tag{8.28a}$$

$$\alpha_t = \frac{4S_1S_2}{(S_1 + S_2)^2} \tag{8.28b}$$

It must be emphasized that these equations are not applicable if either the diameter of S_1 or S_2 approaches a wavelength in size for then the acoustic impedance at the junction is no longer represented by $\rho_0 c/S_2$. Finally, when the wavelength becomes considerably smaller than the diameter of the smaller pipe, the transmission coefficient in going from a pipe of area S_1 into a smaller pipe of area S_2 is essentially equal to the ratio of their areas, S_2/S_1. This relationship arises from the assumption that the fraction of the wave front in the first pipe incident on the opening S_2 is completely transmitted while the remainder is totally reflected by the rigid flange connecting the two pipes. Correspondingly, in going from a small pipe of area S_1 into a larger pipe of area S_2 at high frequencies, the transmission approaches 100 per cent.

If a pipe is terminated in a rigid cap at $x = 0$, then $\mathbf{Z}_0 = \infty$ and hence $\mathbf{B}/\mathbf{A} = 1$. The pressure amplitude of the reflected wave is then equal to that of the incident wave, and at $x = 0$ the incident and reflected pressures are always in phase. On the other hand, the volume currents are always $180°$ out of phase at this position, so that the cap corresponds to a nodal position of volume velocity, as is to be expected.

If the end of the pipe is open and is surrounded by an infinite flange, then the terminal impedance may be considered the same as that acting upon a piston mounted in an infinite baffle, i.e.,

$$R_0 = \frac{\rho_0 c}{S} R_1(2ka) \quad \text{and} \quad X_0 = \frac{\rho_0 c}{S} X_1(2ka)$$

and consequently

$$\frac{\mathbf{B}}{\mathbf{A}} = \frac{R_1(2ka) - 1 + jX_1(2ka)}{R_1(2ka) + 1 + jX_1(2ka)} \tag{8.29}$$

For such high frequencies that $2ka \gg 1$, the piston resistance function $R_1(2ka) \approx 1$ and the reactance function $X_1(2ka) \approx 0$, so that $\mathbf{B}/\mathbf{A} \approx 0$. Little if any power is reflected, and consequently almost all the incident acoustic power is radiated out through the end of the pipe. On the other hand, at such low frequencies that $2ka < 0.5$, $R_1(2ka)$ may be replaced by $k^2a^2/2$ and $X_1(2ka)$ by $8ka/3\pi$, giving

$$\frac{\mathbf{B}}{\mathbf{A}} = -\frac{(1 - k^2a^2/2) - 8jka/3\pi}{(1 + k^2a^2/2) + 8jka/3\pi} \tag{8.29a}$$

When $2ka \ll 1$, $\mathbf{B}/\mathbf{A} \approx -1$, indicating that the pressure amplitude of the reflected wave is only slightly less than that of the incident wave. At $x = 0$ its pressure differs in phase by nearly $180°$, and consequently a condensation is reflected as a rarefaction. In contrast, the incident and reflected volume velocities are nearly in phase at the orifice of the pipe, so that this position is approximately an antinode of volume velocity. In spite of the fact that the amplitude of the volume velocity at the orifice is almost twice as great as that corresponding to the incident wave alone, the acoustic resistance is so small that the sound power transmission coefficient, which is given by

$$\alpha_t = \frac{2k^2a^2}{(1 + k^2a^2/2)^2 + (8ka/3\pi)^2} \tag{8.30}$$

is equally small. If terms of the order of k^2a^2 are neglected as compared with unity, this expression is further simplified to

$$\alpha_t = 2k^2a^2 = 8\pi^2a^2/\lambda^2 \tag{8.30a}$$

When the wavelength λ of the radiated sound is large as compared with the radius a of the pipe, only a small percentage of the incident acoustic power is transmitted out of a flanged pipe, the remainder being reflected back down the pipe. This is in agreement with the results of Sects. 7.5 and 7.14, which indicate that sources whose dimensions are small in comparison with the wavelength of the sound are very ineffective as radiators of acoustic energy.

At such low frequencies that $2ka \ll 1$, both experiment and theory indicate that the acoustic impedance of an unflanged pipe is approximately equal to

$$\mathbf{Z} = \frac{\rho_0 c}{S}\left(\frac{k^2a^2}{4} + 0.6jka\right) \tag{8.31}$$

It may be readily shown that the transmission coefficient at the end of such a pipe is correspondingly

$$\alpha_t = \frac{k^2a^2}{(1 + k^2a^2/4)^2 + (0.6ka)^2} \tag{8.32}$$

or

$$\alpha_t \approx k^2a^2 \approx \frac{4\pi^2a^2}{\lambda^2} \tag{8.32a}$$

so that the presence of a wide flange at the end of a pipe approximately doubles the radiation of sound at low frequencies. It is to be noted that when a pipe is terminated in a horn having a gradual flare from the diameter of the pipe to a much larger diameter, the low-frequency power transmission is still further increased.

8.7 Resonance in Pipes. Assume that the fluid in a pipe of length l and area $S = \pi a^2$ is driven by a vibrating piston located at the left-hand end where $x = 0$ and that the pipe is terminated in an acoustic impedance $\mathbf{Z}_l$ at the right-hand end where $x = l$. Application of equation 8.24a at $x = l$ results in

$$\mathbf{Z}_l = \frac{\rho_0 c}{S} \cdot \frac{\mathbf{A}e^{-jkl} + \mathbf{B}e^{jkl}}{\mathbf{A}e^{-jkl} - \mathbf{B}e^{jkl}} \tag{8.33}$$

This equation in effect determines the reflected pressure amplitude $\mathbf{B}$ in terms of the incident amplitude $\mathbf{A}$. The input impedance $\mathbf{Z}_0$ at $x = 0$ is correspondingly given by

$$\mathbf{Z}_0 = \frac{\rho_0 c}{S} \cdot \frac{\mathbf{A} + \mathbf{B}}{\mathbf{A} - \mathbf{B}} \tag{8.34}$$

Equations 8.34 and 8.33 may be combined to eliminate the complex pressure amplitudes **A** and **B**, and then simplified to give

$$\mathbf{Z}_0 = \frac{\rho_0 c}{S} \cdot \frac{\mathbf{Z}_l + j\,\dfrac{\rho_0 c}{S} \tan kl}{\dfrac{\rho_0 c}{S} + j\mathbf{Z}_l \tan kl} \tag{8.35}$$

It is apparent that the input impedance depends not only on the terminating impedance $\mathbf{Z}_l$ but also on the length of the pipe l and the wavelength constant k.

The resonant frequency of such a pipe may be defined as that at which the reactive component of the input impedance vanishes. At this frequency the input impedance is a minimum and the power radiated out of an open-ended tube is a maximum for a source of constant force or pressure amplitude. If for convenience we replace $\mathbf{Z}_l$ by $(\rho_0 c/S)(\alpha + j\beta)$, then equation 8.35 may be rewritten as

$$\mathbf{Z}_0 = \frac{\rho_0 c}{S} \cdot \frac{\alpha + j(\tan kl + \beta)}{(1 - \beta \tan kl) + j\alpha \tan kl} \tag{8.35a}$$

Application of the condition that $X_0 = 0$ leads to

$$\beta \tan^2 kl + (\beta^2 + \alpha^2 - 1) \tan kl - \beta = 0 \tag{8.36}$$

In the limiting cases at *low frequencies* where both α and β are small as compared to unity, equation 8.36 is approximated by

$$\tan kl = -\beta \tag{8.36a}$$

When a pipe is terminated at $x = l$ in an infinite flange, $\beta \approx 8ka/3\pi$, and the condition $\tan kl = -8ka/3\pi$ is satisfied by

$$\tan (n\pi - kl) = \frac{8ka}{3\pi} \approx \tan\left(\frac{8ka}{3\pi}\right)$$

where n is any integer. Therefore

$$n\pi - kl = \frac{8ka}{3\pi} \tag{8.37}$$

and the fundamental resonance frequency corresponding to $n = 1$ is

$$f_1 = \frac{c}{2(l + 8a/3\pi)} \tag{8.37a}$$

It is apparent that the effective length of such a pipe is not l but rather $l + 8a/3\pi$. This predicted correction for a flanged pipe is in reasonable agreement with experimentally measured values of $0.82a$. The measured correction for an unflanged pipe is $0.6a$ and offers excellent support for our choice in equation 8.31 of $\beta = 0.6ka$. It is to be emphasized that the above expressions for end corrections apply only at those low frequencies where the respective assumed values of β are valid. Within this limitation on the constancy of the end correction, it is to be noted that equation 8.37 indicates that the overtones of an open-ended organ pipe form an integral harmonic group.

If the pipe is closed by a rigid cap located at $x = l$, then $\mathbf{Z}_l = \infty$, and the input impedance reduces to

$$\mathbf{Z}_0 = \frac{\rho_0 c}{S} \cdot \frac{1}{j \tan kl} = -j \frac{\rho_0 c}{S} \cot kl \tag{8.38}$$

The reactance is zero when $\cot kl = 0$, which corresponds to

$$kl = (2n - 1)\pi/2 \qquad n = 1, 2, 3, \cdots$$

or

$$f = \frac{2n - 1}{4} \cdot \frac{c}{l} \tag{8.39}$$

When $n = 1$ this reduces to $f_1 = c/4l$, in agreement with the well-known equation for the fundamental frequency of vibration of a pipe closed at one end. The resonant overtones consist of all odd harmonics of the fundamental but do not include any even harmonics.

8.8 General Theory of a Side Branch. As an introduction to filter theory let us first consider the influence of a side branch on the transmission of acoustic waves through a rigid pipe of infinite length. The presence of such a branch causes the acoustic impedance at the junction to differ from $\rho_0 c/S$, the characteristic value for plane waves in a pipe, and consequently a reflected wave is produced. Furthermore, a portion of the incident acoustic energy may be transmitted into and dissipated in the branch. Both of these factors contribute to a reduction in the energy transmitted through the portion of the pipe lying beyond the branch.

Figure 8.6 represents a pipe of uniform cross section S, to which is attached an arbitrary side branch of input acoustic impedance $\mathbf{Z}_b$. If a plane wave represented by

$$\mathbf{p}_i = \mathbf{A}_1 e^{j(\omega t - kx)} \tag{8.40}$$

is incident from the left on the junction between the main pipe and the branch, it will in general create a reflected wave

$$\mathbf{p}_r = \mathbf{B}_1 e^{j(\omega t + kx)} \tag{8.41}$$

and a transmitted wave

$$\mathbf{p}_t = \mathbf{A}_2 e^{j(\omega t - kx)} \tag{8.42}$$

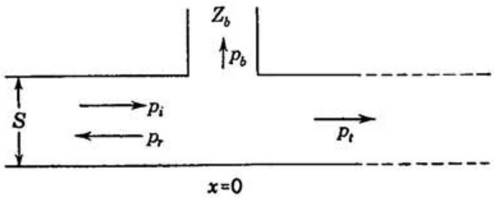

Fig. 8.6. Conditions at a side branch of acoustic impedance, Z_b.

If the junction point is chosen as the origin of the x coordinate, the pressures produced by each of these waves at this point are

$$\mathbf{p}_i = \mathbf{A}_1 e^{j\omega t} \quad \mathbf{p}_r = \mathbf{B}_1 e^{j\omega t} \quad \text{and} \quad \mathbf{p}_t = \mathbf{A}_2 e^{j\omega t}$$

respectively. The pressure at the entrance to the branch may similarly be represented by

$$\mathbf{p}_b = \mathbf{A}_b e^{j\omega t} \tag{8.43}$$

In our entire analysis of the transmission of acoustic waves through pipes it is assumed that the cross-sectional dimensions of all pipes are small in comparison with the wavelength of the sound. Since this is true we may apply the condition of continuity of pressure to the junction and obtain

$$\mathbf{p}_i + \mathbf{p}_r = \mathbf{p}_t = \mathbf{p}_b \tag{8.44}$$

The associated volume velocities in this region are represented by

$$\mathbf{U}_i = \frac{\mathbf{p}_i}{\rho_0 c/S} \quad \mathbf{U}_r = -\frac{\mathbf{p}_r}{\rho_0 c/S} \quad \mathbf{U}_t = \frac{\mathbf{p}_t}{\rho_0 c/S} \quad \text{and} \quad \mathbf{U}_b = \frac{\mathbf{p}_b}{\mathbf{Z}_b} \tag{8.45}$$

The condition of continuity of volume velocity requires that

$$\mathbf{U}_i + \mathbf{U}_r = \mathbf{U}_t + \mathbf{U}_b \tag{8.46}$$

Dividing equation 8.46 by equation 8.44, we obtain

$$\frac{\mathbf{U}_i + \mathbf{U}_r}{\mathbf{p}_i + \mathbf{p}_r} = \frac{\mathbf{U}_t}{\mathbf{p}_t} + \frac{\mathbf{U}_b}{\mathbf{p}_b}$$

which may be written in a simpler form as

$$\frac{1}{\mathbf{Z}} = \frac{1}{\mathbf{Z}_t} + \frac{1}{\mathbf{Z}_b} \tag{8.47}$$

where

$$\mathbf{Z} = \frac{\rho_0 c}{S} \cdot \frac{\mathbf{A}_1 + \mathbf{B}_1}{\mathbf{A}_1 - \mathbf{B}_1} \quad \text{and} \quad \mathbf{Z}_t = \frac{\rho_0 c}{S}$$

Here $\mathbf{Z}$ represents the acoustic impedance at the branch due to the combined effect of the incident and reflected waves, and $\mathbf{Z}_t$ is the acoustic impedance in the transmitted wave. Equation 8.47 shows that the amplitude constant $\mathbf{B}_1$ of the reflected wave is constrained both in magnitude and phase so that the combined *admittance* $1/\mathbf{Z}$ of the incident and reflected waves equals the parallel sum of the admittance $1/\mathbf{Z}_b$ of the branch and the admittance $1/\mathbf{Z}_t$ of the continuing pipe. The electrical analogue of introducing a side branch into an infinite pipe is therefore the connection of an electrical impedance $\mathbf{Z}_E$ across the two wires of an infinite transmission line, as indicated in Fig. 8.7. In the more general case in which the main pipe is not of infinite length but is instead terminated in an impedance $\mathbf{Z}_l$, the impedance $\mathbf{Z}_t$ of the continuing pipe is complex and is given by equation 8.35.

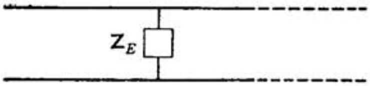

Fig. 8.7. Electrical analogue of attaching a branch to a pipe.

Equation 8.47 may be solved for $\mathbf{B}_1/\mathbf{A}_1$, the ratio of the pressure amplitude of the reflected wave to that of the incident wave, i.e.,

$$\frac{\mathbf{B}_1}{\mathbf{A}_1} = \frac{-\dfrac{\rho_0 c}{2S}}{\dfrac{\rho_0 c}{2S} + \mathbf{Z}_b} \tag{8.48}$$

The corresponding ratios for the transmitted wave and for the pressure at the entrance into the branch are obtained by combining equations 8.48 and 8.44. These are

$$\frac{\mathbf{A}_2}{\mathbf{A}_1} = \frac{\mathbf{A}_b}{\mathbf{A}_1} = \frac{\mathbf{Z}_b}{\dfrac{\rho_0 c}{2S} + \mathbf{Z}_b} \tag{8.49}$$

In deriving expressions for the sound power reflection and transmission coefficients it will prove convenient to replace the branch impedance by $\mathbf{Z}_b = R_b + jX_b$. The reflection coefficient is then

$$\alpha_r = \left(\frac{B_1}{A_1}\right)^2 = \frac{\left(\dfrac{\rho_0 c}{2S}\right)^2}{\left(\dfrac{\rho_0 c}{2S} + R_b\right)^2 + X_b^{\,2}} \tag{8.50}$$

and the transmission coefficient along the pipe is

$$\alpha_t = \left(\frac{A_2}{A_1}\right)^2 = \frac{R_b^{\,2} + X_b^{\,2}}{\left(\dfrac{\rho_0 c}{2S} + R_b\right)^2 + X_b^{\,2}} \tag{8.51}$$

The ratio of the power transmitted into the branch to that in the incident wave is given by $\alpha_b = 1 - \alpha_r - \alpha_t$ and is

$$\alpha_b = \frac{\dfrac{\rho_0 c}{S} R_b}{\left(\dfrac{\rho_0 c}{2S} + R_b\right)^2 + X_b^2} \tag{8.52}$$

It is to be noted that the power transmitted past the junction and along the main pipe is zero only when $\alpha_t = 0$, which in turn requires that both R_b and X_b be zero. A filter for which this is true does not absorb all the sound energy that reaches the junction but, on the contrary, absorbs no energy and merely reflects 100 per cent of the incident energy back through the pipe towards the source. If R_b is greater than zero but is not infinite, some acoustic energy is dissipated in the branch and some is transmitted beyond the junction, irrespective of the particular value of X_b. At the opposite extreme, as either R_b or X_b becomes very large as compared to $\rho_0 c/S$, almost 100 per cent of the incident power is transmitted beyond the branch, and in the limit where $R_b = X_b = \infty$, which corresponds to no branch, the power transmission ratio equals unity. It should also be noted that, if $R_b = 0$, no acoustic power is dissipated in the branch.

8.9 Helmholtz Resonator as a Branch. As an application of the theory developed in Sect. 8.8 we shall now consider the effect of using a Helmholtz resonator as a side branch, Fig. 8.8*a*. If we may neglect viscosity losses, there is no net dissipation of energy from the pipe into the resonator, all energy absorbed by the resonator during some parts of the acoustic cycle being returned to the pipe during other parts of the cycle, so that $R_b = 0$. If the area of the opening into the resonator is $S_b = \pi a^2$, the length of its neck is l, and its volume is V, then the acoustic reactance of the branch is

$$X_b = \rho_0\left(\frac{\omega l'}{S_b} - \frac{c^2}{\omega V}\right) \tag{8.53}$$

where $l' = l + 1.7a$.

A substitution of these values of R_b and X_b into equation 8.51 leads to a transmission coefficient of

$$\alpha_t = \frac{1}{1 + \dfrac{c^2}{4S^2(\omega l'/S_b - c^2/\omega V)^2}} \tag{8.54}$$

This transmission coefficient becomes zero when

$$\omega = \omega_0 = c\sqrt{\frac{S_b}{l'V}}$$

the resonant frequency of the Helmholtz resonator. At this frequency large volume velocity amplitudes exist in the neck of the resonator, but all acoustic energy that is transmitted into the resonator cavity from the incident wave is returned to the main pipe with such a phase relationship as to be reflected back towards the source. This type of acoustic filter is analogous to an electrical system in which a series combination of an inductance and a capacitance is shunted across a transmission line, as shown in Fig. 8.8*b*.

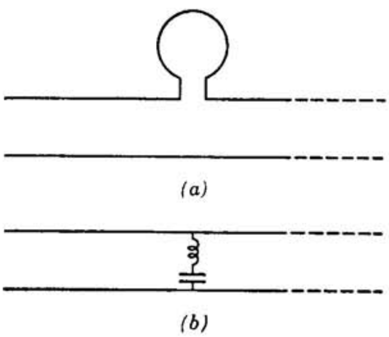

Fig. 8.8. (*a*) Helmholtz resonator as a side branch. (*b*) Electrical analogue of a Helmholtz resonator as a side branch.

Calculated values of the transmission coefficient as a function of frequency are plotted in Fig. 8.9 for a pipe of 0.03-m radius, to which is attached a resonator having a volume of 0.00112 m^3, a neck length of 0.006 m, and an orifice of 0.0155-m radius. Whenever the radius of the neck is rather large, as it is in this example, measured values of the power transmission ratio are found to be in excellent agreement with the values predicted by equation 8.54. For long narrow constrictions, however, computed and measured values are not in agreement unless equation 8.54 is modified to take into account the dissipative forces resulting from

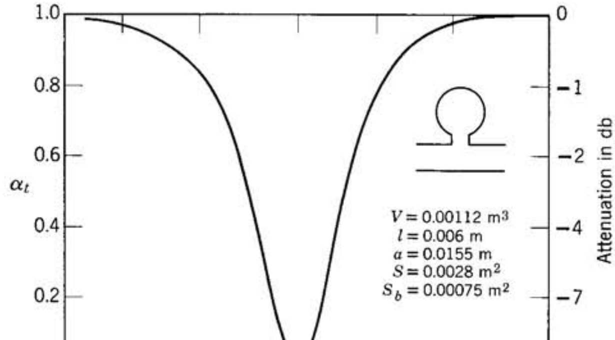

Fig. 8.9. Attenuation produced by a Helmholtz resonator branch.

viscosity. One striking characteristic of the curve of Fig. 8.9 is that it indicates a material reduction in the transmission over a frequency range extending for more than an octave on either side of the resonant frequency. This filtering curve is much broader than that giving the intensity-amplification response of the resonator when it is used in the open, as discussed in Sect. 8.4.

8.10 Orifice as a Branch. Let us next consider the effect of a short length of pipe as a branch. If not only the radius a but also the length l of this pipe are small compared to a wavelength, the branch impedance of such an orifice is

$$\mathbf{Z}_b = \frac{\rho_0 c k^2}{2\pi} + j\,\frac{\rho_0 l'\omega}{\pi a^2} \tag{8.55}$$

where $l' = l + 1.7a$. The first term results from the radiation of sound through the orifice into the external medium, and the second from the inertance of the gas in the orifice.

The transmission coefficient is then

$$\alpha_t = \frac{\left(\dfrac{\rho_0 c k^2}{2\pi}\right)^2 + \left(\dfrac{\rho_0 l'\omega}{\pi a^2}\right)^2}{\left(\dfrac{\rho_0 c}{2S} + \dfrac{\rho_0 c k^2}{2\pi}\right)^2 + \left(\dfrac{\rho_0 l'\omega}{\pi a^2}\right)^2} \tag{8.56}$$

The ratio of the acoustic resistance of the branch to its acoustic reactance is

$$\frac{R_b}{X_b} = \frac{\rho_0 c k^2/2\pi}{\rho_0 l'\omega/\pi a^2} = \frac{ka^2}{2l'}$$

If the branch is merely a hole drilled in the thin wall of the main pipe, $l = 0$ and hence l' has its minimum value of $1.7a$, so that in this extreme case, the above ratio has its maximum value of $R_b/X_b = ka/3.4$. However, the radius of the orifice has been assumed small as compared to the wavelength, i.e., $ka \ll 1$, and therefore the acoustic resistance of such an orifice may be neglected as compared with its acoustic reactance in calculating the transmission coefficient. Upon neglecting $\rho_0 c k^2/2\pi$, equation 8.56 becomes

$$\alpha_t = \frac{1}{1 + (\pi a^2/2Sl'k)^2} \tag{8.56a}$$

This transmission coefficient is very nearly zero at low frequencies and rises to nearly 100 per cent at higher frequencies, as is indicated in Fig. 8.10, which is a graph of calculated values of the power transmission ratio for a pipe of 0.03-m radius, having as an orifice a short pipe 0.0155 m in

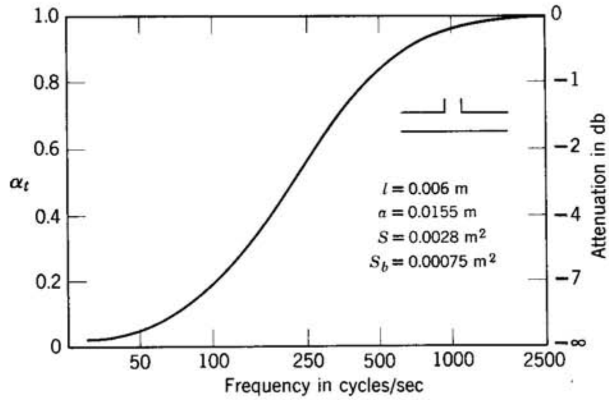

Fig. 8.10. Attenuation produced by an orifice branch.

radius and 0.006 m long. The transmission coefficient equals 50 per cent when the denominator of equation 8.56*a* equals two, i.e., for

$$k = \frac{\pi a^2}{2Sl'} \tag{8.57}$$

The presence of a single orifice converts a pipe into a high-pass filter. As the radius of such an orifice is increased, relative to the radius of the main pipe, the attenuation of the low frequencies is increased, as is the frequency corresponding to 50 per cent power transmission. If the pipe has several orifices, located near enough to one another so that they may be considered as being at a single point, i.e., separated by a small fraction of a wavelength, the action of the group is that of their equivalent parallel impedance. If, on the other hand, the distance between orifices is an appreciable fraction of the wavelength of sound the system becomes analogous to an electrical filter network or to a transmission line across which are shunted a number of widely spaced impedances. The waves reflected from the various orifices are then out of phase with one another, and the power transmission ratio cannot be computed by equation 8.56 but must instead be determined by methods analogous to those of electrical filter theory. In general, the low-frequency attenuation of a number of suitably spaced orifices can be made much greater than that of a single orifice of equal total area.

The sound power transmission coefficient into a single branch is approximately given by

$$\alpha_b = \frac{2k^2S}{\pi[1 + (2Sl'k/\pi a^2)^2]} \tag{8.58}$$

At the frequency corresponding to 50 per cent power transmission this expression is reduced to k^2S/π. For the orifice considered in the above example this ratio is only 1.5 per cent at a frequency of 225 cycles/sec. It is therefore quite apparent that the filtering action of an orifice does not result from the transmission of acoustic energy out of the pipe, but rather from the reflection of energy back towards the source.

The influence of an orifice may be used to explain qualitatively the action of a wind instrument, such as a flute or clarinet. When these instruments are sounded in their fundamental register the player opens all (or nearly all) the orifices lying beyond some particular distance from the mouthpiece. Since the diameters of the orifices are almost as large as the bore of the tube, this effectively shortens the length of the instrument, and the acoustic energy reflected back from the first open orifice sets up a pattern of standing waves between this orifice and the mouthpiece. In a flute, which acts essentially like an open pipe, the wavelength is approximately equal to twice the distance from the opening in the mouthpiece to the first open orifice. In a clarinet, however, the action of the vibrating reed causes the conditions at the mouthpiece to approximate those at the closed end of a tube, and hence the wavelength is nearly four times the distance from the reed to the first open orifice. In both instruments there are also a number of harmonic overtones, those of the clarinet being predominately the odd harmonics, as is to be expected from a closed pipe. When either instrument is played in a high register, the fingering is more complex, some orifices beyond the first open orifice being left closed and others opened, the purpose being to emphasize the desired standing wave pattern.

8.11 Expansion Chamber Type of Filter. A simple type of low-pass acoustic filter may be constructed by inserting an enlarged section of pipe of cross-sectional area S_2 and length l in a pipe of cross section S_1 as shown in Fig. 8.11*a*. At those low frequencies corresponding to $kl \ll 1$, this filter may be looked upon as though it consists of a side branch of acoustic compliance $C = V/\rho_0c^2$, where $V = S_2l$ is the volume of the expansion chamber, in parallel with the continuing pipe. The acoustic impedance of such a branch is a pure reactance and therefore $R_b = 0$ and

$$X_b = -\frac{1}{\omega C} = -\frac{\rho_0c^2}{\omega V} = -\frac{\rho_0c^2}{\omega S_2 l} \tag{8.59}$$

A substitution of these values of R_b and X_b into equation 8.51 leads to a transmission coefficient of

$$\alpha_t = \frac{1}{1 + \left(\dfrac{S_2kl}{2S_1}\right)^2} \tag{8.60}$$

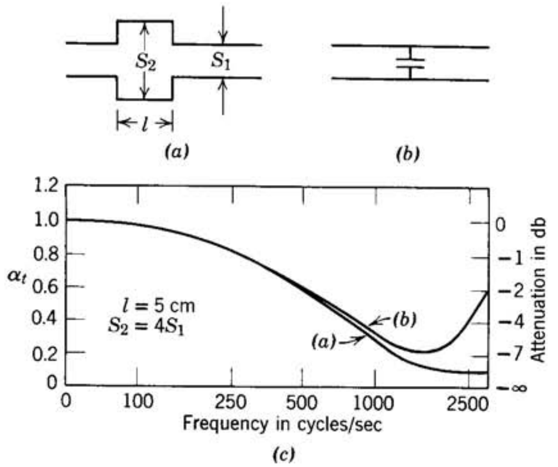

Fig. 8.11. (*a*) Simple low-pass acoustic filter. (*b*) Analogous electrical filter. (*c*) Power transmission curves for filter (*a*).

This equation predicts that at low frequencies the sound power transmission is 100 per cent and then gradually decreases to zero at high frequencies. Curve (*a*) in Fig. 8.11*c* is a graph of values of the transmission coefficient calculated from equation 8.60 for an expansion chamber of 0.05-m length and having a cross section four times that of the original pipe. At first inspection this type of acoustic filter appears to be analogous to the low-pass electrical filter produced by shunting a capacitor across a transmission line as shown in Fig. 8.11*b*. Actually equation 8.60 does not apply when $kl > 1$ and, therefore, the two filters are not truly analogous.

Let us now derive an equation for the above acoustic filter which is valid for $kl > 1$. By considering the various incident, reflected, and transmitted waves present in the three sections of pipes as being related to each other by conditions of continuity of pressure and volume velocity at the two junctions of the expanded pipe with the original pipe, it is possible to derive an equation for the transmission coefficient in a manner similar to that used in Sect. 6.5 for deriving equation 6.37. The resulting equation is

$$\alpha_t = \frac{4}{4\cos^2 kl + \left(\dfrac{S_2}{S_1} + \dfrac{S_1}{S_2}\right)^2 \sin^2 kl} \tag{8.61}$$

Curve (*b*) of Fig. 8.11*c* is a graph of values of the transmission coefficient calculated from equation 8.61 for the same filter section as was used in obtaining curve (*a*). At those low frequencies for which $kl \ll 1$, results given by the two equations are essentially identical. The reader can show that this is to be expected by simplifying equation 8.61 when $kl \ll 1$. However, the more exact equation (8.61) indicates that the transmission coefficient reaches a minimum value of

$$\alpha_t = \left(\frac{2S_1S_2}{S_1^2 + S_2^2}\right)^2 \tag{8.62}$$

for $kl = \pi/2$, i.e., when the length of the filter section is a quarter wavelength. Following this minimum, the sound power transmission gradually increases with increasing frequency until it again reaches 100 per cent for $kl = \pi$. A further increase in frequency causes the transmission coefficient to run through a series of minima and maxima, until finally, when ka_1, where a_1 is the radius of the original pipe, is large in comparison with unity, it remains at 100 per cent. This final attainment of 100 per cent transmission is characteristic of all three of the acoustic filters discussed so far in this chapter. The equations derived for power transmission are valid only when the wavelength is large compared with the radius of the original pipe, or with the dimensions of any filter section.

There exist practical limitations other than those of frequency which must be taken into consideration in applying equation 8.60 to the design of low-pass acoustic filters. For example, it is not applicable when there is an extreme difference between the cross section of the filter and that of the original pipe. In spite of all these limitations, filters of this type are basic to the design of simple automobile mufflers, gun silencers, and sound absorbing plenum chambers as are installed in ventilating systems.

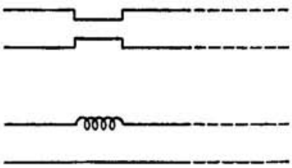

Fig. 8.12. Constriction in a pipe and its electrical analogue.

8.12 Additional Acoustic Filters. Yet another type of simple low-pass electric filter is produced by placing an inductance in series with a transmission line. The acoustic equivalent is a constriction in the pipe, as shown in Fig. 8.12. This system may be thought of as that of introducing an inertance in series with the pipe. However, as is the case with an enlarged section, the analogy between the electric and the acoustic cases is valid only over a limited range of frequencies. Equation 8.61 may be used for calculating the transmission coefficient for this type of filter, since its derivation is independent of whether S_1 or S_2 is the larger.

By employing combinations of resonators, orifices, and enlargements or constrictions of the main pipe, it is possible to construct a wide variety of acoustic filter networks. The design of such networks is greatly facilitated

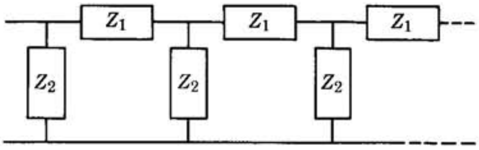

Fig. 8.13. Ladder-type of network used as a filter.

by taking advantage of the analogy between acoustic and electrical filters. For example, the sharpness of cutoff of an electrical filter system can be increased by using a ladder-type network such as is shown in Fig. 8.13. These networks are constructed by using a combination of reactances of one type of impedance $\mathbf{Z}_1$ in series with the line and reactances of another type of impedance $\mathbf{Z}_2$ shunted across the line. It is demonstrated in standard treatises[3] on wave filters, that a nondissipative recurrent structure, such as that of Fig. 8.13, markedly attenuates all frequencies excepting those for which the ratio $\mathbf{Z}_1/\mathbf{Z}_2$ satisfies the condition $0 > \mathbf{Z}_1/\mathbf{Z}_2 > -4$. Three simple ladder-type acoustic filters along with their electrical analogues are shown in Fig. 8.14. An application of the above condition on the

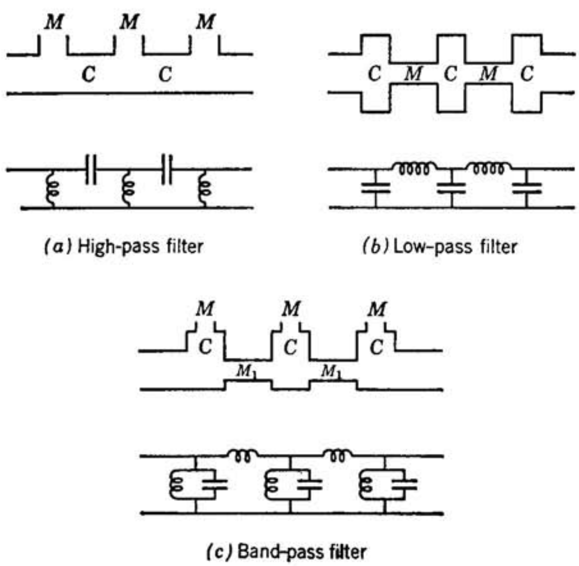

Fig. 8.14. Ladder-type acoustic filters.

[3] Mason, *Electromechanical Transducers and Wave Filters*, pp. 28–31, D. Van Nostrand Co. (1948).

ratio $\mathbf{Z}_1/\mathbf{Z}_2$ leads to cutoff frequencies of

$$f = \frac{1}{4\pi\sqrt{MC}} \tag{8.63}$$

for the high-pass filter of Fig. 8.14*a* and

$$f = \frac{1}{\pi\sqrt{MC}} \tag{8.64}$$

for the low-pass filter of Fig. 8.14*b*. The behavior of the acoustic filters of Fig. 8.14 will begin to deviate more and more from that of their analogous electrical filters as frequency increases. The primary cause of this deviation is that at the higher frequencies, the dimensions of the system ultimately become comparable to a wavelength and the filter begins to have distributed rather than lumped-constant properties. An interested reader will find a wealth of additional information on acoustic filtration in the *Handbook on Noise Control.*[4]

A knowledge of the filtering characteristics of acoustic elements is essential to the design and correction of any mechanoacoustic system such as forced air heating and ventilating systems, exhaust systems for jet engine test cells, and automobile mufflers. However, it is to be emphasized that acoustic filtering is not limited to systems using the nondissipative elements discussed above since additional filtering action is possible by the use of frequency selective sound absorbing materials in such systems. Considerations as to the capabilities and characteristics of such sound absorbing materials will be looked into in subsequent chapters. In electroacoustic systems such as loudspeakers, microphones, etc., consideration also must be given to the action of acoustic filtering. However, the remedial methods used are frequently nonacoustic in that it is usually easier and less expensive to use electrical networks either to provide any desired filtering action or to correct any unwanted acoustic filtering.

PROBLEMS

8.1. The sphere of a Helmholtz resonator has a diameter of 0.1 m. (*a*) What diameter hole should be drilled in the sphere, if it is to resonate in air at a frequency of 320 cycles/sec? (*b*) What must be the pressure amplitude of an incident acoustic plane wave at 320 cycles/sec, if it is to produce an internal excess pressure of 20 microbars in the above resonator? (*c*) What will be the resonant frequency if a hole having twice the cross-sectional area of that of part (*a*) is drilled in the sphere? (*d*) What will be the resonant frequency if two independent holes having the diameter of part (*a*) are drilled in the sphere?

[4] Harris, *Handbook on Noise Control*, Ch. 21, McGraw-Hill Book Company, Inc. (1957).

8.2. A rigid-walled back-enclosed loudspeaker cabinet has inside dimensions of 0.3 m × 0.5 m × 0.4 m. The front panel of the cabinet is 0.03 m thick and has a 0.2-m diameter hole cut in it for mounting a loudspeaker. (*a*) What is the fundamental resonant frequency of the cabinet considered as a Helmholtz resonator? (*b*) If a direct-radiator loudspeaker having a cone of 0.2-m diameter and 0.01-kg mass, and also having a suspension system of 1000-newtons/m stiffness, is mounted in this cabinet, what is the resonant frequency of the cone? Assume that the effective mass of the system is the sum of that of the cone and of the moving air in the opening of the cabinet and that the effective stiffness is the sum of that of the cone and of the cabinet. (*c*) What would be the resonant frequency of the cone if it were not mounted in the cabinet and had no air loading? (*d*) If the cone is driven at the frequency of part (*b*) with an amplitude of 0.002 m, what is the acoustic power radiated? (*e*) Under these same conditions, what is the excess pressure amplitude inside the cabinet and what is the amplitude of the associated force acting upon one of the 0.4 × 0.5-m panels?

8.3. Given a pipe of cross section S_1 to be connected to a pipe of cross section S_2. (*a*) Derive a general expression for the ratio of the intensity of the waves transmitted into the second pipe to that of the incident waves. (*b*) Under what conditions is the transmitted intensity greater than the incident intensity? Explain. (*c*) Derive a general expression for the standing wave ratio SWR produced in pipe S_1 in terms of the relative areas S_1 and S_2.

8.4. A plane sound wave is traveling to the right in a pipe of area S_1 containing a fluid of characteristic impedance $\rho_1 c_1$. At the end of this pipe is attached a second pipe of area S_2 containing a fluid of characteristic impedance $\rho_2 c_2$. The two fluids are separated by means of a thin rubber diaphragm. (*a*) Derive an expression giving the power transmission ratio from the first pipe into the second. (*b*) What is the condition for 100 per cent power transmission?

8.5. Given a plane wave of pressure amplitude P traveling to the right in a pipe of cross-sectional area S_1. At the right-hand end of this pipe is attached a smaller pipe of area S_2 and infinite length. (*a*) What must be the ratio of these two areas if the transmitted pressure amplitude in the second pipe is to be 50 per cent greater than that of the incident wave in the first pipe? (*b*) If the smaller pipe is cut off at a distance of one-quarter of a wavelength from the junction of the two pipes and then covered with a rigid cap, derive an expression giving the pressure amplitude at the cap in terms of that of the incident wave in the large pipe. (*c*) What is the ratio of these two pressures for the area ratio as determined in (*a*)?

8.6. Find the shortest length pipe for which the input acoustic resistance equals the input acoustic reactance at a frequency of 500 cycles/sec when the terminating load impedance is 3 × the acoustic impedance of the air in the pipe.

8.7. The air in a pipe of 1.0-m length and 0.05-m radius is being driven at one end by a piston of negligible mass. The far end of the pipe is open and has a large flange attached to it. (*a*) What is the fundamental resonant frequency of the system? (*b*) If the displacement amplitude of the piston is 0.01-m when driven at the above frequency, what acoustic power is being transmitted by the plane waves moving toward the open end of the pipe? (*c*) What acoustic power is being transmitted out through the open end of the pipe?

8.8. The air in a pipe of 0.05-m radius and 1.0-m length is being driven by a piston of 0.015-kg mass and 0.05-m radius inserted in one end of the pipe. The other end of the pipe is terminated in an infinite baffle. (*a*) At a frequency of 150 cycles/sec, what is the mechanical impedance of the piston, including the loading effect of the air in the pipe? (*b*) What is the amplitude of the force required to drive the piston with a displacement amplitude of 0.005 m at this frequency? (*c*) How much acoustic power in watts will be radiated out through the open end of the pipe?

8.9. A condenser-microphone diaphragm is stretched across one end of a pipe of 0.02-m radius and 0.01-m length, open at the other end. Compute and plot the ratio between the pressure at the diaphragm, considered rigid, and that at the open end as a function of frequency from 100 to 2000 cycles/sec.

8.10. A piston of mass m and radius a is mounted in one end of a pipe of length l and radius a. The other end of the pipe opens into an infinite plane flange. (*a*) Derive an approximate equation giving the acoustic power radiated out through the open end of the pipe when the piston is driven by a force $F \cos \omega t$ at such high frequencies that $ka \gg 1$. (*b*) Also derive an approximate equation that is valid for such low frequencies that both $ka \ll 1$ and $kl \ll 1$.

8.11. The side branch from an infinitely long main pipe of area S is another infinitely long pipe of area S_b. The main pipe is transmitting plane waves at such a frequency that their wavelength is large compared to the diameter of either pipe. (*a*) Assuming the input impedance of the branch pipe to be that of an infinitely long pipe of cross section S_b, derive an equation for the transmission coefficient in the main pipe. (*b*) Also derive an equation for the transmission coefficient into the branch pipe. (*c*) If the area of the main pipe is twice that of the branch pipe, calculate numerical values for the transmission coefficient into each pipe? (*d*) Is the sum of these two coefficients equal to unity? If not, where is the remaining power? Support your explanation by numerical computation.

8.12. A Helmholtz resonator is attached to a pipe of 0.03-m radius. The resonator has a volume of 0.001 m^3 and a neck of 0.003-m length and 0.01-m radius. (*a*) Calculate and plot the sound power transmission coefficient of this filter system over the frequency range between 50 and 500 cycles/sec. (*b*) Over what range of frequencies does this filter reduce the power transmitted by 6 db or more?

8.13. Given a square ventilating duct of 0.3-m length per side. A Helmholtz resonator-type of band filter is constructed around the duct by drilling a hole of 0.08-m radius in one wall of the duct leading into a surrounding closed chamber of volume V. (*a*) What volume V is required in order to most effectively filter sounds at a frequency of 30 cycles/sec? (*b*) What will be the sound power transmission coefficient of the filter at 60 cycles/sec?

8.14. (*a*) If a hole of 1-cm radius is drilled in a thin-walled pipe of 2-cm radius, what is the sound power transmission coefficient along the main pipe at a frequency of 500 cycles/sec? (*b*) What will be the transmission coefficient of the pipe at this frequency if a second hole of 1-cm radius is drilled in the pipe directly across from the first hole?

8.15. Show that the expression giving the radius a of the hole that must be drilled into a thin-walled pipe of radius a_0 in order to result in a 50 per cent sound power transmission coefficient at a frequency f is

$$a = \frac{64 f a_0^2}{3c}$$

8.16. A plane wave of 300-cycles/sec frequency and 0.1-watt power is traveling through an infinitely long pipe of 0.2-m radius. What will be the power reflected, the power transmitted along the pipe, and the power transmitted out through a simple orifice of 0.05-m radius?

8.17. A ventilating duct has a radius of 0.1 m and transports air at a temperature of 50°C. It is desired to reduce the intensity level of plane waves having a frequency of 120 cycles/sec by 13 db as they pass through an inserted low-pass filter section of length l and expanded radius a. (*a*) What length and radius of pipe used as an expansion chamber will most effectively and simply accomplish the required filtering action? (*b*) Compute the filtering action of the above filter at a frequency of 60 cycles/sec.

8.18. A water pipe line has a diameter of 0.04 m. It is desired to filter out plane sound waves traveling in the water by use of sections of pipe of 0.1-m diameter acting as expansion-chamber types of filters. (*a*) Calculate the minimum length of filter section that will most effectively filter out a sound of 900 cycles/sec. (*b*) If the required filtering action is a reduction of 30 db in the level of the intensity, how many sections must be used. Ignore the effects of any interactions between the individual filter sections.

8.19. A simple low-pass filter may be constructed by inserting a short length of pipe of larger radius in a pipe of radius a. If the filter section has a radius $3a$ and is 0.1 m long, compute by means of equation 8.61 the sound power transmission coefficient of the filter as a function of frequency in the interval from 100 to 1500 cycles/sec and plot the results. Similarly, compute the transmission coefficient of the filter by means of equation 8.60, plot, and compare with the above results.

8.20. Show that the attachment of the indicated branch composed of a short section of pipe of volume V with a hole of radius a drilled in its cap is equivalent

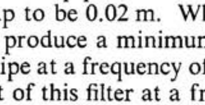

to shunting the main pipe with an inertance $M = 1.7\rho_0/\pi a$ in parallel with a compliance $C = V/\rho_0 c^2$. (*a*) What type of filtering action will result from this filter element? (*b*) Given the main pipe to be of 0.005-m^2 cross section and the radius of the orifice on the cap to be 0.02 m. What must be the volume of the cap, if the filter element is to produce a minimum reduction in transmission of sound waves along the main pipe at a frequency of 400 cycles/sec? (*c*) What will be the transmission coefficient of this filter at a frequency of 200 cycles/sec?

8.21. A rectangular room has internal dimensions of 2.5 m × 4.0 m × 4.0 m and walls of 0.1-m thickness. A door opening into this room has dimensions of 0.8 × 2.0 m. (*a*) Assuming the inertance of the door opening to be equal to that of a circular opening of equal area, calculate the resonant frequency of the room, considered as a Helmholtz resonator. (*b*) What is the acoustic compliance of the room and the inertance of the door opening? (*c*) Considering only the compliance of the room and the inertance of the door opening, what acoustic impedance is presented, at a frequency of 20 cycles/sec, by the room to a sound source within the room?

chapter 9

ABSORPTION OF SOUND WAVES IN FLUIDS

9.1 Introduction. In previous chapters no consideration has been given to the dissipation of energy within sound waves. In many situations such dissipation takes place so slowly that it can be ignored. Ultimately, however, all acoustic energy is degraded into some form of heat energy. The sources of this dissipation may be divided into two general categories, those due to dissipation of acoustic energy in the transmitting medium and those associated with conditions at the boundaries of the medium. The first type of loss is of particular significance when the volume of the fluid is large in comparison with the area of its boundaries, as in the transmission of sound in the earth's atmosphere and oceans, through large ventilating ducts, and within large auditoriums. Losses in the medium may be divided into three basic types, *viscous* losses, *heat conduction* losses, and losses associated with *molecular exchanges* of energy. The viscous losses result from relative motion occurring between various portions of the medium during the compressions and expansions that accompany transmission of a sound wave. A fundamental assumption that has been made in the derivation of the basic equations for acoustic wave motion is that the pressure changes are adiabatic and consequently are accompanied by changes in temperature. Thus there is a tendency for heat to be conducted from regions of condensation where the temperature is raised to neighboring regions of rarefaction where the temperature is lowered. In the process of this heat transfer there is a tendency towards pressure equalization, which reduces the amplitude of a wave as it is propagated through the medium. The dissipation of acoustic energy that is associated with changes in the molecular structure of the medium results from the finite time that is required for these changes to take place. For example, when the period of the acoustic cycle is comparable with the time required for a portion of the compressional energy of the fluid to be converted into internal energy of molecular vibration, then correspondingly during the expansion cycle some of this energy will be delayed in its restoration so as to be returned to the fluid during a time of rarefaction. Such a delay will result in a tendency towards pressure equalization and an attendant reduction in pressure amplitude of the wave.

In our discussions of sound waves in earlier chapters of this book it has been possible to treat the transmitting fluid medium as though it were a simple continuum having certain macroscopic properties such as pressure, density, compressibility, specific heat, and temperature, without being concerned with details as to the molecular structure of its molecules. Similarly, by the use of an additional macroscopic property of fluids, namely viscosity, Stokes[1] in 1845 developed the first successful theory offering a mechanism by which sound waves are attenuated. Kirchhoff[2] in 1868 utilized the macroscopic property of thermal conductivity to develop a theory which provides a second mechanism for explaining sound absorption in fluids. These two mechanisms are commonly referred to as *classical* types of sound absorption in fluids. However, in more recent times, as more and more accurate experimental measurements were made on sound absorption in fluids, it became evident that explanations of sound absorption from the macroscopic viewpoint alone were inadequate. Consequently, it became necessary to adopt a microscopic point of view of fluids and consider such phenomena as the binding energies within and between molecules in order more adequately to explain the absorption mechanism. The latter mechanisms are commonly referred to as *molecular* or *relaxational* types of sound absorption. For a more complete discussion of sound absorption in fluids than is to be presented in this chapter, the reader is referred to the references given below.[3]

The dissipation of acoustic energy at the boundaries of a fluid is of particular significance when the volume of the fluid is small in comparison with the area of its bounding walls, as when sound waves are transmitted through small ventilating ducts lined with a sound-absorbing material or within small rooms. Absorption occurring at the walls of rooms will be given detailed consideration in the chapter on architectural acoustics (Chapter 14).

9.2 Phase Lag Between Pressure and Condensation. From a phenomenological viewpoint, the absorption of energy from sound waves in fluids is associated with a time lag of the condensation s relative to the varying acoustic pressure p. This lag can be shown to depend on a characteristic

[1] Stokes, *Trans. Cambridge Phil. Soc.*, **8,** 287 (1845).

[2] Kirchhoff, *Pogg. Ann. Phys.*, **134,** 177 (1868).

[3] Markham, Beyer, Lindsay, *Reviews of Modern Physics*, **23,** 533, (1951); Herzfeld and Litovitz, *Absorption and Dispersion of Ultrasonic Waves*, Academic Press (1959).

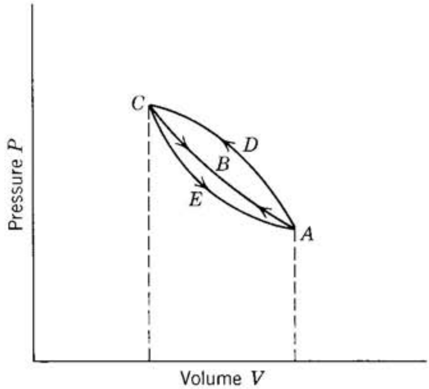

Fig. 9.1. Pressure vs. volume curves representing the work done during a compression-expansion cycle of an acoustic wave.

time or *relaxation* time required for (1) viscous stresses associated with relative fluid particle velocities to tend to equalize these velocities, (2) heat conduction to occur between high pressure (high temperature) and low pressure (low temperature) regions in the fluid, or (3) molecular energy changes to occur. More precisely, the relaxation time is the time required for a process to proceed to within $1/e$ of its equilibrium value.

When acoustic pressure and condensation are always in phase, as was the assumed situation for equation 5.4*b* where $p = \rho_0 c^2 s$, no energy is lost from the sound wave. On the other hand, when condensation lags pressure in phase, it is possible to show that during each cycle of pressure variation a net amount of work is done on the transmitting fluid medium. This work results in an increase in the temperature and heat energy of the medium at the expense of acoustic energy in the sound wave. The above processes are most easily visualized in terms of the PV diagrams shown in Fig. 9.1, where the amount of work W done on a fluid is given by

$$W = -\int P\, dV$$

and is represented by the area under the PV curve. If the pressure and condensation are always in phase, the amount of work done on the fluid in the compression cycle, as represented by the area under the curve ABC, is identical with that returned from the fluid during the expansion cycle along the curve CBA. Since no net amount of work has been done on the fluid, the sound wave does not lose energy and, therefore, is not attenuated in amplitude. On the other hand, if s lags p, the compression cycle may be represented by the curve ADC and the expansion cycle by the curve CEA.

Here the area contained within the loop *ADCEA* is a measure of the net work done on the fluid and correspondingly lost from the sound wave. This loss of energy appears as a reduction in pressure amplitude of the sound wave since in accordance with equation 5.33*b*, the energy density of a sound wave is proportional to the square of its pressure amplitude.

Therefore, in order to introduce dissipative terms into the general wave equation we must modify equation 5.4*b* so that condensation lags behind fluctuations in the acoustic pressure. Experience has shown that an equation after Stokes

$$p = \rho_0 c^2 s + R\frac{\partial s}{\partial t} \tag{9.1}$$

is most useful for this purpose. In this equation, the constant R is some kind of *effective viscosity* constant which will be discussed more fully in later sections of this chapter. In order to show that this equation causes pressure to lead condensation in phase, let us assume that a periodic pressure $\mathbf{p} = P_0 e^{j\omega t}$ is acting in the medium. Now, if $\mathbf{s} = \mathbf{S}e^{j\omega t}$ is assumed for the condensation, a direct substitution into equation 9.1 leads to

$$\mathbf{S} = \frac{P_0}{\rho_0 c^2 + j\omega R} \tag{9.2}$$

which shows that condensation lags pressure by a phase angle ϕ where

$$\tan\phi = \frac{\omega R}{\rho_0 c^2} \tag{9.2a}$$

It is to be noted that, in so far as periodic pressure disturbances are concerned, equation 9.2 indicates that it is possible to introduce dissipation into the wave equation by rewriting equation 5.4*b* as

$$\mathbf{p} = \rho_0 \mathbf{c}'^2 \mathbf{s} \tag{9.3}$$

where $\mathbf{c}'$ is a complex velocity given by the equation

$$\mathbf{c}' = c\left(1 + \frac{j\omega R}{\rho_0 c^2}\right)^{1/2} \tag{9.4}$$

In order further to visualize the significance of equation 9.1, let us assume that at the time $t = 0$, a constant excess pressure of magnitude ΔP_0 is applied to the previously undisturbed medium. When this initial condition is applied to the general solution of the differential equation expressed by equation 9.1

$$s = \frac{\Delta P_0}{\rho_0 c^2}(1 - e^{-\rho_0 c^2 t/R}) \tag{9.5}$$

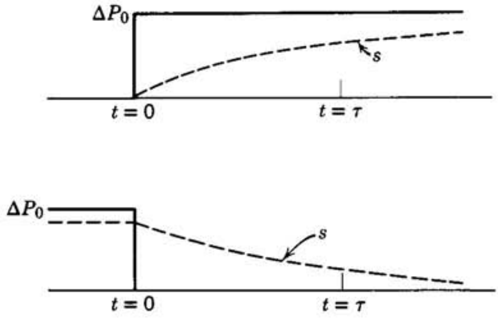

Fig. 9.2. Time delay of the condensation change relative to a step pressure change ΔP_0.

is obtained. The reader will note that this solution is of the same form as that obtained for current when a constant voltage E_0 is applied to a resistance and inductance in series. If after the condensation reaches its final value of $\Delta P_0/\rho_0 c^2$, the pressure ΔP_0 is removed, then the former will return to zero in accordance with the equation

$$s = \frac{\Delta P_0}{\rho_0 c^2} e^{-\rho_0 c^2 t/R} \tag{9.5a}$$

Plotted in Fig. 9.2 are curves representing both equation 9.5 and 9.5*a*. It is to be noted in both cases that condensation does not immediately follow a step change in pressure but instead lags behind so that it has *relaxed* to within $1/e$ of its final value in a time

$$\tau = \frac{R}{\rho_0 c^2} \tag{9.6}$$

This time τ is known as the *relaxation* time and is analogous to the time constant L/R occurring in the electrical circuit equations analogous to equations 9.5 and 9.5*a*. Expressed in terms of this relaxation time, equation 9.4 may be rewritten as

$$\mathbf{c}' = c(1 + j\omega\tau)^{1/2} \tag{9.4a}$$

9.3 Viscous Absorption of Plane Waves. As a relatively simple introduction to the more complicated mechanisms of sound absorption, let us first solve in some detail the case of viscous attenuation of a *plane* wave. If equation 9.1 is combined with the continuity equation 5.3*a*, $s = -\partial\xi/\partial x$, and the force equation 5.8, $-\partial p/\partial x = \rho_0 \partial^2\xi/\partial t^2$, so as to eliminate s and p,

$$\frac{\partial^2 \xi}{\partial t^2} = c^2 \frac{\partial^2 \xi}{\partial x^2} + \frac{R}{\rho_0} \frac{\partial^3 \xi}{\partial x^2\, \partial t} \tag{9.7}$$

is obtained. This equation expresses in analytical form the wave equation for attenuated plane acoustic waves. In the previous section we noted that dissipation of periodic waves could be allowed for by replacing the real velocity c by a complex velocity $\mathbf{c}'$ as given by equation 9.4 or 9.4*a*. Correspondingly, equation 9.7 for attenuated waves may be expressed in complex form by

$$\frac{\partial^2 \xi}{\partial t^2} = \mathbf{c}'^2 \frac{\partial^2 \xi}{\partial x^2} \tag{9.7a}$$

Solutions of either of these two equations may be used for discussing absorption of sound waves. However, in order to carry over techniques used for considering the propagation of electromagnetic waves in dielectrics as well as voltage waves on transmission lines, it will prove advantageous to use methods applicable to the latter equation. Let us assume a periodic solution for equation 9.7*a* in the form

$$\xi = \mathbf{A}e^{j(\omega t - \mathbf{k}'x)} \tag{9.8}$$

where

$$\mathbf{k}' = \frac{\omega}{\mathbf{c}'} \tag{9.9}$$

is a complex wavelength constant which may be expressed in terms of its real and imaginary parts as

$$\mathbf{k}' = k - j\alpha \tag{9.10}$$

When this expression for $\mathbf{k}'$ is substituted into equation 9.8

$$\xi = \mathbf{A}e^{-\alpha x}e^{j(\omega t - kx)} \tag{9.8a}$$

is obtained. This equation is similar in form to equation 5.11 for undamped plane waves excepting that the displacement amplitude is attenuated with distance in accordance with the term $e^{-\alpha x}$.

Explicit expressions for α and k may be obtained upon elimination of $\mathbf{k}'$ and $\mathbf{c}'$ from equation 9.9 by substituting equations 9.10 and 9.4*a*, respectively, into equation 9.9. The result is

$$\omega = c(k - j\alpha)(1 + j\omega\tau)^{1/2} \tag{9.11}$$

By equating the real and imaginary parts of this equation it may be separated into two equations, namely,

$$k^2 - \alpha^2 = \frac{\omega^2}{c^2(1 + \omega^2\tau^2)} \tag{9.11a}$$

and

$$2\alpha k = \frac{\omega^3\tau}{c^2(1 + \omega^2\tau^2)} \tag{9.11b}$$

By eliminating k between these two equations it may be shown that

$$\alpha = \frac{\omega}{c\sqrt{2}}\left(\frac{1}{(1+\omega^2\tau^2)^{1/2}} - \frac{1}{(1+\omega^2\tau^2)}\right)^{1/2} \tag{9.12}$$

In the majority of fluids, the relaxation time τ is so short that even for frequencies in the megacycle region the product $\omega\tau \ll 1$. When this is true, the rather cumbersome expression given in equation 9.12 simplifies to

$$\alpha \approx \frac{\omega^2\tau}{2c} \tag{9.12a}$$

If τ is replaced by $R/\rho_0 c^2$, this equation in turn becomes

$$\alpha \approx \frac{\omega^2 R}{2\rho_0 c^3} \tag{9.12b}$$

Therefore it is evident that, when R is independent of frequency, the attenuation constant α is directly proportional to the square of the frequency. In many liquids and gases such a behavior is observed over a wide range of frequencies and as a consequence it has become the practice to plot experimental data on sound absorption in the form of α/ω^2, or its equivalent, as a function of frequency. When plotted in this manner, any departure from a horizontal straight line is a measure of the deviation of experimental results from the above theory.

It is also possible to eliminate α between equations 9.11a and 9.11b and thereby obtain an equation for k. This expression is no longer simply ω/c. Since ω remains equal to 2π times the frequency, irrespective of whether or not absorption is present, this alteration in the value of k must be attributed to a change in velocity. This changed velocity, known as a *phase* velocity v, may be defined by means of the equation

$$v = \frac{\omega}{k} \tag{9.13}$$

When the value obtained for k above by eliminating α between equations 9.11a and 9.11b is substituted into equation 9.13

$$v = c\left[\frac{2(1+\omega^2\tau^2)}{1+(1+\omega^2\tau^2)^{1/2}}\right]^{1/2} \tag{9.14}$$

is obtained. For such low frequencies that $\omega\tau \ll 1$, this equation may be simplified to

$$v \approx c(1 + \tfrac{3}{8}\omega^2\tau^2) \tag{9.14a}$$

This dependence of phase velocity on frequency indicates that the relaxation behavior of sound waves associated with viscous properties of the medium not only produces *attenuation* in amplitude but also *dispersion* in velocity of propagation.

In order to see when the simplifying condition $\omega\tau \ll 1$ is applicable, we must now investigate the nature of the constant R. When we derive equation 9.7 directly from fundamental hydrodynamic equations,[4] it turns out that

$$R = \chi + 2\eta \tag{9.15}$$

where χ is a *longitudinal* coefficient of viscosity and η is the better known *shear* coefficient of viscosity. Since no direct method existed for measuring χ, Stokes made the assumption that fluids show no viscous reaction to a uniform compression from all directions. Since theory indicates that the *bulk* or *volume* coefficient of viscosity η' associated with uniform compression should be given by $\eta' = \chi + 2\eta/3$, the above assumption of $\eta' = 0$ requires that $\chi = -2\eta/3$. When this theoretical value of χ is substituted into equation 9.15, the latter becomes

$$R = \frac{4\eta}{3} \tag{9.15a}$$

As we shall see later in this chapter, there is reason to believe that some liquids, particularly water, possess a nonvanishing bulk coefficient of viscosity. However, for the present we will follow the classical hypothesis of Stokes and use equation 9.15*a*. Finally when $R = 4\eta/3$ is substituted into equation 9.6

$$\tau = \frac{4\eta}{3\rho_0 c^2} \tag{9.6a}$$

is obtained. Upon substitution into this equation of appropriate numerical values for air at 20°C as obtained from Table I of the appendix

$$\tau = \frac{4 \times 1.81 \times 10^{-5}}{3 \times 1.21 \times 343^2} = 1.7 \times 10^{-10} \text{ sec}$$

Similarly, appropriate numerical values for water at 20°C leads to

$$\tau = \frac{4 \times 0.001}{3 \times 998 \times 1480^2} = 6 \times 10^{-13} \text{ sec}$$

In both cases τ is so small that $\omega\tau \ll 1$ for all practical frequencies. It is only at high ultrasonic frequencies in very viscous liquids that we may anticipate the simplifying condition $\omega\tau \ll 1$ no longer to apply. Therefore, we may assume that in all fluids excepting very viscous liquids, the effects

[4] Mason, *Electromechanical Transducers and Wave Filters*, pp. 298–307, D. Van Nostrand Co. (1948).

of viscosity on acoustic waves are such that the velocity of propagation is independent of frequency and the attenuation is given by

$$\alpha = \frac{2\omega^2\eta}{3\rho_0 c^3} \tag{9.12c}$$

Attenuation in the amplitudes of particle displacement, acoustic pressure, etc. are frequently expressed in *nepers*, a natural logarithmic unit corresponding to a reduction in amplitude to $1/e$ of the initial or reference value. As we have seen in equation 9.8*a*, plane waves are attenuated directly as $e^{-\alpha x}$ and therefore the product αx must have the dimensions of nepers. This in turn indicates that α must have the dimensions of nepers/m. Furthermore, since the intensity of a plane wave is proportional to the square of its displacement amplitude, intensity must vary with distance in accordance with the equation $I_x = I_0\, e^{-2\alpha x}$. Correspondingly, the change in intensity level of the attenuated wave, expressed in decibels, is given by

$$\Delta\text{IL} = 10 \log \frac{I_x}{I_0} = 10 \log e^{-2\alpha x} = -8.7\alpha x$$

Consequently, we may state that 8.7α is a measure of the spatial rate of decrease in intensity level expressed in db/m. It is also a measure of an equal decrease in sound pressure level.

9.4 Heat Conduction as a Source of Acoustic Attenuation. In the preceding section we have examined viscosity as a relaxation mechanism for producing absorption and dispersion of sounds in fluids. Another such mechanism is provided by heat conduction. In the compression of the fluid in the passage of a sound wave, the temperature is raised and a temperature gradient is locally established. This leads to a flow of heat by conduction, which can be of significant magnitude before the subsequent rarefaction is accomplished. Theory indicates that the relaxation time for this process is given by

$$\tau = \frac{\kappa}{\rho_0 c^2 c_p} \tag{9.16}$$

where κ is the thermal conductivity of the fluid and c_p is its specific heat at constant pressure. For most fluids this quantity is so small for all practical frequencies, that the simplified theoretical equation for attenuation associated with heat conduction is given by

$$\alpha = \frac{\gamma - 1}{2c}\, \omega^2\tau \tag{9.17}$$

which upon substitution of τ from equation 9.16 becomes

$$\alpha = \frac{\kappa(\gamma - 1)}{2\rho_0 c^3 c_p}\,\omega^2 \tag{9.17a}$$

A substitution of appropriate values for the constants in this equation will indicate that for gases the attenuation associated with heat conduction is

Table 9.1 Acoustic attenuation in fluids

All Data for $T = 20^\circ$C and $P_0 = 1$ atm	Classical Calculation α/f^2			Observed α/f^2
	Heat Conduction	Viscosity	Total	
Gases	$\times 10^{-11}$	$\times 10^{-11}$	$\times 10^{-11}$	$\times 10^{-11}$
Argon	0.77	1.08	1.85	1.87
Helium	0.22	0.31	0.53	0.54
Oxygen	0.47	1.14	1.61	1.92
Nitrogen	0.39	0.96	1.35	1.64
Air (dry)	0.38	0.99	1.37	2.0
Carbon dioxide	0.31	1.09	1.40	α/f peaks at 20 kc
Liquids	$\times 10^{-15}$	$\times 10^{-15}$	$\times 10^{-15}$	$\times 10^{-15}$
Glycerin	...	3000	3000	3000
Mercury	6	...	6	5
Acetone	0.5	6.5	7.0	30
Water	...	8.1	8.1	24
Sea water	...	8.1	8.1	α/f peaks at 120 kc

somewhat less than that for viscous attenuation but of the same order of magnitude. On the other hand, for liquids the attenuation produced by heat conduction is normally very much less than that produced by viscosity.

When the absorption is small, it is possible to assume that viscosity and heat conduction act independently in producing an attenuation of sound waves. Acting under this assumption, we may add equation 9.12*c* to 9.17*a* to give

$$\alpha = \frac{\omega^2}{2\rho_0 c^3}\left(\frac{4\eta}{3} + \frac{\kappa(\gamma - 1)}{c_p}\right) \tag{9.18}$$

as the theoretical *classical* coefficient of attenuation for acoustic waves.

Table 9.1 contains comparative data on calculated and observed values of the attenuation constant α in nepers/meter for a representative number of gases and liquids. It is to be noted that although the predicted dependence on frequency is confirmed experimentally in most cases over fairly wide ranges of frequency, the magnitude of the measured value is generally in excess of the calculated value excepting for the inert gases, such as helium and argon, for very viscous liquids such as glycerin, and for highly conducting liquids such as mercury. These discrepancies in magnitude along with the abnormal behavior with frequency as indicated for carbon dioxide and sea water suggest that additional types of relaxation phenomena must be considered in order to explain more adequately the absorption of acoustic waves.

9.5 Molecular Thermal Relaxation as a Source of Acoustic Attenuation. In elementary gas theory, the molecules are considered to be perfectly elastic spheres, and the pressure they produce can be explained in terms of their average energy of translation and the number per unit volume. Translational energy of the molecules is assumed on the average to be evenly distributed among the three translational *degrees of freedom* of each molecule, i.e., translation along each of the three coordinate axes. Changes in the translational energy ΔE of 1 kg of gas is in turn related to changes in temperature ΔT by the equation

$$\Delta E = 3(\tfrac{1}{2}r\Delta T) \tag{9.19}$$

where r is the gas constant previously encountered in Section 5.5 and expressed here in joules/kg°C. This equation is in accordance with the classical law of *equipartition of energy* which states that on the average each mechanical degree of freedom of a gas molecule will carry the same amount of energy, $kT/2$, where k is Boltzmann's constant, and is related to r by the equation $r = nk$, where n is the number of molecules per kilogram of the gas. When a monatomic gas such as helium or argon is compressed adiabatically, all of the work done in compressing the gas goes into increasing the temperature of the gas in accordance with equation 9.19. Since this takes place almost instantaneously, changes in pressure, temperature, and density are all in phase and consequently, when sound waves are being propagated in such gases, no excess absorption is present above that resulting from viscosity and heat conduction.

On the other hand, for polyatomic gases, not only must one consider the energy of translation but also the internal energies of *rotation and vibration* of the molecules. For instance, diatomic molecules have three modes of internal energy, two of rotation about axes orthogonal to the molecular axis and one of vibration along this axis. Often, the vibrational modes are not excited at lower gas temperatures. In general, the work done in compressing a gas adiabatically is related to the change in temperature by the equation

$$\Delta E = c_v \Delta T \tag{9.20}$$

where c_v is the specific heat of the gas at constant volume expressed in joules/kg°C. Under equilibrium conditions this specific heat is given by $c_v = Nr/2$, where N is the total number of active degrees of freedom. As we have seen above, N is *three* for the monatomic gases, approximately *five* for the diatomic gases oxygen and nitrogen and *six* for the triatomic gas carbon dioxide. By contrast with the behavior in monatomic gases, when a polyatomic gas is compressed the work done is not immediately equipartitioned amongst the various degrees of freedom, since a finite time is required for molecular collisions to impart additional energy into the rotational and vibrational modes. This delay is normally very short for the rotational modes but quite appreciable for the vibrational modes. It may be taken into consideration by letting

$$c_v = c_e + c_i(1 - e^{-t/\tau}) \tag{9.21}$$

where c_v is the ultimate specific heat at constant volume when equilibrium conditions are reached, c_e is that part of it which remains instantaneously in phase with pressure changes and c_i is that part which is delayed by a fraction $1/e$ from reaching its ultimate value in a *molecular relaxation time* τ.

Let us now inquire as to how the delay in attainment of equilibrium conditions, as discussed above, may affect the propagation of a sound wave. Such a wave involves a momentary compression of the gas which not only increases its density but also increases its temperature and therefore, the mean kinetic energy of translation of its molecules. But the equilibrium increase in density does not occur instantaneously, since as the delayed part of the translational energy is being transferred to the internal modes, a cooling occurs which results in a further increase in density. Thus, just as was the situation with viscosity and heat conduction, this finite time required for molecular interchanges of energy will cause density changes in a fluid to lag behind pressure changes. A similar delay takes place during the expansion part of the acoustic cycle as energy is transferred back from internal states into the translational form. Thus, molecular relaxation will tend to smooth out the sound wave and thereby attenuate it. When the frequency of a sound wave is so low that the relaxation time is much smaller than a period of the wave cycle, equilibrium among the various energy states exists virtually at all times and the attendant difference in phase between pressure and temperature changes is small. Similarly, when the frequency is so high that the relaxation time is much larger than a period of the wave cycle, little or no interchange of energy takes place between external translational states and the delayed internal states and again changes in acoustic pressure and temperature are very nearly in phase. Therefore, it is to be anticipated that this type of relaxation will produce a maximum excess attenuation in one cycle of vibration or in traveling one wavelength at those frequencies having periods nearly equal to the relaxation time. One method of making allowance for the above behavior is to assume a complex frequency-dependent or dynamic specific heat of the form[5]

$$\mathbf{c}_\omega = c_e + \frac{c_i}{1 + j\omega\tau} \tag{9.22}$$

It is to be noted that at such low frequencies that $\omega\tau \ll 1$, this equation is reduced to $c_\omega = c_e + c_i = c_v$, i.e., the dynamic specific heat is identical with the equilibrium specific heat. On the other hand, at such high frequencies that $\omega\tau \gg 1$, $c_\omega = c_e$ which is less than the equilibrium specific heat.

By use of the relationship

$$\gamma = \frac{c_p}{c_v} = \frac{c_v + r}{c_v} = 1 + \frac{r}{c_v}$$

it is possible upon substitution from equation 9.22 to define a complex ratio of specific heats as

$$\boldsymbol{\gamma}' = 1 + \cfrac{r}{c_e + \cfrac{c_i}{1 + j\omega\tau}} \tag{9.23}$$

In equation 5.18 it was shown that the velocity of propagation of sound waves in a gas is directly proportional to $\sqrt{\gamma}$. Therefore, the existence of a complex ratio of specific heats in turn leads to a complex velocity of propagation $\mathbf{c}'$ given by

$$\mathbf{c}' = \frac{c}{\sqrt{\gamma}}\left(1 + \cfrac{r}{c_e + \cfrac{c_i}{1 + j\omega\tau}}\right)^{1/2} \tag{9.24}$$

By use of the techniques of Sect. 9.3, this equation in turn leads to

$$\alpha = \frac{\omega}{2c} \cdot \frac{rc_i}{c_e(c_e + r)} \cdot \frac{\omega\tau}{(1 + \omega^2\tau^2)} \tag{9.25}$$

for the attenuation constant in nepers/meter and

$$v = \frac{c}{\sqrt{\gamma}}\left[1 + \frac{r[c_i + c_e(1 + \omega^2\tau^2)]}{c_v^2 + c_e^2\omega^2\tau^2}\right]^{1/2} \tag{9.26}$$

[5] Vigoureux, *Ultrasonics*, pp. 38–39, John Wiley and Sons (1951).

for the phase velocity. At such low frequencies that $\omega\tau \ll 1$, equation 9.26 simplifies to

$$v_0 = \frac{c}{\sqrt{\gamma}}\left[1 + \frac{r(c_i + c_e)}{c_v^{\,2}}\right]^{1/2} = \frac{c}{\sqrt{\gamma}}\left[1 + \frac{r}{c_v}\right]^{1/2} = c$$

the normal unattenuated sound velocity. On the other hand, at such high frequencies that $\omega\tau \gg 1$, equation 9.26 becomes

$$v_\infty = \frac{c}{\sqrt{\gamma}}\left[1 + \frac{r}{c_e}\right]^{1/2} = c\left[\frac{c_v(c_e + r)}{c_e(c_v + r)}\right]^{1/2} \tag{9.27}$$

which is always greater than c since $c_v > c_e$ unless $c_i = 0$. Thus molecular thermal relaxation not only produces attenuation of sound waves but also a dispersion in phase velocity from c at low frequencies to

$$c\left[\frac{c_v(c_e + r)}{c_e(c_v + r)}\right]^{1/2}$$

at high frequencies.

In plotting graphs of the measured excess attenuation caused by molecular relaxation it is customary either to plot the ratio α/ω against ω or the product $\alpha\lambda$, i.e., the attenuation in nepers per wavelength, against frequency. When this is done, curves similar to that shown in Fig. 9.3 are obtained. A plot of α/ω versus ω is particularly useful since equation 9.25

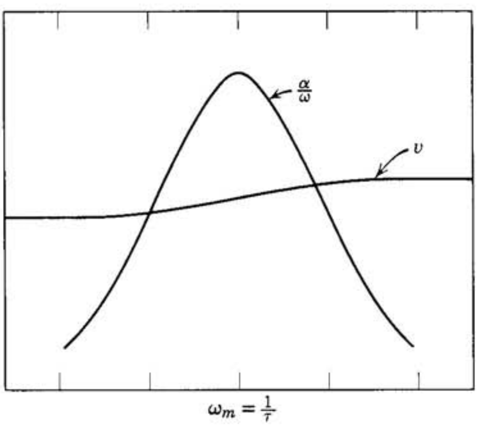

Fig. 9.3. Variation of attenuation and phase velocity, as predicted by molecular relaxation theory.

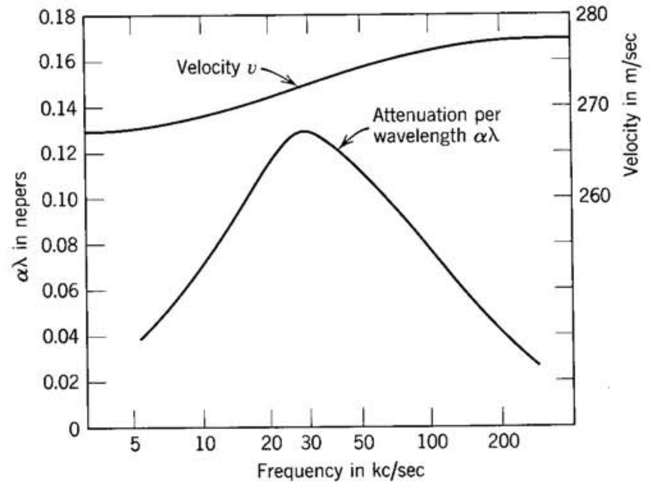

Fig. 9.4. Attenuation and velocity dispersion in carbon dioxide gas.

shows that the peak value of α/ω occurs at a frequency ω_m which is related to the relaxation time by the equation

$$\tau = \frac{1}{\omega_m} \tag{9.28}$$

The magnitude of this maximum value of α/ω is given by

$$\left(\frac{\alpha}{\omega}\right)_m = \frac{rc_i}{4c(c_e + r)c_e} \tag{9.29}$$

An important use of this equation is that through experimental measurement of $(\alpha/\omega)_m$ one is then able to determine a numerical relationship between c_e and c_i. It is to be noted that both the relaxation time τ and the magnitude of $(\alpha/\omega)_m$ are functions of the temperature of a gas, the former decreasing with increased temperature and the latter increasing with increased temperature. If equations 9.28 and 9.29 are combined with equation 9.25, the latter may be written in a simpler form as

$$\left(\frac{\alpha}{\omega}\right) = 2\left(\frac{\alpha}{\omega}\right)_m \frac{\omega\omega_m}{\omega^2 + {\omega_m}^2} \tag{9.30}$$

or

$$(\alpha\lambda) = 2(\alpha\lambda)_m \frac{ff_m}{f^2 + {f_m}^2} \tag{9.30a}$$

The latter two forms of the attenuation equation are particularly useful in plotting and analyzing experimental data.

A classical example of this type of molecular attenuation and dispersion is that of pure carbon dioxide gas. Plotted in Fig. 9.4 are experimental data for carbon dioxide at 20°C. It is to be noted that the excess molecular thermal attenuation at 20 kilocycles/sec is approximately 1200 times the classical attenuation.

Table 9.1 indicates that measured values of acoustic attenuation in dry air follow the square law of dependence upon frequency but are some 50 per cent higher than is predicted by classical theory.[6] Thermal relaxation in the vibrational or rotational energy states of oxygen and nitrogen molecules apparently does not account for this discrepancy and it may well be caused either by experimental errors or relaxational phenomena associated with impurities in the air being measured. By contrast, measured attenuation in *atmospheric* air at the lower ultrasonic and at audible frequencies exceeds the predicted values by a factor that varies from about 5 to 100. Curve *A* of Fig. 9.5 shows the manner in which the attenuation constant varies with frequency in air of 37 per cent relative humidity at a temperature of 27°C. Curve *B* of this figure shows similar measurements taken for completely dry air, and curve *C* gives the attenuation predicted by classical theory. It is apparent that the excess absorption in atmospheric air as shown by curve *A* must be associated with the presence of a small percentage of water-vapor molecules. This excess absorption increases rapidly with temperature and is critically dependent on the relative humidity. Although this phenomenon cannot be explained by classical theory, it is adequately explained in terms of thermal molecular relaxation of the normally unexcited vibrational mode of atmospheric oxygen molecules. In dry air, this relaxation time for oxygen molecules is of the order of several seconds and therefore the vibrational mode is not excited by sound waves. However, the presence of small amounts of water-vapor molecules acts as a sort of catalytic agent which reduces the number of collisions required on the average to excite the vibrational mode of the oxygen molecule. This in turn reduces the relaxation time of the vibrational mode of the oxygen molecule into the range from 10^{-3} to 10^{-5} second, which gives

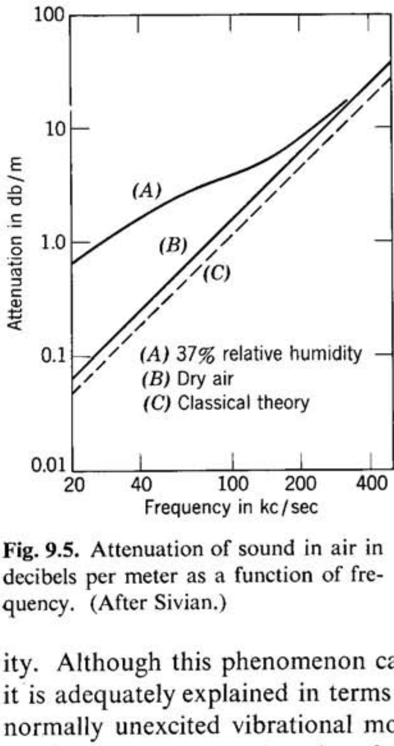

Fig. 9.5. Attenuation of sound in air in decibels per meter as a function of frequency. (After Sivian.)

[6] Sivian, *J. Acoust. Soc. Am.*, **19**, 914 (1947).

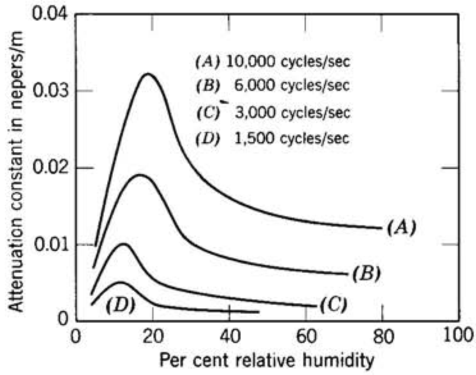

Fig. 9.6. Molecular attenuation in air as a function of relative humidity. (After Knudsen.)

rise to a relatively large excess attenuation per wavelength at frequencies between 1 and 100 kilocycles/sec in accordance with equation 9.30*a*. The magnitude of the maximum excess attenuation per wavelength $(\alpha\lambda)_m$ is observed to be nearly independent of the relative humidity of the air. However, since the frequency at which this maximum attenuation occurs is observed to be nearly a quadratic function of relative humidity, the maximum excess absorption per meter of path is observed to increase rapidly with relative humidity. Measured values[7] of the excess attenuation in air at 20°C are plotted in Fig. 9.6 as a function of relative humidity.

Table 9.2 Molecular attenuation in air

Relative Humidity, %	Frequency of Maximum Attenuation f_m, (cycles/sec)	Molecular Attenuation α_m, (neper/m)	Classical Attenuation α, (neper/m)
9	1500	0.5×10^{-2}	0.0045×10^{-2}
11	3000	1.0×10^{-2}	0.018×10^{-2}
14	6000	1.9×10^{-2}	0.072×10^{-2}
17	10,000	3.2×10^{-2}	0.20×10^{-2}

Data showing conditions corresponding to the frequencies of maximum attenuation per wavelength are summarized in Table 9.2 for various relative humidities. The attenuations in dry air as calculated from the observed constant for α/f^2 listed in Table 9.1 are also given in the last column for purposes of comparison. The constant $(\alpha\lambda)_m$ as empirically

[7] Knudsen, *J. Acoust. Soc. Am.*, **6**, 201 (1935).

determined from this data is 1.14×10^{-3}. It is evident that excess molecular attenuation is most significant in the audible range of frequencies at low relative humidities. Since the effect also increases with temperature, it should be quite noticeable in the hot, relatively dry air over a desert. As the relative humidity increases, the frequency of maximum attenuation is increased, as is the attenuation per meter of path at this frequency. Fortunately, at normal relative humidities of 50 per cent or greater this frequency is in the lower ultrasonic range and consequently, the attenuation in the audible range is less significant. However, the effect definitely attenuates high-frequency sounds coming from a distant band in open air, or the consonant sounds from a speaker in a large auditorium.

The presence of water-vapor has little or no effect upon the attenuation of sound waves in pure nitrogen gas. However, in carbon dioxide gas it has a very pronounced effect upon the vibrational type of relaxation discussed earlier in this section. For instance, the presence of 1 per cent of water-vapoı in carbon dioxide shifts the frequency of maximum molecular attenuation per wavelength to in excess of 2000 kilocycles/sec. As a consequence, carbon dioxide containing a small percentage of water vapor becomes acoustically opaque at frequencies above 1 megacycle/sec.[8]

9.6 Excess Absorption Phenomena in Liquids. One type of excess absorption occurring in liquids is that associated with thermal relaxation of energy between external degrees of translational freedom and internal vibrations. As in the case of gases, it requires that the acoustic waves produce periodic fluctuations in temperature. Thermal relaxation has been applied successfully to explain the excess absorption observed in many nonassociated nonpolar liquids such as carbon disulfide, benzene, and acetone. For instance, it explains the behavior in acetone where the measured attenuation is some 4.3 times the value predicted by classical theory. (See Table 9.1.)

Thermal relaxation, however, has not been successful in accounting for the observed excess absorption in associated polar liquids, such as the alcohols and water. It appears that in these liquids, the intermolecular forces are so strong that they cause any existing thermal relaxation time to be very short. Since in accordance with equation 9.25, the magnitude of the attenuation coefficient is proportional to the relaxation time, the resulting attenuation associated with the process is small. The fact that the excess absorption in water is not due to thermal relaxation has been demonstrated in a striking manner through measurements made in the vicinity of 4°C.[9] If the measured excess absorption in water were caused

[8] Knudsen and Fricke, *J. Acoust. Soc. Am.*, **12**, 255 (1940).

[9] Fox, Rock, *Phys. Rev.*, **70**, 68 (1946).

by thermal relaxation, then this excess should vanish at 4°C, where the coefficient of thermal expansion is zero. At this temperature, compression or rarefaction will not change the temperature and thus thermal relaxation cannot take place. Measurements in water in the vicinity of 4°C give no evidence of any decrease in absorption at this temperature. Therefore, it is necessary to find some other type of relaxation mechanism in order to explain the measured excess absorption in water, which is some three times that predicted by classical theory. (See Table 9.1.) One such explanation is offered by a theory of *structural relaxation*, as applied to water with some success by Hall.[10] This theory assumes the excess absorption in water results from a structural relaxation directly related to volume change and not to temperature change. In this structural relaxation theory, water is assumed to be a two-state liquid. The state of lower energy is the normal state and the state of higher energy is one in which the molecules have a more closely packed structure. Under ordinary static conditions of equilibrium most of the molecules are in the first energy state. However, the passage of a compressional wave is assumed to promote the transfer of molecules from the more open first state to the more closely packed second state. The time delays in this process and in its reversal lead to a relaxational dissipation of acoustic energy.

A detailed analysis of the influence of structural relaxation upon the propagation of acoustic waves in water indicates that it may be taken into consideration by assuming the existence of a nonvanishing volume coefficient of viscosity η'. If this is the case, then the longitudinal coefficient of viscosity χ is not given by $-2\eta/3$, as was originally assumed by Stokes, but instead is given by $(\eta' - 2\eta/3)$ which upon substitution into equation 9.15 leads to

$$R = \eta' - \frac{2\eta}{3} + 2\eta = \eta' + \frac{4\eta}{3} \tag{9.31}$$

When this expression for R is substituted into equation 9.12*b*, the resulting expression for total attenuation in water becomes

$$\alpha = \frac{\omega^2}{2\rho_0 c^3}\left(\tfrac{4}{3}\eta + \eta'\right) \tag{9.32}$$

Direct measurement of the coefficient of volume viscosity by Liebermann[11] indicates that η' in water is approximately three times the coefficient of shear viscosity η. If this measured value of η' is substituted into equation 9.32 and α/f^2 computed, the resulting constant is found to be in satisfactory agreement with the measured value listed in Table 9.1.

[10] Hall, *Phys. Rev.*, **73,** 775 (1948).
[11] Liebermann, *Phys. Rev.*, **75,** 1415 (1949).

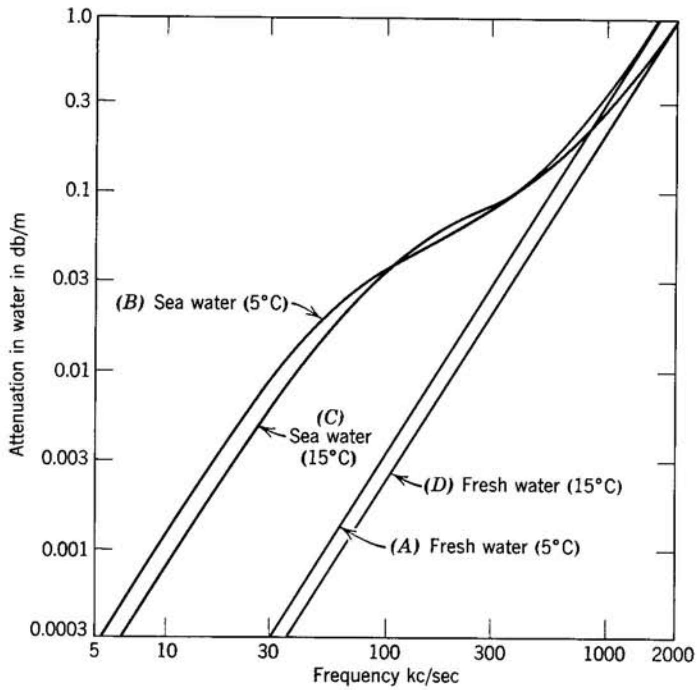

Fig. 9.7. Attenuation at ultrasonic frequencies in (*A*) and (*D*) fresh water; (*B*) and (*C*) sea water.

Plotted in curve *A* of Fig. 9.7 is a line representing the measured attenuation of acoustic waves in fresh water at 5°C expressed in db/meter. Curve *B* of this figure is a plot of measured values of the attenuation in sea water at 5°C. The pronounced difference between these two curves at frequencies below 500 kilocycles/sec makes evident the presence of yet an additional relaxational process and attendant excess absorption in sea water beyond those present in fresh water. It is natural to attribute this additional absorption to the presence of dissolved salts in sea water and to refer to it as a type of *chemical relaxation*. Laboratory measurements by Leonard[12] and co-workers have shown that the excess acoustic absorption of sea water as compared to fresh water is caused almost entirely by the presence of dissolved $MgSO_4$. For instance, as the concentration of $MgSO_4$ is increased in water, the measured excess absorption increases until at a concentration of 0.014 mole per liter it is essentially the same as that of sea water as measured directly in the ocean. The relaxation time of the process may be computed from a measurement of the frequency at which the absorption

[12] Wilson and Leonard, *J. Acoust. Soc. Am.*, **26**, 223 (1954).

per wavelength is a maximum. At 5°C this frequency is near 60 kilocycles/sec which leads to a relaxation time of

$$\tau = \frac{1}{2\pi f_m} = \frac{1}{2\pi \times 60{,}000} = 2.65 \times 10^{-6} \text{ sec}$$

In view of the above discussion, we may anticipate that an equation of the form

$$a = \frac{A f_m f^2}{f^2 + f_m^{\,2}} + B f^2 \quad \text{(decibels/meter)} \tag{9.33}$$

would most likely fit experimental measurements of the attenuation of acoustic waves in sea water. It should be noted that the attenuation a expressed in db/meter is related to α expressed in nepers/meter by the equation $a = 8.7\alpha$. The first term on the right-hand side of this equation is associated with chemical relaxation of the dissolved $MgSO_4$ and the second term with viscous absorption in water. The reader may check by direct substitution that the experimental data of curve B in Fig. 9.7 is quite satisfactorily represented by equation 9.33 when f is expressed in kilocycles/sec, by $A = 6 \times 10^{-4}$, $B = 3.2 \times 10^{-7}$, and $f_m = 60$ kilocycles/sec. A substitution of these constants into equation 9.33 leads to

$$a = \frac{0.036 f^2}{f^2 + 3600} + 3.2 \times 10^{-7} f^2 \quad \text{(db/meter)} \tag{9.34}$$

for the attenuation in sea water at 5°C. It is to be noted that as the temperature of sea water is increased, the relaxation frequency f_m increases. As a consequence, sound absorption in sea water decreases with increased temperature and vice versa. For instance at 15°C, $f_m = 100$ kilocycles/sec which upon substitution into equation 9.33 leads to

$$a = \frac{0.06 f^2}{f^2 + 10{,}000} + 2.4 \times 10^{-7} f^2 \quad \text{(db/meter)} \tag{9.34a}$$

for the attenuation in sea water at 15°C which agrees with measured values as plotted in curve C of Fig. 9.7. Since the coefficient of viscosity in water decreases as the temperature increases, the constant B in equation 9.33 must also decrease with increasing temperature. However, at frequencies below 200 kilocycles/sec, this change has little influence on the total attenuation in sea water.

9.7 Absorption of Sound Within Cylindrical Pipes. Laboratory measurements of acoustic absorption in fluids is frequently made on fluids contained within cylindrical pipes. In one method, probe microphones are used to measure pressure amplitudes of a plane progressive wave at two or more positions along the length of the pipe. If P_1 is the pressure amplitude at x_1 and P_2 that at x_2, then the attenuation constant may be determined from the equation

$$P_2 = P_1\, e^{-\alpha(x_2 - x_1)}$$

When this method is used, steps must be taken to eliminate any effects of reflected waves either through the use of a nonreflecting termination at the end of the pipe or through the use of such short pulses or long pipes that measurements at x_1 and x_2 may be made before a reflected pulse is returned. By contrast, a second method utilizes pressure amplitude measurements at the nodes and antinodes of a pattern of standing waves such as is shown in Fig. 9.8*b*. Let us assume that the reflecting piston *B* of Fig. 9.8*a* is infinitely rigid. Then the amplitude of the reflected wave generated at this piston will equal that of the incident wave impinging on it from the sound source *A*. Accordingly, the steady state acoustic pressure present at any position along the pipe is given by

$$p = P_0 e^{-\alpha x} e^{j(\omega t - kx)} + P_0 e^{\alpha x} e^{j(\omega t + kx)} \tag{9.35}$$

where $x = 0$ at the piston *B*. The resulting pressure amplitude at any position along the pipe may be shown to be

$$P = 2P_0(\cosh^2 \alpha x \cos^2 kx + \sinh^2 \alpha x \sin^2 kx)^{1/2} \tag{9.36}$$

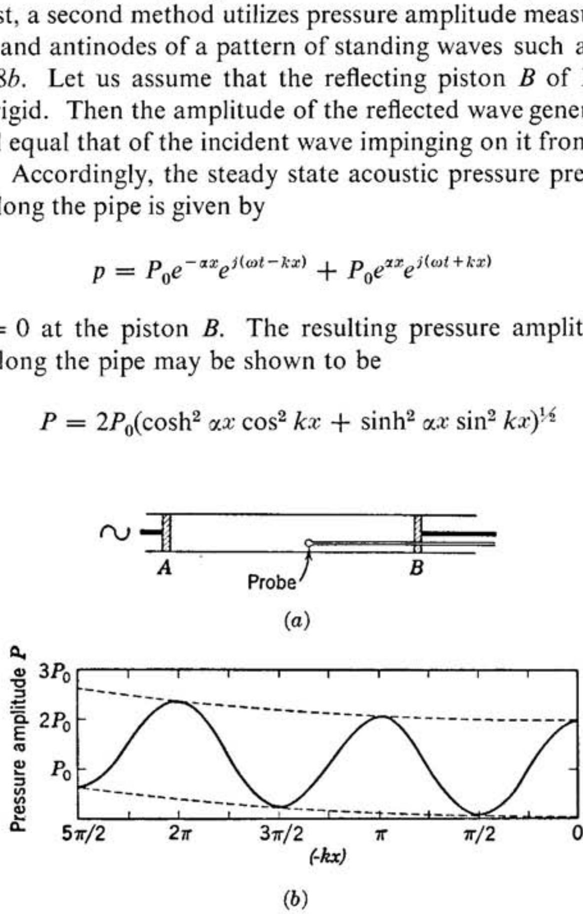

Fig. 9.8. (*a*) Measurement of standing waves. (*b*) Pressure amplitude of damped standing waves.

The nodal points of minimum pressure occur at

$$-kx = \frac{2n-1}{2}\pi \quad n = 1, 2, 3, \cdots$$

and have amplitudes of

$$P_{min} = 2P_0 \sinh \alpha x \approx 2P_0(\alpha x) \tag{9.37}$$

The pressure amplitudes at successive nodes can be measured either directly, by means of a small probe microphone, or by a probe tube attached to a condenser microphone. The value of α may then be determined by drawing a smooth curve through these points, as indicated in Fig. 9.8*b*. The antinodes occur at $-kx = n\pi$, where $n = 0, 1, 2, 3, \cdots$, and give maximum pressure amplitudes of

$$P_{max} = 2P_0 \cosh \alpha x \approx 2P_0(1 + \alpha^2 x^2)^{1/2} \tag{9.38}$$

Experimental determination of acoustic attenuation constants as determined by either of the above methods are always high as compared to those measured in large volumes of the fluid. This is caused by losses taking place at the walls of the pipe which must either be corrected for or made negligible. One source of this increased attenuation in fluids contained within pipes is associated with the viscous resistance offered to fluid motion at the walls of a pipe. This results in a laminar type of motion throughout the cross section of the pipe with the velocity increasing rapidly from zero at the walls to nearly its maximum value at a distance $(2\eta/\rho_0\omega)^{1/2}$ from the walls in accordance with the equation

$$\mathbf{u} = \frac{\mathbf{p}}{\rho_0 c}\left[1 - \frac{J_0(\mathbf{K}r)}{J_0(\mathbf{K}a)}\right] \tag{9.39}$$

In this equation a is the radius of the pipe, r is the radial distance from the center of the pipe, and $\mathbf{K}$ is a complex constant given by

$$\mathbf{K} = (1 - j)\sqrt{\frac{\rho_0\omega}{2\eta}} \tag{9.40}$$

where η is the coefficient of shear viscosity. Plotted in Fig. 9.9 are results obtained from equation 9.39 for the relative fluid velocity amplitude in air as a function of the radial position in a pipe of 0.005-m radius for sound waves having a frequency of 100 cycles/sec. Not only does equation 9.39 result in a radial velocity gradient but it also predicts the existence of a phase difference between fluid particle velocity and acoustic pressure. As a consequence of this phase difference, we may anticipate both attenuation

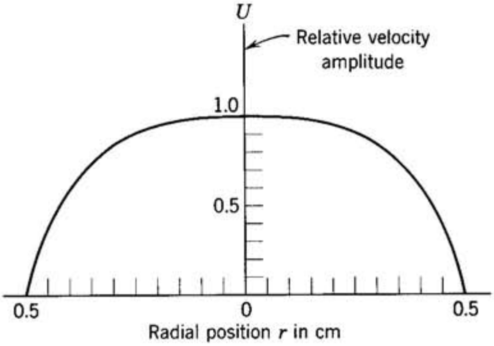

Fig. 9.9. Relative particle velocity amplitude as a function of radial position in a small pipe, $f = 100$ cycles/sec.

and dispersion to be present. This deduction is correct, since it is possible to show[13] that the waves are attenuated in accordance with the equation

$$\alpha = \frac{1}{ac}\sqrt{\frac{\eta\omega}{2\rho_0}} \quad \text{(nepers/m)} \tag{9.41}$$

and have a reduced phase velocity of

$$v = c\left(1 - \frac{1}{2a}\sqrt{\frac{2\eta}{\rho_0\omega}}\right) \tag{9.42}$$

It is to be noted that the effect of viscosity on the propagation of acoustic waves in fluids contained within pipes, as indicated by the above equations, is dependent upon the ratio η/ρ_0, rather than upon η alone. For this reason the ratio η/ρ_0 is sometimes referred to as the kinematic coefficient of viscosity. The coefficient of viscosity of air at 20°C is 1.81×10^{-5} kg/m sec and its density at this temperature is 1.21 kg/m^3, so that its kinematic coefficient is seen to be 1.5×10^{-5} m^2/sec. The coefficient of viscosity of water at 20°C is 0.001 kg/m sec and, since its density at this temperature is 998 kg/m^3, its kinematic coefficient equals 10^{-6} m^2/sec. The effect of viscosity on the propagation of sound waves is therefore greater in air than in water, in spite of the much higher viscosity of water.

Experimentally measured values of the above attenuation constant α for dry air in pipes, are approximately 50 per cent greater than the values predicted by equation 9.41. However, if correction is made for the additional attenuation resulting from heat conduction at the walls of the pipe,

[13] Kinsler and Frey, *Fundamentals of Acoustics*, Section 9.3, John Wiley and Sons, (1950).

the difference between predicted and observed values is greatly reduced.[14] The important effects arising from the generation of heat, and its communication by conduction to and from the walls of a pipe, were first treated by Kirchhoff in 1868. He assumed that the layer of gas in contact with the walls can have neither velocity nor a change in temperature. This analysis, as presented by Rayleigh,[15] shows that the equations above must be modified by replacing the true coefficient of shear viscosity η with an effective coefficient η_e. The latter is defined by

$$\eta_e = \eta\left[1 + \left(\sqrt{\gamma} - \frac{1}{\sqrt{\gamma}}\right)\sqrt{\frac{\kappa}{c_p\eta}}\right]^2 \tag{9.43}$$

where κ is the thermal conductivity of the fluid, γ is the ratio of its specific heats, and c_p is its specific heat at constant pressure.

Experimentally measured values in air indicate that $\gamma = 1.402$, and $\kappa/c_p\eta = 1.29$, so that

$$\eta_e = \eta(1 + 0.39)^2 = 1.93\eta = 3.5 \times 10^{-5}\ \text{kg/m sec}$$

The effect of heat conduction to and from air at the walls of a pipe on the attenuation of sound waves is equivalent to a 93 per cent increase in the coefficient of shear viscosity, and results in a 39 per cent increase in the attenuation constant α of equation 9.41.

Substitution into equation 9.41 of the values corresponding to air at 20°C gives

$$\alpha = \frac{1}{343a}\sqrt{\frac{2\pi f 3.5 \times 10^{-5}}{2 \times 1.21}} = 2.76 \times 10^{-5}\frac{\sqrt{f}}{a} \quad \text{(neper/m)}$$

The attenuation constant given by the above equation for a frequency of 10,000 cycles/sec in air is $\alpha = 2.76 \times 10^{-3}/a$ neper/m. This attenuation is so small that it indicates that viscous and heat conduction losses at the walls are of negligible significance in absorbing sound waves in ventilating ducts. However, small as this attenuation may be, correction must frequently be made for it when acoustic measurements are being made at the higher frequencies in small pipes. For instance, at a frequency of 10,000 cycles/sec in a pipe of 0.01-m radius, it is much larger than attenuation taking place within the body of the gas which in accordance with the data of Table 9.1 is given by $\alpha = 2 \times 10^{-11}f^2$. However, as frequency increases, absorption of acoustic energy within the body of the fluid

[14] Fay, *J. Acoust. Soc. Am.*, **12,** 62 (1940).

[15] Rayleigh, *Theory of Sound*, Sections 348–350, Macmillan and Company, Ltd. (1929).

increases more rapidly than that at the walls and at frequencies above 1 megacycle/sec becomes the dominant type.

The influence of viscosity and heat conduction on the velocity of wave propagation within pipes is in general small. In the region of practical situations to which equation 9.42 applies it is never more than a few per cent. In the treatment of wave propagation through liquids confined within pipes, the influence of heat conduction at the walls is negligible for most liquids, and consequently only the ordinary shear coefficient of viscosity need be considered.

A third mechanism by means of which acoustic energy is extracted from a fluid within a pipe is through direct radiation of acoustic energy into the walls of the pipe. Previously in this section we have assumed that the walls were infinitely rigid so that this type of absorption could be neglected. However, in actual situations some acoustic energy is always irreversibly transmitted into the walls and therefore lost from the fluid. This may be reduced either by using pipes having very thick walls or by using thin-walled pipes which are surrounded by a fluid of much smaller specific acoustic impedance than that of the fluid contained in the pipe. The large mismatch in acoustic impedance provided by either of these arrangements will minimize the loss of acoustic energy from the fluid within the pipe.

Finally, it is sometimes desired to attenuate sound waves rapidly in a fluid, such as those traveling through the air in a ventilating duct. This attenuation may be enhanced by lining the interior walls of the duct with a sound absorbing material so as to increase the loss of acoustic energy from the air within.[16]

9.8 Attenuation in Inhomogeneous Fluids. When a fluid contains inhomogeneities such as suspended particles, thermal microcells of different temperatures, or regions of turbulence, an additional attenuation takes place beyond that occurring in a homogeneous medium. Two primary causes of this excess attenuation are additional absorption mechanisms and *scattering*. Fog and smoke particles produce a decided effect on sound propagation through the atmosphere. In the immediate neighborhood of suspended particles additional viscous and heat conduction losses take place over those effective in the body of a homogeneous fluid. Furthermore, a relaxation process associated with the evaporation of the water in a fog droplet is influenced by the passage of a sound wave. The normal equilibrium between the saturated vapor near the droplet and the surrounding air is disturbed by the sound wave which is followed by a lag in its restoration. Both of these processes lead to losses that increase gradually

[16] Harris, *Handbook of Noise Control*, Ch. 27, McGraw-Hill Book Co. (1957).

with frequency. At 1000 cycles/sec, for example, the measured[17] contribution to attenuation from these sources, in a fog with some 400 droplets/cm^3 having an average radius of 6×10^{-4} cm, is about 2.4×10^{-3} neper/m. This value is some hundred times greater than that measured in dry air and some ten times that measured in humid air. The presence of fog droplets in air also lowers the velocity of sound in the air by amounts down to $0.9c$, where c is the velocity of sound in dry air at the same temperature as the foggy air.

Extremely high attenuations are also produced in water containing suspended gas bubbles. For instance, viscous forces and heat conduction losses associated with the compression and expansion of small gas bubbles by a passing sound wave, results in a loss of energy by the sound wave. A further effect of such inhomogeneities, which is of particular importance in the transmission of directed sonar beams of sound energy, is *scattering*, i.e., the removal of a small amount of energy from the directed beam by each bubble, and its subsequent reradiation in all directions. The presence of gas bubbles also affects the nature of the medium through which the wave is progressing, altering both its density and compressibility and thus changing the velocity of sound. Such changes in velocity and density may result in a considerable amount of acoustic energy being reflected and refracted away from the direction of the initial sound beam. Thus, a beam of sound waves can be attenuated by reflection, refraction, absorption, and scattering as it enters water containing a high concentration of gas bubbles.

Although gas bubbles do not occur in large numbers in the main body of the ocean, high concentrations of bubbles do occur in the wakes of ships and submarines traveling on or near the surface and to modest depths when waves are breaking at the surface. Consequently, there is a tendency for bubbles to be located in specific regions and at high concentrations when they do occur, and such localized groups of bubbles are observed to produce a considerable attenuation of sound waves in the ocean. A single bubble has little effect on the transmission of sound. However, the cumulative effect of many bubbles is quite pronounced. Since large bubbles rise to the surface very rapidly, their life in the medium is too short to be of much significance. However, a large number of bubbles with radii small in comparison with the wavelengths being transmitted produce significant attenuations.

Let us assume that each bubble has an effective attenuating cross section σ expressed in square meters. This effective cross section is a measure of the fraction of energy that the bubble will extract from a sound beam of one square meter cross section. Depending upon frequency, this cross

[17] Knudsen, Wilson, and Anderson, *J. Acoust. Soc. Am.*, **20,** 849 (1948).

section may be either equal to, less than, or greater than the actual cross section πa^2, where a is the radius of the bubble. For instance, at the resonant frequency of radial vibrations of a gas bubble, which is given by the equation[18]

$$f = \frac{1}{2\pi a}\sqrt{\frac{3\gamma P_0}{\rho_0}} \tag{9.44}$$

the effective cross section may be more than a thousand times greater than the actual cross section. In equation 9.44, the frequency is given in cycles/sec when the radius a is expressed in meters, the hydrostatic pressure P_0 of the water in newtons/m^2, the density of the water ρ_0 in kg/m^3, and $\gamma = 1.4$. When the frequency of the sound wave is higher than this resonant frequency, the effective and actual cross sections are nearly equal. On the other hand, at lower frequencies the effective cross section is much less than the actual cross section. If we now assume the bubbles to be concentrated in an amount of N bubbles/m^3 and all to have the same cross section σ, then the loss in intensity experienced by a plane wave in traveling an infinitesimal distance dx is given by

$$dI = -N\sigma I\, dx$$

If this equation is integrated and the constant of integration determined from the assumption that I_0 is the intensity at $x = 0$,

$$I = I_0 e^{-N\sigma x} \tag{9.45}$$

is obtained. Since intensity is proportional to the square of the pressure amplitude P, we may rewrite equation 9.45 as

$$P = P_0 e^{-[(N\sigma/2)x]} \tag{9.45a}$$

Therefore, we see that the attenuation of a beam of sound waves in water containing gas bubbles is given by $\alpha = N\sigma/2$ nepers/m or by $8.7\alpha = 4.35\ N\sigma$ db/m. Of course, all bubbles will not have the same effective cross section and, consequently, some type of summation over all bubble sizes must be carried out in order to compute a realistic attenuation constant. However, in actual practice, only those bubbles having resonant frequencies near that of the sound wave need be taken into consideration in such a summation.

Observed attenuation coefficients, for the relatively fresh wake existing 500 meters astern of a destroyer making 15 knots ranges from 0.8 db/meter at 8 kilocycles/sec, to 1.2 db/meter at 20 kilocycles/sec, to 1.8 db/meter at

[18] NDRC Technical Summary Report, *Physics of Sound in the Sea*, pp. 461–463 (1946).

40 kilocycles/sec.[19] The concentration of bubbles occurring naturally in the main body of the ocean is so small that any attenuation resulting from this source is negligible as compared to that caused by viscous forces and other relaxation phenomena as discussed earlier in this chapter. Finally, it is to be noted that a large school of small fish will produce measureable attenuation in sound beams. The primary source of this attenuation is undoubtedly that of scattering from their internal air sacs.

PROBLEMS

9.1. Using the data in Table 1 in the appendix, (*a*) compute the viscous relaxation time for glycerin. (*b*) For what frequency in cycles/sec is $\omega\tau = 1$? (*c*) Compute and plot α/f^2 over the frequency range between 10 megacycles/sec and that determined in part (*b*).

9.2. (*a*) Assuming the coefficient of viscosity in air to be independent of pressure, what is the viscous relaxation time in air at a pressure of 0.1 atmosphere? (*b*) At what frequency will the product $\omega\tau = 1$ in such air? (*c*) What is the theoretical viscous attenuation constant and phase velocity in such air at this frequency? (*d*) What is the corresponding attenuation and velocity in air of 1-atmosphere pressure at this same frequency?

9.3. Calculate the relaxation time due to heat conduction associated with sound absorption in air. Compare with the corresponding value due to viscosity.

9.4. Given that the ratio of specific heats for CO_2 gas is $\gamma = 1.31$ and that its gas constant is $r = 188$ joules/kg °C, use the data of Fig. 9.4 and the equations of Sect. 9.5 to compute values for c_p, c_v, c_e, and c_i.

9.5. Given air of 13 per cent relative humidity to have its maximum excess molecular attenuation per wavelength at a frequency of 5000 cycles/sec. (*a*) What is the relaxation time? (*b*) If the measured molecular attenuation at 5000 cycles/sec is 0.016 neper/m, compute and plot the excess molecular attenuation per meter of path over the frequency range from 1000 to 10,000 cycles/sec. (*c*) What is the ratio of the excess molecular attenuation in the above air at 1000, 5000, and 10,000 cycles/sec to that in dry air?

9.6. A siren is to operate in air at a frequency of 6000 cycles/sec and at a small height above the level ground. Assuming hemispherical divergence and no absorption by the ground, what must be the acoustic output of the siren in watts if it is to produce an intensity level of 60 db at a distance of 1000 ft for each of the following assumed conditions? (*a*) No absorption by the air. (*b*) Completely dry air. (*c*) Air of 60 per cent relative humidity.

9.7. Show that the attenuation constant α as given by equation 9.32 has the dimensions of a reciprocal length. (*a*) What is the predicted attenuation in decibels for ultrasonic sounds of 40 kc/sec frequency in traversing a path length of 4000 meters in fresh water at 5°C? (*b*) In sea water at 5°C?

9.8. A plane wave having a frequency of 1000 cycles/sec traverses fresh water at 15°C. (*a*) In what distance will it be attenuated by 10 db? (*b*) Work the same problem for a frequency of 20,000 cycles/sec. (*c*) What are the corresponding distances in sea water at 15°C? (*d*) In dry air? (*e*) In air of 37 per cent relative humidity?

[19] NDRC Technical Summary Report, *Physics of Sound in the Sea*, pp. 534 (1946).

9.9. (*a*) Calculate the value of $\sqrt{2\eta/\rho_0\omega}$ for acoustic waves of 200 cycles/sec frequency in air. (*b*) Including the effects of both viscous and heat conduction losses at the walls of the pipe, calculate the phase velocity of 200 cycle/sec plane waves through air in a pipe of 1-cm radius. (*c*) What is the corresponding attenuation constant α in nepers/m? (*d*) What is the decibel attenuation in intensity level produced in a 2-m length of this pipe?

9.10. Calculate and compare the attenuation constant α in dry air for plane waves in a pipe of 1.0-cm radius with that for plane waves in the unbounded medium at frequencies of 1000, 10,000, and 100,000 cycles/sec.

9.11. Calculate a value for the attenuation in decibels/meter at a frequency of 20 kilocycles/sec, (*a*) in fresh water contained in a pipe of 1.0-cm radius, (*b*) in a large body of fresh water at 15°C, (*c*) in a large body of sea water at 15°C.

9.12. Plane waves of sound are being propagated in an air-filled pipe of 0.1-m radius by means of a loudspeaker fitted into one end of the pipe. The far end of the pipe is closed by means of a rigid cap. The frequency radiated by the loudspeaker is 6000 cycles/sec. The measured standing wave ratio of pressure at one position in the pipe is 8. At a second position 0.5 m further down the pipe, the measured standing wave ratio is 9. (*a*) Derive an equation, involving these ratios and the distance between them, that may be used in calculating the absorption constant for waves being propagated within the pipe. Simplify your equation for $\alpha \ll 1$. (*b*) What is the numerical value of α corresponding to the above data? (*c*) Calculate the absorption constant to be anticipated if there were only viscous and heat conduction losses at the walls of the pipe. (*d*) Assuming the remainder of the measured absorption constant to result from the presence of water vapor, use Fig. 9.6 to estimate the relative humidity of the air in the pipe.

9.13. (*a*) What is the resonant frequency of radial vibrations for an air bubble of 0.01-cm radius in water at a depth of 10 m. (*b*) If the effective attenuating cross section for such a bubble is 1000 times its actual cross section, how many bubbles/m^3 will be required in order to produce an attenuation of 0.01 db/m? (*c*) How does this attenuation compare with that of bubble-free sea water at the same frequency? Assume a temperature of 15°C.

9.14. Show that the transverse vibrations $u_0 = U_0 e^{j\omega t}$ of a plane surface along the x direction will produce transverse viscosity waves in an adjacent fluid medium whose wave equation is

$$\frac{\partial^2 u}{\partial z^2} = \frac{\rho_0}{\eta}\frac{\partial u}{\partial t}$$

in which z is the direction of propagation of the waves at right angles to the plane surface, η is the coefficient of viscosity of the medium and ρ_0 its density. Derive the resulting harmonic solution of this wave equation, with the assumed boundary condition that the medium immediately adjacent to the vibrating plane has an identical transverse velocity. Show that these transverse waves are attenuated by $\sqrt{\rho_0\omega/2\eta}$ nepers/m. In the case of air, plot the thickness of the layer of air in which one neper of attenuation takes place as a function of frequency in the range from 10 cycles/sec to 1000 cycles/sec.

chapter 10

LOUDSPEAKERS

10.1 Introduction. In practically all modern acoustical work, the oscillations in sound pressure are picked up by some form of receiving electroacoustic transducer, e.g., a microphone, which converts them into similar electrical current or voltage oscillations. The latter either may be electrically amplified for immediate reconversion into sound energy or may be stored in some form, such as on magnetic tape, for later analysis or playback. After amplification, these oscillations may be converted back into sound vibrations by some form of transmitting electroacoustic transducer, such as the so-called loudspeaker (speaker).

There are a number of interrelated factors that must be considered in the design of an effective transducer for converting electrical energy into airborne acoustic energy. These include electroacoustic efficiency, uniformity of frequency response, linearity of amplitude response, transient response, power handling capacity, size, durability, and cost. An ideal loudspeaker:

(1) Would have an electroacoustic efficiency approaching 100 per cent.
(2) Would have an acoustic output response that is independent of frequency over the entire audible range.
(3) Would introduce neither harmonic nor intermodulation distortion into its output.
(4) Would faithfully reproduce transients, as well as steady input signals.
(5) Would be capable of producing a nondirectional radiation pattern.
(6) Would be of as small a size as is possible considering the required acoustic output.

No single transducer has been designed that is capable of satisfying all the above requirements. Of the many devices developed for the radiation of acoustic energy into air, the two most widely used are the *direct-radiator* or *dynamic loudspeaker* and the *horn loudspeaker*. Both of these loudspeakers utilize the electrodynamic coupling that exists between the motion of a vibrating surface, called the speaker cone or diaphragm, and the current in a so-called *voice-coil*. Additional types of electromechanical coupling that are used for this purpose include electrostatic coupling in electrostatic loudspeakers and electromagnetic coupling in telephone receivers. In this chapter, we will concern ourselves primarily with the characteristics of direct-radiator loudspeakers and to a lesser extent with those of horn loudspeakers.

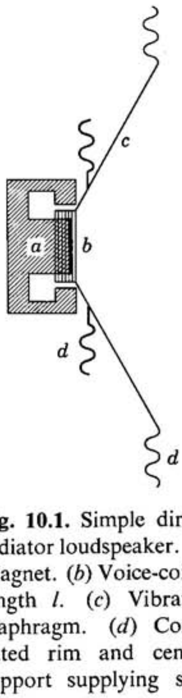

Fig. 10.1. Simple direct-radiator loudspeaker. (*a*) Magnet. (*b*) Voice-coil of length *l*. (*c*) Vibrating diaphragm. (*d*) Corrugated rim and central support supplying stiffness to system.

10.2 Idealized Direct-Radiator Speaker. As an introduction to the problems encountered in the design of a satisfactory direct-radiator speaker, let us first consider a rigid piston-like speaker cone of radius a, mounted in and radiating on *one* side of an infinite plane baffle. The mounting of a loudspeaker in the wall of a room closely approximates this situation. The total mechanical impedance of such a speaker cone is

$$\mathbf{Z}_m = \mathbf{Z}_r + \mathbf{Z}_c \tag{10.1}$$

where $\mathbf{Z}_r$ is associated with acoustic radiation loading of the speaker cone and $\mathbf{Z}_c$ is the lumped-constant mechanical impedance of the cone system. The latter impedance is given by

$$\mathbf{Z}_c = R_m + j[\omega m - (s/\omega)] \tag{10.2}$$

where R_m is a mechanical resistance which is primarily associated with energy losses taking place through the mechanical flexing of the corrugated material used to constrain the cone at its outer edge and near the voice-coil so that it is free to move only in an axial direction (Fig. 10.1). The quantity m represents the total moving mass of the cone system, i.e., the sum of that of the voice-coil and of the speaker cone, and s is the stiffness of the system against axial motion as contributed by the corrugated material at the rim and center of the cone. For high driving frequencies the speaker cone no longer moves as a unit, but instead "breaks up" into zones, some of which move outward while others move inward. When this happens, the simple lumped-constant analysis which follows must correspondingly be modified. The radiation impedance $\mathbf{Z}_r$ is given by

$$\mathbf{Z}_r = R_r + jX_r \tag{10.3}$$

where R_r is the radiation resistance loading of a circular piston as given by equation 7.79 and X_r is the radiation reactance loading as given by equation 7.80. In many types of mounting, the cone of a direct-radiator speaker experiences radiation loading on its rear surface as well as its front surface. Nevertheless, we will ignore any loading of the rear surface in this simple example.

As indicated in Fig. 10.1, the voice-coil of this type of loudspeaker is directly attached to the vibrating surface and is capable of moving to and fro in a radial magnetic field whose direction is perpendicular to the coil winding. If the magnetic field in which the voice-coil moves is assumed uniform, then the driving force f applied to the speaker cone is directly proportional to the current i flowing through the coil and is given by

$$f = Bli \tag{10.4}$$

In this equation, B is the flux density of the magnetic field expressed in webers/m^2, l is the length of conductor in the voice-coil expressed in meters, the current i is expressed in amperes, and the force f in newtons. It is the simplicity of this equation when expressed in MKS units, as well as of additional electromechanical coupling equations to be encountered later, that warrants our use of MKS units in this book.

If we now assume a complex current

$$\mathbf{i} = \mathbf{I}e^{j\omega t}$$

to be flowing in the voice-coil, it will produce a steady-state complex velocity of the speaker cone given by

$$\mathbf{v} = \frac{\mathbf{f}}{\mathbf{Z}_m} = \frac{Bl\mathbf{i}}{\mathbf{Z}_m} \tag{10.5}$$

Since $\mathbf{Z}_m$ is in general complex, the instantaneous velocity may be expected to differ in phase from the driving current. When a loudspeaker is fed an alternating current of rms amplitude I, equation 10.5 may be used to compute the rms velocity amplitude V of the speaker cone at each frequency. In turn, these values of V may be substituted into an rms version of equation 7.85, $W = R_r V^2$, in order to compute the acoustic output of the loudspeaker as a function of frequency

Let us next consider the behavior of the above loudspeaker when a voltage

$$\mathbf{e} = \mathbf{E}e^{j\omega t}$$

is supplied to the terminals of its voice-coil. Also, let us assume that the ordinary electrical impedance of the voice-coil $\mathbf{Z}_E$ is given by

$$\mathbf{Z}_E = R_E + j\omega L_E \tag{10.6}$$

where R_E is the ohmic resistance of the electrical conductor in the voice-coil and L_E is its inductance in henries. Now, if a voltage **e** is applied to the terminals of the voice-coil, it will be observed that the steady-state current is not given by the simple equation $\mathbf{i} = \mathbf{e}/\mathbf{Z}_E$. This results from the fact that a motion of the voice-coil in the magnetic field of the loudspeaker generates a *motional* counter emf in volts as given by the equation

$$e_m = Blv \tag{10.7}$$

where B is expressed in webers/m², l in meters, and v in meters/sec. Upon substitution of **v** from equation 10.5 into this equation, it becomes

$$\mathbf{e}_m = \frac{B^2 l^2}{\mathbf{Z}_m}\,\mathbf{i} = \frac{\phi^2}{\mathbf{Z}_m}\,\mathbf{i} \tag{10.8}$$

where the constant

$$\phi = Bl \tag{10.9}$$

is a *transformation factor* expressed in webers/m relating electrical to mechanical quantities. When this motional emf is taken into consideration, the equation for computing the current in the voice-coil becomes

$$\mathbf{i} = \frac{\mathbf{e} - \mathbf{e}_m}{\mathbf{Z}_E}$$

which may be combined with equation 10.8 and solved for **i** to yield

$$\mathbf{i} = \frac{\mathbf{e}}{\mathbf{Z}_E + (\phi^2/\mathbf{Z}_m)} \tag{10.10}$$

From equation 10.10, it is apparent that the quantity $\phi^2/\mathbf{Z}_m$ must be of the nature of an electrical impedance. As a consequence, we may replace the term $\phi^2/\mathbf{Z}_m$ in equation 10.10 by the so-called *motional impedance* $\mathbf{Z}_M$ as defined by

$$\mathbf{Z}_M = \frac{\phi^2}{\mathbf{Z}_m} = \frac{\phi^2}{\mathbf{Z}_r + \mathbf{Z}_c} = \frac{\phi^2}{(R_r + R_m) + j(X_r + \omega m - s/\omega)} \tag{10.11}$$

It is to be noted that the motional impedance $\mathbf{Z}_M$ has the nature of an electrical impedance, measured in electrical ohms, in contrast with the mechanical impedance $\mathbf{Z}_m$, which is measured in kilograms per second. Whenever it is necessary to indicate the character of an impedance by subscripts, capital-letter subscripts will be used to denote electrical impedances, and small-letter subscripts to denote mechanical impedances.

Equation 10.11 indicates that the larger the mechanical impedance $\mathbf{Z}_m$ of the speaker cone, i.e., the more difficult it is to move, the smaller is the

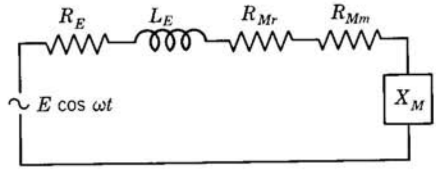

Fig. 10.2. Equivalent series electrical circuit for a direct-radiator loudspeaker.

motional impedance $\mathbf{Z}_M$, i.e., the less counter emf is generated. A little reflection will show the reasonableness of this conclusion, for an infinite mechanical impedance would result in no motion and hence no counter emf, which is equivalent to zero motional impedance. When the speaker cone is blocked so that it cannot move, the only electrical impedance present is that of the voice-coil $\mathbf{Z}_E$. As a consequence, the latter impedance is frequently referred to as the *blocked* impedance.

In the analysis of direct-radiator loudspeakers as well as other electro-acoustic transducers, it is often convenient to replace the actual mechanical system by an equivalent motional electrical system. For instance, currents produced in the voice-coil of the above loudspeaker resulting from an applied voltage may be obtained through use of the circuit of Fig. 10.2. The motional elements R_{Mr}, R_{Mm}, and X_M of this circuit were obtained by a rationalization of the complex equation 10.11. For instance, the reactive component X_M is given by

$$X_M = -\frac{\phi^2(X_r + \omega m - s/\omega)}{Z_m^{\ 2}} \tag{10.12}$$

and the total resistive component R_M by

$$R_M = \frac{\phi^2(R_r + R_m)}{Z_m^{\ 2}} \tag{10.13}$$

Of the total resistive component R_M, only that part given by

$$R_{Mr} = \frac{\phi^2 R_r}{Z_m^{\ 2}} \tag{10.13a}$$

is associated with the transfer of electrical energy into acoustic energy. The remainder

$$R_{Mm} = \frac{\phi^2 R_m}{Z_m^{\ 2}} \tag{10.13b}$$

is associated with the dissipation of energy in flexing the speaker cone and its corrugated supports.

Since the electroacoustic efficiency η of the loudspeaker must be identical with that of the equivalent electrical circuit

$$\eta = \frac{R_{Mr}}{R_{Mr} + R_{Mm} + R_E} \tag{10.14}$$

When the respective expressions for R_{Mr} and R_{Mm} as given by equations 10.13*a* and 10.13*b* are substituted into this equation, the efficiency may finally be expressed as

$$\eta = \frac{\phi^2 R_r}{\phi^2(R_r + R_m) + R_E Z_m{}^2} \tag{10.14a}$$

where

$$Z_m{}^2 = (R_r + R_m)^2 + (X_r + \omega m - s/\omega)^2$$

When an alternating current $I \cos \omega t$ is supplied to the voice-coil, the acoustic power radiated in *watts* is given by

$$W = I^2 R_{Mr} = \frac{\phi^2 R_r I^2}{Z_m{}^2} \tag{10.15}$$

which is the power dissipated in the corresponding part of the equivalent electrical circuit. On the other hand, when an alternating voltage $E \cos \omega t$ is applied to the terminals of the voice-coil, the current is given by

$$I = \frac{E}{Z_I} = \frac{E}{[(R_E + R_M)^2 + (\omega L_E + X_M)^2]^{1/2}} \tag{10.16}$$

where Z_I represents the total input electrical impedance, including the *blocked* impedance $R_E + j\omega L_E$ of the voice-coil, and the *motional* impedance $R_M + jX_M$ associated with motion of the voice-coil. Consequently,

$$W = \frac{\phi^2 R_r E^2}{Z_m{}^2 Z_I{}^2} \tag{10.17}$$

expresses the acoustic output in *watts* when a known voltage E is applied to the terminals of the voice-coil. It is to be noted that the symbols I and E used in the above equations represent rms current and voltage as is customary for these quantities in electrical circuit theory.

An inspection of equation 10.17 shows that an increase in either ϕ, R_r, or E, or a decrease in either Z_m or Z_I will increase the acoustic output of the loudspeaker. Similarly, equation 10.14*a* shows that an increase in either ϕ or R_r increases its efficiency, whereas an increase in either R_m, R_E, or Z_m decreases its efficiency. If the output of acoustic power obtained from a specified electrical input power is to be independent of frequency, it is required that the expression for efficiency (10.14*a*) must also be independent of frequency. Since both the terms R_r and Z_m of this rather complicated

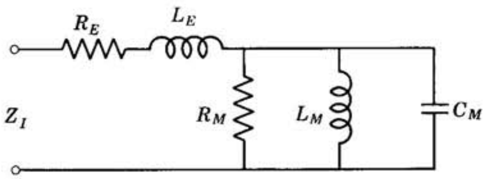

Fig. 10.3. Equivalent parallel electrical circuit for a direct-radiator loudspeaker.

equation are frequency dependent, this requirement is difficult to attain over other than a narrow band of frequencies. It should also be noted, that the situation is equally complicated when a constant amplitude input current I is supplied to equation 10.15 or a constant amplitude input voltage E is supplied to equation 10.17.

The electrical circuit of Fig. 10.2 is but one of a number of circuits that may be used to represent the electrical equivalent of a simple direct-radiator dynamic loudspeaker. Figure 10.3 is another such circuit. The reasonableness of this circuit becomes apparent upon noting that the motional impedance as given by equation 10.11, has a maximum value of $\phi^2/(R_r + R_m)$ at the frequency of mechanical resonance ω_0 as determined by the equation

$$X_r + \omega_0 m - \frac{s}{\omega_0} = 0$$

This behavior is characteristic of the three elements R_M, L_M, and C_M when connected in parallel as shown in Fig. 10.3. When so connected, these three elements have an input electrical impedance $\mathbf{Z}_M$ given by

$$\frac{1}{\mathbf{Z}_M} = \frac{1}{R_M} + \frac{1}{j\omega L_M} + j\omega C_M$$

or

$$\mathbf{Z}_M = \frac{1}{(1/R_M) + j[\omega C_M - (1/\omega L_M)]} \tag{10.18}$$

Comparing this expression for $\mathbf{Z}_M$ with that of equation 10.11 it is seen that they are equivalent if

$$R_M = \frac{\phi^2}{R_r + R_m}, \quad C_M = \frac{(X_r/\omega) + m}{\phi^2}, \quad \text{and} \quad L_M = \frac{\phi^2}{s} \tag{10.19}$$

Use of the parallel type circuit of Fig. 10.3 in order to derive equations for efficiency and acoustic output, leads to essentially the same equations as have previously been derived for the series circuit of Fig. 10.2 and as a consequence will not be repeated. However, it is to be noted that the motional resistance element R_M for the equivalent parallel circuit, as given by equation 10.19, does not equal R_M for the equivalent series circuit, as given by equation 10.13, at any frequency other than the resonant frequency ω_0.

10.3 Numerical Example, Direct-Radiator Loudspeaker. As an illustrative example of the analysis given in Sect. 10.2, let us consider a piston-like speaker mounted in an infinite baffle and having the following physical characteristics.

mass of voice-coil, $m_c = 0.0015$ kg
mass of piston, $m_p = 0.0085$ kg
total mass of moving system, $m = m_c + m_p = 0.01$ kg
radius of piston, $a = 0.1$ m (Equivalent to an 8-inch speaker)
stiffness constant, $s = 2000$ newtons/m
mechanical resistance, $R_m = 1$ mechanical ohm (kg/sec)
inductance of voice-coil, $L_E = 0.2$ millihenry
resistance of voice-coil, $R_E = 5$ ohms
length of conductor in voice-coil, $l = 5$ meters
magnetic flux density, $B = 0.9$ weber/m^2
transformation factor, $\phi = Bl = 4.5$ webers/m

The radiation resistance and reactance are given, respectively, by

$$R_r = \rho_0 c \pi a^2 R_1(2ka) = 415 \times 0.01\pi \times R_1(0.2k) = 13R_1(0.00366f)$$

and

$$X_r = 13X_1(0.00366f)$$

At such low frequencies that $2ka < 1.0$, i.e., $f < 275$ cycles/sec, the two piston impedance functions may be replaced by their approximate values as given by equations 7.72*a* and 7.73*a* without introducing errors in excess of 10 per cent. Therefore at frequencies below 275 cycles/sec, $R_r \approx 0.000022f^2$ and $X_r \approx 0.02f$. At frequencies corresponding to $2ka > 4$, the $R_1(2ka)$ function remains within about 10 per cent of its ultimate value of unity. Therefore, at frequencies above 1100 cycles/sec, $R_r \approx 13$.

The frequency f_0 of mechanical resonance, as determined by

$$(X_r + \omega_0 m - s/\omega_0) = \left(0.02f_0 + 0.0628f_0 - \frac{2000}{6.28f_0}\right) = 0$$

is $f_0 = 62$ cycles/sec.

In order to calculate either the efficiency or the output of this simple piston speaker, it is first necessary to determine the mechanical impedance $\mathbf{Z}_m$ of equation 10.1 as a function of frequency. Plotted in Fig. 10.4 are calculated values of the mechanical resistance $(R_r + R_m)$, the mechanical

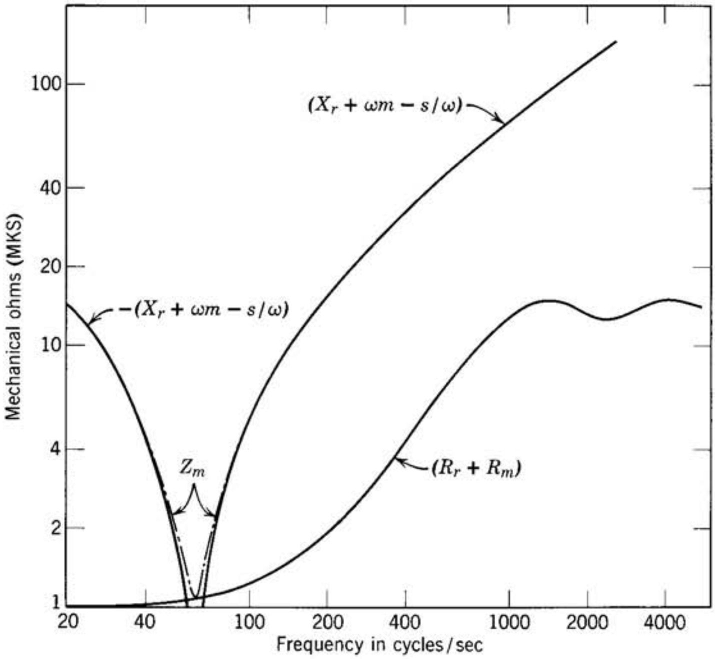

Fig. 10.4. Mechanical impedance of a piston speaker.

reactance $[X_r + \omega m - (s/\omega)]$, and the magnitude of the total impedance Z_m. It is apparent that the mechanical resistance at first rises slowly from its minimum value of 1 mechanical ohm at very low frequencies, experiences a rapid increase between 100 and 1000 cycles/sec, and then fluctuates about the value of 14 mechanical ohms at the higher frequencies. At very low frequencies the reactance has large *negative* values, which results from the stiffness of the suspension system. This reactance is reduced to zero at the resonance frequency of 62 cycles/sec. As the frequency is further increased the reactance becomes positive and rises gradually, until at frequencies above 1000 cycles/sec it may be considered as equal to 0.01ω, that of the mass alone. The magnitude of Z_m has a minimum value of 1.085 mechanical ohms at the resonance frequency, and at all frequencies other than those in this immediate vicinity it may be considered identical to the magnitude of the reactance.

Plotted in Fig. 10.5 are values of the electroacoustic efficiency of the speaker, as calculated by equation 10.14*a*. It is seen that the efficiency rises to a maximum value of 6.1 per cent at the mechanical resonance frequency. Below this frequency the efficiency decreases very rapidly, since R_r is proportional to f^2 and Z_m to $1/f$. In this range the efficiency is therefore

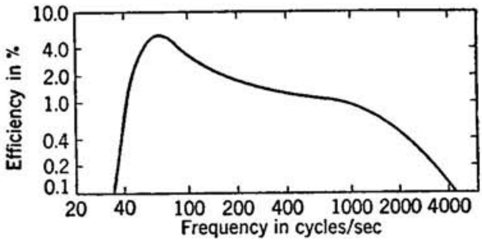

Fig. 10.5. Efficiency of a piston speaker as a function of frequency.

proportional to the fourth power of the frequency. In the interval between 200 and 1000 cycles/sec the rate of increase of radiation resistance R_r with frequency is almost exactly balanced by the increase in the mechanical impedance Z_m, with the result that the efficiency remains fairly constant at a value near 1.5 per cent. At still higher frequencies the radiation resistance remains nearly constant, while Z_m, which is approximately equal to ωm, continues to increase with frequency, so that the efficiency decreases rapidly.

Plotted in Fig. 10.6 are values of the motional impedance Z_M, together with its resistive and reactive components, as computed from equations

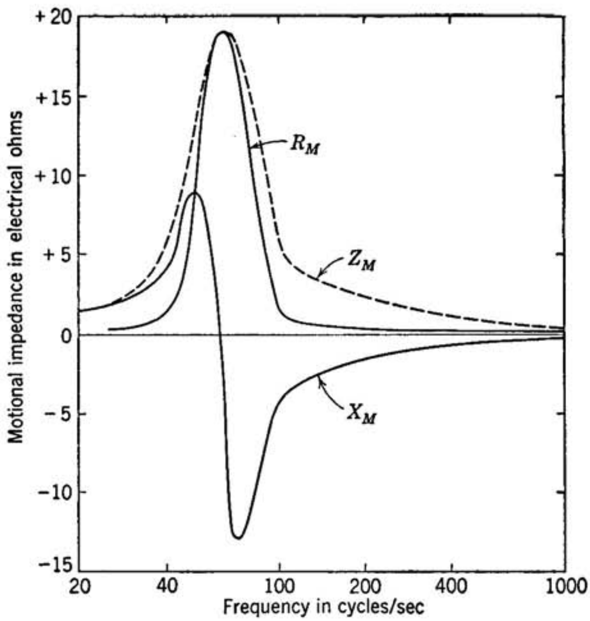

Fig. 10.6. Motional impedance of a piston speaker as a function of frequency.

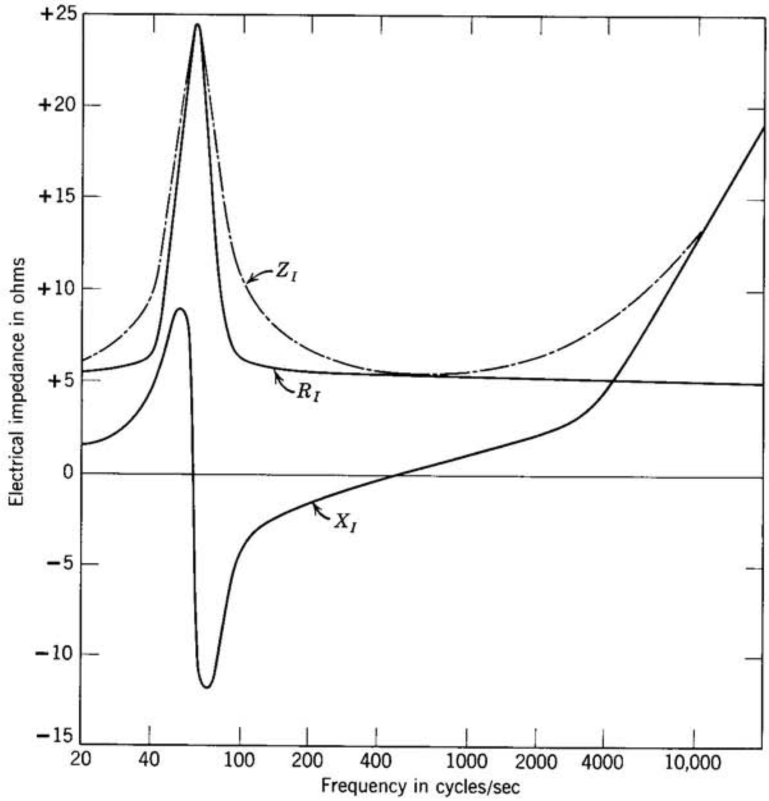

Fig. 10.7. Electrical input impedance of a piston speaker as a function of frequency.

10.11, 10.12, and 10.13. The motional resistance R_M rises to a maximum value of 19.0 electrical ohms at the frequency of mechanical resonance. However, at this particular frequency only 1.5 ohms of this large motional resistance is due to the radiation of sound, the remainder resulting from the mechanical resistance R_m of the suspension system. At frequencies other than those in the immediate vicinity of resonance the motional impedance is seen to be predominantly reactive, positive below resonance and negative above resonance.

Plotted in Fig. 10.7 are values of the total electrical input impedance Z_1 at the terminals of the voice-coil, together with its resistive and reactive components. The resistive component is identical to that of Fig. 10.6, except that all values have been increased by 5 ohms, the d-c resistance of the voice-coil. At low frequencies the reactance is primarily that of the motional impedance. However, at a frequency of 450 cycles/sec the positive inductive reactance ωL_E of the voice-coil equals the negative motional reactance and results in a second frequency at which the electrical reactance is reduced to zero. Finally, at frequencies in excess of 4000 cycles/sec it is observed that the inductive reactance ωL_E is the predominant component of the input electrical impedance. It is to be noted that over the frequency range from 200 to 2000 cycles/sec the input impedance is primarily resistive, and nearly equals the d-c resistance of the voice-coil. Because of this constancy, many loudspeaker manufacturers do not specify the frequency at which the speaker voice-coil has its rated input impedance. In general, it is measured at a frequency somewhat above the resonance frequency and is normally larger than the d-c resistance.

Plotted in Fig. 10.8 are three curves showing computed values of the acoustic output of the speaker expressed in watts as a function of frequency. The computed values plotted in curve A were obtained from equation 10.15 for an assumed input current of 2 amperes. Similarly, curve B has been obtained from equation 10.14a for an assumed input power of 20 watts. Finally, curve C has been obtained from equation 10.17 for an assumed input voltage of 10 volts. It is to be noted, that these three particular values of current, power, and voltage were assumed so as to yield approximately equal acoustic outputs in the frequency range from 400 to 1000 cycles/sec. By contrast, as the frequency of mechanical resonance at 62 cycles/sec is approached, the three outputs differ widely. The output at resonance for an input of 2 amperes is seen to be some 20 times greater than that for an

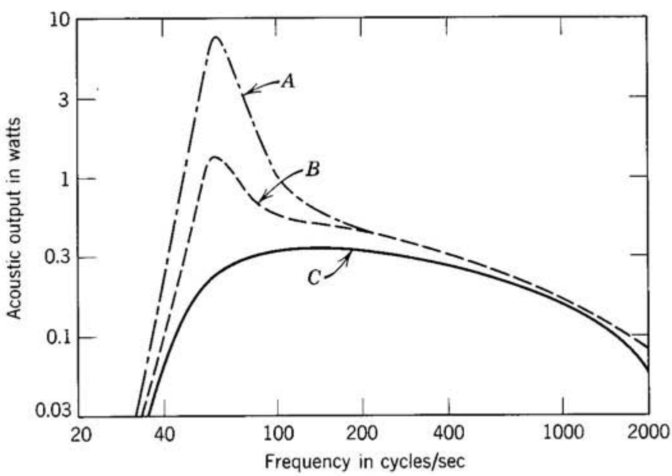

Fig. 10.8. Computed output of idealized loudspeaker as a function of frequency. Curve (A) corresponds to constant current input. Curve (B) corresponds to constant power input. Curve (C) corresponds to constant voltage input.

input of 10 volts. Because of this behavior, it is apparent that if an amplifier were to supply the same current at all frequencies irrespective of the load impedance of the speaker, the latter would produce a distorting peak of acoustic output in the vicinity of 62 cycles/sec. The smoothest acoustic output in this frequency region will be produced by an amplifier that is intermediate between maintaining constant power and constant voltage. Fortunately, such is the behavior of many types of audio-frequency power amplifiers. The large motional impedance of the speaker at resonance results in a mismatch between its impedance and the load impedance for which the amplifier has been designed. In turn, this causes the output power of the amplifier to decrease and its output voltage to increase. The combined effect is to produce a fairly smooth acoustic response curve in the vicinity of resonance, which lies somewhere between curves B and C of Fig. 10.8. Many excellent audio amplifiers employ large amounts of negative voltage feedback in order to reduce distortion. As a consequence, these amplifiers have a very low internal impedance and maintain almost constant voltage output as a load impedance increases. The acoustic output of a loudspeaker connected to this type of amplifier will, therefore, nearly follow curve C.

10.4 Typical Cone Speaker. Let us now consider the characteristics of a typical cone speaker, in comparison with those of our idealized piston-like speaker. Because of the flexibility of the radiating surface, the directional pattern of the radiated sound is somewhat broader than that which would be given by equation 7.54 for a piston of radius a. This effect results from the finite velocity of transverse waves in the cone, which causes the motion of the outer parts of the cone to lag behind that of the voice-coil and central part. The observed decrease in directionality is more pronounced for wide-angle cones than for narrower cones since the effective rigidity of their surface is less. Finally, at frequencies above the fundamental resonant frequency of the cone surface, this lack of rigidity causes the cone to vibrate in oppositely phased circular zones, the effect being similar to that observed in the vibrating circular plate of Sect. 4.12. Consequently, the effective radius of the cone decreases as the frequency increases, which in accordance with equation 7.54 will result in a broadening of the radiated sound pattern. A second effect of this reduction in effective radius of the cone is that of reducing the radiation resistance R_r, which in accordance with equation 7.79 is proportional to the square of this radius. Acting alone, such a reduction in radiation resistance would further reduce the acoustic output of loudspeakers at high frequencies. However, it is to a certain extent counterbalanced by a corresponding reduction in the effective mass of the cone.

The simple speaker cone of Fig. 10.9 consists of a voice coil of mass m_c, attached to a stiff felted paper cone of mass m_p, whose radius at the outer rim is a and whose slant height is l. The resulting cone angle θ is given by

$$\sin\frac{\theta}{2} = \frac{a}{l}$$

Stiffness s is contributed to the system both by s_1, the stiffness of the corrugation at the outer rim of the cone, and by s_2, that of the centering disk or spider attached to the voice coil.

At such low frequencies that the time required for a displacement of the center of the cone to be propagated to the rim is small compared to the period of vibration, the paper cone may be assumed to vibrate as a rigid surface. Its radiation pattern is then similar to that of a piston of mass $m_p + m_c$, stiffness $s_1 + s_2$, and radius a. The velocity of transverse waves in a paper cone is in general a function of its thickness, stiffness, cone angle, etc., as well as of the driving frequency. However, for the cones commonly used in commercial loudspeakers it is observed to have a value of about 500 m/sec. Consequently, about 1/400 of a second will be required for a disturbance to reach the rim of a 0.1-m radius cone having a 120° central angle, so that it is quite reasonable to assume that such a cone moves as a unit at frequencies below 500 cycles/sec.

At high frequencies the cone no longer vibrates as a unit, but instead vibrates in separate zones, separated by nodal circles. The amplitude of vibration in the outer zones is relatively small, so that to a first order of approximation the radiation may be considered to come from a central piston whose radius a' and mass m_p' gradually decrease with increasing frequency. This decrease in effective radius causes the radiation resistance R_r to decrease approximately as $(a'/a)^2$. Since the system is mass-controlled at the higher frequencies, the mechanical impedance Z_m is approximately equal to $(m_c + m_p')\omega$. As a result of the decrease of m_p' with increasing frequency, Z_m does not increase so rapidly as for a rigid piston, where m_p remains constant. The net result of these two effects is to produce some increase in the efficiency of the cone speaker at frequencies above 1000 cycles/sec.

The tendency of a paper cone to vibrate at the higher frequencies more or less like a circular piston of smaller radius is greatly enhanced by constructing the cone with a number of circular corrugations, as indicated in Fig. 10.10. At low frequencies the stiffness reactances s_1'/ω, s_1''/ω, and s_1'''/ω are all large compared to the mass reactances $\omega m_p''$, $\omega m_p'''$, and $\omega m_p''''$, and consequently the cone vibrates as a unit, the effective mass being the mass of the entire cone plus its voice coil, and the effective stiffness being $s_2 + s_1''''$. However, with increasing frequency the stiffness

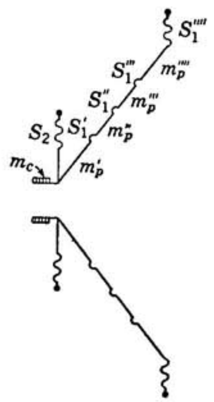

Fig. 10.9. Simple speaker cone and suspension system.

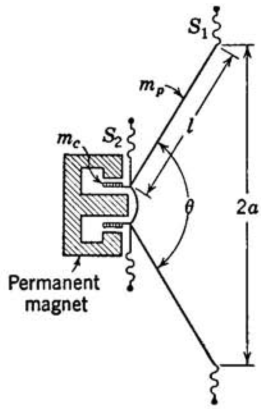

Fig. 10.10. Corrugated speaker cone.

reactances decrease, while the mass reactances increase, so that the outer zones of the cone may be thought of as dropping successively out of motion leaving only the inner zones. Ultimately only the central portion of the cone vibrates, its effective mass being $m_c + m_p'$ and its stiffness $s_2 + s_1'$.

When a loudspeaker is being driven by a vacuum tube amplifier it is difficult to maintain a power input that is independent of frequency. This difficulty is particularly acute at very high frequencies, where the electrical impedance Z_I increases rapidly with the increasing inductive reactance ωL_E. As a result, the actual acoustic response that is obtained when a constant voltage is applied to the input terminals of the amplifier falls off more rapidly than does the response curve for the speaker with an assumed constant input power.

The problem of maintaining a uniform acoustic output from loudspeakers at very low frequencies is more difficult to solve than the corresponding problem at high frequencies. One method of improving the low-frequency response is to increase the radius of the speaker. This increases the radiation resistance in direct proportion to the fourth power of the radius and correspondingly increases the efficiency. However, the increase in efficiency is not so great as might be expected, for the mass of the speaker, and hence Z_m, also increases with the radius. The low-frequency response can also be enhanced by reducing the stiffness of the suspension system and thereby lowering the frequency of mechanical resonance. Reducing the stiffness of the suspension system would be an excellent solution if it were necessary to consider only efficiency and output power. However, if the stiffness of the mechanical system is too greatly reduced, its displacement at low frequencies becomes very large, which may lead to the introduction of *harmonic distortion* into the acoustic output. One source of this type of distortion is nonlinearity between the displacement and the restoring force, which occurs if the elastic limit of the supporting system is exceeded; another is the nonlinearity that accompanies a motion of the voice coil into a nonuniform region of the magnetic field. Even relatively small amounts of harmonic distortion are highly objectionable in the acoustic output, for they result in a sound that is harsh and unnatural, and in extreme cases they may produce rattles closely resembling those that occur if the cone strikes the poles of its field magnet. Unlike nonuniformity in the frequency response, which can be compensated for, at least to some extent, by the introduction of an opposite nonuniformity in the electrical system, harmonic distortion cannot be balanced out and hence must be carefully avoided.

Another method of improving the low frequency acoustic output of a speaker is to mount it in some type of cabinet that will enhance this output. One group of such cabinets enhances the output by increasing the radiation resistance acting upon the cone of the speaker relative to that experienced by a speaker mounted in-a wall. A second group enhances the output by enabling speakers to be used whose voice-coils can make large displacements without producing distortion. These subjects will be considered in detail in later sections of this chapter.

The requirements of an adequate acoustic output at both low and high frequencies are mutually incompatible, and hence a wide-range direct radiator loudspeaker system requires the use of at least two units, one designed for the effective radiation of acoustic power at the lower frequencies, and the other for the higher frequency range. These units are connected to the driving amplifier through a balanced electrical crossover network, which delivers to each unit only those frequencies for which its response is both adequate and relatively uniform.

10.5 Effect of Voice-coil Parameters on Acoustic Output. Except in the immediate vicinity of mechanical resonance, the term $R_E Z_m{}^2$ in equation 10.14*a* is considerably larger than $\phi^2(R_r + R_m)$. Consequently, we may assume that

$$\eta \approx \frac{\phi^2 R_r}{R_E Z_m{}^2}$$

is an approximate equation giving the efficiency of a loudspeaker over the major portion of its useful frequency range. This simplified equation is particularly cogent to a discussion of the influence on the speaker's characteristics of varying different parameters of the voice-coil or of the magnetic field.

Since ϕ is by definition equal to Bl, it is directly proportional to the flux density in the air gap, and it is therefore evident that all factors that increase B will also increase the efficiency, and hence the output of the speaker. The two most feasible methods of accomplishing this are by using a more powerful field magnet and by decreasing the width of the air gap to as small a value as is practicable. The latter method obviously requires the use of a thin voice-coil structure.

An increase in the length of conductor forming the voice-coil winding would be expected to improve the efficiency, for

$$\eta \propto \frac{\phi^2}{R_E} \propto \frac{l^2}{l} = l$$

which indicates that the efficiency is directly proportional to the length l. However, for any specified wire size there exists an optimum length, beyond which the increase in Z_m that results from the increasing mass, and the decrease in B due to the larger air gap required to accommodate the enlarged coil, are more significant than the gain resulting from the increase in l.

If the mass, rather than the diameter, of the conductor to be used in winding the voice-coil is specified, no change in efficiency results from a change in wire size. For example, if the cross-sectional area is halved, the length is doubled and ϕ^2 is increased fourfold. However, as a result of the halved cross-sectional area and the doubled length, the resistance R_E is also increased fourfold, so that the efficiency factor ϕ^2/R_E remains unchanged. The primary consideration involved in the choice of wire size is therefore its current-carrying capacity relative to typical currents supplied by audio amplifiers.

The nature of the conducting material used in winding the voice coil is directly involved in considerations of the speaker's efficiency. If the volume to be occupied by the windings is the limiting factor, then copper wire is more efficient than aluminum, but, if the allowed mass is of primary importance, aluminum is more efficient than copper.

The majority of voice coils are constructed by winding round wire on a cylindrical paper coil form. The use of a self-supporting coil, bound together by a thermosetting cement, eliminates the necessity of a form and thus reduces the space required for the air gap, with a resulting increase in the flux density B, and hence in the efficiency.

10.6 Acoustic Doublet. When a direct radiator loudspeaker is allowed to radiate sound energy from the back of the vibrating cone, this radiation differs in phase by 180° from that coming from the front. If the speaker is mounted in an infinite baffle or its equivalent, the effect of radiation from the back of the cone is merely to increase the mechanical impedance Z_m. A practical example of an equivalent infinite baffle is a speaker mounted in the wall of a room in such a manner that only one face of the cone radiates into the room. If, on the other hand, the dimensions of the baffle are finite, as in effect is true when a speaker is mounted in an open-backed cabinet, the radiation pattern becomes the resultant of the radiations from both sides of the speaker cone. In particular, as the dimensions of the baffle become small as compared with a wavelength, the resultant radiation pattern approaches that of an *acoustic doublet*. The transition between independent operation and doublet operation, which occurs when the dimensions of the baffle are somewhat less than one-half a wavelength, is marked by an abrupt change in the response curve, the response below this frequency falling off rapidly as compared to that of the same speaker mounted in an infinite baffle.

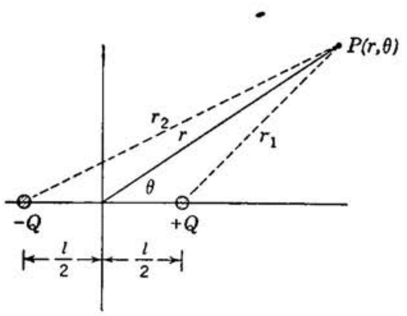

Fig. 10.11. Configuration used in deriving expressions for the sound field of an acoustic doublet.

Let us consider the two small spherical sources of Fig. 10.11 to be of equal strength Q, and to be radiating simultaneously, but pulsating with a difference in phase of 180° between their respective motions. The acoustic pressure produced by a small spherical source of radius a at those low frequencies for which $ka \ll 1$, is given by equation 7.36 as

$$\mathbf{p} = \frac{j\rho_0 ckQ}{4\pi r} e^{j(\omega t - kr)} \tag{7.36}$$

The pressure $\mathbf{p}_d$ at the point $P(r, \theta)$ of Fig. 10.11, due to radiation from both sources, is

$$\mathbf{p}_d = \frac{j\rho_0 ckQ}{4\pi r_1} e^{j(\omega t - kr_1)} - \frac{j\rho_0 ckQ}{4\pi r_2} e^{j(\omega t - kr_2)}$$

or

$$\mathbf{p}_d = \frac{j\rho_0 ckQ}{4\pi} e^{j\omega t} \left(\frac{e^{-jkr_1}}{r_1} - \frac{e^{-jkr_2}}{r_2} \right) \tag{10.20}$$

In the special case where the distance separating the two sources is so small that $l \ll r$ and $kl \ll 1$, equation 10.20 may be simplified to give the pressure field of an acoustic doublet.

In simplifying this expression it is first necessary to replace r_1 and r_2 by

$$r_1^2 = r^2 + \left(\frac{l}{2}\right)^2 - rl\cos\theta$$

and

$$r_2^2 = r^2 + \left(\frac{l}{2}\right)^2 + rl\cos\theta$$

Since r has been assumed to be large as compared to l,

$$r_1 \approx r\left(1 - \frac{l}{r}\cos\theta\right)^{1/2} \approx r\left(1 - \frac{l\cos\theta}{2r}\right)$$

and

$$r_2 \approx r\left(1 + \frac{l}{r}\cos\theta\right)^{1/2} \approx r\left(1 + \frac{l\cos\theta}{2r}\right)$$

Upon utilizing these approximations, equation 10.20 becomes

$$\mathbf{p}_d = \frac{j\rho_0 ckQ}{4\pi}\, e^{j\omega t}\, \frac{e^{-jkr}}{r}\left[\frac{e^{j\frac{kl\cos\theta}{2}}}{1 - \dfrac{l\cos\theta}{2r}} - \frac{e^{-j\frac{kl\cos\theta}{2}}}{1 + \dfrac{l\cos\theta}{2r}}\right]$$

The expression inside the brackets can be somewhat simplified by using the relation $e^{j\theta} = \cos\theta + j\sin\theta$. Then

$$\mathbf{p}_d = \frac{j\rho_0 ckQ}{4\pi r}\, e^{j(\omega t - kr)}\, \frac{2j\sin\left(\dfrac{kl\cos\theta}{2}\right) + \dfrac{l\cos\theta}{r}\cos\left(\dfrac{kl\cos\theta}{2}\right)}{1 - \dfrac{l^2\cos^2\theta}{4r^2}} \tag{10.21}$$

Since kl has been assumed small compared to unity, i.e., since the wavelength radiated is large compared to the distance l, we may use the approximations

$$\sin\left(\frac{kl\cos\theta}{2}\right) \approx \frac{kl\cos\theta}{2} \quad \text{and} \quad \cos\left(\frac{kl\cos\theta}{2}\right) \approx 1$$

Furthermore, since $l \ll r$, the term $l^2\cos^2\theta/4r^2$ in the denominator of equation 10.21 may be neglected. Use of these approximations in equation 10.21 simplifies this equation to

$$\mathbf{p}_d = \frac{j\rho_0 ckQ}{4\pi r}\, e^{j(\omega t - kr)}\left(jkl + \frac{l}{r}\right)\cos\theta \tag{10.22}$$

which may be taken as the general expression for the complex pressure field of an acoustic doublet.

The ratio of the complex pressure of an acoustic doublet to that of one of the spherical sources alone is

$$\frac{\mathbf{p}_d}{\mathbf{p}} = \left(jkl + \frac{l}{r}\right) \cos\theta \tag{10.23}$$

Finally, the ratio of the amplitudes of these two pressures at a point in space is given by

$$\frac{P_d}{P} = \sqrt{(kl)^2 + (l/r)^2}\cos\theta \tag{10.24}$$

Since both kl and l/r are small compared to unity, the magnitude of this ratio is always less than unity and becomes increasingly smaller as the frequency is decreased, as the separation l is decreased, or as the radial distance r is increased. The presence of the term $\cos\theta$ indicates that the pressure in the radiation field is no longer independent of direction but instead has maximum values along the axis of the doublet and zero values at right angles to this direction.

The magnitude of the acoustic pressure P of a small spherical source is given by equation 7.36 as

$$P = \frac{\rho_0 ckQ}{4\pi r}$$

and consequently that of an acoustic doublet is

$$P_d = \frac{\rho_0 ckQ \cos\theta\sqrt{(kl)^2 + (l/r)^2}}{4\pi r} \tag{10.25}$$

In almost all practical applications of this doublet theory the radial distance r is large enough so that $kr \gg 1$. Since this condition is equivalent to $kl \gg l/r$, equation 10.25 simplifies to

$$P_d = \frac{\rho_0 ck^2 Ql\cos\theta}{4\pi r} \tag{10.25a}$$

Therefore, the pressure at points on a spherical surface of large radius r differs from that of a single source by the factor $kl\cos\theta$, which is always less than unity. Since intensity is proportional to the square of the acoustic pressure, the intensities in a doublet field are reduced by the factor $(kl\cos\theta)^2$, as compared with a similar single source. This reduction in intensity must be accompanied by a reduction in the total output of acoustic power, as compared to that of a single source. The ratio of these two outputs of acoustic power is equal to the average reduction in intensity, as obtained by integrating $(kl \cos \theta)^2\, dS$ over the surface of a sphere of radius r and dividing by $4\pi r^2$. Hence,

$$\frac{\text{Power (doublet)}}{\text{Power (single)}} = \frac{\int_0^{\pi} (kl \cos \theta)^2 \cdot 2\pi r^2 \sin \theta \, d\theta}{4\pi r^2} = \frac{k^2 l^2}{3} \qquad (10.26)$$

Figure 10.12 is a polar plot of relative values of the pressure amplitudes in the field of an acoustic doublet. These plotted values correspond to $l = 0.2$ m, $r = 5$ m, and $k = 1.0$ ($f = 55$ cycles/sec). A circle representing the pressure amplitudes produced at this same distance by a single source of strength equal to that of either one of the two sources in the doublet, would have a radius five times the maximum amplitude shown in Fig. 10.12. In addition, the ratio of the total power radiated by the acoustic doublet to that radiated by a similar single source, as given by equation 10.26, is $\frac{(1.0 \times 0.2)^2}{3} = 0.0133$, or down 18.8 db.

The case in which both kl and l/r are of the same order of magnitude and are small compared to unity is more involved than that just considered. The variation of pressure is then quite different from that given by equation 10.25*a* and must be obtained from equation 10.25. It is also to be noted that under these circumstances, the radial particle velocity is no longer in phase with pressure and the intensity is not given by $P^2/\rho_0 c$. Although the individual response patterns may differ as r becomes smaller, the total power output ratio as given by equation 10.26 is still valid, as is to be expected from considerations of the law of conservation of energy.

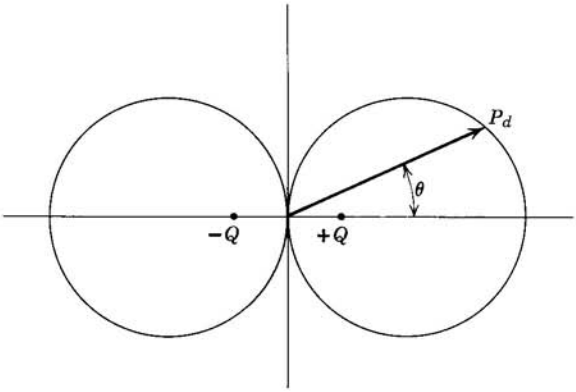

Fig. 10.12. Pressure pattern radiated by an acoustic doublet.

When $kl > 1$, the doublet theory does not apply and the problem must instead be treated as a superposition of radiations; i.e., equation 10.21 must be used without simplification. For instance, it is readily shown that for $l/r \ll 1$ and $kl = \pi$, i.e., $l = \lambda/2$, the pressure response on the axis is double that of one source alone. On the other hand, as kl approaches 2π the pressure response along the axis approaches zero.

10.7 Loudspeaker in a Circular Baffle. Let us consider a direct radiator loudspeaker of radius a to be mounted in a circular baffle of radius l. For such low frequencies that $kl \ll 1$, ka is also small compared to unity, and as a result the radiation pattern of the speaker is nondirectional and may be considered to arise at a simple source. Furthermore, after traveling a distance l to the rim of the baffle, the radiation arising from one side of the speaker cone will spread into the region on the opposite side of the baffle. For this reason, such a speaker may be treated with reasonable accuracy as a doublet of strength $Q = U_0 \pi a^2$ and separation l.

Since the output of a loudspeaker is proportional to the radiation resistance R_r, the reduction of its output by the factor $(kl)^2/3$ when radiating as a doublet at low frequencies may be treated by considering the effective radiation resistance R_r' to be

$$R_r' = R_r \frac{k^2 l^2}{3} \tag{10.27}$$

where

$$R_r = \rho_0 c \pi a^2 R_1(2ka) \approx \frac{\rho_0 c k^2}{2\pi} (\pi a^2)^2$$

Although this equation is strictly applicable only at values of $kl \ll 1$, measurements show it to be reasonably accurate for values up to $(kl)^2 = 3$. Consequently, the reduction in output of a speaker due to mounting it in a plane baffle of finite dimensions may be calculated by using equation 10.27 at frequencies for which $kl < \sqrt{3}$.

Equation 10.27 shows that the size of the baffle used with a direct-radiator loudspeaker is of as great importance in determining the output of the speaker at low frequencies as is its radius or its frequency of mechanical resonance. If the dimensions of the baffle are so small that the frequency corresponding to $kl = \sqrt{3}$ is above the frequency of mechanical resonance, then the output at frequencies below this critical value, as computed by equation 10.17, should be reduced by the factor $k^2l^2/3$, i.e., by 6 db per octave. On the other hand, if the baffle is large enough so that this critical frequency corresponds to the mechanical resonance frequency, the resulting decrease in response is of little importance, since the response of the speaker will in any event fall off at 12 db per octave, even if it is mounted

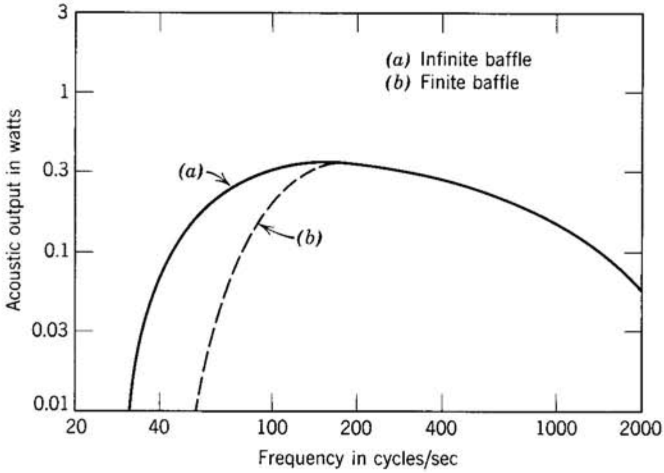

Fig. 10.13. Acoustic output of a piston speaker in a finite baffle for a constant voltage input.

in an infinite baffle. Consequently, the minimum radius of a circular baffle should not be less than

$$l = \frac{\sqrt{3}}{k_0} = \frac{\sqrt{3}\lambda_0}{2\pi} = 0.28\lambda_0 \tag{10.28}$$

where λ_0 is the wavelength corresponding to the frequency of mechanical resonance.

The indicated effective radius of a baffle suitable for use with the speaker treated in Sect. 10.3 is 1.5 m, or about 5 ft. A baffle of such large radius is not in general practicable, and consequently a compromise is usually made by using a smaller baffle, with some sacrifice in low-frequency response. For instance, if a baffle of 2-ft radius is used, the response begins to fall off at a rate of 6 db per octave from that of Fig. 10.5 at frequencies below 155 cycles/sec. This difference between the theoretical response curves for an infinite baffle and a baffle of 2-ft radius is shown by the curves *a* and *b*, respectively, of Fig. 10.13 for an assumed constant voltage input to the speaker.

In addition to the loss in output at frequencies below that given by $kl = \sqrt{3}$, another dip in the response curve is to be expected at $kl = 2\pi$. This dip is analogous to that occurring on the axis of an acoustic doublet under these same conditions. It is most noticeable for small speakers and is greatly reduced by offsetting the speaker from the center of a circular or square baffle.

10.8 Loudspeaker Cabinets. The simplest type of cabinet in which a loudspeaker may be mounted is the back-enclosed cabinet. The only energy radiated into the external medium then is that coming from the front of the speaker cone, as is also true when the speaker is mounted in an infinite baffle. Because of this similarity, the back-enclosed cabinet is frequently referred to as an *infinite-baffle* cabinet.

The primary mechanical loading effect of such a cabinet on the loudspeaker is to contribute additional stiffness to that of its suspension system. The effective stiffness s_c of the cabinet is identical to that previously derived for the cavity of a Helmholtz resonator, or

$$s_c = \frac{\rho_0 c^2 S^2}{V} = \frac{\rho_0 c^2 (\pi a^2)^2}{V} \tag{10.29}$$

This additional stiffness raises the frequency of mechanical resonance of the loudspeaker, and as a result causes the low-frequency response to begin falling off at a higher frequency than when the speaker is mounted in an infinite baffle.

If the loudspeaker of Sect. 10.3 is mounted in a back-enclosed cabinet whose dimensions are $0.5 \times 0.5 \times 0.2$ meters, the stiffness added by the cabinet is

$$s_c = \frac{1.21 \times 343^2 \times (0.01\pi)^2}{0.05} = 2850 \text{ newtons/m}$$

This added stiffness raises the frequency of mechanical resonance from 62 to 96 cycles/sec. The theoretical output of the speaker mounted in this cabinet, as shown in curve (*b*) of Fig. 10.14, is much lower at frequencies below 80 cycles/sec than is that of the same speaker mounted in an infinite baffle, as indicated by curve (*a*).

One alternative to accepting this additional drop in low-frequency acoustic output is the relatively cumbersome one of enlarging the cabinet. A more practical method is to redesign the suspension system of the speaker cone so as to reduce its mechanical stiffness and thereby lower its frequency of mechanical resonance. Furthermore, if the mass of the cone also is increased, it becomes possible to lower the frequency of mechanical resonance to such an extent that acceptable acoustic outputs are produced at frequencies as low as 40 cycles/sec, when speakers of this type are mounted in cabinets of 0.05-m^3 volume or less. However, such a speaker system will have a greatly reduced output at frequencies above 1000 cycles/sec and therefore is restricted to use as the *woofer* in a multi-speaker system.

At frequencies above 400 cycles/sec the radiation from the back of the cone tends to set up patterns of standing waves in the interior of the

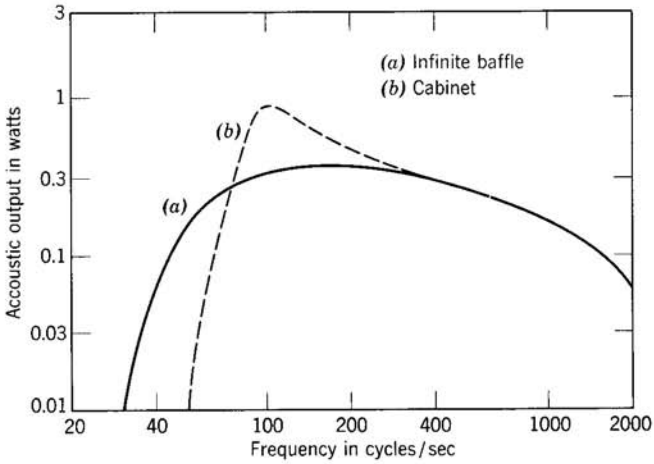

Fig. 10.14. Acoustic output of a piston speaker in a back-enclosed cabinet for a constant voltage input. Volume of cabinet is 0.05 m^3.

cabinet. The resultant reaction on the surface of the cone then results in a curve of motional impedance having sharp peaks and dips, rather than the smooth curve given in Fig. 10.6. In order to reduce these resonances it is necessary to line the inner surfaces of a back-enclosed cabinet with a thick layer of sound-absorbing material. This not only reduces the amplitudes of the standing wave systems set up at the higher frequencies but also reduces the severity of the accentuated response at the fundamental resonance frequency. If the interior of a cabinet of this type is filled completely with a sound absorbing material, the compression and rarefaction of the air contained in the cabinet becomes nearly isothermal. This results from the wide distribution and large heat capacity of the sound absorbing material, which tends to maintain the entrapped air at a constant temperature rather than allowing it to undergo the more normal adiabatic changes. Under these circumstances, the effective stiffness of the cabinet as given by equation 10.29 is reduced by the multiplicative factor of $1/\gamma = 0.7$ which will lead to a further improvement in low-frequency output.

Another common method of mounting a loudspeaker is in an open-back cabinet. This type of speaker installation is characteristic of that in most radio and television sets. Here the coupling between the mechanical speaker system and the acoustical cabinet system becomes important. The electromechanical force $f = Bli$ driving the voice coil acts upon the mechanical system represented schematically in Fig. 10.15. The mass of the speaker cone and coil is represented by m, the stiffness s of the mechanical suspension system is represented by the compliance $C_m = 1/s$, and its mechanical resistance by R_m. The radiation resistance and mass loading acting on the front face of the cone are respectively represented by R_r and m_r. $\mathbf{Z}_{mc}$ represents the complex mechanical impedance acting on the back face of the cone, due to the acoustic impedance of the cabinet. This mechanical impedance is given by

$$\mathbf{Z}_{mc} = (\pi a^2)^2 \mathbf{Z}_{Ac} \tag{10.30}$$

where πa^2 is the cross-sectional area of the cone and $\mathbf{Z}_{Ac}$ is the input acoustic impedance of the cabinet, as seen by the back face of the speaker cone. The impedance $\mathbf{Z}_{Ac}$ is similar to that of the open pipe of equation 8.35.

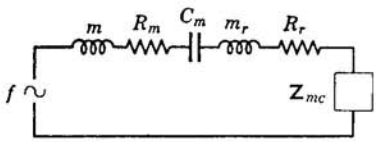

Fig. 10.15. Equivalent mechanical circuit for a speaker mounted in an open-back cabinet.

One of the most troublesome acoustical characteristics of this type of cabinet arises at the fundamental resonance frequency of the cabinet, i.e., at the lowest frequency for which the reactance term in $\mathbf{Z}_{Ac}$ goes to zero. At this frequency the motion of the speaker cone is enhanced, and the output is increased. In the majority of console cabinets this resonant frequency occurs in the region between 100 and 200 cycles/sec, and the increased output results in a "boomy" quality which unfavorably affects the naturalness of reproduced sounds. In addition, the open-back cabinet suffers from the further disadvantage that at frequencies below its fundamental resonance frequency the baffle size is inadequate. Radiation from the back of the cone then combines with that from the front to produce the characteristic doublet radiation, which falls off at 6 db per octave. If the resonant frequency of the speaker's suspension system is lower than that of the cabinet, the resulting increase in response will somewhat compensate for this falling off and thereby both flatten and extend the response curve to lower frequencies.

One factor that limits the acoustic output of all direct-radiator loudspeakers at low frequencies is inefficient coupling between the cone and the air. The use of a larger cone increases the radiation resistance and thereby increases this coupling. An alternative method is to mount the speaker in a *phase-inverter* type of cabinet, which enables radiation from the back of the cone to be added in phase with that from the front, thereby effectively increasing the total radiation resistance. The simplest cabinet of this type is the vented box, or so-called bass-reflex cabinet of Fig. 10.16. The mechanical system of this speaker, which is also represented in the figure, is identical to that of Fig. 10.15, except for the difference in mechanical

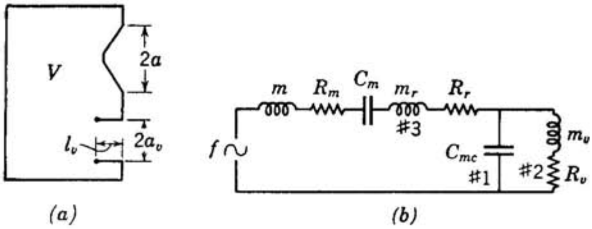

Fig. 10.16. (*a*) Bass-reflex or phase-inverter type of cabinet. (*b*) Equivalent mechanical circuit.

loading due to the acoustic impedance of the cabinet. This acoustic impedance at *low* frequencies consists of the parallel combination of the acoustic capacitance $C_A = V/\rho_0 c^2$ of the cavity, in parallel with the series combination of the inertance $M = \rho_0 l_v'/S_v$ and acoustic resistance R of the vent. If the vent is circular or nearly circular, $l_v' = l_v + 1.7a_v$, where l_v is its length and a_v its radius, $S_v = \pi a_v^2$, and $R = \rho_0 c k^2/2\pi$. The mechanical impedance at the speaker cone due to this acoustic impedance, as given by equation 10.30, is therefore

$$\frac{1}{\mathbf{Z}_{mc}} = j\omega C_{mc} + \frac{1}{R_v + j\omega m_v} \tag{10.31}$$

where

$$C_{mc} = \frac{C_A}{(\pi a^2)^2} = \frac{V}{\rho_0 c^2 (\pi a^2)^2} \tag{10.32}$$

$$R_v = (\pi a^2)^2 R = (\pi a^2)^2 \frac{\rho_0 c k^2}{2\pi} = R_r \tag{10.33}$$

and

$$m_v = (\pi a^2)^2 M = \frac{(\pi a^2)^2 \rho_0 (l_v + 1.7a_v)}{\pi a_v^2} \tag{10.34}$$

In the special case where the radius of the vent equals that of the speaker cone, the last of these equations is simplified to $m_v = (\pi a^2)\rho_0(l_v + 1.7a)$.

At high frequencies the impedance of branch 2 is large and that of branch 1 is small, so that the speaker radiates as though it were mounted in a back-enclosed cabinet. Consequently, it is necessary to line the interior walls with an absorbing material so as to reduce the magnitude of any standing wave patterns that may arise. Since the motion at the vent results from that of the back of the cone, which in turn differs by 180° from that of the front, there must be a phase difference of 180° in the motions of branches 2 and 3, if radiation at the vent is to be in phase with that from the front of the cone. This is approximately true for frequencies above the resonant frequency of the parallel combination of branches 1 and 2, i.e., frequencies above the resonant frequency of the vented box, treated as a Helmholtz resonator. At frequencies below the resonant frequency of the cabinet, however, the phase of the motion of the air in the vent rapidly approaches that of the back of the cone, and the combination of the radiation from the vent with that from the front of the cone then results in the poor low-frequency response characteristic of an acoustic doublet.

Many different factors must be considered in designing a bass-reflex cabinet. However, if the area of the vent is made approximately equal to that of the speaker cone, and if the resonant frequency of the cabinet is made somewhat lower than that of the speaker cone's suspension system, the low-frequency response will be better than that of the same speaker mounted in an infinite baffle. As compared to an open-back cabinet, a bass-reflex cabinet not only extends the low-frequency range but also has a smoother response, and hence it does not exhibit the boomy quality of the former.

A practical problem that arises in the design of any type of speaker cabinet is the mechanical rigidity of its walls. In all the analysis of this section it has been assumed that the walls of the enclosure are perfectly rigid, so that any acoustic loading applied to the speaker cone results exclusively from the motion of the enclosed air. In actual practice this is not strictly true, although it is true to a good approximation for open-back wooden cabinets whose walls are at least a half-inch thick. The design requirements for back-enclosed and bass-reflex cabinets are, however, considerably more severe, since the acoustic pressures in these enclosures are often high enough to set up mechanical vibrations in the larger surfaces, such as the back of the cabinet, and the resulting spurious resonances, which usually occur at the lower audible frequencies, then produce undesirable irregularities in the frequency response. These can be avoided only by making the cabinet very rigid. Its walls should therefore be somewhat thicker than those of an open-back cabinet, and it may also be necessary to brace the larger surfaces with struts.

For more extensive treatments on the enhancement of the acoustic output of loudspeakers by properly designed cabinets and horns, the reader is referred to excellent treatments by Beranek[1] and Olson.[2]

10.9 Horn Loudspeakers. The attachment of a properly shaped horn to a small piston-like sound source is observed to result in a marked increase in its acoustic output at low frequencies. Such a horn is essentially an

[1] Beranek, *Acoustics*, Chapters 8 and 9, McGraw-Hill Book Co. (1954).

[2] Olson, *Acoustical Engineering*, Chapters 6 and 7, D. Van Nostrand Co. (1957).

acoustic transformer, which enables the loading impedance of the low density air to be more effectively matched to that of the relatively massive vibrating piston. In particular, the low-frequency acoustic resistance at the throat of the horn is greater than that which would act on a piston of equal area, vibrating in an infinite baffle, and the output of the horn loaded source is consequently higher. At high frequencies the effect of the horn is almost negligible, for these frequencies are radiated by a piston source as a narrow beam, and hence the confining effect of the walls of the horn is of limited significance.

The most important characteristic of a horn is the manner in which its throat impedance varies with frequency. This throat impedance is also a function of the throat area, of the mouth area, and of the flare, i.e., of the rate of increase of the horn's cross-sectional area. When the area at the mouth is very large, its effect on the throat impedance is negligible, and the variation of this impedance with frequency is then primarily determined by the shape of the horn.

10.10 Approximate Wave Equation in Horns. A rigorous analysis of the propagation of waves in horns is not warranted for the brief treatment of horn speakers given in this book. However, the following simplified derivation of the wave equation leads to many conclusions of practical importance, even though the frequency range to which it may be precisely applied is limited. In deriving this equation it is necessary to make the following assumptions:

(1) The fundamental acoustic equations are applicable; i.e., both pressure and velocity amplitudes are so small that second-order terms may be neglected.

(2) Acoustic energy is propagated through the horn in the form of plane waves moving parallel to its axis. It is further assumed that there are no particle displacements perpendicular to this axis and that pressure, velocity, etc., within the horn are functions only of time t and of the distance x measured along the axis of the horn.

(3) The walls of the horn are perfectly rigid, so that no transverse motions due to pressure release at these walls need be considered.

(4) The horn does not flare so rapidly that the assumed plane waves lose contact with the walls, and instead spread out as spherical waves in free space.

Consider the volume element of length dx and area S_x within the horn of Fig. 10.17. By methods similar to those used in Sect. 5.2, it is possible to show that

$$s = -\frac{1}{S_x}\frac{\partial(S_x\xi)}{\partial x} \tag{10.35}$$

represents the equation of continuity for plane waves being propagated along the axis of the horn. It is to be noted that when S_x is constant, equation 10.35 reduces to the simple form, $s = -(\partial\xi/\partial x)$, of equation 5.3*a*. Upon using equation 5.4*b*, the resulting expression for pressure becomes

$$p = -\frac{\rho_0 c^2}{S_x}\frac{\partial(S_x\xi)}{\partial x} \tag{10.36}$$

If we now equate $-(\partial p/\partial x)\,dx$, the net force acting on a volume element of unit cross section and length dx, to the product of the elements mass $\rho_0\,dx$ by its acceleration $\partial^2\xi/\partial t^2$

$$\frac{\partial^2\xi}{\partial t^2} = c^2\frac{\partial}{\partial x}\left(\frac{1}{S_x}\frac{\partial(S_x\xi)}{\partial x}\right) \tag{10.37}$$

is obtained. This equation is a general equation for propagation of plane waves along the axis of a horn. It is to be noted that when S_x is constant, this equation simplifies to the simple plane wave equation (5.9).

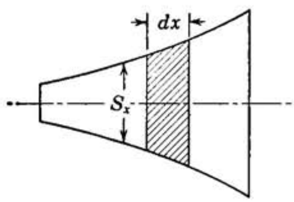

Fig. 10.17. Volume element $S_x\,dx$ of a horn.

10.11 Infinite Exponential Horn. Experience has shown that the most effective horns are those whose rate of flare, dS_x/dx, increases from throat to mouth. Various functions, such as hyperbolas, catenaries, and exponentials have been used in constructing such horns, with the most common horn being one whose cross-sectional area increases exponentially with distance from its throat. In this so-called *exponential horn*, which is illustrated in Fig. 10.18, the cross-sectional area S_x at any distance x from the throat is given by

$$S_x = S_0 e^{mx} \tag{10.38}$$

where S_0 is the throat area and m is the *flare constant*. When this function for S_x is substituted into equation 10.37

$$\frac{\partial^2\xi}{\partial t^2} = c^2\left[\frac{\partial^2\xi}{\partial x^2} + m\frac{\partial\xi}{\partial x}\right] \tag{10.39}$$

is obtained as the wave equation for plane waves in an exponential horn. If a solution of the type

$$\boldsymbol{\xi} = \mathbf{A}e^{j(\omega t + \gamma x)}$$

is assumed for this equation, it can be shown that γ must satisfy the relation

$$\gamma^2 - jm\gamma - k^2 = 0 \tag{10.40}$$

where $k = \omega/c$. The allowed values of γ are therefore

$$\gamma = j\frac{m}{2} \pm \sqrt{k^2 - \frac{m^2}{4}} \tag{10.41}$$

Consequently, the general harmonic solution of equation 10.39 is

$$\boldsymbol{\xi} = e^{-\alpha x}(\mathbf{A}e^{j(\omega t - \beta x)} + \mathbf{B}e^{j(\omega t + \beta x)}) \tag{10.42}$$

where

$$\alpha = \frac{m}{2} \quad \text{and} \quad \beta = \sqrt{k^2 - \frac{m^2}{4}} \tag{10.43}$$

This solution represents plane waves whose amplitudes decrease exponentially with increasing x and which progress with a phase velocity c' given by

$$c' = \frac{\omega}{\beta} = \frac{c}{\sqrt{1 - \dfrac{m^2}{4k^2}}} \tag{10.44}$$

Here it is to be noted that the term $e^{-\alpha x}$ does not represent a damping of waves due to absorption, as discussed in Sect. 9.3, but rather a decrease in amplitude that results as the waves spread over an increasing cross-sectional area within the horn. The phase velocity c' represents the velocity with which a condition of maximum pressure is propagated through the horn. Since c' is a function of frequency, the exponential horn is a dispersive medium for sounds of different frequencies.

As the frequency being transmitted is decreased, k decreases, and ultimately equals $m/2$. The frequency f_c corresponding to this condition is

$$f_c = \frac{mc}{4\pi} \tag{10.45}$$

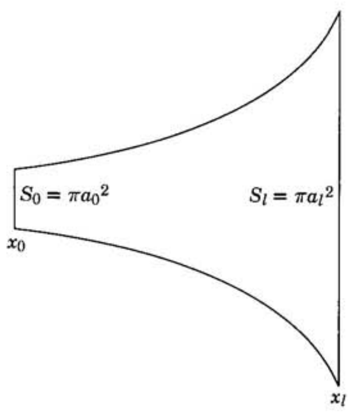

Fig. 10.18. Exponential horn.

This frequency, which is known as the *cut-off frequency*, marks the lowest frequency at which the exponential horn provides a significant gain in acoustic output. At the cut-off frequency the phase velocity c' becomes infinite, which indicates that all parts of the medium within the horn move in phase as a unit; i.e., the motion at the mouth is in phase with the motion at the throat. Similar conclusions are reached if the condition $\beta = 0$ is substituted into equation 10.42.

In contrast to the simple theory developed above, experimental observations indicate that acoustic waves are propagated through an exponential horn both at and below the cut-off frequency, although the acoustic power transmitted is greatly reduced. The source of this discrepancy lies undoubtedly in the failure of some of the simplifying assumptions made in the derivation of the approximate wave equation (10.37).

The usual equations $p = -\rho_0 c^2 s$ and $u = \partial\xi/\partial t$ may be used to obtain pressures and particle velocities within the horn. If these expressions are substituted into $\mathbf{Z} = \mathbf{p}/\mathbf{U} = \mathbf{p}/(S_x\mathbf{u})$, the equation defining acoustic impedance, then

$$\mathbf{Z}_x = \frac{\rho_0 c}{S_x} \cdot \frac{1}{k} \cdot \frac{(\beta + j\alpha)\mathbf{A}e^{-j\beta x} - (\beta - j\alpha)\mathbf{B}e^{j\beta x}}{\mathbf{A}e^{-j\beta x} + \mathbf{B}e^{j\beta x}} \tag{10.46}$$

This is a general expression for the acoustic impedance at any coordinate position x within the horn. The constants **A** and **B**, representing the respective displacement amplitudes for waves being propagated in the $+x$ and $-x$ directions, are in general complex and are determined by boundary conditions at the throat x_0 and mouth x_l of the horn.

The magnitude of the constant **B** is a measure of the amplitude of the wave reflected at the mouth of the horn. If x_l were truly infinite, there would be no reflected wave, and therefore **B** would equal zero. In actual practice the amplitude is small compared to that of the incident wave whenever the radius of the mouth a_l is so large that $ka_l > 3$, so that such horns may be treated as infinite horns. For instance, if the mouth of the horn opens into an infinite baffle, then equation 8.29 predicts that for $ka_l > 3$, **B** will always be less than 10 per cent of **A**. If we set $\mathbf{B} = 0$ in equation 10.46, the acoustic impedance at the throat becomes

$$\mathbf{Z}_0 = \frac{\rho_0 c}{S_0 k}(\beta + j\alpha) \tag{10.47}$$

or upon substitution of the values of α and β from equation 10.43,

$$\mathbf{Z}_0 = \frac{\rho_0 c}{S_0}\left(\sqrt{1 - \frac{m^2}{4k^2}} + j\,\frac{m}{2k}\right) \tag{10.47a}$$

In order to compare the throat impedance of an "infinite" exponential horn with that acting on the driving piston-like speaker when mounted in an infinite baffle, let us assume that the exponential horn of Fig. 10.18 flares from a radius of 0.02 m at its throat to one of 0.4 m at its mouth and that its length is 1.6 m. The flare constant of this horn is $m = 3.7$, which corresponds to a cut-off frequency of 100 cycles/sec. The curves of Fig.

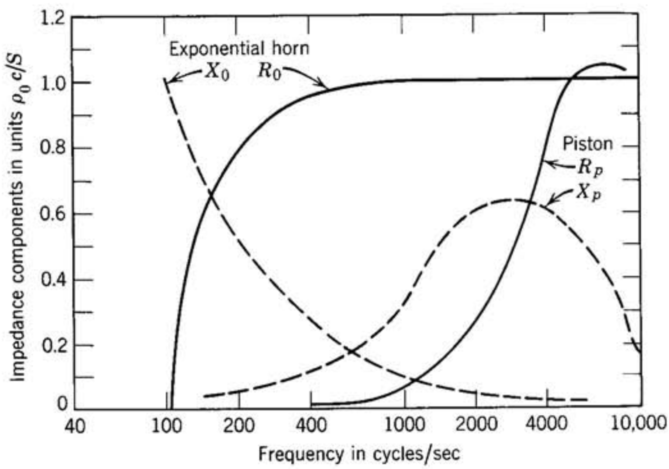

Fig. 10.19. Curves showing the acoustic resistance and reactance acting at the throat of an infinite exponential horn and on a piston mounted in an infinite baffle. Values are expressed relative to $\rho_0 c/S$, the acoustic resistance of an infinite pipe of area S.

10.19 show computed values of the throat resistance R_0 and reactance X_0 in units of $\rho_0 c/S_0$, as a function of frequency. Although these curves are calculated on the assumption that the horn is of infinite length, they are applicable to the finite horn of length 1.6 m with no appreciable error for frequencies such that $0.4k > 3$, i.e., at frequencies above 400 cycles/sec. Below this frequency reflections from the mouth of the horn set up resonances that cause the throat resistance and reactance to fluctuate about their values as computed for an infinite horn. The figure also shows computed values of the acoustic resistance and reactance for a piston of 0.02-m radius, mounted in an infinite baffle. It is apparent that in the frequency interval from 100 to 3000 cycles/sec the resistance loading at the throat of the horn is considerably greater than that of the piston of equal area. As a consequence, the attachment of the horn to the above piston speaker will greatly enhance acoustic output at the lower frequencies.

10.12 Acoustic Output of Horn Speakers. A small cone speaker, mounted so as to radiate directly into the throat of the horn, is sometimes used as a driver for a horn speaker. The equations used to calculate the efficiency, motional impedance, and acoustic output of such a horn speaker are identical in form with those of Sect. 10.2, the only difference being that the mechanical radiation resistance R_r and reactance X_r, are obtained from the throat acoustic impedance $\mathbf{Z}_0$ of the horn. Since an acoustic impedance is converted to a mechanical impedance by multiplying the former by the square of the surface upon which it acts,

$$R_r = S_0^2 R_0 \quad \text{and} \quad X_r = S_0^2 X_0 \tag{10.48}$$

The effect of the horn is to produce a large increase in R_r at low frequencies, and such a horn speaker is therefore much more efficient at these frequencies than is its small driving speaker alone. As was noted previously in this chapter, the high-frequency output of a direct radiator speaker increases as its size is reduced, since the accompanying decrease in mass results in a lower mechanical impedance $\mathbf{Z}_m$. The driver of the above horn speaker behaves as a direct radiator speaker at high frequencies, and consequently the efficiency is greater than that of a large direct radiator speaker of comparable low-frequency output. Horn speakers of this type can readily be built, having efficiencies in excess of 20 per cent over a wide range of frequencies above the cut-off frequency of the horn. The primary difficulty with this type of horn speaker is that in order to produce high outputs at low frequencies the displacements of the small driving unit must be very large, so that it is difficult to construct a suspension system and housing for the cone which will not introduce nonlinear distortion.

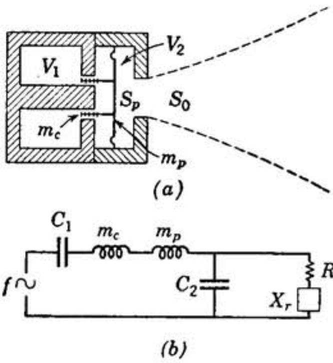

Fig. 10.20. (*a*) Idealized driver unit for a horn speaker. (*b*) Equivalent mechanical circuit.

A more common type of driver for use with horn speakers is represented schematically in Fig. 10.20*a*. In this type of design the area S_p of the piston surface is much greater than the area S_0 of the throat, with the result that much smaller displacements are required to produce a given acoustic output than when the piston is mounted directly in the throat of the horn. Furthermore, the housing completely screens the external medium from any radiation coming from the back of the piston surface, so that the problems arising through doublet radiation are nonexistent.

Figure 10.20*b* is a schematic mechanical circuit showing the various elements that contribute to the mechanical impedance of the moving piston. The electromechanical driving force produced by currents in the voice coil is represented by $f = Bli$. The mechanical compliance C_1 represents the effect of both the stiffness s of the suspension system and the reaction due to the compression and expansion of the air in the volume V_1 behind the piston. At such low frequencies that the dimensions of this air chamber are less than a quarter wavelength, its stiffness as given by equation 8.2*a* is $\rho_0 c^2 S_p^{\,2}/V_1$, and the mechanical compliance C_1 is therefore

$$C_1 = \frac{1}{s + \dfrac{\rho_0 c^2 S_p^{\,2}}{V_1}} \tag{10.49}$$

The masses of the voice coil and the piston are represented by m_c and m_p, respectively. The mechanical compliance C_2 due to the air chamber of volume V_2 in front of the vibrating piston is given by the equation

$$C_2 = \frac{V_2}{\rho_0 c^2 S_p^{\,2}} \tag{10.50}$$

The reactance due to this compliance acts in parallel with the radiation impedance $\mathbf{Z}_r$ of the horn. The latter is given by

$$\mathbf{Z}_r = R_r + jX_r = S_p^{\,2}\mathbf{Z}_0 = S_p^{\,2}R_0 + jS_p^{\,2}X_0 \tag{10.51}$$

Additional mechanical impedances acting on the piston include those due to the mechanical resistance of the suspension system and to radiation and mass loading resulting from radiation into the air contained in V_1. However, the impedances due to these causes are in general small and will be neglected.

The motional impedance, speaker efficiency, power output, etc., can be computed from this mechanical circuit and the known electrical characteristics of the voice coil by application of the equations and methods developed in Sect. 10.2. Rather than attempt a detailed general discussion of this type of speaker, let us instead consider two special examples.

The simplest possible case is that in which the contributions of C_1, C_2, m_c, m_p, and X_r to the mechanical impedance of the system are negligible in comparison with R_r. Then the motional impedance as given by equation 10.11 is

$$R_M = \frac{\phi^2}{R_r} = \frac{\phi^2}{S_p^{\,2}R_0} \tag{10.52}$$

and is a pure resistance. The corresponding efficiency as given by equation 10.14*a* is, therefore,

$$\eta = \frac{\phi^2}{\phi^2 + S_p^{\,2}R_0R_E} \tag{10.53}$$

It is to be noted that R_E in this equation represents the resistance of the voice-coil, expressed in electrical ohms, whereas R_0 represents the acoustic resistance at the throat of the horn and is expressed in acoustic ohms, i.e., kg/m^4 sec. The efficiency of a horn speaker, as given by equation 10.53, is analogous to the resonant efficiency of a direct-radiator speaker.

As an illustrative example, let us assume that the voice-coil of the speaker discussed in Sect. 10.3 is attached to a piston-like diaphragm having a mass of 0.0015 kg and a radius of 0.04 m, and that this diaphragm is connected to the "infinite" exponential horn of Fig. 10.18 in a manner similar to that shown in Fig. 10.20. Then at frequencies above the cut-off frequency of this horn

$$R_0 \approx \frac{\rho_0 c}{S_0} = \frac{415}{\pi \times 0.02^2} = 3.3 \times 10^5$$

Since $\phi = 4.5$ and $R_E = 5$ ohms, the maximum or resonant efficiency as given by equation 10.53 is

$$\eta = \frac{4.5^2}{4.5^2 + (0.0016\pi)^2 \times (3.3 \times 10^5) \times 5} = 0.33 = 33\%$$

In the immediate vicinity of the cut-off frequency the mechanical impedance of the remaining elements of the mechanical circuit is of greater importance than R_r, and consequently the efficiency falls below its maximum value as given by equation 10.53. In the region of high frequencies the motion of the piston is mass-controlled, and its mechanical impedance is effectively equal to the positive reactance $j\omega(m_c + m_p)$ associated with the sum of the masses of the voice-coil and the piston. Therefore efficiency at high frequencies is

$$\eta = \frac{\phi^2 R_0 S_p^{\ 2}}{\phi^2 R_0 S_p^{\ 2} + R_E \omega^2 (m_c + m_p)^2} \tag{10.54}$$

At a frequency of 1000 cycles/sec the efficiency of the horn speaker considered above as computed from equation 10.54 is 0.09 or 9 per cent.

As the frequency is still further increased, a frequency is eventually reached at which the reactance $1/(j\omega C_2)$, due to the volume V_2, is small compared to the radiation resistance R_r of the horn. Under these conditions the compliance C_2 effectively short-circuits the horn, and the efficiency falls off rapidly. This high-frequency cut-off can be raised above the designated range of operating frequencies of the speaker by decreasing the volume V_2 of the air chamber in front of the piston.

Another factor limiting the output at high frequencies is the requirement that distances from different elements of the piston's surface to the throat of the horn must not differ from one another by more than a quarter wavelength. Violation of this requirement results in serious phase differences and in destructive interference which reduces the volume flow at the throat. The simplified driver of Fig. 10.20*a* will not function properly at frequencies for which $\lambda/4 < 0.02$ m, i.e., for frequencies in excess of 4000 cycles/sec. This difficulty can be partially overcome by shaping the vibrating diaphragm and the forward air chamber so that disturbances arising from different elements of the diaphragm's surface arrive at the throat in phase with one another. One method of accomplishing this is indicated in Fig. 10.21.

The efficiency and power output of a horn speaker are generally much higher than those of a direct-radiator speaker, so that high levels of sound intensity can be reached without the use of excessively powered driving amplifiers. This factor accounts for the use of horn speakers in public-address and motion-picture sound systems.

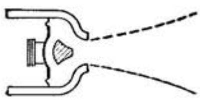

Fig. 10.21. Driver construction used to reduce phase differences at the throat of a horn speaker.

The acoustic power output of a horn speaker can be determined from the product of its efficiency and the electrical power input. It is given in watts either by equation 10.17, or by the equation

$$W = R_r V^2 = R_r \omega^2 \xi_0{}^2 \qquad (10.55)$$

where R_r is the radiation resistance acting on the diaphragm and ξ_0 is the rms displacement amplitude of this diaphragm. The constructional details of the driver unit determine the maximum allowable value of this displacement amplitude, which is in turn one factor limiting the maximum power output at low frequencies. For example, if the horn speaker previously considered is to radiate 20 watts of acoustic power at 160 cycles/sec, the required rms displacement amplitude of the driver is

$$\xi_0 = \left(\frac{20}{3.3 \times 10^5 (0.0016\pi)^2 \times 1000^2}\right)^{1/2} = 0.00155 \text{ m}$$

which is entirely reasonable. However, at frequencies below the cut-off frequency of 100 cycles/sec, ω^2 is somewhat reduced and R_r is greatly reduced, so that the required amplitudes become so large that they are impossible of attainment. These required amplitudes can be reduced by increasing the area S_D of the vibrating diaphragm, but this will necessarily increase the mass of the vibrating system and will also introduce difficulties arising from phase differences at the throat when the speaker is operated at high frequencies. It is therefore apparent that the requirements of high output at both high and low frequencies are mutually contradictory in horn speakers, just as they are in direct radiator speakers. As a consequence, wide range systems of this type are usually designed with two horn speakers, one of which is large and radiates only the lower frequencies, whereas the other is a small horn unit radiating only frequencies higher than about 500 or 1000 cycles/sec. As in the corresponding direct radiator system, electrical filter networks are employed to deliver to each unit only

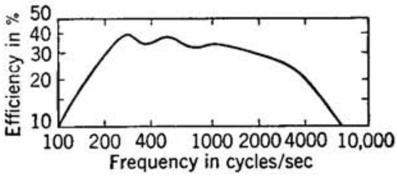

Fig. 10.22. Typical frequency response of an exponential horn speaker.

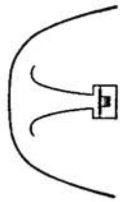

Fig. 10.23. Method of folding a horn so as to decrease its overall length.

that range of frequencies for which its acoustic efficiency is relatively high.

Figure 10.22 is a typical response curve showing how the efficiency of an exponential horn speaker varies with frequency. The peaks and dips in the low-frequency response result from resonances due to the finite length of the horn, which in turn affect the throat impedance. If it were possible to increase the length of the horn to about 10 ft such peaks and dips would be eliminated, but space limitations usually make this impossible. One indirect method of gaining many of the advantages of a long horn is through the use of a *folded horn*, such as that shown in Fig. 10.23. Unfortunately, however, one effect of folding the horn is to introduce differences in the length of the path traversed by the waves as they travel around the bends, and the resulting destructive interference produces some attenuation of the higher frequencies.

10.13 Measurement of Pressure Response of a Loudspeaker. Loudspeakers are commonly rated both as to the total acoustic power radiated and as to the acoustic pressures produced. The *pressure response* of a loudspeaker is a measure of the sound pressure produced at designated positions in the medium, with the electrical input, the frequency, and the acoustic conditions specified. One method of specifying pressure response is to give the effective or rms sound pressure measured at a specified position for one volt input to the terminals of the voice-coil. It is given by the equation

$$S_E = \frac{P}{E} \tag{10.56}$$

where P is the measured effective sound pressure in microbars and E is the voltage applied to the voice-coil. The resulting behavior with frequency, as calculated from equation 10.56, represents the sound pressure that would be obtained from the speaker if it were fed from an amplifier that automatically delivered an output of 1 volt irrespective of the loading impedance of the voice-coil. Additional, but usually less significant responses, are obtained if a constant current of one ampere or a constant power of one watt is supplied to the voice-coil.

The pressure response may also be expressed in *decibels*, relative to an arbitrary response of 1 microbar per volt of electrical input, by the equation

$$n_s = 20 \log \frac{P}{E} \tag{10.57}$$

If it is desired to express the level of pressure response in terms of the commonly used acoustic reference pressure of 0.0002 microbar, the response levels as computed from equation 10.57 must be increased by the addition of +74 db.

When a source of sound is present in a room, the resultant sound at any point is a combination of the direct and the reflected sound. The direct sound is independent of the room and is characteristic only of the source. The reflected sound, however, depends not only on the source but also on the geometrical configuration of the room and the absorption characteristics of its walls, and on the coordinates of the source and point of observation. It is obvious, therefore, that, unless the measuring conditions are identical, the response characteristics obtained in an ordinary room will vary considerably. Hence the outdoor or free-space measurement of the frequency-response characteristic offers the simplest method for making loudspeaker measurements that may be duplicated and compared among various laboratories. For this reason, outdoor measurements are considered as a standard test for showing the performance of a loudspeaker. In practice it is observed that measurements made in large sound-deadened or *anechoic* chambers are equivalent to outdoor measurements at all frequencies except those below about 100 cycles/sec.

A general schematic circuit arrangement showing one specific way to obtain the factor P/E in equation 10.56 is given in Fig. 10.24. This particular arrangement has the desirable feature that it does not require an *absolute* calibration of the measuring system. However, it necessitates the use of a calibrated microphone having a known open-circuit response n_m in decibels, relative to a reference level of 1 volt produced by a pressure of

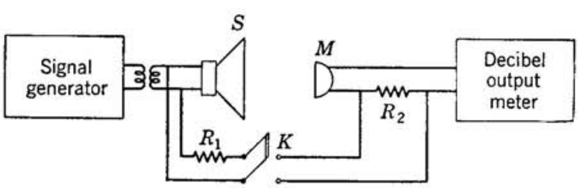

Fig. 10.24. Measurement of output pressure level of a loudspeaker.

1 microbar in a free progressive wave. It can be shown that the pressure response of the speaker in decibels is

$$n_s = A - B - n_m - 20 \log \frac{R_1 + R_2}{R_2} \tag{10.58}$$

where A is the output of the measuring system in decibels, with K open and the microphone M picking up sound from the loudspeaker S, and B is the output of the measuring system with K closed and the microphone shielded from sound. The resistance R_2 should be small enough compared to the internal impedance of the microphone so that the measured output of M does not change when R_2 is short-circuited. In order to reduce errors resulting from inaccuracies in the relative readings of the measuring system, R_1 should be so selected as to obtain a value of B in the range of values obtained for A. The loudspeaker should be mounted either in the cabinet with which it is to be used or, if the speaker unit alone is to be tested, in a rigid baffle of adequate size. The microphone should be placed at a distance of at least 5 ft from the speaker, or at some designated greater distance.

Acoustic pressure responses measured on the axis of a loudspeaker are in general higher than those measured in other directions. For instance, when a loudspeaker is mounted in a wall, equation 7.54 indicates that the radiated directional pattern is essentially nondirectional as long as $ka < 1$. However, at higher frequencies the directionality of the pattern increases and, as a consequence, the axial pressure response is no longer a good measure of the total acoustic output of the loudspeaker. For example, at a frequency such that $ka = 1$, the axial response is about 10 per cent higher than the average hemispherical response. By contrast, at frequencies such that $ka > 2$, the ratio of the axial response to the average response is approximately equal to $ka/1.4$.

10.14 Measurement of Acoustic Power Output of a Loudspeaker. The sound power output from a speaker driven at any particular frequency may be obtained by measuring the rate of flow of acoustic energy through any arbitrary surface that entirely encloses the sound source. When a loudspeaker is mounted in a wall, this surface is normally that of a hemisphere centered on the loudspeaker. For speakers mounted in cabinets or horns, it is normally a sphere centered on the loudspeaker. The surface of the sphere (or hemisphere) is divided into incremental areas, and the power transmitted through each is determined by the product of the intensity I and the area of the surface element dS. If the effective acoustic pressure response measurements, as made by a microphone, are taken at a sufficient distance so as to be external to the so-called near-field, then $I = P^2/\rho_0 c$, and the total power in acoustic watts transmitted through the surrounding surface is given by

$$W = \frac{1}{\rho_0 c} \iint P^2 \, dS \tag{10.59}$$

The acoustic output characteristics of a loudspeaker may also be determined by measurement of the resistive component of the input electrical impedance under various conditions of loading. For instance, if R_{Mr}, R_M, and R_E could be measured separately, then equation 10.14 could be used to compute the electroacoustic efficiency of the speaker. The first step in such a procedure is to *block* the voice-coil so that it cannot move. The resistance R_B measured under this condition is a direct measurement of the resistance R_E of the voice-coil. A second step is to measure the input resistance R_A under normal conditions of *air* loading. The motional resistance R_M, which is given by the difference between these two resistances is therefore

$$R_M = R_A - R_B \tag{10.60}$$

By combining equations 10.13, 10.13*a*, and 10.14 with this equation it is possible to show that the efficiency of the loudspeaker will be given by

$$\eta = \left(1 - \frac{R_B}{R_A}\right)\left(\frac{R_r}{R_m + R_r}\right) \tag{10.61}$$

The first bracketed term in this equation is a measure of the efficiency with which electrical power is converted into mechanical power and the second is a measure of the efficiency of conversion of mechanical into acoustic power.

The ratio of the mechanical resistances expressed by $R_r/(R_r + R_m)$ can only be measured solely by electrical means at the frequency of mechanical resonance. At this frequency, equation 10.13 simplifies to

$$R_M = R_A - R_B = \frac{\phi^2}{R_r + R_m} \tag{10.62}$$

As a third step, the input resistance R_V is measured when the acoustic radiation loading R_r is removed, either by driving the speaker in a *vacuum* or by removing it from its normal cabinet or wall installation. Under either of these conditions

$$R_{Mm} = R_V - R_B = \frac{\phi^2}{R_m} \tag{10.63}$$

Equations 10.62 and 10.63 may be combined so as to eliminate ϕ and yield

$$\frac{R_r}{R_m + R_r} = \frac{R_V - R_A}{R_V - R_B} \tag{10.64}$$

which upon substitution into equation 10.62 gives

$$\eta = \left(1 - \frac{R_B}{R_A}\right)\left(\frac{R_V - R_A}{R_V - R_B}\right) \tag{10.65}$$

for the efficiency at resonance. Finally, since the input reactance is zero at this frequency, the normal input power is E^2/R_A, which upon being multiplied by the efficiency as given by equation 10.65 gives the acoustic output in watts as

$$W = \frac{E^2}{R_A}\left(1 - \frac{R_B}{R_A}\right)\left(\frac{R_V - R_A}{R_V - R_B}\right) \tag{10.66}$$

An inspection of Fig. 10.4 will show that at frequencies in excess of 400 cycles/sec, $R_r \gg R_m$. This behavior is typical of most loudspeaker installations in their higher range of operating frequencies. Under such circumstances, the ratio $R_r/(R_r + R_m)$ approaches unity, and consequently

$$\eta = \left(1 - \frac{R_B}{R_A}\right) \tag{10.67}$$

may be used to compute the efficiency of a loudspeaker at frequencies well above that of mechanical resonance.

PROBLEMS

10.1. (*a*) Show that for frequencies well above that of mechanical resonance, equation 10.14*a* simplifies to

$$\eta = \frac{\phi^2 R_r}{m^2\omega^2 R_E}$$

What terms are neglected and what is the justification for so doing? (*b*) For the simple speaker discussed in Sect. 10.3, what is the ratio of the efficiency as computed from this equation at a frequency of 1000 cycles/sec to that computed from equation 10.14*a*?

10.2. Derive a simplified version of equation 10.17 for computing the acoustic output of a direct-radiator loudspeaker mounted in an infinite baffle, at frequencies well below that of mechanical resonance. For constant voltage input, how does the acoustic power vary with frequency in this region?

10.3. (*a*) Show that when the voice-coil of a loudspeaker is short-circuited that the effective mechanical impedance of the loudspeaker cone is increased by an amount ϕ^2/Z_E. (*b*) For the loudspeaker discussed in Sect. 10.3, what is this additional mechanical impedance at the frequency of mechanical resonance?

10.4. The driving voice-coil of a direct-radiator speaker is 0.03-m in diameter and has 80 turns. Its blocked resistance is 3.2 ohms and its blocked inductance is 0.2 millihenry. It operates in a magnetic field of 1 weber/m^2. The total mass of the cone and voice-coil is 0.015 kg, the mechanical resistance R_m is 1 kg/sec, the radiation resistance R_r is also 1 kg/sec, and the stiffness of the cone system is 1500 newtons/m. (*a*) Assuming the radiation reactance X_r to be negligible, what are the blocked electrical impedance Z_E, the motional impedance Z_M, and the total electrical input impedance Z_I at a frequency of 200 cycles/sec? (*b*) What rms driving voltage is required in order to produce an rms displacement amplitude of the speaker cone of 0.1 cm at this frequency? (*c*) What acoustic output in watts will be produced by the above driving voltage? (*d*) Calculate values for R_M, L_M, and C_M of the parallel electrical circuit having an impedance equivalent to the motional impedance of the above speaker.

10.5. (*a*) What is the frequency of mechanical resonance for the speaker of Problem 10.4? (*b*) What is the mechanical quality factor Q (see Sect. 1.16) of the above speaker cone system? (*c*) What is the rms displacement amplitude of the cone for an applied voltage of 5 volts at resonance? (*d*) If the driving circuit is opened at an instant of maximum displacement, what will be the rms displacement amplitude at the end of 0.02 sec?

10.6. Given a simple direct-radiator loudspeaker to have a mass $m = 0.01$ kg, a mechanical resistance $R_m = 2$ kg/sec, a radiation resistance $R_r = 2$ kg/sec, a transformation factor $\phi = 3.5$ webers/m, and a frequency of mechanical resonance of 200 cycles/sec. Assuming $X_r = 0$, (*a*) What is the stiffness constant of the suspension system of the speaker cone? (*b*) Compute the motional resistance R_M and the motional reactance X_M at 100, 150, 180, 200, 220, 250, and 400 cycles/sec. (*c*) For each of the above frequencies plot the computed value of X_M as an ordinate against R_M as an abscissa. (*d*) Show that the curve obtained when X_M is plotted against R_M as in part (*c*), is a circle of radius $\phi^2/2(R_r + R_m)$.

10.7. A direct-radiator loudspeaker has a voice-coil of 5 ohms resistance and negligible inductance. The transformation factor is $\phi = 10$ webers/m. The motional impedance of the speaker cone system is equivalent to a resistance of 20 ohms in parallel with a capacitance of 100 microfarads and an inductance of 0.04 henry. (*a*) What are the numerical values for the mechanical constants $(R_m + R_r)$, s, and m of the loudspeaker? (*b*) If $R_m = 3R_r$, what will be the electroacoustic efficiency of this speaker at a frequency of 159 cycles/sec?

10.8. A direct-radiator loudspeaker is mounted in an infinite baffle. It has a radius of 0.2 m, a mass of 0.04 kg, a voice-coil having a resistance of 4 ohms, an inductance of 0.0001 henries, and a transformation factor ϕ of 10 webers/m. The suspension system of the cone has a stiffness of 2000 newtons/m and a mechanical resistance of 2 kg/sec. (*a*) If an alternating voltage of 10 volts rms and 200 cycles/sec frequency is applied to the voice-coil, what is the acoustic power output of the speaker? Assume radiation loading on just one side of the speaker cone. (*b*) Assuming the radiated beam pattern to be that of a circular piston in an infinite baffle, what axial pressure level will be produced at a distance of 10 meters?

10.9. Design a small direct-radiator loudspeaker capable of at least 0.005 watt of acoustical output for an electrical input power of 1 watt over the frequency range from 2000 cycles/sec to 8000 cycles/sec. Give specifications as to mounting (wall or cabinet); radius and mass of speaker cone; stiffness constant of suspension system; radius, turns, resistance, and mass of voice-coil; and flux density of magnetic field. Show by calculation that the acoustic output capabilities of the designed speaker meet the specified requirements. What practical difficulties if any, might be encountered in constructing the designed speaker?

10.10. Design a direct-radiator loudspeaker capable of at least 1 watt of acoustic output at an efficiency of at least 10 per cent over the frequency range from 100 to 1000 cycles/sec. Give specifications as follows: (*a*) mass, resistance, turns, radius, and inductance of voice-coil. (*b*) mass, radius, mechanical resistance, and stiffness constant of speaker cone. (*c*) type of mounting (wall or cabinet), if cabinet mounting give dimensions and added stiffness constant. (*d*) flux density of magnetic field. Show by calculations that the above requirements regarding acoustic output are met by the speaker of your specifications. (*e*) What input voltage would be required for this speaker to produce 1 watt of acoustic output at a frequency of 100 cycles/sec? (*f*) Calculate the acoustic output of this speaker at 1000 cycles/sec for this same input voltage.

10.11. A corrugated speaker cone is so designed that its effective piston-like radius is given by $a = (2 + 100/\sqrt{f})$ cm in the region from 100 to 10,000 cycles/sec. If the velocity amplitude of the speaker cone is assumed to remain constant over this frequency range, compute and plot a curve showing the relative acoustic output of the speaker from 100 to 10,000 cycles/sec. Assume the radiation resistance loading of the speaker cone to be that of a flat piston of radius a, as given above, when mounted in an infinite baffle.

10.12. A corrugated speaker cone is so designed that its effective piston-like radius is given by $a = (5 + 100/\sqrt{f})$ cm in the region from 100 to 10,000 cycles/sec. (*a*) Assuming the radiation pattern of the speaker to be that of a flat piston of radius a, as given above, when mounted in an infinite baffle, compute and plot its radiated beam pattern at 100, 1000 and 10,000 cycles/sec. (*b*) If the velocity amplitude of the speaker cone over the above frequency range is assumed to be given by $V = 2/\sqrt{f}$ cm/sec, compute and plot a curve showing the relative acoustic output of the speaker from 100 to 10,000 cycles/sec. Assume the radiation resistance loading of the speaker cone to that of a flat piston of radius a when mounted in an infinite baffle.

10.13. Two identical loudspeakers are mounted in a wall with a distance of 0.4 m between their centers. They are normally driven in phase so that their acoustic outputs are additive. If the acoustic output of an individual speaker at 100 cycles/sec is 0.05 watts, what is the output of the combination when they are mistakenly connected so as to radiate in phase opposition? Assume the radiation coming from each speaker to have hemispherical symmetry and apply the acoustic doublet theory.

10.14. A direct-radiator loudspeaker has a radius of 0.15 m. When mounted in a wall its measured frequency of mechanical resonance is 25 cycles/sec. When mounted in a small back-enclosed cabinet of 0.1-m^3 volume, its frequency of mechanical resonance is raised to 50 cycles/sec. (*a*) What is the stiffness constant of the suspension system of the speaker cone? (*b*) What is the mass of the speaker cone? In each case consider the speaker cone to be air loaded with radiation reactance X_r on just one side.

10.15. The cone of a large direct-radiator loudspeaker has a radius of 0.2 m, a mass of 0.04 kg, and a mechanical resistance of 1 kg/sec. (*a*) Considering the cone to be equivalent to a flat piston of equal radius, what must be the stiffness of the suspension system in newtons/m, if it is to have a frequency of mechanical resonance of 20 cycles/sec when mounted in an infinite baffle? Consider the speaker to be radiation loaded on just one side. (*b*) When mounted in an enclosed-back cabinet, the frequency of mechanical resonance is observed to increase to 80 cycles/sec. What is the volume of the cabinet? (*c*) If the transformation factor ϕ of the voice-coil is 10 webers/m, what must be the rms current supplied to the voice-coil, if the speaker is to radiate 0.5 watt of acoustic power at 40 cycles/sec when mounted in the above cabinet?

10.16. A direct-radiator loudspeaker has the following physical characteristics: mass = 0.01 kg, stiffness = 1000 newtons/m, mechanical resistance = 1.5 kg/sec, radius = 0.15 m, a voice-coil of 1.5 cm radius having 150 turns of No. 34 copper wire, a flux density of the magnetic field in the air gap of 0.8 weber/m^2, and 0.4-millihenry inductance. The speaker is mounted in an enclosed-back cabinet $0.2 \times 0.5 \times 1.0$ m. (*a*) Considering the speaker cone to be radiation loaded on just one side, what is the frequency of mechanical resonance? (*b*) If an rms voltage of 10 volts is applied to the voice-coil, what is the acoustic output in watts at the resonant frequency, at 200 cycles/sec, and at 1000 cycles/sec?

10.17. Consider the direct-radiator speaker of problem 10.16 to be mounted in a bass-reflex cabinet. (*a*) If the vent is a circular hole of 0.15-m radius and negligible length, what must be the volume of the cabinet if its Helmholtz resonance frequency is to equal that of the speaker cone and suspension when mounted in an infinite baffle? (*b*) What is the ratio of the acoustic output at 75 cycles/sec of the speaker when mounted in this cabinet, to that when mounted in an infinite baffle? Assume the displacement of the speaker cone to be the same in each case.

10.18. (*a*) Show that the pressure amplitude P of plane progressive waves being propagated along the axis of an infinite exponential horn is given by $P = P_0 e^{-\alpha x}$, where P_0 is the pressure amplitude at $x = 0$. (*b*) Show that the acoustic pressure $\mathbf{P}$ for a wave moving in the positive x direction in this horn leads the particle velocity $\mathbf{u}$ by an angle θ, where $\tan\theta = \alpha/\beta$. (*c*) Show that the intensity of plane waves being propagated along the axis of this horn is given by

$$I = \frac{P^2}{2\rho_0 c} \cdot \sqrt{1 - m^2/4k^2}$$

(*d*) Show that the volume velocity U for a wave moving in the positive x direction in this horn is given by $U = U_0 e^{\alpha x}$, where U_0 is the volume velocity at $x = 0$.

10.19. One watt of acoustic power is being radiated at a frequency of 250 cycles/sec from an infinite exponential horn. The horn has a radius of 0.03 m at its throat and has a flare constant $m = 5$. (*a*) What is the cut-off frequency of the horn? (*b*) What is the required peak volume velocity at the throat in order to produce one watt of acoustic output? (*c*) If the radius of the diaphragm in the driver unit attached to this horn is 0.05 m, what must be its peak displacement amplitude if it is to produce the above volume velocity?

10.20. A small circular piston has a radius of 0.03 m and a mass of 0.002 kg. The stiffness of its suspension system is such that its free oscillation frequency is 300 cycles/sec. An exponential horn having a radius of 0.03 m at its throat, a length of 1.0 m, and a radius of 0.3 m at its mouth is fitted over the piston. (*a*) What is the new mechanical resonance frequency of the piston? Consider the mass loading of the piston by the horn to be that of an infinite horn having the same flare constant as the actual horn. (*b*) If the rms amplitude of the driving force acting upon the piston is 5 newtons, what acoustic power will be radiated by this infinite horn at a frequency of 300 cycles/sec?

10.21. Derive a general expression for the sound power transmission coefficient α_t (see Sect. 8.6) for plane waves in a circular pipe of cross section S entering into an infinite exponential horn of flare constant m.

10.22. Given an exponential horn of 10-cm radius at its mouth, 2-cm radius at its throat, and 20-cm length along its axis. The throat of the horn is closed by means of the relatively rigid diaphragm of an attached microphone. A plane wave of 2000 cycles/sec frequency and 74 db pressure level, relative to 0.0002 microbar, is incident on the mouth of the horn in a direction parallel to the axis of the horn. Assuming no reflections to take place at the mouth of the horn, what is the acoustic pressure level produced by this plane wave at the throat as it is converged by the horn and reflected by the relatively rigid diaphragm?

10.23. The exponential horn of a small "tweeter" loudspeaker has a radius of 0.01 m at its throat. The diaphragm of the driver unit has a radius of 0.03 m, a stiffness of 5000 newtons/m, and a mass of 0.001 kg. The voice-coil has a resistance of 1.6 ohms, an inductance of 0.0001 henry, and a transformation factor ϕ of 4 webers/m. (*a*) What must be the flare constant of the horn if it is to have a cut-off frequency of 500 cycles/sec? (*b*) What must be the peak volume-velocity amplitude at the throat of the horn, if the acoustic output is to be 0.2 watt at a frequency of 1000 cycles/sec? (*c*) What displacement amplitude of the diaphragm will produce this volume velocity at a frequency of 1000 cycles/sec? (*d*) What is the efficiency of the speaker at this frequency? (*e*) What voltage must be applied to the voice-coil in order to produce the above acoustic output?

10.24. A direct-radiator loudspeaker of 0.2-m radius is mounted flush in a large flat wall. When the speaker is being driven at a frequency of 1000 cycles/sec, the sound intensity at a point 5 meters from the speaker and directly out from the wall is 0.1 watt/m^2. (*a*) What is the intensity level at this point? (*b*) Assuming the speaker to have the same directional pattern as a flat piston of equal radius, what is the intensity level at this same distance directly along the wall? (*c*) in a direction 30° from the wall? (*d*) in a direction 60° from the wall? (*e*) What is the total acoustic output of the speaker in watts?

10.25. Given a loudspeaker flush-mounted in a large flat wall. The measured effective acoustic pressures at a radial distance of 2 meters from the speaker are observed to be represented by the equation $P = 20 \cos \theta$ newtons/m^2, where θ is the polar angle between the direction of measurement and the axis of the speaker. By integration of equation 10.59 over the surface of a hemisphere of radius 2 meters, using an annular ring surface element $2\pi r^2 \sin \theta \, d\theta$ for dS, compute the total acoustic output in watts.

10.26. When the voice-coil of a certain loudspeaker is blocked, the resistive component of its measured input impedance is found to be 5 ohms. When flush mounted in a large wall and driven at its frequency of mechanical resonance, the resistive component of its measured input impedance is found to be 10 ohms. Upon removing the speaker from the wall in order approximately to eliminate the acoustic radiation loading R_r, the measured input resistance is found to be 12 ohms at the frequency of mechanical resonance. (*a*) What is the electro-acoustic efficiency of the above speaker when mounted in the wall? (*b*) What is the acoustic output of the speaker in watts, when 0.6 ampere is supplied to the voice-coil at the frequency of mechanical resonance? (*c*) Assuming hemispherically symmetrical radiation, what is the intensity level at 5 meters from the above speaker?

10.27. (*a*) Considering R_A as a variable in equation 10.65, what value of R_A expressed in terms of R_B and R_V will result in a maximum efficiency? (*b*) Substitute this value of R_A into equation 10.65 and derive an expression for the maximum possible efficiency, expressed in terms of R_B and R_V. (*c*) The maximum efficiency of part (*b*) corresponds to an optimum radiation loading R_r. Derive an expression for R_r expressed in terms of R_m, R_B, and R_V, which will result in this maximum efficiency at resonance.

chapter 11

MICROPHONES

11.1 Introduction. In the preceding chapter we have considered two important types of electroacoustic transducers which are capable of converting electrical energy into acoustic energy. Of equal importance are those electroacoustic transducers used to convert acoustic energy into electrical energy. When operating in air such transducers are known as *microphones*, and when operating in water as *hydrophones*. Microphones serve two principal purposes. First, they are used for converting music or speech into electrical signals which are transmitted or processed in some manner and then reproduced. Second, they serve as measuring instruments, converting acoustic signals into electrical currents which actuate indicating meters.

Numerous physical phenomena have been used to convert acoustic energy into electrical energy. These include electromagnetic induction, the piezoelectric effect, magnetostriction, variations in the capacitance of a capacitor, and variations in the resistance of packed carbon granules. Before the development of the vacuum-tube amplifier, the inherent insensitiveness of all but the last of these methods precluded their practical application to sound systems, and all such systems employed carbon microphones. At present, however, the voltage and power gains that can be obtained from vacuum-tube amplifiers make it possible to employ microphones of much lower sensitivity, such as electrodynamic microphones, crystal microphones, and condenser microphones, and thus to take advantage of the greater uniformity of response and the absence of internal noise that is characteristic of these types.

All microphones are used to convert the periodic variations of acoustic pressure in the medium into similar variations in voltage or current in an associated electrical circuit. If this electrical response corresponds to the variations in acoustic pressure, the microphone is classified as a *pressure microphone*; if the response corresponds to variations in the pressure-gradient, it is known as a *pressure-gradient microphone*. Microphones may also be classified as either *sound-powered* or *sound-controlled*. In sound-powered microphones the acoustic energy of the incident wave supplies the electrical energy generated in the microphone; in sound-controlled microphones the acoustic waves merely control the flow of electrical energy from a battery or other source of electrical power.

11.2 Carbon Microphone. The carbon microphone is widely used for telephone and radio communication purposes where its high electrical output, low cost, and durability are of greater significance than fidelity of response. It depends for its operation on the variation in resistance of a small enclosure filled with carbon granules, which is known as the carbon button. Figure 11.1*a* gives a schematic diagram of this type of microphone. As the diaphragm is displaced, the plunger attached to it varies the pressure applied to the carbon granules, and hence the resistance from granule to granule, so that the total resistance across the carbon button, which is ordinarily about 100 ohms, varies in an approximately linear manner with the acoustic pressure applied to the diaphragm.

In the simple equivalent circuit shown in Fig. 11.1*b*, let us assume that for small displacements of the diaphragm the resistance R_c of the carbon button varies linearly with the displacement y of the center of the diaphragm, i.e.,

$$R_c = R_0 + hy \tag{11.1}$$

where R_0 is the zero-displacement resistance of the button and h is its resistance constant in ohms per meter of displacement of the plunger. At frequencies well below the fundamental resonant frequency of the diaphragm, its motion is stiffness-controlled, so that it may be treated as a simple oscillator of stiffness s and negligible mass. If an impinging sound wave of frequency ω produces a pressure amplitude P on the face of the diaphragm, then

$$y = \frac{PS}{s} \cos \omega t = y_0 \cos \omega t \tag{11.2}$$

where S is the effective area of the diaphragm and y_0 is the displacement amplitude at its center. Therefore

$$R_c = R_0 + hy_0 \cos \omega t \tag{11.3}$$

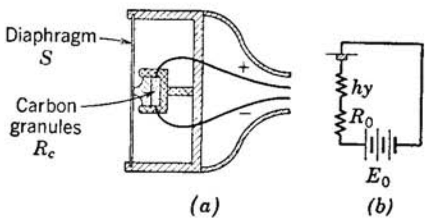

Fig. 11.1. (*a*) Simple carbon microphone. (*b*) Equivalent electrical circuit.

This variation in resistance causes the current in the circuit to vary as

$$i = \frac{E_0}{R_0 + hy_0 \cos \omega t} \tag{11.4}$$

where E_0 is the voltage of the battery. If $hy_0 \ll R_0$, then equation 11.4 may be expanded and simplified to

$$i \approx \frac{E_0}{R_0}\left[1 - \frac{hy_0 \cos \omega t}{R_0} + \left(\frac{hy_0}{R_0}\right)^2 \frac{\cos 2\omega t}{2} + \cdots\right] \tag{11.5}$$

Equation 11.5 indicates the presence of a steady direct current E_0/R_0, an alternating current $i_c = -(E_0 hy_0/R_0^2) \cos \omega t$, and higher harmonics of this current.

The alternating current component i_c of frequency ω may be thought of as arising from an alternating emf

$$e_c = i_c R_0 = -\frac{E_0 hy_0 \cos \omega t}{R_0} \tag{11.6}$$

generated internally in the microphone. This treatment is somewhat analogous to that in which the effect of a grid voltage e_g applied to a vacuum tube is replaced by an equivalent voltage $-\mu e_g$ generated in the plate circuit. The amplitude of the equivalent voltage of the microphone is therefore

$$E_c = \frac{E_0 hy_0}{R_0} = \frac{E_0 hSP}{R_0 s} \tag{11.7}$$

The ratio E_c/P is a measure of the sensitivity of the microphone and is known as the *open-circuit voltage response*. It may be expressed either in volts per newton/m², i.e.,

$$M_c = \frac{E_c}{P} = \frac{E_0 hS}{R_0 s} \tag{11.8}$$

or upon multiplying the right-hand side of equation 11.8 by 0.1, it may be expressed in volts per microbar. The response may also be expressed as a decibel level relative to some arbitrary reference level. The commonly used reference level is one volt per microbar (one volt per 0.1 newton/m²). Expressed in terms of this reference level, the db response of the above carbon microphone is

$$n = 20 \log \frac{E_c}{10P} = 20 \log \frac{E_0 hS}{10 R_0 s} \tag{11.8a}$$

The response evidently increases as the battery voltage E_0 is increased or as the total resistance R_0 of the circuit is decreased. It also increases directly with the area S and inversely with the stiffness s of the diaphragm.

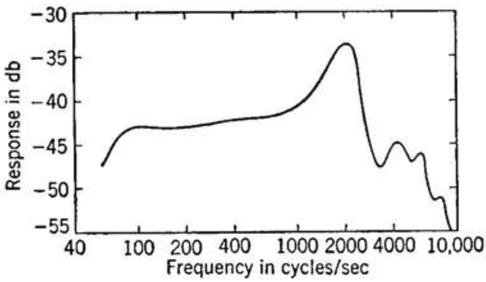

Fig. 11.2. Typical constant-pressure frequency-response characteristic of a carbon microphone in decibels relative to 1 volt per microbar.

However, there are practical limitations to such methods of increasing the sensitivity, since high values of E_0 cause excessive heating and internal noise in the carbon button, and decreasing s tends to lower the fundamental frequency of the diaphragm, thus reducing the useful frequency range of the microphone.

The ratio of second-harmonic voltage to fundamental voltage, as obtained from equation 11.5, is $hy_0/2R_0$. Since increasing the ratio h/R_0 in an attempt to increase the sensitivity also increases the relative amplitude of the second harmonic, it is apparent that some sensitivity must be sacrificed if distortion is to be reduced, and vice versa. It is also apparent that very intense sound waves, for which the amplitude y_0 is large, will introduce considerable harmonic distortion into the output of a carbon microphone. Finally, the assumption that h is constant, i.e., that the resistance varies uniformly with the displacement, is undoubtedly in error for large amplitudes and will act as a further source of distortion. The distortion arising from even-harmonic terms in equation 11.5 can be balanced out by using a double-button carbon microphone connected in a push-pull type of circuit, but this type of microphone will still have odd-harmonic distortion when the amplitude of the impressed sound wave is too great.

A measured frequency-response characteristic for a single-button carbon microphone is shown in Fig. 11.2, which gives the open-circuit response n in decibels as a function of frequency. In this particular response curve, which is known as a *constant-pressure* curve, the pressure actuating the diaphragm is uniformly distributed over its surface and is measured directly. When a microphone is inserted into a sound field the sound pressure acting on the microphone is not necessarily equal to that of the undisturbed sound wave, for the presence of the microphone will produce diffraction effects which may either increase or decrease the pressure as compared with that in the free wave. Response curves showing the ratio of the open-circuit voltage to the pressure in the undisturbed sound wave are known as free-field curves; they will be considered further in Sect. 11.7.

The peak response in Fig. 11.2, which occurs near 2000 cycles/sec, is associated with the fundamental resonant frequency of the diaphragm, and the uneven response above this frequency is due to the breaking up of the diaphragm into various overtone modes of vibration. If the diaphragm is tightly stretched, instead of being merely clamped at its rim, its effective stiffness can be increased, with a corresponding increase in the fundamental frequency. The use of a stretched diaphragm makes it possible to extend the region of relatively uniform response to about 8000 cycles/sec, but only at the expense of a decreased sensitivity.

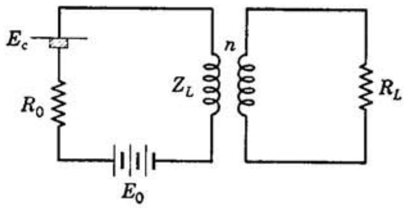

Fig. 11.3. Transformer coupling of the output of a carbon microphone to a load R_L. ($Z_L = n^2R_L$.)

In using a carbon microphone it is necessary to insert a load $\mathbf{Z}_L$ into the simple circuit of Fig. 11.1*b*. An efficient method of obtaining maximum output is to couple the microphone through a transformer, as shown in Fig. 11.3. Here the signal voltage $\mathbf{E}_L$ developed in the primary of the transformer is

$$\mathbf{E}_L = E_c \frac{\mathbf{Z}_L}{R_0 + \mathbf{Z}_L} \qquad (11.9)$$

As is to be expected, the maximum power is developed in this load when the impedance $\mathbf{Z}_L$ is a pure resistance of magnitude R_0.

11.3 Condenser Microphone. A condenser microphone is one that depends for its operation on the variation in capacitance between a fixed plate and a tightly stretched metal diaphragm. Its development by Wente in 1917 represents an important milestone in the history of modern electroacoustics, and for a number of years this type of microphone was the accepted standard for high-quality sound systems. However, the condenser microphone has a number of disadvantages, such as a very high internal impedance, which necessitates locating a preamplifier in the immediate vicinity of the microphone and leads to the generation of noise in the high-impedance circuit required to couple it to the grid of the preamplifier tube. The microphone also requires a polarizing voltage ranging from about 200 to 400 volts, which must be supplied by batteries or by a rectifier having an exceptionally well-filtered output. As a consequence of these disadvantages, condenser microphones have been supplanted by either crystal or electrodynamic microphones in many sound systems, but their extensive use as primary standards for calibration

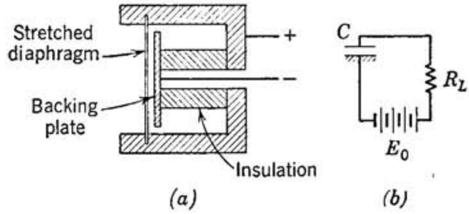

Fig. 11.4. (*a*) Simplified cross section of a condenser microphone. (*b*) Simplified output circuit of a condenser microphone.

purposes, in acoustic research, and for high-fidelity recording of sound, still justifies a somewhat detailed analysis.

The simple condenser microphone shown in Fig. 11.4*a* consists of a thin stretched metal diaphragm, usually of steel or aluminum, having a radius a, and separated by a small distance d from a parallel rigid plate. The rigid plate is insulated from the remainder of the microphone, and a polarizing voltage E_0 is applied between it and the diaphragm, as indicated in the accompanying circuit diagram. When a sound wave impinges upon the diaphragm, the resulting displacement of the latter alters the electrical capacitance C of the microphone, causing a signal voltage e_L to appear across the load resistor R_L. Let us assume that the capacitance at any instant is given by

$$C = C_0 + C_1 \sin \omega t \tag{11.10}$$

where C_0 is the capacitance in the absence of any applied pressure, and C_1 is the amplitude of the change in capacitance resulting from the application of a sinusoidal pressure variation. In the circuit of Fig. 11.4*b*

$$E_0 - iR_L = \frac{\int i\,dt}{C} \tag{11.11}$$

Substitution of equation 11.10 into equation 11.11 and differentiation with respect to time t gives

$$(C_0 + C_1 \sin \omega t)R_L \frac{di}{dt} + (1 + R_L C_1 \omega \cos \omega t)i - E_0 C_1 \omega \cos \omega t = 0 \tag{11.12}$$

A series solution of this equation is most readily obtained by assuming

$$i = \sum A_n \sin (n\omega t + \phi_n) \tag{11.13}$$

In all practical condenser microphones $C_1 \ll C_0$, even for very intense sounds, and consequently the amplitudes A_2, A_3, A_4, $\cdots$ of the higher harmonic overtones are negligible compared to A_1. Then

$$i \approx \frac{E_0 C_1}{C_0} \cdot \frac{\sin(\omega t + \phi_1)}{\sqrt{(1/\omega C_0)^2 + R_L{}^2}} \tag{11.14}$$

where

$$\tan \phi_1 = \frac{1}{\omega C_0 R_L} \tag{11.14a}$$

The voltage drop across the resistor R_L resulting from this current is

$$e_L = R_L i = \frac{E_0 C_1}{C_0} \cdot \frac{R_L \sin(\omega t + \phi_1)}{\sqrt{(1/\omega C_0)^2 + R_L{}^2}} \tag{11.15}$$

Equation 11.15 indicates that a condenser microphone may be considered as equivalent to a generator having an open-circuit voltage amplitude

$$E_c = \frac{E_0 C_1}{C_0} \tag{11.16}$$

and an internal capacitive impedance $1/j\omega C_0$.

When the radius a and distance d are expressed in meters, the capacitance C_0 of the microphone in *farads* is given by

$$C_0 = \frac{\epsilon_0 \pi a^2}{d} \tag{11.17}$$

where $\epsilon_0 = 8.85 \times 10^{-12}$ farad/meter is the permittivity of free space. Upon multiplying by 10^{12} this equation becomes

$$C_0 = 27.8 \frac{a^2}{d} \tag{11.17a}$$

which gives the capacitance in $\mu\mu f$. Let us now assume that the pressures in the sound wave displace the stretched diaphragm in a manner analogous to that of the forced vibrations of a membrane, as discussed in Sect. 4.8. Then for such low driving frequencies that $ka < 1$, or, as given by equation 4.35, that

$$f < \frac{1}{2\pi a}\sqrt{\frac{T}{\sigma}}$$

equation 4.34 shows that the average displacement $\bar{y}$ of the surface of the diaphragm is

$$\bar{y} = \frac{Pa^2}{8T} \sin \omega t \tag{11.18}$$

In this equation P represents the pressure amplitude in newtons per square meter, and T the tension in the diaphragm in newtons per meter. Displacing the diaphragm of the microphone an average distance $\bar{y}$ from its normal position towards the fixed plate will change its capacitance from C_0 to C, where

$$C = \frac{\epsilon_0 \pi a^2}{(d - \bar{y})} = \frac{C_0 d}{d - \bar{y}} \tag{11.19}$$

Since the amplitude of $\bar{y}$ is always small compared to d, equation 11.19 may be expanded as a series

$$C = C_0 \left[1 + \frac{\bar{y}}{d} + \left(\frac{\bar{y}}{d} \right)^2 + \cdots \right]$$

Neglecting $(\bar{y}/d)^2$ and higher-order terms, this becomes

$$C = C_0 + \frac{C_0 \bar{y}}{d} = C_0 + \frac{C_0 P a^2}{8dT} \sin \omega t \tag{11.20}$$

A comparison of this equation with the previously assumed equation (11.10) shows that

$$C_1 = \frac{C_0 P a^2}{8dT} \tag{11.21}$$

so that the theoretical amplitude of the open-circuit voltage of this idealized simple condenser microphone, as defined by equation 11.16, is

$$E_c = \frac{E_0 P a^2}{8dT} \tag{11.22}$$

As a typical numerical example let us consider a microphone constructed with an aluminum diaphragm 0.00004 m thick, having a radius $a = 0.01$ m and stretched to a tension of $T = 20{,}000$ newtons/m. If the spacing between the diaphragm and the backing plate is $d = 0.00004$ m and the polarizing voltage is $E_0 = 300$ volts, then the theoretical open-circuit voltage response is

$$M_c = \frac{E_c}{P} = \frac{300 \times 0.01^2}{8 \times 0.00004 \times 20{,}000} = 4.7 \times 10^{-3} \frac{\text{volts}}{\text{newton/m}^2}$$
$$= 4.7 \times 10^{-4} \text{ volts/microbar}$$

Using the same reference level as for the carbon microphone, i.e., one volt per microbar, the response level in decibels is

$$n = 20 \log 4.7 \times 10^{-4} = -66.6 \text{ db}$$

Measured values of the constant-pressure response of such a microphone are observed to agree with the predicted response to within a small percentage of error in the frequency range below 8000 cycles/sec. This is to be anticipated, since the limiting frequency, as predicted by equation 4.35, is

$$f = \frac{1}{2\pi \times 0.01}\sqrt{\frac{20{,}000}{2700 \times 0.00004}} = 6800 \text{ cycles/sec}$$

In this expression the area density σ of the aluminum diaphragm is represented by the product of its volume density $\rho = 2700 \text{ kg/m}^3$ and its thickness, 0.00004 m. The fundamental frequency of the diaphragm, as given by equation 4.14, is 2.405 times the above frequency, or 16,400 cycles/sec. In the vicinity of the latter frequency the microphone will be observed to have a maximum response, which is some 5 to 10 db above the low-frequency response, with the exact amount of this increase depending

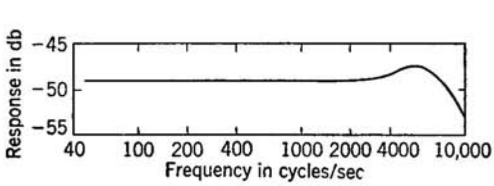

Fig. 11.5. Typical constant-pressure frequency-response characteristic of a condenser microphone in decibels relative to 1 volt per microbar.

upon the magnitude of the damping forces. Above this frequency the response falls off rapidly, since the motion of the diaphragm then becomes mass-controlled, with the result that the average displacement $\bar{y}$ is no longer independent of frequency but instead decreases inversely with increasing frequency.

Figure 11.5 shows an open-circuit constant-pressure frequency-response curve typical of the WE 640AA condenser microphone, a widely used microphone for making acoustic measurements. It is to be noted that this curve shows only a small rise in response in the vicinity of its fundamental resonant frequency of 6000 cycles/sec. This desirable feature is obtained by constructing the microphone so that the viscous damping associated with the motion of air to and from the region adjacent to the diaphragm through special slots in the fixed backing plate becomes effective at this frequency.

The capacitance C_0 of the microphone considered in the above numerical example is

$$C_0 = 27.8\,\frac{0.01^2}{0.00004} = 69.5\,\mu\mu\text{f}$$

Because of this small capacitance the internal impedance $1/\omega C_0$ is very high at audio frequencies. For example, its value at 100 cycles/sec is

$$\frac{10^{12}}{200\pi \times 69.5} = 23 \text{ megohms}$$

Consequently, the load resistor R_L must be about 50 megohms if the voltage across it is to be approximately equal to that generated in the microphone.

Because of this high internal impedance it is necessary to provide at least one stage of preamplification located in the immediate vicinity of the microphone, as indicated in Fig. 11.6. If this is not done and the microphone is instead connected through a long cable to its amplifier, the electrical capacitance of the cable is in parallel with the capacitance C_0 of

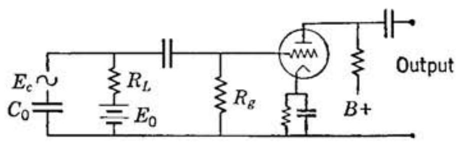

Fig. 11.6. Simple single-stage preamplifier for use with condenser microphone C_0.

the microphone. Since the capacitance of ordinary shielded microphone cable is about 20 to 40 $\mu\mu$f per foot, the total capacitance of even relatively short runs will be greater than C_0, thus effectively increasing the latter and hence decreasing the sensitivity of the microphone, as is apparent from equation 11.16. Since the internal impedance of the microphone is a capacitance, the primary effect of the cable capacitance is attenuation, without appreciable frequency discrimination.

Currently, condenser microphones are commonly used as standards for calibration purposes. For this application the requirement of incorporating a preamplifier in the microphone housing is not particularly disadvantageous, except that the resulting increase in physical size may produce diffraction effects that distort the sound waves being measured. An advantage of the condenser microphone for standardization work is that it does not require a coupling transformer, as do electrodynamic microphones, and thus avoids the variations in voltage ratio of the transformer which always occur with variations in the frequency or load. Furthermore, the open-circuit response of a condenser microphone is independent of such variable physical quantities as resistance and magnetization. This makes it possible to construct microphones which are nearly exact physical duplicates, and whose calibration may also be expected to remain constant with the elapse of time, thus permitting the precise calibration of one instrument to serve for the others.

11.4 Piezoelectric Microphones. Piezoelectric microphones employ crystals or dielectrics which upon being distorted by the action of incident sound waves become electrically polarized and produce voltages linearly related to the mechanical strains. A precise mathematical analysis of the piezoelectric type microphone is not warranted in this book. Instead, we must be satisfied with a nonmathematical discussion of their characteristics. The *direct* piezoelectric effect was discovered by the brothers Curie in 1880. As an illustration of this effect, let us consider Fig. 11.7. If the orientation of the crystal cut is such that compression along the indicated axis causes the upper face to become positive with respect to the lower, the polarity of the charge and corresponding electrical potential will be reversed if the crystal is subjected to a tension force along this same axis. By an *inverse* effect, a crystal will become strained when it is polarized by the application of an externally supplied electrical potential across the crystal. In a discussion of *crystal* and *ceramic* microphones, one is concerned solely with the direct piezoelectric effect. In the following chapter, by contrast, upon discussing the radiation of sound into liquids by crystal and ceramic sonar transducers, we will be concerned primarily with the inverse piezoelectric effect. However, since the piezoelectric effect is reversible, it is to be noted that all types of piezoelectric microphones will function as weak sources of sound when an alternating voltage is applied to their terminals.

Rochelle salt crystals have the strongest piezoelectric effect of any piezoelectric material and consequently have been widely employed in the design of crystal microphones. Unfortunately, crystals cut from this substance are subject to deterioration in the presence of moisture and are permanently damaged if subjected to temperatures in excess of 115°F. Furthermore, the 45° X-cut Rochelle salt crystal, which is frequently used

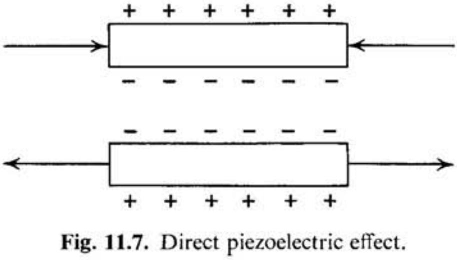

Fig. 11.7. Direct piezoelectric effect.

because of its high electromechanical coupling coefficient, is subject to large variations in its dielectric constant, which also affects the sensitivity or voltage output of the crystal. Crystals cut from the synthetic crystal ammonium dihydrogen phosphate, which are usually designated as ADP crystals, are commonly used in constructing microphones that must operate over a wide range of temperatures, for although they are somewhat less sensitive than Rochelle salt crystals, they can be raised to a temperature in excess of 200°F without deterioration and also exhibit much less variation in their piezoelectric and dielectric properties with changes in temperature. Another useful piezoelectric substance is a ceramic material made from barium titanate. This ceramic is rendered piezoelectric by permanently polarizing it electrically with a high electrostatic potential gradient of about 20,000 volts/cm for a period of several minutes. The permanent polarization of this material is enhanced by raising its temperature above its Curie temperature of 120°C and then applying the external polarizing voltage during the cooling cycle. Microphones using this form of polarized barium titanate and similar materials are known as *ceramic* microphones. They may be used interchangeably with crystal microphones, except that their sensitivity is about 10 db below that of the Rochelle salt or ADP types. On the other hand, ceramic microphones have an advantage as compared to crystal microphones in that they may withstand much higher temperatures and are not as readily damaged by moisture or high humidity.

The magnitude of the resulting potential difference produced in a piezoelectric material depends upon the type of deformation and its orientation relative to the various axes of the crystal. Deformations of bending, shear, and compression types have been utilized. The deformation may be brought about by having the sound waves act directly upon the piezoelectric material. The principal disadvantage of a microphone of this type is associated with the large mechanical impedance of its vibrating element. For use in liquids, such a large impedance is not objectionable and transducers (hydrophones) of this type are commonly used, but in air because of the large mechano-acoustic impedance mismatch, very small output voltages would be obtained from normal acoustic pressures. As a consequence, piezoelectric microphones are usually constructed in a manner similar to that shown in Fig. 11.8. Here, the sound waves act upon a light diaphragm whose center is in turn linked to an end or corner of the piezoelectric element by means of a driving pin. Although the piezoelectric element of such a microphone could be constructed with a single crystal as the voltage-generator, two crystals are usually sandwiched together to form an assembly known as a *Bimorph*. In general, a Bimorph element has a smaller mechanical impedance than does a single crystal

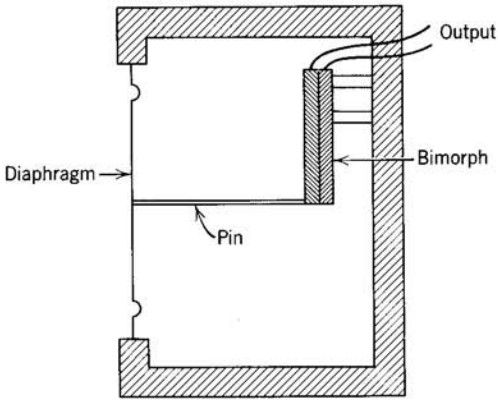

Fig. 11.8. Diaphragm actuated crystal microphone.

producing the same voltage output. Each crystal of the Bimorph is plated on both faces in order to facilitate the making of electrical connections. Either a series or a parallel connection of the two crystals may be used, the series connection giving a larger voltage output and the parallel connection giving a lower internal impedance.

The voltage output of a Bimorph element is proportional to the amplitude of its deformation. Hence, as for condenser microphones, the moving elements of the microphone must be designed as a stiffness-controlled system. Consequently, it is necessary to arrange that the fundamental frequency of mechanical resonance of the entire vibrating system, including the diaphragm, connecting pin, and Bimorph, be at a frequency above that of the desired range of relatively uniform response. This is readily accomplished through a proper choice of stiffness of the Bimorph and mass of the vibrating system.

Piezoelectric microphones are widely used in public-address systems, with sound-level meters, and for hearing aids. They have a satisfactory frequency response for such applications, are relatively high in sensitivity, low in cost, and small in size. Inexpensive diaphragm actuated types are available which cover the frequency range from 20 to 10,000 cycles/sec with a maximum variation in sensitivity of less than 5 db from their average sensitivity. A typical average sensitivity is -50 db relative to 1 volt per microbar. The electrical impedance of a piezoelectric microphone is that of a dielectric capacitor. A typical value for this capacitance is 3000 $\mu\mu$f. This is a relatively large capacitance, as compared to that of a condenser microphone, so that these microphones may be connected to an audio amplifier by a cable of moderate length without an intervening preamplifier being required.

11.5 Moving-Coil Electrodynamic Microphone. The simple moving-coil or "dynamic" microphone consists of a light diaphragm, to which a small coil is rigidly attached. The action of sound waves on the diaphragm causes the coil to move in the radial field of a permanent magnet, thus generating an emf expressed in volts of

$$e = Blv \tag{11.23}$$

where B is the flux density of the magnetic field in webers/m^2, l is the length of wire in the coil expressed in meters, and v is its velocity in meters per second. Basically, a moving-coil microphone is similar to a direct-radiator loudspeaker, except that it converts acoustic energy into electrical energy, instead of the reverse. As a matter of fact, the small direct-radiator loudspeakers of an interoffice communications system usually serve as the microphones of the system.

As an introduction to the problem of designing a satisfactory moving-coil microphone, let us consider its mechanical system as equivalent to a simple oscillator of mass m_0, stiffness s_0, and resistance R_0. The velocity of the coil is then

$$\mathbf{v} = \frac{\mathbf{f}}{\mathbf{Z}_m} = \frac{PSe^{j\omega t}}{R_0 + j(\omega m_0 - s_0/\omega)} \tag{11.24}$$

where S is the area of the diaphragm and P is the pressure amplitude acting on the diaphragm. Consequently, if the voltage output for constant sound pressure on the diaphragm is to be independent of frequency, the mechanical impedance $\mathbf{Z}_m$ must also be independent of frequency. This requires that R_0 be large, i.e., that the system be resistance-controlled. On the other hand, a high voltage sensitivity can be obtained only by making the velocity amplitude as large as possible, which requires a small mechanical impedance. Therefore, it is impossible to satisfy both the requirement of high sensitivity and uniformity of response by employing a mechanical system equivalent to a simple oscillator. Instead, additional mechanical elements are utilized to compensate for the increase in mass reactance ωm_0 at high frequencies and in stiffness reactance s_0/ω at low frequencies, and thus to provide a fairly uniform response, and yet a low mechanical impedance.

It is possible to design electrical networks capable of transmitting wide bands of frequencies by combining a number of resonant circuits. In 1931 Wente and Thuras[1] published a paper showing how the same expedient could be resorted to in the design of a satisfactory mechanical system for the moving-coil microphone. The success of their efforts is but one of many examples illustrating the fruitfulness of the application of electrical network techniques to acoustic problems.

[1] Wente and Thuras, *J. Acoust. Soc. Am.*, **3**, 44 (1931).

Let us consider the mechanical circuit of Fig. 11.9. It can be shown that the input impedance is

$$\mathbf{Z}_m = R_m + jX_m \tag{11.25}$$

where

$$R_m = \frac{s_1^2 R_1}{R_1^2\omega^2 + m_1^2(\omega_1^2 - \omega^2)^2} + R_0 \tag{11.25a}$$

$$X_m = \frac{s_1\omega[m_1^2(\omega_1^2 - \omega^2) - R_1^2]}{R_1^2\omega^2 + m_1^2(\omega_1^2 - \omega^2)^2} + m_0\omega - \frac{s_0}{\omega} \tag{11.25b}$$

and

$$\omega_1^2 = \frac{s_1}{m_1} \tag{11.25c}$$

The mechanical constants R_0, m_0, s_0, R_1, m_1, and s_1 can be chosen so that the absolute value of the mechanical impedance $\mathbf{Z}_m$ is fairly uniform over a rather wide range of frequencies. Curve A of Fig. 11.10 shows its value in the range of frequencies from 40 to 10,000 cycles/sec for the following values of the mechanical constants: $R_0 = 1$, $R_1 = 24$, $s_0 = 10{,}000$, $s_1 = 1{,}000{,}000$, $m_0 = 0.0006$ kg, and $m_1 = 0.0003$ kg. For purposes of comparison, the mechanical impedance of the simple oscillator $R_0 m_0 s_0$ alone has been plotted in curve B, and that of a similar oscillator for which R_0 is 25 in curve C. It is evident that curve A is flatter than either curve B or curve

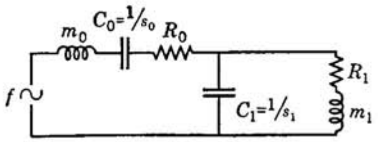

Fig. 11.9. Mechanical circuit of a moving-coil microphone.

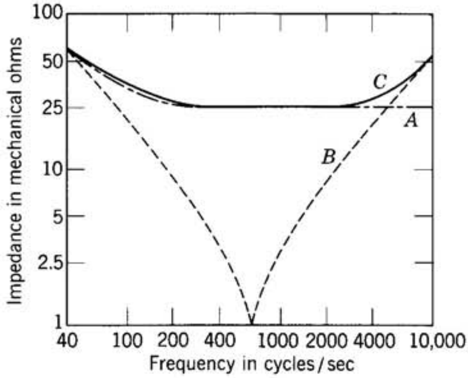

Fig. 11.10. Possible mechanical impedances for the moving element of a moving-coil microphone.

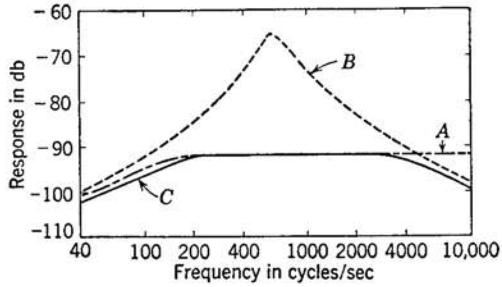

Fig. 11.11. Constant-pressure frequency-response characteristics in decibels relative to 1 volt per microbar for simple moving-coil microphones having impedances as indicated in Fig. 11.10.

C, and consequently the corresponding mechanical system will lead to a more uniform response of the microphone.

Upon combining equation 11.23 with equation 11.24 the expression for the open-circuit response M_m of a moving-coil microphone expressed in volts per newton/m^2 becomes

$$M_m = \frac{E_m}{P} = \frac{BlS}{Z_m} \tag{11.26}$$

The open-circuit voltage response for a diaphragm of 0.0004-m^2 effective area attached to a coil of 10-m length, and operating in a field of 1.5 webers/m^2 is plotted in Fig. 11.11 for each of the three mechanical systems considered above.

A cross-sectional view of a moving-coil microphone having the mechanical characteristics of the circuit of Fig. 11.9 is shown in Fig. 11.12. The diaphragm is composed of a spherical shell which vibrates as a rigid piston in the useful range of frequencies. The stiffness s_0 and the resistance R_0 are contributed by the corrugated annulus supporting the diaphragm. The stiffness s_1 is due primarily to compression of the air trapped in the chamber beneath the diaphragm. The mass m_1 and the resistance R_1 arise from viscous forces opposing the flow of air through the capillaries of the silk cloth. The stiffness due to the air chamber below the silk cloth is relatively small and may be neglected.

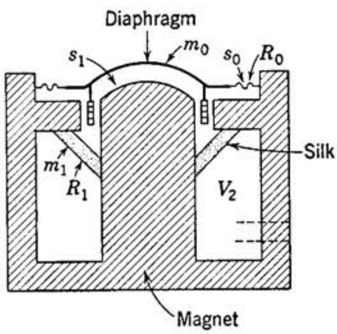

Figs. 11.12. Schematic cross section of a moving-coil microphone.

The low-frequency response of this microphone can be still further improved by the addition of a tube connecting the lower chamber to outer air, as indicated by dotted lines in Fig. 11.12. At low frequencies the phase of the acoustic pressure introduced into V_2 by this tube is shifted 180° before acting on the rear of the diaphragm, thus increasing the force on the diaphragm and hence the output of the microphone. Fundamentally, this procedure is similar to enhancing the low-frequency output of a loudspeaker through the use of a phase-inverter type of cabinet.

The open-circuit voltage sensitivity of the above moving-coil microphone is about 2.4×10^{-5} volt per microbar, or -92.4 db, which is much lower than that of the condenser and crystal microphones previously considered. However, the internal impedance of the microphone is quite low, about 10 ohms, and hence a transformer having a step-up voltage ratio can be used to match this impedance to the high input resistance of the first stage of a following amplifier. If the turns ratio of this transformer is n, the effective open-circuit voltage of the microphone is increased by the factor n, its internal impedance by n^2, and its open-circuit response, as measured at the secondary terminals of the transformer, by $20 \log n$ decibels. In general, when a transformer is used to match a moving-coil microphone to the high-impedance loads that must be used with condenser and crystal microphones, the effective open-circuit voltage response and power output of the moving-coil microphone are each some 10 db greater.

A further advantage of the moving-coil microphone is that if it is connected to a microphone cable through a transformer having a secondary to primary turns ratio of from three to one to ten to one, its output can be transmitted over fairly long distances without serious frequency discrimination or attenuation. At the far end of the line a second transformer is used to further step up the voltage, and to match the impedance to the input of a vacuum-tube amplifier.

11.6 Diffraction of Sound Waves by a Sphere. When low-frequency sound waves of known pressure amplitude impinge on the diaphragm of a condenser or moving-coil microphone, the measured responses are observed to agree with the predictions of equations 11.22 and 11.26. Furthermore, since pressure is a scalar quantity the low-frequency response is observed to be independent of the direction of the incident wave. However, at higher frequencies for which the linear dimensions of the microphone housing are no longer small compared to a wavelength, the measured response at normal incidence is observed to exceed the predicted response by as much as 6 db and is no longer independent of direction. One source of these discrepancies lies in the *diffraction* effects of the microphone.

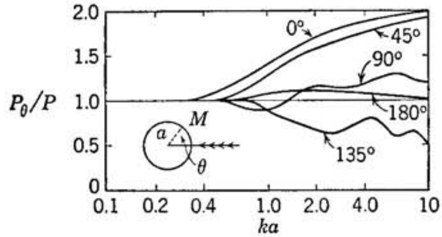

Fig. 11.13. Influence of diffraction on sound pressures produced at the surface of a sphere of radius a.

In general, the shapes of microphones and their housings are so irregular that it is impossible to predict theoretically their effect as diffractors of sound. However, a brief consideration of the diffraction effects of a spherical housing will show us roughly what to expect in more complicated situations. The diffraction of plane sound waves around a rigid sphere was first investigated mathematically by Rayleigh, and later extended by Ballantine.[2] Figure 11.13 show how the acoustic pressure at a point on the surface of a sphere varies with frequency for various angles of incidence of the acoustic waves. In this figure the ordinates are the ratio P_θ/P, where P_θ is the acoustic pressure amplitude at a point M on the surface whose polar angle to the direction of incidence of the plane waves is θ and where P is the pressure amplitude in the undisturbed sound wave. The abscissas are the parameter $ka = 2\pi a/\lambda$, where a is the radius to the sphere. The curves are computed from the equation derived by Ballantine.

Fig. 11.14. Moving-coil pressure microphone mounted in a spherical housing of radius a.

It is to be noted that P_θ/P has a maximum value of two for normal incidence at high frequencies. Therefore, we may expect that, for normal incidence, diffraction effects will increase the high-frequency response of a pressure microphone by $20 \log 2 = 6$ db, as compared to the predicted constant-pressure responses of the previous sections. For sounds incident at either 90° or 180° diffraction effects are less than one decibel and are consequently entirely negligible. Diffraction is seen to reduce the response to waves incident in the vicinity of 135°.

As an example let us consider a pressure microphone housed in a sphere of 0.04-m radius, as shown in Fig. 11.14. Commerical microphones of this shape and approximate dimensions are commonly available. For this radius the condition $ka = 1$ corresponds to a frequency of 1400 cycles/sec.

[2] Ballantine, *Physics Rev.*, **32**, 988 (1928).

The microphone begins to enhance the response of sounds incident normally on its diaphragm at frequencies above 700 cycles/sec and becomes quite directional at frequencies above 2800 cycles/sec. It is evident that, if the effects of diffraction are to remain small throughout the audible range of frequencies, both the microphone and its housing must be small. A pressure microphone fulfilling this requirement will be quite nondirectional in its response.

A second source of directivity in a pressure microphone is the difference in phase between the forces exerted on its diaphragm by different segments of the incident wave when the direction of propagation is not perpendicular to its surface. In general this effect becomes pronounced when the frequency is such that $2a \sin \theta > \lambda$, where a is the radius of the diaphragm and θ is the angle between the incident sound wave and the normal to the diaphragm. When the above condition is satisfied, the average phase of the force acting on one half of the diaphragm is approximately opposite to that acting on the other half, while their amplitudes are nearly equal, with the result that the driving force is materially reduced. If the diaphragm of the microphone shown in Fig. 11.14 is assumed to have a radius of 0.02 m, the above condition indicates a sharp drop in the response in the vicinity of 7500 cycles/sec for waves incident at an angle of 90°.

When a pressure microphone is used to pick up sound from a large orchestra, or from some similar broad source, the sound reaching the diaphragm at normal incidence is only a small part of the total. Since the high-frequency response of the microphone varies with direction, its output will not truly represent the sound at the point of pick-up and will consequently contain a type of distortion. The situation can be somewhat improved by orienting the microphone so that its diaphragm is horizontal, thereby giving a response that is symmetrical about a vertical axis, although the microphone still remains directional with respect to positions in a vertical plane. Directivity could be completely avoided by making the microphone small enough, but calculations show that the entire instrument would have to be approximately one centimeter in diameter to reduce directional effects to a negligible value at 10,000 cycles/sec. Nondirectional microphones of this and even smaller size have been built and, although their sensitivity is rather low for some uses, they are admirably suited for use as *probe microphones* for measuring fairly intense sound fields without distorting them in the process.

11.7 Free-Field Response. As we have just seen, both diffraction and the finite size of the diaphragm produce differences between the sound pressure in the incident wave and that effective on the diaphragm of the microphone. Yet another phenomenon contributing to this difference arises

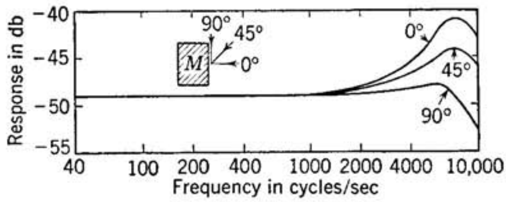

Fig. 11.15. Free-field frequency-response characteristics of a condenser microphone for various angles of incidence. (In decibels *re* 1 volt per microbar.)

from resonance in the cylindrical cavity or mouthpiece in front of the diaphragm. These resonances are similar to those of a closed pipe. At the resonant frequency, the pressure at the closed end immediately above the diaphragm may become very large compared to the free-space pressure of the sound actuating the system. Although the constant-pressure response of a microphone is more readily computed and measured, the free-space or free-field response determined under actual operating conditions is a more valid indication of the practical utility of a microphone.

By definition, the *free-field response* of a microphone is the ratio of the open-circuit voltage of the microphone to the free-field sound pressure existing at the microphone location before the microphone was introduced into the sound field. Plotted in Fig. 11.15 are typical free field response curves for the condenser microphone whose constant-pressure response was previously given in Fig. 11.5. Since the free-field response depends on the angle of incidence, this angle should always be specified. A comparison of the curves of Fig. 11.15 with that of Fig. 11.5 shows that, for this microphone, the latter curve is almost identical with the 90° free-field curve.

11.8 Pressure-Gradient Microphone. All the microphones previously considered in this chapter are classified as pressure microphones. The acoustic pressure acts on only one side of the moving diaphragm, and the resulting driving force is proportional to and in phase with this pressure. It is also possible to construct *pressure-gradient* microphones in which the driving force is proportional to the difference between the pressures acting on the two sides of a moving element.

As an introduction to the theory of this type of microphone, let us consider the net axial force exerted by a plane wave on a cylinder, when the sound is incident at an angle to the axis. In Fig. 11.16 let the axis of the cylinder of length l coincide with the x axis, and assume that a plane wave is incident from the left making an angle θ with the axis. The pressure in such a wave, as given by equation 6.48 is

$$\mathbf{p} = Pe^{j(\omega t - kx\cos\theta - ky\sin\theta)}$$

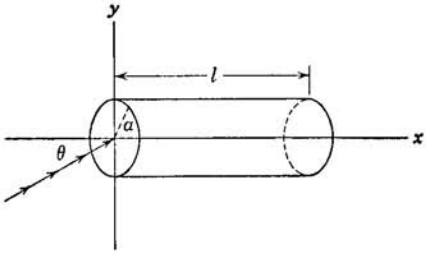

Fig. 11.16. Figure used in deriving axial pressure-gradient forces on a cylinder.

If the radius a of the cylinder is small compared to a wavelength λ, i.e., if $ka \ll 1$, and if the axis of the cylinder is chosen as the x axis, then variations in $ky \sin \theta$ over the ends of the cylinder may be neglected. Consequently,

$$\mathbf{p} \approx P e^{j(\omega t - kx \cos \theta)} \tag{11.27}$$

When the length l of the cylinder is so small that $kl \ll 1$, the *net* force acting to displace the cylinder in the x direction is

$$\mathbf{f} = -\frac{\partial \mathbf{p}}{\partial x} lS \tag{11.28}$$

where $S = \pi a^2$, the cross-sectional area of the cylinder. Upon substitution of equation 11.27 into equation 11.28 we obtain

$$\mathbf{f} = jklS\mathbf{p} \cos \theta \tag{11.29}$$

As compared to the force $\mathbf{f}_0 = S\mathbf{p}$ acting on the left face of the cylinder, this gradient force is seen to lead the acoustic pressure by 90°, to be proportional to frequency, as is indicated by the multiplication factor k, and to depend on the direction θ of the incident wave.

If the piston is so supported that it is mass-controlled, i.e., if the stiffness reactance and mechanical resistance are negligible compared to the mass reactance $j\omega m$, then

$$\mathbf{v} = \frac{\mathbf{f}}{j\omega m} = \frac{jklS\mathbf{p} \cos \theta}{j\omega m} = \frac{lS \cos \theta}{cm} \mathbf{p} \tag{11.30}$$

Since the amplitude of this complex velocity is independent of frequency and since the electrodynamic voltage generated in a conductor of length l_c moving across a magnetic field of strength B is $Bl_c v$, the open-circuit voltage generated by an idealized mass-controlled pressure-gradient microphone element is also independent of frequency, and is given by

$$\mathbf{e} = \frac{Bl_c lS \cos \theta}{cm} \mathbf{p} \tag{11.31}$$

The sensitivity of this microphone may be expressed in volts per newton/m^2 as

$$M = \frac{E}{P} = \frac{Bl_c lS \cos\theta}{cm} \tag{11.32}$$

11.9 Velocity-Ribbon Microphone. One practical example of a pressure-gradient microphone is the simple velocity-ribbon microphone of Fig. 11.17. It consists of a light corrugated metallic ribbon suspended between the magnetic polepieces N and S and freely accessible to acoustic pressures on both sides. This structure is indicated as mounted in a circular baffle of radius l, which in effect determines the length of the air path between the two sides of the ribbon. In actual instruments the shape of this baffle is primarily that of the magnetic field structure and is consequently quite irregular, so that a theoretical calculation of the difference in pressure would be extremely complex. However, if the baffle area is roughly circular or square, the distance l of equation 11.31 may be considered to equal the radius of a circular baffle or the half width of a square baffle.

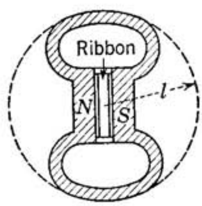

Fig. 11.17. Simple velocity-ribbon microphone mounted in a circular baffle of radius l.

The stiffness of the suspension system of the ribbon is made so small that its natural frequency is below the audible frequency range. As a result, the low-frequency response is quite uniform; however, it is limited in its magnitude by the maximum allowable physical displacement of the ribbon. As the frequency increases above 1000 cycles/sec, the response falls off from that predicted by equation 11.31, the decrease becoming more pronounced as kl approaches unity. This drop in response results from the fact that at the higher frequencies the dimensions of the microphone are no longer small as compared to the wavelength of the sound, so that the approximations made in deriving equation 11.28 are no longer valid. Instead, the net force is equal to the difference between the forces acting on the two ends of the cylinder, or

$$\mathbf{f} = PSe^{j\omega t}(e^{-jk0} - e^{-jkl\cos\theta}) = PSe^{j\omega t}(1 - e^{-jkl\cos\theta}) \tag{11.33}$$

The velocity is then

$$\mathbf{v} = \frac{\mathbf{f}}{j\omega m} = \frac{S(1 - e^{-jkl\cos\theta})}{j\omega m}\,\mathbf{p} \tag{11.34}$$

and the voltage is

$$\mathbf{e} = \frac{Bl_c S(1 - e^{-jkl\cos\theta})}{j\omega m}\,\mathbf{p} \tag{11.35}$$

The voltage response, as given by the magnitude of **e**/**p**, is

$$M_v = \frac{E}{P} = \frac{Bl_cS}{\omega m}\left[(1 - \cos(kl\cos\theta))^2 + \sin^2(kl\cos\theta)\right]^{1/2} \quad (11.36)$$

which may be reduced to

$$M_v = \frac{2Bl_cS}{\omega m}\sin\left(\frac{kl\cos\theta}{2}\right) \quad (11.36a)$$

It is evident that when $(kl\cos\theta)/2 = \pi$, $\sin[(kl\cos\theta)/2] = 0$. For normal incidence this condition is equivalent to $l = \lambda$, which indicates that the voltage response of the microphone will drop to zero at the frequency $f = c/l$. Curve *A* of Fig. 11.18 shows the open-circuit voltage response of a ribbon microphone having the following constants: $m = 10^{-6}$ kg, $S = 0.00005$ m^2, $l_c = 0.02$ m, $B = 0.5$ weber/m^2, and $l = 0.03$ m, as computed from equation 11.36*a* for normal incidence, i.e., for $\theta = 0°$. It will be seen that the response is quite uniform out to a frequency of 3000 cycles/sec, but falls off rapidly as the zero response frequency of $343/0.03 = 11{,}550$ cycles/sec is approached. Curve *B* shows measured values of the response of a microphone of this type. The increased response of the latter in the region from 2000 to 9000 cycles/sec is caused by diffraction effects. The upper limit of practical usefulness of this particular microphone is seen to be about 9000 cycles/sec, an entirely reasonable value.

Although the open-circuit voltage generated in the ribbon is very small, the internal impedance of a ribbon microphone is even less than that of a dynamic microphone, so that still higher turns ratios may be used in the transformer employed to match the microphone to the high input impedance of the following amplifier. When this is done, its output compares

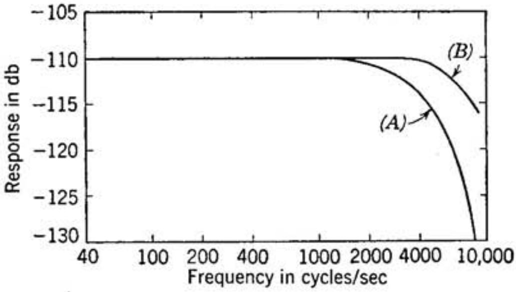

Fig. 11.18. Frequency-response characteristics of a velocity-ribbon microphone. (*A*) Computed. (*B*) Measured free-field. (In decibels *re* 1 volt per microbar.)

quite favorably with those of the pressure microphones previously considered.

Diffraction effects resulting from the presence of the assumed circular baffle, or the actual field-magnet structure, cause the pressure amplitudes acting on the front and back surfaces of the ribbon to differ from that of the incident wave. For normal incidence, the effective pressure amplitude P_0 on the front of a ribbon mounted in a circular baffle is

$$P_0 = P\sqrt{5 - 4\cos kl} \tag{11.37}$$

while that on the back remains equal to the amplitude P of the incident wave. Therefore, the pressure at the front rises to a value *three* times that in free space when $kl = \pi$, i.e., for $l = \lambda/2$. In the above microphone this corresponds to a frequency of about 5750 cycles/sec and at least partially accounts for the difference between curves A and B. The pressure P_0 falls back to its free-space value at $l = \lambda$, so that diffraction effects will not tend to produce any anomalous effects in this region of anticipated zero output.

The above type of pressure-gradient microphone is commonly referred to as a *velocity* microphone. When the microphone is receiving progressive plane waves this terminology has no significance, for in such waves the amplitudes of acoustic pressure and velocity are proportional to each other and are in phase. However, in the immediate vicinity of a source of spherical waves this is not true, and under these conditions it is possible to show that the velocity and the output of the moving element of a ribbon microphone coincide more nearly in amplitude and phase with the particle velocity than with the pressure. Since the ratio of particle velocity amplitude to pressure amplitude in a spherical wave increases as the source of sound is approached (Sect. 7.4), there will be a corresponding increase in the relative response of a velocity microphone as compared to that of a pressure microphone. This gain is more pronounced at low frequencies than at high frequencies, as is evident from the curves of Fig. 11.19. Each curve shows the relative gain in response at a particular frequency for a velocity microphone over a pressure microphone, as the distance of both microphones from the source is varied. The sensitivities of the microphones are assumed equal at a distance of 10 ft from the source. It is to be noted that the difference between the responses is negligible at frequencies above 500 cycles/sec.

There is another important case in which there is a pronounced difference between the responses of pressure and velocity microphones. This occurs when the microphones are used to measure a pattern of standing waves. Consider plane waves of wavelength λ to be incident normally on a rigid wall. At the wall the combination of incident and reflected waves results in a velocity node and a pressure antinode, whereas at a distance of a

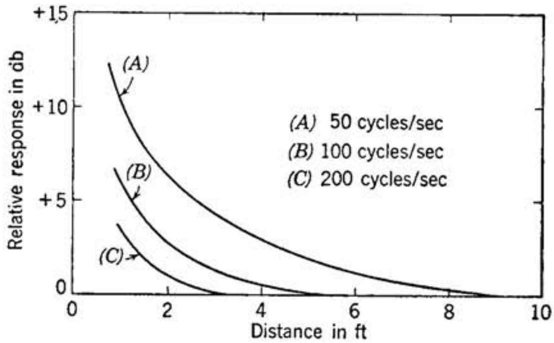

Fig. 11.19. Increase in response of a velocity microphone relative to that of a pressure microphone as a function of source distance.

quarter of a wavelength from the wall the conditions are reversed, giving rise to a pressure node and a velocity antinode. The observed response of a pressure microphone at the latter position is zero, whereas that of a velocity microphone reaches a maximum. This difference is readily explained if we consider the net force exerted on a pressure-gradient element of length l by both waves. The net force exerted by a wave traveling in the negative x direction is

$$\mathbf{f}_- = -jklS\mathbf{p}_- \tag{11.38}$$

and combining this with equation 11.29 we obtain for the net force exerted by both waves

$$\mathbf{f} = \mathbf{f}_+ + \mathbf{f}_- = jklS(\mathbf{p}_+ - \mathbf{p}_-) \tag{11.39}$$

This force is a maximum when the total pressure $\mathbf{p}_+ + \mathbf{p}_-$ is a minimum or zero. Consequently, if contradictory results are to be avoided, it is necessary to exercise care as to the type of probe microphone used to investigate a standing wave pattern.

11.10 Directional Characteristics of a Velocity-Ribbon Microphone. The velocity-ribbon microphone is *bidirectional* in its response, i.e., it favors waves incident in the vicinity of 0° or 180° and discriminates against those incident in the vicinity of 90° or 270°. One method of presenting the directional characteristics of a microphone is by a polar plot of its *relative response* $R(\theta)$ where the latter is defined by the equation

$$R(\theta) = \frac{(E/P)_\theta}{(E/P)_0} \tag{11.40}$$

In this equation, $(E/P)_\theta$ is the response of the microphone for waves arriving at an angle θ from the principal axis of the microphone and

$(E/P)_0$ is that for waves arriving along this axis. In order to derive the relative response of a velocity-ribbon microphone it becomes necessary to consider diffraction effects such as those just discussed in the previous section. The resulting relative response is somewhat similar to that of the idealized pressure-gradient element of Fig. 11.16 which may be derived from equation 11.36a to be

$$R(\theta) = \frac{\sin\left(\dfrac{kl\cos\theta}{2}\right)}{\sin(kl/2)} \tag{11.41}$$

In the low frequency region corresponding to $kl < \pi/2$, this expression may be simplified to

$$R(\theta) \approx \cos\theta \tag{11.41a}$$

Curve A of Fig. 11.20 shows a polar plot of the relative response of the microphone used as an example in Sect. 11.9 as measured at low frequencies, and curve B a similar plot of the relative response at a frequency of 6000 cycles/sec. It is to be noted that even at 6000 cycles/sec the relative response does not differ markedly from a plot of $\cos\theta$.

The directional characteristics of the response of a microphone are frequently expressed in terms of a *directivity factor* D, whose definition is analogous to that given for sound sources in Sect. 7.11. The directivity

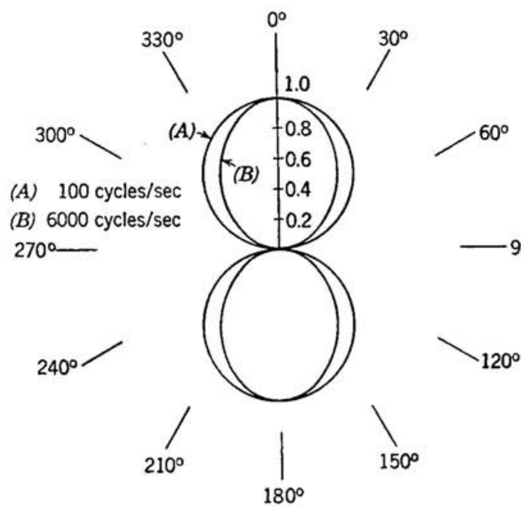

Fig. 11.20. Measured directivity characteristics of a velocity-ribbon microphone element mounted in a circular baffle.

factor of a microphone is the ratio of the square of the open-circuit voltage generated by sound waves arriving in a direction parallel to the principal axis of greatest response, to the square of that generated in a perfectly diffuse sound field having the same total mean square pressure. Since this ratio is a function of frequency, the frequency should be stated. An alternative definition states that the directivity factor is a measure of the ratio of electrical power generated in a nondirectional microphone by a diffuse sound field arriving uniformly from all directions, to that generated in a directional microphone having an axial response equal to the uniform response of the nondirectional microphone. In effect, the directivity factor measures the ability of a directional microphone to improve the signal to noise ratio for sound signals received along its principal axis relative to a diffuse noise field.

The *directivity index* d of a microphone is defined by

$$d = 10 \log D \tag{11.42}$$

It is a measure, expressed in decibels, of the extent to which a directional microphone raises the apparent pressure level of sounds arriving along its principal axis, as compared to that of sounds arriving uniformly from all directions.

The above definition of the directivity factor may be expressed mathematically by means of the equation

$$D = \frac{4\pi}{\displaystyle\int_0^{4\pi} R^2(\theta)\, d\Omega} \tag{11.43}$$

where $d\Omega$ is an element of solid angle. When the relative response $R(\theta)$ is symmetrical with respect to the principal axis, as is commonly the situation, the element of solid angle may be taken as $d\Omega = 2\pi \sin\theta\, d\theta$ and equation 11.43 simplfies to

$$D = \frac{2}{\displaystyle\int_0^{\pi} R^2(\theta) \sin\theta\, d\theta} \tag{11.43a}$$

For a velocity ribbon microphone $R(\theta) \approx \cos\theta$ which upon substitution into equation 11.43*a* and integration leads to a directivity factor of $D = 3$ and a corresponding directivity index of $10 \log 3 = 4.8$ db.

The bidirectional velocity microphone has three principal advantages. Since it discriminates by a factor of three against all-around background noise or reverberation, it allows speakers to stand at $\sqrt{3}$ times as great a distance from the microphone as from a nondirectional microphone, and yet to generate an electrical output having the same signal to noise ratio.

Secondly, its bidirectional characteristic permits speakers to face each other from opposite sides of the microphone, and have their speech picked up with equal efficiencies. Finally, the sharp nulls at 90° and 270° make it possible to orient the microphone so that the regions of zero response are pointed towards particularly annoying sources of noise, thus completely eliminating direct pick-up from them.

11.11 Unidirectional Cardioid Microphone. If the output of a pressure element is combined in series with that of a velocity element, the resulting response favors the reception of sounds coming from one hemisphere and discriminates against those arriving from the opposite hemisphere. If the axial response $(E/P)_0$ of the velocity element is made equal to the nondirectional response of the pressure element, then the net response of the two elements in series is

$$\left(\frac{E}{P}\right)_{UD} = \left(\frac{E}{P}\right)_0 \cos\theta + \left(\frac{E}{P}\right)_0 = \left(\frac{E}{P}\right)_0 (1 + \cos\theta) \quad (11.44)$$

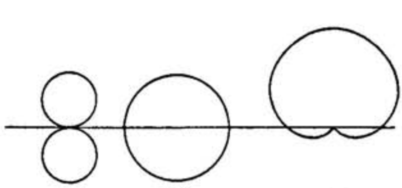

(a) (b) (c)

Fig. 11.21. Directional response characteristics of various microphones. (*a*) Velocity or bidirectional microphone. (*b*) Pressure or nondirectional microphone. (*c*) Cardioid or unidirectional microphone.

Figure 11.21*a* shows the directional response of a velocity ribbon element, Fig. 11.21*b* that of an equally sensitive pressure element, and Fig. 11.21*c* that of the combination. The combined directional characteristic is a cardioid of revolution, with the axis of revolution normal to the plane of the ribbon element. Microphones having a response of this type are commonly known as *unidirectional* or *cardioid* microphones. The principle on which they are based is similar to that used in combining the output of a vertical antenna with that of a loop, thus forming a radio direction finder which is capable of determining the sense of the incoming signal.

Numerous commercial forms of this microphone have been devised. One form employs a single-ribbon element, the upper part being velocity-operated and the lower part pressure-operated. The magnetic field structure is similar to that of a standard velocity-ribbon microphone, but, although the rear of the velocity portion of the ribbon is exposed to the sound waves, the rear of the pressure portion is enclosed, and thus shielded from acoustic pressures. Since the velocity and pressure sections are formed from a single continuous ribbon, their outputs are automatically combined in series. In another form a ribbon-velocity element is mounted in the same housing with a moving-coil pressure element of conventional design, together with an electrical equalizer unit which adjusts the amplitude and phase of the moving-coil element to conform with that of the velocity element.

By methods similar to those employed with a velocity microphone, it can be shown that the directivity factor of a unidirectional cardioid microphone is also three. As a result of the large solid angle over which a cardioid microphone receives sound without appreciable discrimination, it is possible to cover widely separated speakers or musical instruments by a single microphone. Furthermore, if such a microphone is placed near the front of a stage, its directional characteristics are exceptionally well suited to picking up sounds from the stage, while excluding those from the audience.

11.12 Rating of Microphone Responses. There are an almost unlimited number of ways in which the response characteristics of a microphone may be expressed, and manufacturers exercise a considerable amount of individuality in their ratings. One of the most significant and precise methods of expressing the response of a microphone is to state the free-field open-circuit voltage generated in its primary element, relative to a reference response of one volt per microbar. This voltage is given as a function of frequency and is usually expressed in decibels by the equation

$$n = 20 \log (E/P) \tag{11.45}$$

where E is in volts and P in microbars. Since this response is also a function of direction, the orientation of the principal axis of the microphone with respect to the source of sound should also be specified. In addition, if the internal impedance of the element in which the voltage is generated is low enough so that a matching transformer is desirable, this impedance should be specified, for it will then be possible to design a transformer capable of matching the microphone to any given load and to calculate the voltage and power generated in this load.

The first two columns of Table 11.1 give typical values of the free-field open-circuit response and internal impedance of a few of the most commonly used microphones, operating at a frequency of 1000 cycles/sec. It is to be noted that the relatively low responses of the moving-coil, velocity, and cardioid microphones are all generated in low impedances. Sometimes the response of a low-impedance microphone is given in terms of the voltage generated in the secondary of the transformer used to match its impedance to that of a 250-ohm line or to the high input impedance of a vacuum-tube amplifier. This procedure is to be deprecated, for the response then depends on the turns ratio of the particular transformer and hence does not truly represent the capabilities of the microphone.

A second method of rating microphones is in terms of the power that they are capable of delivering to a matched load. The most commonly used reference level for response ratings of this type is to assume that a zero decibel microphone is one having an output of 0.001 watt when it is

Table 11.1 Microphone response ratings at 1000 cycles per second

Type	Voltage Response, db	Internal Impedance, ohms	Power Response, db
Carbon	−45	100	−21
Condenser	−50	500,000	−63
Crystal	−50	100,000	−56
Moving-coil	−85	10	−51
Velocity	−105	<1	−54
Cardioid	−82	10	−48

located in a sound field of 10 microbars rms pressure. The reference pressure of 10 microbars is used instead of 1 microbar for the purely practical reason that it is more nearly representative of the actual pressure that is generated at the microphone by normal speech. The power in watts generated in a properly matched effective load resistance R_L is

$$W = \frac{E^2}{4R_L} = \left(\frac{E}{P}\right)^2 \frac{P^2}{4R_L} \tag{11.46}$$

so that the response level, relative to 0.001 watt from 10 microbars, is

$$n = 10 \log \left[\frac{\left(\frac{E}{P}\right)^2 \frac{10^2}{4R_L}}{0.001} \right] = 20 \log \left(\frac{E}{P}\right) - 10 \log R_L + 44 \tag{11.47}$$

The power response levels of the various types of microphones, as computed by this equation from the data of the first two columns of Table 11.1, are listed in the third column. It is apparent that, in spite of their lower voltage responses, the power responses of the moving coil, velocity, and cardioid microphones are considerably higher than those of the crystal or condenser microphones. As a matter of fact, since condenser and crystal microphones must be operated into loads of one megohm or more in order to produce useful outputs at the lower frequencies, their actual power outputs are some 10 db lower than those listed in the table. The primary advantage of rating microphones in terms of their power response levels is that the rating immediately indicates the gain that must be supplied by the amplifier to raise the signal generated in the microphone to any specified output level. For example, an amplifier having a gain of 90 db will raise the power generated in the moving-coil microphone of Table 11.1 by a 10-microbars sound wave to

$$-51 + 10 \log 0.001 + 90 = +9 \text{ db}$$

which corresponds to about 8 watts of electrical power.

A third method of rating microphones is in terms of the power that they deliver to a matched load relative to 0.001 watt when acted upon by a sound pressure of one microbar. Because of the variety of methods used in rating the responses of microphones, a decibel rating of a microphone is meaningless unless the zero level reference conditions and the impedance in which the voltage or power is generated are precisely specified.

11.13 Acoustical Reciprocity Theorem. The problem of making experimental measurements of the response and directivity curves of microphones, as well as those of underwater transducers, can be greatly simplified through the use of certain reciprocity theorems. One of them is a generalized acoustical reciprocity theorem which was first stated by Rayleigh and can be expressed in the following form: "Let an enclosed region have bounding surfaces S_1, S_2, S_3, $\cdots$, and let two separate distributions, generally different, of normal velocities v' and v'' over the bounding surfaces produce pressure fields p' and p'', respectively, over these surfaces. Then the surface integral of $(p''v' - p'v'')$ over all the bounding surfaces S_1, S_2, S_3, . . . vanishes." An equivalent brief mathematical statement of this theorem is

$$\iint_{(S_1,S_2,S_3,\cdots)} (p''v' - p'v'')\, dS = 0 \tag{11.48}$$

If the region being considered contains only one simple source, the general reciprocity theorem may be reduced to a form ascribed to Helmholtz, i.e., "In a region partially bounded and partially unbounded, a simple source at any point A produces the same sound pressure at another point B as would have been produced at A had the source been located at B." Therefore, at least for simple sources, the transmission characteristics of any sound path are the same in either direction.

As a specific example, let us apply the general theorem to show that the directivity pattern of a rigid plane piston, acting as a radiator of sound, is identical with its receiving response pattern when it is acting as the diaphragm of a microphone. Assume that all the bounding surfaces forming the enclosed region referred to in this theorem are fixed, except for the area S_p of the piston and a small spherical surface of radius a, where $ka \ll 1$. Then all bounding surfaces other than those of the piston and the sphere may be neglected, since they do not move. If the piston is acting as a source of sound, and the sphere as a receiver, then only the velocity v_p' at the surface of the piston has a value, whereas, if the conditions are reversed and only the sphere is acting as a source, then only v_s'', the radial velocity of the surface of the sphere, differs from zero. An application of equation 11.48 to this situation leads to

$$\iint_{S_p} p_p'' v_p' \, dS_p - \iint_{S_s} p_s' v_s'' \, dS_s = 0 \qquad (11.49)$$

where p_p'' is the pressure produced at the piston by motion of the spherical source, and p_s' is that produced at the spherical source by the motion of the piston. However, since the surface of the piston is assumed to be rigid, and hence moves as a unit, v_p' is independent of dS_p and may be removed from behind the first integral sign. Similarly, for a small spherical source, p_s' is constant over dS_s and likewise may be removed from behind the second integral sign. Finally, since $\iint_{S_p} p_p'' \, dS_p = F_p''$, the force acting on the piston, and since $\iint_{S_s} v_s'' \, dS_s = Q_s''$, the source strength of the sphere, equation 11.49 reduces to

$$\frac{Q_s''}{F_p''} = \frac{v_p'}{p_s'} \qquad (11.50)$$

This equation indicates that, for each relative position of piston and sphere, the receiving characteristic Q_s''/F_p'' of the piston, acting as a microphone, is identical with its transmitting characteristic v_p'/p_s', acting as a loudspeaker. For instance, if surrounding a piston by an infinite plane baffle doubles its output as a loudspeaker, it may also be expected to double its receiving response M as a microphone. Furthermore, if the directivity pattern and directivity index of a reciprocal transducer are measured in transmission, then we may assume an identical receiving pattern and directivity index, and vice versa. This reciprocity principle is satisfied by the commonly used crystal, condenser, and electrodynamic transducers, both microphones and loudspeakers.

11.14 Electroacoustical Reciprocity Theorem. The statement after Helmholtz of the acoustical reciprocity theorem may be restated in the form, "If a simple source of strength Q_1 at point A produces a sound pressure P_2

at point B, then a simple source of strength Q_2 at point B will produce a sound pressure P_1 at point A such that

$$\frac{Q_1}{P_2} = \frac{Q_2}{P_1}\text{''} \tag{11.51}$$

In this form the acoustical reciprocity theorem is seen to be analogous to a commonly used reciprocity theorem for linear passive electrical networks. For example, if a voltage E_1 in the first mesh of the circuit of Fig. 11.22 produces a current I_2 in the second mesh, then a voltage E_2 inserted into the second mesh where the current I_2 was measured, will produce a current I_1 in the first mesh such that

$$\frac{E_1}{I_2} = \frac{E_2}{I_1} \tag{11.52}$$

Since the principle of reciprocity applies separately to both electrical and acoustical systems and since acoustical and mechanical elements of an electroacoustic transducer may be transferred into equivalent electrical elements (see Sect. 10.2), we may anticipate that linear electroacoustic transducers will also satisfy an electroacoustic version of a reciprocity theorem. In one form the latter states that: "The *magnitude* of the ratio of the open-circuit voltage at the output terminals of a transducer, when it is used as a sound receiver, to the free-field sound pressure at any arbitrarily selected reference point near the transducer, divided by the *magnitude* of the ratio of the sound pressure produced at a distance d from this reference point, to the current flowing at the transducer input terminals when it is used as a sound emitter, is a *constant*." This constant is called the *reciprocity constant*, and equals

$$\frac{2d\lambda}{\rho_0 c}$$

where $\rho_0 c$ is the specific acoustic resistance of the medium, and λ is the wavelength being transmitted. This constant is seen to be independent of

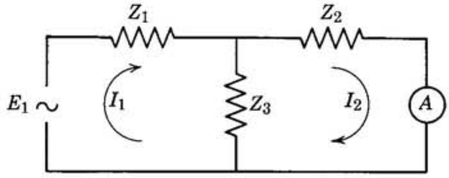

Fig. 11.22. Circuit diagram illustrating the reciprocity principle for a linear passive electrical network.

the type or constructional details of any particular transducer. In mathematical form this reciprocity principle may be stated as

$$\frac{M}{S} = \frac{2d\lambda}{\rho_0 c} \tag{11.53}$$

where M is the free-field microphone response of the transducer, expressed in volts per newton/m^2, and S is its speaker response, expressed in newtons/m^2 per ampere.

Rather than attempting a general proof[3] of this relationship, let us instead show that it is satisfied by the electrodynamic type of transducer. Consider a piston of surface area S_p and mechanical impedance Z_m, attached to a coil of electromechanical coupling given by $f = Bli$, and mounted in an infinite baffle. The axial pressure amplitude produced by such a piston at a distance d is given by equation 7.54 as

$$P = \frac{\rho_0 ckS_p}{2\pi d} U_0$$

where

$$U_0 = \frac{BlI}{Z_m}$$

and the speaker response $S = P/I$ of the piston is therefore

$$S = \frac{\rho_0 ckBlS_p}{2\pi dZ_m} \tag{11.54}$$

Its free-field response as a microphone is given by equation 11.26 as

$$M = \frac{2BlS_p}{Z_m} \tag{11.55}$$

where the factor 2 has been introduced to allow for the doubling of the free-field pressure in the sound wave at the surface of the piston. In the previous section this pressure doubling, which results from the presence of the infinite baffle, was explained by use of the reciprocity theorem. It can also be explained in terms of standing waves, since reflection at the baffle sets up a pressure antinode at its surface, and the pressure amplitude in this antinode is twice the pressure amplitude in the incident wave. If equation 11.55 is divided by equation 11.54 we obtain equation 11.53.

11.15 Reciprocity Calibration of a Microphone. The experimental calibration of microphones is greatly facilitated by the application of the electroacoustical reciprocity theorem. In one method three transducers

[3] See Beranek, *Acoustic Measurements*, pp. 113–120, John Wiley and Sons (1949).

are employed—the microphone A to be calibrated, a reversible transducer B which obeys the reciprocity principle, and a loudspeaker C. A convenient type of reversible transducer is a small back-enclosed direct-radiator loudspeaker. In step one of the calibration, the reversible transducer B is placed at a specific position in the sound field of the speaker C, as shown in Fig. 11.23a, and the open-circuit voltage generated in B by C is measured. This voltage is

$$E_B = M_B P_C \tag{11.56}$$

where M_B is the microphone response of B, and P_C is the sound pressure produced at B by speaker C. In step two the microphone A is substituted for the transducer B, as shown in Fig. 11.23b, and its open-circuit voltage E_A is measured for the same sound pressure P_C employed in step one. Then

$$E_A = M_A P_C \tag{11.57}$$

where M_A is the desired microphone response of A. These two equations may be combined to give

$$M_A = M_B \frac{E_A}{E_B} \tag{11.58}$$

In the final step of the calibration, the reversible transducer B is substituted for the speaker C, as indicated in Fig. 11.23c, and the output E_A' of microphone A is measured for a current I_B in transducer B. Then $E_A' = M_A P_B$. Combining this expression with $P_B = S_B I_B$, which gives

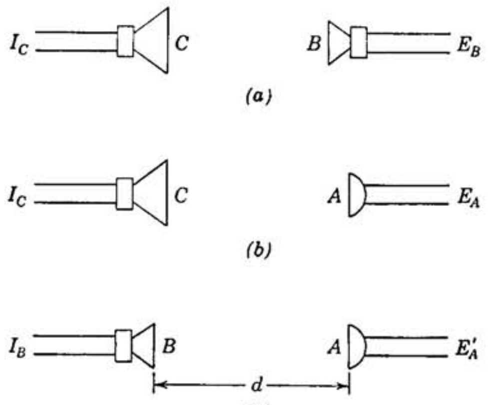

Fig. 11.23. Schematic representation of the three steps used in the reciprocity calibration of microphone A.

the pressure P_B produced by the transducer B as a function of its speaker response S_B, we obtain

$$E_A' = M_A S_B I_B \tag{11.59}$$

Then from equations 11.58 and 11.59

$$M_A^2 = \frac{M_B}{S_B} \cdot \frac{E_A E_A'}{E_B I_B} \tag{11.60}$$

The open-circuit voltage response M_A of microphone A, expressed in volts per newton/m^2, can now be obtained by substituting the reciprocity constant of equation 11.53 for M_B/S_B, which leads to

$$M_A = \left[\frac{2d\lambda E_A E_A'}{\rho_0 c E_B I_B}\right]^{1/2} \tag{11.61}$$

This method has the advantage of avoiding the necessity of attempting to produce measurable or calculable sound pressures, since all the basic measurements, other than the distance d, are electrical in nature. These measurements should be made either in a sound-deadened room such as an anechoic chamber, in large rooms where reflections are negligible, or outdoors at a considerable distance from reflecting surfaces. It is customary to convert the results obtained by use of equation 11.61 to volts per microbar by multiplying by the factor 0.1.

If two *identical* reversible microphones are available, the reciprocity principle makes it possible to calibrate both microphones by a single set of measurements involving only one setup. Here $E_A = E_B$, so that equation 11.61 reduces to

$$M_A = M_B = \left[\frac{2d\lambda E_A}{\rho_0 c I_B}\right]^{1/2} \tag{11.62}$$

Finally, it is possible to self-calibrate a microphone at high frequencies by using short pulse techniques. The microphone is first used as a sound source, and the voltage generated in it by reflection of the pulse from a 100 per cent reflecting surface is then determined.

PROBLEMS

11.1. The open-circuit voltage response of a carbon microphone is -40 db *re* 1 volt per microbar when connected to a 12-volt battery and its internal impedance is 100 ohms. Its diaphragm has an area of 0.001 m^2 and an effective stiffness of 10^6 newtons/m. (*a*) What is the numerical value of the resistance constant h for this microphone? (*b*) For an incident sound wave of 100 microbars pressure amplitude, what will be the ratio of the second harmonic to fundamental voltage developed in this microphone?

11.2. A condenser microphone diaphragm of 0.02-m radius and 0.00002-m spacing between diaphragm and backing plate is stretched to a tension of 10,000 newtons/m. (*a*) If the polarizing voltage is 200 volts, what is the low-frequency open-circuit voltage response of the microphone in volts per newton/m^2? (*b*) What is the corresponding response level in db relative to 1 volt per microbar? (*c*) When acted upon by a sound pressure of 1 newton/m^2 amplitude, what is the amplitude of the average displacement of the diaphragm? (*d*) What voltage will be generated in a load resistance of 5 megohms by this condenser microphone at a frequency of 100 cycles/sec when acted upon by a sound wave of 10 microbars pressure amplitude?

11.3. A small condenser microphone having a diameter of 0.8 cm is to be used as a probe microphone. The steel diaphragm is 0.001-cm thick and is stretched to the maximum allowable tension of 10,000 newtons/m. The spacing between the diaphragm and backing plate is 0.001 cm, and the polarizing voltage is 150 volts. (*a*) What is the fundamental frequency of the diaphragm? (*b*) What is the open-circuit constant-presssure response level and internal impedance of the microphone at 10,000 cycles/sec? (*c*) Considering diffraction effects of the microphone to be equivalent to that of a sphere of equal diameter, what is the free-field response level at this frequency?

11.4. A certain crystal microphone is rated as having an open-circuit voltage response level of -54 db *re* 1 volt per microbar and an internal capacitive impedance of 200,000 ohms at 400 cycles/sec. (*a*) If a plane wave of this frequency and 70 db pressure level *re* 0.0002 microbar is incident on the microphone, what voltage will be generated in a 500,000-ohm load resistor connected across the output terminals of the microphone? (*b*) What power will be generated in this resistor? (*c*) If the area of the diaphragm of the microphone is 0.0004 m^2, what is the ratio of this electrical power to the acoustic power incident on the microphone?

11.5. A crystal microphone of -60 db open-circuit constant-pressure voltage response level *re* 1 volt per microbar and having a diaphragm of 0.02-m diameter is inserted into the throat of an exponential horn of 1 meter length. The diameter of the throat of the horn is 0.02 m and that of its mouth is 0.25 m. For a frequency of 450 cycles/sec, compute the free-field response level of the microphone when mounted in the horn. Assume the plane waves to be incident along the axis of the horn and that the infinite horn equations apply as the waves progress from the mouth to the throat of the horn.

11.6. A small direct-radiator moving-coil loudspeaker is used both as a microphone and as a loudspeaker in an interoffice communication system. The constants of the speaker are as follows: $m = 0.003$ kg, $a = 0.05$ m, $R_m = 10$ kg/sec, $s = 50{,}000$ newtons/m, $B = 0.75$ weber/m^2, $l = 10$ m, $R_E = 1$ ohm, and $L_E = 0.01$ mh. (*a*) Calculate its open circuit voltage response level *re* 1 volt per microbar at a frequency of 1100 cycles/sec. (*b*) What is its power response level in decibels *re* 0.001 watt per 10 microbars at a frequency of 1100 cycles/sec?

11.7. A simple moving-coil microphone has a moving element of 0.0004-m^2 cross section, 0.001-kg mass, 10,000-newtons/m stiffness, and 20-kg/sec mechanical resistance. The coil has a resistance of 5 ohms, a length of 5 meters and moves in a magnetic field of 1.0-weber/m^2 flux density. (*a*) What is its open-circuit constant-pressure response level at 1000 cycles/sec? (*b*) What is its power response level into a matched impedance load of 5 ohms? (*c*) What is the ratio of this electrical power to the acoustical power incident on the diaphragm of the microphone?

11.8. A velocity-ribbon microphone is constructed by mounting a thin aluminum strip in a circular baffle of 4-cm radius. The aluminum strip is 0.001-cm thick, 0.4-cm wide, and 2.5-cm long. The magnetic field has a flux density of 0.25 weber/m^2. A plane wave of 250-cycles/sec frequency and 2-newtons/m^2 acoustic pressure is incident normally on the face of the ribbon. (*a*) What voltage is developed in the ribbon? (*b*) What is the open-circuit voltage response level at this frequency? (*c*) What is the amplitude of the displacement of the ribbon under the above conditions?

11.9. The moving element of a velocity-ribbon microphone is mounted in a circular baffle of 0.04-m radius. (*a*) Compute and plot a curve showing the amplitude of the pressure on the front surface of the element as a function of frequency from 400 to 4000 cycles/sec. Express this amplitude relative to that of an assumed constant incident amplitude as given by equation 11.37. (*b*) Compute and plot the angle of phase difference kl between the front and back surfaces of the ribbon in this same frequency interval. (*c*) Compute the net force acting on the ribbon in this same interval and then compute and plot the velocity amplitude of the ribbon. (*d*) What does this last curve indicate as to the nature of the voltage response curve of this microphone?

11.10. The ribbon element of a velocity microphone is mounted in a circular baffle of radius l. Assuming plane waves in the frequency range from 100 to 5000 cycles/sec to be normally incident on the baffle, compute and plot the relative responses for baffles of 5-cm radius, 10-cm radius, and 15-cm radius, respectively. Neglect any effects due to diffraction.

11.11. Given a pattern of standing plane waves as represented by $p = 2P \cos \omega t \sin kx$. Derive an expression giving the net axial force acting on the cylinder of an idealized pressure-gradient microphone element. Consider only the special case in which the direction of propagation of the waves is along the axis of the cylinder. Show that this force is zero at the antinodes of pressure and a maximum at the antinodes of velocity.

11.12. A certain microphone has a directivity such that the response in any direction making an angle θ with the principal axis is proportional to $\cos^2 \theta$. (*a*) Compute the numerical value of the directivity factor for such a microphone. (*b*) What is its directivity index?

11.13. Two identical reversible microphones are set up for a reciprocity type of calibration. The spacing between microphones is 2 meters. For a frequency of 2000 cycles/sec, the measured open-circuit voltage output of one microphone is 0.0001 volt for an input current of 0.01 amp to the other. What is the open-circuit voltage response level of the microphones in decibels *re* 1 volt per microbar?

11.14. A microphone is to be calibrated. From initial measurements, it is determined that its sensitivity is 5 times as great as a certain reversible transducer. When the reversible transducer is used as a source at a distance of 1.5 m from the microphone, the microphone is observed to have an open-circuit output of 0.001 volt when a driving current of 1 ampere is supplied to the transducer at a frequency of 500 cycles/sec. (*a*) What is the open-circuit voltage response of the microphone? (*b*) What is the acoustic pressure acting on the microphone during the above experiment?

11.15. A condenser microphone has a diaphragm of 2-cm radius and the separation between the diaphragm and the backing plate is 0.002 cm. The diaphragm is stretched to a tension of 5000 newtons/m. The polarizing voltage is 200 volts. (*a*) What is the low-frequency open-circuit voltage response level of the microphone? (*b*) Using the electroacoustical reciprocity theorem, compute the acoustic pressure produced by the microphone, acting as a loudspeaker, at a distance of 1 meter when being driven by a current of 0.01 amperes at a frequency of 1000 cycles/sec.

chapter 12

ULTRASONIC AND SONAR TRANSDUCERS

12.1 Introduction. In the preceding two chapters we have considered important types of electroacoustic transducers used for the production and reception of airborne sounds at audible frequencies. In this chapter we will be concerned with equally important transducers used for the production and reception of acoustic waves in liquids and solids. They include (1) ultrasonic transducers used in experimental work for investigating the propagation of high-frequency acoustic waves in liquids and in measuring the elastic properties of solids; (2) ultrasonic transducers used in industry as a potent microagitator of liquids for such purposes as degassing, emulsifying, and coagulation; (3) ultrasonic transducers used to locate flaws in metal castings and laminated plastics; and (4) sonar transducers used in naval operations and warfare for the production and reception of underwater sounds in order to detect the presence of submerged submarines, communicate with submerged submarines, actuate the homing systems of acoustic torpedoes, and determine the depth of water.

Because of the high characteristic specific acoustic impedance of liquids as compared to air, the vibrating elements of transducers designed for use in liquids must be capable of producing large forces at small displacements in order to match the impedance of the liquid efficiently. The most widely used type of element for such transducers depends upon the piezoelectric effect for its action. Commonly used piezoelectric vibrators include ones constructed from crystals of quartz, Rochelle salt, and ammonium dihydrogen phosphate (ADP), and from cast ceramic materials such as barium titanate and similar dielectrics having strong ferroelectric properties. The vibrating elements of a second group of transducers utilize the strong magnetostrictive effect of nickel and certain of its alloys. The action of yet a third type of transducer depends upon the varying attractive force between an electromagnet, in whose coil is flowing an alternating current, and a rigid circular steel plate in contact with the liquid.

12.2 Quartz Crystal Vibrators. Much work has been done in ultrasonics with transducers that depend for their operation on the piezoelectric properties of crystalline quartz. The type of crystal most commonly used is the so-called X-cut crystal, which is cut from the natural crystal as shown in Fig. 12.1. The axis along the longest dimension of the natural crystal is called the *optic* or z-axis. An axis perpendicular to the z axis and passing through any two opposite prism edges is known as the *electric* or x-axis. A third axis perpendicular to the x and z axes, and passing normally through any two of the major faces of the natural crystal is called the *mechanical* or y-axis. It will be noted from Fig. 12.1 that in an X-cut crystal the two major surfaces of the cut crystal are perpendicular to the x-axis.

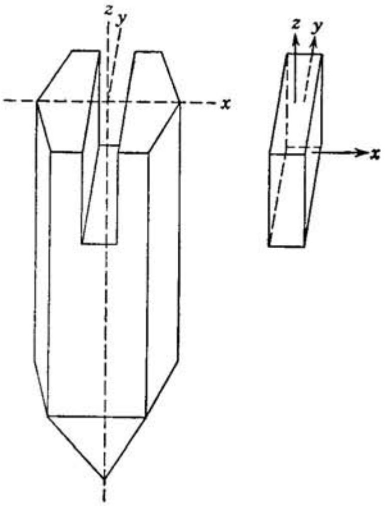

Fig. 12.1. Quartz crystal, X-cut.

Whenever an applied stress produces a strain along either the x-axis or the y-axis of an X-cut crystal, the crystal becomes electrically polarized and piezoelectric charges of opposite sign appear on the two surfaces perpendicular to the x-axis. Conversely, if these two surfaces are covered by a metal film, or are placed between contiguous electrodes, and an electric field is applied parallel to the x-axis, the crystal will either expand along the y-axis and contract along the x-axis or will experience a reverse behavior, depending on the direction of the applied field.

If an alternating electrical field is applied along the x-axis, the resulting mechanical deformations along the y-axis may be used to set up longitudinal vibrations along this axis. In particular, as the frequency of the applied electrical field approaches the natural frequency of any longitudinal mode of vibration of the crystal, the amplitude of the mechanical vibration becomes large. Mechanical vibrations of this type in quartz or other piezoelectric crystals have been utilized to produce ultrasonic vibrations in liquids at frequencies ranging from 5 kc/sec to several hundred kc/sec. Similarly, the mechanical deformations produced along the x-axis may be used to set up thickness vibrations parallel to this axis. Since the thickness of a quartz crystal plate can be made less than 1 mm, the thickness mode of vibration is particularly suited to the radiation of ultrasonic energy at frequencies in excess of 1 megacycle/sec. Up to about 10 megacycles/sec such crystals may be driven in their fundamental mode of thickness vibration; the use of harmonic modes makes possible ultrasonic radiation at frequencies as high as 500 megacycles/sec.

Since the radiating surface available is considerably greater for thickness vibrations than for longitudinal vibrations, the electroacoustic efficiency of this type of vibration is relatively high, and as a consequence crystal radiators operated in their thickness modes are the most common laboratory source of ultrasonic radiations in gases, liquids, and solids. Furthermore, the dimensions of the radiating surface are large in comparison with the wavelength radiated, and hence these radiators produce ultrasonic beams of small angular divergence.

12.3 Longitudinal Piezoelectric Vibrator. In general, nine linear equations are required to express the various relationships between the mechanical stresses and strains and the electrical fields and polarization charges existing in a piezoelectric crystal. However, if a plated X-cut quartz crystal is cut in the form of a bar whose length l_y along the mechanical axis is at least three times as great as either l_x or l_z, Fig. 12.2, and if the crystal is caused to vibrate longitudinally, then only the longitudinal stresses and strains parallel to the y-axis are significant. Under these circumstances only two of the nine equations are required for a discussion of the longitudinal vibrations, and these may be somewhat simplified. They are

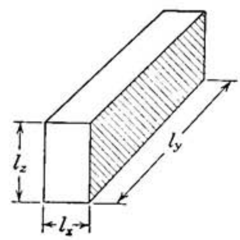

Fig. 12.2. Longitudinal vibrator, X-cut.

$$\sigma_x = \frac{\epsilon_x \epsilon_0 E_x}{l_x} - d_{12}\left(\frac{F_y}{S_y}\right) \tag{12.1}$$

and

$$\frac{\partial \eta}{\partial y} = -s_{22}\left(\frac{F_y}{S_y}\right) + \frac{d_{12}E_x}{l_x} \tag{12.2}$$

where:

σ_x is the surface charge density appearing on the plated surfaces of the crystal in coulombs/m^2;

ϵ_x is the *free* dielectric constant of quartz, measured parallel to the x axis when the crystal is free of external stresses;

$\epsilon_0 = 8.85 \times 10^{-12}$ farads/meter is the permittivity of free space;

E_x is the potential difference in volts between the plated surfaces of the crystal;

F_y is the *compressional* force in newtons applied parallel to the y-axis;

$S_y = l_x l_z$ is the cross-sectional area perpendicular to the y-axis;

l_x, l_y, and l_z are, respectively, the thickness, length, and width of the crystal;

$\partial\eta/\partial y$ is the longitudinal strain in the y direction, where η represents longitudinal displacements parallel to the y-axis;

d_{12} is one of the piezoelectric *strain* coefficients of quartz, expressed either in meters/volt or coulombs/newton;

$s_{22} = 1/Y_y$, is one of the elastic *compliance* coefficients of quartz, expressed in meters^2/newton. In this particular example it is equivalent to, and may be replaced by, $1/Y_y$, the reciprocal of Young's modulus as measured parallel to the y-axis.

The first term of equation 12.1, $\epsilon_x\epsilon_0 E_x/l_x$, is the familiar expression for the surface charge density appearing on the plates of a parallel plate capacitor having a dielectric whose constant is ϵ_x. The second term, $-d_{12}(F_y/S_y)$, represents the additional charge density generated on these plates by the *direct* piezoelectric effect. The first term of equation 12.2, $-s_{22}(F_y/S_y)$, is the usual longitudinal strain produced by a compressional stress F_y/S_y. The second term, $d_{12}E_x/l_x$, represents the additional strain in the y direction produced by the *inverse* piezoelectric effect, i.e., by the deforming action of an applied electric field E_x/l_x.

It is sometimes convenient to express equation 12.1 in an alternative form, i.e., in terms of strain $\partial\eta/\partial y$ rather than stress F_y/S_y. Eliminating F_y/S_y between equations 12.1 and 12.2 we obtain

$$\sigma_x = \frac{\epsilon_x'\epsilon_0 E_x}{l_x} + \frac{d_{12}}{s_{22}}\left(\frac{\partial\eta}{\partial y}\right) \tag{12.3}$$

where

$$\epsilon_x' = \epsilon_x - \frac{d_{12}^{\;2}}{\epsilon_0 s_{22}} \tag{12.4}$$

The quantity ϵ_x' is known as the longitudinally *clamped* dielectric constant of the crystal. It is the dielectric constant that would be measured if the crystal were so clamped as to make $\partial\eta/\partial y$ zero, i.e., if the crystal were constrained from expanding or contracting in the y-direction.

Equation 12.4, which expresses the relationship between the free and the clamped dielectric constants, may also be written in the form

$$\epsilon_x' = \epsilon_x\left(1 - \frac{d_{12}^{\;2}}{\epsilon_x\epsilon_0 s_{22}}\right) = \epsilon_x(1 - k^2) \tag{12.4a}$$

where the parameter k, which is known as the *coefficient of electromechanical coupling* of the crystal, is defined by

$$k = \sqrt{\frac{d_{12}^{\;2}}{\epsilon_x\epsilon_0 s_{22}}} \tag{12.5}$$

In the following sections it will be shown that the electromechanical activity of the crystal as well as other important characteristics can be conveniently expressed in terms of this parameter k.

Table 12.1 Mechanical and electrical constants of quartz

Quantity	Symbol	Magnitude	Units
Density	ρ	2650	kg/m^3
Compliance coefficient	s_{22}	1.27×10^{-11}	m^2/newton
Stiffness coefficient	c_{11}	8.55×10^{10}	newtons/m^2
Piezoelectric strain coefficient	d_{12}	2.3×10^{-12}	meters/volt
Piezoelectric stress coefficient	e_{11}	0.17	coulombs/m^2
Free dielectric constant	ϵ_x	4.50	—
Clamped dielectric constant	ϵ_x'	4.45	—
Electromechanical coupling coefficient	k	0.1	—
Longitudinal wave velocity	c_y	5450	m/sec
Thickness wave velocity	c_x	5750	m/sec
Longitudinal characteristic impedance	ρc_y	1.45×10^7	rayls (MKS)
Thickness characteristic impedance	ρc_x	1.53×10^7	rayls (MKS)

Listed in Table 12.1 are measured values for a number of the more important electrical and mechanical constants of an X-cut quartz crystal. It should be noted that the two dielectric constants ϵ_x and ϵ_x' differ by 0.05, i.e., by approximately 1 per cent of the free dielectric constant. The relative magnitude of this difference offers another measure of the electromechanical activity of a piezoelectric crystal.

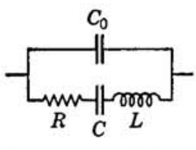

Fig. 12.3. Equivalent electrical circuit for a crystal vibrator.

12.4 Equivalent Electrical Circuit of a Piezoelectric Vibrator. The analysis of the operation of a piezoelectric vibrator as a component of an electroacoustic transducer is greatly simplified if the crystal and its electrodes are replaced by an equivalent electrical circuit. It will now be demonstrated that this equivalent circuit consists of a capacitor C_0 connected in parallel with a series resonant circuit, i.e., a series circuit containing resistance, inductance, and capacitance, Fig. 12.3. This procedure of replacing mechanical constants of an electroacoustic vibrator by their electrical equivalents is similar to that used in Sect. 10.2 in the analysis of a moving-coil loudspeaker.

Let us first assume that the longitudinal periodic waves moving along the y axis of the crystal with a velocity

$$c_y = \sqrt{\frac{1}{\rho s_{22}}} \tag{12.6}$$

may be represented in complex form by an equation equivalent to equation 3.9, i.e., by

$$\boldsymbol{\eta} = (\mathbf{A}e^{-jky} + \mathbf{B}e^{jky})e^{j\omega t} \tag{12.7}$$

Now, if a complex driving voltage

$$\mathbf{E}_x = Ee^{j\omega t} \tag{12.8}$$

is applied between the plates of the crystal, the constants **A** and **B** may be determined, provided that the boundary conditions existing at the ends of the crystal are known. As a specific example, let us assume that the crystal is rigidly clamped at $y = 0$ and is radiating plane waves into a fluid medium of specific acoustic impedance $\rho_0 c_0$ at $y = l_y$.

Application of the first condition that $\boldsymbol{\eta} = 0$ at $y = 0$ to equation 12.7 results in

$$\mathbf{A} + \mathbf{B} = 0$$

Consequently, equation 12.7 is reduced to

$$\boldsymbol{\eta} = (-2j\mathbf{A} \sin ky)e^{j\omega t} = (\mathbf{A}' \sin ky)e^{j\omega t} \tag{12.9}$$

where $\mathbf{A}'$ is a new arbitrary constant replacing $-2j\mathbf{A}$.

At high frequencies the radiation impedance loading of the fluid medium at $y = l_y$ is largely resistive and may be represented by $\rho_0 c_0 S_y$. Therefore, at $y = l_y$

$$\mathbf{Z}_{ly} = \frac{(\mathbf{F}_y)_{ly}}{\left(\dfrac{\partial \boldsymbol{\eta}}{\partial t}\right)_{ly}} = \rho_0 c_0 S_y \tag{12.10}$$

Upon substitution of $\mathbf{F}_y$ from equation 12.2 and $\boldsymbol{\eta}$ from equation 12.9 into equation 12.10 there results

$$\mathbf{A}' = \frac{\phi E}{\omega S_y} \cdot \frac{1}{\rho c_y \cos kl_y + j\rho_0 c_0 \sin kl_y} \tag{12.11}$$

where ϕ is defined by the equation

$$\phi = \frac{d_{12} l_z}{s_{22}} \tag{12.12}$$

Later in this section we shall learn that ϕ serves as a *transformation factor* relating electrical to mechanical quantities for piezoelectric coupling in a manner similar to that of the corresponding factor defined by equation 10.9 for the electrodynamic coupling of a moving-coil loudspeaker.

When the angular frequency ω of the applied potential difference $Ee^{j\omega t}$ is equal to the fundamental frequency ω_1 of longitudinal vibration of a fixed-free bar, as given by equation 3.21, i.e., when $\omega = c_y\pi/2l_y$, then

$$\cos k_1 l_y = \cos \frac{\omega_1 l_y}{c_y} = \cos \frac{\pi}{2} = 0$$

Correspondingly, $\sin k_1 l_y = 1$, and equation 12.11 simplifies to

$$\mathbf{A}_1' = -\frac{j\phi E}{\omega_1 S_y \rho_0 c_0} \tag{12.13}$$

The complex longitudinal displacement $\boldsymbol{\eta}_1$ of the crystal, when driven at its fundamental resonant frequency, is obtained by substituting equation 12.13 into equation 12.9. It is

$$\boldsymbol{\eta}_1 = -\frac{j\phi \sin k_1 y}{\omega_1 S_y \rho_0 c_0} Ee^{j\omega_1 t} \tag{12.14}$$

and the fundamental resonant frequency is

$$f_1 = \frac{c_y}{4l_y} = \frac{1}{4l_y}\sqrt{\frac{1}{\rho s_{22}}} \tag{12.15}$$

As previously, the actual physical displacements are given by the real part of equation 12.14.

If a *static* potential difference E_s is applied to this same crystal, the resulting strain, which is given by

$$\left(\frac{\partial \eta}{\partial y}\right)_s = d_{12}\left(\frac{E_s}{l_x}\right)$$

is constant and the displacement of the free end of the bar becomes

$$(\eta_s)_{ly} = \frac{d_{12}E_s l_y}{l_x} \tag{12.16}$$

The ratio of $(\eta_1)_{ly}$, the dynamic amplitude of the free end of the bar at resonance, to $(\eta_s)_{ly}$, the static displacement of this same end, is

$$r = \frac{E}{s_{22}\rho_0 c_0 \omega_1 E_s l_y} \tag{12.17}$$

In particular, if the peak voltage E equals the static voltage E_s, then

$$r = \frac{2\rho c_y}{\pi \rho_0 c_0} \tag{12.17a}$$

in which s_{22} has been replaced by $1/\rho c_y^2$ and ω_1 by $c_y\pi/2l_y$. Equation 12.17*a* shows that when the characteristic longitudinal impedance ρc_y of the quartz crystal is large in comparison with the characteristic impedance $\rho_0 c_0$ of the fluid medium, the ratio r is also large. As a consequence, when quartz crystals are driven in air, care must be taken to ensure that the dynamic amplitudes are not excessive, as otherwise the crystal may fracture.

The complex velocity $\mathbf{v}_1$ at resonance is

$$\mathbf{v}_1 = \frac{\partial \boldsymbol{\eta}_1}{\partial t} = \frac{\phi \sin k_1 y}{S_y \rho_0 c_0} E e^{j\omega_1 t} \tag{12.18}$$

Therefore, the velocity amplitude V_1 of the free end of the crystal is

$$V_1 = \frac{\phi E}{S_y \rho_0 c_0} \tag{12.19}$$

Since this end of the crystal has been assumed to be working against a radiation resistance $\rho_0 c_0 S_y$, the acoustic power radiated in watts is given by a rms version of equation 7.85 as

$$W = \rho_0 c_0 S_y V_1^2 = \frac{\phi^2 E^2}{\rho_0 c_0 S_y} \tag{12.20}$$

where the voltage E is expressed in rms volts. If this energy is assumed to be radiated uniformly over the radiating face of the vibrator of cross section S_y, then the radiated intensity at the surface of the vibrator in watts/m^2 is

$$I = \frac{\phi^2 E^2}{\rho_0 c_0 S_y^2} \tag{12.21}$$

Substitution of equation 12.14 into equation 12.3 gives for the complex resonant surface charge density $\boldsymbol{\sigma}_{x_1}$ appearing on the plated surfaces of the crystal

$$\boldsymbol{\sigma}_{x_1} = \left(\frac{\epsilon_x' \epsilon_0}{l_x} - j\,\frac{\phi^2 \cos k_1 y}{\rho_0 c_0 S_y c_y l_z}\right) E e^{j\omega_1 t} \tag{12.22}$$

The total charge $\mathbf{q}_1$ appearing on the plates of the crystal may in turn be obtained by integrating $\boldsymbol{\sigma}_{x_1}(l_z\, dy)$ over the plated surface. Finally, the current flowing into the plated crystal is

$$\mathbf{i}_1 = \frac{d\mathbf{q}_1}{dt} = j\omega_1 \mathbf{q}_1 = j\omega_1 \int_0^{l_y} \boldsymbol{\sigma}_{x_1} l_z\, dy$$

$$= j\omega_1 \left(\frac{\epsilon_x' \epsilon_0 l_y l_z}{l_x} - j\,\frac{\phi^2}{\rho_0 c_0 S_y \omega_1}\right) E e^{j\omega_1 t} \tag{12.23}$$

At the resonant frequency ω_1, the electrical admittance $\mathbf{Y}_1$ that would be observed at the terminals of the plated crystal is therefore

$$\mathbf{Y}_1 = \frac{\mathbf{i}_1}{Ee^{j\omega_1 t}} = j\omega_1 \frac{\epsilon_x'\epsilon_0 l_y l_z}{l_x} + \frac{\phi^2}{\rho_0 c_0 S_y} \tag{12.24}$$

This expression is of the same form as

$$\mathbf{Y}_1 = j\omega_1 C_0 + \frac{1}{R} \tag{12.25}$$

which is the equation for the admittance of an electrical circuit consisting of a capacitor C_0 in parallel with a resistance R. Consequently, when the plated crystal is driven at its fundamental resonant frequency it may be replaced, in so far as its electrical input characteristics are concerned, by a capacitance

$$C_0 = \frac{\epsilon_x'\epsilon_0 l_y l_z}{l_x} \qquad \text{farads} \tag{12.26}$$

connected in parallel with a resistance

$$R = \frac{\rho_0 c_0 S_y}{\phi^2} \qquad \text{ohms} \tag{12.27}$$

Equation 12.26 expresses the usual dependence of the capacitance of a parallel plate capacitor upon its physical dimensions and dielectric material. The expression for R is a *motional* resistance associated with the electrical power absorbed by the crystal from the electrical generator and radiated into the adjacent fluid medium as acoustic power. It is to be noted that equation 12.27 indicates that the mechanical loading resistance $\rho_0 c_0 S_y$ of the fluid medium is transformed into an electrical resistance upon being divided by the square of the transformation factor ϕ. When $\rho_0 c_0 \to \infty$, $R \to \infty$, the former indicating that there is no vibration of the free end of the crystal, and the latter that no power is being dissipated by the crystal. Considering the above electrical circuit, the power dissipated by the vibrating crystal is given by

$$W = \frac{E^2}{R} = \frac{\phi^2 E^2}{\rho_0 c_0 S_y} \tag{12.28}$$

This is identical with the expression for the acoustic power radiated (equation 12.20), as should be anticipated, since it has been assumed that the crystal has no internal losses. Although this assumption is not strictly true, the internal losses in quartz are extremely small.

When the frequency ω of the applied voltage differs from the fundamental resonant frequency ω_1 of the crystal, equation 12.13 is no longer applicable, and the general expression (12.11) must be used in deriving equations for the admittance of the crystal, the acoustic power radiated, etc. When this is done, the admittance is found to be that of the capacitor C_0 in parallel with a branch having an impedance

$$\mathbf{Z} = \frac{\rho_0 c_0 S_y}{\phi^2} - j\frac{\rho c_y S_y \cot kl_y}{\phi^2} \tag{12.29}$$

At the frequency of fundamental resonance, i.e., for $kl_y = \pi/2$, this expression is seen to reduce to equation 12.27. At all frequencies below this frequency, the second term is a negative reactance, and immediately above this frequency changes to a positive reactance. The latter behavior corresponds to that of an inductance and a capacitance in series. It is left as an exercise for the reader to show (Problem 12.4) that the reactive term of equation 12.29 may be represented by a capacitance

$$C = \frac{8\phi^2 s_{22} l_y}{\pi^2 S_y} \qquad \text{farads} \tag{12.30}$$

in series with an inductance

$$L = \frac{\rho l_y S_y}{2\phi^2} \qquad \text{henries} \tag{12.31}$$

It is to be noted that, in contrast with R, the equivalent capacitance C and inductance L of the crystal are independent of the properties of the medium into which the crystal is radiating and depend only on the physical dimensions of the crystal, its density, its elastic compliance, and the transformation factor ϕ. Excellent agreement exists between the measured electrical admittance of a crystal vibrator in the vicinity of its fundamental resonant frequency and that computed for the above electrical elements in the circuit of Fig. 12.3. However, it is not possible to use the same numerical values for all of the elements over a wide range of frequencies. For instance, the loading mechanical impedance of the fluid medium at low frequencies becomes less than $\rho_0 c_0 S_y$ and consequently R is reduced. Of a more fundamental significance is the requirement that the capacitance C must be given by

$$C = \frac{\phi^2 s_{22} l_y}{S_y} \tag{12.30a}$$

at low frequencies, if the impedance of the RLC branch is to represent that given by equation 12.29. Finally, in the vicinity of each of the higher resonant frequencies of the crystal, the capacitance C is given by

$$C = \frac{8\phi^2 s_{22} l_y}{\pi^2 S_y} \cdot \frac{1}{n^2} \tag{12.30b}$$

where n is an integer giving the ratio of each higher resonant frequency to that of the fundamental.

The magnitudes of the elements of the equivalent circuit are often rather striking. For example, the values for an X-cut quartz crystal, $0.03 \times 0.004 \times 0.0015$ meters in dimensions, mounted in air, are $C_0 = 3.15\ \mu\mu f$, $R = 4750$ ohms, $C = 0.0268\ \mu\mu f$, $L = 457$ henries, and $f_1 = 45.5$ kc/sec. Even if a coil having an inductance of this magnitude could be constructed, its physical dimensions would be enormous in comparison with those of the crystal, and its losses also would be very much greater.

One interesting feature of the equivalent circuit is that the ratio C/C_0 turns out to be a constant for any given type of crystal cut and mode of vibration, i.e., it is independent of the particular physical dimensions of the crystal. This ratio C/C_0 is a measure of the ratio of mechanical to electrical energy stored in the vibrating crystal, and it therefore should serve as a measure of the electromechanical *activity* or coupling of the crystal. For a longitudinally vibrating X-cut quartz crystal it is

$$\frac{C}{C_0} = \frac{8\phi^2 s_{22} l_y}{\pi^2 S_y} \cdot \frac{l_x}{\epsilon_x' \epsilon_0 l_y l_z} = \frac{8 d_{12}^{\ 2}}{\pi^2 \epsilon_x' \epsilon_0 s_{22}} = \frac{8k^2}{\pi^2(1 - k^2)} \qquad (12.30c)$$

where k is the coefficient of electromechanical coupling as defined by equation 12.5. It is this relationship between C/C_0 and k that justifies calling k the electromechanical coupling coefficient. From Table 12.1 it is seen that $k^2 \approx 0.01$ for an X-cut quartz crystal, and therefore $C/C_0 \approx 0.008$. As compared to some of the crystal cuts for other commonly used piezoelectric crystals, this electromechanical activity is quite low. For example, $C/C_0 \approx 0.08$ for a 45° Y-cut Rochelle salt crystal.

12.5 Generalized Theory of Equivalent Circuits for Piezoelectric Transducers. Rather than discussing each additional type of piezoelectric vibrator with the same detail as has been carried out for the longitudinal quartz vibrator in the preceding section, let us instead proceed by generalizing the relationships between the mechanical and electrical elements of a piezoelectric transducer. Such a transducer can be represented by a four-terminal network with two electrical input terminals and two mechanical output terminals as shown in Fig. 12.4. If an alternating voltage $\mathbf{E}$ is applied to the input terminals, then a current $\mathbf{I}$ will flow such that

$$\mathbf{I} = \mathbf{Y}_E \mathbf{E} - \phi \mathbf{U} \qquad (12.32)$$

where $\mathbf{Y}_E$ is the so-called *blocked* electrical input admittance corresponding to $\mathbf{U} = 0$, and ϕ is a *transformation factor* relating the piezoelectrically generated current in the short-circuited electrical side of the transducer, i.e., for $\mathbf{E} = 0$, to the generating velocity $\mathbf{U}$ in the mechanical side.

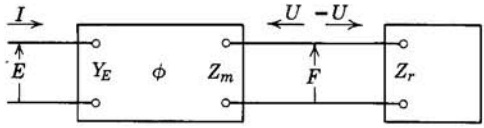

Fig. 12.4. Four-terminal electromechanical network of transducer with attached acoustic load Z_r.

Correspondingly, if an alternating force **F** is applied to the mechanical side of the transducer, then

$$\mathbf{F} = \phi\mathbf{E} + \mathbf{Z}_m\mathbf{U} \tag{12.33}$$

where $\mathbf{Z}_m$ is the *short-circuited* mechanical impedance corresponding to $\mathbf{E} = 0$ and ϕ is a *transformation factor* relating the piezoelectrically generated force in the transducer when its motion is blocked, i.e., for $\mathbf{U} = 0$, to the generating voltage **E**. In essence, equation 12.32 is a generalized form of equation 12.3 appropriate for alternating voltages, currents, etc. Similarly, equation 12.33 is a generalized form of equation 12.2. Finally, by use of equations 12.2 and 12.3 one may show that the two terms containing the transformation factor ϕ in equations 12.32 and 12.33 should have the opposite algebraic signs as given. Furthermore, the generalized piezoelectric transformation factor ϕ of these equations is dimensionally identical with that defined by equation 12.12 for the longitudinal quartz vibrator.

In addition, the mechanical force acting *on* the transducer face of area S must be related to the particle motion of velocity **U** in the adjacent fluid medium by the equation

$$\mathbf{Z}_r = \frac{\mathbf{F}}{-\mathbf{U}} \tag{12.34}$$

where $\mathbf{Z}_r$ is the mechanical radiation impedance loading of the latter. In this equation $-\mathbf{U}$ is used to represent the positive velocity in the fluid associated with a positive force **F** in the transducer in accordance with the definition of $\mathbf{Z}_r$ (Sect. 7.14).

If equations 12.32, 12.33, and 12.34 are combined so as to eliminate **F** and **U**, the result may be expressed as

$$\mathbf{Y}_I = \frac{\mathbf{I}}{\mathbf{E}} = \mathbf{Y}_E + \frac{\phi^2}{\mathbf{Z}_m + \mathbf{Z}_r} \tag{12.35}$$

where $\mathbf{Y}_I$ is the input electrical admittance of the transducer. This equation shows that the input admittance is the sum of the blocked admittance $\mathbf{Y}_E$ and a motional admittance as defined by the equation

$$\mathbf{Y}_M = \frac{\phi^2}{\mathbf{Z}_m + \mathbf{Z}_r} \tag{12.36}$$

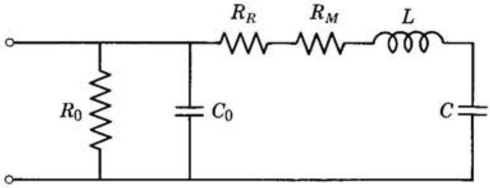

Fig. 12.5. Equivalent circuit of piezoelectric transducer.

Let us now formulate generalized expressions for the various terms occurring in equation 12.35. The blocked admittance $\mathbf{Y}_E$ is that of a dielectric parallel plate capacitor, which normally is represented by a capacitor C_0 in parallel with a dielectric leakage resistance R_0, and is given by

$$\mathbf{Y}_E = \frac{1}{R_0} + j\omega C_0 \tag{12.37}$$

The mechanical impedance $\mathbf{Z}_m$ of the transducer may be represented in lumped constant form by

$$\mathbf{Z}_m = R_m + j[\omega m - (s/\omega)] \tag{12.38}$$

where R_m is a resistance term associated with mechanical losses in a crystal vibrator or in constraints in its method of mounting, m is the effective mass of a vibrator element, and s is the effective stiffness. Finally, the loading impedance $\mathbf{Z}_r$ is largely resistive and may be represented by R_r. Upon substitution of these expressions into equation 12.35, it becomes

$$\mathbf{Y}_I = \frac{1}{R_0} + j\omega C_0 + \frac{\phi^2}{R_r + R_m + j[\omega m - (s/\omega)]} \tag{12.39}$$

which in turn may be represented by the electrical circuit of Fig. 12.5, where the electrical elements in the motional admittance part of the circuit are given by

$$R_R = \frac{R_r}{\phi^2}, \quad R_M = \frac{R_m}{\phi^2}, \quad L = \frac{m}{\phi^2}, \quad \text{and} \quad C = \frac{\phi^2}{s} \tag{12.40}$$

The resistance R_R appearing in this circuit represents a generalized form of equation 12.27. When a voltage is applied to the input terminals of the transducer, only that power dissipated in this element of the equivalent circuit is converted into acoustic radiation. Power dissipated in the resistance R_M is converted into heat by means of internal mechanical losses in the crystal vibrator. The inductance L must be equivalent to that given by equation 12.31. A comparison of the latter equation with that for L in equation 12.40 indicates that the effective mass of the crystal

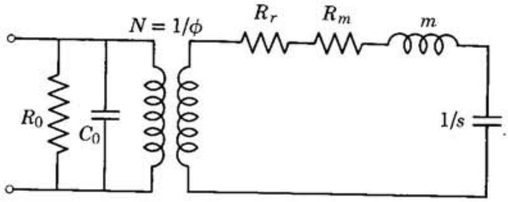

Fig. 12.6. Equivalent circuit with transformer between electric and mechanical sides of transducer.

vibrator is given by $\frac{1}{2}(\rho Sl)$, i.e., one half of its actual mass. Such a behavior is reasonable since all parts of the vibrator do not move with equal displacements. Finally, a comparison of the expression for C given in equation 12.40 with those previously given in equations 12.30, 12.30*a*, and 12.30*b* shows that the effective stiffness does not remain constant as the frequency changes. For instance, at low frequencies

$$s = \frac{S}{ls_{22}} \tag{12.41}$$

while near a resonant frequency f_n

$$s = \frac{n^2\pi^2 S}{8ls_{22}} \tag{12.41a}$$

and has intermediate values between such resonances.

By use of appropriate expressions for m, s, R_m, R_r, ϕ, C_0, and R_0 for any given piezoelectric transducer, it becomes possible to compute values for the various circuit elements of Fig. 12.5. Standard methods of electrical analysis of the circuit may then be used to predict the behavior of the transducer as a sound source. It is to be noted that the input admittance of a piezoelectric transducer, as given by equation 12.39, may also be represented by the circuit of Fig. 12.6. When this circuit is used, the transformer has a turns ratio of $1/\phi$ and the numerical values of the indicated electrical elements m, $1/s$, R_m, and R_r are now identical with their mechanical values.

12.6 Quality Factor or Q of Piezoelectric Vibrators. By analogy with the similar definition of the quality factor or Q of an inductor, let us define the Q of a piezoelectric vibrator by

$$Q = \frac{\omega_1 L}{R_R + R_M} \tag{12.42}$$

This definition is seen to represent the electrical Q of the motional admittance branch of Fig. 12.5. When signals of constant voltage but varying frequency are applied to a transducer, consideration of equation 1.31 shows that Q also serves as a measure of the acoustic half-power bandwidth of the transducer.

As a numerical example, let us consider the longitudinal quartz vibrator of Sect. 12.4. For such vibrators, R_M is usually small compared to R_R and may be neglected without serious error. Upon substitution of the expressions for ω_1, L, and R_R as given respectively by equations 12.15, 12.31, and 12.27

$$Q = \frac{\pi \rho c_y}{4\rho_0 c_0} \tag{12.43}$$

When the free end of a longitudinally vibrating quartz crystal is radiating into water of characteristic impedance $\rho_0 c_0 = 1.48 \times 10^6$ rayls, equation 12.43 predicts a quality factor of

$$Q = \frac{\pi \times 1.45 \times 10^7}{4 \times 1.48 \times 10^6} \approx 7.5$$

This relatively low Q is typical of the measured values for ultrasonic and sonar piezoelectric transducers when used to generate acoustic waves in liquids.

On the other hand, if the fluid medium in contact with the free end of the crystal is air, rather than a liquid, then

$$Q = \frac{\pi \times 1.45 \times 10^7}{4 \times 415} \approx 27{,}500$$

This Q is very large and indicates that the resonance curve of a driven quartz crystal in air should be sharply peaked. By contrast, the Q of a well-designed oscillator coil for operation in the range from 10 to 100 kc/sec is less than 300. Because of their high values of Q, properly mounted quartz crystals are excellently suited as circuit elements for electronic oscillators and in wave filter networks designed to have sharp cut-off characteristics.

When a carefully mounted quartz crystal is placed inside an evacuated chamber, losses resulting from the radiation of acoustic energy are absent, leaving only the mechanical and dielectric losses in the quartz, which are extremely small. As a consequence, the Q of such a vibrator is of the order of magnitude of 1,000,000.

12.7 Piezoelectric Constants of Common Transducer Materials. The equations derived in the preceding sections of this chapter have been concerned with longitudinal vibrations along the y-axis of an X-cut quartz crystal. These equations also may be applied to longitudinal vibrations in other crystals by use of appropriate equivalent constants for d_{12} and s_{22}.

In order to obtain a maximum piezoelectric effect, a crystal should be cut so as to use the strongest possible coupling between mechanical strain and associated electrical polarization as produced by an applied electrical field. For quartz, this occurs when an electrical field applied along the x-axis is coupled with mechanical deformation along the y-axis and is measured by the piezoelectric strain constant d_{12}. Table 12.2 lists the principal piezoelectric strain constants for quartz, Rochelle salt, and ammonium dihydrogen phosphate (ADP). The tensor constants d_{ij} given in this table relate mechanical strain to the voltage gradient components $\partial E/\partial x$, $\partial E/\partial y$, $\partial E/\partial z$ of the applied field by three longitudinal strain equations

$$\begin{aligned} \frac{\partial \xi}{\partial x} &= d_{11}\frac{\partial E}{\partial x} + d_{21}\frac{\partial E}{\partial y} + d_{31}\frac{\partial E}{\partial z} \\ \frac{\partial \eta}{\partial y} &= d_{12}\frac{\partial E}{\partial x} + d_{22}\frac{\partial E}{\partial y} + d_{32}\frac{\partial E}{\partial z} \\ \frac{\partial \zeta}{\partial z} &= d_{13}\frac{\partial E}{\partial x} + d_{23}\frac{\partial E}{\partial y} + d_{33}\frac{\partial E}{\partial z} \end{aligned} \tag{12.44}$$

and three shear strain equations

$$\begin{aligned} \frac{\partial \eta}{\partial z} &= d_{14}\frac{\partial E}{\partial x} + d_{24}\frac{\partial E}{\partial y} + d_{34}\frac{\partial E}{\partial z} \\ \frac{\partial \zeta}{\partial x} &= d_{15}\frac{\partial E}{\partial x} + d_{25}\frac{\partial E}{\partial y} + d_{35}\frac{\partial E}{\partial z} \\ \frac{\partial \xi}{\partial y} &= d_{16}\frac{\partial E}{\partial x} + d_{26}\frac{\partial E}{\partial y} + d_{36}\frac{\partial E}{\partial z} \end{aligned} \tag{12.45}$$

Fortunately, many of the 18 piezoelectric strain constants d_{ij} are zero for the common transducer materials listed in Table 12.2. This greatly simplifies the problem of determining the effective strain constant d for the significant modes of longitudinal vibration.

Table 12.2 Principal piezoelectric strain constants for several crystals

Crystal Material	d_{11}	d_{12}	d_{14}	d_{25}	d_{26}	d_{36}
Quartz (20°C)	−2.3	2.3	0.57	−0.57	−4.6	...
ADP (20°C)	...	...	1.45	...	...	−48
Rochelle salt (30°C)	...	...	550	−54	...	12

The above constants should be multiplied by 10^{-12} in order to express them in meters/volt.

In ADP the principal constant is d_{36}, which leads to a strong shear strain in the xy-plane upon application of an electrical field along the z-axis. Thus a cut normal to the z-axis, a so-called Z-cut, is required for maximum piezoelectric coupling. If a rectangular plate is cut in this plane in such a manner that its longest dimension extends at 45° between the x and y crystallographic axes, a strong longitudinal motion will result from the above shearing action (Fig. 12.7). In fact, every shear strain in a solid involves longitudinal compression and expansion strains along 45° diagonals equal to one half of the shear strain. Hence, for a 45° Z-cut ADP crystal, the effective longitudinal piezoelectric strain constant d is given by $d_{36}/2 = 24 \times 10^{-12}$ meter/volt.

Similarly, in Rochelle salt the principal constant is d_{14}, which requires a cut in the yz-plane normal to the crystallographic x-axis. Hence, a 45° X-cut crystal can be used for longitudinal vibrations with an effective piezoelectric strain constant of $d_{14}/2 = 275 \times 10^{-12}$ meter/volt. A somewhat weaker coupling occurs in Rochelle salt between electrical fields applied along the y-axis and longitudinal deformations produced 45° between the x and z axes. This cut is known as a 45°Y-cut and has an effective longitudinal strain constant of $d_{25}/2 = 27 \times 10^{-12}$ meter/volt. Although the constant for the 45° Y-cut is much smaller than that for the 45° X-cut, the latter changes rapidly with temperature in the region from 20°C to 30°C and, consequently, the 45° Y-cut must be used whenever a Rochelle salt crystal having stable temperature characteristics is required.

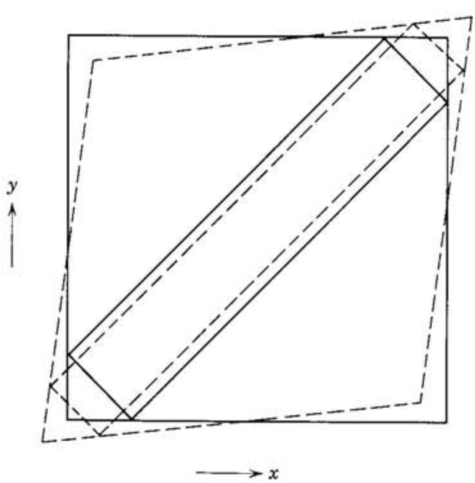

Fig. 12.7. Longitudinal vibrator cut at 45° from Z-cut ADP plate.

Numerical values for the important electromechanical constants of those piezoelectric materials commonly used as longitudinal vibrators are listed in Table 12.3. It is important to bear in mind that all of these constants change to some extent as temperature is varied. Therefore, if the vibrator

Table 12.3 Electromechanical constants of transducer materials

Quantity	Symbol	Quartz X-cut	ADP (20°C) 45° Z-cut	Rochelle salt (30°C) 45° X-cut	45° Y-cut	Barium Titanate (25°C)	Units
Density	ρ	2650	1800	1770	1770	5500	kg/m^3
Compliance coefficient	s	1.27×10^{-11}	5.2×10^{-11}	5.6×10^{-11}	9.6×10^{-11}	0.9×10^{-11}	m^2/newton
Piezo strain coefficient	d	2.3×10^{-12}	24×10^{-12}	275×10^{-12}	27×10^{-12}	56×10^{-12}	m/volt
Free dielectric constant	ϵ	4.5	15.3	350	10	1200	...
Coupling coef	k	0.1	0.29	0.67	0.3	0.18	...
Longitudinal velocity	c	5450	3280	3150	2430	4500	m/sec
Longitudinal impedance	ρc	14.5×10^6	5.9×10^6	5.6×10^6	4.3×10^6	25×10^6	rayls (MKS)
$\frac{\text{Trans. factor}}{\text{Unit width}}$	d/s	0.18	0.46	4.9	0.28	6.2	$\frac{\text{newtons}}{\text{m volt}}$

element heats up during operation, the constants may change and limit the stability of operation. For instance, if the longitudinal velocity c changes with temperature, this variation will in turn alter the frequency of fundamental resonance. In quartz, this velocity is practically constant between 0°C and 60°C. In ADP, it increases by 2.5 per cent in the same interval. In pure barium titanate ceramic vibrators, this velocity has a minimum at one of its crystallographic transition points near 10°C which is some 10 per cent lower than that listed in Table 12.3 at 25°C. This rapid change in velocity with temperature change may be reduced by adding small percentages of either calcium titanate or lead titanate to the ceramic mix from which the vibrator is formed. Many of the electromechanical constants of Rochelle salt are quite unstable in the vicinity of 24°C where it has a Curie point. In particular, the longitudinal velocity in a 45° X-cut crystal decreases some 20 per cent in this vicinity as compared to the value listed in Table 12.3. By contrast, the change in longitudinal velocity in a 45°Y-cut vibrator is relatively small in the vicinity of this temperature.

The free dielectric constants and piezoelectric strain coefficients listed in Table 12.3 are also subject to considerable variation with change in temperature. The behavior of the 45° X-cut of Rochelle salt is most pronounced in that measured values of ϵ and d at 24°C are more than double the values listed in the table. Finally, it should be noted that the constants listed for barium titanate are only approximate since they depend both upon the pretreatment and remanent polarization of the ceramic.

12.8 Mosaic Type of Piezoelectric Transducer. When an individual longitudinal piezoelectric vibrator is driven at its fundamental frequency, the wavelength produced in an adjacent liquid is always greater than the transverse cross-sectional dimensions of the vibrator. As a consequence, the radiation loading impedance acting on the free end of a single vibrator would not be given by $\rho_0 c_0 S$, which requires that $S > \lambda^2$. However, if a large number of such vibrators are mounted in a mosaic pattern such as that shown in Fig. 12.8, then the cumulative effect of all vibrators being driven in phase will result in individual loadings of $\rho_0 c_0 S$ and the equations derived earlier in this chapter may be used.

One common method of assembling a mosaic of piezoelectric vibrators in a "searchlight" type of sonar transducer is shown in Fig. 12.9*a*. The elements of the mosaic are cemented to a metal backing plate which holds them firmly and maintains their alignment. This plate is actually an integral part of the vibrating system. Its dimensions, and physical material will influence the resonance frequency, mechanical quality factor, and input electrical impedance of the transducer. However, when its thickness approaches a quarter of a wavelength, it will for all practical purposes rigidly *clamp* the vibrators and prevent any longitudinal motion where they are cemented to the plate. Normally, the mosaic of individual vibrators are electrically driven in parallel and consequently, the input admittance of N such vibrators is N times that of one vibrator alone. Because of their solubility in water, ADP and Rochelle salt crystals must be operated under

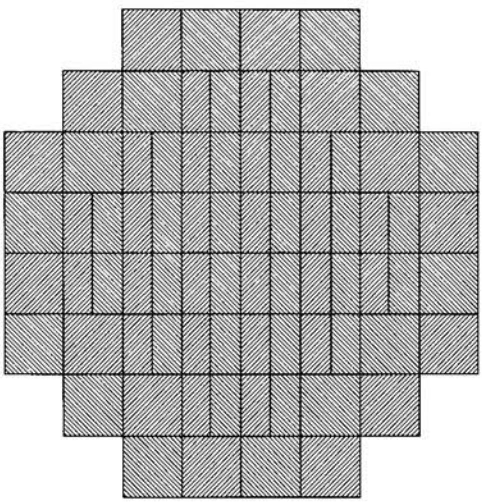

Fig. 12.8. Mosaic array of vibrator elements.

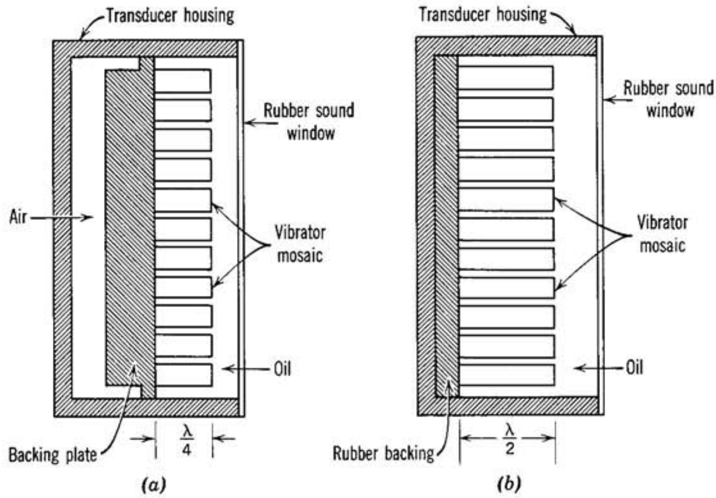

Fig. 12.9. Typical mosaic transducers. (*a*) Quarter-wave vibrators with metal backing plate. (*b*) Half-wave vibrators with pressure release rubber backing.

oil, such as electrical-grade castor oil from which air and water vapor have been removed. The active transducer face and surrounding oil are in turn sealed off from the adjacent water by means of a sound-transparent window made of *rho-c* rubber whose characteristic impedance is matched to that of water.

Often transducers are constructed so that the vibrators in the outer part of the mosaic are thicker than those in the central region (Fig. 12.8). When the same voltage is applied to all vibrators of such a transducer, those in the outer regions will be driven with a lesser amplitude. Such a transducer is said to be *shaded* and will produce a beam pattern having lower minor lobes than one which is driven uniformly over its entire radiating surface. It is also possible to construct a mosaic type of transducer from half wavelength vibrators in the manner shown in Fig. 12.9*b*. Here, both ends of each vibrator are relatively free to vibrate. However, only that end in contact with the oil radiates sound. It is possible to show that the mechanical Q of these vibrators is twice that of the quarter wavelength vibrators previously considered. Mosaic types of transducers may also be constructed from individual vibrators so as to produce cylindrical and spherical radiating surfaces. For a comprehensive discussion of sonar transducers utilizing longitudinal crystal vibrators the reader is referred to the reference given below.[1]

[1] *Design and Construction of Crystal Transducers*, Summary Technical Report of Division 6, Vol. 12, National Defense Research Committee (1946).

12.9 Thickness Vibrators. Transducers employing longitudinal vibrators are commonly used when it is desired to produce ultrasonic waves at frequencies below one hundred kilocycles/sec. However, at higher frequencies it becomes more practical to employ vibrators using the thickness vibrations of thin slabs. The most widely used vibrators of this type are constructed either from X-cut quartz crystals or from polarized ceramic wafers of barium titanate or other strongly ferroelectric materials.

As an example of this type of vibrator, let us consider thickness vibrations of the thin X-cut quartz crystal of Fig. 12.10. A discussion of this mode of vibration is facilitated by expressing the pertinent piezoelectric equations in terms of the *stress* coefficient e_{11}, rather than in terms of the *strain* coefficient d_{11}. Then

$$\sigma_x = \frac{\epsilon_x' \epsilon_0 E_x}{l_x} + e_{11}\left(\frac{\partial \xi}{\partial x}\right) \tag{12.46}$$

and

$$\frac{F_x}{S_x} = -c_{11}\left(\frac{\partial \xi}{\partial x}\right) + e_{11}\left(\frac{E_x}{l_x}\right) \tag{12.47}$$

where:

$\partial\xi/\partial x$ is the thickness strain resulting from displacements ξ parallel to the x axis,

$S_x = l_y l_z$, the cross-sectional area perpendicular to the x axis,

F_x is the compressional force parallel to the x-axis,

e_{11} is one of the piezoelectric *stress* coefficients of quartz, expressed in coulombs per square meter,

c_{11} is one of the elastic *stiffness* coefficients of quartz, expressed in newtons per square meter. Numerical values for these two coefficients are given in Table 12.1. The remaining quantities are identical in definition with those previously defined for equations 12.1 and 12.2.

In order to obtain the maximum transfer of energy from the crystal into an adjacent liquid, it is customary to mount the crystal in a manner such as that indicated schematically in Fig. 12.11. Because of the poor acoustic impedance match between air and quartz, only an insignificant amount of energy is radiated from the face A in contact with the air. An expression for the ultrasonic acoustic power radiated into the adjacent liquid by the crystal face B may be obtained by methods similar to those used in Sect. 12.4 for the longitudinal vibrator. The acoustic output is a maximum when the crystal is driven at its fundamental frequency of free-free vibrations, i.e., when the frequency is such that the thickness of the crystal equals $\lambda/2$. This frequency is given by the equation

$$f_1 = \frac{c_x}{2l_x} = \frac{1}{2l_x}\sqrt{\frac{c_{11}}{\rho}} \tag{12.48}$$

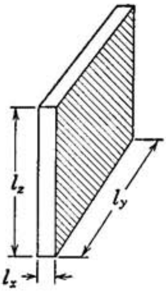

Fig. 12.10. Thickness vibrator, X-cut.

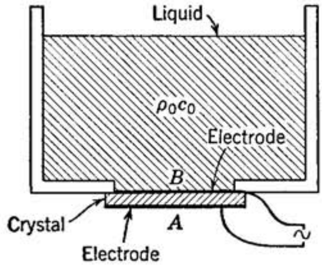

Fig. 12.11. Ultrasonic radiation into a liquid.

The corresponding acoustic output in watts is

$$W = \frac{\phi^2 E_x^{\ 2}}{\rho_0 c_0 S_x} \tag{12.49}$$

where the transformation factor ϕ, appropriate for thickness vibrations of a half wavelength vibrator, is defined by

$$\phi = \frac{2e_{11} S_x}{l_x} \tag{12.50}$$

and $\rho_0 c_0$ is the characteristic impedance of the liquid.

Furthermore, by methods similar to those used in Sect. 12.4, it is possible to show that the input electrical admittance of the thickness vibrator may be represented near its frequency of fundamental resonance by the circuit of Fig. 12.3 where

$$C_0 = \frac{\epsilon_x' \epsilon_0 l_y l_z}{l_x} \qquad \text{farads} \tag{12.51}$$

$$R = \frac{\rho_0 c_0 S_x}{\phi^2} \qquad \text{ohms} \tag{12.52}$$

$$C = \frac{2\phi^2 l_x}{\pi^2 S_x c_{11}} \qquad \text{farads} \tag{12.53}$$

and

$$L = \frac{\rho l_x S_x}{2\phi^2} \qquad \text{henries} \tag{12.53a}$$

As an example, let us calculate the acoustic power radiated into water by a quartz crystal of 2.0-mm thickness and 10-cm² cross section, when an rms voltage of 1000 volts is applied between the two plated surfaces at its fundamental resonant frequency. The resonant frequency of the crystal is

$$f_1 = \frac{5750}{2 \times 0.002} = 1.44 \text{ megacycles/sec}$$

The transformation factor for the crystal is

$$\phi = \frac{2 \times 0.17 \times 0.001}{0.002} = 0.17 \text{ coulomb/m}$$

and the corresponding acoustic output is

$$W = \frac{(0.17)^2 \times 1000^2}{1.48 \times 10^6 \times 0.001} = 19.5 \text{ watts}$$

If we now make the reasonable asssumption that this acoustic power is radiated uniformly over the surface of the crystal, the corresponding acoustic intensity in the water immediately above the crystal is 1.95 watts/cm^2 or 19,500 watts/m^2. In turn, equation 5.38 may be used to show that this intensity corresponds to peak pressure amplitudes in the adjacent water of

$$P = (2\rho_0 c_0 I)^{1/2} = (2 \times 1.48 \times 10^6 \times 19{,}500)^{1/2}$$
$$= 2.4 \times 10^5 \text{ newtons/m}^2 = 2.4 \text{ atmospheres}$$

It is to be anticipated that cavitation bubbles and other unusual physical phenomena may be observed in ultrasonic beams of such high intensities and pressure amplitudes.

Typical values for those coefficients required for making computations regarding the thickness vibrations of barium titanate wafers, polarized in the direction of these vibrations, are $e_{11} = 16$ coulombs/m^2 and $c_{11} = 15 \times 10^{10}$ newtons/m^2. It is to be noted that since the stress coefficient e_{11} for barium titanate is some 100 times greater than that of quartz, only about 10 volts would be required for a barium titanate wafer of 2 mm thickness to produce the same acoustic output as that of the quartz crystal discussed above.

12.10 Piezoelectric Receivers or Hydrophones. Let us now consider how the piezoelectric effect may be used to construct simple receivers or *hydrophones* for converting the pressure changes associated with acoustic waves in liquids into similar voltage changes. Although both thickness and longitudinal vibrators may be used as the transducing element in such receivers, we will confine this discussion to longitudinal vibrators and in particular to the X-cut quartz crystal of Fig. 12.2.

Equations 12.32 and 12.33 are admirably suited for derivation of general equations applicable to the receiving response of an open-circuited vibrator element. Under these circumstances, $\mathbf{I} = 0$ and equation 12.32 simplifies to

$$\mathbf{U} = \frac{\mathbf{Y}_E\mathbf{E}}{\phi} = \frac{\mathbf{E}}{\mathbf{Z}_E\phi}$$

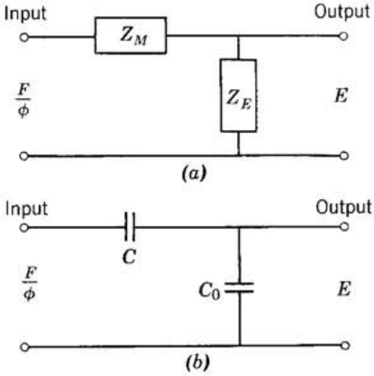

Fig. 12.12. Equivalent circuits of a piezoelectric receiver. (*a*) General circuit. (*b*) Low-frequency circuit.

When this expression for $\mathbf{U}$ is substituted into equation 12.33, there results

$$\mathbf{F} = \phi\mathbf{E} + \frac{\mathbf{Z}_m\mathbf{E}}{\mathbf{Z}_E\phi} = \phi\mathbf{E}\left(1 + \frac{\mathbf{Z}_m}{\mathbf{Z}_E\phi^2}\right)$$

Upon replacing $\mathbf{Z}_m/\phi^2$ by the equivalent motional impedance $\mathbf{Z}_M$ and solving for $\mathbf{E}$

$$\mathbf{E} = \left(\frac{\mathbf{F}}{\phi}\right)\frac{\mathbf{Z}_E}{\mathbf{Z}_E + \mathbf{Z}_M} \tag{12.54}$$

is obtained. The output voltage $\mathbf{E}$ of the vibrator is identical with that produced across the impedance $\mathbf{Z}_E$ of the circuit of Fig. 12.12*a* by an input voltage $(\mathbf{F}/\phi)$ inserted into the motional impedance or $\mathbf{Z}_M$ part of the circuit.

As an example of the utility of equation 12.54, let us apply it to the special case of relatively uniform response that occurs at frequencies well below the fundamental frequency of resonance of the vibrator. The circuit is then represented by Fig. 12.12*b* in which the blocked electrical impedance $\mathbf{Z}_E$ has been replaced by the capacitor C_0 whose capacitance is given by equation 12.26 and the motional impedance $\mathbf{Z}_M$, by the capacitor C whose low-frequency capacitance is given by equation 12.30*a*. By considering the two capacitors of Fig. 12.12*b* to act as a potential divider, one may show that

$$E = \left(\frac{F}{\phi}\right)\frac{C/C_0}{1 + (C/C_0)} \tag{12.55}$$

In turn, when the respective defining expressions for C and C_0 are substituted into the ratio C/C_0, the result may be expressed as

$$C/C_0 = \frac{k^2}{1 - k^2}$$

which upon being substituted into equation 12.55 leads to

$$E = \left(\frac{F}{\phi}\right)k^2 \tag{12.56}$$

Finally, if the pressure acting on the driven end of the vibrator in contact with the adjacent liquid is P, then $F = S_y P$, where S_y is the cross section of the vibrator, and equation 12.56 may be rewritten as

$$\frac{E}{P} = \frac{k^2}{\phi} S_y \tag{12.57}$$

Equation 12.57 gives the open-circuit receiving response of a longitudinal vibrator in volts per newton/m^2. It must, of course, be multiplied by 0.1 in order to express the response in volts per microbar.

Equation 12.57 indicates that, when crystal elements of identical dimensions are constructed from different piezoelectric materials, the open-circuit low-frequency receiving responses will be proportional to the quantity k^2/ϕ. Numerical values for this ratio are listed in Table 12.4

Table 12.4 Receiving response constants of transducer materials

Crystal	k^2/ϕ (volts/newton)	$\epsilon k^2/\phi$ (volts/newton)
X-cut Quartz	$0.058/l_z$	$0.26/l_z$
45° Z-cut ADP	$0.178/l_z$	$2.7/l_z$
45° X-cut Rochelle salt	$0.089/l_z$	$31.0/l_z$
45° Y-cut Rochelle salt	$0.305/l_z$	$3.05/l_z$
Barium Titanate	$0.0053/l_z$	$6.35/l_z$

for those crystal cuts commonly used as longitudinal vibrators in piezoelectric receivers. It is to be noted that k^2/ϕ depends on the width l_z of the crystal. However, a cursory consideration of the relative magnitudes of this ratio alone, will yield misleading information as to the practical sensitivities obtained from these various crystal elements. The open-circuit voltages given by equation 12.57 are essentially generated in impedances equal to that of a capacitor whose capacitance is the sum of C plus C_0. This capacitance is in turn proportional to the free dielectric constant ϵ. A more realistic parameter expressing the relative responses of the various crystals is given by the quantity $\epsilon k^2/\phi$. This parameter measures the relative magnitudes of the voltage outputs obtained from crystals having the same width and length but of different thicknesses so that their capacitances are identical. The tabulated values of this parameter $\epsilon k^2/\phi$ show that the 45° X-cut of Rochelle salt will produce the highest sensitivity when referred to crystal elements having equal capacitances.

Since the right-hand term of equation 12.57 is independent of frequency, the low-frequency response of piezoelectric receivers is independent of frequency. However, as the fundamental frequency of mechanical resonance is approached, Z_m decreases to a minimum and the response increases to a maximum. Calculations as to the receiving response of a piezoelectric vibrator in the vicinity of this resonance may be made by inserting a voltage SP/ϕ into the motional impedance branch of Fig. 12.5 and computing the output voltage E appearing across the capacitor C_0.

12.11 Characteristics of Ceramic Cylinders as Transducers. When the lateral dimensions of the surface either of a mosaic of longitudinal vibrators or of a single thickness vibrator are small compared to a wavelength in the adjacent liquid, both the transmitting and the receiving responses of the transducer are essentially nondirectional. Nondirectional transducers are also obtained when *small* ceramic cylinders of barium titanate are used. When operating as a receiving hydrophone, the choice of dimensions of the cylinder is determined by the frequency range in which a flat response is desired. The upper limit of this flat range is somewhat below the frequency of the lowest natural mode of vibration of the cylinder. When operating as a sound source, the choice of dimensions is determined by the frequency at which the peak acoustic output is desired since it will occur at the fundamental frequency of radial vibrations.

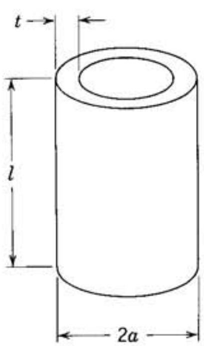

Fig. 12.13. Important dimensions of a ceramic cylinder type of vibrator.

The cylinder of Fig. 12.13 has three distinctly different possible modes of vibration. They are:

1. *Radial mode.* The mean radius of the cylinder becomes larger and smaller. The fundamental resonant frequency is determined primarily by the mean radius a and is given approximately by the equation

$$f \approx \frac{c}{2\pi a} \tag{12.58}$$

where c is the velocity of longitudinal waves in the material of the cylinder.

2. *Length mode.* The length of the cylinder becomes longer and shorter. The fundamental resonant frequency is determined primarily by the length l and is given approximately by the equation

$$f \approx \frac{c}{2l} \tag{12.59}$$

where c is the velocity of longitudinal waves in the material of the cylinder.

3. *Thickness mode.* The vibrating wall becomes thicker and thinner. The fundamental resonant frequency is determined primarily by the wall

thickness t and is given approximately by the equation

$$f \approx \frac{c'}{2t} \tag{12.60}$$

where c' is the velocity of thickness waves in the material of the cylinder.

Some coupling is always present between the various modes of vibration. For example, when the mean radius of the cylinder is compressed radially by an external pressure, the walls of the cylinder become thinner and its length increases. In particular, the coupling between the radial and length modes becomes strong when the length is approximately three times the mean radius, i.e., for $l \approx 3a$. As an example, let us consider a barium titanate cylinder to be polarized radially outward across the wall of the cylinder. When an alternating electric field is produced along this direction by application of an alternating voltage between electrodes plated on the inner and outer walls of the cylinder, it is possible to excite each of the three basic modes of vibration. The amount that any given mode is excited will be determined by the nearness of its frequency to that of the driving voltage. Conversely, when acting as a receiving hydrophone, the application of a uniform external pressure produces radial, longitudinal, and thickness strains and as a consequence the voltage output may be obtained either as a longitudinal voltage gradient along the axis of the cylinder, as a circumferential voltage gradient around the cylinder, or as a thickness voltage gradient across the walls of the cylinder. Of course, when the cylinder is polarized radially outward, the voltage will be obtained between the plated walls of the cylinder. Since the above uniform external pressure involves both radial and tangential strains, two piezoelectric strain constants are involved in the resulting electric fields generated. These two constants have opposite signs and therefore, the electric fields generated partly cancel each other. The degree of this cancellation depends upon the ratio of the thickness t to the mean radius a. For barium titanate cylinders having a ratio of $t/a = 0.58$, this cancellation effect is complete and reduces the voltage output to zero. Correspondingly, as this ratio ranges from about 0.4 to 0.7 the receiving response of radially polarized barium titanate cylinders is relatively low.

As an example of a typical cylindrical ceramic hydrophone element, let us consider one of 4-cm length, 2-cm mean radius, and 0.3-cm wall thickness. The resonant frequency of such a cylinder vibrating in its fundamental radial mode is approximately 36 kc/sec, the fundamental length mode is approximately 57 kc/sec, and the fundamental thickness mode is approximately 870 kc/sec. The resulting coupling coefficient is $k = 0.16$, the receiving response is about -104 db relative to 1 volt per microbar, and the response is relatively uniform up to a frequency of 30 kc/sec. The electrical capacitance in which the above voltage is generated is that of a cylindrical tube fully electroded on its inside and outside surfaces and as given by the usual equation for coaxial cylindrical conductors separated by a medium of dielectric constant ϵ is

$$C = \frac{2\pi\epsilon\epsilon_0 l}{\ln\left(\dfrac{a_2}{a_1}\right)} = \frac{2\pi \times 1200 \times 8.85 \times 10^{-12} \times 0.04}{\ln\left(\dfrac{0.0215}{0.0185}\right)} = 0.018\ \mu\text{f}$$

In the final assembly, the cylindrical element is usually covered with a pressure-molded neoprene sheath bonded to the cylinder so as to insulate it electrically and also to cover the ends so as to prevent any liquid pressure from acting on the inner wall of the cylinder.

Extremely small ceramic cylinders of barium titanate of millimeter dimensions have been constructed as probes for measurements at ultrasonic frequencies up to a few megacycles per second. Although the output of such probes is both relatively uniform and nondirectional up to frequencies in excess of one megacycle/sec, the electrical voltage generated is so low that considerable care must be taken in designing amplifiers for use with such probes.

12.12 Piezoelectric Transducer Measurements. The transmitting and receiving characteristics of piezoelectric sonar and ultrasonic transducers may be measured by methods similar to those described in earlier chapters for loudspeakers and for microphones. For instance, the receiving response of a hydrophone may be obtained by application of the reciprocity method described for microphones in Sect 11.15. Similarly, measurement of either the input electrical impedance or admittance, first in air and then in water, enables one to compute the transmitting efficiency of a sonar transducer at a resonant frequency.

When making such measurements on piezoelectric transducers, it is usually more advantageous to measure the input admittance rather than the input impedance. If we consider the electrical input of such a transducer to be represented by that of the circuit of Fig. 12.5, then the *motional admittance* is that of the branch containing R_R, R_M, L, and C and is independent of the *blocked admittance*, which is that of R_0 in parallel with C_0. By contrast, the motional impedance contributed by this branch to the total impedance is also dependent on R_0 and C_0. Consequently, it is easier to analyze the circuit of Fig. 12.5 and to compute its blocked and motional components in terms of admittance rather than in terms of impedance.

It is possible to show that the complex vector

$$\mathbf{Y}_M = G_M + jB_M = \frac{1}{(R_R + R_M) + j(\omega L - 1/\omega C)} \qquad (12.61)$$

representing the motional admittance of the circuit of Fig. 12.5, describes a circle in the complex plane as frequency is changed. The diameter of this circle is equal to $1/(R_R + R_M)$ and its measurement under various loading conditions enables one to determine the magnitudes of R_R and R_M. For instance, the diameter D_W of the motional admittance circle measured when the transducer is immersed in water is given by the equation

$$D_W = \frac{1}{R_R + R_M} \qquad (12.62)$$

However, if the motional admittance circle is measured when the transducer is in air, $R_R \approx 0$, since it is proportional to the relatively small characteristic impedance $\rho_0 c_0$ of the air. Therefore, the measured diameter D_A in air should be given by the equation

$$D_A = \frac{1}{R_M} \qquad (12.63)$$

The electroacoustic efficiency of a piezoelectric transducer represented by the circuit of Fig. 12.5 is determined by the ratio of the power dissipated in R_R to the total power consumed by R_R, R_M, and R_0. By application of simple electrical circuit theory, one may show that at the resonant frequency of the motional admittance branch, this efficiency is given by

$$\eta = \frac{R_R R_0}{(R_R + R_M)(R_R + R_M + R_0)} \qquad (12.64)$$

Finally, if equations 12.62 and 12.63 are used to eliminate R_R and R_M from equation 12.64, and if $1/R_0$ is replaced by the measured blocked conductance G_E, then

$$\eta = \frac{D_W(D_A - D_W)}{D_A(D_W + G_E)} \qquad (12.65)$$

is obtained for the *resonant* efficiency.

Plotted in Fig. 12.14, for frequencies near resonance, are measured values of the input conductance G_I and susceptance B_I of a typical sonar transducer constructed from ADP crystals. The curves of Fig. 12.14*a* correspond to measurements taken when the transducer is in air and of Fig. 12.14*b* for measurements in water. Also shown are dashed straight

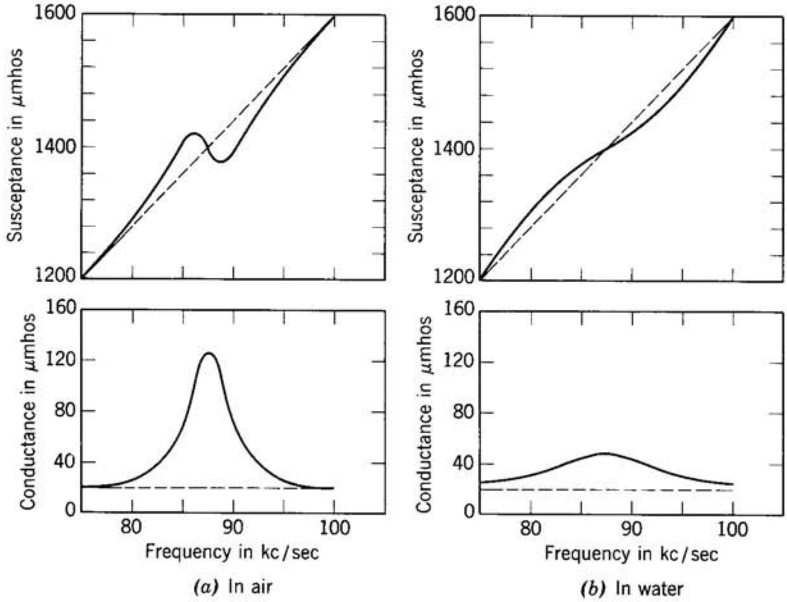

Fig. 12.14. Measured susceptance and conductance curves for a piezoelectric transducer resonating at 87.5 kc/sec.

lines connecting low and high frequency values for each of these quantities which represent their *blocked* values. The departure of each of these curves from the corresponding dashed line is a measure of the associated motional admittance component. In order to compute the efficiency of the transducer, it is convenient to replot the data of Fig. 12.14 in the manner of Fig. 12.15. Here, at each frequency, the motional susceptance is plotted as ordinate against the total input conductance as abscissa. The large circle corresponds to measurements taken in air and the small one to measurements in water. It is to be noted that each of these circles is displaced by a distance G_E from the origin. The indicated resonant efficiency of this transducer, as computed from values of G_E, D_A, and D_W obtained from Fig. 12.15, is

$$\eta = \frac{30(110 - 30)}{110(30 + 20)} = 0.44$$

Of the many kinds of measurements made on piezoelectric transducers, only one more will be considered in this section. This is one whereby measurement of the frequencies of *resonance* and *antiresonance* of the unloaded transducer enables one to compute the piezoelectric activity of the material involved. The frequency of mechanical resonance is that which results in the electrical reactance of the motional admittance branch of Fig. 12.5 becoming zero and, therefore, is given by the equation

$$\omega_r = \sqrt{\frac{1}{LC}} \tag{12.66}$$

At this frequency, both the efficiency and the acoustic output of the transducer for constant voltage input are a maximum. In addition, for an unloaded transducer, i.e., when operating in air, the magnitude of the admittance is near its maximum. Another frequency of considerable interest is the parallel antiresonant frequency ω_a. This frequency is defined by the equation

$$\left(\omega_a L - \frac{1}{\omega_a C}\right) = \frac{1}{\omega_a C_o}$$

which may be rewritten as

$$\left(\frac{\omega_a}{\omega_r}\right)^2 = 1 + \frac{C}{C_0} \tag{12.67}$$

At this frequency, as defined above, the reactances of the blocked and motional branches of Fig. 12.5 are equal in magnitude and of opposite sign. Consequently, if no resistance terms were present, i.e., if the transducer were completely unloaded, the input admittance would be zero. In actual practice, an air-loaded transducer has its minimum admittance at

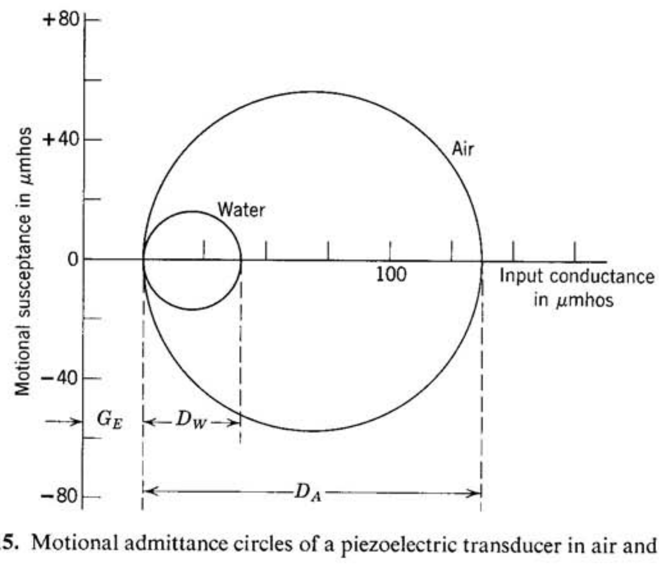

Fig. 12.15. Motional admittance circles of a piezoelectric transducer in air and in water.

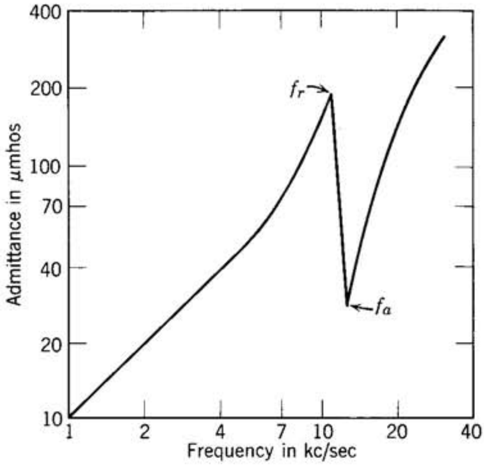

Fig. 12.16. Admittance vs. frequency curve for Rochelle salt vibrator.

a frequency only slightly in excess of the frequency defined by equation 12.67. Therefore, if one measures the frequencies of maximum and minimum admittance of an unloaded transducer and assumes these frequencies respectively to be ω_r and ω_a, equation 12.67 may be used to compute the capacitance ratio C/C_0 which in turn is one measure of the piezoelectric activity of a material.

Plotted in Fig. 12.16 are measured values of the input admittance of a 45° X-cut Rochelle salt longitudinal vibrator. Upon substituting the respective values of 12.2 kc/sec and 10.7 kc/sec for the frequencies of minimum and maximum admittance into equation 12.67

$$\frac{C}{C_0} = \left(\frac{12.2}{10.7}\right)^2 - 1 = 0.30$$

is obtained. Finally, the corresponding coefficient of electromechanical coupling k may be computed from equation 12.30*c* as $k = 0.52$. For further information on measurement and calibration of electroacoustic transducers used in liquids, the reader is referred to the complete discussion given in the American Standards Association publication on this topic.[2]

12.13 Magnetostriction. When a ferromagnetic material is magnetized, certain changes occur in its internal structure, and the resulting stresses in the specimen produce small changes in its physical dimensions. This phenomenon is referred to as *magnetostriction* or the *magnetostrictive*

[2] *Calibration of Electroacoustics Transducers*, Z24.24–1957, American Standards Association (1957).

effect. It is widely used in constructing vibrating elements for sonar transducers and hydrophones, and a limited treatment of the fundamental principles involved is therefore justified.

In the most common method of producing longitudinal vibrations in a magnetostrictive vibrator, an alternating magnetic field is applied parallel to the axis of the vibrator, which produces corresponding changes in its length. If the vibrator is initially unmagnetized, the resulting changes in its length are independent of the direction of the applied field and may be either an increase or a decrease, depending upon the material from which it is constructed. The magnitude of the effect is actually a function of the intensity of magnetization produced in the material, but for flux densities B which are well below that corresponding to magnetic saturation the static strain produced may be considered as being proportional to the square of the flux density. We may therefore write

$$\left(\frac{\partial \xi}{\partial x}\right)_m = KB^2 \qquad (12.68)$$

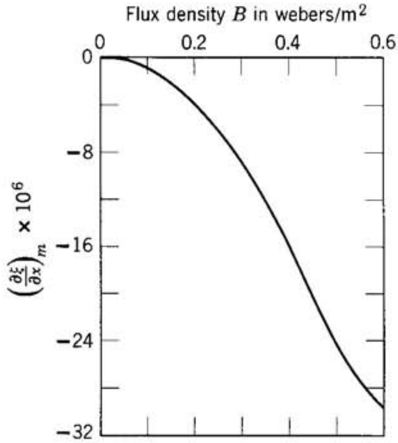

Fig. 12.17. Static magnetostrictive strain in nickel as a function of flux density.

where K is a material constant (m⁴/webers²) that is positive for a material that expands upon magnetization and negative for one that contracts. Permalloy expands, so that K is positive, whereas nickel contracts, giving a negative value for K. Nickel and certain of its alloys, such as Invar and Permendur, exhibit the magnetostrictive effect to a greater degree than other materials and are consequently most commonly used in magnetostrictive vibrators. Figure 12.17 is a typical curve showing the relation between the static magnetostrictive strain $(\partial \xi/\partial x)_m$ in a bar of annealed nickel and the flux density B in webers/m². At flux densities of less than 0.5 webers/m² the value of the proportionality constant K corresponding to this curve is $K = -1.0 \times 10^{-4}$. For greater flux densities the magnetostrictive strain is no longer represented by equation 12.68, but instead attains a maximum value of about -40×10^{-6} when B exceeds 1.0 webers/m².

If an alternating current is passed through a coil of wire A wound around a nickel rod, as shown in Fig. 12.18, the resulting alternating magnetic field causes the rod to shorten periodically. Since the shortening is independent of the direction of the applied field, it is apparent that the frequency of mechanical vibration will be twice that of the applied current. If, as is usually true, it is desired that the frequency of mechanical vibration be the same as that of the current, a steady polarizing magnetic field must be applied to the bar. This field may be produced either by a direct current flowing through a second coil B, or by the use of adjacent permanent magnets. Then, if the magnitude of the polarizing field is greater than the amplitude of the alternating field, the mechanical and electrical frequencies will be identical. Equation 12.68, which gives the relationship between magnetostrictive strain and flux density, may be used to obtain the equations of motion for such a rod.

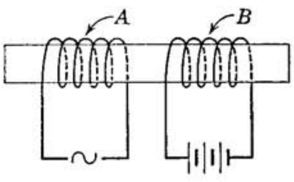

Fig. 12.18. Magnetostrictive vibrator.

With a slight modification, equation 3.5, which gives the relation between the internal longitudinal force in a rod and its strain, may be applied to this case. Here the longitudinal force F_x is proportional only to that portion of the total strain $\partial\xi/\partial x$ in excess of the strain KB^2 produced by the magnetostrictive effect, so that

$$F_x = -SY\left(\frac{\partial \xi}{\partial x} - KB^2\right) \tag{12.69}$$

where B is the net flux density resulting from both the steady and the alternating current. If the net flux density B in the rod changes from the polarizing flux density B_0 to $B_0 + \delta B$, the internal force changes from F_{x0} to $F_{x0} + \delta F_x$, and the strain from $(\partial\xi/\partial x)_0$ to $(\partial\xi/\partial x)_0 + \delta(\partial\xi/\partial x)$. Then

$$\delta F_x = -SY\left[\delta\left(\frac{\partial \xi}{\partial x}\right) - 2KB_0\delta B\right] \tag{12.70}$$

If we agree to let F_{xi}, $(\partial\xi/\partial x)_i$, and B_i represent alternating or incremental changes in these various quantities, each small as compared to its respective static or polarizing value F_{x0}, $(\partial\xi/\partial x)_0$, and B_0, then equation 12.70 may be rewritten as

$$F_{xi} = -SY\left(\frac{\partial \xi}{\partial x}\right)_i + \Lambda SB_i \tag{12.71}$$

where the quantity Λ, which is known as the *magnetostriction constant* of the rod, is

$$\Lambda = 2YKB_0 \tag{12.72}$$

It is to be noted that the magnitude of this constant increases with the polarizing flux, B_0, provided that K remains constant.

Equation 12.71 shows that incremental changes in the strain of a magnetostrictive material arise from two causes, i.e., changes in stress F_{xi}/S and changes in flux density B_i. Conversely, it may be shown through conservation of energy considerations that the magnetostrictive effect is reversible, i.e., changes in the incremental flux density B_i also arise from two causes, either a change H_i in the external magnetizing field or a change $(\partial\xi/\partial x)_i$ in the strain. The total change in flux density B_i is thereby expressed as

$$B_i = \mu_i\mu_0 \left[H_i + \Lambda\left(\frac{\partial\xi}{\partial x}\right)_i\right] \tag{12.73}$$

where μ_i is the incremental or reversible permeability of the material and $\mu_0 = 4\pi \times 10^{-7}$ henries/m is the permeability of free space. The incremental permeability is determined by the slope of the familiar B versus H curve at the operating point, i.e., the point at which $B = B_0$. Hence $\mu_i\mu_0 = dB_i/dH_i$, evaluated at B_0.

The two equations 12.71 and 12.73 may be used to derive wave equations for calculating longitudinal strains and forces produced in a magnetostrictive vibrator which is driven by an alternating current flowing in a surrounding coil. Conversely, they may be used to compute voltages induced in the coil when the dimensions of the vibrator are altered by the application of external forces, such as those due to acoustic waves.

As a simple illustration let us consider the free oscillations of a rod of length l which is clamped at one end and free at the other. If the external magnetic field is constant, i.e., if $H_i = 0$, then equation 12.73 is reduced to

$$B_i = \mu_i\mu_0\Lambda\left(\frac{\partial\xi}{\partial x}\right)_i \tag{12.74}$$

Substitution of this equation into equation 12.71 yields

$$F_{xi} = -S(Y - \mu_i\mu_0\Lambda^2)\left(\frac{\partial\xi}{\partial x}\right)_i \tag{12.75}$$

The effective Young's modulus of the rod is reduced from Y to

$$Y' = Y(1 - k^2) \tag{12.76}$$

where k, the *coefficient of electromechanical coupling* of a magnetostrictive vibrator, is given by

$$k = \sqrt{\mu_i\mu_0\Lambda^2/Y} = 2KB_0\sqrt{\mu_i\mu_0 Y} \tag{12.77}$$

Equation 12.76 expresses the important physical fact that the induction of a polarizing flux of density B_0 in a magnetostrictive material lowers the value of Young's modulus. The reduced stiffness Y' of the material causes a corresponding reduction in the velocity of longitudinal waves which in turn reduces the fundamental frequency of vibrations of the rod.

If a coil of wire is wound around the rod, equation 12.74 may be used to compute the voltage induced in the coil when the rod is caused to vibrate. It is to be noted that when no polarizing flux is present, the magnetostriction constant Λ is zero. Therefore, when a magnetostrictive material is *demagnetized*, forced vibrations of the material will not induce a voltage in a surrounding coil.

Similarly, the magnetostriction equations 12.71 and 12.73 may be used to show that if an alternating current from an external generator flows through the surrounding coil of a vibrator, the amplitude of the resulting vibration has its maximum value when the impressed frequency equals the

Table 12.5 Typical magnetostriction constants for annealed nickel

B_0	μ_i	Λ	k
0.25	137	-4.8×10^6	0.14
0.4	78	-12.5×10^6	0.27
0.5	41	-20.0×10^6	0.31
0.6	25	-15.0×10^6	0.18

resonant frequency of the vibrator. In particular, when the vibrator is driven at its frequency of fundamental resonance, the amplitude of the dynamic strains produced are markedly greater than those resulting from the application of static magnetizing fields of equal magnitude and may range up to 100×10^{-6}. Although the numerical magnitude of such a strain is small, the associated internal stress is quite large. Young's modulus for nickel is 2.1×10^{11} newtons/m^2, so that a strain of 100×10^{-6} corresponds to a stress of 2.1×10^7 newtons/m^2 which is equivalent to a pressure of 210 atmospheres. These high stresses indicate that magnetostrictive vibrators are excellently suited to act as the driver elements of sonar transducers.

The coefficient k as defined by equation 12.77 acts as a measure of the magnetostrictive coupling of a magnetostrictive vibrator in much the same manner as does the similar coefficient (Equation 12.5) for piezoelectric vibrators. It measures the degree of coupling that may be obtained between the mechanical motion of a magnetostrictive vibrator and the currents and voltages in a surrounding coil. In magnetostrictive sonar transducers both the efficiency and the quality factor Q, i.e., the sharpness of frequency response, are found to depend upon k. Since both the magnetostriction constant Λ and the incremental permeability μ_i are functions of the polarizing flux density B_0, it is apparent that the coefficient k will have its maximum value when the material is polarized so as to make the product $\mu_i \Lambda^2$ a maximum. Typical values for these various quantities are shown in Table 12.5 for a sample of annealed nickel.

12.14 Magnetostrictive Transducers. In the interests of efficiency, magnetostrictive sonar transducers are usually operated at or near a resonant frequency of their driving elements. This is required since the quality factor or Q associated with the bandwidth characteristics of their transmitting response curves, usually exceeds 50. One common type of transducer employs the longitudinal vibrations of tubes or laminations attached to a driven plate in contact with the water. For most efficient transfer of energy from the driving elements into the water it is essential that the latter present the optimum acoustic impedance to the motion of the driver. A *tube-and-plate* design, as illustrated in Fig. 12.19, provides one method of attaining this match. Here the driving elements are nickel tubes, each having a length equal to one-quarter of the wavelength (in nickel) of the sound to be radiated. Hundreds of such tubes are employed in a single transducer, one end of each tube being free, and the other being embedded in one side of a circular steel plate of such dimensions that the resonant frequency of the entire system is near that of the tubes alone. Each tube is surrounded by its own driving coil, and all are driven in phase by the current from a power amplifier. Polarizing fields are supplied either by a d-c component of the driving current or more commonly by permanent magnets mounted inside the watertight housing containing the tubes. The alternating forces exerted on the plate by the reaction to the stresses in the driving elements are transmitted by the plate into the adjacent water. In other designs, laminated stacks are used as driving elements instead of tubes, but solid rods are avoided because of their higher eddy current losses. Transducers using laminated stacks as vibrator elements are also designed so that the free end of each vibrator makes direct contact with the

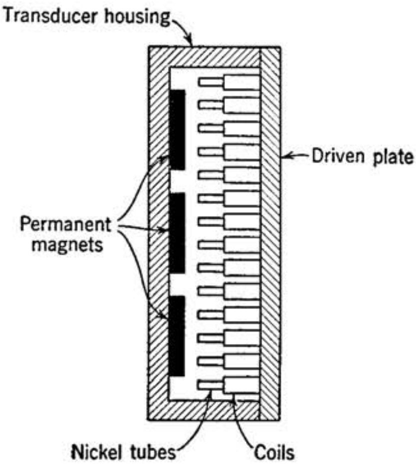

Fig. 12.19. Cross section of a typical magnetostrictive transducer.

adjacent water through a surrounding thin rubber boot. A mosaic of such laminated stacks may be mounted to supporting structures in such manners as to produce flat, cylindrical, or spherical radiating surfaces.

The primary advantages of magnetostrictive transducers over piezoelectric transducers of similar overall dimensions are their greater ruggedness and higher power-handling capacity. They also have a higher Q and a correspondingly sharper resonance curve, which is advantageous in reducing the disturbing effects of ambient background noise, but restricts their frequency range of efficient operation to a relatively narrow band. A disadvantage of the magnetostrictive type of transducer is the necessity of insuring the presence of a permanent polarization of the proper magnitude in order to attain optimum operating conditions. The reader is referred to the reference given below for a complete discussion of the magnetostrictive effect and its application to sonar transducers.[3]

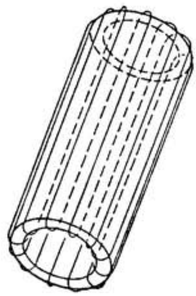

Fig. 12.20. Cylindrical magnetostrictive hydrophone.

12.15 Magnetostrictive Hydrophones. Because of the reversibility of the magnetostrictive effect, the transducer of Fig. 12.19 may also be used as a receiver. Sound waves impinging on the plate set it into vibration and correspondingly set up stresses and strains in the attached tubes. The resulting alternating voltages induced in the surrounding coils may be amplified and used to activate some portrayal device such as an oscilloscope or voltmeter. As in transmission, the receiving sensitivity of a magnetostrictive transducer is high only over a relatively narrow band of frequencies centered on its resonant frequency.

The active receiving element in the most widely used type of magnetostrictive hydrophone is a cylinder such as that shown in Fig. 12.20. Such a hydrophone has its maximum receiving response at its fundamental frequency of radial vibrations as given by the equation

$$f_0 = \frac{c}{2\pi a} \tag{12.78}$$

where c is the velocity of longitudinal waves in the magnetostrictive material composing the cylinder and a is its radius. However, these hydrophones are normally used at frequencies well below this resonant frequency and consequently, the receiving response equation derived in the next paragraph is limited in its application to frequencies below that given by equation 12.78.

[3] *Design and Construction of Magnetostriction Transducers*, Summary Technical Report of Division 6, Vol. 13, National Defense Research Committee (1946).

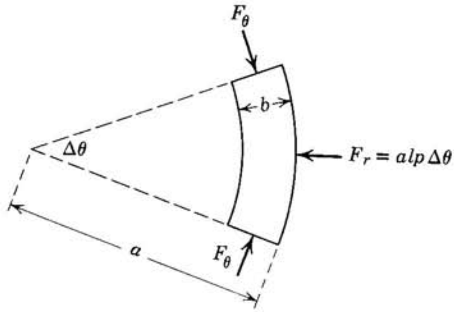

Fig. 12.21. Figure used to relate radial stresses in a cylinder to circumferential stresses.

Consider an acoustic pressure $p = P \cos \omega t$ to act uniformly inward on the surface of a cylinder of radius a, length l, and wall-thickness b. This acoustic pressure will in turn generate a circumferential force

$$F_\theta = alP \cos \omega t \tag{12.79}$$

in the cylinder. Equation 12.79 may be derived by considering the three forces acting on an angular segment $\Delta\theta$ of the cylinder, shown in Fig. 12.21, to be in static equilibrium. Then

$$2F_\theta \sin \frac{\Delta\theta}{2} \approx alp\Delta\theta$$

which upon letting $\Delta\theta \to 0$ leads to equation 12.79. The force F_θ in turn produces a circumferential strain $-F_\theta/blY'$ which upon being substituted for $(\partial\xi/\partial x)_i$ in equation 12.74 gives

$$B_i = -\frac{a}{b} \cdot \frac{\mu_i \mu_0 \Lambda}{Y'} P \cos \omega t \tag{12.80}$$

Finally, this changing flux density will induce a voltage e into the coil of N turns wound toroidally around the cylinder, where

$$e = N\frac{d\phi}{dt} = Nbl\frac{dB_i}{dt} = \frac{N\omega alP\mu_i\mu_0\Lambda}{Y'} \sin \omega t \tag{12.81}$$

The corresponding open-circuit voltage sensitivity is

$$\frac{E}{P} = \frac{N\omega al\mu_i\mu_0\Lambda}{Y'} \tag{12.82}$$

expressed in volts per newton/m^2.

The receiving response given by equation 12.82 is limited to low frequencies for three different reasons. They are:

(1) The frequency must be sufficiently low so that the diameter of the cylinder is small compared with a wavelength of sound in the fluid in which it is immersed in order that the acoustic pressure may be considered as acting uniformly and in the same phase over the entire surface of the cylinder.

(2) The frequency must be well below the frequency of fundamental radial vibrations of the cylinder in order to consider the circumferential strain to be that produced by a static force acting solely against the elastic stiffness of the cylinder. As the resonant frequency is approached, strains in the cylinder must be treated as dynamic ones depending upon its mass and mechanical resistance in addition to stiffness. Because of its smaller mass, equation 12.82 may be applied to a thin-walled cylinder at higher frequencies than to a thick-walled cylinder having the same external radius.

(3) Finally, the frequency must be sufficiently low so that eddy current losses in the material of the cylinder are negligible.

As an example of a typical cylindrical nickel magnetostrictive hydrophone element let us consider one of 15-cm length and 1-cm radius. The radial resonant frequency of such a cylinder is approximately 80 kc/sec and its receiving response at a frequency of 20 kc/sec is about -120 db relative to 1 volt per microbar. The electrical impedance in which the above voltage is generated is that of a resistance in series with an inductance. This impedance is normally of the order of magnitude of a hundred ohms and is much lower than the impedance in which the voltage is generated in ceramic hydrophones. In some hydrophones the circumferential polarizing flux is produced by flash-polarizing the cylinder by a short d-c current pulse which will generate a remanent internal flux. A stronger flux may be generated by cutting the cylinder lengthwise and inserting a narrow Alnico bar magnet in the cut. Of course, the Alnico magnet must be magnetized crosswise in order to generate the circumferential flux. It is to be noted that both μ_i and Λ are functions of the polarizing flux density B_0. Consequently, as B_0 changes, the sensitivity of a magnetostrictive hydrophone will change. For this reason, the sensitivity of a calibrated magnetostrictive hydrophone may change with time and, therefore, they are not used when acoustic measurements of high accuracy are required.

12.16 Impedance Measurements of Magnetostrictive Transducers. Methods used for the measurement of the characteristics of magnetostrictive transducers are very similar to those described in Sect. 12.12 for piezoelectric transducers excepting that it is more convenient to analyze magnetostrictive transducers from the electrical impedance concept than from the admittance concept. For instance, Fig. 12.4 may be used to represent a magnetostrictive transducer. Then

$$\mathbf{E} = \mathbf{Z}_E\mathbf{I} + \boldsymbol{\phi}_m\mathbf{U} \tag{12.83}$$

where $\mathbf{Z}_E = 1/\mathbf{Y}_E$ is the blocked electrical input impedance corresponding to $\mathbf{U} = 0$, and $\boldsymbol{\phi}_M$ is a *complex* transformation factor relating the magnetostrictively generated voltage in the open-circuited electrical side of the transducer to the generating velocity $\mathbf{U}$. Because of eddy current and magnetic hysteresis phenomena, the generated voltage is not in phase with the generating velocity and consequently, $\boldsymbol{\phi}_m$ must be complex. The corresponding equation giving the force on the mechanical side of the transducer is

$$\mathbf{F} = -\boldsymbol{\phi}_m\mathbf{I} + \mathbf{Z}_m\mathbf{U} \tag{12.84}$$

By combining equations 12.83 and 12.84 with equation 12.34 so as to eliminate $\mathbf{F}$ and $\mathbf{U}$ it is possible to show that the input impedance of the transducer is given by

$$\mathbf{Z}_I = \mathbf{Z}_E + \frac{\boldsymbol{\phi}_m^{\ 2}}{\mathbf{Z}_m + \mathbf{Z}_r} \tag{12.85}$$

The last term in this equation represents the *motional* impedance of the transducer and is identical to equation 12.36 for the motional admittance, excepting that $\boldsymbol{\phi}_m$ is complex and depends on different parameters.

By methods similar to that used for deriving equation 12.65, one can derive an equation that may be used to compute the resonant efficiency of a magnetostrictive transducer from measured values of its input impedance in air and in water. The resulting equation is

$$\eta = \frac{D_W(D_A - D_W)}{R_I D_A} \tag{12.86}$$

where D_A is the diameter of the motional impedance circle in air, D_W is its diameter in water, and R_I is the resistive component of the total input impedance in water. Plotted in Fig. 12.22 are typical curves for the motional impedance of a magnetostrictive transducer in air and in water. It is to be noted that since the transformation factor $\boldsymbol{\phi}_m$ is complex, the motional impedance vector at resonance is not horizontal but dips by an angle ψ_m below the horizontal. Consequently, the input resistance at resonance is not merely R_E, the blocked resistance, plus D_W but is instead given by

$$R_I = R_E + D_W \cos \psi_m \tag{12.87}$$

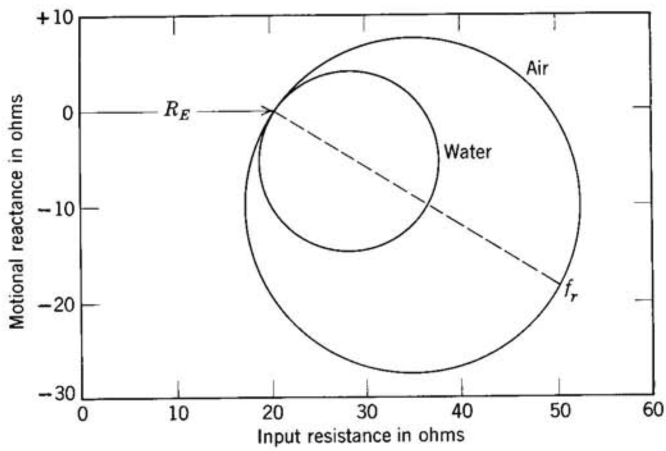

Fig. 12.22. Typical motional impedance circles for a magnetostrictive transducer in air and in water.

Upon substituting measured values from Fig. 12.22 into equation 12.86, the resulting resonant efficiency is

$$\eta = \frac{17(35 - 17)}{(20 + 17\cos 30)35} = 0.25$$

which is typical of magnetostrictive transducers. Finally, since $\boldsymbol{\phi}_m$ is a function of the electromechanical coupling coefficient k and as a consequence all terms in equation 12.86 are also dependent on this constant, it is observed that the efficiency of a magnetostrictive transducer increases as k is increased. Therefore, in order to maximize the efficiency of a magnetostrictive type of transducer it is necessary to choose an optimum polarizing flux B_0.

PROBLEMS

12.1. A plated X-cut quartz crystal has the following dimensions, $l_x = 0.005$ m, $l_y = 0.03$ m, and $l_z = 0.01$ m. (*a*) If a constant potential difference of 100 volts is applied between the plated surfaces, what is the longitudinal strain $\partial\eta/\partial y$ in the unconstrained crystal? (*b*) If the crystal is clamped so that it may not expand longitudinally, what stress is set up in the crystal? (*c*) What is the energy of mechanical deformation of the unconstrained crystal?

12.2. (*a*) Derive an expression giving the charge density appearing on the plates of a short-circuited X-cut quartz crystal when a constant longitudinal force F_y is applied along the y-axis. (*b*) Given an X-cut quartz crystal 5.0-cm long, 1.0-cm wide, and 0.5-cm thick, what total charge is generated on one of the short-circuited plates when a longitudinal force of 1000 newtons is applied? (*c*) If the plates were not short-circuited, what would be the difference in potential between the plates when the above force is applied?

12.3. If the crystal of Problem 12.1 is clamped at one end and free at the other: (*a*) What is its fundamental frequency of longitudinal vibrations? (*b*) Compute numerical values for the electrical elements in the equivalent electrical circuit of Fig. 12.3. Assume the mechanical resistance loading of the crystal to be of such a magnitude that its quality factor Q is 20,000.

12.4. (*a*) Show that the LC combination given by equations 12.30 and 12.31 may be used to represent the reactance term in equation 12.29 in the vicinity of the frequency of fundamental resonance, i.e., for kl_y near $\pi/2$. (*b*) Derive a general equation expressing the ratio of the reactance of the above LC combination to that of equation 12.29. (*c*) Compute the numerical value of this ratio for $kl_y = \pi/4$.

12.5. Show that the complex vector Y_M of equation 12.36, representing the motional admittance of a piezoelectric vibrator, traces a circle of diameter $\phi^2/(R_r + R_m)$ as frequency is increased from 0 to ∞.

12.6. (*a*) Given the individual X-cut quartz crystals in a mosaic type of sonar transducer are of 0.06-m length, 0.02-m width and 0.006-m thickness. What is their fundamental frequency of longitudinal vibrations? Assume each crystal vibrator to be fastened to a rigid backing plate at one end and radiating into water at the other end. (*b*) If the transducer is composed of a mosaic of 400 such crystals driven in parallel, what total acoustic power is radiated when the crystals are driven at the above frequency by an rms voltage of 100 volts? (*c*) What is the resonant value of the input admittance of this transducer?

12.7. Make the same calculations as requested in Problem 12.6 for a similar transducer having the individual crystal vibrators constructed from 45° Z-cut ADP.

12.8. Make the same calculations as requested in Problem 12.6 for a similar transducer having the individual crystal vibrators constructed from barium titanate ceramic bars.

12.9. Repeat the calculations of Problem 12.2 for a 45° X-cut Rochelle salt crystal of $5.0 \times 1.0 \times 0.5$ cm dimensions and compare the results with those obtained for a similar X-cut quartz crystal.

12.10. Repeat the calulations of Problem 12.3 for a 45° Y-cut Rochelle salt crystal of $0.03 \times 0.01 \times 0.005$ meter dimensions and compare the results with those obtained for a similar X-cut quartz crystal.

12.11. A square type of mosaic transducer, 25 cm $\times$ 25 cm, is constructed from 250 individual vibrators. Each individual vibrator is a 45° Z-cut ADP crystal 4.0-cm long, 2.5-cm wide, and 1.0-cm thick and is rigidly clamped to a backing plate on one end and radiates into water on the other. (*a*) What is the resonant frequency of the transducer? (*b*) Assuming the individual vibrators to be connected in parallel, what is the input admittance of this transducer at resonance? (*c*) What voltage must be applied to this transducer if it is to radiate 625 watts at resonance? (*d*) For a constant voltage input, at what frequencies will its output be down 3 db from the resonance value? (*e*) What is the diameter of the motional admittance circle of this transducer? (*f*) What is the quality factor or Q of this transducer?

12.12. (*a*) What is the thickness strain $\partial\xi/\partial x$ produced by a potential difference of 100 volts in the unconstrained crystal of Problem 12.1. (*b*) What thickness stress is produced, if the crystal is prevented from expanding along its thickness direction? (*c*) If a static force of 100 newtons is applied across the thickness dimension of the crystal, what difference in potential is generated between the plated surfaces of the crystal?

12.13. (*a*) What is the fundamental frequency of thickness vibrations of a 3-mm thick X-cut half-wave quartz crystal vibrator? (*b*) What voltage must be applied between the plated surfaces of this crystal at its resonant frequency, if it is to radiate 5 watts/cm^2 into water? (*c*) If the amplitude of the plated surface in contact with air is assumed to be the same as that in contact with the water, how many watts/cm^2 will be radiated into the air?

12.14. Repeat parts (*a*) and (*b*) of Problem 12.13 for a 3-mm thick barium titanate ceramic vibrator.

12.15. (*a*) By eliminating $(\partial\xi/\partial x)$ between equations 12.46 and 12.47, show that the electromechanical coupling coefficient of a thickness vibrator is given by

$$k = \sqrt{\frac{e_{11}^{\ 2}}{\epsilon_x \epsilon_0 c_{11}}}$$

(*b*) Compute the numerical value of *k* for an X-cut quartz thickness vibrator and compare with the value of *k* for a longitudinal vibrator. (*c*) Compute the numerical value of *k* for a barium titanate thickness vibrator and compare with the value of *k* for a longitudinal vibrator.

12.16. Given a square transducer, 0.05 m on a side and 0.01 m thick, to be constructed from barium titanate. The transducer is air-backed on one side and radiates into water on the other. (*a*) What is the frequency of fundamental resonance of this transducer? (*b*) What voltage must be applied to this transducer if it is to radiate 100 watts of acoustic power at its resonant frequency? (*c*) What is the input admittance of this transducer at resonance? (*d*) What is the width of the band of frequencies over which the output of this transducer, for a constant voltage input, will not be down by more than 3 db from its resonant output?

12.17. (*a*) Show that $k^2/\phi = d_{12}/\epsilon_x\epsilon_0 l_z$ for a longitudinal quartz vibrator clamped at one end. (*b*) Show that the voltage output of a longitudinal quartz crystal receiving element is proportional to its thickness. (*c*) What is the low-frequency open-circuit voltage response of a longitudinal quartz receiving element of 0.5-cm thickness, 1.0-cm width, and 5.0-cm length?

12.18. (*a*) Show that the low-frequency receiving response of a longitudinal X-cut quartz vibrator clamped at one end is given by $E/P = d_{12}l_x/\epsilon_x\epsilon_0$. (*b*) Show that the resonant receiving response of this vibrator is given by

$$\frac{E}{P} = \frac{d_{12}l_x}{\epsilon_x\epsilon_0 k^2(1 + \omega_1^{\ 2}C_0^{\ 2}R^2)^{1/2}}$$

where *R* is the motional resistance. (*c*) Compute the ratio of the resonant to the low-frequency receiving response for the longitudinal vibrator of part (*c*) of Problem 12.17.

12.19. (*a*) Derive a general expression for the low-frequency receiving response of a thickness vibrator of area *S* and thickness *t*, when the sound pressure acts on both faces of the crystal. (*b*) What is the numerical value of this type of receiving response for a barium titanate wafer of 0.0004-m^2 cross section and 0.002-m thickness?

12.20. An X-cut quartz crystal vibrator is 0.04-m long, 0.0075-m wide, and 0.0015-m thick. The quality factor or Q of the crystal when vibrating in air is measured to be 50,000. (*a*) What is the fundamental resonant frequency of longitudinal vibrations in air? Assume the crystal to be clamped at one end and free at the other. (*b*) At what frequency will the input admittance be a minimum? (*c*) What is the motional resistance R in ohms?

12.21. Given the following measured data for a crystal vibrator in air. At 20 kc/sec, the input conductance is negligible and the susceptance is 400 μmhos. At 45 kc/sec, the input admittance is a maximum with $G_I = 500$ μmhos and $B_I = 900$ μmhos. At 46.5 kc/sec, the input admittance is a minimum. (*a*) From the above data compute approximate numerical values for C_0, C, L, and R of the equivalent electrical circuit. (*b*) What is the quality factor Q of this crystal? (*c*) What is the coefficient of electromechanical coupling k of this crystal?

12.22. (*a*) If $K = -1.0 \times 10^{-4}$, plot values of the static magnetostrictive strain in a bar of nickel as a function of the flux density B, and compare with Fig. 12.17. (*b*) What is the magnitude of the resulting magnetostriction constant Λ at a flux density of 0.3 weber/m^2? (*c*) If $\mu_i = 100$, what is the magnitude of the coefficient of electromechanical coupling k under the above conditions? (*d*) If the above nickel bar is magnetized to a flux density of 0.3 weber/m^2 without being allowed to contract, what static stress is set up in the bar?

12.23. A longitudinal magnetostrictive vibrator is constructed from a nickel tube of 0.06-m length, 0.005-m inner radius, and 0.0005-m wall thickness. The tube is polarized to a flux density of 0.4 weber/m^2, the resulting incremental permeability is $\mu_i = 80$, and the magnetostriction constant is $\Lambda = -12.0 \times 10^6$. (*a*) What is the numerical value of the proportionality constant K? (*b*) What permanent change in length takes place as the tube is polarized to a flux density of 0.4 weber/m^2? (*c*) What stretching force will be required if this change in length is to be prevented? (*d*) If an additional external magnetizing field $H_i = 600$ ampere-turns/meter is applied so as to act uniformly along the axis of the tube, what additional change in length takes place? (*c*) What additional stretching force is required, if the change in length of part (*d*) is to be prevented?

12.24. Derive a general expression for the incremental change in longitudinal strain produced in a polarized magnetostrictive vibrator by a static increment in the magnetizing field H_i. Assume the vibrator to be free at both ends.

12.25. (*a*) Given that the nickel magnetostrictive tube of Problem 12.23 is rigidly clamped at one end to the relatively immobile driven plate of a sonar transducer and free at the other end. What is the fundamental frequency of longitudinal vibrations of the polarized tube? (*b*) When acting as a receiver, the forced longitudinal vibrations of the tube may be represented by the equation $\xi = A \sin (\pi x/2l) \cos \omega_1 t$, where l is the length of the tube, A is the displacement amplitude at the free end, and ω_1 is the resonant frequency. If $A = 10^{-6}$ meter, what open-circuit voltage will be induced in a 200-turn single-layer coil uniformly wound along the entire length of the above tube?

12.26. (*a*) By considering the effective radial restoring force associated with the accompanying circumferential forces in the shell, show that the fundamental frequency of radial vibrations of a thin cylindrical shell is given by equation 12.78. This problem may be worked by treating the cylinder as a simple oscillator, whose frequency of radial vibrations is determined by the ratio of the effective radial stiffness of the cylinder to its mass. (*b*) What must be the mean radius of an unpolarized nickel cylinder, if its fundamental frequency of radial vibrations is to be 50 kc/sec? (*c*) What will be the change in this frequency, if the nickel is polarized so that the magnetostriction constant $\Lambda = -25 \times 10^6$ and the incremental permeability is $\mu_i = 30$?

12.27. Given a nickel magnetostrictive hydrophone to be constructed from a cylindrical shell of 20-cm length and 5-cm mean diameter. The nickel is polarized so that its magnetostriction constant $\Lambda = -5 \times 10^6$ and the incremental permeability is $\mu_i = 100$. A coil of 100 turns is wound toroidally around the circumference of the cylinder. (*a*) What is the fundamental frequency of radial vibrations of the cylinder? (*b*) What is the low-frequency open-circuit voltage response of the hydrophone in volts per newton/m^2? (*c*) Express the answer of part (*b*) as a decibel response relative to 1 volt per microbar.

12.28. Show that equations 12.83 and 12.84 may be used to describe the electrical behavior of a direct radiator loudspeaker. What is the appropriate expression for $\mathbf{\Phi}_m$ for a loudspeaker?

12.29. Given a magnetostriction transducer to have a blocked resistance R_E of 20 ohms, a measured motional impedance circle in air having a diameter D'_A of 35 ohms which at resonance dips below the horizontal by an angle ψ_m of 30°. (*a*) By maximizing equation 12.86, determine the numerical value of the motional impedance circle in water that will lead to a maximum efficiency. (*b*) What is the resulting maximum potential efficiency?

chapter 13

SPEECH, HEARING, AND NOISE

13.1 Introduction. In previous chapters in this book we have considered the fundamentals of production, transmission, and reception of sound waves. Speech, music, and noise are three categories into which practically all important natural sounds may be grouped. Hearing is the natural method for the reception of such sounds, and in particular is the ultimate significant termination of most acoustic systems involving the artificial reproduction of sound. Therefore, in order properly to design acoustical systems for the reproduction of sound, one must know something about the basic characteristics of speech and hearing. An enormous amount of valuable physical, physiological, and psychological data relating to these subjects has been collected. However, it is beyond the intent of this book to present all possible pertinent material. For a wealth of information beyond that given in this chapter, the reader is advised to consult the references given below.[1,2,3]

The treatment in this chapter will be limited primarily to a consideration of the characteristics of sounds produced by the human voice, the capabilities of the human ear for receiving these sounds as well as other wanted sounds such as musical sounds, and interference produced in this reception by unwanted sounds or noise. The acoustical characteristics of speech sounds as well as those of music and noise may be measured with considerable precision by use of standard acoustical instrumentation including microphones, frequency analyzers, oscilloscopes, etc. The results of such measurements may be expressed in terms of precise physical parameters including frequency, power, pressure level, time duration, etc. By contrast, the ultimate interpretative characteristics of the human hearing mechanism

[1] Fletcher, *Speech and Hearing in Communication*, D. Van Nostrand Co. (1953).

[2] Rosenblith and Stevens, *Handbook of Acoustic Noise Control*, Vol. II, "Noise and Man," WADC Technical Report 52-204 (1953).

[3] Harris, *Handbook of Noise Control*, Chs. 4-9, McGraw-Hill Book Co. (1957).

are not expressible in terms of objectively determined physical parameters. Instead they must be determined by operational experiments leading to statistical predictions as to the capabilities of an average ear under assumed or known conditions. As an example, in attempting to measure the psychological sensation of *loudness*, one finds that it is possible to get listeners to agree with surprising accuracy as to the relative loudness of two sounds of different frequency, and as a result to construct conversion curves relating the physical parameters of intensity and frequency to psychological loudness. Similar investigations enable one to determine typical values for just noticeable differences in frequency or intensity, for minimum perceptible intensities, for onset of pain, etc. Such experimentation, being psychological in its nature, suffers from the uncertainty as to whether or not all pertinent independent variables, including any mental bias or attitude toward the experiment, are being held constant. Therefore, in reading the material on hearing that follows and in interpreting the curves that are presented, one should bear in mind that the data presented were obtained by particular experimenters using particular stimuli, presented to particular listeners under particular background conditions. As a result, other experimenters in attempting to repeat a given experiment may obtain substantially different results unless great care is used to repeat all factors involved in the initial experiment.

13.2 The Voice Mechanism. The acoustic energy associated with speech originates in the chest muscles which, by contraction, force air from the lungs up through the various components of the vocal mechanism (Fig. 13.1). This steady stream of air may be looked upon as a *carrier* of energy which must be modulated in its velocity and correspondingly in pressure in order to produce sounds. The requisite modulation is accomplished in two basic ways leading respectively to *voiced* and *unvoiced* sounds.

Voiced sounds include the vowels of ordinary speech as well as the tones characteristic of the singing voice. The primary modulating agent for voiced sounds is the *larynx*, across which are stretched the *vocal cords*. The vocal cords are two membranelike bands forming a diaphragm with a slit-like opening which modulates the air stream as it vibrates open and shut. The length of this opening (about 2.5 cm in men and 1.5 cm in women) and the tension to which the vocal cords are stretched determines the fundamental frequency of this modulation. The action of the vocal cords produces a *sawtooth* type of variation in velocity and correspondingly of pressure in the modulated stream of air, Fig. 13.2*a*, which, upon analysis into a Fourier series of sinusoidal waves is found to contain a large number of harmonically related frequency components.

The numerous resonating cavities and orifices of the nose, mouth, and

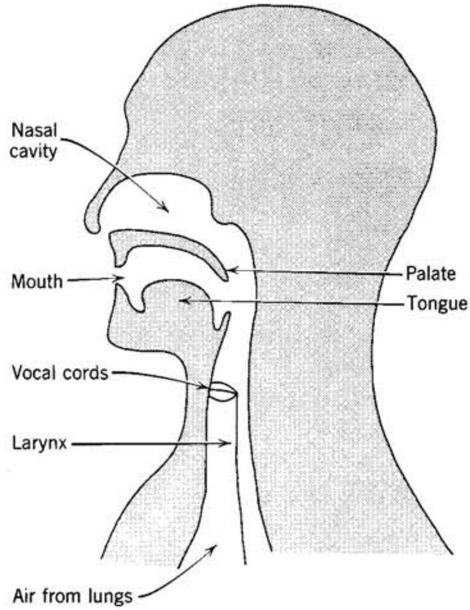

Fig. 13.1. Sectional view of the head, showing the important elements of the voice mechanism.

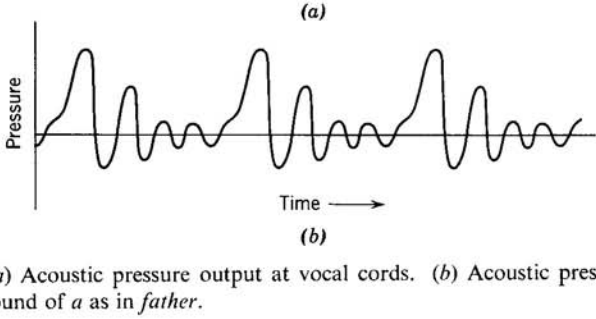

Fig. 13.2. (*a*) Acoustic pressure output at vocal cords. (*b*) Acoustic pressure output for vowel sound of *a* as in *father*.

throat form an acoustic network which further modulates the pressure wave of Fig. 13.2*a*. Many of these parameters are controllable at will, i.e., by changing the position of the tongue or altering the configuration of the lips, and thereby a wide variety of voiced sounds may be produced. Fig. 13.2*b* shows how the output at the vocal cords may be modified so as to produce the vowel sound *a* as in father.

It is also possible for the voice mechanism to produce sounds without use of the vocal cords. Such sounds are called breath sounds. For instance, a steady forcible exhaling of the breath will produce a hissing sound like that of escaping steam. This is apparently caused by turbulences set up in the flow of air through the numerous irregularities along the vocal tract. Additionally, they include such unvoiced *fricative* consonants as *f* and *s* as well as the unvoiced *stop* consonants *p*, *t*, and *k*. Here the basic vibrations are produced by modulating the air stream by means of the lips, teeth, or tongue. An analysis of the unvoiced types of sounds reveals a band of practically continuous frequency coverage largely confined to the upper portion of the audible frequency range.

13.3 Acoustic Power Output of Speech. The average speech power emitted by a speaker at a conversational level is about 10 microwatts, when the power is averaged over a long time interval, i.e., from two to four seconds. When one talks as loudly as possible without straining the vocal cords, this average speech power rises to about 200 microwatts and upon shouting to

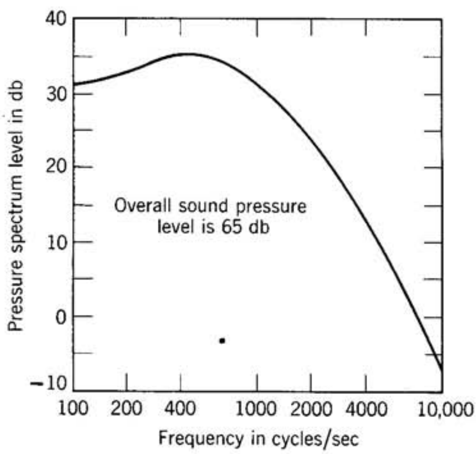

Fig. 13.3. Spectrum level curve for average conversational speech. Spectrum levels are expressed in decibels *re* 0.0002 microbar and are measured at 1 meter from the mouth of the talker.

about 1000 microwatts. By contrast the speech power associated with whispering is about 0.001 microwatt.

When the power of conversational level speech is averaged over a time interval that is short compared to the duration of a syllable (about 0.2 sec), sizeable fluctuations in the level are observed as different speech sounds are uttered. For example, the power of the vowel *o* as in *low* is about 50 microwatts, whereas the weak consonant *v* has an average power of only 0.03 microwatt.

The distribution of speech power with frequency (averaged over long time intervals) has been measured by several investigators.[4] A typical average speech spectrum for male talkers is shown in Fig. 13.3. In this curve the ordinate represents the *pressure spectrum level.* i.e., the sound pressure level in bands of one cycle/sec width, measured at a distance of one meter from the lips of the talker. The integrated overall sound pressure level of the entire band of frequencies from 100 to 10,000 cycles/sec is about 65 db. The total acoustic output computed by assuming the intensity to be uniformly distributed over a hemisphere of one meter radius centered on the mouth of the talker, is about 20 microwatts.

13.4 Anatomy of the Ear. The range of acoustic pressures over which the ear can operate is truly phenomenal. It not only can withstand intense sounds having pressure amplitudes in excess of 1000 microbars, but at the other extreme it responds to sound pressures which are as small as 0.0001 microbar. These very small sound pressures produce a displacement of the eardrum that is of the order of 10^{-9} cm for frequencies near 1000 cycles/sec. This distance is approximately one-tenth the diameter of a hydrogen molecule. It is also capable of responding over a frequency range extending from approximately 20 to 15,000 cycles/sec for normal ears. However, the ear functions as more than an extremely sensitive microphone. It also acts as a frequency analyzer of considerable selectivity. In conjunction with the nervous system, it is able to detect sounds of particular frequencies in the presence of intense backgrounds of wide-band noise, i.e., it appears to operate as though it contained a set of continuous band-filters.

In view of the above capabilities it is not surprising that the hearing mechanism is undoubtedly the most intricate and delicate mechanical structure in the human body. It consists of three main divisions, the *outer*, the *middle*, and the *inner ear*. The outer ear includes the visible ear or *pinna*, the *auditory canal*, and the *drum membrane* or *eardrum*. Inside the drum membrane is the middle ear, an airfilled chamber containing a linkage of three tiny bones, the *ossicles*, which transmit the vibrations of this membrane to the inner ear. The inner ear is a liquid-filled cavity of

[4] Dunn and White, *J. Acoust. Soc. Am.*, **11**, 278 (1940).

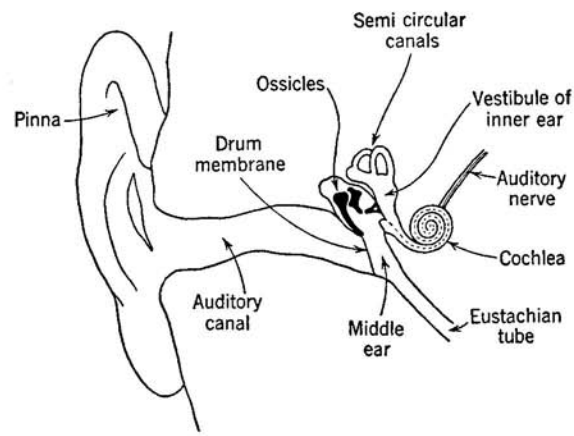

Fig. 13.4. Sketch of hearing mechanism.

complex shape lying within the bony structure of the skull, and containing the membranes and nerve endings by which acoustic pressure changes are detected, analyzed, and transmitted to the auditory nerve. Figure 13.4 is a sketch and Fig. 13.5 is a schematic diagram of the entire hearing mechanism.

The *pinna* of the outer ear serves as a horn to receive acoustic energy and lead it into the auditory canal. In a human being the pinna is a relatively ineffective device, and from an acoustical point of view is almost useless. In some animals, however, it supplies an appreciable gain, particularly over certain frequency ranges. The *auditory canal* is an approximately straight tube, about 0.7 cm in diameter and 2.5 cm long, closed at its inner end by a stretched membrane. Both calculations and measurements indicate that

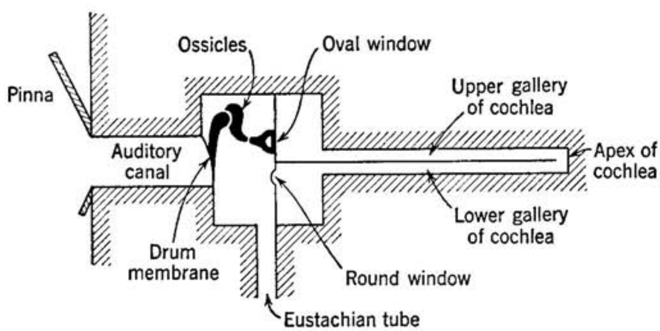

Fig. 13.5. Schematic representation of hearing mechanism.

resonance in this tube causes the acoustic pressure at the drum membrane to differ from that at the entrance to the auditory canal. Assuming that the auditory canal acts like a closed pipe, and adding to its length an end correction of 0.85 times its radius, the computed resonant frequency of the pipe at a sound velocity of 34,300 cm/sec is approximately 3000 cycles/sec. Experimental measurements made by inserting into the auditory canal a thin probe tube connected to a microphone confirm the fact that resonance does occur at about this frequency and show that under resonant conditions the acoustic pressure levels at the drum are about 10 db higher than those at the entrance to the canal. Since the resonance curve is quite broad, appreciable gains in pressure are observed over a frequency range extending from below 2000 to over 6000 cycles/sec. If the effects of the diffraction of sound waves by the head are also taken into account, the pressure levels at the drum may exceed the free-field pressure levels by 15 or 20 db at some frequencies.

The drum or *tympanic membrane* has the shape of a flat cone, lying somewhat obliquely across the auditory canal, with its apex facing inwards. It is quite flexible and is attached around its edges to the end of the canal. Inside this membrane is the cavity of the *middle ear*, which has a volume of between 1 and 2 cm^3, and contains the three ossicles, the *malleus* (hammer), the *incus* (anvil), and the *stapes* (stirrup), together with their supporting muscles and ligaments. This cavity is connected to the throat through the *Eustachian tube*, which is normally closed, thus sealing the cavity, but which opens during the acts of swallowing or yawning to permit air to enter or leave, and so to establish equilibrium between the external and internal air pressures. The handle of the malleus is attached to the tympanic membrane, and it is the tension supplied by the ligaments of the malleus that gives the membrane its conical shape. Vibrations of the membrane are transmitted to the malleus, through the incus, and thence to the stapes, which, as implied by its name, has the shape of a stirrup. The footplate of the stirrup covers an opening, known as the *oval window*, connecting the middle and inner ear. The footplate is attached to one edge of this window by a hinge-like support which permits it to rock back and forth, thus transmitting pressure waves to the liquid filling the inner ear.

It is believed that this linkage of bones, in combination with the area ratio of about 30 to 1 between the tympanic membrane and the oval window, supplies an approximate impedance match between the air in the auditory canal and the liquid in the inner ear. Various attempts have been made to measure or compute the impedance ratio, but there are so many unknown factors, such as the relative motions of the ossicles and the tensions in their supporting ligaments, that the results are inconclusive. It is known, however, that this ratio is not constant but varies with the intensity of the received sound. For high intensities the muscles controlling the motion of the ossicles change their tensions in such a manner as to reduce relative amplitude of motion of the stapes, as compared with that of the handle of the malleus, and thus help to protect the delicate mechanism of the inner ear from damage.

Measurements have been made of the natural frequency of vibration of the entire middle ear, including the tympanic membrane and the ossicular chain. The results indicate that this frequency lies between about 800 and 1500 cycles/sec and that the system is quite highly damped. Since the mechanism is required to respond faithfully to acoustic waves having very irregular shapes and rapidly varying frequencies, this high damping is quite desirable if prolonged transient vibrations are to be avoided.

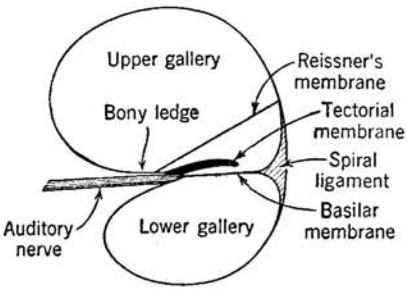

Fig. 13.6. Cross section of cochlea.

The inner ear, or *labyrinth*, has three parts, the *vestibule* or entrance chamber, the *semicircular canals*, and the *cochlea*. The vestibule connects with the middle ear through two openings, the *oval window* mentioned above and the *round window*. Both of these windows are sealed to prevent the escape of the liquid filling the inner ear, the former by the stapes and its supports, and the latter by a thin membrane. The semicircular canals need not concern us here, for they play no part in the process of hearing, their function being instead to provide us with a sense of balance. The cochlea, as implied by its name, is a tube of roughly circular cross section, wound in the shape of a snail shell. The overall dimensions of the shell are about 5 mm from base to apex, with a width across the base of about 9 mm. The tube makes $2\frac{3}{4}$ turns, and has a total length of 3.1 cm, measured from the oval window to the apex. Its mean diameter is about 1.5 mm, and its cross-sectional area decreases in a somewhat irregular manner from its basal to its apical end.

The tube of the cochlea is divided by the *cochlear partition* into two longitudinal channels, the *upper gallery* or *scala vestibuli* and the *lower gallery* or scala *tympani*, the only communication between these two galleries being through a small opening at the apical end of the cochlea. The other ends of the upper and the lower galleries connect with the oval and the round windows, respectively. The cochlear partition is a complex structure consisting of a *bony ledge* and three membranes. A typical cross section of one of the turns of the cochlea is shown in Fig. 13.6. The *bony ledge* projects from the central portion of the shell-like structure into the liquid-filled tube and carries the auditory nerve. At the termination of the bony ledge the nerve fibers enter the *basilar membrane*, which continues across the tube to the farther side, where it is attached to the *spiral ligament*. In the basilar membrane the nerve fibers terminate in minute *hair cells*, which project from its upper surface. Lying above the basilar membrane is the *tectorial membrane*, which is attached along one edge to the bony ledge, with its opposite edge floating freely in the cochlear liquid. The hair cells projecting from the basilar membrane touch, or are imbedded in, the tectorial membrane. Running somewhat diagonally across the cochlear canal from the bony ledge to the opposite wall is a third thin membrane, known as *Reissner's membrane*.

13.5 Mechanism of Hearing. There is good general agreement between theorists and experimenters as to the manner in which acoustic waves impinging upon the pinna travel down the auditory canal and set up vibrations in the ear drum, which are in turn transferred to the inner ear by the movement of the ossicles. The principal matters still in doubt as to this part of the hearing mechanism are its degree of linearity, and the extent to which it supplies an accurate impedance match between the external air and the cochlear liquid. On the other hand, the details of the process by which vibrations of this liquid are analyzed and converted into nerve impulses are not as yet completely understood and require further investigation. Factors such as the small size of the cochlea, its location in the bony structure of the skull, and the delicacy of its components, all contribute to the difficulty of this type of investigation. In spite of these facts there are some phases of the problem upon which there is now complete agreement.

One of the questions that has been of particular interest ever since the earliest investigations were made as to the structure of our auditory mechanism is the manner in which the ear distinguishes one frequency from another. In 1683 Duverney, a French anatomist, proposed the first *resonance theory* of hearing. He and his predecessors had observed that the width of the bony ledge decreases progressively from the basal end of the cochlea towards its apical end, and he suggested that vibrations of the cochlear liquid set up resonant vibrations in portions of this bony ledge, the lower frequency vibrations being particularly effective in producing motion of its wider and heavier basal end, and the higher frequencies stimulating its apical end. Although we now know that his conclusions were in error and that it is vibrations of the basilar membrane rather than of the bony ledge that are responsible for our sense of pitch, his theory is of interest as the first that proposed a plausible mechanism for pitch perception. It was not until more than a century later that Helmholtz built up a theory of hearing that is in reasonable agreement with current ideas. He assumed that the basilar membrane has a fibrous structure, the fibers being relatively independent of one another and being stretched across the width of the cochlear canal somewhat like the strings of a piano. The bony ledge projects farther into the canal at its basal end than at its apical end, so that the basilar membrane is narrowest near the stapes. From this Helmholtz concluded that for the higher frequencies the sympathetic vibrations of this membrane should be most pronounced near its basal end, a conclusion directly opposed to that of Duverney. Investigations have shown that Helmholtz was correct in assuming that the basilar membrane is the organ that serves to analyze a complex wave motion into its component frequencies and that its region of maximum high-frequency response is located at its basal end, but they indicate that neither his postulate that the membrane has a transverse fibrous structure nor that it is in tension is in agreement with experimental findings. Microscopic examination gives no evidence of this fibrous structure, and the shapes assumed by minute depressions or incisions made in the membrane are not typical of a stressed film. Any tuned properties that the membrane may exhibit are therefore thought to be the result of its dimensions, mass, and stiffness, rather than of its structure and tension.

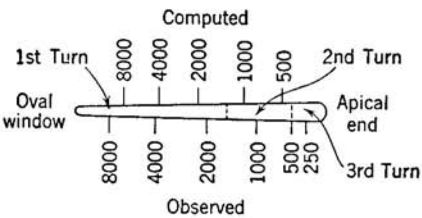

Fig. 13.7. Computed and observed locations of maximum frequency response on basilar membrane. (After de Rosa.)

One of the difficulties inherent in any resonance theory of pitch discrimination is the high degree of damping that should be expected to accompany the transmission of acoustic waves through the narrow cochlear channel. As a consequence of this damping, it appears improbable that there are reflections of sufficient magnitude to establish a standing wave pattern which would in turn set up resonant vibrations in the basilar membrane. In 1947 de Rosa made a mathematical investigation of the propagation of acoustic waves through a structure similar in shape and dimensions to the cochlea.[5] The details of his analysis are too involved to be considered here, but the results indicate that in the presence of damping there should be two coexistent pressure waves, which are propagated along the scala vestibuli with different velocities. Stimulation of the nerve endings in the

[5] de Rosa, *J. Acoust. Soc., Am.*, **19**, 623 (1947).

basilar membrane may be assumed to be a maximum in any region where coincidence occurs between compression cycles of the more rapidly and more slowly moving waves. Figure 13.7 is a representation of the basilar membrane, showing the locations of the regions of maximum response at various frequencies as determined experimentally and as computed from this theory. It will be seen that the agreement is reasonably satisfactory in the frequency range from 500 to 8000 cycles/sec, particularly in view of the various simplifying assumptions that were essential to the analysis.

A more naive approach to this problem is illustrated in Fig. 13.8. Since the walls of the cochlea are essentially rigid and the enclosed fluid is nearly incompressible, any inward motion of the stapes must be accompanied by a corresponding outward motion of the membrane covering the round window of the lower gallery. At very low frequencies the flow of liquid is predominantly through the opening between the upper and lower galleries at the apex of the cochlea. At higher frequencies, however, the inertia of the cochlear liquid causes the basilar membrane to deflect downward as the stapes moves inward, thus forming a sort of hydraulic short circuit. With increasing frequency the position of maximum deflection shifts towards the stapes, and for very high frequencies only the portion of the liquid close to the stapes is in motion. Although this explanation does not lend itself well to quantitative prediction of the relation between frequency and region of maximum motion, it serves as a convenient physical picture in analyzing the action of the basilar membrane. It should be mentioned in passing that the function of Reissner's membrane is not understood and that its presence is ignored in current theories of hearing.

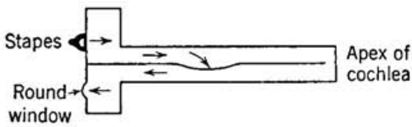

Fig. 13.8. Motion of basilar membrane.

The actual organs by which motions of the basilar membrane are transferred to the auditory nerve are believed to be the hair cells. These cells, of which approximately 23,000 are spaced along the entire length of the basilar membrane, are known to exhibit a type of piezoelectric effect. When a motion of one part of the basilar membrane stresses the hair cells connecting this portion to the tectoral membrane, a measurable difference in potential is set up. This so-called *cochlear potential* can be observed by connecting one input terminal of a high-gain amplifier to any convenient portion of the muscular structure of the head, and either immersing the other in the cochlear fluid or placing it in contact with the external surface of the membrane sealing the round window. Evidence that it is the hair cells that are responsible for the cochlear potentials is supplied by the fact that in certain congenitally deaf animals having normal hearing structures except for the absence of hair cells, no cochlear potentials have been detected.

The precision with which these cochlear potentials reproduce the fluctuations in acoustic pressure corresponding to sound waves is surprisingly high. If electrodes are attached to the neck and round window of an anesthetized cat, and the output of the associated amplifier is connected to a loudspeaker or telephone receivers, speech sounds reaching the ear of the cat are reproduced in a completely intelligible manner. The study of cochlear potentials has been of great assistance in investigations of the hearing process. For example, one method of experimentally determining the regions of the basilar membrane that are stimulated by particular frequencies is to observe the changes that appear in a cochlear potential vs. frequency-response curve, when one or another part of the basilar membrane is cut or otherwise damaged. This method is simpler and more satisfactory than other possible methods, such as direct microscopic observation of the vibration of the membrane.

There is as yet no definite answer to the question whether the potentials developed in the hair cells are directly responsible for the resulting impulses in the auditory nerve fibers to which they are connected, or whether they generate chemical effects in the intervening ganglions, which in turn stimulate the nerve fibers. In any event, it seems highly probable that these potentials play a basic part in our hearing process.

13.6 Thresholds of the Ear. One of the simplest measurements that can be made of our hearing ability is to determine the manner in which the minimum perceptible intensity level varies with frequency. The acoustic intensity that can be barely detected at any particular frequency is known as the *threshold of hearing* or *threshold of audibility* for that frequency. Measurements have been made of this threshold by numerous observers. As is to be expected, the results vary to a considerable extent from one individual to another, even when all have what is commonly considered normal hearing, and the threshold intensity is also a function of the age of the listener, a progressive loss in sensitivity at the higher frequencies being customary with increasing age. In addition, the exact shape of the threshold curve varies with the manner in which the incident sound level is measured, i.e., at the pinna of the ear or in the free sound field, the observer's head being absent. It also depends on the direction of incidence of the sound and on whether the listening is done with both ears or with only one ear. Figure 13.9 shows a typical response for both ears, the level being measured in a free sound field of random horizontal direction. Although the thresholds are expressed in terms of decibel intensity levels, it is to be noted that the ordinate scale would have been nearly the same if the thresholds were expressed in terms of pressure levels relative to 0.0002 microbar.

The frequency of maximum sensitivity is in the vicinity of 3000 cycles/sec for normal ears. To some extent this is accounted for by resonance in the auditory canal, as was pointed out in Sect. 13.4, but other factors are undoubtedly of greater importance. The threshold curve crosses the 0 db level at about 1000 cycles/sec and rises in a regular manner with decreasing frequency, the minimum power required to produce an audible sound at 50 cycles/sec being nearly a million times as great as it is at 3000 cycles/sec. Measurements of the threshold curve below about 30 cycles/sec are quite unreliable, as the required intensities become so great that it is difficult to avoid the presence of small percentages of harmonics in the source. Since the pitch-discriminating ability of the ear is relatively poor in this frequency range, the harmonics may be mistaken for the fundamental. Even when the source is known to develop a strictly pure sine wave, nonlinearity in the hearing mechanism itself, as will be discussed in Sect. 13.9, may give the illusion of hearing a fundamental that is actually inaudible.

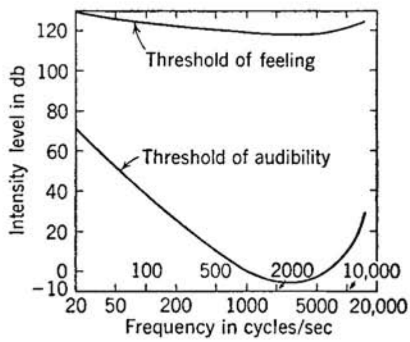

Fig. 13.9. Thresholds of the ear in decibels relative to 10^{-12} watt/m^2.

For high frequencies the threshold curve also rises, the rate of increase near the upper limit being often so rapid as to constitute a sharp cut-off. It is in this frequency region that the greatest variability is observed between different listeners, particularly if some of them are over 30 years of age. The cut-off frequency for a young man or woman may be as high as 20,000 or even 25,000 cycles/sec, but people who are 40 or 50 years of age can seldom hear frequencies in excess of 15,000 cycles/sec, and in some the cut-off is below 10,000 cycles/sec. In the range below 1000 cycles/sec, the threshold is essentially independent of the age of the observer.

The sensitivity of the human ear to sounds of low intensity is quite phenomenal. In the range from about 1000 to 5000 cycles/sec the minimum perceptible acoustic pressures are less than 0.0002 microbar, and as has been previously noted the resulting amplitude of vibration of the drum membrane is approximately 10^{-9} cm. Calculations show that in this frequency range the changes in pressure due to the thermal agitation of the air molecules are very nearly as great as the minimum audible acoustic pressures, so that any appreciable increase in the sensitivity of our hearing mechanism would also result in our observing a background of thermal noise, a hissing or rushing sound that would interfere with the perception of low-intensity acoustic waves. It is consequently improbable that there are any animals whose hearing is more acute than ours in this frequency range, for they too would be susceptible to the masking produced by thermal noise. On the other hand, it is well known that many animals, such as dogs, are readily capable of perceiving sounds of appreciably higher frequency than can human beings.

As the intensity of the incident acoustic waves is increased, the resulting sound grows louder and eventually produces a tickling sensation rather than a sensation of hearing. This level, which is also shown in Fig. 13.9, is less dependent on frequency than is the threshold of audibility and has a value of approximately 120 db. It is called the *threshold of feeling*. As with the lower threshold, it varies somewhat from individual to individual, but not to so great an extent. As the intensity is still further increased, the tickling sensation becomes one of *pain* at about 140 db. Prolonged stimulation at appreciably higher intensity levels will cause permanent damage to the hearing mechanism. Finally, immediate damage will result when the hearing mechanism is exposed to intensity levels greater than 160 db.

It is to be noted that the above thresholds are given for pure tones. Similar results have been reported for noises having a continuous spectrum. However, in the case of a continuous wide-band noise, the thresholds are reached when the intensity level in any one *critical bandwidth* (Sect. 13.11) at some point along the frequency scale reaches the levels given above.

13.7 Loudness. In elementary treatments of acoustics it is often stated that the subjective characteristic of a sound which is commonly known as its *loudness* is determined by its intensity. When properly interpreted, this statement is strictly correct, but it is somewhat misleading, for it may appear to imply that loudness and intensity are synonymous. An inspection of Fig. 13.9 shows immediately that this is not true. For example, a pure tone having an intensity level of 20 db and a frequency of 1000 cycles/sec is plainly audible, whereas one having the same intensity but a frequency of 100 cycles/sec is well below the threshold of audibility and cannot be heard at all. The loudness of such a tone is therefore a function not only of of its intensity but also of its frequency.

Although our hearing mechanism is not well-adapted to making quantitative measurements of the relative loudness of different sounds, there is fair agreement between observers as to when two pure tones of different frequency appear to be equally loud. It is therefore possible to plot contour curves of equal loudness, such as those shown in Fig. 13.10. The data for these curves are obtained by alternately sounding a reference tone of 1000 cycles/sec and a second tone of some other frequency. The intensity level of the second tone is then adjusted to the value that makes the two tones appear equally loud. The unit of loudness level is the *phon*, the loudness level (in phons) of any sound being taken as numerically equal to the intensity level in decibels of a pure 1000-cycle tone that is judged by the average observer to be equally loud. For example, a pure tone having a frequency of 100 cycles/sec and an intensity level of about 50 db sounds as loud as a pure 1000-cycle tone whose intensity level is 20 db, and hence the loudness level of this 100-cycle tone is by definition 20 phons. It is to be noted that in accordance with the definition of loudness level, all loudness level curves of Fig. 13.10 intersect the corresponding intensity level lines at a frequency of 1000 cycles/sec.

The loudness level of a sound does not reach an instantaneous maximum at the onset of a sound. Its magnitude increases rapidly for a brief interval

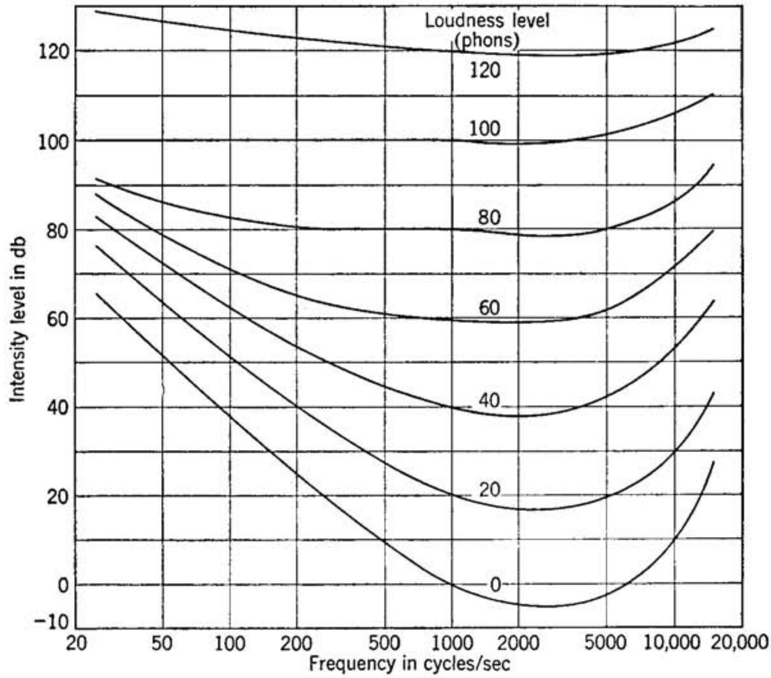

Fig. 13.10. Equal loudness level contours expressed in decibels relative to 10^{-12} watt/m^2.

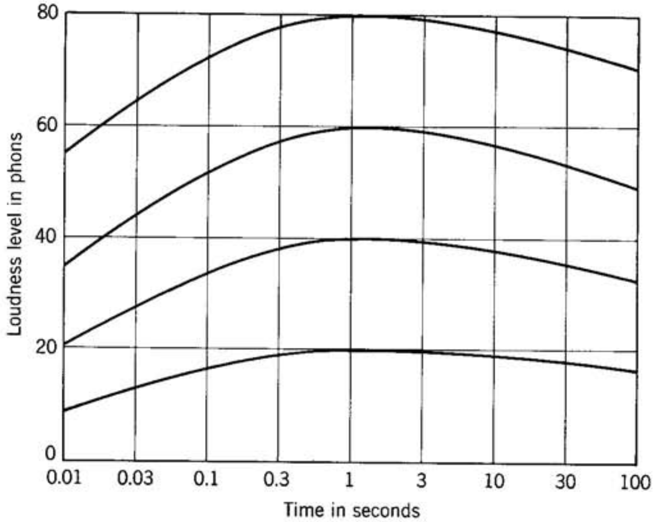

Fig. 13.11. Relation between loudness level and duration time. (After Munson.)

after onset, then gradually approaches a steady value and finally decreases slowly for long duration sounds.[6] Since the mechanical elements of the ear are believed to be too highly damped to account for the observed rate of growth of loudness level, it is probably determined by the response characteristics of the neural components of the auditory system. Figure 13.11 shows the relation between loudness level and the duration time, with the loudness level in phons of a one-second stimulating tone serving as a reference.

It is to be emphasized that although two sounds having the same loudness level in phons appear to the average observer to be equally loud, this does not imply that the apparent loudness of a sound is directly proportional to its level in phons, i.e., that a sound having a level of 60 phons will seem to be twice as loud as one whose level is 30 phons. It is not always possible to obtain agreement among different observers as to when one sound is twice as loud as a similar one of lower level, but even simple experiments of this type prove conclusively that apparent loudness is not directly proportional to loudness level. More exact determinations made by various indirect methods also show that loudness ratios are not proportional to the *increment* in loudness level, as might be expected from the logarithmic nature of the definition of the phon. For example, increasing the loudness level by 10 phons from 10 to 20 phons increases the apparent loudness by a factor

[6] Munson, *J. Acoust. Soc. Am.*, **19**, 584 (1947).

of approximately 6, whereas a similar increase from 50 to 60 phons increases the loudness by a factor of only about 2.

In a true loudness scale doubling the number of loudness units should double the subjective loudness. Similarly increasing the number of loudness units by a factor of 10 should increase the subjective loudness by the same factor, etc. One indirect method of establishing such a scale depends on the assumption that a sound heard by both ears will appear to be exactly twice as loud as the same sound heard by only one ear. A sound of relatively low level is introduced through telephone receivers to both ears of an observer and is alternated with the same sound introduced into a single ear at a somewhat higher level. The observer is then required to adjust the level of the sound entering only one ear to such a value that it appears as loud as the sound entering both ears. When this has been accomplished it is assumed that, if these two levels were listened to alternately by both ears, they would appear to have a subjective loudness ratio of 2 to 1. The experiment is then repeated at successively higher and higher initial levels throughout the intensity range of hearing.

Another indirect procedure is based upon the assumption that, since two pure tones of quite different frequencies stimulate different portions of the basilar membrane, the subjective response to both acting at once should be additive. Two such tones are first adjusted to the same loudness and are then superimposed upon each other. The resulting complex sound is presented to the observer and is alternated with one of its components. As before, the observer is required to equalize the loudnesses of the two sounds by adjusting the level of the simple tone, and the resulting value for this component is taken as just twice that of either of the components of the complex sound. Similar experiments have been made employing as many as ten superimposed pure tones, thus making possible subjective determinations of loudness ratios of 10 to 1.

The results of experiments such as those described above have been used by Fletcher to establish the relation between loudness level in phons and subjective loudness in *sones*.[7] The unit of loudness is a *sone* which is defined as being the loudness of a 1000-cycle tone of 40 db intensity level. It is also equal to the loudness of any sound having a loudness level of 40 phons. The conclusions of Fletcher are summarized by the graph shown in Fig. 13.12, in which loudness in sones is plotted as ordinate against loudness level in phons. It will be seen that, although the lower portion of this graph is noticeably curved, the portion corresponding to loudnesses in excess of one sone is relatively straight. In this upper region, where the levels correspond to sounds whose loudnesses range from comfortably audible to unpleasantly loud, an increase in loudness level of 10 phons is

[7] Fletcher, *J. Acoust. Soc. Am.*, **9**, 5 (1937).

approximately equivalent to doubling the subjective loudness, and an increase of about one-half phon corresponds to the minimum perceptible change in loudness.

If we let L be the loudness in sones and LL the loudness level in phons then an empirical equation which holds to a reasonably close approximation over the range from 40 to 100 phons is

$$\log L = 0.033(\text{LL} - 40) = 0.033\,\text{LL} - 1.32 \quad (13.1)$$

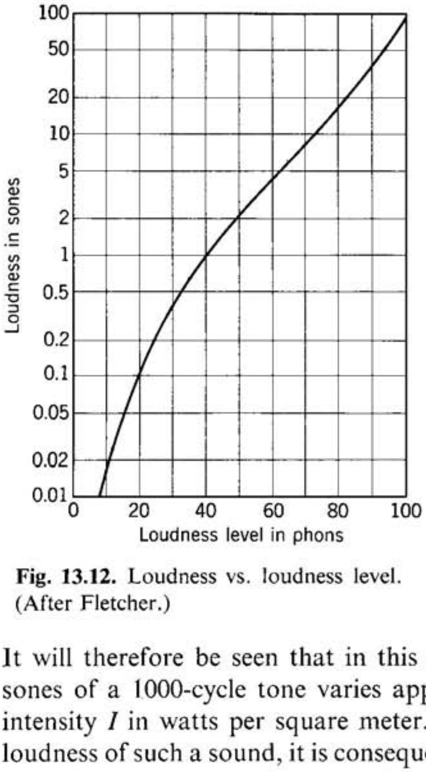

Fig. 13.12. Loudness vs. loudness level. (After Fletcher.)

For a frequency of 1000 cycles/sec the loudness level LL in phons is by definition numerically equal to the intensity level IL in decibels, so that equation 5.44 may be rewritten as

$$\text{LL} = 10 \log (I/I_0)$$

or since $I_0 = 10^{-12}$ watt/m^2,

$$\text{LL} = 10 \log I + 120$$

Substitution of this value of LL into equation 13.1 gives

$$\log L = 0.033(10 \log I + 120) - 1.32 = 0.33 \log I + 2.64$$

which reduces to

$$L = 445\, I^{0.33} \qquad (13.2)$$

It will therefore be seen that in this range, the subjective loudness L in sones of a 1000-cycle tone varies approximately as the cube root of the intensity I in watts per square meter. In order to double the subjective loudness of such a sound, it is consequently necessary to increase the power supplied to the sound source by a factor of eight.

Up to the present we have been concerned solely with factors influencing the loudness sensation of individual pure tones. Let us next consider the loudness of stimuli that are more realistic than pure tones, i.e., wide-band noise, speech, combinations of pure musical tones, factory noise, etc. The loudness of these sounds could be evaluated by tedious psychophysical tests. However, it is also possible to *estimate* their loudness on the basis of physical measurements, utilizing the pure-tone loudness curves of Fig. 13.12. Several investigators[8] have measured the subjective loudness of

[8] Beranek et al, *J. Acoust. Soc. Am.*, **23**, 261 (1951).

complex sounds and have found that the loudness can be predicted by adding the loudnesses (but not the intensities) of the individual components. This procedure fails when too much interaction exists between the individual components. For instance, the individual components whose loudnesses are being added must be separated widely enough in frequency so that they are not competing on the basilar membrane for the same neural stimuli.

One objective procedure for determining the loudness of any type of complex sound with reasonable accuracy is as follows.

1. Divide the sound spectrum into bands of frequencies, each at least greater in width than a critical bandwidth for hearing, but not greater in width than a half-octave.

2. Determine the intensity level (or pressure level) in decibels for each band.

3. By means of the curves of Fig. 13.10, find the loudness level in phons for each band corresponding to its intensity level as determined in step 2 and the mean frequency of the band.

4. Using the relation between loudness and loudness level of Fig. 13.12, determine the loudness in sones contributed by each band.

5. Add the individual values of loudness to obtain the total loudness in sones.

As an example of this procedure, let us proceed to determine the composite loudness of six pure tones of frequencies 125, 250, 500, 1000, 2000, and 4000 cycles/sec respectively and all having the same intensity level of 60 decibels. Data used in making this computation is summarized in the accompanying table.

Frequency f (cycles/sec)	Intensity Level IL (db)	Loudness Level LL (phons)	Loudness L (sones)
125	60	35	0.7
250	60	54	3.0
500	60	59	4.3
1000	60	60	4.5
2000	60	62	5.0
4000	60	60	4.5
			Total 22.0

The final result of 22.0 sones is equivalent to about 80 phons which in turn corresponds to an intensity level of 80 db for a 1000-cycle tone. Since the sum of the intensities of the six individual tones corresponds to an intensity level of only 67.8 db, it is apparent that sound energy appears to be louder when it is distributed over a wide range of frequencies as compared to being concentrated at one frequency.

No instrument exists which is capable of truly measuring the loudness of a composite sound containing many frequency components. However, commerical instruments known as *sound level meters* are available which are capable of making precise measurements of the intensity level of such sounds and reasonably accurate measurements of their loudnesses. All these meters operate on essentially the same principle, although there are variations in design between different manufacturers. Any sound level meter consists of a sensitive microphone of good stability, a linear amplifier, one or more attenuators, a set of frequency-weighting networks, and an indicating meter. The electrical voltages corresponding to sounds picked up by the microphone are first amplified, the amount of amplication being determined by the attenuator settings. They are next passed through a suitable frequency-weighting network and are then used to operate the indicating meter, which is usually calibrated to read sound levels in decibels above the standard reference intensity of 10^{-12} watt/m^2. The purpose of a frequency-weighting network is to make the readings of the sound level meter correspond as closely as possible to observed loudness levels. As can be seen from Fig. 13.10, the numerical values of loudness levels in phons and intensity levels in decibels are nearly equal for quite loud sounds of any frequency, but they vary widely for low-intensity sounds whose frequencies differ appreciably from 1000 cycles/sec. Therefore, at high intensity levels no frequency-weighting network is required, but at low intensities a network should be used that attenuates both high and low frequencies by an amount just sufficient to make the meter readings for these frequencies correspond to the loudness levels as heard by ear. The ideal arrangement would be to employ a continuously variable frequency-weighting network, but this would be very difficult and expensive to construct, and it is found that in actual practice it is sufficient to include only two fixed networks, one for use at loudness levels below about 55 phons and the other for the range from about 55 to 85 phons.

For further information on the frequency-weighting and other characteristics of sound level meters, the reader is referred to the American Standards Association publication on this topic.[9]

13.8 Pitch and Timbre. From a subjective point of view, a continuous sound has in general three different characteristics that distinguish it from other continuous sounds. One of these characteristics, its loudness,

[9] *Sound Level Meters for Measurement of Noise and Other Sounds*, Z24.3–1944, American Standards Association (1944).

has been discussed in the previous section. The second subjective characteristic is its *pitch*. Pitch, like loudness, is a complex characteristic and is not dependent on any single physical quantity, the pitch of a musical sound being determined *primarily* by its frequency but being also a function of its intensity and wave form. For example, if a pure tone having a sinusoidal wave form and a frequency of about 100 or 200 cycles/sec is first sounded at a moderate and then at a high loudness level, nearly all observers will agree that the louder sound has a lower pitch, in spite of the fact that its frequency remains unchanged. Experiments of this type show that the most pronounced decrease in pitch with increasing loudness occurs for tones of low frequency, and that when the loudness of such a tone is increased from a level of 40 to one of 100 phons, it may be necessary to increase the frequency by as much as 10 per cent in order to maintain the pitch at a constant value. This change in pitch with loudness is most pronounced at a frequency of about 100 cycles/sec. It is also most apparent for pure sinusoidal tones. For frequencies between about 1000 and 5000 cycles/sec, i.e., over the range for which the ear is most sensitive, the pitch of a tone is relatively independent of its loudness.

It should be emphasized that the appreciable changes in pitch with loudness that have just been discussed are characteristic only of pure tones. For ordinary musical tones, such as those produced by violins, clarinets, trumpets, etc., the changes in pitch are much smaller, usually not more than one-fifth as great. This is to be expected, since Fourier's theorem shows that the complex acoustic waves produced by these instruments may be resolved into a fundamental frequency and a series of harmonics, some of which have amplitudes that are quite large, and may even exceed that of the fundamental. Consequently, even if the fundamental lies in the frequency range where a pure tone shows a large decrease in pitch, the harmonics will have frequencies for which the pitch changes very little, or increases with increasing loudness, so that the ear judges the entire series of components as remaining at essentially the same pitch.

Several different approaches have been employed in an attempt to establish a relationship between our subjective sense of pitch and the physical property of frequency. One method is to present alternately to an observer two pure tones of the same loudness level, usually 40 or 60 phons, and to require the observer to adjust the frequency of one of the tones until its pitch appears to be exactly half that of the other. The experiment is then repeated for a series of frequencies covering the entire audible range. As is to be expected, the agreement between different observers is by no means exact, but the average results show clearly that pitch and frequency are not proportional. For example, the frequency that is judged to be half as great as one of 200 cycles/sec is about 100 cycles/sec, but the frequency that sounds half as high as 5000 cycles/sec is less than 2000 cycles/sec. It should be clearly understood that in making tests of this type the two frequencies are presented alternately, and not at the same time. If a pair of tones that are judged to have a pitch ratio of two to one are sounded simultaneously the result is in general very discordant, so that if the tones had originally been presented together the observer would have instinctively adjusted the lower frequency to exactly half that of the upper, i.e., to an octave below, and would thus have avoided the discord.

If we select some reference frequency, it becomes possible to assign a series of numbers to the subjective determinations of pitch, and thus establish a pitch scale. The commonly chosen reference frequency is 1000 cycles/sec, and the tone corresponding to this frequency is said to have a pitch of 1000 subjective units, sometimes called *mels*, from the word melody. The observations can then be integrated graphically to obtain a curve giving the relation between subjective pitch and frequency, such as that shown in Fig. 13.13. This particular curve was taken at a loudness level of 60 phons.

Another method of obtaining data for a curve of this type depends on determining the value of the minimum perceptible change in frequency Δf and observing the manner in which Δf varies with the mean frequency f. In one such set of experiments a pure tone was maintained for about a second at a constant frequency, was next shifted smoothly to a slightly different frequency, which was also maintained for the same length of time, and was then shifted smoothly back to the original value. The frequency

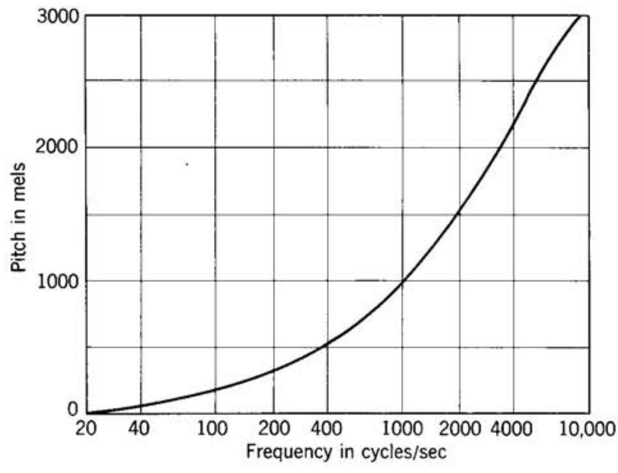

Fig. 13.13. Pitch vs. frequency.

shift Δf was at first made so small as to be imperceptible and was then gradually increased. At frequencies below 500 cycles/sec the minimum perceptible values of Δf are found to be nearly constant and for a loudness level of 60 phons are approximately equal to 3 cycles/sec. For the higher frequencies, however, the *ratio* $\Delta f/f$ is more nearly constant and ranges between about 0.002 and 0.003 at this same loudness. If we now make the bold assumption that for any particular loudness level all minimum values of Δf, regardless of their *absolute* magnitudes, are of equal *subjective* magnitude, i.e., that they correspond to the same number of mels, we may use graphical integration to obtain the relation between pitch and frequency. The resulting curve is in surprisingly good agreement with that obtained by the method of half pitch, indicating that the asssumption made above has at least considerable validity.

It is of interest to compare the results of pitch vs. frequency determinations with the manner in which the physical position of the region of maximum stimulation on the basilar membrane varies with frequency. A comparison of this type shows that when any two tones differ in pitch by a barely discernable amount, the distance in millimeters between the corresponding regions of maximum stimulation has a constant value. In other words, when an observer is required to reduce the pitch of any particular pure tone to one-half, he automatically reduces the frequency by such an amount as to shift the position of maximum stimulation on the basilar membrane approximately half way from its original location towards the apical end of the membrane.

The subjective pitch of a *complex tone* containing overtones of appreciable magnitude depends not only on the frequency of its lowest component but also on the frequencies and amplitudes of its overtones. For example, if a complex tone is built up out of the series of frequencies 100, 200, 300, 400, and 500 cycles/sec, with all components of equal loudness, the apparent pitch will be approximately 160 mels, but, if the 100-cycles/sec component is now omitted, all others remaining the same, the apparent pitch will still appear to be 160 mels. Similarly, a set of equal components of frequencies 400, 600, 800, and 1000 cycles/sec gives a pitch of about 300 mels, but, if the frequencies 500, 700, and 900 are now added, the pitch drops to about 160 mels. It is apparent from the above examples that the pitch of a complete series of harmonics of equal loudness is determined by the minimum frequency difference, rather than by the frequency of the lowest component. The same phenomenon is observed, although to a somewhat lesser extent, in a musical tone whose harmonics have amplitudes considerably lower than that of its fundamental. Effects of this type have their origin in the nonlinear characteristics of hearing and will be further discussed in Sect. 13.9, which deals with this topic.

When the frequency components of a complex sound are so numerous and so closely spaced as to stimulate relatively large areas of the basilar membrane, the sound ceases to have the property of pitch, and is identified as a noise. A typical example is thermal noise, all of whose frequency components have approximately the same intensity and are distributed in a continuous manner over the entire audible range. Such a noise has a typical sizzling or rushing sound and is commonly referred to as *white noise.*

The *timbre* of a musical sound is the subjective characteristic that makes it possible for us to distinguish between two tones having the same intensity level and fundamental frequency but different wave forms. In other words, it expresses our ability to recognize the sound of a violin as different from that of a trumpet, even when the two instruments are sounding the same note with equal loudness. Like loudness and pitch, timbre is a complex characteristic, for, although is is *primarily* dependent on the wave form of the tone being heard, it is also a function of its intensity and frequency. For example, if a note played by a violin is recorded and then reproduced at approximately the same loudness level by a high-fidelity sound-recording system, the reproduction is nearly indistinguishable from the original sound. If, on the other hand, the loudness level is raised 20 or more phons, all other factors remaining the same, the tone no longer sounds natural, indicating that its timbre has changed. Similarly, if the disk or film upon which the note is recorded is played back at a considerably higher velocity than that at which the recording was made, thus raising the fundamental frequency of the tone but leaving its wave form and harmonic structure unchanged, the reproduced sound is no longer recognizable as that of a violin. Various adjectives, such as mellow, brilliant, reedy, brassy, etc., have been used by musicians to describe different types of tones, but no serious attempt has been made to establish a set of subjective units of timbre, similar to those established for loudness and pitch, nor in view of the complexity of the problem does it appear probable that any such attempt would be likely to succeed.

13.9 Beats, Aural Harmonics, and Combination Tones. In Sect. 1.11 it was pointed out that when two simple-harmonic tones having approximately the same intensity, but differing by a few cycles per second in frequency, are linearly combined, the resulting amplitude of vibration fluctuates at a rate equal to the difference between their frequencies. If the tones are within the audible range, the resulting sound is heard as a single tone whose loudness varies smoothly and rhythmically at the difference rate, and is it said that the tones *beat* with each other, or that we hear *beats.* This phenomenon is readily explained in terms of our present knowledge of the hearing process, for the two frequencies are so nearly alike that they stimulate the same part of the basilar membrane and hence have the same pitch. As the tones swing in and out of phase they set up vibrations of greater or smaller amplitude in this membrane, which are in turn heard as increases or decreases in loudness. Observation of the beat rate between two tones forms the basis of a highly precise method of adjusting the tones to the same frequency, i.e., to zero beat, and is the method employed in tuning many types of musical instruments.

As the difference between the two frequencies increases, the beat rate also increases, and up to a rate of 6 or 7 beats per second the sound retains its smoothly varying characteristic. For higher beat rates the loudness no longer appears to vary smoothly, but in an intermittent, throbbing manner, and a considerably greater increase in the difference frequency causes the sound to appear harsh and discordant. The beat rate at which harshness appears depends, among other factors, on the mean frequency, and for a frequency in the vicinity of 1000 cycles/sec is about 170 beats per second. The physiological reasons for the throbbing or harsh characteristics of the higher beat frequencies are not so well understood as are those for the smooth, rhythmical beats, but they are presumably associated with the stimulation of more and more widely separated portions of the basilar membrane.

When two pure tones in the audible range differ in frequency by an amount that itself lies within the audible range we may hear a note corresponding to this difference frequency, particularly if the tones are sounded at a fairly high loudness level. The resulting note is called a *difference tone*, and its presence is a direct result of the nonlinear characteristics of the ear, for as has been noted in Sect. 1.10 a *linear* combination of two frequencies does not result in any periodicity of the nature of the difference of the component frequencies. On the other hand, if two frequencies are supplied to a nonlinear system, for example one in which the response varies as the square rather than as the first power of the stimulation, it can be shown by a straightforward trigonometric transformation that the response will contain not only the original frequencies, but also frequencies corresponding to both their sum and their difference. Nonlinear electrical circuits are commonly used in radio receivers and transmitters for generating such sum or difference frequencies. Mathematical proof of the generation of sum and difference tones by nonlinear mechanisms will be left as an exercise for the reader (Problem 13.6).

Before continuing the discussion of *combination tones* of the type considered above, it wiil be well to review some of the evidence proving that our hearing mechanism does actually have nonlinear characteristics. There are two kinds of experimental approach to this problem, one based on subjective observation and the other on the measurement of cochlear potentials. As an illustration of the former method, consider the subjective response to be expected when a single pure tone of some moderately low frequency, such as 200 cycles/sec, is sounded at a fairly high loudness level. If the ear were strictly linear the only tone heard would be that corresponding to the impressed frequency, but a trigonometric analysis of the type mentioned in the preceding paragraph shows that in the presence of any appreciable nonlinearity we should also hear other frequencies that are integral multiples of the 200-cycle tone. These higher frequencies, which are known as *aural harmonics*, can actually be detected by any observer having a well-trained ear. A method of making such an aural harmonic more apparent is to introduce an additional tone of approximately the same frequency as that of the anticipated aural harmonic. For example, if this second tone has a frequency of 603 cycles/sec, it will beat three times a second with the third aural harmonic of the 200-cycle tone, and the resulting fluctuations in loudness can readily be observed. Since any beat is most apparent when the amplitudes of its component tones are equal, the subjective loudness of an aural harmonic may be assumed to be the same as that of the additional tone that produces the most pronounced beats.

A second method of obtaining data as to the nonlinearity of the ear is through the measurement of cochlear potentials. Since this method requires the use of operative techniques, it is applicable only to animals, but the anatomical resemblance between their hearing mechanism and our own makes it highly probable that if measurements of this kind were made on human ears the results would be quite similar. As has been pointed out in Sect. 13.5, the close association between cochlear potentials and hearing gives us confidence that the amplitudes, frequencies, and wave forms of the cochlear potentials represent quite accurately those of the sounds actually heard by the animals being tested. If a pure tone of low intensity arrives at the ear, the cochlear potential has a sinusoidal wave form and a frequency identical with that of the received sound, but as the incident intensity is increased the wave becomes distorted, indicating the generation of aural harmonics. Electrical devices known as harmonic analyzers can be employed to determine the frequencies and relative amplitudes of the harmonic components of such a distorted wave, and thus to measure quantitatively the relative intensities of the corresponding aural harmonics.

The results of both types of measurement show that tones having frequencies above 500 cycles/sec and loudness levels below 40 phons do not generate aural harmonics of appreciable magnitude. For frequencies around 100 cycles/sec, however, the loudness level at which distortion first appears is much lower, about 20 phons. With increasing loudness the aural harmonics appear in order, initially the second harmonic, then the third, then the fourth, etc. In general the subjective loudnesses of all aural harmonics are less than that of the fundamental, and they decrease progressively with increasing order, the second harmonic being louder than the third, and so on. However, in an intense, low-pitched sound, such as a 60-cycle tone sounded at an intensity level of 100 db, the second harmonic may be louder than the fundamental, and a number of the higher harmonics may also approach the fundamental in loudness.

The existence of combination tones of the sum and difference type can be investigated by either of the methods discussed above. In general, difference tones appear at somewhat lower intensity levels than do summation tones, but both are observed. Typical results as obtained by Newman, Stevens, and Davis[10] are given in Fig. 13.14, where the curves show how the combination-tone response varies with stimulus for four combination tones. Data for these curves were obtained by measuring the cochlear potentials developed in the ear of a cat when it was stimulated by two pure tones having frequencies of 700 and 1200 cycles/sec, respectively. It will be observed that for moderate stimuli the 500-cycle difference tone (1200 − 700) is the most intense and that it appears at the lowest stimulus level. Next in prominence is the 1900-cycle sum tone (1200 + 700). Also shown in the figure are curves for two higher-order combination tones, the 1700-cycle difference tone (2 × 1200 − 700) and the 3100-cycle sum tone (2 × 1200 + 700). It will be seen that, although these tones first appear at a considerably higher stimulus level than do the first-order combination tones, their response is greater at the high stimulus levels. Other higher-order combination tones having frequencies of 200, 300, 1000, 2200, 2600, and 3300 cycles/sec are also observed.

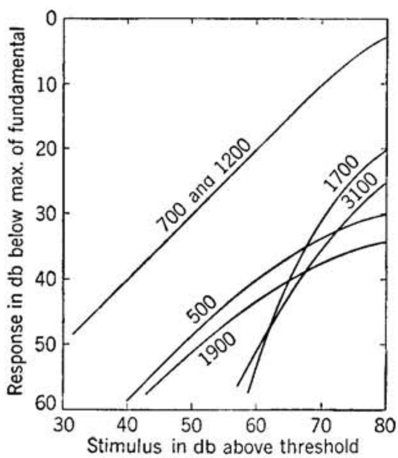

Fig. 13.14. Aural combination tones. (After Newman, Stevens, and Davis.)

The existence of combination tones supplies an explanation for the anomalous relation between the pitch of a complex tone and its harmonic content pointed out in Sect. 13.8, where it was stated that a tone having only the frequency components 200, 300, 400, and 500 cycles/sec appears to

[10] Newman, Stevens, and Davis, *J. Acoust. Soc. Am.*, **9**, 107 (1937).

have a pitch of about 160 mels. It should now be apparent that the missing 100-cycle frequency is built up as a combination tone in the ear of the listener from differences between the other components. Designers of low-priced a-c radio receivers often take advantage of this phenomenon. The 120-cycle hum that results when 60-cycle alternating current is rectified by a full-wave rectifier would be highly objectionable if it appeared in the sound output. Since the electrical circuit elements required to eliminate this hum are bulky and expensive, the problem is usually avoided by designing the circuits and speaker of the receiver so as to prevent it from radiating any appreciable acoustic energy at frequencies below about 140 cycles/sec. This frequency is less than an octave below middle C, and the resulting sound reproduction would consequently be almost completely lacking in bass notes if the missing frequencies were not resupplied in the ear of the listener from differences between the higher harmonics.

The source of the nonlinearity of our hearing mechanism is not yet completely determined. It was at first believed that the distortion arose primarily in the middle ear and was the result of a purely mechanical nonlinearity in the ossicular linkage connecting the drum membrane and the oval window. Although it is true that this linkage introduces some distortion, particularly at very high intensity levels, experimental evidence indicates that the primary source of the distortion is presumably in the inner, rather than the middle, ear and may be associated with nonlinearity in the hair cells.

13.10 Masking by Pure Tones. Everyone is familiar with the fact that it is difficult to hear and understand speech in the presence of a background of some other loud sound, such as the whine of a large generator or the roar of an airplane engine. Under such circumstances we say that the desired sound or signal is *masked* by the background and define the degree of masking as the extent to which the masking sound raises the threshold of audibility of the desired sound, the increase being customarily expressed in decibels. In general both the masked sound and the masking sound have highly complex wave forms and frequency structures. However, an understanding of the basic principles underlying this phenomenon is most readily obtained through a study of the special case in which both sounds are pure sinusoidal tones. In performing experiments of this type the masking tone is operated steadily at some particular intensity level, and the intensity of the signal tone is raised from a level below audibility to one that is just distinguishable. Typical results of experiments of this type are shown in Fig. 13.15 for two masking frequencies, (*A*) 400 cycles/sec and (*B*) 2000 cycles/sec. In each the frequency of the masked tone is indicated along the axis of abscissas, and the threshold shift in decibels for various

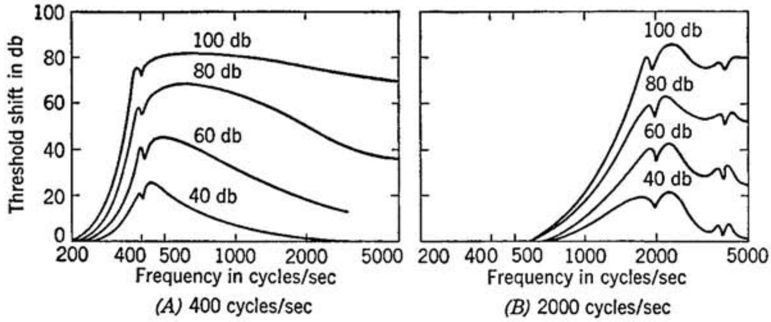

Fig. 13.15. Masking of one pure tone by another.

intensities of the masking tone along the axis of ordinates. It will be observed that the masking of one pure tone by another is most apparent when the two tones are of approximately the same frequency and also that in general a tone masks signals of higher frequency more effectively than it does those of lower frequency. For example, a signal having a frequency of 1000 cycles/sec and an intensity level of 40 db is completely masked by a 400-cycle tone whose intensity level is 80 db, but it is well above the threshold of audibility in the presence of a 2000-cycle tone of the same intensity. A consideration of the aural harmonics generated by the masking tone supplies an explanation of this effect. For the 400-cycle, 80-db tone these harmonics have frequencies of 800, 1200, 1600, etc., cycles/sec and have loudnesses approaching that of the fundamental, so that, since one or another of these harmonics will be of approximately the same frequency as any signal in the upper audible range, it will provide effective masking. On the other hand, the aural harmonics of the 2000-cycle tone have frequencies of 4000 cycles/sec or more and hence do not mask the 1000-cycle signal. The notch observed in each of the curves when the signal frequency is approximately the same as the masking frequency is due to the generation of beats, which aid in recognition of the presence of a signal.

From the results of experiments such as that described above it is possible to make qualitative predictions as to the manner in which pure tones should be expected to mask complex signals, such as speech. The complete spectrum of speech frequencies extends from below 200 to above 10,000 cycles/sec, but articulation tests have shown that the band of speech frequencies most important for intelligibility is that extending from about 1000 to 2500 cycles/sec. If only this band is reproduced, the remaining frequencies being suppressed by filter networks, the intelligibility is not seriously affected, although the speech sounds unnatural, and it is difficult to distinguish a male from a female voice. In telephone practice it is customary to transmit the band extending from about 250 to 2750 cycles/sec, but the lower frequencies in this band add little to the intelligibility, their primary function being to improve the naturalness of the reproduction. From the above considerations it should be expected that a pure tone would be most effective in masking speech when its frequency was about 500 cycles/sec, for its more intense harmonics would then be spread across the frequency band required for good articulation. We should also conclude that distorted waves, such as square waves or series of pulses, would be more effective in masking speech than are pure tones, for such masking signals are themselves rich in harmonic frequencies. Actual experiments confirm both of these deductions.

13.11 Masking by Noise. The kind of masking sound most commonly encountered in real situations is noise, which has an essentially continuous frequency spectrum. In an electrical communications system, such as radio or telephone, this type of interference may be due to ordinary room noise at either the transmitting or the receiving end of the line, or it may be generated in the transmitting system itself as thermal, tube, or atmospheric noise. It is obviously of great interest to the communications engineer to determine the amount of masking that is tolerable and to investigate methods of reducing this type of interference. Room noise can, of course, be reduced by suitable sound insulation, and circuit noise by proper electrical design, but in practical situations there will almost always be a residual background of masking noise.

Although the energy in almost all types of noise background is continuously distributed over a wide band of frequencies, this distribution is not necessarily uniform. The manner in which the intensity varies with frequency may be represented by a graph showing the *sound spectrum* of the noise. The abscissas of such a graph are the frequencies, and the ordinates give the so-called *spectrum level* of the sound at each frequency. For any specified frequency f, the *intensity* spectrum level is defined as the intensity level of the sound contained within a band of frequencies 1 cycle/sec wide, centered on the frequency f. Similarly, the *pressure* spectrum level is defined as the pressure level in a 1-cycle band. In theory, the sound spectrum of a noise could be measured by picking up the noise with a linear microphone and amplifier system, and then passing the resulting voltage through an electrical filter network whose transmission band was 1 cycle/sec wide and whose center frequency was adjustable over the audible range. In actual practice it is difficult to construct a filter network having such a narrow pass band, together with the assumed sharp cutoff, and consequently it is usually necessary to employ a filter having a wider pass band. If the pass band is reasonably narrow, however, and if the sound spectrum does not contain any sharp peaks, it is observed that for any particular center frequency f the ratio of the intensity I, measured through the actual filter network, to the bandwidth of the filter is nearly constant. Hence the intensity spectrum level ISL at any frequency can be measured by observing the intensity I, as transmitted through this wide filter, and then computing the spectrum level from the equation

$$\text{ISL} = 10 \log \frac{I}{I_0 \, \Delta f} \tag{13.3}$$

where I_0 is the reference intensity of 10^{-12} watt/m^2 and Δf is the bandwidth of the filter in cycles/sec. Since 10 log (I/I_0) is actually the measured intensity level IL of the band Δf, equation 13.3 may also be expressed as

$$\text{ISL} = \text{IL} - 10 \log \Delta f \tag{13.4}$$

It is left as an exercise for the reader to show that the pressure spectrum level PSL is similarly given by the equation

$$\text{PSL} = \text{SPL} - 10 \log \Delta f \tag{13.5}$$

where SPL is the sound pressure level measured in the band of Δf cycles/sec width.

The spectrum level of noise is in general a function of frequency f. Figure 13.16 exemplifies three typical dependences of spectrum level on

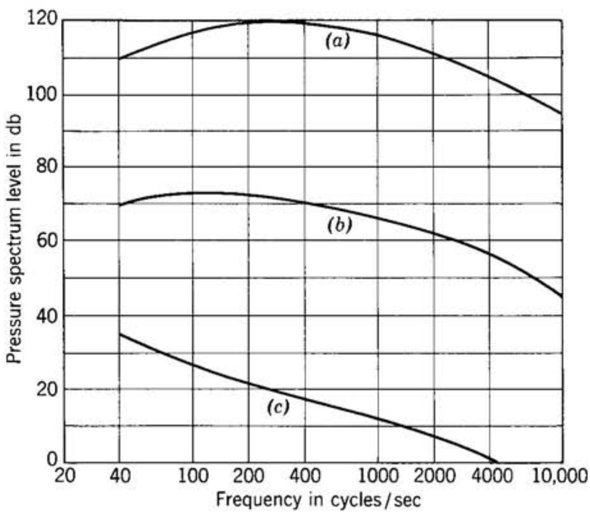

Fig. 13.16. Typical pressure spectrum levels in decibels relative to 0.0002 microbar. (*a*) 10 feet from turbo-jet engine of 150 db overall pressure level. (*b*) Noisy factory of 102 db overall pressure level. (*c*) Average room noise of 50 db overall pressure level.

frequency. Actually all three of the curves were obtained from measurements made with filters having half-octave rather than one-cycle pass bands. If one-cycle pass band filters had been used, undoubtedly both the jet engine spectrum and the factory noise spectrum would show one or more sharp peaks superimposed upon the given curves. It is to be noted that the spectrum level for all three of the noises illustrated in Fig. 13.16 ultimately reaches a region where the level falls off regularly with increasing frequency. This behavior is typical of all naturally produced sounds. However, it is possible by electrical means to generate noise having a constant spectrum level over the entire band of audible frequencies. Such a noise is referred to as "white" noise.

From each of the curves of Fig. 13.16 it is possible to compute an *overall* sound pressure level for the entire band of frequencies between 40 and 10,000 cycles/sec. Although the overall pressure level is much less significant than a plot of spectrum levels, it does provide a single number type of rating of the noise and consequently is frequently used. It is directly measured by means of sound level meters. It can also be computed from spectrum level curves. One method of making this computation is as follows:

(1) Divide the frequency scale into convenient bandwidths for estimating the mean pressure spectrum level PSL in each band.

(2) Estimate the mean pressure spectrum level in each band.

(3) Compute the pressure band level PBL for each of the above bands. This operation is essentially the reverse of that leading to equation 13.5 and is given by

$$\text{PBL} = \text{PSL} + 10 \log \Delta f \tag{13.6}$$

where Δf is the width of the band in cycles/sec.

(4) Convert each pressure band level to an intensity (or relative intensity).

(5) Add the intensities (or relative intensities) to obtain an overall intensity.

(6) Convert the overall intensity to an overall sound pressure level. The method outlined above may be used with equal facility to convert a curve of intensity spectrum levels to an overall intensity level. Various nomographs have been devised for adding decibels. These devices may be used to combine the decibel band levels of part (3) directly without converting to intensities and thereby obtain an overall level.

As an example of the procedure outlined above, let us proceed to determine the overall pressure level of the factory noise given by curve (*b*) of Fig. 13.16. Data used in making this computation is summarized in the accompanying table. Finally an intensity of 15×10^{-3} watt/m^2 is equivalent to a pressure level of 102 db.

Frequency Band (cycles/sec)	Bandwidth Δf (cycles/sec)	Spectrum Level PSL (db)	Band Level PBL (db)	Intensity I (watt/m^2)
40–100	60	72	90	1×10^{-3}
100–200	100	73	93	2×10^{-3}
200–400	200	72	95	3×10^{-3}
400–1000	600	68	96	4×10^{-3}
1000–2000	1000	64	94	2.5×10^{-3}
2000–4000	2000	59	92	1.5×10^{-3}
4000–10,000	6000	52	90	1×10^{-3}
			Total	15×10^{-3}

Masking of a pure tone by a very narrow band of noise, i.e., a band of only a few cycles/sec width, is essentially the same as that of an equally intense pure tone having the same frequency as that at the center of the band. Consequently, when the spectrum level of noise is relatively constant, the intensity of a narrow band of this noise is directly proportional to the bandwidth Δf and correspondingly, the masking expressed in decibels increases directly as $10 \log \Delta f$. However, ultimately a bandwidth will be reached, known as the *critical bandwidth*,[11] beyond which any further increase in the width of the pass band of the noise has little or no influence on the amount of masking produced on a pure tone at the center of the band. The critical bandwidth apparently is reached when it includes all frequencies in the noise that excite the same region of the basilar membrane as does the pure tone being masked. The addition of noise outside the critical band may be unpleasant but it does not increase the masking of the pure tone. Plotted in Fig. 13.17 are critical bandwidths as a function of the frequency of the pure tone being masked. A second and very important characteristic associated with the concept of critical band masking is that the normal threshold of audibility of the masked tone is raised to the decibel level of the critical band, i.e., the band level of the noise in a critical band. Once the width of the critical band Δf_c and the mean spectrum level has been determined, the *critical band level* CBL may be computed from equation 13.6 rewritten in this special case as

$$\text{CBL} = \text{PSL} + 10 \log \Delta f_c \tag{13.7}$$

As an example, let us compute the amount that the normal threshold of audibility of a 1000-cycle tone is raised by the room noise of Fig. 13.16*c*. The critical bandwidth of a 1000-cycle tone, as given by Fig. 13.17, is 40

[11] Fletcher and Munson, *J. Acoust. Soc. Am.*, **9**, 1 (1937).

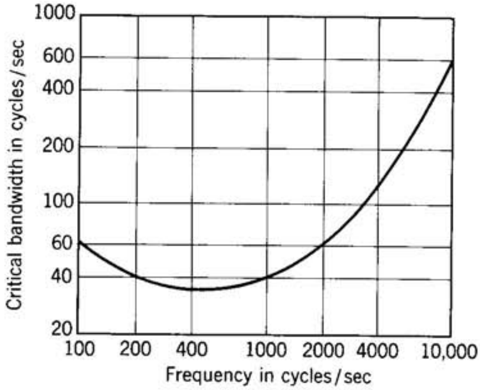

Fig. 13.17. Critical bandwidths for masking of pure tones.

cycles/sec. The pressure spectrum level of the room noise at 1000 cycles/sec, as given by Fig. 13.16*c*, is 13 db. Therefore the critical band level is CBL = $13 + 10 \log 40 = 29$ db and consequently, the masked threshold of audibility of the 1000-cycle tone will be 29 db instead of the normal 0 db, as given in Fig. 13.9. Of course, if the critical band level of the masking noise had been below the normal threshold of audibility of the frequency being considered, no masking would have occurred.

The presence of a background of noise also raises the detection threshold for other noise sources. Here, the normal detection threshold of the masked noise in a critical band is raised to the level of the masking noise in this same band. Since speech has both tonal and noise characteristics, its per cent *articulation* or *intelligibility* will be degraded by masking sounds. Space is not available to discuss this topic in the detail required. An interested reader is referred to the general references given at the beginning of this chapter and to that listed below.[12]

13.12 Binaural Localization. It is well known that we are able to determine, to a considerable degree of precision, the direction of a source of sound. Numerous experimenters have attempted to analyze the method by which this so-called *binaural localization* is accomplished. Regarding the problem from a fundamental viewpoint, there are two primary factors that might assist us to determine the direction of arrival of a sound: (1) its relative intensity in our two ears, and (2) its relative time of arrival at the ears, or, for a sustained tone, the difference in phase between the waves arriving at the right and the left ears. As has been pointed out, most of the ordinary sounds that we hear have a complex wave form and

[12] French and Steinberg, *J. Acoust. Soc. Am.*, **19**, 90 (1947).

frequency structure. However, the relative importance of the two factors mentioned above can be most readily determined by somewhat artificial experiments in which a pure sustained tone is supplied to each ear of an observer through telephone receivers, and either the relative intensity or the relative phase of one tone is varied with respect to the other.

From a consideration of the refraction of sound waves around a small obstacle, such as the human head, it can be shown both theoretically and experimentally that for frequencies below about 1000 cycles/sec the intensity of the sound from a distant source reaching one ear of an observer differs from that arriving at the other ear by a completely negligible amount and hence that, if we were forced to rely on considerations of intensity alone, we should be unable to determine the direction of arrival of a low-pitched tone. At higher frequencies, however, the observer's head casts a distinct sound shadow, and the intensity of the sound in the ear more nearly directed towards the source is considerably greater than that in the opposite ear, so that for tones in this frequency range the relative intensities as heard by the two ears should provide a cue as to the direction of the source. Not only is this true, but for frequencies above about 3000 cycles/sec the sound shadow cast by the pinna of the ear is sufficiently pronounced to indicate that it might be possible to distinguish between tones arriving from sources located in front of or behind the observer.

Confirmation of these conclusions is provided by experiments in which a pure tone is supplied to each ear of an observer through a telephone receiver, and the intensity of the sound transmitted to one ear is made somewhat greater than that transmitted to the other ear, all other factors remaining identical. The observer is then required to judge whether the source of sound appears to be on one side or the other of a median plane between his two ears. At low frequencies the results are in general inconsistent, but for frequencies above 1000 cycles/sec most observers tend to locate the direction of the source towards the side of the median plane that includes the ear receiving the louder sound.

Turning now to the effect of the relative phase of sounds arriving at the ears, it is apparent that the phase difference is a function not only of the distance between the ears and the orientation of the head but also of the wavelength of the sound. For pure tones of very low frequency and correspondingly long wavelength the difference in phase between sounds reaching the two ears is a comparatively small fraction of a wavelength, even if one ear is turned directly towards the source. For example, the distance between the ears is approximately 20 cm, which is only about 3 per cent of a wavelength at a frequency of 50 cycles/sec. It seems improbable that the phase difference corresponding to such a small fraction of a wavelength could be observed. With increasing frequency the wavelength decreases, with a resulting increase in the phase difference, until at about 850 cycles/sec the separation between the ears is equal to a half wavelength of the sound; i.e., the phase difference is 180° when one ear is facing directly towards the source. At still higher frequencies it will not appear that the phase of the sound in the ear nearer the source *leads* that in the other ear by more than 180°, but rather that it *lags* by some angle less than 180°. Consequently, for high frequencies, judgments of the source direction based only on phase difference should be expected to become ambiguous.

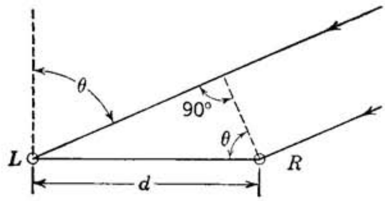

Fig. 13.18. Binaural localization by phase difference.

Figure 13.18 illustrates the relation existing between phase lag and angle of arrival for a sound coming from a distant source. In this figure d represents the separation of the observer's ears, and θ the angle between the direction of arrival of the sound and the median plane. Then the additional distance traveled by a wave crest in reaching the left ear, as compared to that traveled in reaching the right ear, is $d \sin \theta$, so that the relative delay in time of arrival of the crest at the left ear is

$$\Delta t = \frac{d \sin \theta}{c} \tag{13.8}$$

where c is the velocity of sound. The angle of phase lag $\Delta\phi$ is equal to $\omega \, \Delta t$, and hence

$$\Delta\phi = \omega \, \Delta t = \omega \frac{d \sin \theta}{c} = kd \sin \theta \tag{13.9}$$

where k is equal to ω/c. It will be observed that since $\Delta\phi$ decreases with θ, the phase lag is less when the observer is facing somewhat towards the source of the sound than it is when one of his ears is directly towards the source. It is therefore to be expected that under such circumstances it should be possible to estimate the direction of the source of a pure tone even when its frequency is greater than 850 cycles/sec.

From the above considerations it would appear that auditory localization by phase difference should be most definite for a band of frequencies ranging from about 200 to 800 cycles/sec. Numerous experiments have been made in which the phase of a pure tone supplied to one ear of an observer through a telephone receiver is varied with respect to that entering his other ear. In general the observer tends to locate the sound towards the side of leading phase, but the results are far from consistent, some observers reporting a pronounced directional effect under conditions in which others report none at all.

Taking the effects of both relative loudness and relative phase into account, we should expect that our ability to localize a pure tone would be least accurate at intermediate frequencies, too low to produce pronounced sound shadows, and at the same time too high to permit satisfactory localization by phase differences. This conclusion has been confirmed by experiments in which a loudspeaker producing a continuous tone is located at a distance from a blindfolded observer; either the observer's chair is rotated, or the loud-speaker is swung around his head on the end of the long boom. Such experiments indicate that the errors made in estimating the direction of the source are greatest for frequencies of about 1500 cycles/sec. They also show that at low frequencies we are unable to distinguish between sounds coming from sources located in front of and behind the head, whereas at frequencies above 5000 cycles/sec the confusion between the front and rear quadrants is relatively slight, thus indicating that front-back estimates are made on the basis of intensity differences. It should be emphasized that all such experiments must be made either outdoors or in a room whose walls have very high sound-absorbing properties, as otherwise the effects of reflections would invalidate the conclusions.

The foregoing discussion has been limited to continuous pure tones, and it has also been assumed that the observer is unable to turn his head to assist himself in finding the azimuth of the source. In common practice neither of these restrictions applies, and as a consequence we are able to determine the direction of arrival of an ordinary sound to a considerably higher degree of accuracy than is indicated by artificial experiments involving pure tones. The complex nature of such sounds causes them to have frequency spectra that extend over most of the audible range, so that differences in both loudness and phase may be used simultaneously to locate their sources. In addition, when we try to find out where a sound originates, we usually turn our heads back and forth so as eventually to face the source, thus employing a type of null method that is more precise than estimating the angle from the difference in either the phase or the loudness.

PROBLEMS

13.1. (*a*) From the curves of Figs. 13.10 and 13.12 determine the loudness level and loudness of a pure tone having a frequency of 100 cycles/sec and an intensity level of 60 db. (*b*) To what intensity level must this tone be reduced in order to reduce its loudness to one-tenth of the value obtained above? (*c*) To what intensity level must it be increased in order to raise its loudness to ten times the value determined in part (*a*)?

13.2. Given six pure tones with the following frequencies and intensity levels: 50 cycles/sec at 85 db, 100 cycles/sec at 80 db, 200 cycles/sec at 75 db, 500 cycles/sec at 80 db, 1000 cycles/sec at 75 db, and 10,000 cycles/sec at 70 db. (*a*) Determine the loudness level for each of the tones. (*b*) Assume the intensity level of each of the tones to be decreased by 30 db. Determine the new values of the loudness level for each of the tones. (*c*) Compute the decrease in loudness level in phons for each of the tones as brought about by a decrease in intensity level of 30 db.

13.3. (*a*) Compute the overall intensity level for the six tones of Problem 13.2. (*b*) What is the total loudness in sones of these six tones? (*c*) What is the required intensity level of a single 1000-cycle/sec tone having the loudness of part (*b*)?

13.4. Given three pure tones with the following frequencies and sound pressure levels relative to 0.0002 microbar: 100 cycles/sec at 60 db, 200 cycles/sec at 60 db, and 500 cycles/sec at 55 db. (*a*) Which tone is the loudest? (*b*) What is the overall sound pressure level of these three tones when sounded simultaneously? (*c*) What is their total loudness level in phons?

13.5. Let the pressure exerted by acoustic waves upon the drum membrane of the ear be represented by $p = P \cos \omega t$, where P is the pressure amplitude. Assuming that the subjective response r in the auditory nerve may be represented by the three terms

$$r = a_1 p + a_2 p^2 + a_3 p^3$$

where all the a's are constants, prove that the response contains a constant term, and a set of three terms having frequencies ω, 2ω, and 3ω, respectively. Compute the amplitude of each term as a function of P and the constants a.

13.6. Assume that for moderate instantaneous pressures p the response of the ear may be represented by only the two terms

$$r = a_1 p + a_2 p^2$$

where p and the a's are as defined in Problem 13.5. If the incident sound consists of two wave motions of frequencies ω_1 and ω_2, which produce a pressure p given by

$$p = P_1 \cos \omega_1 t + P_2 \cos \omega_2 t$$

determine the frequencies and amplitudes of the response.

13.7. Determine the origin of the combination tones of frequencies 200, 300, 1000, 2200, and 3300 cycles/sec indicated in Sect. 13.9.

13.8. Using Fig. 13.15, (*a*) what must be the intensity level of a 1000 cycle/sec tone if it is to be heard in the presence of a 2000 cycle/sec tone at an intensity level of 80 db? (*b*) What must be the intensity level of a 5000 cycle/sec tone in order to be heard in the presence of the 2000 cycle/sec tone?

13.9. When a condenser microphone is used to measure the spectrum level of a noise, the measured open-circuit voltage is 0.001 volt. The open-circuit voltage response rating of the microphone is -50 db relative to 1 volt per microbar. If the width of the pass band of the filter used with the microphone is 50 cycles/sec, what is the pressure spectrum level of the noise relative to 0.0002 microbar?

13.10. A certain noise has a spectrum such that the intensity I_1 in each one-cycle band is given by the equation $I_1 = 10^{-6}/f$ watt/m^2, where f is the center frequency of the band in cycles/sec. (*a*) Compute the intensity spectrum level at

100, 500, and 1000 cycles/sec. (*b*) What is the intensity level of the entire band of frequencies between 100 and 1000 cycles/sec? (*c*) What is the loudness of the entire band of frequencies between 100 and 1000 cycles/sec?

13.11. Given a certain noise to be represented by an rms acoustic pressure $P_1 = 500/f$ microbar, where P_1 is the pressure in a one-cycle band centered on the frequency f in cycles/sec. (*a*) Derive a general expression for the pressure spectrum level PSL of this sound. (*b*) How does the pressure spectrum level change with frequency expressed in decibels per octave? (*c*) What is the band level of this noise in a band of 50 cycles/sec width centered on a frequency of 2500 cycles/sec?

13.12. (*a*) Compute the overall sound pressure level in the band of frequencies from 200 to 2000 cycles/sec for the speech spectrum of Fig. 13.3. (*b*) Compute the loudness of this band of frequencies. (*c*) What is the loudness level of this band of frequencies?

13.13. What must be the pressure level of a pure tone of 200-cycles/sec frequency if it is to be audible in the factory noise spectrum of Fig. 13.16*b*?

13.14. (*a*) Using Figs. 13.16*c* and 13.17, compute critical band levels for the room noise at 100, 200, 400, 1000, 2000, and 4000 cycles/sec and plot the results as a function of frequency. (*b*) At what frequency will this noise have the maximum effect on raising the detection threshold of a pure tone?

chapter 14

ARCHITECTURAL ACOUSTICS

14.1 Introduction. Although the acoustics of enclosed spaces has been of obvious importance ever since people first began to gather in large auditoriums or churches, it was not until after the institution of quantitative measurements by Sabine[1] in 1895 that the maze of superstitions concerning the subject began to be replaced by a firm foundation of scientific knowledge. Through extensive experimental studies of the acoustical properties of a room, Sabine arrived at an empirical relation between the reverberation characteristics of an enclosure, its size, and the amount of absorbing material present. His definition of the *reverberation time* T of an enclosure, i.e., the time in seconds required to reduce the intensity from a level 60 db above the threshold of audibility to the threshold, is still the most important single parameter used in judging the acoustical quality of a room.

The simple Sabine equation

$$T = \frac{0.049V}{a} \tag{14.1}$$

used for calculating the reverberation time of a room, requires a knowledge only of its volume V and a parameter a which measures its total capability of absorbing acoustic energy. Theoretical derivations of this equation are usually based on the concept of *geometric* or *ray* acoustics, in which sound energy emanating from a source in a room is assumed to travel outward from the source along diverging rays. At each encounter with the boundaries of the room the rays are partially reflected and partially absorbed in accordance with the equations derived in Chapter 6. After a large number of successive reflections the sound in the room may be assumed to become *diffuse*, i.e., the average energy density $\mathcal{E}$ is then the same throughout the entire volume of the enclosure, and all directions of propagation are equally probable. This theory oversimplifies the actual behavior of sound

[1] Sabine, *Collected Papers on Acoustics*, Harvard University Press (1922).

waves in a room, particularly at low frequencies, for it neglects entirely such important factors as the normal modes of vibration of the room, the particular locations of the various absorptive materials, interference and diffraction, and parameters associated with the shape of the room, such as focusing effects. Nevertheless, it frequently leads to valid general conclusions, and, since Sabine's approach is much simpler than that of *wave* acoustics, it will be considered first.

When a simple source of sound is present in an enclosed space, sound rays originating from the source are in general partially reflected each time they strike the walls of the enclosure and consequently the waves proceeding along the direct sound ray to any particular point in the room are followed by a multitude of reflected waves. It may be assumed that the phases and amplitudes of these reflected waves are randomly distributed, so that the cancellation resulting from destructive interference is negligible. If the source is operated continuously, the acoustic intensity at any point in the room builds up to higher values than would be true if the source were operated in open air, or far from reflecting surfaces, the gain in intensity often being greater than tenfold. For any given enclosure this gain is nearly proportional to the reverberation time; hence a large reverberation time is desirable if a weak source of sound is to be everywhere audible.

If the sound source is now shut off, reception of sound by the direct ray path ceases after the lapse of a short time interval $t = d/c$, where d is the distance from the source to the point of observation and c is the velocity of sound in air. However, the reflected waves continue to be received in the form of a rapid succession of randomly oriented waves of gradually decreasing intensity. The presence of this reverberant acoustic energy tends to mask the immediate recognition of any new source of sound, unless sufficient time has elapsed for the reverberation to have fallen some 5 to 10 db below its initial level. Since the reverberation time T is a direct measure of the persistence of such sounds, it is obvious that a small reverberation time is desirable, so as to minimize these masking effects. The choice of the best reverberation time for a particular enclosure must therefore be a compromise between two extremes.

One additional acoustic factor of importance in the design of a room or other enclosure is its ability to screen out external sounds and thus reduce their annoyance or masking effects. Although the acoustic transmission of the walls of the enclosure (Sect. 6.5) is the most significant factor to be considered in this respect, it should also be noted that the existence of a small reverberation time with its attendant high total internal acoustic absorption will tend to minimize the ambient noise level produced by those sounds that do penetrate into the enclosure.

14.2 Growth of Sound Intensity in a Live Room—Classical Ray Theory. If a source of sound is operated continuously in an enclosure, it is apparent that only absorption, either in the medium or at the surrounding surfaces, will prevent the intensity from becoming infinitely large. In small and medium sized enclosures, absorption in the medium is negligible, so that both the rate at which the acoustic intensity increases, and its ultimate magnitude, are controlled by the absorptive power of the bounding surfaces. If this absorptive power is large, the intensity quickly reaches its ultimate value which at any point is only slightly in excess of that produced by the direct wave. By contrast, if the absorptive power is small, the growth is slow and a considerable time will elapse before the ultimate intensity is attained. Rooms of this latter type are known as *live* rooms, and application of the acoustic ray theory to such rooms yields results that are in fairly good agreement with experimental measurements.

When a source of sound is started in a live room, reflections at the walls produce a sound energy distribution that becomes more and more uniform with increasing time. Ultimately, except in close proximity to the source, this energy distribution may be assumed to be completely uniform and to have a direction of flow that is essentially random. Actually, if the source of sound is a pure tone of just one frequency, standing wave patterns may be set up in the room, and large fluctuations in intensity will then be observed from point to point. However, if the source of sound consists of a uniform band of frequencies, at least one-half an octave wide, or is a pure tone that is warbled over a similar frequency band, the interference effects mentioned above are largely overcome and may be neglected.

Let us now derive a relationship between *energy flow* or *intensity* and *energy density* for such randomly distributed sound energy. In particular, let us determine the rate at which sound energy strikes the walls of the

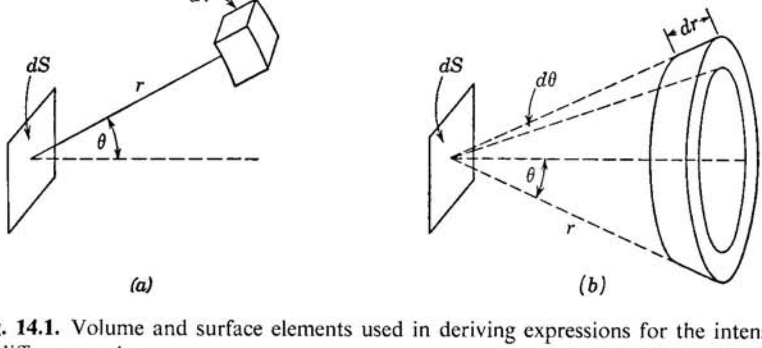

Fig. 14.1. Volume and surface elements used in deriving expressions for the intensity of diffuse sounds.

room. Consider Fig. 14.1*a*, in which dS is an element of wall surface, and dV an element of volume in the medium at a distance r from dS, where r makes an angle θ with the normal to dS. Let the average acoustic energy density, which is assumed uniform throughout the region being considered, be represented by $\mathcal{E}$. The acoustic energy present in dV is then $\mathcal{E}\, dV$. The surface area of a sphere of radius r surrounding dV is $4\pi r^2$, and the projected area of dS on any portion of this sphere is $dS \cos \theta$. Hence the ratio $(dS \cos \theta)/(4\pi r^2)$ represents the fraction of the energy in dV that will ultimately strike dS by direct transmission, and the energy from dV that impinges directly upon dS is therefore

$$\Delta E = \frac{\mathcal{E}\, dV\, dS \cos \theta}{4\pi r^2} \tag{14.2}$$

Now assume that the volume element dV is part of a hemispherical shell of radius r and thickness dr, centered upon dS. The acoustic energy ΔE contributed to dS by this entire shell can then be obtained by considering a circular zone of radius $r \sin \theta$, for which θ is a constant, Fig. 14.1*b*, and then integrating over the entire surface of the shell. The volume of this zone is $2\pi r \sin \theta\, r\, dr\, d\theta$, so that integration from $\theta = 0$ to $\theta = \pi/2$ gives

$$\Delta E = \frac{\mathcal{E}\, dS\, dr}{2} \int_0^{\pi/2} \sin \theta \cos \theta\, d\theta = \frac{\mathcal{E}\, dS\, dr}{4} \tag{14.3}$$

Since this energy arrives during the time interval $\Delta t = dr/c$, the rate at which sound energy falls on dS from all directions is

$$\frac{\Delta E}{\Delta t} = \frac{\mathcal{E} c\, dS}{4} \tag{14.4}$$

or $\mathcal{E}c/4$ per unit area. The intensity I of such diffuse sound at the walls is therefore

$$I = \frac{\mathcal{E} c}{4} \tag{14.5}$$

which is seen to be one-quarter of that given by equation 5.37 for a plane wave of equal energy density incident normally upon a surface.

Now if $\alpha_1, \alpha_2, \alpha_3, \cdots$ are the respective *absorption coefficients* representing the fraction of *randomly* incident energy absorbed by the different materials of areas $S_1, S_2, S_3, \cdots$ forming the interior walls of the room as well as any other absorbing surfaces, then the rate at which energy is being absorbed by these surfaces is

$$\frac{\mathcal{E} c}{4} (\alpha_1 S_1 + \alpha_2 S_2 + \alpha_3 S_3 + \cdots)$$

Defining the total absorptive power a of a live room as

$$a = \sum \alpha_i S_i \tag{14.6}$$

the above rate of absorption can be more simply represented by

$$\frac{\mathcal{E} c a}{4}$$

This rate at which sound energy is absorbed at the bounding surfaces of the room, plus the rate $V\, d\mathcal{E}/dt$ at which it increases in the medium throughout the interior of the room, must equal the rate W at which it is being produced. The fundamental differential equation governing the growth of sound energy in a live room is therefore

$$V\frac{d\mathcal{E}}{dt} + \frac{ac\mathcal{E}}{4} = W \tag{14.7}$$

Assuming the sound source to have been started at the time $t = 0$, the solution of this differential equation is

$$\mathcal{E} = \frac{4W}{ac}\left(1 - e^{-\frac{ac}{4V}t}\right) \tag{14.8}$$

and using equation 14.5, this equation may be rewritten in terms of the intensity I as

$$I = \frac{W}{a}\left(1 - e^{-\frac{ac}{4V}t}\right) \tag{14.8a}$$

or using equation 5.33b, in terms of the mean square acoustic pressure P^2 as

$$P^2 = \frac{4W\rho_0 c}{a}\left(1 - e^{-\frac{ac}{4V}t}\right) \tag{14.8b}$$

These results are identical in form with that giving the growth of a direct current in an electrical circuit containing an inductance L and a resistance R. In particular, the time constant of the process is $4V/ac$. Therefore, if a is small the time constant is large, and a relatively long time will be required for the intensity to approach its ultimate value of

$$I_\infty = \frac{W}{a} \tag{14.9}$$

as was to have been anticipated from our discussion in Sect. 14.1. Correspondingly, equation 14.9 indicates that a small value of a is associated with a large value for the ultimate intensity. The ultimate values of the energy density and mean square pressure are given respectively by

$$\mathcal{E}_\infty = \frac{4W}{ac} \tag{14.9a}$$

and

$$P_\infty{}^2 = \frac{4W\rho_0 c}{a} \tag{14.9b}$$

Since the mathematical developments of this section are based upon an assumed diffuse distribution of acoustic energy, certain limitations apply to the resulting derived equations. For instance, equation 14.8 may not be used until a sufficient time t has elapsed to permit each initial ray to have experienced several reflections at the boundaries. For a small room this time is of the order of 0.05 sec, whereas for a large auditorium it may approach 1.0 sec. Equation 14.9*a* indicates that the final energy density is independent of the volume and shape of the room, is the same at all points in the room and depends only upon the total absorption a as defined by equation 14.6. Of course, this is not true for spherical or curved rooms having well-defined sound-focusing properties. Neither can the equations be applied to odd-shaped rooms having deep recesses, nor to rooms coupled together by an opening. Furthermore, they are not valid if some of the surfaces of the room have abnormally large coefficients α, for the energy density near such walls is then considerably lower than elsewhere.

14.3 Decay of Sound in Live Rooms. The differential equation governing the decay of uniformly distributed diffuse sound in a live room is obtained directly by letting W equal zero in equation 14.7. Assuming that the source is shut off at the time $t = 0$ and letting $\mathcal{E}_0$ represent the assumed uniformly distributed energy density at this instant, then as t increases

$$\mathcal{E} = \mathcal{E}_0 e^{-\frac{ac}{4V}t} \tag{14.10}$$

Similarly, the intensity I at any time t is related to the initial intensity I_0 by

$$\frac{I}{I_0} = e^{-\frac{ac}{4V}t} \tag{14.10a}$$

If we now apply the operator 10 log to both sides of this equation, it becomes

$$\Delta\mathrm{IL} = 10 \log e^{-(ac/4V)t} = \frac{10}{2.3} \ln e^{-(ac/4V)t} = -\frac{1.087act}{V}$$

where $\Delta \text{IL} = 10 \log (I/I_0)$ represents the change in intensity level in decibels. It is apparent that the intensity level in a live room, and correspondingly the sound pressure level, decreases with elapsed time at a constant *decay rate* D in decibels per second given by

$$D = \frac{1.087ac}{V} \tag{14.11}$$

In accordance with the original proposal of Sabine, let us define the reverberation time T as the time required for the level of the sound in the room to decay by 60 db; then

$$T = \frac{60}{D} = \frac{55.2V}{ac} \tag{14.12}$$

Expressing the volume V in cubic meters and the areas S_i used in computing a in square meters, and introducing $c = 343$ m/sec, equation 14.12 becomes

$$T = \frac{0.161V}{a} \tag{14.12a}$$

In acoustical engineering practice it is customary to express V in cubic feet and a in *sabins*, where the sabin is an absorption unit representing a surface capable of absorbing sound at the same rate as does 1 sq ft of perfectly absorbing surface. Equation 14.6 may be used to compute the total absorption in sabins provided that S_i is measured in square feet. In these units equation 14.12 becomes

$$T = \frac{0.049V}{a} \tag{14.12b}$$

It is apparent from these equations that the reverberation time of a live room can be calculated at once if its volume and total absorption are known. Since the latter can be readily changed by the insertion or removal of absorptive materials at the walls, the magnitude of the reverberation time of a live room is subject to precise control. Furthermore, the measured change in reverberation time produced by the addition of a definite area of absorbing material in specially constructed live rooms, known as reverberation chambers, is commonly used as the standard method of determining absorption coefficients.

14.4 Influence of Reverberation Time upon Articulation. As an illustration of the validity of the various assumptions made in deriving the reverberation equation for a live room, let us consider a rectangular room $10 \times 15 \times 30$ ft in dimensions, whose interior boundaries have an average absorption coefficient of $\bar{\alpha} = 0.1$. Then $V = 4500$ ft^3 and $a = 2(10 \times 15 + 10 \times 30 + 15 \times 30) \times 0.1 = 180$ sabins, so that

$$T = \frac{0.049 \times 4500}{180} = 1.23 \text{ sec}$$

which corresponds to a fairly live room. Equation 14.9 gives the ultimate intensity developed by a 10-microwatt source in the room as

$$I = \tfrac{10}{180} = 0.055 \text{ microwatt/ft}^2 = 0.59 \text{ microwatt/m}^2$$

which corresponds to an intensity level of 58 db. For comparison, the intensity produced by direct transmission at a distance of 15 ft from a source located in the center of the room, i.e., at the most distant wall, is

$$I = \frac{10}{4\pi \times 15^2} = 0.0035 \text{ microwatt/ft}^2 = 0.038 \text{ microwatt/m}^2$$

or 46 db, which is considerably lower.

Figure 14.2 presents a graphical representation of the growth and decay of the intensity level in such a room. In the figure it is assumed that the source of sound consists of successively spoken syllables, each of 10 microwatts power and each emitted for 0.2 sec, with a silent period of 0.05 sec between the termination of one syllable and the beginning of the next. The initial sound is seen to build up to a level of nearly 58 db in 0.2 sec. It then falls off at a rate of about 50 db/sec, reaching a level nearly 7.5 db below that of the second syllable at the latter's midpoint, i.e., at the time $t = 0.35$ sec. At this instant the first syllable may be regarded as a masking noise having a level some 7.5 db below that of the syllable to which one is listening. This amount of masking is readily tolerable.

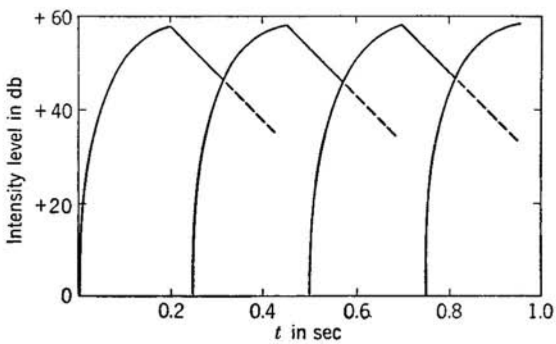

Fig. 14.2. Intensity level in a live room as produced by successively spoken syllables.

However, if these same syllables are spoken at double the above rate, the masking differential due to preceding syllables would be reduced to about 3 db, which would manifest itself as a confusing background and would interfere with the intelligibility of the speech. As a consequence, the room considered in this example verges on being overly reverberant.

In general, a room of the size just considered is more satisfactory from an acoustic viewpoint if the absorption is increased so as to reduce the reverberation time to about 0.6 sec. The distribution of sound energy in rooms having reverberation times of this magnitude no longer satisfies the conditions assumed in deriving equation 14.12*b*, so that such rooms are more appropriately classified as *dead* rooms, and a slightly modified equation (14.18) must be used in calculating their reverberation times.

Let us now consider the effect of the size of a room upon the sound level produced. Assume that the volume of the room previously considered is increased to ten times its original value, without altering the reverberation time of 1.23 sec. From equation 14.12*b* it is apparent that this will also necessitate an increase in the total absorption a by a factor of ten. The sound levels produced by the pattern of syllables previously considered will now be down 10 db to a level of 48 db, with the result that they are likely to be masked by the general background noise level in the room or may even fall below the threshold of audibility for some listeners. This difficulty may be readily overcome if the speaker increases his power output tenfold, and thereby raises the level to the previous value of 58 db.

On the other hand, if the volume of the original room is considered as increased by a factor of 100, i.e., if its volume becomes equivalent to that of a large auditorium, it is difficult, if not impossible, for the speaker to increase his power output sufficiently to maintain the original intensity level of 58 db. In such an auditorium it is necessary to use a public address system in order to produce an adequately high intensity level without excessive reverberation.

14.5 Decay of Sound in Dead Rooms. In deriving equation 14.12*b* for the reverberation time of a live room it was assumed that the number of reflections occurring during the growth or decay of sound as well as the fractional amount of energy reflected at each reflection was sufficient to provide a uniform energy density distribution. It is obvious that the previously derived equations for growth and decay of sound are not applicable to the limiting case in which the absorption coefficient of the materials constituting each of the boundaries is unity, for here the reflected energy must be zero. The only energy present is that of the direct wave diverging from the sound source. Under these conditions the reverberation time must be zero, whereas equation 14.12*b* gives a finite value of $0.049\,V/S$, where S is merely the area of the interior surface of the room. Similarly, it is to be anticipated that this equation will also give increasingly incorrect results as the average sound absorption coefficient exceeds 0.2, where it is in error by approximately 10 per cent. A new approach to the problem is therefore essential to the discussion of the growth and decay of sound in such *dead* rooms.

One such approach is that of Eyring,[2] who considers the multiplicity of reflections from the walls as equivalent to a set of *image sources*, all of which come into existence the instant the real source starts. The building up of acoustic energy at any point then consists of the accumulation of successive increments from the true source, from the first-order or single-reflection images whose strengths are $(1 - \bar{\alpha})W$, from the second-order or double-reflection images whose strengths are $(1 - \bar{\alpha})^2 W$, etc., until all the image sources of any appreciable strength have made their contribution. Similarly, when the true source in the room is stopped, all the images of this source are assumed to be simultaneously extinguished. The decay in energy density in the room therefore results from the successive losses of acoustic radiation, first from the source, then from the first-order images, the second-order images, etc.

If this process of explaining the growth and decay of acoustic energy in a room is assumed to be correct, and it is certainly more nearly correct than that based on an assumed uniform distribution of energy, it may be shown that the equation for the growth in acoustic energy density is

$$\mathcal{E} = \frac{4W}{-cS \ln (1 - \bar{\alpha})} \left[1 - \exp \frac{cS \ln (1 - \bar{\alpha})t}{4V} \right] \tag{14.13}$$

This equation is seen to be similar to the corresponding live-room equation (14.8) excepting that the total room absorption is now given by

$$a = -S \ln (1 - \bar{\alpha}) \tag{14.14}$$

where S is the total area of the interior surfaces of the room and $\bar{\alpha}$ is an average sound absorption coefficient as defined by the equation

$$\bar{\alpha} = \frac{\sum \alpha_i S_i}{S} \tag{14.15}$$

Similarly, the equation for decay of sound energy in such a room is given by

$$\mathcal{E} = \mathcal{E}_0 \exp \frac{cS \ln (1 - \bar{\alpha})t}{4V} \tag{14.16}$$

[2] Eyring, *J. Acoust. Soc. Am.* **1.** 217 (1930).

that for the decay rate in decibels per second by

$$D = -\frac{1.087cS \ln(1 - \bar{\alpha})}{V} \tag{14.17}$$

and that for the reverberation time (expressed in the customary engineering units) by

$$T = \frac{0.049\ V}{-S \ln(1 - \bar{\alpha})} \tag{14.18}$$

Another approach to the problem of decay of sound energy in a room is that of Norris,[3] who assumes that the energy density is reduced to $(1 - \bar{\alpha})$ of its incident value upon each reflection. Furthermore, the mean free path L, defined as the average distance which a sound ray travels through the air between successive encounters with the boundaries of the room, has been shown both in theory[4] and by experiment to be given by the equation

$$L = \frac{4V}{S} \tag{14.19}$$

so that the number n of reflections experienced by an average individual ray in a time interval t is

$$n = \frac{ct}{L} = \frac{Sct}{4V} \tag{14.20}$$

Therefore in a time t, the average energy density will decrease from its initial value of $\mathcal{E}_0$ to $\mathcal{E}$ in accordance with the equation

$$\mathcal{E} = \mathcal{E}_0(1 - \bar{\alpha})^{\frac{Sct}{4V}} \tag{14.21}$$

It is left as an exercise for the reader to show that this equation is equivalent to equation 14.16 and that as a consequence, it leads to the same reverberation equation (14.18) as does the approach of Eyring.

In general, equation 14.18 gives shorter reverberation times than does equation 14.12*b*. Fundamentally, this results from the fact that the discrete energy losses $\bar{\alpha}\mathcal{E}$ experienced at each individual reflection and leading to equation 14.18 are greater on the average than that obtained in the average interval between reflections in the process of continuous absorption leading to equation 14.12*b*. For example, the reverberation time of the room considered in Sect. 14.4, as calculated from equation 14.18, is 1.18 sec instead of 1.23 sec. This slight difference is of little practical significance. However, in dead rooms, i.e., ones for which $\bar{\alpha} > 0.2$, the measured reverberation

[3] Knudsen, *Architectural Acoustics*, p. 603, John Wiley and Sons (1932).

[4] Kosten, *Acustica*, **10**, 245 (1960).

times are in much better agreement with equation 14.18 than with equation 14.12*b*. Furthermore, equation 14.18 gives the proper *zero* reverberation time for the limiting case of $\bar{\alpha} = 1$, i.e., for a room bounded by completely absorptive surfaces. It should be mentioned that one weakness of the theories leading to equation 14.18 is that the equation is strictly correct only for rooms in which all the boundaries have the same absorption coefficient.

A still different approach to the problem of decay of sound in a dead room is that of Millington and Sette.[5] Their theory indicates that the total room absorption is given by

$$a = \sum -S_i \ln (1 - \alpha_i) \tag{14.22}$$

which leads to

$$T = \frac{0.049\, V}{\sum - S_i \ln (1 - \alpha_i)} \tag{14.23}$$

for the reverberation time. It is to be noted that dead room equation 14.23 may be derived from live room equation 14.12*b* by substitution of an *effective* sound absorption coefficient α_e, as defined by

$$\alpha_e = -\ln (1 - \alpha_i) \tag{14.24}$$

for α_i in equation 14.6. This indicates that in so far as influencing reverberation time is concerned, highly absorbing materials are more effective than would be anticipated from their true absorption coefficients α_i as defined in Chapter 6. For instance, when $\alpha_i > 0.63$, equation 14.24 indicates that $\alpha_e > 1$.

Experience shows that when materials having a wide variety of absorption coefficients are present in a room, equation 14.23 is the best equation to use in predicting the reverberation time. In computing reverberation times in rooms, it will be the practice in this book to use whichever of equations 14.12*b*, 14.18, or 14.23 seems most appropriate for each particular case. For a detailed analysis of the relative validities of the various theories describing the decay of sound in enclosures, the reader is referred to a comprehensive discussion by Young.[6]

14.6 Effect of the Absorption of Sound in Air upon Reverberation. In the previously considered theories of reverberation, any absorption of sound in the air has been neglected. However, as has been discussed in Chapter 9, all sound waves lose some energy during their propagation through a fluid medium. In particular, the intensity of a plane wave decreases in accordance with the equation

$$I = I_0 e^{-2\alpha x} = I_0 e^{-mx} \tag{14.25}$$

[5] Millington, *J. Acoust. Soc. Am.*, **4,** 69 (1932); Sette, *J. Acoust. Soc. Am.*, **4,** 193 (1932)
[6] Young, *J. Acoust. Soc. Am.* **31,** 912 (1959)

In this chapter $m = 2\alpha$ will be used as an attenuation constant of the medium, so as to avoid confusion between α as used in Sect. 9.5 for attenuation in a fluid and α as used in this chapter to represent the absorption coefficient of a surface. During a time t, an acoustic wave travels a distance $x = ct$, and consequently equation 14.25 may be rewritten as

$$I = I_0 e^{-mct} \tag{14.25a}$$

If the effect of this absorption in air is introduced into equation 14.10*a* which describes the decay of sound in a room, the resulting equation is

$$I = I_0 e^{-(a/4V + m)ct} \tag{14.25b}$$

Correspondingly, the expression for the reverberation time becomes

$$T = \frac{0.049V}{a + 4mV} \tag{14.26}$$

where the attenuation constant m must be expressed in units of ft^{-1}. It is to be noted that in using this equation, the total absorption a is given either by equation 14.6 or by 14.14 or 14.22 depending upon whether the room is classified as live or dead. The relative importance of absorption in the air is determined by the relative magnitudes of the second and first terms in the denominator of equation 14.26. As is to be anticipated, air absorption is of greater significance in rooms of large volume V, where the path lengths between successive reflections at the walls are relatively large. Since m increases with frequency, air absorption is also greater at frequencies above 1000 cycles/sec than it is at lower frequencies. Finally, in extremely reverberant rooms, for which $\bar{\alpha}$ approaches zero, the major portion of the sound absorption may occur in the air, rather than at the walls. Measured values of the reverberation times in such rooms offer an excellent experimental means for determining the attenuation constants of gases, as discussed in Chapter 9.

14.7 Measurement of Reverberation Time. Although numerous techniques have been devised for measuring the reverberation time of an enclosure, most procedures may be classified as belonging to one or the other of two basic types. One such group includes those procedures depending on the subjective judgment of an observer as to the time interval required for the intensity level to fall 60 db to the threshold of audibility. In the second group some form of high-speed recorder is employed, capable of recording changes in the intensity level as a function of time.

Included in the first group is the classical method of Sabine, in which a stop watch is used to determine the interval required for sounds produced by an organ pipe to decay from a level 60 db above the threshold of audibility to the threshold. Many refinements have been added to this original method. One primary difficulty encountered in all reverberation measurements is the existence of local anomalies resulting from the formation of patterns of standing waves. Sabine's method of overcoming this difficulty was to place near the center of the reverberation chamber a number of large reflecting surfaces, which were rotated while measurements were being made, thus varying the standing wave patterns and averaging out the local anomalies. Another procedure is to make measurements at a large number of different points in the chamber. The method most commonly employed at present is to use a warble oscillator, which by slowly warbling the frequency of the sound emitted by a loudspeaker produces continuous changes in the standing wave patterns and thus averages out the anomalies. The usual method of attaining the desired initial intensity level of 60 db above the threshold of audibility is first to drive the loudspeaker or loudspeakers at such a low power level that the sound produced throughout the enclosure is barely audible and then to increase the power input by a factor of 10^6, i.e., by 60 db. After steady conditions have been reached, the driving power is cut off, and the reverberation time is measured directly, either by a stop watch or by an electrical timer.

A more objective method involves some form of high-speed sound-level recorder. Sound waves picked up by a calibrated microphone are amplified, rectified, and their level recorded by a stylus on a moving strip of paper. Recorders of this type have been developed that are capable of following rates of change of intensity level in excess of 1000 db/sec. The curve shown in Fig. 14.3 is a typical record of the decay in intensity level as recorded in this manner. In this example the paper was run past the stylus at a rate of 5 cm/sec, so that each centimeter of distance along the abscissa represents 0.2 sec. The rate of decay in decibels per second can be obtained directly

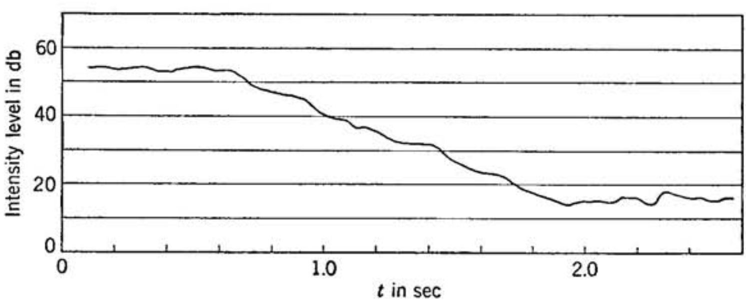

Fig. 14.3. Reverberation decay curve.

from the slope of the curve, and from this the reverberation time. For the curve illustrated in Fig. 14.3 the decay rate is approximately 30 db/sec, corresponding to a reverberation time of $\frac{60}{30} = 2$ sec. An advantage of this method is that errors of personal judgment are largely eliminated. Furthermore, it provides a permanent record of the rate of decay in intensity level, which may be checked and rechecked if necessary. Reverberation times of less than 0.1 sec can be measured by this method. Another type of recorder consists of a cathode-ray oscillograph having a slow sweep rate and a long-persistence screen. A permanent record from which the reverberation time can be computed may be obtained by photographic means.

The initial work of Sabine on reverberation was limited to a single frequency 512 cycles/sec, although his later experiments included measurements in octave steps between 64 and 4096 cycles/sec. Custom has attached so much importance to the frequency 512 cycles/sec that, when the expression *reverberation time* is used, without specification of any particular frequency, it is generally understood to refer to a pure or warbled tone or a band of noise centered on this frequency or more recently on 500 cycles/sec. Measurements of reverberation time made at a single frequency suffice to characterize the reverberation characteristics of an enclosure at other frequencies if the absorption coefficients of the absorptive materials present are approximately independent of frequency, but this is obviously not true if these absorption coefficients vary widely with frequency. Under these circumstances it becomes necessary to specify the reverberation time for representative frequencies covering the entire range of importance to speech and music. The representative frequencies usually chosen are 125, 500, 1000, and 2000 cycles/sec.

An ever-present question is, what is the *optimum* reverberation time for a given enclosure? Important factors that must be considered in answering this question include information both as to the size (volume) of the enclosure and its primary use. For example, in small to medium-sized rooms used for office work it is found possible to carry on conversations, conferences, and routine office work with the minimum of difficulty and interference when the reverberation time is approximately 0.5 sec. We might expect that an enclosure designed specifically for public speech should have a short reverberation time, to avoid overlap of syllables and to provide good articulation. This is the condition that is to be found in an open-air theater, where reverberation is absent, and the only difficulty that faces a speaker is one of generating sufficiently intense sounds. However, a speaker does not prefer such highly absorbing conditions, for the enclosure appears dead and unresponsive to him. In addition, the absence of the gain in intensity associated with reverberation puts a considerable vocal strain on the speaker. The most acceptable conditions for speaker and audience seem to correspond to a reverberation time of about 0.8 sec for a small auditorium of 50,000 ft^3 volume, increasing to about 1.5 sec or more for large auditoriums whose volume exceeds 1,000,000 ft^3. Since rapidity of speech is as important a factor as loudness, a speaker who talks slowly can make himself intelligible in an auditorium having a reverberation time far above the optimum value.

The problem of specifying an optimum reverberation time for enclosures primarily designed for the playing or reproduction of music is even more complex than for speech, for the optimum time may vary with type of music or with the effect desired. In a broad sense the enclosure and its reverberation characteristics are a part of each musical instrument being played in the room, and this factor should be, consciously or unconsciously, in the minds of the composer, conductor, or artist when the music is composed and played. In general, enclosures designed primarily as music rooms should be more reverberant than similar-sized rooms designed primarily for speech. The optimum reverberation time is found to range from 1.0 sec in small rooms used for soloists or chamber music to about 2.5 sec for organ music and oratorios in large churches.

In designing an enclosure for recording purposes or as a television broadcast studio, it is generally considered advisable to hold the reverberation time to somewhat lower values than those given above for music rooms of equal volume, since the reverberation characteristics of the listening room are then superimposed on those of the room in which the music is originally produced.

One factor that must be considered in designing an auditorium is the effect on its reverberation time of the presence of an audience. Since the sound-absorbing power of an average human being is about 4.5 sabins, variations in the size of the audience may produce large changes in the reverberation time. The change is particularly apparent when an empty auditorium is used for rehearsals, and orchestra conductors who are unfamiliar with this effect are sometimes led to completely erroneous conclusions as to the most desirable loudness and balance of the music. The influence of variations in the size of the audience can be materially reduced by using seats whose backs are upholstered with a material having a fairly large sound absorption coefficient, for the total absorption of an unoccupied seat is then nearly the same as that of one which is occupied.

For further information on the utility of the concept of reverberation time in designing satisfactory enclosures from an acoustical viewpoint, the reader is referred to the following books.[7]

[7] Knudsen, *Architectural Acoustics*, John Wiley and Sons (1932); Knudsen and Harris, *Acoustical Designing in Architecture*, John Wiley and Sons (1950).

14.8 Sound Absorption Coefficients. The standard method of measuring the effective sound absorption coefficient α_e of a material is through an investigation of its effect on the reverberation time or the decay rate of sound pressure level in an enclosure. Specially constructed enclosures known as *reverberation chambers* are generally used for this purpose. The primary requirements of such a chamber are that its wall surfaces should be highly reflecting, so as to produce a large reverberation time when the test sample is not present, that its volume should be large enough so as to reduce the importance of any single pattern of standing waves, and that it should have irregular wall surfaces, or be equipped with large rotating vanes, so as to increase the rate at which the sound waves become diffuse.

In the absence of absorbing material, the reverberation time T of such a chamber is given by the live room equation of

$$T = 0.049V/a \tag{14.27}$$

where V is the volume of the room in cubic feet, and a is the total absorption in sabins as given by equation 14.6. If an area of S square feet of the wall surface is covered by the absorbing material being investigated, then the new reverberation time T' will equal

$$T' = \frac{0.049V}{a + S(\alpha_e - \alpha_0)} \tag{14.28}$$

where α_e is the effective absorption coefficient of the material being investigated and α_0 is that of the wall surface covered. If these two equations are combined so as to eliminate a, then

$$\alpha_e = \frac{0.049V}{S}\left(\frac{1}{T'} - \frac{1}{T}\right) + \alpha_0 \tag{14.29}$$

It is to be emphasized that the measurements indicated in equation 14.29 are not a direct measurement of α, the energy absorption coefficient of the material for randomly incident sound, but instead merely measure its influence upon reverberation time in a particular reverberation chamber. Since the reverberation time also depends on such parameters as the diffuseness of sound in the room, as well as size and location of the sample of absorbing material, measurement in different chambers of supposedly identical materials frequently leads to modestly different values for their absorption coefficients. If it is desired to obtain a value for the randomly incident energy absorption coefficient α, a modification of the Millington-Sette equation is perhaps most appropriate. Then α is given by

$$-\ln(1 - \alpha) = \frac{0.049V}{S}\left(\frac{1}{T'} - \frac{1}{T}\right) + \alpha_0 \tag{14.30}$$

Frequently, the quantity measured in reverberation chambers is the decay rate of sound pressure level in decibels per second rather than the reverberation time. Under such circumstances, it is advantageous to use equation 14.12 in order to eliminate T and T' from equation 14.29 and thereby obtain

$$\alpha_e = \frac{0.00081V}{S}(D' - D) + \alpha_0 \tag{14.31}$$

where D' is the measured decay rate when the material being investigated is present and D is that measured when it is absent.

Table 14.1 Effective absorption coefficients

Material	Frequency, cycles/sec 125	500	2000
Acoustic paneling	0.16	0.50	0.80
Acoustic plaster	0.30	0.50	0.55
Brick wall, unpainted	0.02	0.03	0.05
Draperies, light	0.04	0.11	0.30
Draperies, heavy	0.10	0.50	0.82
Felt	0.13	0.56	0.65
Floor, concrete	0.01	0.02	0.02
Floor, wood	0.06	0.06	0.06
Floor, carpeted	0.11	0.37	0.27
Glass	0.04	0.05	0.05
Marble or glazed tile	0.01	0.01	0.02
Plaster	0.04	0.05	0.05
Rock wool	0.35	0.63	0.83
Wood paneling, pine	0.10	0.10	0.08

Listed values are only representative in that actual values also depend on mounting and thickness of the material.

Table 14.1 lists representative effective sound absorption coefficients α_e for various commonly used materials, as determined from reverberation chamber measurements made by a number of different observers. For more detailed information on sound absorption coefficients of specific materials, the reader is referred to the bulletin on "Sound Absorption Coefficients of Architectural Acoustical Materials" as published annually by the Acoustical Materials Association. It is to be noted that the absorptive ability of most materials increases with increasing frequency and that this is particularly noticeable in the more highly absorbing materials. Correspondingly, the reverberation time in most enclosures is considerably shorter at high frequencies than at low frequencies.

14.9 Measurement of the Acoustic Output of Sound Sources in Live Rooms. Although the most accurate methods of measuring the acoustic output of sound sources are carried out in anechoic chambers as discussed in Sect. 10.13, such outputs may also be measured with considerable accuracy in reverberation chambers. When the sound energy in such a room is completely diffuse, the acoustic power output W as given by equation 14.9*b* is

$$W = \frac{P^2 a}{4\rho_0 c} \tag{14.32}$$

where the final steady-state rms effective acoustic pressure P is assumed to be uniformly distributed throughout the room. This pressure can be measured directly by means of a calibrated microphone. If P were truly uniform throughout the room, one measurement of its magnitude would be sufficient. When it is not, either a number of measurements must be made and averaged or the microphone may be rapidly rotated on an arm by mechanical means so as to measure a mean pressure averaged over a distance of at least a quarter wavelength. The only other unknown parameter in equation 14.32 is the total absorption constant of the room a. If the absorption coefficients of the materials constituting the walls of the room are known, a may be computed from the equations presented earlier in this chapter. If not, it may be determined from equation 14.12 by measuring the reverberation time T of the room. Upon eliminating the constant a between equations 14.12 and 14.32, the acoustic output in watts is given by

$$W = \frac{13.9 P^2 V}{\rho_0 c^2 T} \tag{14.33}$$

where P is expressed in newtons/m^2, V is the volume of the room in cubic meters, and T is the measured reverberation time in seconds. After substituting the appropriate value for $\rho_0 c^2$ in air, this equation may be converted into a practical engineering form in which W is expressed in watts, V in cubic feet, P in microbars, and T in seconds. The resulting equation is

$$W = 2.8 \times (P^2 V/T) \times 10^{-8} \tag{14.34}$$

14.10 Use of Sound Absorbing Materials for Noise Reduction in Rooms. Whenever a continuous source of sound is present in a room, such as that from a fan or motor, two sound fields are produced. One is the direct sound field diverging from the source. The other, is the reverberant sound field associated with reflections from the walls. The rms acoustic pressure P_d produced by the direct sound field, assumed to be radiated uniformly in all directions, is given in MKS units by the equation

$$\frac{P_d^2}{\rho_0 c} = I = \frac{W}{4\pi r^2} \tag{14.35}$$

where r is the radial distance from the effective center of the sound source, and W is the acoustic output of the source in watts. On the other hand, the rms acoustic pressure P_r of the reverberant sound field, as obtained upon rewriting equation 14.32, is

$$P_r^2 = \frac{4\rho_0 c W}{a} \tag{14.36}$$

If we add these two equations the total mean squared pressure $P^2 = P_d^2 + P_r^2$ is given by

$$P^2 = \rho_0 c W \left(\frac{1}{4\pi r^2} + \frac{4}{a}\right) \tag{14.37}$$

This equation shows that for locations very close to the sound source, i.e., when r is so small that $4\pi r^2 \ll (a/4)$, that increasing or decreasing the amount of sound absorbing material on the walls of the room will have little influence on measured sound pressure levels. By contrast, at distances such that $4\pi r^2 \gg (a/4)$, the sound pressure level will be reduced by 3 db for each doubling of the total sound absorption a. For example, a workman whose head is very near a noisy machine will receive very little benefit from increasing the magnitude of the total absorption of the room. However, those workmen at some distance from the machine will be exposed to 3 db less sound pressure level for each doubling of a. As another example, when two people are alone in a room and relatively close together, the acoustical characteristics of the surrounding room have negligible influence upon their ability to carry on a conversation. However, if many talkers are present in the room, the reverberant sound pressure level will increase by 10 log N, where N is the number of talkers, and make conversation difficult unless the total absorption a is large. This explains the frequently experienced difficulty of carrying on a conversation in a large ballroom or dining hall when many people are talking.

As an illustration of the utility of the above equations, let us work out the following example. We will assume one hundred talkers, each with an acoustic output of 100 microwatts, to be present in a room 5 × 20 × 40 meters and having a reverberation time of 3 seconds. A substitution into equation 14.12a leads to a total absorption of

$$a = \frac{0.161 \times 4000}{3} = 215 \text{ metric sabins}$$

The reverberant sound pressure, as given by equation 14.36, is then

$$P_r = \left[\frac{4 \times 415 \times 0.01}{215}\right]^{1/2} = 0.28 \text{ newtons/m}^2$$

which corresponds to a sound pressure level of 83 db. This background level is much too high for carrying on normal conversation. For instance, a substitution into equation 14.35 will show that this same pressure is reached in the direct pressure field of an individual talker at a distance of

$$r = \left[\frac{415 \times 0.0001}{4\pi}\right]^{1/2} \cdot \frac{1}{0.28} = 0.2 \text{ meters}$$

It is to be noted that if all talkers in the room were to reduce their acoustic outputs to 10 microwatts, the background level of reverberant sound would be reduced to a more pleasant 73 db without altering the relative pressure level of the direct sound field. Unfortunately, when a large number of talkers are present in a room of the above acoustic characteristics, the so-called "cocktail party effect"[8] comes into existence as each talker raises his individual acoustic output in order to be heard. On the average, this does not increase the intelligibility of conversation, but merely serves to increase the background level to an unpleasantly high value.

For further information on problems of noise control and noise reduction in enclosures, the reader is referred to the following books.[9]

14.11 Standing Waves in an Enclosure. In Sect. 14.7 it was pointed out that in order to avoid the inconsistencies arising from the presence of standing waves it is necessary, in making reverberation measurements, to employ certain averaging procedures, such as rotating large reflecting surfaces, warbling the sound source, or observing the pressure level at a large number of different locations. By 1930 it was becoming apparent that even such methods were not always sufficient and that the entire approach of geometric or ray acoustics was inadequate as the basis for a completely satisfactory theory of the behavior of sound in an enclosure. A more adequate but unfortunately more difficult approach is that based upon wave acoustics, i.e., upon the motion of waves in a three-dimensional bounded space. In particular, it has been found possible to apply the mathematical techniques of wave acoustics to problems of architectural acoustics in simple enclosures, such as rectangular boxes, cylindrical tubes, or spherical shells, and thus develop several new equations and concepts

[8] MacLean, *J. Acoust. Soc. Am.*, **31**, 79 (1959).

[9] Harris, *Handbook of Noise Control*, McGraw-Hill Book Co. (1957); Beranek, *Noise Reduction*, McGraw-Hill Book Co. (1960).

for discussing the transient and steady-state behavior of sound in enclosures. Furthermore, even in those enclosures of such a complicated shape that wave acoustics can not supply an explicit solution, it has been used to clarify and supplement results predicted by the more conventional equations of geometric acoustics.

From the wave acoustic viewpoint, a room may be treated as a complex resonator having numerous allowed modes of vibration, each with its own characteristic frequency of damped free vibration. When a sound source is started in such a resonator, a steady-state vibration having the frequency of the source is set up, together with a transient free vibration composed of the various *normal modes* of vibration in the room. This transient vibration will be composed of the normal modes required to satisfy the initial acoustic conditions in the room. If the sound source is operated continuously, each component frequency of the transient dies out exponentially at its own particular rate, eventually leaving only the steady-state vibration.

When the source is shut off, the steady-state waves having the frequency of the impressed sound almost immediately disappear. However, at any instant, the steady-state vibration can be considered as being compounded of a large number of standing waves characteristic of the room, just as the forced or initial motion of a string can be built up out of a Fourier series. The amplitude of each of these standing waves depends primarily on the frequency of the source, the acoustic impedance of each wave with respect to this frequency, and the position of the source in the room. Consequently, when the source is shut off the acoustic energy in the room is considered to reside in these standing waves, largely in those having natural frequencies near that of the source. As these waves damp out exponentially according to their individual free-vibration properties, they often interfere with one another and thus produce beat notes. The resulting damped pulsations of these free vibrations constitute the phenomenon of reverberation.

Unless all the excited modes of vibration decay at the same rate, it is not to be expected that wave acoustics will predict a unique value for the reverberation time of a room. Instead, it is to be anticipated that the rate of decay of acoustic energy will at first be rapid, corresponding to a short reverberation time, and that it will then decrease stepwise with correspondingly longer and longer reverberation times as the more rapidly damped waves successively die out. This latter behavior is readily observable at low impressed frequencies in reverberant chambers whose walls differ markedly in their absorption characteristics.

The characteristic frequencies of vibration of the standing waves in a room depend primarily on the shape and size of the room; whereas their rates of damping depend chiefly on the boundary conditions, i.e., on either the normal specific acoustic impedance or the absorption coefficient at the walls. This is fortunate, for it enables us to use the simplest possible boundary condition, that of perfectly rigid walls and no damping, in deriving expressions for the characteristic frequencies. The effect of the acoustic conditions at the walls on the damping of the vibrations may then be considered as a perturbation of these simple conditions.

Let us consider the simplest sort of enclosure, a rectangular room whose sides have lengths l_x, l_y, and l_z. The general expression for a plane wave (6.46) may now be written in the form

$$\mathbf{p} = \mathbf{A}e^{j(\omega t - k_x x - k_y y - k_z z)} \tag{14.38}$$

If this equation is to satisfy the general wave equation

$$\nabla^2 \mathbf{p} = \frac{1}{c^2}\frac{\partial^2 \mathbf{p}}{\partial t^2} \tag{14.39}$$

the constants k_x, k_y, and k_z must satisfy

$$k = \frac{\omega}{c} = \sqrt{k_x^{\,2} + k_y^{\,2} + k_z^{\,2}} \tag{14.40}$$

as the reader can show by direct substitution of equation 14.38 into equations 14.39. Furthermore, k_x/k, k_y/k, and k_z/k represent the direction cosines made by the direction of propagation of the waves with respect to the x, y, and z axes. If we replace any one, any two, or all three of the negative signs in equation 14.38 by positive signs, we obtain seven additional wave equations similar to equation 14.38, all of which have identical values of k_x, k_y, and k_z. This array of eight wave equations represents the family of plane waves generated by the original wave as successive reflections occur at the six bounding walls.

Since the walls have been assumed rigid, the velocity of the air particles near any wall must be parallel to that wall; i.e., the normal component must be zero. If we chose one corner of the room as the origin of the coordinate system, the above boundary condition is equivalent to

$$u = 0 \text{ for } x = 0 \text{ and for } x = l_x$$

$$v = 0 \text{ for } y = 0 \text{ and for } y = l_y$$

$$w = 0 \text{ for } z = 0 \text{ and for } z = l_z$$

Before applying the above boundary conditions, we must first obtain expressions for **u**, **v**, and **w** in terms of the pressure **p**. For periodic wave motion, equation 5.8 may be rewritten as

$$-\frac{\partial \mathbf{p}}{\partial x} = \rho_0 \frac{\partial \mathbf{u}}{\partial t} = j\omega\rho_0\mathbf{u}$$

and therefore

$$\mathbf{u} = -\frac{1}{j\omega\rho_0}\cdot\frac{\partial \mathbf{p}}{\partial x} \tag{14.41}$$

with similar equations for $\mathbf{v}$ and $\mathbf{w}$ in terms of $(\partial\mathbf{p}/\partial y)$ and $(\partial\mathbf{p}/\partial z)$. Application of the boundary conditions at $x = 0$, $y = 0$, and $z = 0$ to the respective equations for particle velocities obtained from the array of eight wave equations similar to and including equation 14.38 results in the standing wave equation

$$\mathbf{p} = P\,(\cos k_x x \cos k_y y \cos k_z z)e^{j\omega t} \tag{14.42}$$

It should be noted that pressure antinodes exist at the wall surfaces $x = 0$, $y = 0$, and $z = 0$, as was to have been anticipated.

Upon substituting equation 14.42 into equation 14.41, the particle velocity in the x direction becomes

$$\mathbf{u} = \frac{k_x P}{j\omega\rho_0}(\sin k_x x \cos k_y y \cos k_z z)e^{j\omega t} \tag{14.43}$$

which is, of course, zero for $x = 0$. If the additional condition of $\mathbf{u} = 0$ for $x = l_x$ is applied to equation 14.43, then $\sin k_x l_x = 0$, or

$$k_x = \frac{n_x\pi}{l_x} \qquad n_x = 0, 1, 2, 3, \cdots \tag{14.44}$$

Similarly

$$k_y = \frac{n_y\pi}{l_y} \qquad n_y = 0, 1, 2, 3, \cdots \tag{14.44a}$$

and

$$k_z = \frac{n_z\pi}{l_z} \qquad n_z = 0, 1, 2, 3, \cdots \tag{14.44b}$$

Therefore equation 14.42 is a general expression for pressures in any of the allowed standing waves produced inside a rigid-walled rectangular enclosure, and the *component* wavelength constants k_x, k_y, and k_z in this expression are limited to the values given by equations 14.44, 14.44*a*, and 14.44*b*, respectively. This limitation in turn restricts the characteristic frequencies corresponding to the allowed normal modes of vibration, as obtained upon substitution into equation 14.40, to

$$f = \frac{\omega}{2\pi} = \frac{c}{2}\left[\left(\frac{n_x}{l_x}\right)^2 + \left(\frac{n_y}{l_y}\right)^2 + \left(\frac{n_z}{l_z}\right)^2\right]^{1/2} \tag{14.45}$$

It should be noted that in the special case of $n_y = n_z = 0$, both equation 14.45 and equation 14.42 are reduced to the more familiar forms for acoustic plane waves within a pipe lying along the x axis and terminated with rigid caps at $x = 0$ and $x = l_x$.

A particular normal mode of vibration corresponding to any set of values of n_x, n_y, and n_z can be produced by starting a wave in the direction given by any combination of the direction cosines $\pm k_x/k$, $\pm k_y/k$, and $\pm k_z/k$ and letting it be reflected from the various walls until it becomes a standing wave. On the other hand, if a wave starts out in a direction not satisfying the above conditions as to its direction cosines and frequency, the reflected waves will interfere with each other in a nonperiodic manner, and consequently no regular pattern of standing waves will be set up.

Table 14.2 Characteristic frequencies below 100 cycles/sec for a rectangular room 10 × 15 × 20 ft

n_x	n_y	n_z	f, cycles/sec	n_x	n_y	n_z	f, cycles/sec
0	0	1	27.5	1	0	2	77.5
0	1	0	36.6	0	2	1	78.5
0	1	1	45.9	0	0	3	82.5
1	0	0	55.0	1	1	2	86.0
0	0	2	55.0	0	1	3	90.2
1	0	1	61.5	0	2	2	91.5
0	1	2	66.0	1	2	0	91.5
1	1	0	66.0	1	2	1	95.5
1	1	1	71.5	1	0	3	99.0
0	2	0	73.2				

As an example let us consider the normal modes of vibration inside a rectangular room 10 × 15 × 20 ft in dimensions. Table 14.2 contains a list of all the characteristic frequencies below 100 cycles/sec, as calculated for an assumed velocity of sound in air of 1100 ft/sec.

A knowledge of the characteristic frequencies of a room is essential to a complete understanding of its acoustic properties, for the room will act as a resonator and respond strongly to those impressed sounds having frequencies in the immediate vicinity of any of these characteristic frequencies. For instance, the data tabulated in Table 14.2 indicates that two different modes of vibration have the identical characteristic frequency of 55 cycles/sec, and therefore this particular room should be expected to respond strongly to 55 cycles/sec. It is just this characteristic that affects the output of a loudspeaker, as measured in a reverberant room and causes the results to have limited significance as a true criterion of the speaker's properties. Furthermore, when $n_x = 1$, the term cos $k_x x$ in equation 14.42 is zero for $x = l_x/2$ and consequently, the 100 standing wave has a pressure node along a plane through the center of the room perpendicular to the x-axis. Therefore, although measured sound pressures along the two yz-wall surfaces at a frequency of 55 cycles/sec may be large, those along a parallel plane through the center of the room will be much smaller. By contrast, the 002 standing wave of identical frequency will produce large sound pressures both at the xy-wall surfaces and along a plane through the center of the room parallel to these walls. In effect, every room or enclosure superimposes its own characteristics on those of any sound source present, so that the fluctuations in sound pressure which occur as a microphone is moved from one point to another, or as the frequency of the source is varied, may completely conceal the true output characteristics of the source. As has previously been mentioned, it is for this reason that measurements of the response curves of loudspeakers should be carried out either in the open air or in specially constructed dead rooms known as anechoic chambers. If the absorption coefficient at the walls of an anechoic chamber is greater than 0.99, the sound pressures resulting from any standing waves that are present are negligible as compared to those produced by the direct wave transmitted to the microphone from the source.

Each of the individual normal modes of vibration of an enclosure can only be excited to its fullest extent by a sound source located in those regions where the particular standing wave pattern has a maximum of pressure amplitude. Equation 14.42 indicates that the pressure amplitudes of all patterns of standing waves in a rectangular enclosure are at a maximum in the corners of the room. Therefore, if the source is at the corner of such a room, it will be possible for it to excite every allowed mode of vibration to its fullest extent. Correspondingly, if a microphone is located in the corner of the room, it will measure the peak sound pressure for every normal mode of vibration that has been excited. By contrast, when a source is located in a region where a particular mode of vibration has a pressure node, that mode will be excited only weakly, if at all. For instance, if a loudspeaker is located in the center of a rectangular room, only about 10 per cent of the modes will be excited as the driving frequency is slowly varied from low to high frequencies. In fact, only those modes of vibration having even numbers simultaneously for n_x, n_y, and n_z will be excited.

An example typical of the transmission of sound from a loudspeaker located in one corner of a rectangular room 10 × 15 × 20 ft to a microphone located in a diagonally opposite corner is given in Fig. 14.4. These curves were obtained by slowly increasing the pure tone frequency supplied by the loudspeaker from 20 to 100 cycles/sec and simultaneously recording

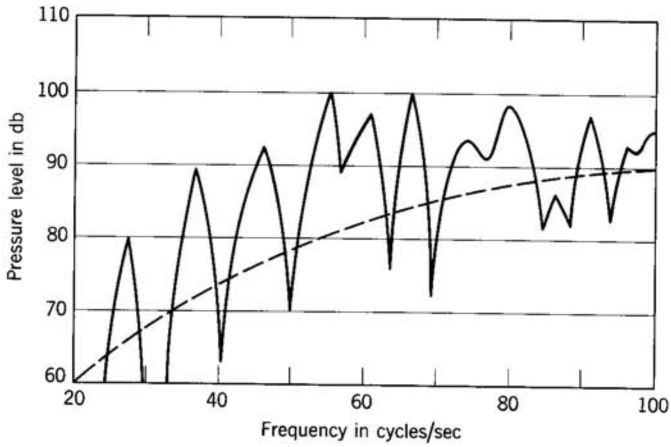

Fig. 14.4. Normal mode response of a rectangular room at low frequencies.

the output of the microphone. The dashed line corresponds to a similarly determined output of the loudspeaker as measured in an anechoic chamber. The marked influence of the room is quite apparent. When either the loudspeaker or microphone is located in the center of the room, only those peaks corresponding to the 002 mode at 55 cycles/sec, the 020 mode at 73.2 cycles/sec, and the 022 mode at 91.5 cycles are observed.

14.12 Frequency Distribution of Normal Modes. Equation 14.45 suggests that each of the characteristic frequencies f may be considered as a vector in *frequency space*, having components $n_x c/2l_x$, $n_y c/2l_y$, and $n_z c/2l_z$. A normal mode of vibration may therefore be represented by a point in this frequency space, the x component of this point being an integral number of unit lengths $c/2l_x$, its y component an integer times $c/2l_y$, etc. The length of the line joining the point to the origin is a measure of the characteristic frequency of this particular normal mode. A few of these *characteristic points* are shown in Fig. 14.5. It is evident that they correspond to the intersections of a rectangular lattice having f_x, f_y, and f_z spacings equal to $c/2l_x$, $c/2l_y$, and $c/2l_z$, respectively. Furthermore, all the normal modes of characteristic frequency f and below are included among the points contained within the octant of frequency space between the positive f_x, f_y, and f_z axes and a spherical surface of radius f.

This method of representing the normal modes of vibration by a lattice of characteristic points in frequency space is extremely useful in computing the number and types of modes having characteristic frequencies lying within any specified frequency interval. The direct computation and counting of the individual characteristic frequencies below any given frequency is quite tedious, so that it is advantageous to obtain equations giving approximate values for such counts. One simple approach is to consider each lattice point as occupying a rectangular block in frequency space of dimensions $c/2l_x$, $c/2l_y$, $c/2l_z$, and volume $c^3/8l_xl_yl_z = c^3/8V$. Then the number of points can be obtained by dividing $\pi f^3/6$, the volume of an octant of radius f, by $c^3/8V$. Accordingly, the number N of normal modes of frequency below f is approximately

$$N = \frac{4\pi V}{3c^3} f^3 \tag{14.46}$$

where V is the volume of the room.

As an example, let us consider the number of modes below 100 cycles/sec in the room of dimensions 10 × 15 × 20 ft previously discussed. Then

$$N = \frac{4\pi \times 3000}{3 \times 1100^3} 100^3 = 9.5$$

A comparison with the correct number, 19, as given in Table 14.2, indicates a considerable error. A more accurate expression for N is

$$N = \frac{4\pi V}{3c^3} f^3 + \frac{\pi S}{4c^2} f^2 + \frac{L}{8c}\, i \tag{14.47}$$

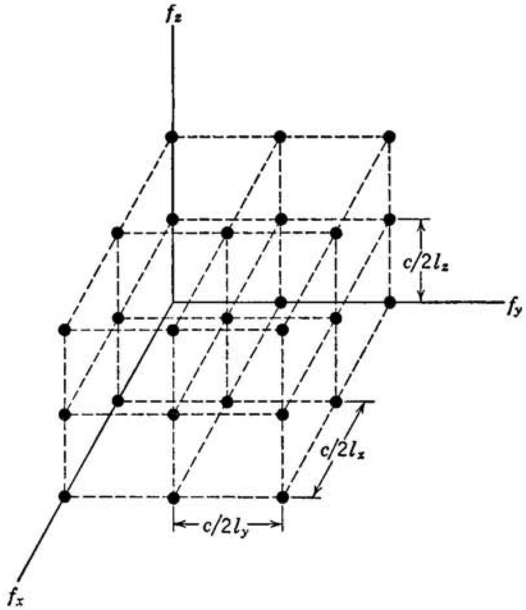

Fig. 14.5. Characteristic points in frequency space.

where S is the total surface area of the walls, as given by

$$S = 2(l_x l_y + l_y l_z + l_x l_z)$$

and L is the sum of the lengths of all edges of the room, i.e.,

$$L = 4(l_x + l_y + l_z)$$

The additional terms of this equation result from the inclusion of that part of frequency space outside the octant $\pi f^3/6$ which is associated with lattice points lying on the f_x, f_y, and f_z axes, or in the planes formed by these axes. The computed number of normal modes below 100 cycles/sec in the room considered above, as given by equation 14.47, is 18.5, which is in excellent agreement with the accurate value 19.

A still more useful quantity is the number of normal modes having frequencies in a band of width Δf centered on f. An approximate expression for this quantity ΔN is obtained by differentiating equation 14.47 with respect to f. The result is

$$\Delta N = \left(\frac{4\pi V}{c^3} f^2 + \frac{\pi S}{2c^2} f + \frac{L}{8c}\right) \Delta f \tag{14.48}$$

This equation indicates that the number of normal modes of vibration in a given frequency band of width Δf increases rapidly as the center frequency of the band, or the size of the enclosure, is increased. For instance, within the room considered above the indicated value in a 10-cycle band centered on 1000 cycles/sec is 286, as compared with *three* for a band centered on 100 cycles/sec. As a result, the spacing of the characteristic frequencies at 1000 cycles/sec in this room is so close that specific resonances may be neglected, and the room may instead be considered as capable of carrying all frequencies in this region with equal readiness.

Since the standing wave pattern corresponding to each characteristic frequency is in general associated with some particular set of direction cosines, any increase in ΔN indicates an increase in the randomness of direction of the associated waves. This deduction is supported by the observation that those reverberation equations which are based on an assumed random distribution of sound energy, such as equation 14.12*b*, are in better agreement with experiment at high frequencies and in large enclosures, two factors that tend to increase ΔN.

Finally, the response of a room is observed to become less uniform as its symmetry is increased. This results from the increase in the number of *degenerate* normal modes, i.e., standing waves having different individual n's but the same characteristic frequency. Table 14.2 shows that in the room being considered there are three cases of such a degeneracy at frequencies below 100 cycles/sec, namely, at 55, 66, and 91.5 cycles/sec. If similar calculations are made for the characteristic frequencies of a cubical room of equal volume, the degeneracy becomes much worse. Threefold and even sixfold degeneracies are not uncommon. The response then becomes very irregular, since the grouping of characteristic frequencies leaves large intervals within which there is no characteristic frequency.

14.13 Damping of Standing Waves. In order to discuss the damping of standing waves in a rectangular enclosure it will prove advantageous to separate them into three groups. One group is composed of *axial* waves, for which two of the n's are zero. Such axial waves move parallel to either the x, the y, or the z axis, and each is more readily damped by the wall surfaces perpendicular to its axis. A second group is composed of *tangential* waves, for which only one n is zero. These waves, which travel parallel to the surfaces of *one* pair of walls, strike and are primarily absorbed by the remaining four walls. Finally, the third group is composed of *oblique* waves, for which no n is zero. Since the array of individual waves forming an oblique standing wave strikes all six walls, the rate of damping is influenced by the absorption characteristics of all the walls.

A damping term $e^{-\beta t}$ can be introduced into the undamped standing wave equation (14.42) by replacing $j\omega$ by the complex quantity $j\omega - \beta$. The resulting damped standing wave equation is

$$\mathbf{p} = P \cosh\left[(\beta_x - j\omega_x)\frac{x}{c} + \phi_x\right] \cosh\left[(\beta_y - j\omega_y)\frac{y}{c} + \phi_y\right] \times \cosh\left[(\beta_z - j\omega_z)\frac{z}{c} + \phi_z\right] e^{(j\omega-\beta)t} \quad (14.49)$$

where ϕ_x, ϕ_y, and ϕ_z are phase constants determined by the particular boundary conditions that must be satisfied at $x = 0$, $y = 0$, and $z = 0$, respectively. A direct substitution of equation 14.49 into the general wave equation (14.39) shows that the various ω's and β's are restricted to certain allowed values, in that they must satisfy the relation

$$(j\omega - \beta)^2 = (j\omega_x - \beta_x)^2 + (j\omega_y - \beta_y)^2 + (j\omega_z - \beta_z)^2 \quad (14.50)$$

A more useful form of equation 14.50 is obtained by separately equating its real and imaginary parts. The resulting equations are

$$\omega^2 - \beta^2 = (\omega_x^2 + \omega_y^2 + \omega_z^2) - (\beta_x^2 + \beta_y^2 + \beta_z^2) \quad (14.50a)$$

and

$$\beta = \beta_x\frac{\omega_x}{\omega} + \beta_y\frac{\omega_y}{\omega} + \beta_z\frac{\omega_z}{\omega} \quad (14.50b)$$

It should be noted that if $\beta_x = \beta_y = \beta_z = 0$, then $\beta = 0$. The wave motion is therefore undamped, and equation 14.50*a*, the equation giving the characteristic frequencies of the normal modes, is reduced to

$$\omega = \sqrt{\omega_x^2 + \omega_y^2 + \omega_z^2}$$

which is equivalent to equation 14.40.

In theory, it should be possible to apply the boundary conditions at the various wall surfaces and thus determine allowed values for the imposing array of constants ω_x, ω_y, ω_z, β_x, β_y, β_z, ϕ_x, ϕ_y, ϕ_z, etc. In practice, the problem becomes so involved that at present it can be solved only for limited frequency ranges, or for particularly simple physical configurations of sound-absorbing materials.

As a simple special case let us consider only that mode of vibration corresponding to x-axial waves. Then $\omega_y = \omega_z = 0$. Furthermore, we shall assume that the wall surfaces perpendicular to the y and z axes are rigid, and therefore nonabsorbing. Consequently, $\beta_y = \beta_z = \phi_y = \phi_z = 0$. These simplifying assumptions reduce equation 14.49 to

$$\mathbf{p} = P \cosh \left[(\beta - j\omega) \frac{x}{c} + \phi_x \right] e^{(j\omega - \beta)t} \tag{14.51}$$

in which the subscripts have been dropped from β_x and ω_x, since the latter are now equal to β and ω, respectively.

By utilizing the usual relationships between pressure and particle velocity, the reader may show that

$$\mathbf{u} = \frac{P}{\rho_0 c} \sinh \left[(\beta - j\omega) \frac{x}{c} + \phi_x \right] e^{(j\omega - \beta)t} \tag{14.52}$$

In turn, the specific acoustic impedance $\mathbf{z}_x$ at any point in the standing wave is

$$\mathbf{z}_x = \frac{\mathbf{p}}{\mathbf{u}} = \rho_0 c \coth \left[(\beta - j\omega) \frac{x}{c} + \phi_x \right] \tag{14.53}$$

The question now arises as to what physical property of the wall should be used in applying boundary conditions to the standing wave. The absorption coefficient α, as previously defined, is not a suitable property, for it represents the average absorption for waves striking the wall from all directions. Another possibility would be to define and use an appropriate α_θ for each angle of incidence θ. However, the simplest and most direct procedure is to ignore the concept of an absorption coefficient and instead consider the absorbing characteristics of the wall as being determined by its *normal specific acoustic impedance* $\mathbf{z}_n$, the ratio of pressure to normal air velocity at the surface of the wall. It is customary to express the normal specific acoustic impedance of a material relative to air by the equation

$$\mathbf{z}_n = (r_n + jx_n)\rho_0 c \tag{14.54}$$

in which $\rho_0 c$ is the characteristic impedance of air, i.e., $\rho_0 c = 415$ kg/m^2 sec or MKS rayls.

If the above boundary condition is applied to equation 14.53 at $x = 0$, then

$$-(r_n + jx_n) = \coth \phi_x \tag{14.55}$$

in which the negative sign is used because a positive pressure at this wall will produce a negative particle velocity. In general, ϕ_x is complex. Fortunately, however, many of the materials used for wall surfaces are characterized by $r_n \gg x_n$ and $r_n \gg 1$. If we assume this to be true in our particular example, then

$$\phi_x \approx -\frac{1}{r_n} \tag{14.56}$$

Now applying the boundary condition that $\mathbf{z}_x \approx r_n \rho_0 c$ at $x = l_x$, we obtain

$$r_n \approx \coth \left[(\beta - j\omega)\frac{l_x}{c} - \frac{1}{r_n}\right] \tag{14.57}$$

The right-hand term in this expression may be expanded to give

$$r_n \approx \frac{1 - j \tanh \left(\dfrac{\beta l_x}{c} - \dfrac{1}{r_n}\right) \tan \dfrac{\omega l_x}{c}}{\tanh \left(\dfrac{\beta l_x}{c} - \dfrac{1}{r_n}\right) - j \tan \dfrac{\omega l_x}{c}} \tag{14.58}$$

Since r_n is a real quantity the right-hand term of equation 14.58 must also be real. This requirement is satisfied by setting

$$\tan \frac{\omega l_x}{c} = 0$$

or

$$\frac{\omega l_x}{c} = n\pi \qquad n = 0, 1, 2, 3, \cdots \tag{14.59}$$

The latter equation is equivalent to $f = nc/2l_x$, indicating that the characteristic frequencies of the damped axial waves are identical with those of the corresponding undamped waves obtained by substitution of $n_y = n_z = 0$ into equation 14.45. It should be noted that if the normal specific acoustic impedance of the wall is such that r_n is *not* large with respect to both x_n and unity, then the damped and undamped waves will no longer possess the same characteristic frequencies.

If we equate the remaining real parts of equation 14.58 we obtain

$$r_n = \frac{1}{\tanh\left(\dfrac{\beta l_x}{c} - \dfrac{1}{r_n}\right)}$$

or

$$\frac{1}{r_n} = \tanh\left(\frac{\beta l_x}{c} - \frac{1}{r_n}\right) \tag{14.60}$$

Since $1/r_n \ll 1$, the hyperbolic tangent may be replaced by the first term of its series expansion, i.e.,

$$\frac{1}{r_n} = \frac{\beta l_x}{c} - \frac{1}{r_n}$$

which, upon solving for β, becomes

$$\beta = \frac{2c}{r_n l_x} \tag{14.61}$$

Since the energy density $\mathcal{E}$ at any point in the standing wave is proportional to the square of the pressure, the energy density of a freely vibrating damped wave decreases exponentially with time as $(e^{-\beta t})^2 = e^{-2\beta t}$. Therefore

$$\mathcal{E} = \mathcal{E}_0 e^{-2\beta t} = \mathcal{E}_0 e^{-[(4c/r_n l_x)t]} \tag{14.62}$$

where $\mathcal{E}_0$ is the energy density in the wave at the time $t = 0$ when the source of sound is shut off. The corresponding decay rate in decibels per second is

$$D = -10 \log e^{-(4c/r_n l_x)} = \frac{17.3c}{r_n l_x} \tag{14.63}$$

The reverberation time T as obtained from the equation $T = 60/D$ is

$$T = \frac{3.45 r_n l_x}{c} \tag{14.64}$$

In order to compare this expression for reverberation time with those previously derived in this chapter, it is necessary to obtain some sort of relationship between the relative normal specific acoustic resistance r_n of the wall and its coefficient of absorption α. Unfortunately, there exists no simple general relationship between these two quantities. However, in our particular example where $r_n \gg 1$ and $r_n \gg x_n$, the sound transmission coefficient of a wall as given by equation 6.66, which is assumed equal to the absorption coefficient α_θ, may be simplified to give

$$\alpha_\theta = \frac{4 r_n \cos\theta}{(r_n \cos\theta + 1)^2} \tag{14.65}$$

It should be noted that the definition used for r_n in equation 6.66 differs from that used in this section.

In defining the average absorption coefficient α of Sect. 14.2, a diffuse distribution of directions was assumed for the waves impinging on the wall. By a process of reasoning similar to that used in deriving equation 14.3, it can be shown that the fractional amount of energy $(\Delta E)_{\text{abs}}$ absorbed by a surface element dS is

$$(\Delta E)_{\text{abs}} = \frac{\mathcal{E}\, dS\, dr}{2} \int_0^{\pi/2} \alpha_\theta \sin\theta \cos\theta \, d\theta \tag{14.66}$$

If the value of α_θ from equation 14.65 is substituted into equation 14.66, and the indicated integration carried out, we obtain

$$(\Delta E)_{\text{abs}} = \frac{\mathcal{E}\, dS\, dr}{4} \cdot \frac{8}{r_n}\left[1 + \frac{1}{1 + r_n} - \frac{2}{r_n}\ln(1 + r_n)\right] \tag{14.67}$$

From equation 14.3, the fractional amount of energy incident on the surface element dS is $\Delta E = \mathcal{E}\, dS\, dr/4$, and hence the absorption coefficient α is equal to equation 14.67 divided by this expression for ΔE, or

$$\alpha = \frac{8}{r_n}\left[1 + \frac{1}{1 + r_n} - \frac{2}{r_n}\ln(1 + r_n)\right] \tag{14.68}$$

When $r_n > 100$, this equation may be simplified to

$$\alpha \approx \frac{8}{r_n} \tag{14.68a}$$

without being in error by more than 10 per cent. The latter equation represents the simplest possible relationship between the randomly incident sound absorption coefficient α and the normal specific acoustic resistance ratio r_n. Unfortunately, this simple relationship may be applied only at surfaces of large r_n, i.e., to those having small absorption coefficients, and it is therefore limited to the discussion of standing waves in *live* rooms.

A substitution of r_n from equation 14.68*a* into equation 14.64 leads to

$$T = \frac{27.6 l_x}{\alpha c} \tag{14.69}$$

If both numerator and denominator of this expression are multiplied by $2l_y l_z = 2S_x$, where S_x is the area of one of the walls perpendicular to the x-axis, then

$$T = \frac{55.2V}{2S_x \alpha c} = \frac{0.049V}{a_x} \tag{14.69a}$$

where $a_x = 2S_x\alpha$ represents the absorption due to the walls perpendicular to the x-axis. A comparison with equation 14.12*b* shows that the x-axial standing waves in this particular room are damped out at the same rate as is predicted by geometric acoustics for randomly distributed sound waves in an enclosure of equal volume and the same total surface absorption.

By contrast, the rate of damping of y-axial or z-axial waves is only half that of the x-axial waves. Correspondingly, their reverberation times, as indicated by equation 14.70, are twice as large, i.e.,

$$T_{y,z} = \frac{0.049V}{0.5a_x} \tag{14.70}$$

This smaller damping of the y-axial and z-axial waves results from the fact that the average mean square pressures produced by these modes at the absorbing S_x surfaces are only half those produced on the nonabsorbing S_y and S_z surfaces, respectively. This behavior illustrates an important general principle derived from the wave acoustics theory, namely, an absorbing surface is most effective in damping a standing wave if it is located in a region of maximum mean square pressure. The most effective method of reducing any particular undesirable mode of vibration is therefore to place absorbing material on those parts of the walls where the pressures corresponding to this mode are the greatest. Consequently, absorbing material placed near the corners of a room is twice as effective, on the average, as if it were placed elsewhere, for all standing waves have pressure maxima at these points.

It is possible to derive more general forms of equations 14.69*a* and 14.70 which are applicable to oblique and tangential waves in live rooms, as well as to axial waves. One such form is

$$T \approx \frac{0.049V}{\epsilon_{nx}a_x + \epsilon_{ny}a_y + \epsilon_{nz}a_z} \tag{14.71}$$

The factors ϵ_n equal 0.5 for $n = 0$, and 1.0 for $n > 0$. It is these factors that cause this equation to differ from equation 14.12*b*, which assumes a uniform distribution of sound. The quantities a_x, a_y, and a_z represent the total absorptions of those walls perpendicular to the x-, y-, and z-axes, respectively.

Since all three ϵ_n's are unity for an oblique standing wave, the reverberation time of all such waves in a live room is identical with that given by the classical equation of Sabine (14.1). On the other hand, for tangential or axial waves one or more of the ϵ_n's equals 0.5, so that the reverberation times for these waves are always somewhat greater than that for oblique waves. For example, in a room having all six walls covered with identical absorbing material the respective reverberation times for axial, tangential, and oblique waves are related to one another as 6:5:4. In such a room the reverberation time, as measured for low driving frequencies, may vary rapidly with changes in frequency as first one and then another type of standing wave is strongly excited, and hence at such frequencies the term *reverberation time* has a specific meaning only in connection with the damping out of some particular type of normal mode. In the middle range of frequencies the measured decay in intensity level may be expected to approximate a broken line, such as that indicated in Fig. 14.6. Here the steeper initial part corresponds to the decay rate of the oblique waves, the middle part to the decay of tangential waves, and the less steep final part to the decay of axial waves. The actual length of time required for the intensity level to drop 60 db will therefore depend on the relative amounts of acoustic energy possessed by the various types of standing waves.

At such high frequencies that most of the acoustic energy residues in oblique waves, the break in the curve giving the rate of decay of intensity level comes late enough so that the first 20 or 30 db of the curve is nearly a straight line. The slope of this line may then be used to determine the reverberation time associated with the major portion of the acoustic energy present. Consequently, it is only in this frequency range that the concept of reverberation time is, by itself, a sufficient criterion for judging the acoustic characteristics of an enclosure.

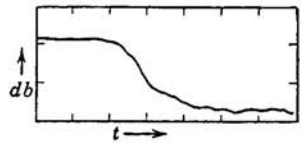

Fig. 14.6. Influence of standing waves on a reverberation decay curve.

In spite of the greater complexity of the mathematical techniques involved, the application of the methods of wave mechanics to architectural acoustics has markedly broadened our knowledge of the behavior of sounds in enclosures. It lends itself admirably to a consideration of such important factors as the shape of the enclosure, the effects of different distributions of absorbing surfaces, the behavior of sound in dead rooms, the effect of the position of source or receiver, etc. The interested reader will find numerous examples of such applications and developments in the research literature of acoustics.[10]

With the advent of wave acoustics, the importance of the concept of an absorption coefficient has been somewhat diminished. If the normal specific acoustic impedances of the various wall surfaces of an enclosure are known, it becomes possible to discuss in considerable detail the behavior of sound waves in the enclosure, without any reference to a table of absorption coefficients. Actually, the normal specific acoustic impedance of a material is a more fundamental, as well as more readily measured, quantity than is its absorption coefficient.

[10] Morse and Bolt, *Revs. Modern Phys.*, **16**, 69 (1944).

Before concluding this chapter, it should be pointed out that the normal specific acoustic impedance of a material is itself not truly a fundamental physical property. Instead, it merely serves as a convenient parameter for discussing the influence of the wall surfaces on the behavior of sound waves in an enclosure. However, a successful theory has been developed which treats of the propagation of damped waves through solid materials in terms of such fundamental physical properties as *density*, *porosity*, and *flow resistance*.[11] As a by-product of this theory, it is now possible to derive expressions giving the normal specific acoustic impedance in terms of these more fundamental quantities and thus to further our ability to design and produce materials for wall surfaces having specified acoustic properties.

PROBLEMS

14.1. (*a*) Using equation 14.8*a*, derive a general expression for the growth rate of intensity level in a live room in db/sec. (*b*) What is this growth rate at $t = 0$, and $t = \infty$. (*c*) At what time t is the growth rate equal to the constant decay rate given by equation 14.11?

14.2. When steady state conditions are reached in a live room, the measured sound pressure level is 74 db relative to 0.0002 microbar. (*a*) If the average sound absorption coefficient of the walls is 0.05, what is the rate at which sound energy is being absorbed per square meter of wall surface in watts/m^2? (*b*) If the total area of absorbing wall surface in the room is 50 m^2, at what rate in watts is sound power being generated in the room?

14.3. A small reverberation chamber is constructed with concrete walls. Its internal dimensions are $6 \times 7 \times 8$ ft. (*a*) Calculate the final steady-state sound pressure level in decibels produced by a 2000 cycles/sec source of 7.5 microwatts acoustic output. Assume the absorption coefficient of the concrete to be 0.02. (*b*) How many seconds will be required from the time the source is turned on until the pressure level reaches within 3 db of the value of part (*a*)? (*c*) When an observer enters the chamber, the steady-state sound pressure level is observed to decrease by 3 db. What is the equivalent absorbing ability of the observer in sabins?

14.4. A room $10 \times 10 \times 4$ m has an average sound absorption coefficient $\bar{\alpha} = 0.1$. (*a*) Calculate its reverberation time. (*b*) What must be the acoustic output of a source, if it is to produce a steady-state sound pressure level of 60 db relative to 0.0002 microbar? (*c*) At what rate in watts/m^2 is sound energy incident on the walls of the room?

14.5. An auditorium is observed to have a reverberation time of 2.0 seconds. Its dimensions are $7 \times 15 \times 30$ m. (*a*) What acoustic power is required to produce a steady-state sound pressure level of 60 db relative to 0.0002 microbar? (*b*) What is the average sound absorption coefficient of the materials making up the various surfaces in the auditorium? (*c*) If 400 people are present in the auditorium, each adding 0.5 metric sabins (0.5 sq m of perfectly absorbing surface) to its total absorption, what is the new reverberation time? (*d*) What will be the new sound pressure level produced by the sound source of part (*a*)?

[11] Zwikker and Kosten, *Sound Absorbing Materials*, Elsevier Publishing Co. (1949).

14.6. A rectangular room is 10 ft high, 20 ft wide and 30 ft long. The walls are of plaster, wood, and glass having an average absorption coefficient of 0.05. The floor is covered with a rug ($\alpha = 0.2$), and the ceiling with an acoustical tile ($\alpha = 0.6$). Ten people are present in the room, each equivalent to 4.5 sabins. (*a*) Compute the reverberation time by using the live room equation 14.12*b*. (*b*) Compute the reverberation time by using the Eyring-Norris dead room equation 14.18. (*c*) Compute the reverberation time by using the Millington-Sette dead room equation 14.23.

14.7. The interior surfaces of an auditorium $200 \times 50 \times 30$ ft have an average sound absorption coefficient $\bar{\alpha} = 0.25$. (*a*) What is the reverberation time of the auditorium? Use the Eyring-Norris equation. (*b*) What must be the power output of a source, if it is to produce a steady-state sound pressure level of 65 db relative to 0.0002 microbar? (*c*) What average sound absorption coefficient would be required, if a speaker having an acoustic output of 100 microwatts is to produce a steady-state pressure level of 65 db? (*d*) Would the latter conditions be practicable? Consider reverberation time, articulation, audience allowed, etc., in answering this question.

14.8. A cubical room 10 ft on a side has acoustic paneling on its walls, acoustic plaster on its ceiling, and a carpeted floor. (*a*) Using the effective coefficients listed in Table 14.1 and equation 14.12*b*, calculate its reverberation time at a frequency of 500 cycles/sec. (*b*) Repeat the calculations at a frequency of 125 cycles/sec. (*c*) At a frequency of 2000 cycles/sec.

14.9. Given a noise source of 10 microwatts acoustic output at a frequency of 125 cycles/sec. (*a*) What ambient background sound pressure level in decibels will it generate in the room of problem 14.8? (*b*) What will be the loudness level of this sound in phons? (*c*) Repeat parts (*a*) and (*b*) for a similar noise source of 500-cycles/sec frequency.

14.10. Given a rectangular room $12 \times 18 \times 30$ ft. (*a*) What is the mean free path of a sound ray in this room? (*b*) If the average decrease in intensity level per encounter with the walls of the room is 1 db, what is the average sound absorption coefficient of the room? (*c*) Compute the decay rate of sound in the room in db/sec by considering the number of encounters with the walls per second. (*d*) Compute the decay rate by means of equation 14.17 and compare the result with that of part (*c*).

14.11. Given a cubical room 10 ft on a side. (*a*) What is the mean free path of a sound ray in this room? (*b*) How many reflections per second does an average ray make with the walls? (*c*) If the loss in intensity level per reflection is 1.5 db, what is the reverberation time of the room? (*d*) What is the average sound absorption coefficient for the walls? (*e*) Using the value of $\bar{\alpha}$ determined in part (*d*), compute the reverberation time of the room and compare with that determined in part (*c*).

14.12. (*a*) Show that the reverberation time equations for dead rooms (14.18 or 14.23) may be obtained from the live-room equation (14.12*b*), if we assume an effective absorption coefficient $\alpha_e = -\ln(1 - \alpha)$ where α is the true random incidence energy absorption coefficient. (*b*) Compute values for the effective absorption coefficient α_e for $\alpha = 0.1$, 0.5, and 0.75. (*c*) For what value of $\bar{\alpha}$ is the reverberation time as computed by means of equation 14.18, one half of that computed by means of the live room equation (14.12*b*)? (*d*) What is the effective sound absorption coefficient corresponding to the average coefficient determined in part (*c*)? Explain any correlation between the answers of parts (*c*) and (*d*).

14.13. By use of the identity $(1 - \alpha) = e^{\ln(1-\alpha)}$, show that equation 14.21 is equivalent to equation 14.16.

14.14. The reverberation time T measured at 6000 cycles/sec in a small reverberation chamber containing completely dry air is found to be 20 seconds. When moist air is present in the room, the measured reverberation time T' is 5 seconds. (*a*) Derive an equation involving these two reverberation times and the respective medium absorption coefficients m and m', that is independent of the surface characteristics and volume of the room. (*b*) Using your equation, compute a value for m' in ft^{-1} as determined from the measured values of T and T' and m as computed from Table 9.1.

14.15. (*a*) Show that the constant m in equation 14.26 must have the units of ft^{-1}. (*b*) Using the curves of Fig. 9.6 and data from Table 9.1, compute a value for m at 6000 cycles/sec in air of 40 per cent relative humidity. (*c*) Upon considering only absorption at the walls, the computed reverberation time at a frequency of 6000 cycles/sec in a room of 10,000-ft^3 volume is 1.2 seconds. What would be the computed reverberation time of this room, if absorption in 40 per cent relative humidity air is taken into consideration?

14.16. The normal reverberation time in a small reverberation chamber $9 \times 10 \times 11$ ft is 4.0 sec. (*a*) What is the effective sound absorption coefficient of the surfaces of the chamber? (*b*) When 50 ft^2 of one wall is covered with an acoustic tile, the reverberation time is reduced to 1.3 sec. What is the effective sound absorption coefficient of the tile? (*c*) What would be the reverberation time, if all surfaces of the chamber were covered with this acoustic tile?

14.17. (*a*) Derive equation 14.34 from equation 14.33. (*b*) What mean sound pressure level will be produced in a cubical room of 1000-ft^3 volume by a source of 0.001 watt acoustic output? The measured reverberation time of the room is 0.3 sec. (*c*) What is the effective sound absorption coefficient of the walls of this room?

14.18. Given a directional sound source having a directivity factor of 10 and an acoustic output of 100 microwatts in a room of 5000-ft^3 volume having a reverberation time of 0.7 sec. What is the maximum distance from the sound source at which the sound pressure level in the direct field will be 10 db above that of the reverberant field?

14.19. Given a motor to produce a steady state reverberant sound pressure level of 74 db relative to 0.0002 microbar in a room $10 \times 20 \times 50$ ft. The measured reverberation time of the room is 2 seconds. (*a*) What is the acoustic output of the motor? (*b*) How many additional sound absorbing units in sabins must be added to this room in order to lower the above ambient sound level by 10 db? (*c*) What is the new reverberation time of the room?

14.20. A cubical room is 5 meters on a side. (*a*) What is the characteristic frequency of the normal mode corresponding to the lowest-frequency axial wave? (*b*) the lowest-frequency tangential wave? (*c*) the lowest-frequency oblique wave?

14.21. A rectangular corridor is 2-m wide, 3-m high, and 10-m long. (*a*) Compute and plot the average number of allowed frequencies in the enclosure per one cycle/sec band at frequencies of 100, 200, 300, 400, 500, and 600 cycles/

sec. (*b*) Above what frequency does the average number of allowed frequencies always exceed *two* per one cycle/sec band?

14.22. Given a room of $4 \times 6 \times 10$ meters dimensions. (*a*) What is the frequency of the 111 mode of vibration in this room? (*b*) If the average sound absorption coefficient at this frequency is 0.1, what is the reverberation time for this 111 mode? (*c*) What is the minimum frequency for which the average number of normal modes per 1 cycle/sec band will exceed 5?

14.23. Given all the walls of a rectangular room $10 \times 15 \times 20$ ft to have a relative normal specific acoustic impedance $r_n = 20$. (*a*) What is the sound absorption coefficient of these walls for randomly incident sound waves? (*b*) What is the reverberation time of the room for oblique waves? (*c*) What is the reverberation time for axial waves parallel to the longest dimension of the room?

14.24. A cubical room is 5 m on a side. (*a*) Compute and list all the characteristic frequencies between 30 and 70 cycles/sec. (*b*) Locate the nodal planes for each of these characteristic frequencies. (*c*) If all surfaces of the room have an effective sound absorption coefficient $\alpha_e = 0.1$, what is the reverberation time for each of the above normal modes of vibration?

14.25. A cubical room is 15 ft on a side and has an effective absorption coefficient of 0.25 for the floor and ceiling and 0.05 for the walls. (*a*) What is the reverberation time for those axial waves that strike the floor and ceiling? (*b*) What is the reverberation time for those tangential waves that strike all four walls? (*c*) What is the reverberation time of the oblique waves striking all surfaces?

14.26. The velocity of sound in concrete is 3500 m/sec and its density is 2700 kg/m^3. (*a*) What is the normal specific acoustic resistance of concrete relative to water? (*b*) Applying equation 14.68, calculate the random incidence sound absorption coefficient of concrete relative to water. (*c*) If a concrete-walled cubical tank 3 m on a side is filled with water, what is the indicated reverberation time for water-borne sounds? Assume the upper surface of the water in contact with the air to reflect all incident energy.

14.27. Given a certain wall surface to have a normal specific acoustic resistance relative to air of $r_n = 4$. (*a*) By means of equation 14.65, compute and plot the absorption coefficient of this wall for plane waves incident at angles from 0 to 90°. (*b*) By means of equation 14.68, compute the sound absorption coefficient of the wall for randomly incident sound waves.

14.28. Given the two yz walls of a rectangular room to have a normal specific acoustic resistance of r_n relative to air. All other walls are assumed to be perfect reflectors. (*a*) What is the sound absorption coefficient of these two walls α_n for normally incident sound waves? (Use equation 14.65) (*b*) Using the method of Norris (Sect. 14.5), derive a general expression for the decay rate in db/sec for axial waves moving parallel to the x axis. Assume that upon each encounter with the yz walls, these axial waves are reflected with a fractional amount $(1 - \alpha_n)$ of their incident energy. (*c*) Show that your equation derived in part (*b*) is equivalent to equation 14.63 for $r_n \gg 1$.

14.29. A certain back-enclosed loudspeaker cabinet has internal dimensions of $2 \times 3 \times 4$ ft. Its internal surfaces are lined with an absorbing material having an effective absorption coefficient of 0.2. (*a*) The influence of internal resonances of the cabinet on the output of the loudspeaker may be assumed to become negligible when the average number of normal modes of vibration per one cycle/sec band becomes greater than one. What is this frequency for the interior volume of the above cabinet? (*b*) The duration of any spurious transient vibrations of the loudspeaker will be in part influenced by the length of reverberation time of the cabinet. What is the reverberation time of oblique waves in the interior volume of the cabinet? (*c*) Steady state sounds radiated into the interior of the cabinet may produce very large sound pressures within the interior volume of the cabinet. If 0.1 watt of acoustic power is radiated into the interior of the cabinet, what is the steady-state sound pressure level produced within the cabinet? (*d*) What are the frequencies of the three lowest normal modes of vibration of standing waves in the interior of the cabinet?

chapter 15

UNDERWATER ACOUSTICS

15.1 Introduction. As is to be anticipated, the use of sound waves in water for the transmission of intelligence has been of interest primarily to nautical and naval personnel. One of the early applications was the installation of submerged bells on lightships. Underwater sound from these bells could be detected at a considerable distance through a stethoscope or simple microphone mounted in the hull of a ship, or, if two such detecting devices were located on opposite sides of the hull, and the sounds received by each were transmitted separately to the right and the left ears of an observer, it became possible to employ the directional properties of hearing to determine the approximate bearing of the lightship. This simple device was of considerable assistance in avoiding navigational dangers under conditions of poor visibility.

In 1912 Fessenden developed an electrodynamic type of underwater sound source, the so-called Fessenden Oscillator, which operated in the frequency range between 500 and 1000 cycles/sec. The greatly increased output of this source correspondingly increased the range of underwater sound signaling and permitted vessels to communicate with one another by Morse code. As improved transmitting and receiving transducers were developed it was a natural step to apply them to the problem of rapidly measuring the depth of water, by timing echoes from the ocean bottom. One outgrowth of these early developments is the modern ultrasonic *fathometer*, in which the time required for short sound pulses to travel from the transmitting transducer to the ocean bottom and return is presented as a sequence of depth indications on a moving recording paper.

Upon development of the various types of "searchlight" transducers, as previously described in Sects. 12.8 and 12.14, capable of transmitting ultrasonic frequencies whose wavelengths in water are small compared to the lateral dimensions of the radiating face of the transducer, it became possible to produce narrow beams of sound which could be directed like the beam of a searchlight. As has been noted in Chapter 12, transducers of this type are also satisfactory for use as receiving hydrophones, and consequently in many installations a single transducer is used for both purposes. With equipment of this kind it is possible to determine the bearing of a sound-reflecting target by observing the direction of the sound beam that leads to the strongest echoes, and the range by measuring the time required for a short pulse of energy to return as an echo. Ultrasonic transducers as well as individual sonic hydrophones and arrays of such hydrophones are also used in *passive* listening, in which the source of sound being detected is that radiated by some distant ship. Under wartime conditions this type of listening is at times highly advantageous, for it permits determining the bearing, although not the range, of the radiating ship or submarine, without revealing the presence of the listening vessel.

The most interesting developments and applications as well as the greatest effort in underwater acoustics have been those associated with the problems of detecting, tracking and classifying submarines and surface vessels in naval warfare. It is customary to apply the generic name *sonar* (SOund NAvigation and Ranging) to this phase of underwater acoustics. In attacking this problem it has been found necessary to develop new means for the efficient conversion of electrical power into high intensity beams of water-borne acoustic power and to develop detection systems capable of detecting weak signals in the presence of a masking noise background. Of equal importance has been a study of the influence of such fundamental phenomena as divergence, absorption, reflection, refraction, scattering, diffraction, etc. on the transmission of sound waves in sea water. It is the primary purpose of this chapter to investigate the fundamental acoustic properties of sea water and to demonstrate its peculiar capabilities and limitations as a medium for transmitting sound energy to considerable distances. A secondary purpose is that of describing and defining some of the system parameters that must be considered when designing a sonar system to any given specifications.

The most comprehensive summary of underwater acoustics and sonar systems is that contained in the declassified Summary Technical Reports of Division 6 of the National Defense Research Committee as published shortly after the end of World War II. Important volumes dealing with basic problems of an acoustic nature include: (1) Volume 6A, Military Oceanography; (2) Volume 7, Principles of Underwater Sound, (3) Volume 8, Physics of Sound in the Sea. Additional volumes concerned with the fundamental parameters and characteristics of the various sonar systems include: (4) Volume 9, Recognition of Underwater Sounds; (5) Volume 14, Sonar Listening Systems; (6) Volume 15, Sonar Echo-Ranging Systems; (7) Volume 16, Scanning Sonar Systems; (8) Volume 17, FM Sonar Systems. Three additional references that delve deeper into the subject of underwater acoustics than is possible in this chapter are listed below.[1]

15.2 Velocity of Sound in Sea Water. In Sect. 5.5 it was pointed out that the velocity of sound in fresh water is a function of temperature. There are two additional factors that influence the velocity of sound in sea water, i.e., salinity and the changes in pressure associated with changes in depth. Each of these factors tends to increase the velocity, their composite effect being represented by the empirical equation

$$c = 1449 + 4.6t - 0.055t^2 + 0.0003t^3 + (1.39 - 0.012t)(S - 35) + 0.017d \quad (15.1)$$

where c is the velocity in meters per second, t is the temperature of the water in °C, S is its salinity expressed in parts per thousand, and d is the depth below the surface in meters. This equation is a simplification of more complicated equations obtained by Wilson[2] and others as the best fits to experimentally measured data. Equation 15.1 is accurate to within about one meter/sec for those conditions of temperature, salinity, and pressure commonly occurring in the various oceans. It is to be noted that the velocity of sound in surface sea water of 35 parts per thousand salinity is 1449 m/sec at 0°C as contrasted with 1403 m/sec for fresh water under similar conditions of temperature and pressure.

In making calculations involving the transmission of sound through sea water it is frequently quite adequate to use a *standard* velocity, rather than the more accurate value given by equation 15.1. In this book we will use 1500 m/sec as a standard velocity. This velocity is typical of those measured in surface waters overlying the continental shelves in middle latitudes. It corresponds to the velocity of surface sea water having a temperature of 13°C and a salinity of 35 parts per thousand, as can be seen by a substitution of these quantities into equation 15.1.

Associated with the adoption of a standard velocity is that of a concomitant standard characteristic impedance $\rho_0 c$. Since the density of sea water having the pressure, temperature, salinity given above is 1026.4 kg/m³, the corresponding standard characteristic impedance is

$$\rho_0 c = 1.54 \times 10^6 \text{ kg/m}^2 \text{ sec or MKS rayls}$$

It will be the practice in this book to use the above value in obtaining numerical relationships between acoustic pressure, particle velocity, and intensity in sea water.

[1] Officer, *Introduction to the Theory of Sound Transmission*, McGraw-Hill Book Co. (1958); Horton, *Fundamentals of Sonar*, U.S. Naval Institute (1959); Albers, *Underwater Acoustics Handbook*, Pennsylvania State University Press (1960).

[2] Wilson, *J. Acoust. Soc. Am.*, **32**, 641 (1960).

15.3 Sound Transmission Losses in Sea Water. If the water composing the oceans were both unbounded and homogeneous, only divergence and absorption would contribute to a decrease in pressure level as a sound beam was propagated away from its source. For instance, a wave diverging spherically in such a medium may be represented by the equation

$$P_2 = P_1(r_1/r_2)e^{-\alpha(r_2-r_1)} \tag{15.2}$$

where P_2 and P_1 are the acoustic pressures measured respectively at distances r_2 and r_1 from the apparent center of origin of the wave and α is the absorption constant of the medium in nepers/meter. Upon applying the operation, 20 log, to both sides of equation 15.2, the latter becomes

$$20 \log P_2 = 20 \log P_1 + 20 \log (r_1/r_2) - 8.7\alpha(r_2 - r_1)$$

which upon rewriting and replacing 8.7α by a, where a is the absorption constant in db/m, becomes

$$20 \log P_1 - 20 \log P_2 = 20 \log (r_2/r_1) + a\,(r_2 - r_1)$$

The left-hand side of the latter equation represents the *decrease* in sound pressure level as the wave is propagated from r_1 to r_2 and may be replaced by the expression H, where H represents a transmission loss in decibels. Then,

$$H = 20 \log (r_2/r_1) + a\,(r_2 - r_1) \tag{15.3}$$

It is customary to refer transmission losses to a given distance r as being relative to the sound pressure level existing at one meter from the effective center of the sound source. When this is done, the sound transmission loss from the reference distance at one meter to any distance r is given by

$$H = 20 \log r + ar \tag{15.4}$$

The absorption constant a for sound waves in sea water has already been discussed in Sect. 9.6. Its dependence on frequency and temperature is represented by equation 9.33. Numerical values of its magnitude as a function of frequency at either 5°C or 15°C may be obtained either from equations 9.34 and 9.34*a* or from Fig. 9.7. For instance, in sea water at 5°C, $a = 0.00001$ db/m at 1 kc/sec, $a = 0.001$ db/m at 10 kc/sec, and $a = 0.015$ db/m at 50 kc/sec.

Plotted in Fig. 15.1 are curves computed from equation 15.4, showing the transmission loss as a function of distance r for each of the above three frequencies. An inspection of curve A of this figure shows that at low frequencies such as 1 kc/sec, the entire transmission loss is caused by spherical divergence of the sound beam. However, as the frequency and range increase, curves B and C show that the absorption loss becomes of

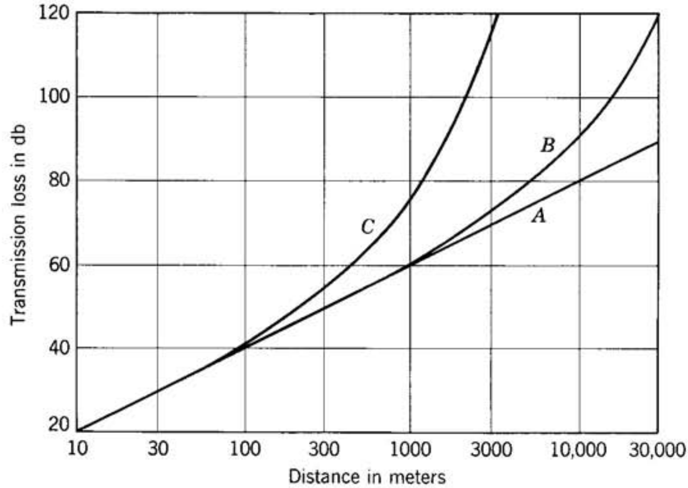

Fig. 15.1. Curves showing dependence of transmission loss on distance and frequency. Curve *A* at 1 kc/sec. Curve *B* at 10 kc/sec. Curve *C* at 50 kc/sec.

greater and greater significance. If we differentiate equation 15.4 with respect to r, then

$$\frac{dH}{dr} = \frac{20}{2.3} \cdot \frac{d(\ln r)}{dr} + a = \frac{8.7}{r} + a \tag{15.5}$$

is obtained for the spatial rate of transmission loss in decibels/meter. Let us now define a *crossover range* r_c as one within which the rate of attenuation caused by divergence is greater than that caused by absorption and vice versa for ranges greater than r_c. Upon equating $(8.7/r)$ to a, this crossover range is given as

$$r_c = \frac{8.7}{a} \tag{15.6}$$

For 10 kc/sec, the crossover range is 8700 m while at 50 kc/sec it is reduced to 600 m. From the above discussion it is evident that low frequencies must be used if sound energy is to be transmitted through sea water to great distances with a minimum of transmission loss.

When sound transmission loss measurements are made in the ocean, they are frequently observed to be at a considerable variance (usually larger) with those predicted by equation 15.4. Factors contributing to this variance include additional divergence or partial convergence caused by *refraction*, destructive and constructive *interference* associated with multipath types of propagation including reflections from the surface and bottom of the sea, *diffraction* and *scattering* caused by the presence of inhomogeneities in the water (see Sect. 9.8). It is possible to derive equations and compute precise values for the changes in transmission loss associated with each of these additional factors for certain idealized situations. However, the oceans are so variable in their characteristics that it is customary to lump together contributions of the above factors into a single term A, known as the *transmission anomaly*. The total transmission loss in decibels is then given by

$$H = 20 \log r + ar + A \tag{15.7}$$

Although many factors produce limitations on our ability to transmit sound energy through sea water, it should be noted that sound is immensely superior to the various classes of electromagnetic waves as a means for transmitting energy through sea water. For example, the lowest frequency radio waves in commercial use, 30 kc/sec, are attenuated by one decibel in a distance of 30 cm, and the higher frequencies are attenuated even more rapidly. Similarly, the diffusion and scattering of a beam of light passing through sea water is so great that the medium is for all practical purposes opaque at distances in excess of 200 m, and the most penetrating γ-rays are reduced by one decibel for every 1.5 cm of path. In comparison with other available means, the use of sound waves for transmitting energy through sea water is therefore vastly superior, and it suffers only when contrasted with the far more efficient transmission of radio and light waves through air or a vacuum.

15.4 Refraction Phenomena. The most important phenomenon that interferes with simple spherical divergence and straight line propagation of sound beams in sea water is the refraction resulting from variations in velocity. As can be seen from equation 15.1, the principal factors influencing the velocity of sound in sea water are temperature, salinity, and depth. Variations in salinity are of importance near the mouths of large rivers, where appreciable amounts of fresh water run into the sea, in the vicinity of large ocean currents such as the Gulf Stream, and in water close to the surface where rain and evaporation will have a maximum effect. Variations in velocity with depth, as caused by the increased pressure, are quite regular, i.e., 0.017 m/sec increase per meter increase in depth. The resulting increase in velocity with depth is quite modest for moderate depths and often may be ignored when a considerable variation in temperature is present. For example, the change in velocity at a depth of 100 m as caused by the pressure increase is only about 0.1 per cent. By contrast, variations in velocity resulting from changes in temperature are normally quite large and are subject to wide fluctuation, especially near the surface where such factors as the season of the year, time of the day, cloudiness,

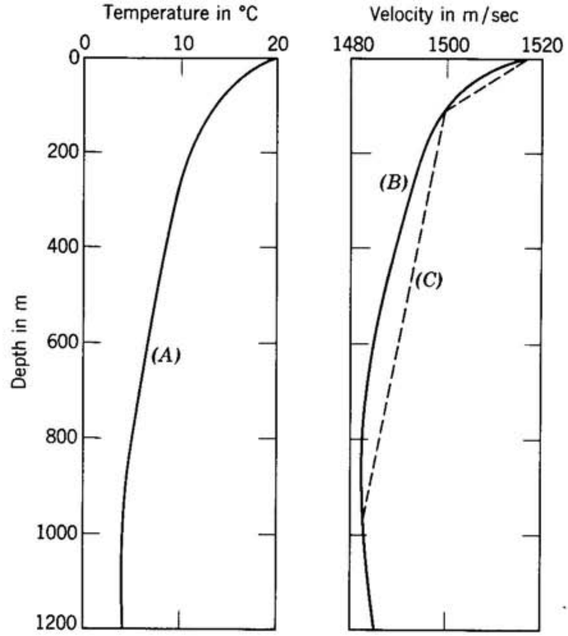

Fig. 15.2. (*A*) Typical thermocline. (*B*) Velocity of sound vs. depth curve. (*C*) Simplified velocity of sound vs. depth curve.

wind velocity, and sea state, all have their effect on the temperature gradient. Differentials of more than 5°C are common in the first 100 m, and since the change in velocity with temperature is about 0.2 per cent per °C for a temperature in the vicinity of 15°C, this effect makes the prediction of the exact path of a sound beam quite difficult. The influence of the resulting refraction on the transmission of sound waves is in many respects similar to that of heated air on the transmission of light rays.

Below 100 m in deep water the temperature in general decreases more regularly until at depths ranging from 500 to 1500 m it reaches a temperature near 4°C and then decreases very slowly until the bottom is reached. Curve *A* of Fig. 15.2 is a typical *thermocline* illustrating the manner in which the temperature of sea water varies with depth, and curve *B* of this figure shows the corresponding variation in velocity. It is to be noted that when the near constant temperature water is reached at a depth of 1000 m, the velocity then increases in accordance with the pressure effect rate of 0.017 m/sec per meter.

The path of a ray of sound through a medium in which the velocity varies with depth can be calculated by the application of Snell's law. In one form this law states that the ray must take such a path that

$$\frac{\cos\theta}{c} = \frac{1}{c_0} \tag{15.8}$$

where θ is the angle made with the horizontal at a depth where the velocity of sound is c, and c_0 is the velocity at a depth, real or extrapolated, where the ray would become horizontal. In tracing the path of any given ray through a complicated velocity gradient such as that of Fig. 15.2 it is advantageous to simplify the analysis by breaking up the path into separate segments, each short enough so that the velocity gradient may be assumed constant over its length.

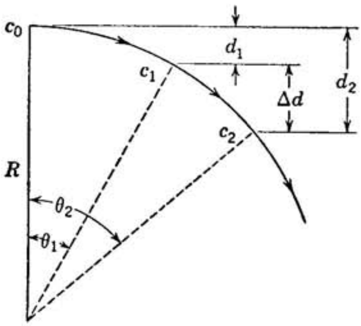

Fig. 15.3. Diagram used in deriving relation between velocity gradient g and the radius of curvature R of a sound ray.

Let us now demonstrate that the path of a sound ray through a layer of water of constant sound velocity gradient g, is an arc of a circle. Consider a circle of radius R, as shown in Fig. 15.3. Then $d_1 = (1 - \cos\theta_1)R$ and $d_2 = (1 - \cos\theta_2)R$, so that

$$\Delta d = d_2 - d_1 = R(\cos\theta_1 - \cos\theta_2) \tag{15.9}$$

But $c_2 = c_1 + g\Delta d$, and hence

$$\Delta d = \frac{c_2 - c_1}{g} \tag{15.10}$$

Combining these two equations with Snell's law (15.8) and eliminating Δd, c_1, c_2, $\cos\theta_1$, and $\cos\theta_2$, we obtain

$$R = \frac{c_0}{-g} = \frac{c}{-g\cos\theta} \tag{15.11}$$

It should be noted that for the situation illustrated in Fig. 15.3, the velocity gradient is intrinsically negative, and hence R is positive. If the velocity gradient were positive, R would be negative and the path would curve upward rather than downward.

Once the radius of curvature of each segment of the path is known, the actual path can either be traced graphically or computed from familiar equations of trigonometry. Useful equations for such computations include equation 15.9 and

$$\Delta x = R(\sin\theta_2 - \sin\theta_1) \tag{15.12}$$

where Δx is the horizontal distance traveled by the sound ray of Fig. 15.3 while traveling the vertical distance Δd, and

$$\Delta x = \Delta d \cot\left(\frac{\theta_1 + \theta_2}{2}\right) \tag{15.12a}$$

As an example consider a ray that is initially horizontal at the surface of sea water having the velocity structure indicated in curve C of Fig. 15.2. Since

$$g' = \frac{1500 - 1518}{100} = -0.18$$

the radius of curvature of this ray in the upper layer is

$$R' = \frac{1518}{0.18} = 8400 \text{ m}$$

At a depth of 100 m this ray will make a downward angle with the horizontal of $\theta_1 = 8.8°$, as given upon substitution into equation 15.8 by

$$\cos\theta_1 = \frac{c_1}{c_0} = \frac{1500}{1518} = 0.9881$$

Finally, the horizontal distance x_1 traveled in attaining this depth is given by

$$x_1 = R' \sin\theta_1 = 8400 \sin 8.8° = 1300 \text{ m}$$

When the ray enters the second layer the velocity gradient becomes

$$g'' = \frac{1482 - 1500}{900} = -0.02$$

so that the radius of curvature of the path changes to

$$R'' = \frac{1518}{0.02} = 75{,}100 \text{ m}$$

At the bottom of the second layer at a depth of 1000 m, the velocity of sound has its minimum value of 1482 m/sec, and consequently the ray makes a maximum angle with the horizontal of 12.4°. Upon substituting into equation 15.12

$$\Delta x''' = 75{,}100\,(\sin 12.4° - \sin 8.8°) = 4900 \text{ m}$$

is obtained for the horizontal distance traveled in the second layer.

At depths below 1000 m the temperature is nearly constant, but the velocity begins to increase with depth because of the increasing pressure and produces a positive velocity gradient of +0.017. Hence, the ray begins to follow a circular path which curves upward, its radius of curvature being

$$R''' = \frac{1518}{-0.017} = -89{,}000 \text{ m}$$

An upward curving path of this radius of curvature is typical of all sound rays in isothermal layers of water. The resulting path of the ray to a depth of 2000 m is shown in Fig. 15.4. The ray in the third layer will ultimately become horizontal and reach its maximum depth of 3100 m when the velocity increases to 1518 m/sec, that existing at the surface. The horizontal distance traveled in the third layer is

$$\Delta x''' = 89{,}000 \sin 12.4° = 19{,}000 \text{ m}$$

The total horizontal distance traveled by the ray in reaching its maximum depth is therefore

$$x = 1300 + 4900 + 19{,}000 = 25{,}200 \text{ m}.$$

After reaching its maximum depth, the ray will return to the surface as a horizontal ray by traversing a path symmetrical to that followed in reaching its maximum depth. Upon returning to the surface it will have traveled a total horizontal distance of 50,400 m.

Two different types of transmission anomalies, as produced by refraction, exist when sound rays are propagated along paths such as that of Fig. 15.4. For instance, a shallow-depth hydrophone located at a distance of 6000 m from the sound source will receive a very weak signal since the main axis of the sound beam will be at a depth of 1000 m at this distance. Typical values of A for this situation range from 30 to 50 db. By contrast, those rays returning to the surface region at a range of about 50,000 m will tend to converge and lead to a stronger signal than would be present at the same distance for rays diverging spherically in isovelocity water. Under

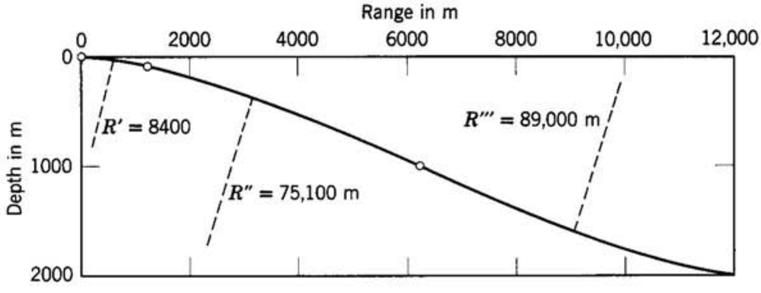

Fig. 15.4. Typical sound-ray path as influenced by refraction.

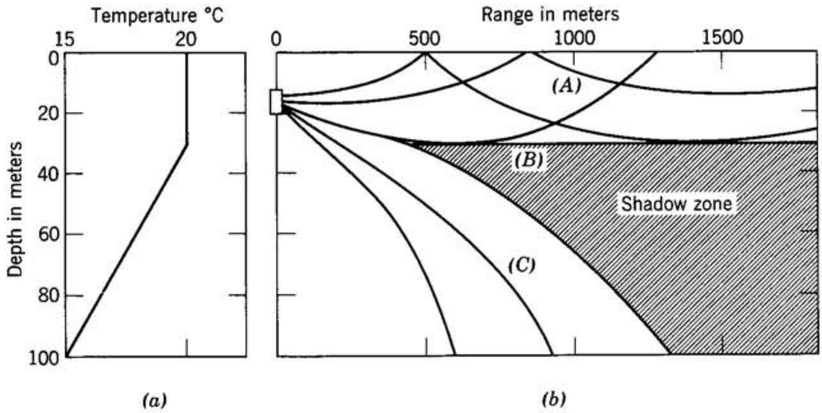

Fig. 15.5. (*a*) Thermocline. (*b*) Paths of typical sound rays.

this circumstance *A* may have negative values of a considerable magnitude, i.e., the transmission loss will be less than that given by equation 15.4.

Let us now consider the manner in which the refraction of sound rays traveling within another typical temperature-gradient structure, such as that of Fig. 15.5, may produce transmission anomalies. In this example we assume that there is an upper layer of isothermal water extending to a depth of 30 m, and that below this depth the temperature decreases at a rate of 0.07°C per meter. The paths of several sound rays originating from a source located 15 m below the surface are indicated in the figure. At a point such as *A* the signal received will be very nearly that calculated for an assumed simple spherical divergence, and hence the transmission anomaly will be negligible. Below *A* there is a so-called *shadow zone B*, in which the sound pressure is theoretically zero, since no rays are indicated as entering this region. In actual practice, however, sound pressures measured in the shadow zone are never strictly zero, owing to such factors as irregularities in the temperature gradient, diffuse scattering from the surface of the water when roughened by wave action, scattering by inhomogeneities within the body of the water, etc. However, their levels may be as much as 30 db below that predicted on the assumption of simple spherical divergence, with a corresponding value for the transmission anomaly. Below the shadow zone there is a third region, *C*, where the measured sound pressures are intermediate between those at similar horizontal distances in *A* and *B*. The decrease in sound pressure in this region results from further refraction in the lower layer, which causes the rays to spread more rapidly than they would for simple spherical divergence.

The increased divergence observed in region *C* of Fig. 15.5 is but one example of an increased transmission loss generated as sound rays are refracted in passing from water of one velocity structure into water of a considerably different structure. This phenomenon is commonly referred to as the *layer effect*. Another example of this effect is illustrated in Fig. 15.6 where the velocity is observed to suddenly decrease from a value c_1 to a value c_2 at a depth d, the so-called *layer depth*. An estimate of the transmission anomaly for the latter situation may be obtained by simplifying equations developed in Sect. 6.6 for the oblique transmission of plane waves from one medium to a second medium. By combining equations 6.54 and 6.56 one may show that the pressure amplitude P_2 of the transmitted wave is given relative to the pressure amplitude P_1 of the incident wave by

$$P_2 = P_1 \frac{2\rho_2 c_2 \cos \theta_i}{\rho_2 c_2 \cos \theta_i + \rho_1 c_1 \cos \theta_t} \tag{15.13}$$

Upon replacing $\cos \theta_i$ by $\sin \theta_1$ and $\cos \theta_t$ by $\sin \theta_2$ and assuming that $\rho_1 c_1 \approx \rho_2 c_2$, equation 15.13 is reduced to

$$P_2 = P_1 \frac{2 \sin \theta_1}{\sin \theta_1 + \sin \theta_2} \tag{15.14}$$

The corresponding transmission anomaly as given by $A = 20 \log (P_1/P_2)$ is

$$A = 20 \log \frac{\sin \theta_1 + \sin \theta_2}{2 \sin \theta_1} \tag{15.15}$$

As an example, let us assume that $c_1 = 1500$ m/sec, $c_2 = 1490$ m/sec, and $\theta_1 = 1°$. A substitution of these values into equation 15.8 leads to a refracted angle $\theta_2 = 6.7°$ which upon substitution into equation 15.15 yields a transmission anomaly of 12 db.

Under wartime conditions the question whether the temperature gradients are such as to produce either shadow zones or layer effects is obviously of the highest importance to commanders of both submarines and antisubmarine vessels. For example, in the situation illustrated in

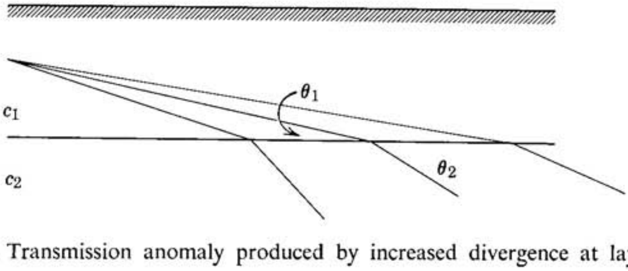

Fig. 15.6. Transmission anomaly produced by increased divergence at layer depth.

Fig. 15.5 a submarine located at a distance of 1500 m from a sonar-equipped destroyer would probably escape undetected at a depth of 50 m, whereas it would be easily detected if its depth were 20 m.

15.5 Sound Channels. A type of refraction of particular interest exists at great depths, where the temperature decreases steadily towards a nearly constant value of about 4°C. At these depths the conditions are very stable and uniform throughout the year. As has been pointed out in Sect. 15.4, it is at such depths that the velocity of sound attains its minimum value, increasing at lesser depths because of the increase in temperature and at greater depths because of the increase in pressure. As a consequence of these conditions, all rays that originate in this region of minimum velocity and make a small angle with the horizontal will tend to curve back toward this level without reaching either the surface or the bottom, forming what is known as the *deep sound channel.*

Sound waves propagated in this channel are constrained to remain in the channel, and as a consequence they do not diverge as rapidly as do waves in isovelocity water. Their initial divergence is spherical out to a distance r_1 where the channel is said to be filled, but from there on the divergence is more nearly cylindrical. Under these conditions, the transmission loss associated with divergence is given by the equation

$$H = 20 \log \frac{r_1}{1} + 10 \log \frac{r}{r_1} = 10 \log r_1 + 10 \log r \qquad (15.16)$$

which is less than 20 log r, that for spherical divergence out to a distance r. Since the absorption of audio frequencies in sea water is quite small, the low-frequency components of sound signals from explosive charges detonated in this channel are propagated to tremendous distances. Such signals have been received at distances in excess of 3000 km and require about an hour for transit. The use of the deep sound channel offers considerable promise as a means for facilitating rescue work at sea. According to this technique, which is known as SOFAR (SOund Fixing And Ranging), anyone in need of rescue drops overboard a small depth charge (4 pounds of TNT is adequate), set to explode in the deep sound channel. The location of the explosion can then be determined from the differences in transit time to three or more listening stations.

To analyze this type of transmission, let us assume that the velocity increases at a uniform rate of g' meters/sec per meter above the *axis* of the sound channel, i.e., the depth of minimum velocity c_m, and likewise increases at a rate of g'' meters/sec per meter below this axis. When the velocity gradient g' is constant, rays crossing the axis of the sound channel in an upward direction at an angle θ_0 with the horizontal, will travel on an arc of a circle of radius R' and recross the axis of the sound channel at a horizontal distance

$$\Delta x' = 2R' \sin \theta_0 = \frac{2c_m}{g' \cos \theta_0} \sin \theta_0 = \frac{2c_m}{g'} \tan \theta_0 \qquad (15.17)$$

Correspondingly, rays crossing the axis of the sound channel in a downward direction at an angle θ_0 will recross in a horizontal distance

$$\Delta x'' = 2R'' \sin \theta_0 = \frac{2c_m}{g''} \tan \theta_0 \qquad (15.18)$$

In general, any ray that once crosses the axis of the sound channel at an angle θ_0 will continue to recross the axis at this same angle, first in one direction and then in the other, at intervals given alternately by equations 15.17 and 15.18. It is to be noted that when the angle of crossing θ_0 is so large that the ray in the upper layer approaches the surface, it may no longer be possible to treat this ray as traveling in water having a constant velocity gradient. Instead, the path may have to be broken up into separate segments as was done with the example discussed in Sect. 15.4.

Figure 15.7 shows the paths of a few representative rays in a deep sound channel having a velocity gradient of 0.027 m/sec per meter above its axis and 0.018 m/sec per meter below its axis. It is interesting to note that the time required for the axial ray to travel a given horizontal distance

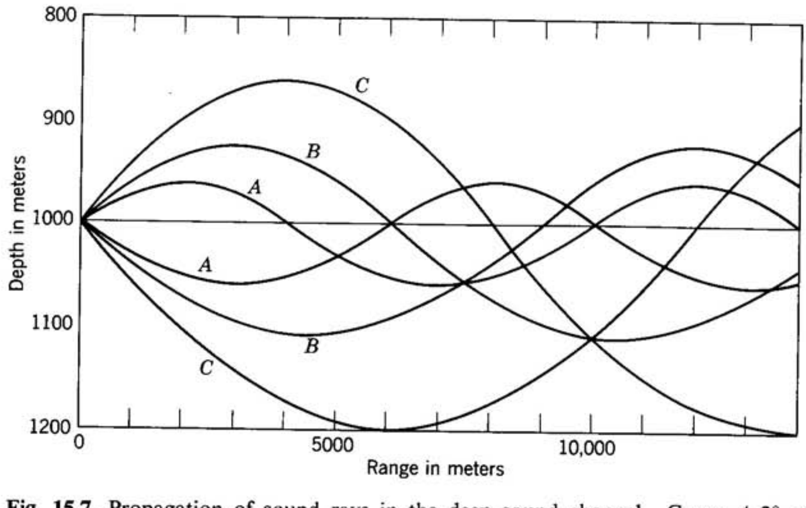

Fig. 15.7. Propagation of sound rays in the deep sound channel. Curve *A*–2° ray. Curve *B*–3° ray. Curve *C*–4° ray.

is greater than that for rays crossing the axis at a finite angle, such as *B* or *C*. This phenomenon can readily be observed when one is listening to a sofar signal, which rumbles in with growing intensity for up to as much as 10 sec and then ends abruptly as the slowest ray, that traveling along the axis of the channel, finally arrives. In order to explain this behavior, let us derive an expression for the mean horizontal velocity of of rays crossing the axis at an angle θ_0. The instantaneous velocity of propagation of the wave as given by Snell's law is

$$c = \frac{c_m \cos \theta}{\cos \theta_0}$$

where c_m is the minimum velocity occurring at the axis of the channel. The horizontal component of this velocity, $c \cos \theta$, is then given by

$$c_x = \frac{c_m \cos^2 \theta}{\cos \theta_0} \tag{15.19}$$

From this equation it is apparent that $c_x > c_m$ when $\cos^2 \theta > \cos \theta_0$ and vice versa. However, if we compute the average value of $\cos^2 \theta$ over the path as θ goes from θ_0 to 0 and returns to θ_0, and substitute this expression into equation 15.19, the mean horizontal velocity during 1 cycle of the path becomes

$$\bar{c}_x = \frac{c_m}{2}\left(\frac{1}{\cos \theta_0} + \frac{\sin \theta_0}{\theta_0}\right) \tag{15.20}$$

The thermal structure of the oceans is such that rays may not cross the axis of the deep sound channel at angles greater than 13° without striking either the surface or the bottom. Therefore, we may simplify equation 15.20 by replacing $\cos \theta_0$ and $\sin \theta_0$ by the first two terms of their respective series expansions, which leads to

$$\bar{c}_x = c_m\left(1 + \frac{\theta_0^2}{6}\right) \tag{15.21}$$

where θ_0 is expressed in radians. This equation shows that the mean horizontal velocity of all rays is greater than c_m excepting, of course, that corresponding to $\theta_0 = 0$.

Less pronounced sound channels also exist near the surface whenever either an isothermal layer or one having a positive velocity gradient underlies one having a negative gradient. Figure 15.8 is a typical example of a near-surface sound channel. The range r_1 indicated in this figure corresponds to that at which the divergence may be considered to change from spherical to cylindrical.

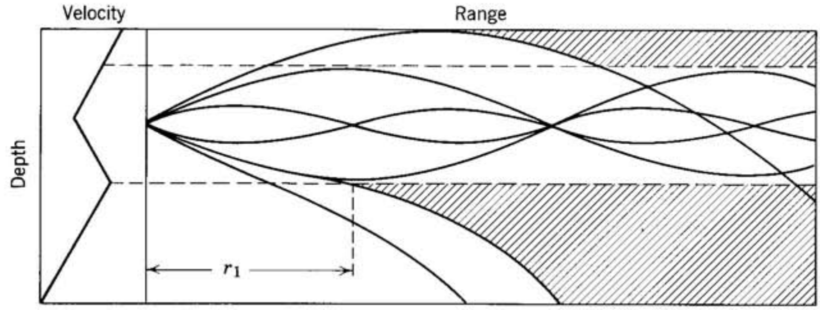

Fig. 15.8. Diagram illustrating the formation of a near-surface sound channel.

15.6 Influence of Surface Reflections on Transmission Loss. Whenever a source of diverging acoustic waves is present in sea water, both surface-reflected and bottom-reflected waves may arrive at a given point and combine their effects with that of the direct wave. Depending upon their respective phases, this multiplicity of waves may either reinforce each other so as to produce greater pressure amplitudes than that of the direct wave alone or partially cancel each other so as to produce a lesser pressure. In shallow water, the influence of surface-reflected and bottom-reflected waves is of equal importance. By contrast, in deep water the bottom-reflected waves are relatively weak when both the source of sound and the receiving hydrophone are near the surface. Under these circumstances the observed interference phenomena may be considered to arise from the presence of just the direct and surface-reflected waves.

We will now derive equations giving the result of combining waves traveling along the direct path SH of Fig. 15.9 with those traveling along the surface-reflected path SRH. For the purpose of computing the length of the path SRH, it is convenient to assume that the reflected waves have their origin at an *image* source I at the position shown in Fig. 15.9. It is

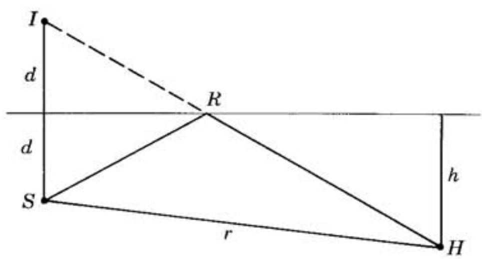

Fig. 15.9. Diagram for computing surface image effects.

for this reason that phenomena associated with the influence of the reflected wave in combination with the direct wave are frequently referred to as *image effects*. The complex pressure $\mathbf{p}_1$ of the direct wave is represented by the usual spherical wave equation as

$$\mathbf{p}_1 = \frac{A_1}{r} e^{j(wt-kr)} \tag{15.22}$$

Similarly, the pressure $\mathbf{p}_2$ of the reflected wave may be represented by

$$\mathbf{p}_2 = \frac{-\mu A_1}{r + \Delta r} e^{j[wt-k(r+\Delta r)]} \tag{15.23}$$

where $(r + \Delta r)$ is the total distance from the image position I to the hydrophone position H. The negative sign is required in order to allow for the 180° phase shift taking place upon reflection at the water-air interface and μ is the pressure reflection coefficient of the surface, i.e., the ratio B_1/A_1 of equation 6.56. For smooth sea surfaces, i.e., smooth relative to a wavelength of the incident sound, the reflection is specular and $\mu \approx 1$. When the surface of the sea is rough, however, the reflection becomes diffuse and $\mu \rightarrow 0$.

The total complex acoustic pressure at the position of the measuring hydrophone, as given by $\mathbf{p} = \mathbf{p}_1 + \mathbf{p}_2$, is

$$\mathbf{p} = \frac{A_1}{r} e^{j(wt-kr)} \left[1 - \frac{\mu e^{-jk\Delta r}}{1 + (\Delta r/r)}\right] \tag{15.24}$$

In the general case, the ratio of the pressure amplitude of the combined waves to that of the direct wave alone is given by the magnitude of the complex term contained within the square bracket of equation 15.24. However, if the depth d of the source and h of the hydrophone are both small compared to the distance r, it is possible to show that

$$\Delta r \approx \frac{2hd}{r} \tag{15.25}$$

Under these circumstances, the term $\Delta r/r \ll 1$ and may be neglected where it occurs in the denominator of equation 15.24. When the magnitude of the bracketed term of equation 15.24 is now computed, the resulting pressure amplitude P of the combined waves becomes

$$P = \frac{A_1}{r}(1 + \mu^2 - 2\mu \cos k\Delta r)^{1/2} \tag{15.26}$$

This equation shows that depending upon the particular phase relationship existing between the two waves, the pressure amplitude of their combination ranges between $(1 + \mu)P_1$ and $(1 - \mu)P_1$, where $P_1 = A_1/r$ is the pressure amplitude of the incident wave alone. The corresponding transmission anomaly as defined by $A = 20 \log (P_1/P)$ is

$$A = -10 \log (1 + \mu^2 - 2\mu \cos k\Delta r) \tag{15.27}$$

As a special example, let us consider $\mu = 1$. Then equation 15.26 simplifies to

$$P = 2P_1 \sin \frac{k\,\Delta r}{2} = 2P_1 \sin \frac{khd}{r} \tag{15.28}$$

It is evident that the two waves will reinforce each other to a maximum extent when

$$\frac{khd}{r} = \frac{\pi}{2}, \frac{3\pi}{2}, \frac{5\pi}{2}, \text{etc.}$$

and cancel each other when

$$\frac{khd}{r} = \pi, 2\pi, 3\pi, \text{etc.}$$

The most important practical situation occurs when $khd/r \ll 1$. Then

$$P = \frac{2P_1 khd}{r} \tag{15.29}$$

and since $P_1 = A_1/r$, this becomes

$$P = \frac{2A_1 khd}{r^2} \tag{15.29a}$$

It is to be noted that for those large distances r at which equation 15.29a is applicable, the pressure amplitude decreases as $1/r^2$ rather than as $1/r$. Correspondingly, the transmission loss is given by $40 \log r$ rather than by $20 \log r$, i.e., it increases by 12 db each time the distance is doubled rather than by 6 db as is characteristic for simple spherical divergence. It should be noted that when $\mu = 1$, the sound field of the above source-image pair

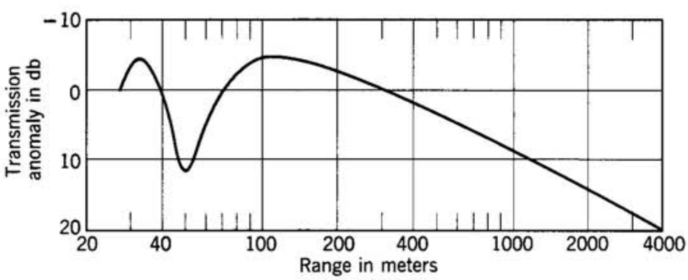

Fig. 15.10. Example of the transmission anomaly produced by the surface image effect.

is essentially the same as that of the acoustic doublet previously discussed in Sect. 10.6.

Figure 15.10 is a plot of computed values of the transmission anomaly as obtained from equation 15.27 for an assumed frequency of 200 cycles/sec, a source depth of 10 meters, a receiving hydrophone depth of 20 meters, and a pressure reflection coefficient of $\mu = 0.8$. Experimentally measured values of the transmission loss at low frequencies agree quite well with the predictions of equation 15.27. However, at high frequencies, e.g., above 5 kc/sec, interference between direct and surface-reflected waves becomes less significant and is likely to be masked by refraction effects. Nevertheless, even at these frequencies it undoubtedly accounts for some of the rapid fluctuations in transmission loss that are often observed.

15.7 Bottom Reflection Phenomena. The influence of bottom reflections on transmission loss is somewhat more involved than that of surface reflections. For instance, the bottom varies much more in its acoustical nature and slope than does the surface. In deep water, rays reflected from the bottom become significant only when either the direct rays are canceled by combination with surface-reflected rays or are sharply refracted downward. These bottom-reflected rays may be assumed to experience a reflection loss of $10 \log \alpha_r$, where α_r is the reflection coefficient as discussed in Sect. 6.7. This coefficient depends both upon the angle with which the ray is incident on the bottom and the acoustical nature of the bottom, i.e., its specific acoustic impedance. Typical values of this reflection loss range from 10 to 20 db for sound waves incident normally on the bottom to less than 5 db when incident at grazing angles.

As a consequence of the multiplicity of reflections taking place both at the surface and bottom, prediction as to the characteristics of sound transmission in shallow water is more complicated than for deep water. One theoretical attack on the problem involves a *ray* solution in which the sound field is made up of contributions from an infinite set of images of the source in the surface and bottom. Figure 15.11 is a diagram showing a portion of the infinite set of images of a near-surface source *S*. This source *S* may be considered to form an acoustic doublet in combination with the first surface-reflected image *I*. This doublet is then repeated as $S'I'$, $S''I''$, etc. upon repeated reflections from the bottom and surface. As a consequence, the resulting sound field will have much the same characteristics as that of the single source-image pair discussed in Sect. 15.6. At distances large compared to the depth of the bottom and for wavelengths greater than this depth, the acoustic pressure will decrease as $1/r^2$, pressures near the surface will be small, pressures will go through one or more maxima as the bottom is approached, etc.

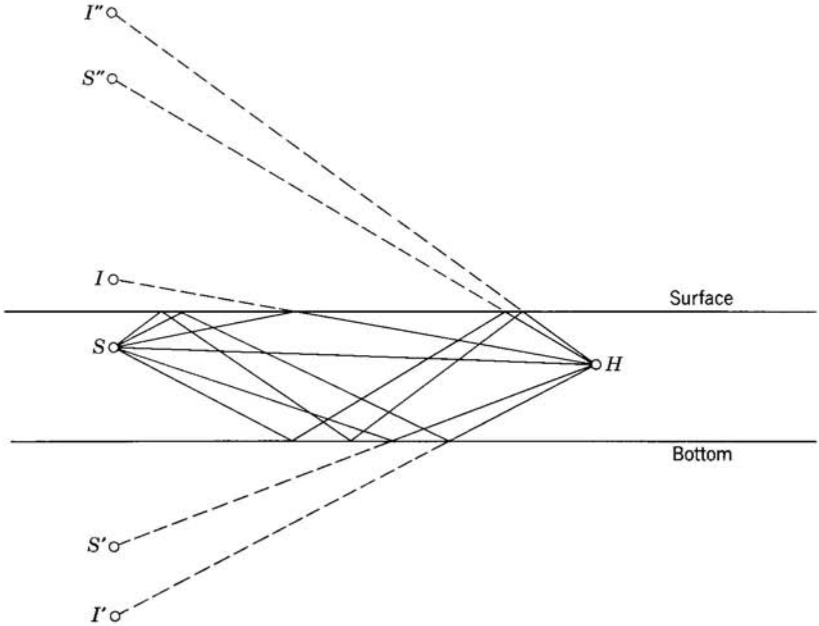

Fig. 15.11. Doublet-pairs produced by multiple reflections from surface and bottom in shallow water.

Another theoretical solution to shallow water propagation is called the *normal mode* solution. Here the sound field is described by an infinite set of functions, called normal modes, each of which is a solution of the wave equation and satisfies the assumed boundary conditions. Although the form of the solution of shallow water propagation is quite different when expressed in terms of normal modes than when expressed in terms of rays, it can be shown that they are actually equivalent. The ray solution lends itself to computing sound fields out to distances of from two to three times the depth of the water, while the normal mode solution is easier to apply at greater distances. For further information on the details of the normal mode type of solution, the reader is referred to the references given below.[3]

15.8 Source Level. In all of our discussions of transmission loss, it has been measured or computed with respect to a reference position at a distance of *one* meter from the effective center of the sound source. Consequently, if we are to predict actual signal levels produced at any distance

[3] Officer, *Introduction to the Theory of Sound Transmission*, pp. 117–145, McGraw-Hill Book Co. (1958); Pekeris, *Theory of Propagation of Explosive Sound in Shallow Water*, *Geol. Soc. Amer.*, Mem. 27 (1948).

from a specific sound source, we must know the sound pressure level generated by the source at the reference position. The sound pressure level, in decibels relative to *one* microbar, generated at the reference position is defined to be its *source level*, S. The source level depends fundamentally on just two parameters, the acoustic output W of the source and its transmitting directivity index d_t.

For an omnidirectional source of spherical waves, the intensity I in watts/m^2 at a distance of one meter from the effective center of a source having an output of W watts is $I = W/4\pi$. The associated effective (rms) acoustic pressure P in newtons/m^2 is given by

$$P^2 = \frac{\rho_0 c W}{4\pi} = \frac{1.54 \times 10^6 W}{4\pi}$$

which leads to a source level of

$$S = 20 \log 10P = 71 + 10 \log W \tag{15.30}$$

in decibels relative to 1 microbar. It is to be noted, that in order for equation 15.30 to yield sound pressure levels in decibels relative to 1 microbar, i.e., 0.1 newton/m^2, one must substitute $10P$ into this equation when P is given intrinsically in newtons/m^2.

When a sound source is directional, the source level along its axis will be increased by its transmitting directivity index d_t (Sect. 7.11) as compared to an omnidirectional source of equal total acoustic output. Therefore, the axial source level of a directional sound source is given by

$$S = 71 + 10 \log W + d_t \tag{15.31}$$

Two common types of directional transducers are used in sonar systems. One type either has a plane radiating surface, or the individual elements on a curved surface are phased so as to be equivalent to a plane radiating surface. When the lateral dimensions of the radiating surface of such a transducer are greater than one wavelength, its directivity index is given by equation 7.61*a* as

$$d = 10 \log \frac{4\pi S}{\lambda^2} \tag{15.32}$$

where S is the area of the radiating surface of the transducer and λ is the wavelength radiated. The other common type of transducer is one having a cylindrical radiating surface. Such a transducer radiates a cylindrical beam which has directionality only in planes through the axis of the cylinder. The directivity index of a cylindrical transducer of height h and radius a is given by

$$d = 10 \log \frac{2h}{\lambda} \tag{15.33}$$

when $h > \lambda$.

In measuring the source level of sound sources it is often necessary to measure the sound pressure level at a distance greater than one meter from the effective center of the source. This practice becomes necessary whenever the sound source is so large that the reference position at one meter from the effective center of the source is within the source, e.g., a spherical source of 2-meter radius. Another reason for making measurements at distances greater than one meter is in order to avoid complicating factors associated with the near-field, as discussed in Sect. 7.11. However, if the sound pressure level generated by a given source is measured at a distance of r meters from the effective center of the souce, it may be converted to source level by addition of the term 20 log r.

15.9 Factors Influencing Echo Levels. Equipment designed to echo-range on underwater targets (Fig. 15.12) must satisfy three basic requirements:

(1) It must generate underwater sounds of sufficient source level to make the relatively weak echoes from a distant target recognizable above background noises.

(2) The time required for an emitted sound pulse to proceed to the target and return must be measured, and this information must be presented in some manner as a range, expressed either in meters or in yards.

(3) The direction from which the echo returns, i.e., the bearing angle and sometimes the depression angle of the target, must be determined to an accuracy of about 1°.

The sound pressure level E (*re* 1 microbar) of the returning echo is given by

$$E = S - H + T - H = S + T - 2H \qquad (15.34)$$

where S is the source level of the transmitting transducer, T is the *target strength* of the reflecting object, and H is the one-way transmission loss between source and target.

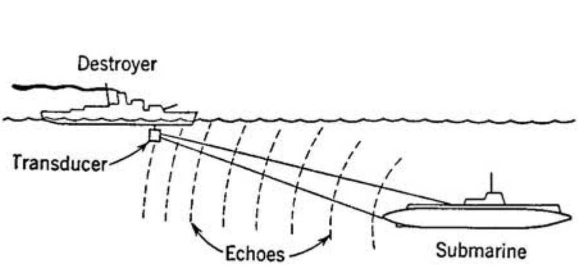

Fig. 15.12. Echo ranging on a submarine.

The target strength of a reflecting object may be defined by the equation

$$T = 20 \log (P_s/P_i) \tag{15.35}$$

where P_i is the sound pressure incident on the target, and P_s is the sound pressure scattered back by the target as measured at a distance of *one* meter from the effective center of the scattered sound. Target strength is expressed in decibels. It measures the amount by which the apparent source level of sound scattered by the target exceeds the sound pressure level of the incident sound.

The target strength of a reflecting object is determined primarily by its size, its shape, and the fraction of the incident acoustic energy that is reradiated. For example, one may show that the target strength of a perfectly reflecting sphere of radius a meters, which reradiates the intercepted sound energy uniformly in all directions, is given by the equation

$$T = 20 \log (a/2) \tag{15.36}$$

This equation indicates that a sphere of 2-meter radius will have a target strength of 0 db. Such a 0 db target merely corresponds to one that reradiates sound with an effective source level that is equal to the pressure level of the incident sound. For larger spheres, the radiated source level is greater than the level of the incident sound and vice versa.

The target strength of an irregularly shaped object, such as a submarine, may be expected to depend on its orientation with respect to the incident sound. For each particular orientation, the target may be assumed to present a different effective scattering cross section of σ square meters. One may show that the corresponding target strengths are given by

$$T = 10 \log (\sigma/4\pi) \tag{15.37}$$

The above dependence of target strength on orientation has been verified by experimental measurements. For instance, the measured target strengths of World War II fleet type submarines are at a minimum of about 10 db for sounds incident on the bow, increase gradually to about 25 db on the beam, and then decrease to about 15 db on the stern.

As an example of a typical echo level, let us compute that returned from a submarine of 20 db target strength at a distance of 5000 m when the transmitting transducer radiates 2000 watts at a frequency of 20 kc/sec in a beam of 20 db directivity index. The source level as given by equation 15.31 is

$$S = 71 + 10 \log 2000 + 20 = 124 \text{ db}$$

The sound absorption coefficient of sea water at 20 kc/sec as given by equation 9.34 is 0.004 db/meter. Substitution into equation 15.7 yields a one way transmission loss of

$$H = 20 \log 5000 + 0.004 \times 5000 + A = 94 + A$$

Finally, upon substitution into equation 15.34

$$E = 124 + 20 - 2(94 + A) = -44 - 2A$$

is obtained for the echo level. It is evident that even if no transmission anomaly losses are present, i.e., if $A = 0$, the echo level being returned under the above assumed conditions corresponds to a sound pressure of less than 0.01 microbar. Factors influencing the detectability of such a weak signal will be discussed in the following two sections.

15.10 Masking by Noise. Two basic types of noise tend to mask echoes returned from underwater targets. One type consists of those noises present even when no sound is being radiated by the transducer. These include such noises as ambient sea noise, machinery and propulsion noises generated by the echo-ranging ship, and turbulence noises generated in the vicinity of the sonar transducer. The second type consists of a multiplicity of weak echoes returned from small scatterers located in the sound beam and near the target. This second type of masking noise is referred to as *reverberation* and will be discussed in Sect. 15.11.

Ambient sea noise results from the summation of all noises generated within the body of the ocean. However, its principal source is associated with wind and wave action at the surface of the sea.[4] Figure 15.13 is a plot of average values of the pressure spectrum level of ambient sea noise as a

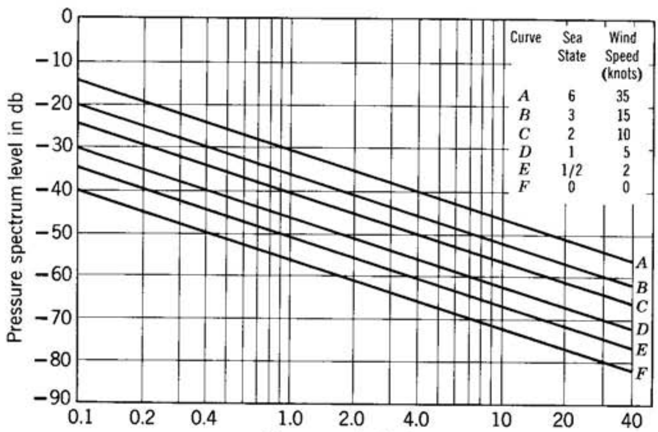

Fig. 15.13. Pressure spectrum level of ambient sea noise for various sea states and wind speeds expressed in decibels relative to 1 microbar. (After Knudsen.)

[4] Knudsen, Alford, and Emling, *J. Marine Research*, 7, 410 (1948).

function of frequency for six different conditions of wind speed and sea state. It is to be emphasized that the lines shown are merely statistical averages since the standard deviation of individual measurements is about 5 db. It is interesting to note that neither wind speed nor sea state appear to have any systematic effect on the spectral distribution since all lines show the same uniform decrease in spectrum level with frequency of about 5 db per octave. This behavior may be represented by the equation

$$N_f = N_1 - 17 \log f \qquad (15.38)$$

where N_f is the spectrum level at a frequency of f kc/sec and N_1 is the spectrum level at a frequency of 1 kc/sec. Ambient sea noise appears to be essentially isotropic at depths up to a few hundred meters, i.e., it comes equally from all directions and does not vary appreciably with depth.

Ambient sea noise, which is always present, sets an ultimate limit on the detectability of wanted sonar echoes. When an echo-ranging ship is moving at appreciable speeds, its own self-noise is usually greater than the ambient sea noise. This self-noise increases as the ship's speed is increased. It may increase by more than 2 db per knot at speeds in excess of 15 knots in the case of destroyers. It also depends on the location of the receiving transducer, the type of ship, and the direction from which echoes are being received. In essence, it differs so widely from one situation to another that typical values cannot be given.

In all echo-ranging systems a directional receiving transducer is used. This may be either the same transducer used in transmission or a separate transducer. Because of the directionality of the receiving transducer, the effective pressure level of the masking noise will be reduced by the transducer's receiving directivity index d_r. One additional factor influences the effective level of the masking noise, namely, the bandwidth w in cycles/sec of the receiving system. A finite bandwidth is required in order to allow the short echo-pulse to attain full value and to allow for shifts produced in the echo frequency by the doppler effect. The effective level of the masking noise L_N in decibels is therefore given by

$$L_N = N_f + 10 \log w - d_r \qquad (15.39)$$

where the term $10 \log w$ converts the spectrum level N_f to a band level in accordance with equation 13.6.

For each particular sonar detection system, whether the echo signal is presented audibly or visually, the echo level E leading to a 50 per cent probability of detection may be related to the effective noise level L_N by the equation

$$E = L_N + M_N \qquad (15.40)$$

The quantity M_N is known as the *recognition differential* of the detection system for masking noise. It is expressed in decibels and may be either positive or negative, depending upon the particular detection system.

As an example of the use of equation 15.40, let us assume that the receiving system of the example previously presented in Sect. 15.9 has a bandwidth of 1000 cycles/sec, that its recognition differential is +3 db, that the same transducer is used for receiving as for transmitting so that $d_r = 20$ db and that the masking noise corresponds to a sea state of 3. From Fig. 15.13 it is seen that the spectrum level is $N_f = -57$ db in this sea state at a frequency of 20 kc/sec. Therefore

$$L_N + M_N = -57 + 10 \log 1000 - 20 + 3 = -44 \text{ db}$$

Upon comparing this level with the previously computed echo level of $(-44 - 2A)$, we see that the probability of detection will be about 50 per cent provided the transmission anomaly A is zero. However, if $A = 10$ db, a very modest figure for a range of 5000 m, the deficiency of the actual echo level of -64 db relative to the required echo level of -44 db is so large that the probability of detection would be nil.

The equations developed in this section and the preceding two sections may be combined in many different ways so as to produce equations that are useful in designing sonar systems and predicting their capabilities. One such equation is obtained by substituting the expressions for E and L_N from equations 15.34 and 15.39 into equation 15.40 and solving for the two-way transmission loss, $2H = 40 \log r + 2ar + 2A$. The result is

$$40 \log r + 2ar + 2A = S + T + d_r - N_f - M_N - 10 \log w \qquad (15.41)$$

This transcendental equation for range r is the basic echo-ranging equation and has a multiplicity of uses. For instance, the influence on detection range may be computed for changes in each of the various parameters on the right-hand side of the equation. Since many of the terms in the equation are dependent on frequency, curves may be computed showing how the detection range depends on frequency and thereby determine optimum frequencies to be used in various situations.

15.11 Masking by Reverberation. When a short pulse of sound energy is radiated into a room, the sound echoes and re-echoes from the walls, ceiling, and floor for a considerable time. This phenomenon was discussed in Chapter 14 and is called reverberation. When an echo-ranging pulse of sound is emitted into the ocean, a superficially similar phenomenon is observed to which the name *reverberation* is also applied. However, while the ocean has a surface and a bottom it lacks an equivalent of the four

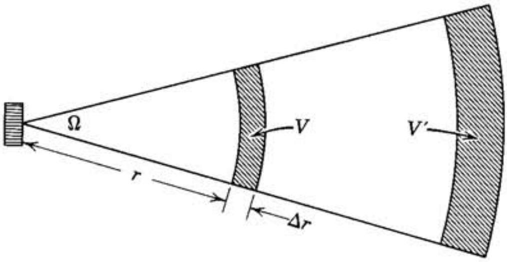

Fig. 15.14. Active volume V producing reverberation at the time $t = 2r/c$.

walls of a room, and both the equations and causes of underwater reverberation are somewhat different from those produced in the air within a room. If the sea surface and bottom were mirror-flat and it if were also free from internal reflectors such as air bubbles, fish, or small thermal inhomogeneities, no sound would be scattered back to the transmitting transducer and no reverberation would be observed. However, there are many irregularities on the ocean bottom, each little wavelet on the ocean surface scatters sound, and the body of the ocean contains many scatterers. The combined effect of echoes from all of these scatterers produces a level of reverberation at the transducer that will tend to mask the returning individual echo from any wanted target, such as that from a submarine.

As a specific example, let us derive an expression for the reverberation level that exists when the scattering is produced by a large number of small scatterers, assumed uniformly distributed throughout the body of the ocean. In addition, let us assume that the transducer emits a short pulse of energy of Δt seconds duration and that the sound energy is radiated uniformly over a sound beam subtending a solid angle of Ω steradians, with no energy being radiated or received outside of this solid angle. This pulse will produce a train of waves of length $\Delta r' = c\,\Delta t$. At any time t thereafter, the remaining nonscattered portion of the radiated sound energy will lie within that part of a spherical shell of radius $r' = ct$ and thickness $\Delta r'$ intercepted by the sound beam and represented by the volume V' of Fig. 15.14. Let us now assume that the same transducer is used for receiving as for transmitting. Since the returning waves producing reverberation at the time t have traveled out to a scatterer and back within this time, they must have been reflected at an earlier time from scatterers located within a shell of radius $r = ct/2$ and thickness $\Delta r = c\,\Delta t/2$ as represented by the volume V of Fig. 15.14. This volume is known as the active volume and is given by the equation

$$V = \Omega r^2\,\Delta r \tag{15.42}$$

Let us next assume that: (1) the average number of scatterers per unit volume is n; (2) each scatterer in effect intercepts sounds over a cross-sectional or *target area* σ; (3) the sound intercepted by each scatterer is reradiated uniformly in all directions. Under these assumptions, one may show that the resulting reverberant sound scattered back to the transducer at a time t after emission, has on the average the same pressure level as that returned by a single target of target strength

$$T_R = 10 \log \frac{n\sigma V}{4\pi} = 10 \log \frac{n\sigma r^2 \Delta r \Omega}{4\pi} \tag{15.43}$$

The sound pressure level L_R (*re* 1 microbar) of the returning reverberations is therefore given by an equation similar to 15.34 as

$$\begin{aligned} L_R &= S + T_R - 2H \\ &= S + 10 \log n\sigma + 10 \log \Delta r + 10 \log \frac{\Omega}{4\pi} + 20 \log r - 2H \\ &= S + 10 \log n\sigma + 10 \log \frac{c\,\Delta t}{2} - d_r - 20 \log r - 2ar - 2A' \end{aligned} \tag{15.44}$$

in which $10 \log (\Omega/4\pi)$ has been replaced by $-d_r$, the receiving directivity index of the transducer, and A' is the transmission anomaly for reverberations. It is to be noted that the transmission anomaly A' associated with reverberations from a multitude of scatterers at a distance r may be quite different from the anomaly A associated with an individual target at this same range.

A number of important conclusions may be drawn from equation 15.44, the most obvious being:

(1) The reverberation level L_R increases directly with the source level S. Since the echo level E also increases directly with the source level, the difference $E - L_R$ is independent of S. Therefore when reverberations are masking the echo, no improvement can be gained by increasing the acoustic output of the transducer.

(2) The reverberation level increases as the pulse duration Δt is increased. Therefore, the difference $E - L_R$ may be increased by decreasing Δt and thereby increase the detectability of the echo providing this decrease in Δt does not degrade the detectability of the echo by some other mechanism.

(3) The decrease in reverberation level with increasing range is given by the term $-(20 \log r + 2ar + 2A')$. This is at a lesser rate than that of the echo level which is as $-(40 \log r + 2ar + 2A)$. Therefore, if the reverberation masks the echo at a range r, the masking will be even greater at increased ranges.

(4) The reverberation level increases as either the number of scatterers per unit volume or their average cross section increases. Typical values of

the product $n\sigma$ range from 10^{-6} to 10^{-7} m^{-1}, which indicates that the scatterers are both small in size and rather sparsely distributed throughout the body of the ocean.

As an example of the use of equation 15.44, let us compute the reverberation level produced at the transducer discussed in Sect. 15.9 when the pulse duration is 0.1 sec and the product $n\sigma = 10^{-6}$ m^{-1}. Then

$$L_R = 124 + 10 \log 10^{-6} + 10 \log \frac{1500 \times 0.1}{2} - 20$$
$$- 20 \log 5000 - 2 \times 0.004 \times 5000 - 2A'$$
$$= -51 - 2A'$$

As was the case with masking noise, in order for the echo level to have a 50 per cent probability of detection, it must be related to the reverberation level by the equation

$$E = L_R + M_R \tag{15.45}$$

where M_R is the recognition differential of the detection system for masking reverberation. It is in general different from M_N, that for masking noise. The numerical value of M_R may range from positive values when the reverberation level is fluctuating widely to negative ones when the speed of the target through the water is high enough to cause an appreciable difference between its doppler-shifted frequency and that of the reverberations. If we now substitute $-(44 + 2A)$ for E in equation 15.45 and $-(51 + 2A')$ for L_R, the required recognition differential of the detection system for a 50 per cent probability of detection is

$$M_R = 7 + 2(A' - A) \text{ db}$$

With a slight modification, the above theory of volume reverberation may be applied to scattering that occurs at either the surface or the bottom of the sea, the primary difference being that we are dealing with reflections originating in an active area S, rather than an active volume V. The area S is that intercepted at either the surface or the bottom by the active volume V. A second difference between the two types of reverberation arises from the fact that the active area S does not come into existence until the volume V first intercepts the surface or bottom.

Figure 15.15 shows a typical reverberation decay curve, such as might be observed at a transducer at a depth of 10 m in deep water. After a lapse of approximately 0.3 sec the initial high-level reverberations caused by nearby volume scattering are supplemented by reverberations from the surface, and about 1 second after the initiation of the pulse there is a second increase in reverberation due to scattering from the bottom. If a highly directional source is beamed horizontally, the active volume of the beam will not reach either the surface or the bottom until a much longer time has elapsed, and the supplemental surface and bottom reverberations will be much weaker than those of Fig. 15.15. By contrast, surface and bottom reverberations in very shallow water are usually of a higher level than volume reverberation.

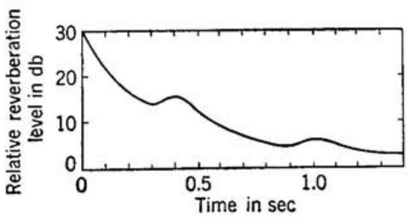

Fig. 15.15. Decay of reverberation in deep water.

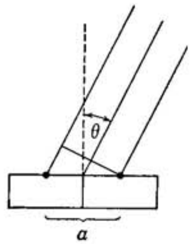

Fig. 15.16. Use of a split transducer in determining direction.

15.12 Additional Parameters Significant to Echo-Ranging Sonars. As has already been noted, the time interval t between the transmission of a radiated pulse and the reception of a returning echo includes intervals of $t/2$ seconds duration on both the outward and return paths. Therefore the range is given by

$$r = \frac{ct}{2} = 750t \text{ m} \tag{15.46}$$

The ability to separate echoes from two distinct targets located on the same bearing is a function of the pulse duration Δt. Echoes from two such targets may be separated provided their difference in range is greater than

$$\Delta r = \frac{c\,\Delta t}{2} = 750\,\Delta t \text{ m} \tag{15.47}$$

Two principal methods are available for determining the bearing of a target from which echoes are being received. The simplest is that of training the sound beam to the direction from which the strongest echoes are received. Since a transducer has similar directional characteristics both in reception and in transmission, the observed echo level will be a maximum when the axis of the transducer is centered on the target. If a so-called *split* transducer is used, a somewhat more complicated but considerably more accurate method may be employed. In such a transducer the radiating surface are divided along a vertical line into two equal areas, which are driven in synchronism during radiation of the pulse. During reception, however, the two halves act separately, and the phase relationship between the two received signals is compared in an appropriate electrical network. If the echo returns from a direction making an angle θ to the right of the central axis of the transducer (Fig. 15.16), the signal in the right half leads that in the left half by

$$\Delta\phi = \frac{2\pi a}{\lambda} \sin\theta \text{ radians} \tag{15.48}$$

where a is the distance between the effective centers of the two halves of the transducer, and λ is the wavelength in water. For a rectangular transducer, a is one half its width. For a circular transducer, a is slightly less than its radius. The bearing of a target can be determined to a high degree of precision by rotating the transducer to such a position that $\Delta\phi = 0$. Furthermore, the sense of the phase difference corresponding to an off-axis target, i.e., leading or lagging phase in the right half, can be used to inform the sonar operator of the direction in which the transducer should be trained in order to center the sound beam on the target. The use of a split transducer for determining the direction of underwater sounds has much in common with our use of two ears in the binaural localization of the direction towards a source of sound. The phase angle $\Delta\phi$ observed at any particular angle θ is greater for sounds of short wavelength, i.e., high frequency, so that the direction of arrival of a high-frequency sound can be determined more precisely than that of a low-frequency sound.

Frequencies normally used in echo-ranging are so high that they are either above the normal audible range or are at least so high as to be above those frequencies near 1000 cycles/sec where our hearing capability is most acute. When the echoes are portrayed visually, either by a brightening or displacement of a spot on the face of a cathode-ray tube or by some other means, the signal is merely the detected envelope of the high-frequency echo and the latter's frequency has no significance. When, on the other hand, an audible presentation is desired, the echo frequency is lowered by beating it against that of a local oscillator in the receiving amplifier, thus producing a difference frequency in the desired audible range, usually one of about 800 cycles/sec.

In general, the observed frequency of the returning echo is not identical with that radiated by the transducer. This change in frequency is caused by the familiar *doppler effect*, which arises whenever either or both the transducer and the target are moving with respect to the water. It is left as an exercise for the reader to show that the doppler frequency f_d returning to the transducer is given approximately by

$$f_d = f_0 \left[1 + \frac{2(v_s \cos\theta_s - v_t \cos\theta_t)}{c}\right] \tag{15.49}$$

where v_s is the velocity of the source with respect to the water, and v_t is that of the target. In this equation θ_s and θ_t are the respective angles between the directions of the velocities and a radius vector from the source to the target, while f_0 is the driving frequency supplied to the transducer. When the velocity of the source is known, information as to the velocity of the target can be obtained from the frequency of the returning echo. It should be noted that in the process of beating an ultrasonic frequency down to a frequency near 800 cycles/sec, the *difference* in frequency between the transmitted and received signals remains unaltered, with the result that the *ratio* of their frequencies changes materially. This leads to a highly exaggerated doppler effect, which facilitates recognition of the motion of the target.

15.13 Fundamental Characteristics of Passive Listening Sonars. The use of passive listening for detecting and locating enemy ships differs from echo-ranging in several ways. In echo-ranging, the searching vessel intentionally projects a sound signal into the water in the expectation that the sound will strike a target ship and that enough of the energy will be reflected back from the target to make it detectable. The primary source of sound is that transmitted by the searching vessel with the target acting only as a secondary source. The associated transmission loss is that of a two-way process. In listening, by contrast, the source of the signal is sound emitted directly and involuntarily by the target vessel itself. The associated transmission loss is that of a one-way process. A consideration of the latter suggests that losses by transmission will be much smaller in the case of listening, and that detection should be possible at longer ranges by listening than by echo-ranging, provided only that the sound output of the target is not too small as compared with that of a standard echo-ranging transducer. The sound output of both submarines and surface vessels cruising at normal speeds are usually of such a magnitude that they can be detected by listening sonars at considerably greater ranges than by echo-ranging. Echo-ranging, however, enables both the range and bearing of the target to be determined accurately, whereas listening sonars in their normal configuration give only bearing information.

Listening is used chiefly by submarines. A surface vessel produces considerably more noise than does a submarine, and this noise interferes with the detection of sounds from other ships. On the other hand, the relatively quiet submarines are able to detect the presence of surface vessels rather easily without in turn being detected by the latter. Listening also plays an important part in the detection of submarines by harbor and coastal defense stations. It is also used for detecting the presence of submarines by means of expendable radio sonobuoys. The latter are dropped from aircraft and consist of a listening hydrophone and radio that transmit the received sounds back to the aircraft.

Physical factors involved in listening are essentially the same as those in echo-ranging. The target ship acts as a source of sound that must be transmitted through the water to the receiving hydrophone system and detected against a background of masking noise. The ability to detect the received signal depends upon the following factors:

1. The nature of the sound signal radiated by the source.
2. The magnitude of the one-way transmission loss of sound in the water between the source and receiver.
3. The nature of the masking noise.
4. The directivity index of the receiving hydrophone system.
5. The recognition differential and bandwidth of the detection system.

15.14 Acoustic Output of Ships. The radiated sound output of ships arises primarily from two sources. One is the so-called *cavitation* noise generated at its propellers and the other is *machinery* noise. In general, the sound has a continuous spectrum which decreases in level with increasing frequency, upon which are superposed strong lines associated with individual machinery components. The main propulsion system is usually the predominant source of the strongest of such lines. Cavitation noise arises when the propellers are turning so rapidly that the reduced pressures in the water near the blades, as produced by the Bernoulli effect, cause air and vapor bubbles to form. Upon leaving the immediate vicinity of the propellers, the pressure of the water returns to its normal hydrostatic value causing the vapor bubbles to collapse and generate a continuous-spectrum sound much like that of frying fat. At low shaft rates, cavitation noise is not present. However, when a shaft rate is reached at which cavitation begins, the resulting noise is usually the predominant contributor to the overall sound pressure level radiated by the ship. Since the onset of propeller cavitation is retarded by an increase in hydrostatic pressure, submerged submarines may prevent the onset of cavitation noise by operating at increased depths as their speed is increased.

Figure 15.17 is an idealized spectrum plot of the acoustic output of a submerged submarine. Values given are *source spectrum levels* assumed to be measured at one meter from the effective center of the source of radiated sound. It is to be noted that superposed on the straight line representing the continuous spectrum are individual spikes corresponding to higher pressure levels at discrete frequencies as produced by individual machinery items. The acoustic outputs of other types of ships are usually considerably higher than that shown in Fig. 15.17 for a submarine. For

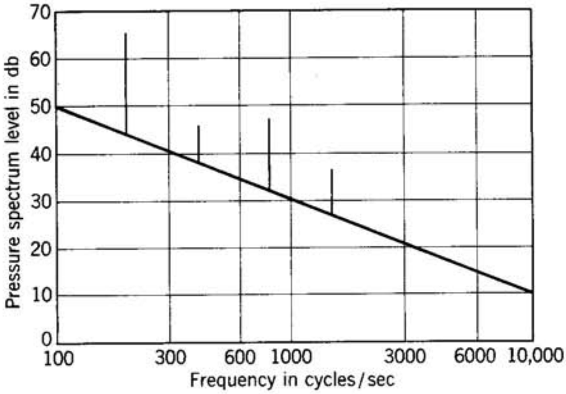

Fig. 15.17. Idealized acoustic output of a medium-speed submarine in decibels relative to 1 microbar.

instance, that of a destroyer would average at least 10 db higher and that of an aircraft carrier some 25 db higher.

The spectrum levels plotted in Fig. 15.17 are in decibels relative to 1 microbar. Frequently, the noise output of ships is measured and plotted in decibels relative to 0.0002 microbar, leading to pressure levels 74 db greater than those shown in Fig. 15.17. However, so as to use pressure levels consistent with those used earlier in this chapter for the echo-ranging systems, we have chosen to express the acoustic output of ships in pressure levels relative to 1 microbar.

The acoustic output of a ship, such as that presented in Fig. 15.17, will generate two basic kinds of signals at a distance r from the ship. One will consist of individual frequency components having sound pressure levels L_S (*re* 1 microbar) given by the equation

$$L_S = S - H \tag{15.50}$$

where S is the source level of any one of the individual spikes shown in Fig. 15.17 and H is the one-way transmission loss between source and receiver. The other will consist of band pressure levels L_w given by the equation

$$L_w = S_f + 10 \log w - H \tag{15.51}$$

where S_f is the source spectrum level at the center frequency f of a continuous spectrum of bandwidth w.

15.15 Prediction of Passive Detection Ranges. Two basic types of noises will tend to mask detection of the signals given by equations 15.50 and 15.51. One is self-noise generated by the listening vessel. Since its influence will depend on such specific factors as the particular type of ship, the location of the receiving hydrophone system on the ship, the speed of the ship, etc., a general discussion is not possible. However, as was the case with active sonars, the ambient sea noise sets an ultimate limit on the detectability of signals with passive sonars. The effective level of this masking noise L_N is given by equation 15.39 as previously derived in Sect. 15.10. Also, for a 50 per cent probability of detection the signal levels L_S and L_w must respectively satisfy the equations

$$L_S = L_N + M_N \tag{15.52}$$

and

$$L_w = L_N + M_N \tag{15.52a}$$

where M_N is the recognition differential of the detection system for masking noise.

Upon substituting appropriate expressions for the various terms in equation 15.52,

$$20 \log r + ar + A = S + d_r - N_f - M_N - 10 \log w \tag{15.53}$$

is obtained for computing the detection range of a line component of source level S in the acoustic output of the target ship. Similarly, the detection range equation for the continuous spectrum output level S_f is

$$20 \log r + ar + A = S_f + d_r - N_f - M_N \tag{15.54}$$

For visual types of detection systems, M_N may be either positive or negative and the bandwidth w may range from about 1 cycle/sec to 1000 cycles/sec. In audible detection systems, the operator listens directly to an amplified reproduction of the sounds being received at the hydrophone and as a consequence, $M_N = 0$ and w is the critical bandwidth of the human ear as given by Fig. 13.17.

When the passive detection of low-frequency machinery line components is being computed by means of equation 15.53, the small changes occurring in the terms ar and d_r as the frequency is changed are relatively unimportant. Therefore, the greatest detection range is usually obtained at that frequency for which the expression $(S - N_f)$ has a maximum value. By contrast, when the range of passive detection of cavitation or other continuous-spectrum noise is being computed, the difference $(S_f - N_f)$ occurring in equation 15.54 is often nearly independent of frequency and therefore, the maximum range will be obtained at that frequency which maximizes the difference $(d_r - ar)$.

15.16 Passive Detection Hydrophone Systems. Both equations 15.53 and 15.54 indicate that an increase in the receiving directivity index d_r will also increase the detection range, if all other parameters remain fixed.

The simple line hydrophone, shown in Fig. 15.18, has been widely used as a receiving hydrophone for passive sonars. Such hydrophones are usually constructed from a number of collinear cylindrical ceramic or magnetostrictive elements (Sects. 12.11 and 12.15) whose electrical outputs are connected in series. When sounds are incident on such a line hydrophone of length L from a direction making an angle θ with respect to a perpendicular plane through the center of the hydrophone (Fig. 15.18), the voltage generated E_θ is given by

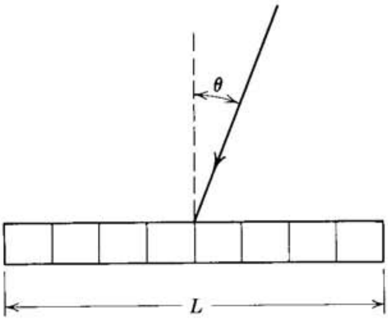

Fig. 15.18. Segmented cylindrical line hydrophone.

$$E_\theta = E_0 \frac{\sin\left(\frac{\pi L}{\lambda}\sin\theta\right)}{\frac{\pi L}{\lambda}\sin\theta} \tag{15.55}$$

where E_0 is the voltage generated when $\theta = 0$ and λ is the wavelength of the waves being received. When $L \ll \lambda$, $E_\theta \approx E_0$ for all angles of incidence θ and consequently, the receiving pattern of the hydrophone is omnidirectional and $d_r \approx 0$. By contrast, when $L > \lambda$, the receiving directivity index d_r is given by

$$d_r = 10 \log \frac{2L}{\lambda} \tag{15.56}$$

Equation 15.56 indicates that in order to have a large receiving directivity index at low frequencies and thereby increase the detection range, L must be large compared to a wavelength. In actual practice, L does not exceed about 2 meters for true line hydrophones. However, a receiving system may be constructed that is equivalent to a long line hydrophone. Such a system, known as a *line array*, is constructed from a large number of equally spaced small omnidirectional hydrophones as shown in Fig. 15.19. If the outputs of n such hydrophones, spaced at intervals a, are connected in series, the voltage E_θ generated by sound incident along a direction θ is given by

$$E_\theta = E_0 \frac{\sin\left(\frac{n\pi a}{\lambda}\sin\theta\right)}{n\sin\left(\frac{\pi a}{\lambda}\sin\theta\right)} \tag{15.57}$$

where E_0 is the voltage generated when $\theta = 0$. It is left as an exercise for the reader to show that when $a < \lambda/4$, the directivity pattern given by

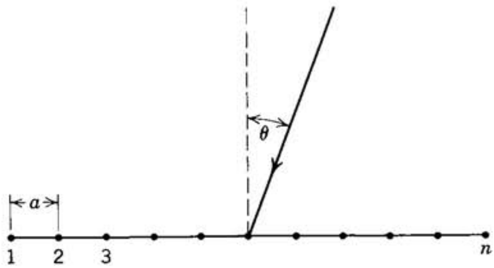

Fig. 15.19. Line array of small hydrophones.

equation 15.57 is essentially the same as that given by equation 15.55 for a line hydrophone of length $L = na$. Correspondingly, the receiving directivity index of such a line array will be given by

$$d_r = 10 \log \frac{2na}{\lambda} \tag{15.58}$$

when $na > \lambda$. By use of long line-arrays constructed from a large number of properly spaced hydrophone elements, it is possible to obtain a significant receiving directivity index at frequencies as low as 100 cycles/sec.

In order to rotate the axis of greatest receiving sensitivity to the direction from which the sound waves are being received, a line hydrophone is usually rotated about an axis through its center until its length is parallel to the incident wave surfaces. Such a procedure is not feasible for a long line-array of individual hydrophones. They are instead steered electrically by inserting controlled electrical time delays into the signals from adjacent hydrophone elements before they are combined in series. For instance, if the separation between adjacent hydrophone elements is a, one may show that the insertion of successive phase differences $\Delta\phi$ radians between adjacent hydrophone signals will steer the main axis of the beam by an angle θ as given by equation 15.48.

It is also possible to use as passive receivers, either individual transducers or hydrophone array systems having an effective plane surface area S. The receiving directivity index of such a system may be computed from equation 15.32.

As an example of passive detection ranges, let us compute the audible detection range of the 200-cycle/sec noise spike in the acoustic output of the submarine shown in Fig. 15.17. The receiver system is assumed to be a line array composed of 20 small hydrophones spaced 1 meter apart. The masking noise is assumed to be that of a sea state of 2. An inspection of Fig. 15.13 shows that $N_f = -28$ db at 200 cycles/sec in a sea state of 2.

The noise spike at 200 cycles/sec in Fig. 15.17 is seen to have a source level of $S = 65$ db. At 200 cycles/sec, the wavelength in water is

$$\lambda = \frac{1500}{200} = 7.5 \text{ m}$$

Therefore the receiving directivity index of the line array at this frequency, as given by equation 15.58 is

$$d_r = 10 \log \frac{2 \times 20}{7.5} = 7 \text{ db}$$

Since audible means are being used for detection, w is determined by the critical bandwidth of the human ear at 200 cycles/sec, which is given by Fig. 13.17 as 40 cycles/sec. Finally, for audible presentation $M_V = 0$. When all of these various quantities are substituted into equation 15.53, the result is

$$20 \log r + ar + A = 65 + 7 - (-28) - 0 - 10 \log 40 = 84 \text{ db}$$

Upon assuming that both the terms ar and A are negligible at a frequency of 200 cycles/sec, the predicted passive detection range is

$$r = 16{,}000 \text{ m}$$

which is typical of those obtained in actual practice.

15.17 Additional Applications of Underwater Acoustics. Many additional military and commercial uses have been found for underwater acoustic waves. For instance, both active and passive acoustic torpedoes have been designed to home on ships. Acoustic mines may be actuated by the noise output of nearby ships and may be swept by sound sources of an equivalent output. Fathometers may be used to measure the depth of the water below the keel of a ship or to locate schools of fish. Finally, acoustic waves may be employed as a means of underwater speech communication. One method used for such communication is, in its essentials, identical with that used for radio communication. Here the water serves as a medium for transmitting an 8 kc/sec carrier wave, which is modulated at audio frequencies. Any of the types of modulation common to radio transmission may be employed, e.g., amplitude modulation, suppressed-carrier single-side-band amplitude modulation, frequency modulation, or phase modulation, and ranges in excess of 10 miles have been obtained.

PROBLEMS

Note: In all problems below assume the transmission anomaly $A = 0$ and the sound absorption constant a to be that in 5°C water unless otherwise specified. All sound pressure levels are expressed in decibels relative to 1 microbar.

15.1. (*a*) By means of equation 15.1, compute the velocity of sound in sea water at a depth of 500 m, if the temperature is 5°C and the salinity is 32 parts per thousand. (*b*) By means of equation 9.34, compute the sound absorption coefficient a in this water for a frequency of 15 kc/sec.

15.2. A 30-kc/sec sonar transducer produces an axial sound pressure level of 40 db at a distance of 1000 m in sea water. (*a*) What is the axial pressure level at one meter? (*b*) at 2000 m? (*c*) At what distance will the axial pressure level be reduced to 0 db? (*d*) At what distance will the total transmission loss resulting from spherical divergence be equal to that caused by absorption? (*e*) At what distance is the rate of transmission loss associated with spherical divergence equal to that associated with absorption?

15.3. Show that $x = \sqrt{2c_0d/g}$ is an approximate equation giving the horizontal distance x in which an initially horizontal ray will reach a depth d in a layer of water having a constant negative velocity gradient of magnitude g.

15.4. The velocity of sound in sea water of 35 parts per thousand salinity decreases uniformly from a value of 1540 m/sec at the surface to 1520 m/sec at a depth of 50 m. (*a*) What is the velocity gradient? (*b*) What is the average temperature gradient? (*c*) What horizontal distance is required for a horizontal ray at the surface to reach a depth of 50 m? (*d*) What will be the downward angle of such a ray upon reaching this level?

15.5. An isothermal layer of sea water has a temperature of 20°C, a salinity of 35 parts per thousand, and extends to a depth of 40 m. A sonar transducer is located at a depth of 10 m in this isothermal layer. (*a*) In what horizontal distance will a ray leaving the transducer in a horizontal direction, reach the surface of the water? (*b*) What is the downward angle from the transducer of a ray that will become horizontal at the bottom of the isothermal layer? (*c*) In what horizontal distance will the ray of part (*b*) reach the bottom of the isothermal layer? (*d*) The velocity of sound decreases below the isothermal layer at a rate of 0.2 m/sec per meter. What is the depth below the surface of a ray originally starting downward at an angle of 3° from the transducer, upon traveling a horizontal distance of 2300 m?

15.6. A sonar transducer is at a depth of 5 m in shallow water having a flat bottom at a depth of 35 m. The velocity of sound in the water decreases regularly from a value of 1500 m/sec at the surface to 1493 m/sec at the bottom. (*a*) Calculate and plot the path for a ray leaving the transducer in a horizontal direction, until it strikes the bottom a second time. Assume the first reflection from the bottom to be specular. (*b*) Similarly calculate and plot the paths for rays initially 1° above and 1° below the horizontal.

15.7. A sonar transducer is at a depth of 10 m in water having a constant negative velocity gradient of 0.2 m/sec per meter. The velocity of sound at the transducer depth is 1500 m/sec. When the axis of the transducer is tilted down 6° from the horizontal, its beam appears to be centered on a target submarine at a horizontal distance of 1000 m. (*a*) What is the apparent depth of the submarine? (*b*) What is the true depth of the submarine?

15.8. A surface sound channel is formed by a layer of water in which the velocity of sound decreases uniformly from 1500 m/sec at the surface to 1498 m/sec at a depth of 10 m and then increases uniformly to reach 1500 m/sec again at a depth of 100 m. (*a*) What is the maximum angle with which a ray may cross the axis of the channel and still remain in the channel? (*b*) What is the horizontal distance between crossings for such a ray in the upper part of the channel? (*c*) in the lower part of the channel? (*d*) Derive a general expression giving all angles of departure θ from a sound source on the axis of the above sound channel which will result in rays recrossing the channel axis at a distance of 3000 m.

15.9. (*a*) Derive equation 15.21 from equation 15.20. (*b*) What is the difference in time for a ray along the axis to travel the horizontal distance of part (*c*) of Problem 15.8 compared to that required for a ray crossing the axis at the maximum possible downward angle? (*c*) At what depths does the horizontal component of the velocity of the latter ray exceed that of the axial ray?

15.10. The velocity of sound in sea water decreases regularly from a value of 1500 m/sec at the surface to a value of 1470 m/sec at a depth of 600 m and then increases regularly to again reach a value of 1500 m/sec at a depth of 2400 m. (*a*) What is the maximum angle with which a sound ray may cross the axis of the resulting sound channel and not come within 100 m of the surface? (*b*) What are the two maxima angles with which rays may cross the axis of the channel so as first to recross it at a horizontal distance of 10,000 m? (*c*) What difference in time will be required for each of the rays of part (*b*) to travel this horizontal distance? (*d*) If a ray starts out initially at an upward angle of 0.5° at the axis of the channel, how many times will it cross the axis in traveling a horizontal distance of 10,000 m?

15.11. (*a*) Derive equation 15.25. (*b*) If $d = 10$ m, $h = 10$ m, and $r = 100$ m, what is the difference between the correct value of Δr and that given by equation 15.25?

15.12. Given a sound source of spherically diverging waves of 1000-cycles/sec frequency located 5 m below the surface in sea water. The acoustic output of the source is such as to produce an rms pressure amplitude of 200 microbars at 1 m distance from the center of the source. (*a*) Assuming 100 per cent reflection at the surface, i.e., $\mu = 1$, what is the sound pressure level produced at a distance of 200 m at a depth of 1 m? (*b*) At a depth of 5 m? (*c*) at a depth of 10 m? (*d*) What would be the sound pressure level produced by the direct wave alone at a distance of 200 m? (*e*) Repeat the problem for $\mu = 0.5$.

15.13. (*a*) Assuming $\mu = 1$, derive an equation for the distance r, expressed in terms of k, h, and d, beyond which the transmission anomaly caused by the surface image effect is always greater than 10 db. (*b*) What is this distance when $f = 500$ cycles/sec, $d = 10$ m, and $h = 20$ m?

15.14. Given a sound source of diverging spherical waves of 50-cycles/sec frequency to be located at a depth of 30 m in water having a hard bottom at a depth of 60 m. The acoustic pressure produced at a distance of 1 m from the center of the source is 1000 microbars. The magnitude of the pressure reflection coefficient at the surface is $\mu = 0.8$ and that at the bottom is $\mu = 0.5$. (*a*) Compute the pressures produced at a horizontal distance of 100 m from the source at a depth of 30 m, for the direct ray and for the reflected rays coming from the images I, S', I', and S'' of Fig. 15.11. (*b*) Considering the velocity of sound to be 1500 m/sec, compute the phase differences between the above rays and the resultant pressure amplitude of their combination.

15.15. A sonar transducer of 30-cm radius radiates 5000 watts of acoustic power at a frequency of 15 kc/sec in the form of a beam similar to that generated by a circular piston mounted in an infinite baffle. (*a*) What is the transmitting directivity index of the transducer? (*b*) What is the axial source level of the transducer? (*c*) What is the width of the beam to the -10 db direction?

15.16. Given a cylindrical transducer, having a height of h cm and a radius of a cm, to radiate I_s watts/cm² from its surface at a frequency of f kc/sec. (*a*) Derive a general equation for computing its source level S in terms of these quantities. (*b*) Compute S, if $I_s = 2$ watts/cm², $f = 25$ kc/sec, $a = 20$ cm, and $h = 30$ cm. (*c*) What is the acoustic output of this transducer in watts? (*d*) What is its directivity index?

15.17. A sonar transducer produces a beam having a source level of 120 db. The transmitted frequency is 15 kc/sec. (*a*) What will be the sound pressure level produced at a distance of 3000 m? (*b*) What will be the echo level returned from a spherical target of 20 m radius at a distance of 3000 m?

15.18. (*a*) Derive equation 15.37 from the general equation defining target strength as given by equation 15.35. (*b*) Show that equation 15.36 is a special case of equation 15.37.

15.19. A certain sonar equipment is capable of echo-ranging at a frequency of 30 kc/sec out to a maximum detection range of 3000 m on a given submarine target. (*a*) If the source level of the transducer is increased by 20 db, what will be the new maximum detection range of the sonar equipment for the same submarine target? (*b*) If the transmitted frequency is lowered to 15 kc/sec, without changing the physical dimensions of the transducer or its acoustic output in watts from that leading to a 3000-m detection range, what will be the new maximum detection range? Assume the transducer to produce a searchlight type of beam and that the detection is masked by ambient noise.

15.20. (*a*) Give the radius and acoustic output for a searchlight type of sonar transducer having a directivity index of 25 db and source level of 115 db at a frequency of 40 kc/sec. (*b*) What would be the level of a returning echo from a one meter diameter spherical mine case at a distance of 500 m? (*c*) Estimate the audible detectability of this echo when masked by ambient noise corresponding to a sea state of 3. Assume $M_x = +10$ db for sound in a critical bandwidth of 40 cycles/sec.

15.21. If the sonar equipment of Problem 15.20 generates an output pulse of 0.05 sec duration, at what range will the reverberation level produced by scatterers of a density and size such that $n\sigma = 10^{-6}\ \text{m}^{-1}$ be equal to the echo level from the mine case at the same range?

15.22. (*a*) Derive a general equation for the echo level returned from the ocean bottom at a depth of r meters for a fathometer having a transducer of source level S and directivity index d. Assume the bottom to have a sound power reflection coefficient α_r and to diffusely reflect the incident sound, i.e., uniformly over a hemisphere. (*b*) If $S = 100$ db, $d = 20$ db, $f = 30$ kc/sec, and $\alpha_r = 0.1$, what echo level will be returned from the bottom at a depth of 1000 m?

15.23. Derive equation 15.49 by use of the fundamental doppler-effect equation

$$f_d = f_o\left(\frac{c \pm v'}{c \pm v''}\right)$$

where v' is the velocity of an observer and v'' that of a source with respect to the medium. Assume both source ship and target ship velocities to be small as compared to that of sound. What must be the relative velocity between source and target in order to produce a total doppler shift of 200 cycles/sec at a frequency of 20 kc/sec?

15.24. (*a*) Calculate the source level of the continuous-spectrum band of frequencies between 100 and 300 cycles/sec for a submarine having an acoustic output as shown in Fig. 15.17. (*b*) Including the noise spike at 200 cycles/sec, what is the overall source level in this band? (*c*) What is the overall source level in the band of frequencies between 1000 and 10,000 cycles/sec? (*d*) What is the total acoustic output of the above submarine in watts?

15.25. Given a submarine to produce a sound output as indicated in Fig. 15.17. (*a*) If the detection system consists of an omnidirectional hydrophone, filters out all sounds outside of a band from 300 to 600 cycles/sec, and has a recognition differential of $M_N = 5$ db, at what distance will the submarine have a 50 per cent probability of detection in a sea state of 3? (*b*) Similarly, compute the audible detection range of the noise spike at 200 cycles/sec. For such detection, assume that $M_N = 0$ db and that the filtering action is that associated with the critical bandwidth of the human ear.

15.26. The receiving transducer of a passive acoustic homing torpedo is assumed to have a directivity index of 10 db and to receive frequencies in a band between 9 and 10 kc/sec. (*a*) What is the effective band pressure level of the ambient noise picked up by this transducer in a sea state of 6? (*b*) If the level of a signal in the above band required to actuate the homing mechanism of the torpedo is 5 db above that of the masking noise, what is the maximum range at which the torpedo will home on a submarine having an output corresponding to Fig. 15.17?

15.27. (*a*) Derive an expression for determining the optimum frequency f in kc/sec to be used in reaching a given detection range r with a line hydrophone type of passive detection system. Assume the continuous-spectrum noise S_f of the target to have the same dependence on frequency as the masking noise N_f and that the sound absorption constant of the water is given by $a = 0.00001 f^2$ db/m. (*b*) What frequency is optimum for reaching a range of 10,000 meters? (*c*) What range will be reached most effectively at a frequency of 1 kc/sec?

15.28. Given two small hydrophones to be separated by a distance a and that their electrical outputs are connected in series. (*a*) Derive a general expression showing how the series voltage generated by the pair depends upon the angle θ made by an incident ray with a perpendicular plane through the center of the line connecting the two hydrophones. (*b*) Show that your result is equivalent to equation 15.57 for $n = 2$. (*c*) If $a = \lambda$, from what directions θ is the output voltage a maximum? (*d*) What is the angular beam width to the -6 db directions for the major lobe centered on $\theta = 0$?

15.29. Given a line array to consist of 40 small hydrophones spaced at 0.5-m intervals and connected in series. (*a*) What is its receiving directivity index at a frequency of 500 cycles/sec? (*b*) What is the angular beam width to the -6 db directions for the major lobe of the receiving pattern? (*c*) What is the direction and amplitude of voltage response of the first side lobe relative to the major lobe? (*d*) What must be the recognition differential of a visual detection system of 1-cycle/sec bandwidth, if it is to detect a single frequency 500-cycle/sec noise source of 60 db source level at a distance of 100,000 m, when masked by the noise of a sea state of 3?

APPENDIX

Table I Elastic constants, velocity of sound, characteristic impedance

(*a*) SOLIDS

Solid	Density kg/m³ ρ_0	Young's Modulus newtons/m² Y	Shear Modulus newtons/m² G	Bulk Modulus newtons/m² B	Poisson's Ratio σ	Velocity m/sec c		Characteristic Impedance MKS rayls $\rho_0 c$	
						Bar	Bulk	Bar	Bulk
		$\times 10^{10}$	$\times 10^{10}$	$\times 10^{10}$				$\times 10^6$	$\times 10^6$
Aluminum	2700	7.1	2.4	7.5	0.33	5150	6300	13.9	17.0
Brass	8500	10.4	3.8	13.6	0.37	3500	4700	29.8	40.0
Copper	8900	12.2	4.4	16.0	0.35	3700	5000	33.0	44.5
Iron (cast)	7700	10.5	4.4	8.6	0.28	3700	4350	28.5	33.5
Lead	11300	1.65	0.55	4.2	0.44	1200	2050	13.6	23.2
Nickel	8800	21.0	8.0	19.0	0.31	4900	5850	43.0	51.5
Silver	10500	7.8	2.8	10.5	0.37	2700	3700	28.4	39.0
Steel	7700	19.5	8.3	17.0	0.28	5050	6100	39.0	47.0
Glass (Pyrex)	2300	6.2	2.5	3.9	0.24	5200	5600	12.0	12.9
Quartz (X-cut)	2650	7.9	3.9	3.3	0.33	5450	5750	14.5	15.3
Lucite	1200	0.4	0.14	0.65	0.4	1800	2650	2.15	3.2
Concrete	2600	—	—	—	—	—	3100	—	8.0
Ice	920	—	—	—	—	—	3200	—	2.95
Cork	240	—	—	—	—	—	500	—	0.12
Oak	720	—	—	—	—	—	4000	—	2.9
Pine	450	—	—	—	—	—	3500	—	1.57
Rubber (hard)	1100	0.23	0.1	0.5	0.4	1450	2400	1.6	2.64
Rubber (soft)	950	0.0005	—	0.1	0.5	70	1050	0.065	1.0
Rubber (rho-c)	1000	—	—	0.24	—	—	1550	—	1.55

Table I (continued)

Table I (continued)

(*b*) LIQUIDS

Liquid	Temperature °C t	Density kg/m³ ρ_0	Bulk Modulus newtons/m² B_T	Ratio of Specific Heats γ	Velocity m/sec c	Characteristic Impedance MKS Rayls $\rho_0 c$	Coefficient of Viscosity newton sec/m² η
			$\times 10^9$			$\times 10^6$	
Water (fresh)	20	998	2.18	1.004	1481	1.48	0.001
Water (sea)	13	1026	2.28	1.01	1500	1.54	0.001
Alcohol (ethyl)	20	790	—	—	1150	0.91	0.0012
Caster oil	20	950	—	—	1540	1.45	0.96
Mercury	20	13600	25.3	1.13	1450	19.7	0.0016
Turpentine	20	870	1.07	1.27	1250	1.11	0.0015
Glycerin	20	1260	—	—	1980	2.5	1.2

(*c*) GASES
(at a pressure of 1.013×10^5 newtons/m²)

Gas	Temperature °C t	Density kg/m³ ρ_0	Ratio of Specific Heats γ	Velocity m/sec c	Characteristic Impedance MKS rayls $\rho_0 c$	Coefficient of Viscosity newton sec/m² η
Air	0	1.293	1.402	331.6	428	0.000017
Air	20	1.21	1.402	343	415	0.0000181
Oxygen	0	1.43	1.40	317.2	453	0.00002
CO_2 (low freq.)	0	1.98	1.304	258	512	0.0000145
CO_2 (high freq.)	0	1.98	1.40	268.6	532	0.0000145
Hydrogen	0	0.09	1.41	1269.5	114	0.0000088
Steam	100	0.6	1.324	404.8	242	0.000013

Table II Trigonometric and hyperbolic functions

x radians	$\sin x$	$\cos x$	$\sinh x$	$\cosh x$	e^x	e^{-x}
0.0	0.0000	1.0000	0.0000	1.0000	1.0000	1.0000
0.2	0.1987	0.9801	0.2013	1.0201	1.2214	0.8187
0.4	0.3894	0.9211	0.4108	1.0811	1.4918	0.6703
0.6	0.5646	0.8253	0.6367	1.1855	1.8221	0.5488
0.8	0.7174	0.6967	0.8881	1.3374	2.2255	0.4493
1.0	0.8415	0.5403	1.1752	1.5431	2.7183	0.3679
1.2	0.9320	0.3624	1.5095	1.8107	3.3201	0.3012
1.4	0.9854	+0.1700	1.9043	2.1509	4.0552	0.2466
1.6	0.9996	−0.0292	2.3756	2.5775	4.9530	0.2019
1.8	0.9738	−0.2272	2.9422	3.1075	6.0496	0.1653
2.0	0.9093	−0.4161	3.6269	3.7622	7.3891	0.1353
2.2	0.8085	−0.5885	4.4571	4.5679	9.0250	0.1108
2.4	0.6755	−0.7374	5.4662	5.5569	11.023	0.09072
2.6	0.5155	−0.8569	6.6947	6.7690	13.464	0.07427
2.8	0.3350	−0.9422	8.1919	8.2527	16.445	0.06081
3.0	+0.1411	−0.9900	10.018	10.068	20.086	0.04979
3.2	−0.0584	−0.9983	12.246	12.287	24.533	0.04076
3.4	−0.2555	−0.9668	14.965	14.999	29.964	0.03337
3.6	−0.4425	−0.8968	18.285	18.313	36.598	0.02732
3.8	−0.6119	−0.7910	22.339	22.362	44.701	0.02237
4.0	−0.7568	−0.6536	27.290	27.308	54.598	0.01832
4.2	−0.8716	−0.4903	33.336	33.351	66.686	0.01500
4.4	−0.9516	−0.3073	40.719	40.732	81.451	0.01228
4.6	−0.9937	−0.1122	49.737	49.747	99.484	0.01005
4.8	−0.9962	+0.0875	60.751	60.759	121.51	0.00823
5.0	−0.9589	0.2837	74.203	74.210	148.41	0.00674
5.2	−0.8835	0.4685	90.633	90.639	181.27	0.00552
5.4	−0.7728	0.6347	110.70	110.71	221.41	0.00452
5.6	−0.6313	0.7756	135.21	135.22	270.43	0.00370
5.8	−0.4646	0.8855	165.15	165.15	330.30	0.00303
6.0	−0.2794	0.9602	201.71	201.72	403.43	0.00248
6.2	−0.0831	0.9965	246.37	246.38	492.75	0.00203
6.4	+0.1165	0.9932	300.92	300.92	601.85	0.00166
6.6	0.3115	0.9502	367.55	367.55	735.10	0.00136
6.8	0.4941	0.8694	448.92	448.92	897.85	0.00111
7.0	0.6570	0.7539	548.32	548.32	1096.6	0.00091
7.2	0.7937	0.6084	669.72	669.72	1339.4	0.00075
7.4	0.8987	0.4385	817.99	817.99	1636.0	0.00061
7.6	0.9679	0.2513	999.10	999.10	1998.2	0.00050
7.8	0.9985	+0.0540	1220.3	1220.3	2440.6	0.00041
8.0	0.9894	−0.1455	1490.5	1490.5	2981.0	0.00034

Table III Bessel functions

x	$J_0(x)$	$J_1(x)$	$J_2(x)$	$I_0(x)$	$I_1(x)$	$I_2(x)$
0.0	1.0000	0.0000	0.0000	1.0000	0.0000	0.0000
0.2	0.9900	0.0995	0.0050	1.0100	0.1005	0.0050
0.4	0.9604	0.1960	0.0197	1.0404	0.2040	0.0203
0.6	0.9120	0.2867	0.0437	1.0921	0.3137	0.0464
0.8	0.8463	0.3688	0.0758	1.1665	0.4329	0.0843
1.0	0.7652	0.4401	0.1149	1.2661	0.5652	0.1358
1.2	0.6711	0.4983	0.1593	1.3937	0.7147	0.2026
1.4	0.5669	0.5419	0.2074	1.5534	0.8861	0.2876
1.6	0.4554	0.5699	0.2570	1.7500	1.0848	0.3940
1.8	0.3400	0.5815	0.3061	1.9895	1.3172	0.5260
2.0	0.2239	0.5767	0.3528	2.2796	1.5906	0.6890
2.2	0.1104	0.5560	0.3951	2.6292	1.9141	0.8891
2.4	+0.0025	0.5202	0.4310	3.0492	2.2981	1.1111
2.6	−0.0968	0.4708	0.4590	3.5532	2.7554	1.4338
2.8	−0.1850	0.4097	0.4777	4.1575	3.3011	1.7994
3.0	−0.2601	0.3391	0.4861	4.8808	3.9534	2.2452
3.2	−0.3202	0.2613	0.4835	5.7472	4.7343	2.7884
3.4	−0.3643	0.1792	0.4697	6.7848	5.6701	3.4495
3.6	−0.3918	0.0955	0.4448	8.0278	6.7926	4.2538
3.8	−0.4026	+0.0128	0.4093	9.5169	8.1405	5.2323
4.0	−0.3971	−0.0660	0.3641	11.302	9.7594	6.4224
4.2	−0.3766	−0.1386	0.3105	13.443	11.705	7.8683
4.4	−0.3423	−0.2028	0.2501	16.010	14.046	9.6259
4.6	−0.2961	−0.2566	0.1846	19.097	16.863	11.761
4.8	−0.2404	−0.2985	0.1161	22.794	20.253	14.355
5.0	−0.1776	−0.3276	+0.0466	27.240	24.335	17.505
5.2	−0.1103	−0.3432	−0.0217	32.584	29.254	21.332
5.4	−0.0412	−0.3453	−0.0867	39.010	35.181	25.980
5.6	+0.0270	−0.3343	−0.1464	46.738	42.327	31.621
5.8	0.0917	−0.3110	−0.1989	56.039	50.945	38.472
6.0	0.1507	−0.2767	−0.2429	67.235	61.341	46.788
6.2	0.2017	−0.2329	−0.2769	80.717	73.888	56.882
6.4	0.2433	−0.1816	−0.3001	96.963	89.025	69.143
6.6	0.2740	−0.1250	−0.3119	116.54	107.31	84.021
6.8	0.2931	−0.0652	−0.3123	140.14	129.38	102.08
7.0	0.3001	−0.0047	−0.3014	168.59	156.04	124.01
7.2	0.2951	+0.0543	−0.2800	202.92	188.25	150.63
7.4	0.2786	0.1096	−0.2487	244.34	227.17	182.94
7.6	0.2516	0.1592	−0.2097	294.33	274.22	222.17
7.8	0.2154	0.2014	−0.1638	354.68	331.10	269.79
8.0	0.1716	0.2346	−0.1130	427.57	399.87	327.60

Table IV Directivity and impedance functions for a circular piston

x	Directivity Functions ($x = ka \sin \theta$)		Impedance Functions ($x = 2ka$)	
	Pressure	Intensity	Resistance	Reactance
	$\frac{2J_1(x)}{x}$	$\left[\frac{2J_1(x)}{x}\right]^2$	$R_1(x)$	$X_1(x)$
0.0	1.0000	1.0000	0.0000	0.0000
0.2	0.9950	0.9900	0.0050	0.0847
0.4	0.9802	0.9608	0.0198	0.1680
0.6	0.9557	0.9134	0.0443	0.2486
0.8	0.9221	0.8503	0.0779	0.3253
1.0	0.8801	0.7746	0.1199	0.3969
1.2	0.8305	0.6897	0.1695	0.4624
1.4	0.7743	0.5995	0.2257	0.5207
1.6	0.7124	0.5075	0.2876	0.5713
1.8	0.6461	0.4174	0.3539	0.6134
2.0	0.5767	0.3326	0.4233	0.6468
2.2	0.5054	0.2554	0.4946	0.6711
2.4	0.4335	0.1879	0.5665	0.6862
2.6	0.3622	0.1326	0.6378	0.6925
2.8	0.2927	0.0857	0.7073	0.6903
3.0	0.2260	0.0511	0.7740	0.6800
3.2	0.1633	0.0267	0.8367	0.6623
3.4	0.1054	0.0111	0.8946	0.6381
3.6	0.0530	0.0028	0.9470	0.6081
3.8	+0.0068	0.00005	0.9932	0.5733
4.0	−0.0330	0.0011	1.0330	0.5349
4.5	−0.1027	0.0104	1.1027	0.4293
5.0	−0.1310	0.0172	1.1310	0.3232
5.5	−0.1242	0.0154	1.1242	0.2299
6.0	−0.0922	0.0085	1.0922	0.1594
6.5	−0.0473	0.0022	1.0473	0.1159
7.0	−0.0013	0.00000	1.0013	0.0989
7.5	+0.0361	0.0013	0.9639	0.1036
8.0	0.0587	0.0034	0.9413	0.1219
8.5	0.0643	0.0041	0.9357	0.1457
9.0	0.0545	0.0030	0.9455	0.1663
9.5	0.0339	0.0011	0.9661	0.1782
10.0	+0.0087	0.00008	0.9913	0.1784
10.5	−0.0150	0.0002	1.0150	0.1668
11.0	−0.0321	0.0010	1.0321	0.1464
11.5	−0.0397	0.0016	1.0397	0.1216
12.0	−0.0372	0.0014	1.0372	0.0973
12.5	−0.0265	0.0007	1.0265	0.0779
13.0	−0.0108	0.0001	1.0108	0.0662
13.5	+0.0056	0.00003	0.9944	0.0631
14.0	0.0191	0.0004	0.9809	0.0676
14.5	0.0267	0.0007	0.9733	0.0770
15.0	0.0273	0.0007	0.9727	0.0880
15.5	0.0216	0.0005	0.9784	0.0973
16.0	0.0113	0.0001	0.9887	0.1021

Table V Conversion factors

Quantity	MKS Unit	Multiply Value in MKS Units by	To Obtain Value in CGS Units of
Length	meter	10^2	centimeter
Mass	kilogram	10^3	gram
Force	newton	10^5	dyne
Energy	joule	10^7	erg
Power	watt	10^7	erg/sec
Density	kilogram/meter^3	10^{-3}	gram/centimeter^3
Pressure	newton/meter^2	10	dyne/centimeter^2 or microbar
Velocity	meter/sec	10^2	centimeter/sec
Energy density	joule/meter^3	10	erg/centimeter^3
Elastic modulus	newton/meter^2	10	dyne/centimeter^2
Coef. of viscosity	newton sec/meter^2	10	dyne sec/centimeter^2
Volume velocity	meter^3/sec	10^6	centimeter^3/sec
Intensity	watt/meter^2	10^3	erg/sec centimeter^2
Mechanical impedance	MKS mechanical ohm	10^3	CGS mechanical ohm
Specific impedance	MKS rayl	10^{-1}	CGS rayl
Acoustic impedance	MKS acoustic ohm	10^{-5}	CGS acoustic ohm
Acoustic compliance	meter^4 sec^2/kilogram	10^5	centimeter^4 sec^2/gram
Acoustic inertance	kilogram/meter^4	10^{-5}	gram/centimeter^4
Mechanical stiffness	newton/meter	10^3	dyne/centimeter
Flux density	weber/meter^2	10^4	gauss

GLOSSARY OF SYMBOLS

Listed below are the commonly used symbols, together with their various meanings, units, and references to the page where defined or first used.

Symbol	*Meaning*	*Units*	*Page*
a	Acceleration	m/sec^2	7
	Attenuation constant	db/m	237
	Radius	m (meter)	
	Total absorption	sabin	424
A	Amplitude		3
	Transmission anomaly	db	464
B	Amplitude		43
	Bulk modulus	newton/m^2	117
	Magnetic flux density	weber/m^2	249
c	Wave velocity	m/sec, ft/sec	35
C	Acoustic compliance	m^{4}sec^2/kg	191
	Electrical capacitance	farad	26
d	Distance or depth	m, ft	
	Directivity index	db	174
	Piezoelectric strain coefficient	meter/volt	336
D	Decay rate	db/sec	424
	Directivity factor		174
e	Base of natural logarithms	2.718	5
	Instantaneous voltage	volt	249
E	Amplitude of voltage	volt	26
	Echo level	db	480
	Energy	joule	9
f	Frequency	cycle/sec	3
	Instantaneous force	newton	2
F	Amplitude of force	newton	20
g	Velocity gradient	m/sec per meter	466
H	Magnetic field strength	ampere turn/m	367
	Transmission loss	db	462
i	Instantaneous current	ampere	26

Symbol	*Meaning*	*Units*	*Page*
I	Acoustic intensity	watt/m^2	121
	Amplitude of current	ampere	249
IL	Intensity level	db	125
j	Imaginary unit	$\sqrt{-1}$	5
k	Coefficient of electromechanical coupling		336
	Wavelength constant	m^{-1}	40
l	Length	m	
L	Electrical inductance	henry	26
	Loudness	sone	396
	Mean free path	m, ft	428
L_N	Noise level	db	483
L_R	Reverberation level	db	486
LL	Loudness level	phon	396
m	Attenuation constant	ft^{-1}	430
	Horn flare constant	m^{-1}	276
	Mass	kg	3
M	Acoustic inertance	kg/m^4	190
	Microphone response	volt/microbar	296
	Moment of force	newton meter	66
M_N, M_R	Recognition differential	db	484, 487
m, n	Integers		
N_f	Noise spectrum level	db	483
p	Instantaneous acoustic pressure	newton/m^2	109
P	Amplitude of acoustic pressure	newton/m^2, microbar	94
	Absolute pressure	newton/m^2	91
	Effective or rms pressure	newton/m^2, microbar	121
q	Instantaneous electrical charge	coulomb	26
Q	Quality factor		25
	Source strength	m^3/sec	164
r	Gas constant	joule/kg °C	117, 227
	Radius, radial distance	m	
	Specific acoustic resistance	kg/m^2 sec (MKS rayl)	122
R	Acoustic resistance	kg/m^4 sec	189
	Electrical resistance	ohm	26
	Radius of curvature	m	66
R_m	Mechanical resistance	kg/sec	18
R_M	Motional resistance	ohm	251
R_r	Radiation resistance	kg/sec	181
s	Compliance coefficient	m^2/newton	336
	Condensation		109
	Mechanical stiffness constant	newton/m	2
S	Source level	db	479
	Surface or cross-sectional area	m^2	57
SPL	Sound pressure level	db	125

Symbol	*Meaning*	*Units*	*Page*
SWR	Standing wave ratio		135
t	Temperature	°C (centigrade)	117
	Time	sec	
T	Absolute temperature	°K (Kelvin)	117
	Period of vibration	sec	4
	Reverberation time	sec	418
	Target strength	db	481
	Tension in membrane	newton/m	82
	Tension in string	newton	34
TL	Transmission loss	db	139
u, v, w	Components of velocity	m/sec	
v	Phase velocity	m/sec	70
U, V	Amplitude of velocity	m/sec	48
U	Volume velocity	m^3/sec	188
V	Volume	m^3, ft^3	
w	Bandwidth	cycle/sec	483
W	Acoustic power	watt	165
	Electrical power	watt	26
	Mechanical power	watt	23
x, y, z	Rectangular coordinates	m	
x	Specific acoustic reactance	kg/m^2 sec (MKS rayl)	122
X	Acoustic reactance	kg/m^4 sec	190
	Electrical reactance	ohm	26
	Volume displacement	m^3	188
X_m	Mechanical reactance	kg/sec	21
X_r	Radiation reactance	kg/sec	181
X_M	Motional reactance	ohm	251
Y	Electrical admittance	mho	341
	Young's modulus	newton/m^3	57
Y_M	Motional admittance	mho	344
z	Specific acoustic impedance	kg/m^2 sec (MKS rayl)	122
Z	Acoustic impedance	kg/m^4 sec	189
	Electrical impedance	ohm	26
Z_m	Mechanical impedance	kg/sec	21
Z_r	Radiation impedance	kg/sec	180
Z_M	Motional impedance	ohm	250
α	Damping constant	neper/sec	19
	Absorption coefficient	sabin/ft^2	421
	Attenuation constant	neper/m	225
α_r	Sound power reflection coefficient		131
α_t	Sound power transmission coefficient		131
γ	Exponential time constant	sec^{-1}	5
	Ratio of specific heats		91
	Wave propagation constant	m^{-1}	70
δ	Linear density	kg/m	34

Symbol	*Meaning*	*Units*	*Page*
$\mathscr{E}$	Energy density	joule/m^3	119
ϵ	Dielectric constant		335
ϵ_0	Permittivity of free space	farad/m	300
η	Efficiency		252
	Shear coefficient of viscosity	newton sec/m^2	224
θ	Angle	radian, degree	
κ	Radius of gyration	m	66
	Thermal conductivity	joule/m sec °C	225
λ	Wavelength	m	42
Λ	Magnetostriction constant		366
μ	Magnetic permeability		367
	Pressure reflection coefficient		475
μ_0	Permeability of free space	henry/m	367
ξ, η, ζ	Components of displacement	m	
ρ	Volume density	kg/m^3	58
σ	Area density	kg/m^2	82
	Electrical charge density	coulomb/m^2	335
	Poisson's ratio		100
	Target area	m^2	481
τ	Decay modulus	sec	19
	Relaxation time	sec	221
ϕ	Angle	radian, degree	
	Transformation factor	weber/m	250
ω	Angular frequency	radian/sec	3
Ω	Solid angle	steradian	485

ANSWERS TO ODD-NUMBERED PROBLEMS

Chapter 1

1.1. Proof

1.3. (*a*) $-T\left(\frac{x}{\sqrt{x^2 + a^2}} + \frac{x}{\sqrt{x^2 + (l - a)^2}}\right)$

(*b*) $\frac{1}{2\pi}\sqrt{\frac{Tl}{m(l - a)a}}$ (*c*) $l/2$

1.5. 124 kg **1.7.** Proof

1.9. $a\left(\frac{1}{2} + \frac{2}{\pi}\sin\frac{2\pi t}{T} + \frac{2}{3\pi}\sin\frac{6\pi t}{T} + \frac{2}{5\pi}\sin\frac{10\pi t}{T} + \cdots\right)$

1.11. $R_m = 1.0$ kg/sec; $\omega_d = 9.85$ rad/sec;
$A = 0.0402$ m; $\phi = -5.8°$

1.13. Proof. **1.15.** $\sqrt{\omega_0^2 + R_m^2/4m^2} \pm R_m/2m$

1.17. (*a*) $-(\omega F/Z_m)\sin(\omega t - \phi)$ (*b*) $\omega_0\bigg/\left(1 - \frac{R_m^2}{2\omega_0^2 m^2}\right)^{1/2}$ (*c*) Proof

Chapter 2

2.1. (*a*) 11.2 cycles/sec (*b*) 0.00494 joule (*c*) 0.99 m/sec
2.3. Proof; plot; shows wave velocity **2.5.** $(9h/n^2\pi^2)\sin(n\pi/3)$
2.7. $B_1 = 0.151\, v_0 l^2/c$; $B_3 = -0.0325\, v_0 l^2/c$
$B_2 = B_4 = 0$
2.9. (*a*) 111.8 cycles/sec (*b*) 0.97 newton
2.11. (*a*) 54.2 cycles/sec (*b*) 183 cycles/sec

Chapter 3

3.1. (*a*) $(2n - 1)c/4l$ (*b*) Proof (*c*) 2525 cycles/sec (*d*) Proof
(*e*) $A_1 = 0.000208$ m; $A_3 = -0.000023$ m; $A_5 = 0.0000083$ m

3.3. (*a*) $A = \frac{F\cos k(l - x)}{YSk\sin kl}$ (*b*) $Z - j\rho cS\tan kl$

(*c*) $Z = \rho cS$ (*d*) Plot

3.5. (*a*) 1780 cycles/sec (*b*) 350 newtons (*c*) 1800 cycles/sec

3.7. (*a*) 6800 cycles/sec (*b*) $x = 0.185$ m
(*c*) 1.91 (*d*) 15,930 cycles/sec
3.9. $0.35M$ **3.11.** Proof
3.13. $A = 0.5a$; $B = -0.365a$; $C = -0.5a$; $D = 0.365a$
3.15. Proof **3.17.** (*a*) 36 cycles/sec (*b*) 2000 newtons

Chapter 4

4.1. (*a*) $0.406A$ (*b*) $0.5 = \sin(\pi x/a)\sin(\pi z/a)$ (*c*) Plot; no
4.3. (*a*) 0.0284 m (*b*) 0.0485 m
(*c*) square—395 cycles/sec, 500 cycles/sec
circular—574 cycles/sec, 900 cycles/sec
4.5. Proof
4.7. (*a*) 11,100 cycles/sec (*b*) 0.00555 m; 0.01275 m (*c*) 0.00000624 m
4.9. (*a*) 4000 newtons/m (*b*) 6950 cycles/sec
(*c*) 2.84×10^{-8} m (*d*) 1.41×10^{-8} m
4.11. (*a*) 153 cycles/sec (*b*) 194 cycles/sec
4.13. (*a*) Plot (*b*) Plot (*c*) 3.15 per cent; 47 per cent
(*d*) 1060 cycles/sec
4.15. (*a*) 242 cycles/sec; 555 cycles/sec; 870 cycles/sec; 1185 cycles/sec
(*b*) none; 0.109 m; 0.072 and 0.1595 m; 0.051, 0.117 and 0.183 m
4.17. 1230 cycles/sec (*b*) double the frequency
(*c*) quarter the frequency
4.19. (*a*) -0.0025

(*b*) $y_2 = A_2 \cos(\omega_2 t + \phi_2)\left[J_0\left(\frac{6.3r}{a}\right) - 0.0025\, I_0\left(\frac{6.3r}{a}\right)\right]$

(*c*) Plot (*d*) 0.38

Chapter 5

5.1. Proof; $p = \rho_0 c u$

5.3. (*a*) $\Delta T = \frac{(\gamma - 1)\, Tp}{\gamma P}$ (*b*) 0.076°C **5.5.** Proof

5.7. (*a*) 0.0795 watt/cm^2 (*b*) 48,500 newtons/m^2
(*c*) 0.0328 m/sec (*d*) 2.18×10^{-7} m
(*e*) 2.22×10^{-5} (*f*) 34,300 newtons/m^2 (*g*) 110.7 db
5.9. (*a*) 2.92×10^{-8} joule/m^3; 0.0632 newton/m^2
(*b*) 4.55×10^{-5} joule/m^3; 316 newtons/m^2
5.11. (*a*) Proof (*b*) 430 rayls; 378 rayls
(*c*) 13.8 per cent increase (*d*) 0.56 db increase; none

Chapter 6

6.1. (*a*) 0.0281 newton/m^2 (*b*) 0.00169 watt/m^2; 0.0000019 watt/m^2
(*c*) 29.5 db decrease
(*d*) 66.5 newtons/m^2; 0.0015 watt/m^2; 0.5 db decrease (*e*) 0.109
6.3. (*a*) 0.25 (*b*) 4,440,000 rayls
6.5. (*a*) 12.3 (*b*) 0.385 m and 1.245 m from tile
6.7. (*a*) 1 db (*b*) 0.2 (*c*) TL = 0.2 db; 0.05
6.9. 51.3 db **6.11.** (*a*) 65.5° (*b*) 0.96

6.13. (*a*) 28.5° (*b*) 104 newtons/m^2 (*c*) 4.2 newtons/m^2 (*d*) 0.00176
6.15. (*a*) 69.65° (*b*) 65.4° (*c*) 0.077

6.17. $\alpha_r = \dfrac{\rho_1^2 c_1^2(\cos\theta - 1)^2 + \omega^2\sigma^2\cos^2\theta}{\rho_1^2 c_1^2(\cos\theta + 1)^2 + \omega^2\sigma^2\cos^2\theta}$

Chapter 7

7.1. Proof; Derivation
7.3. 89°, 80°, 28.5°; 7.5, 72, and 365 rayls
7.5. (*a*) 2000 microbars (*b*) 0.027 watt/m^2
(*c*) 0.68 watt (*d*) 0.000023 m
7.7. (*a*) 0.628 watt
(*b*) 5 watts/m^2; 64.5 newtons/m^2; 0.87 m/sec
(*c*) 0.2 watt/m^2; 12.9 newtons/m^2; 0.046 m/sec
7.9. $P = \rho_0 c a U_0/r$; $U = aU_0/r$; $I = \rho_0 c a^2 U_0^2/2r^2$; $W = 2\pi\rho_0 c a^2 U_0^2$
7.11. Proof **7.13.** Plot; 800 cycles/sec
7.15. (*a*) 14.8° (*b*) 114 db

7.17. (*a*) $R_r = \dfrac{4\pi\rho_0 c k^2 a^4}{1 + k^2a^2}$; $X_r = \dfrac{4\pi\rho_0 c k a^3}{1 + k^2 a^2}$

(*b*) $W = \dfrac{2\pi\rho_0 c k^2 a^4 U_0^2}{1 + k^2 a^2}$

7.19. (*a*) 12.7 watts (*b*) 0.0098 watt/m^2 (*c*) 5.9 db (*d*) 0.001 kg
7.21. (*a*) 0.31 m/sec (*b*) 15.2 newtons

Chapter 8

8.1. (*a*) 1.94 cm (*b*) 0.34 microbar
(*c*) 452 cycles/sec (*d*) 452 cycles/sec
8.3. (*a*) $I_t/I_i = 4S_1^2/(S_1 + S_2)^2$ (*b*) $S_1 > S_2$
(*c*) SWR $= S_1/S_2$ for $S_1 > S_2$; SWR $= S_2/S_1$ for $S_1 < S_2$
8.5. (*a*) $S_2 = 0.33S_1$ (*b*) $P_c = 2S_1P/S_2$ (*c*) 6
8.7. (*a*) 164 cycles/sec (*b*) 174 watts (*c*) 7.8 watts
8.9. Plot
8.11. (*a*) $\alpha_t = 4S^2/(2S + S_b)^2$ (*b*) $\alpha_b = 4SS_b/(2S + S_b)^2$
(*c*) $\alpha_t = 0.64$; $\alpha_b = 0.32$ (*d*) no; reflected since $\alpha_r = 0.04$
8.13. (*a*) 0.49 m^3 (*b*) 0.5 **8.15.** Proof
8.17. (*a*) length = 0.75 m; radius = 0.298 m (*b*) 10.2 db
8.19. Plot
8.21. (*a*) 9.55 cycles/sec (*b*) $C = 0.00028$ m^4 sec/kg; $M = 1.0$ kg/m^4
(*c*) $-15.1j$ kg/m^4 sec

Chapter 9

9.1. (*a*) 2.43×10^{-10} sec (*b*) 657 megacycles/sec (*c*) Plot
9.3. 1.66×10^{-10} sec; slightly smaller
9.5. (*a*) 3.18×10^{-5} sec (*b*) Plot (*c*) 61.5; 32; 12.8
9.7. (*a*) 2 db (*b*) 45 db
9.9. (*a*) 0.000154 m (*b*) 339.4 m/sec (*c*) 0.039 neper/m (*d*) 0.68 db
9.11. (*a*) 0.147 db/m (*b*) 0.000096 db/m (*c*) 0.0024 db/m
9.13. (*a*) 46.2 kc/sec (*b*) 73 bubbles/m^3 (*c*) 10 per cent less

Chapter 10

10.1. (*a*) Proof (*b*) 1.32
10.3. (*a*) Proof (*b*) $(4.05 - j0.063)$ kg/sec
10.5. (*a*) 50.4 cycles/sec (*b*) 2.37 (*c*) 0.00189 m (*d*) 0.0005 m
10.7. (*a*) 5 kg/sec; 2500 newtons/m; 0.01 kg (*b*) 13.8 per cent
10.9. Design problem **10.11.** Plot **10.13.** 0.00885 watt
10.15. (*a*) 1040 newtons/m (*b*) 0.144 m^3 (*c*) 4.75 amperes
10.17. (*a*) 0.68 m^3 (*b*) 1.27
10.19. (*a*) 136.5 cycles/sec (*b*) 0.004 m^3/sec (*c*) 0.000327 m
10.21. $\alpha_t = \dfrac{2\sqrt{1-(m/2k)^2}}{1+\sqrt{1-(m/2k)^2}}$
10.23. (*a*) 18.3 (*b*) 0.00059 m^3/sec (*c*) 0.0000335 m
(*d*) 31.4 per cent (*e*) 1.22 volts
10.25. 8.05 watts
10.27. (*a*) $R_A = \sqrt{R_B R_V}$ (*b*) $\eta = \dfrac{\sqrt{R_V} - \sqrt{R_B}}{\sqrt{R_V} + \sqrt{R_B}}$ (*c*) $R_r = R_m\sqrt{\dfrac{R_V}{R_B}}$

Chapter 11

11.1. (*a*) 8.33×10^8 ohms/m (*b*) 0.0417
11.3. (*a*) 34,800 cycles/sec (*b*) -70.4; 360,000 ohms (*c*) -67.8 db
11.5. -32 db
11.7. (*a*) -100 db (*b*) -63 db (*c*) 0.0005
11.9. (*a*) Plot (*b*) Plot (*c*) Plot (*d*) Peaks at 2150 cycles/sec
11.11. $F = 2PSkl \cos kx \cos \omega t$; proof **11.13.** -68 db
11.15. (*a*) -40 db (*b*) 0.605 newton/m^2

Chapter 12

12.1. (*a*) 4.6×10^{-8} (*b*) 3620 newtons/m^2 (*c*) 1.24×10^{-10} joule
12.3. (*a*) 45.4 kilocycles/sec
(*b*) $C_0 = 2.36\ \mu\mu$f; $C = 0.02\ \mu\mu$f; $L = 607$ henrys; $R = 8660$ ohms
12.5. Proof
12.7. (*a*) 13.67 kilocycles/sec (*b*) 1.92 watts (*c*) $192 + j840$ micromhos
12.9. (*a*) $\sigma = dF_y/S_y$ (*b*) 2.75×10^{-6} coulomb (*c*) 8880 volts
12.11. (*a*) 20.5 kilocycles/sec (*b*) $90 + j\,400$ micromhos
(*c*) 2635 volts (*d*) 24.08 kilocycles/sec; 17.44 kilocycles/sec
(*e*) 90 micromhos (*f*) 3.13
12.13. (*a*) 958 kilocycles/sec (*b*) 2400 volts (*c*) 0.0014 watt/cm^2
12.15. (*a*) Proof (*b*) 0.092 for thickness; 0.1 for longitudinal
(*c*) 0.4 for thickness; 0.18 for longitudinal
12.17. (*a*) Proof (*b*) Proof (*c*) 0.00029 volt per newton/m^2
12.19. (*a*) $E/P = e_{11}t/\epsilon\epsilon_0 c_{11}$ (*b*) 0.00002 volt per newton/m^2
12.21. (*a*) $C_0 = 3180\ \mu\mu$f; $C = 216\ \mu\mu$f; $L = 0.058$ henry; $R = 2000$ ohms
(*b*) 8.2 (*c*) 0.277
12.23. (*a*) -0.715×10^{-4} (*b*) contracts 6.85×10^{-7} m
(*c*) 39.5 newtons (*d*) contracts 2.07×10^{-7} m
(*e*) 11.9 newtons

12.25. (*a*) 19.65 kilocycles/sec (*b*) 8.2 volts (peak)
12.27. (*a*) 31 kilocycles/sec (*b*) $9.43f \times 10^{-9}$ volt per newton/m^2
(*c*) $-180.5 + 20 \log f$
12.29. (*a*) 13.5 ohms (*b*) 26.2 per cent

Chapter 13

13.1. (*a*) 36 phons; 0.7 sone (*b*) 48 db (*c*) 75 db
13.3. (*a*) 87.7 db (*b*) 80 sones (*c*) 99 db
13.5. $a_2P^2/2$; $(a_1P + 3a_3P^3/4)$; $a_2P^2/2$; $a_3P^3/4$
13.9. 47 db
13.11. (*a*) $\text{PSL} = 128 - 20 \log f$
(*b*) decreases 6 db per octave increase in frequency (*c*) 77 db
13.13. 89 db

Chapter 14

14.1. (*a*) $\dfrac{d\text{IL}}{dt} = \dfrac{1.087ac}{V(e^{act/4V} - 1)}$ (*b*) infinite; zero (*c*) $2.76V/ac$
14.3. (*a*) 77.6 db (*b*) 0.0141 sec (*c*) 5.85 sabins
14.5. (*a*) 0.000061 watt (*b*) 0.154 (*c*) 1.12 sec (*d*) 57.5 db
14.7. (*a*) 1.47 sec (*b*) 0.000635 watt (*c*) 0.045 (*d*) No
14.9. (*a*) 66 db (*b*) 52 phons (*c*) 62 db; 60 phons
14.11. (*a*) 6.67 ft (*b*) 168 (*c*) 0.238 sec (*d*) 0.29 (*e*) 0.238 sec
14.13. Proof **14.15.** (*a*) Proof (*b*) 0.00592 ft^{-1} (*c*) 0.76 sec
14.17. (*a*) Derivation (*b*) 84.2 db (*c*) 0.272
14.19. 0.00014 watt (*b*) 2200 sabins (*c*) 0.2 sec
14.21. (*a*) 0.356; 1.07; 2.15; 3.6; 5.4; 7.6 (*b*) 288 cycles/sec
14.23. 0.406 (*b*) 0.217 sec (*c*) 0.354 sec
14.25. (*a*) 1.22 sec (*b*) 1.63 sec (*c*) 1.05 sec
14.27. (*a*) Plot (*b*) 0.79
14.29. (*a*) 1950 cycles/sec (*b*) 0.113 sec (*c*) 116 db
(*d*) 138 cycles/sec; 184 cycles/sec; 230 cycles/sec

Chapter 15

15.1. (*a*) 1475.1 m/sec (*b*) 0.00215 db/m **15.3.** Proof
15.5. (*a*) 1340 m (*b*) 1.48° (*c*) 2330 m (*d*) 308 m
15.7. (*a*) 115 m (*b*) 183.5 m
15.9. (*a*) Derivation (*b*) 0.002 sec (*c*) at depths between 55 and 100 m
15.11. (*a*) Derivation (*b*) 0.02 m
15.13. (*a*) $r = 6.3\, khd$ (*b*) 2640 m
15.15. (*a*) 25.5 db (*b*) 133.5 db (*c*) 16.66°
15.17. (*a*) 44 db (*b*) −12 db
15.19. (*a*) 4000 m (*b*) 4600 m **15.21.** 725 m
15.23. Derivation; 7.5 m/sec **15.25.** (*a*) 1260 m (*b*) 5000 m
15.27. (*a*) $f = 470/\sqrt{r}$ (*b*) 4.7 kilocycles/sec (*c*) 220,000 m
15.29. (*a*) 11.2 db (*b*) 10.4° (*c*) 12.3°; $0.22E_0$ (*d*) +2 db

INDEX